Multipoint Lightcone Bootstrap from Conformal Block Integrability

Dissertation
zur Erlangung des Doktorgrades
an der Fakultät für Mathematik, Informatik und Naturwissenschaften
Fachbereich Physik
der Universität Hamburg

vorgelegt von

Jeremy A. Mann

Hamburg

2022

Gutachter/innen der Dissertation:	Prof. Dr. Volker Schomerus Prof. Dr. Gleb Arutyunov
Zusammensetzung der Prüfungskommission:	Prof. Dr. Volker Schomerus Prof. Dr. Gleb Arutyunov Prof. Dr. Sven-Olaf Moch Dr. Pedro Liendo Dr. Christof Weitenberg
Vorsitzende/r der Prüfungskommission:	Prof. Dr. Sven-Olaf Moch
Datum der Disputation:	01.02.2023
Vorsitzender Fach-Promotionsausschusses PHYSIK:	Prof. Dr. Günter H. W. Sigl
Leiter des Fachbereichs PHYSIK:	Prof. Dr. Wolfgang J. Parak
Dekan der Fakultät MIN:	Prof. Dr.-Ing. Norbert Ritter

Zusammenfassung

Konforme Feldtheorien sind allgemeine Beschreibungen skaleninvarianter Systeme. Letztere reichen von kontinuierlichen Phasenübergängen bis zu Quantengravitationstheorien. Der Lichtkegel Bootstrap bezeichnet in diesem Kontext einen analytischen Ansatz zum Herausfiltern physikalischer Daten aus der Gleichung der Kreuzungssymmetrie der Korrelationsfunktion. Die Gleichung ist gelöst in der Nähe von Lichtkegel Singularitäten, wobei manche Einfügepunkte zu lichtartigen Trennungen tendieren. In dieser Arbeit wird ein Fortschritt in der Erweiterung vom Lichtkegel Bootstrap der Korrelationsfunktionen bis zu mehr als vier Feldern erzielt. Die Annäherung stützt sich hauptsächlich auf die Integrabilitätstheorie von konformen Partialwellen, die den größten Teil dieser Arbeit einnimmt. Die Partialwellen, hier die kinematischen Bestandteile von Korrelationsfunktionen, sind neu umgestaltet zu Wellenfunktionen eines mehrkörperlichen Quanten-Integrabelsystems. Nach der Konstruktion dieser Integrabelsysteme im Allgemeinen wird das entsprechende System von Differenzialgleichungen für Mehrpunkt-Partialwellen berechnet. Durch die detaillierte Analyse der Differenzialgleichungen bestimmen wir die präzisen Beziehungen zwischen Partialwellen höherer und niedrigerer Punkte sowie explizite Lösungen für verschiedene Grenzwerte. Auf Grundlage dieser Ergebnisse lösen wir in den ersten führenden Ordnungen die Fünf-Punkt-Kreuzungsgleichung und legen damit im sogenannten Kammkanal den Grundstein für den Lichtkegel Bootstrap mit sechs Punkten.

Abstract

Conformal field theories are universal descriptions of scale-invariant systems, ranging from critical phenomena all the way to theories of quantum gravity. In this context, the lightcone bootstrap program is an analytic approach to extracting physical data from the crossing symmetry equation of correlation functions. The equation is solved near lightcone singularities, where insertion points tend to lightlike separation. In this thesis, we make progress in extending the lightcone bootstrap to correlation functions of more than four fields. Our approach relies primarily on the integrability based theory of multipoint conformal blocks, which occupies the largest part of this work. The blocks, that is to say the kinematical constituents of a correlation function, are recast as wavefunctions of a many-body quantum integrable system. After constructing these integrable systems in full generality, we determine the corresponding system of differential equations that they entail for so called comb channel blocks. Following a detailed analysis of these differential equations, we then derive precise relations between higher and lower point blocks, as well as explicit solutions in various limits. Based on these results, we solve the five-point crossing equation at the first leading orders and lay the groundwork for the six-point comb channel lightcone bootstrap.

Eidesstattliche Versicherung / Declaration on Oath

Hiermit versichere ich an Eides statt, die vorliegende Dissertationsschrift selbst verfasst und keine anderen als die angegebenen Hilfsmittel und Quellen benutzt zu haben.

Hamburg, den 19.09.2022

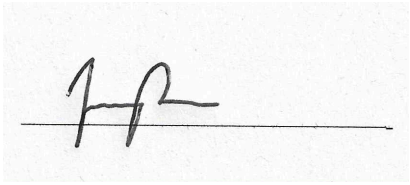

Unterschrift des Doktoranden

Für Selina und unsere drei Jahre zusammen in Hamburg.

Acknowledgements

I would first like to thank my supervisor, Volker Schomerus, for his steadfast support and guidance throughout these last three years. In my first experience navigating through the uncertainties of a long-term research project, I was given the freedom to explore my own ideas whilst greatly benefitting from his experience and intuition. It has been a pleasure working together, and I look forward to our continued collaboration in the future.

Next, I would like to thank my co-authors Ilija Burić, Sylvain Lacroix, Lorenzo Quintavalle and Apratim Kaviraj. This research project, mixing Conformal Field Theory and Integrability, analytics and numerics, kinematics and bootstrap, was only successful as a collective enterprise. Aside from the papers we have written together, our numerous extended discussions have been an indispensable source of insight. Our collaborations have been a truly enriching experience, and I'm excited to continue them in the future.

Throughout my time in Hamburg, I have profited from the vibrant and stimulating research environment that the DESY Theory Group has to offer, and I am grateful to all of the members and faculty that make it that way. With professors, postdocs and fellow Ph.D. students, I have always greatly enjoyed and gained a lot from our countless lunch discussions, seminars and social events. Relatedly, it would be remiss of me not to mention the numerous interactions and colloquia with the Center for Mathematical Physics of the University of Hamburg, which have undeniably enhanced my academic experience here.

Finally, I am grateful to my parents and my sister for their unwavering support and encouragement in all of my higher education pursuits and, by the same token, to Selina for her invaluable support during these three years.

Statement of Originality

The first three chapters review known results in the literature, although the presentation is original. Chapters four through six are based on the following works.

1. I. Burić, S. Lacroix, J. A. Mann, L. Quintavalle, and V. Schomerus, "*Gaudin models and multipoint conformal blocks III: comb channel coordinates and OPE factorisation*", JHEP 06, 144 (2022), arxiv:2112.10827.

2. I. Burić, S. Lacroix, J. A. Mann, L. Quintavalle, and V. Schomerus, "*Gaudin models and multipoint conformal blocks. Part II. Comb channel vertices in 3D and 4D*", JHEP 11, 182 (2021), arxiv:2108.00023.

3. I. Burić, S. Lacroix, J. A. Mann, L. Quintavalle, and V. Schomerus, "*Gaudin models and multipoint conformal blocks: general theory*", JHEP 10, 139 (2021), arxiv:2105.00021.

4. I. Burić, S. Lacroix, J. A. Mann, L. Quintavalle, and V. Schomerus, "*From Gaudin Integrable Models to d-dimensional Multipoint Conformal Blocks*", Phys. Rev. Lett. 126, 121603 (2021), arxiv:2009.11882.

All authors contributed equally to the above publications. Finally, chapter seven is based on the following forthcoming work.

5. A. Kaviraj, J. A. Mann, L. Quintavalle, and V. Schomerus, "*Multipoint comb channel lightcone bootstrap*", in preparation (2022).

The author's last publication, not included in this thesis, is stated below.

6. M. R. Gaberdiel and J. A. Mann, "*Stringy CFT duals with* $\mathcal{N} = (2, 2)$ *supersymmetry*", JHEP 2001, 160 (2020), arxiv:1910.10427.

Contents

1 Introduction **1**
- 1.1 Conformal symmetry in physics 1
- 1.2 The conformal bootstrap 4
- 1.3 The conformal bootstrap at higher points 7
- 1.4 Plan of the thesis 8

I Conformal Field Theory Review **11**

2 Foundations of Conformal Field Theory **13**
- 2.1 Conformal symmetry 13
  - 2.1.1 The conformal group 14
  - 2.1.2 The conformal algebra 16
  - 2.1.3 Conformal completions and embedding space 19
  - 2.1.4 Primaries and descendants 22
- 2.2 Unitarity 23
  - 2.2.1 Positive energy representations 23
  - 2.2.2 Reflection positivity 25
  - 2.2.3 Unitarity bounds 25
- 2.3 The operator product expansion 26
  - 2.3.1 State operator correspondence and OPE 26
  - 2.3.2 Three-point functions and OPE coefficients 27
  - 2.3.3 Higher point functions from the OPE 29
- 2.4 The conformal bootstrap 31
- 2.A Derivation of unitarity bounds 32

3 Conformal Correlators and Blocks **35**
- 3.1 The embedding space formalism 35
  - 3.1.1 Tensor representations of the conformal algebra 35
  - 3.1.2 Back to tensor representations in position space 39
- 3.2 Conformal invariance of correlation functions 39
  - 3.2.1 Two-point functions 41
  - 3.2.2 Three-point functions and tensor structures 42
  - 3.2.3 Scalar N-point functions 43
- 3.3 The conformal block decomposition 44

3.3.1 Casimir differential equations 45
3.3.2 Integral representations 47

II The Integrability Based Theory of Multipoint Blocks 51

4 Multipoint Conformal Blocks from Gaudin Integrable Models 53
4.1 Summary of Results 53
4.2 The Vertex Integrable System 59
4.2.1 Reduction to the vertex systems 59
4.2.2 The vertex system and Gaudin models 61
4.2.3 Restricted vertices and relations between vertex operators 64
4.3 OPE channels and limits of Gaudin models 69
4.3.1 N sites Gaudin model and OPE limits 69
4.3.2 Examples 72
4.3.3 Recursive proof of the limits 75
4.4 Example: five-point conformal blocks 77
4.5 Outlook 79
4.A Proof of the induction in the limits of Gaudin models 80
4.A.1 Reference vertex 80
4.A.2 Vertices in V'. 82
4.A.3 Vertices in V'' 83
4.B Proof of relations using embedding space formalism 84
4.B.1 Classical Embedding space 84
4.C Relations among vertex differential operators 84

5 Three-Point Vertex Integrable Systems 87
5.1 Review and Summary of Results 87
5.1.1 Reduction to vertex systems via shadow integrals 88
5.1.2 From Gaudin Hamiltonians to Lemniscatic CMS models 89
5.2 Three-Point Functions in Embedding Space 91
5.2.1 Spinning 3-point functions in embedding space 91
5.2.2 Embedding space construction in $d = 4$ dimensions 94
5.3 The Single Variable Vertex Operator 99
5.3.1 Construction of the reduced vertex operator 100
5.3.2 Relation with vertex operator for 5-point functions 103
5.4 Vertex Operator and Generalized Weyl algebras 107
5.4.1 Single variable vertices and the Gegenbauer scalar product 107
5.4.2 A generalized Weyl algebra acting on tensor structures 109
5.5 Map to the Lemniscatic CMS model 112
5.5.1 The elliptic $\mathbb{Z}/4\mathbb{Z}$ CMS model 113
5.5.2 Construction of the map 115
5.5.3 CMS multiplicities from weights and spins 117
5.6 Outlook 119
5.A Map from $\mathfrak{so}_{\mathbb{C}}(6)$ embedding space to $\mathfrak{sl}_{\mathbb{C}}(4)$ twistors 120
5.B Comments on scalar products and unitarity 122

5.B.1 Integral formula for the SO($d+2$)-invariant scalar product 122
5.B.2 Generalizations to different real forms of $\mathfrak{so}_{\mathbb{C}}(d+2)$ 124
5.B.3 Iterated integration over Poincaré patches 126
5.B.4 Application to the scalar products of 3-point vertex systems 127
5.B.5 Relationship with boundary and projective space in CFT_{d-2}: 132
5.C The d-deformation of the MST_2-MST_2-scalar vertex operator 133
5.C.1 Comparison with one-dimensional vertex systems 133
5.C.2 The constant shift for the CMS Operator 134

6 OPE Limits and Cluster Decomposition 137
6.1 Summary of results 138
6.2 Cross ratios for multipoint correlation functions 142
6.2.1 Prologue: Cross ratios for four-point blocks 142
6.2.2 Polynomial cross ratios for comb channel multipoint blocks 145
6.2.3 Five-point OPE cross ratios 147
6.2.4 Six-point OPE cross ratios 149
6.2.5 Generalization to higher number of points 150
6.3 OPE limits and factorization for six-point blocks 151
6.3.1 Preliminaries on comb channel six-point blocks 152
6.3.2 The OPE limit from embedding space 153
6.3.3 OPE limits of six-point blocks 156
6.A Construction of a six-point conformal frame 159
6.B Middle leg OPE limit in embedding space 162
6.C OPE limit factorization of six-point blocks in one-dimensional CFT 163

III Applications to the Multipoint Lightcone Bootstrap 165

7 Multipoint Comb Channel Lightcone Bootstrap 167
7.1 Applications of OPE and Polynomial Cross Ratios 167
7.2 Lightcone Bootstrap for Four Points 169
7.2.1 Preliminaries on blocks and lightcone limits 169
7.2.2 Lightcone blocks in the direct channel 170
7.2.3 Lightcone blocks in the crossed channel 173
7.2.4 Review of the four-point lightcone bootstrap 174
7.3 Lightcone Bootstrap for Five Points 177
7.3.1 Preliminaries on blocks and lightcone limits 178
7.3.2 Lightcone blocks: general strategy 179
7.3.3 Lightcone blocks in the direct channel 182
7.3.4 Lightcone blocks in the crossed channel 184
7.3.5 Five-point lightcone bootstrap revisited 189
7.4 Outlook 197
7.4.1 Five points 197
7.4.2 Six points 198
7.A Five-point lightcone blocks 201
7.A.1 Integral representation from lightcone OPE 201

7.A.2 Power series expansion of lightcone blocks 202
7.A.3 Further limits 204
7.B Double integral computation 208

8 Conclusion and Future Perspectives 209

Chapter 1

Introduction

> It was quite obvious to me that the critical phenomena are equivalent to relativistic quantum field theory, continued to imaginary time. I felt that they provided an invaluable opportunity to study elementary particle physics at small distances. The "imaginary time" didn't bother me at all; on the contrary I felt that it is the most natural step, ultimately uniting space and time, and making the ordinary time just a matter of perception.
>
> — A.M. Polyakov [1]

Symmetries play a fundamental role in physics. By Noether's theorem, they imply universal conservation laws. In statistical and quantum physics, they give rise to robust classification schemes for phases of matter, particles and fields, leading to the spectacular successes of the Landau theory of phase transitions and of the Standard Model of particle physics. In this context, be it in condensed matter or high energy physics, the enhancement of distance preserving (isometric) to angle preserving (conformal) transformations of space or spacetime carries a plethora of far reaching implications that physicists continue to explore to this day.

The importance of conformal symmetry in condensed matter and particle physics was not well understood until the second half of the 20th century[1]. Indeed, most physical systems are characterized by intrinsic length scales, like the de Broglie wavelength of a particle, or the correlation length of a thermodynamical system. The system will behave very differently when it is probed at a resolution near to or far from the intrinsic lengths, such that conformal symmetry emerges only when the lengths vanish or diverge. Remarkably, such conditions are met in a wide variety of physical systems and models: critical points of continuous phase transitions, quantum field theories at fixed points of the renormalization group (RG) flow, and quantum field or gravity theories in Anti de Sitter space. All of these realizations share one common description: that of a conformal field theory (CFT).

1.1 Conformal symmetry in physics

Continuous phase transitions. Continuous phase transitions are characterized by the divergence of the correlation length at the critical point. In this context, the phenomenon of critical opalescence in binary mixtures of liquids and/or gases was perhaps the first visible manifestation of conformal

[1] See [2] for a comprehensive and authoritative review of the early history of conformal transformations (and closely related Weyl transformations) in physics, starting from Lord Kelvin's observation that the Laplace equation is invariant under conformal inversion [3].

symmetry in nature. There, the near divergence of the correlation length translates to large fluctuations of the liquid/gas densities. As Smoluchowski first explained in 1908 [4, Sec. 7], once these fluctuations reach scales comparable to wavelengths of visible light, Rayleigh scattering in the medium will cause the otherwise transparent liquid/gas mixture to appear cloudy. At the quantitative level, the emergence of conformal symmetry is demonstrated by the scaling behavior of thermodynamic quantities. For example, the two point correlation function of the order parameter[2] $\phi(x)$, measured in scattering experiments, takes the form $\langle\phi(x)\phi(0)\rangle \sim (x^2)^{-\Delta_\phi}$, where Δ_ϕ is one example of a critical exponent[3], also called a scaling dimension in this case. Critical exponents are insensitive to the microscopic details of the system — this property was first observed experimentally in the case of binary mixtures, in accordance with the "law of corresponding states", see Fig. 1. Even more surprisingly, these binary mixtures share the same critical exponents as the uniaxal magnetic phase transitions described by the $d = 3$ Ising model (see Fig. 2a). This family of critical points with common exponents is said to define a *universality class*. Ultimately, these classes can be fully characterized by only a few common properties of the system, such as the dimension d and the internal symmetry group[4].

RG fixed points. Wilson's theory of renormalization, building on the insights of scaling theory, explains the emergence of conformal symmetry and universality in critical systems at the microscopic level. At the same time, it generalizes those insights to the relativistic quantum field theories (QFTs) of particle physics and cosmology. In the Wilsonian paradigm, a QFT is a trajectory, called renormalization group (RG) flow, in the space of all possible couplings $g \int \mathrm{d}^d x\, \mathcal{O}(x)$ that can be included in the Hamiltonian. Starting from a specific point, one moves along this trajectory by integrating out all short distance (UV) degrees of freedom in the partition function below a certain factor. After rescaling fields and space(time) according to that same factor, the resulting Hamiltonian is the RG transformation of the former. At fixed points of the RG flow, the Hamiltonian is manifestly scale invariant. In the neighborhood of this fixed point, the RG transformation can be linearized and subsequently diagonalized with eigenvalues $d - \Delta_\mathcal{O}$, where $\Delta_\mathcal{O}$ is the scaling dimension of the corresponding operator/coupling. In particular, two trajectories differing only by *irrelevant* operators $\Delta_\mathcal{O} > d$ will flow to the *same* fixed point — this mechanism underlies the phenomenon of universality, as illustrated in Fig. 2b.

In particle physics, RG fixed points can be constructed from quantum theories of massless fields. In this language, the linearized RG flow is encoded in the β functions of the couplings. There is a fixed point only if conformal symmetries are not broken by quantum fluctuations, that is to say, if the conformal symmetry enjoyed by the classical field theory is not anomalous. One important example is QCD with N_c colors and N_f flavors, which is known to have a vanishing β function for a specific N_c dependent interval of N_f at the perturbative level [7, 8]. A precise determination of this conformal window at finite N_c remains an important open problem in theoretical physics. In general, exploiting conformal symmetry may be the best way to improve our understanding of quantum field theory (QFT). In this context, the uncontested "harmonic oscillator" of QFT is the maximally supersymmetric Yang-Mills

[2] In Ginzburg-Landau theory, this is a local observable like the relative density of a binary mixture or the magnetization of a solid that provides an effective description of the system, typically at mesoscopic scales.

[3] To quote [5, p. 13], "there are essentially as many exponents as there are singular functions [correlation length, specific heat, etc.], and the Greek alphabet is fast being exhausted." After Wilson's theory of renormalization made all of the relations between critical exponents clear, this Greek alphabet was replaced with a much shorter list of scaling dimensions associated to relevant, marginal and irrelevant operators.

[4] The $d = 3$ Ising universality class has $\mathbb{Z}_2$ symmetry, corresponding to the flip $M \leftrightarrow -M$ of the magnetization in the case of uniaxal magnets. This same symmetry only emerges asymptotically close to the critical point in the case of binary mixtures, c.f. Fig. 1.

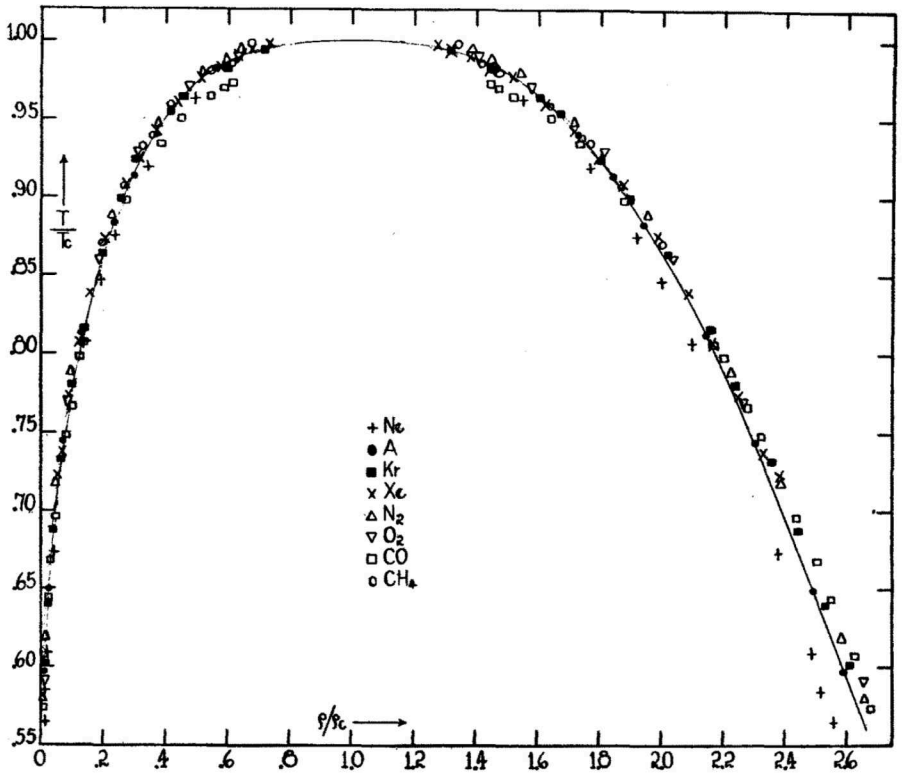

Figure 1: Experimental evidence of the principle of corresponding states for the liquid-gas phase transition of various chemical substances, compiled by E.A. Guggenheim in 1945. Reprinted from [6], with the permission of AIP Publishing. The vertical axis is the reduced temperature T/T_c, while the horizontal axis is the reduced density ρ/ρ_c. In the neighborhood of the critical point $T \sim T_c$, the fit from [6, Eq. (6.4)] is $\rho_{\text{liq}} - \rho_{\text{gas}} \propto (T_c - T)^\beta$, with critical exponent $\beta \sim 1/3$, providing the first manifestation of scaling behavior near the critical point.

theory in $d = 4$. Conformal at *all* values of the coupling and integrable in the planar limit, its study has yielded unprecedented insight into the non-perturbative structures of gauge theories. It is also the best understood example of a CFT holographically dual to a theory quantum gravity.

AdS/CFT correspondence. The equivalence between conformal transformations of d dimensional flat space and isometries of $d+1$ dimensional Anti de Sitter space (AdS) was known at least since Dirac's work [9], where he constructed irreducible representations in terms of fields on AdS for $d = 3$. These "singletons" (see [10] and references therein) were later generalized and related to massless free fields on the conformal boundary of AdS, namely the Lorentzian cylinder (depicted in Fig. 9). In parallel, Lüscher and Mack [11] gave convincing evidence that CFTs extend from the Penrose diagram of Minkowski spacetime to the whole Lorentzian cylinder, where the conformal group acts transitively and preserves a causal ordering. These findings set the stage for the seminal work of Maldacena [12], followed by Gubser-Klebanov-Polyakov [13] and Witten [14], establishing the holographic correspondence between certain quantum gravity or field theories in AdS and CFTs at the boundary. Starting with Maldacena's example of $\mathcal{N} = 4$, SU(N_c) Yang-Mills theory at large N_c, it is now believed (and has been checked in myriad cases) that any CFT with a sparse spectrum and an analogous large N

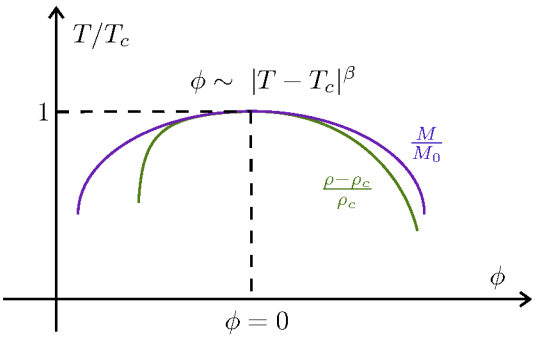

(a) Universal scaling laws.

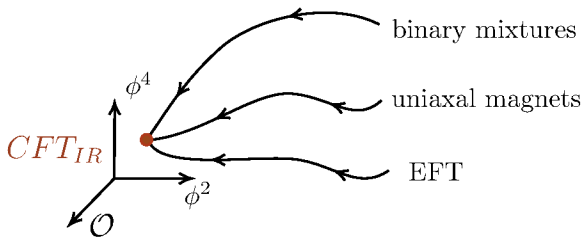

(b) Renormalization group flows.

Figure 2: Illustration of the concept of universality. Left: scaling of the order parameter (reduced magnetization and relative density for uniaxal magnets and binary mixtures respectively) in the neighborhood of the critical temperature $T \sim T_c$. Right: RG flows to the $d = 3$ Ising CFT. The microscopic theories differ only up to irrelevant operators $\mathcal{O}$.

expansion is dual to a local field or gravity theory in the bulk[5]. In this way, CFTs constitute the most rigorous non-perturbative formulation of quantum gravity that we know. This discovery led to an explosion of interest in the subject, playing arguably a key role in the revival of the conformal bootstrap program for $d > 2$.

1.2 The conformal bootstrap

The phenomenon of universality implies an inherent redundancy in the standard microscopic description of physical systems near a critical point. In this setting, the conformal bootstrap discards this redundancy of microscopic models for an equally universal description of criticality.

Foundations. The conformal bootstrap is a non-perturbative approach to CFT, aiming to constrain the physical data without recourse to an explicit Hamiltonian or Lagrangian. After the classification of observables based on scaling dimensions, the operator product expansion (OPE) is the second fundamental ingredient of this framework[6]. The notion that a product of two operators expands into a linear combination thereof at short distances originated in perturbation theory, but was then generalized by Wilson[7] [24], Kadanoff [25] and Polyakov [26]. In the presence of conformal symmetry, the OPE converges even at finite distances and is fixed entirely up to a set of numbers called *OPE coefficients*, similar to the structure constants of an infinite dimensional Lie algebra.
The OPE can be consistently applied to correlation functions if and only if it is associative. Inside of a four-point function, this leads to an infinite set of quadratic equations for the OPE coefficients analogous to a Jacobi identity, viz. Fig. 3. On both sides of this crossing symmetry equation (CSE), the kinematical dependence on spacetime positions and spin degrees of freedom is fixed by conformal

[5] see [15, p. 7] for a more precise statement of the conjecture.

[6] The older incarnation of the bootstrap named after Migdal [16] and Polyakov [17, 18] did not rely on an OPE, imposing instead conformal invariance of the skeleton expansion of N-point vertex functions (see [19, 20] for more details). While less agnostic about the microscopic details of the theory (c.f. the introduction of [21]), this approach was recently revisited in [22] with some promising results.

[7] Interestingly enough, in contrast to Kadanoff and Polyakov, Wilson developed the OPE for the theory of strong interactions and did not envisage its applications to critical systems [23]

symmetry and repackaged entirely into the *conformal blocks*. These intricate functions of external fields' space(time) and spin degrees of freedom, represented graphically by the diagrams of Fig. 3, are also called *conformal partial waves* in analogy to plane waves for translation invariant systems. Together, the CSEs of the four-point functions encode the fundamental constraints on the scaling dimensions and OPE coefficients that the bootstrap program endeavors to solve, as first described in [21, Sec. 2] and [27, Sec. 6].

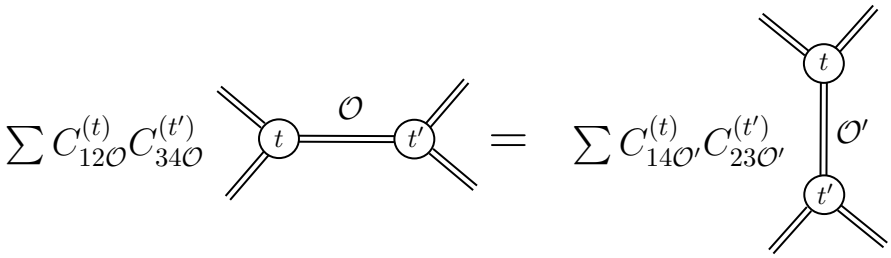

Figure 3: Graphical representation of a crossing symmetry equation with OPE diagrams. The numbers $C^{(t)}_{ijk}$ denote the OPE coefficients, while the diagrams represent the kinematical constituents of the correlation function, the conformal blocks. The internal legs of the diagram are labeled by the operators appearing in the OPE, and the vertex labels t, t' distinguish multiple occurrences of the same operator in an OPE.

The bootstrap's first major success was [28], where Belavin, Polyakov and Zamolodchikov exploited the infinite dimensional enhancement of conformal symmetry in $d = 2$ dimensions to determine exact results for critical exponents and correlation functions in a family of CFTs called minimal models. Since their breakthrough paper, two dimensional CFT has grown into its own independent field of research, with immediate connections to the worldsheet description of string theory and the mathematics of vertex operator algebras.

Numerical bootstrap. For $d > 2$, the first explorations of the bootstrap in the 70s fell short of recasting the CSEs into a concrete computational scheme. However, in the aftermath of AdS/CFT, Dolan and Osborn [29, 30] made significant progress in computing the conformal blocks. Their closed form expressions in $d = 4$ were then used in the first numerical implementation of crossing symmetry constraints by Rattazzi, Rychkov, Tonni and Vichi [31] that gave birth to the modern numerical bootstrap program. Since then, further improvements in the evaluation of blocks and the further development of efficient numerical algorithms have continued to increase the numerical bootstrap's precision and scope (see [32] for a comprehensive review). One of the greatest successes of this program has been the determination of the scaling dimensions and OPE coefficients of the $d = 3$ Ising universality class at hitherto unattainable levels of precision [33].

Analytic/lightcone bootstrap. In parallel, the large N expansion of CFTs with an AdS bulk dual had gone under intense investigation, producing new insights into the analytic structure of the crossing symmetry equations. The operators in their OPEs were understood in terms of two-particle states in AdS, and the observation that these particle pairs become non-interacting at large spin[8] suggested a novel perturbative approach to the bootstrap. The lightcone bootstrap, anticipated in [34] and initiated in [35, 36], built on this idea to solve the CSE of four scalars near lightcone limits. As

[8]Spin refers here to the eigenvalue of the Casimir operator for the rotation or Lorentz subgroup of the conformal group. This will be explained in detail in later chapters.

Ferrara et al. [37–39] had shown in the 70s, the lightcone limit only suppresses the *twist* of exchanged operators, that is to say the scaling dimension minus the spin. The decoupling of two-particle states translates to the additivity of twist in the large spin limit, such that the CSE in lightcone limits is solved by a large spin expansion of double-twist CFT data — see Fig. 4. Contrary to the more traditional

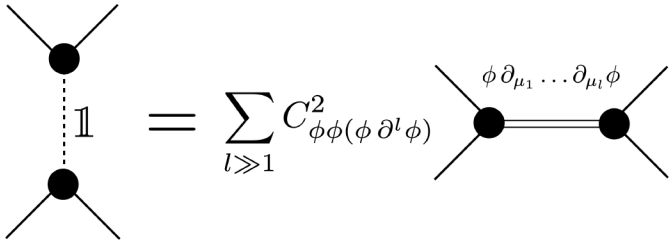

Figure 4: Crossing symmetry equation of the four-point function of a scalar field ϕ at leading order in the lightcone limits. A black vertex indicates that every operator appears only once in the OPE, so that its associated OPE coefficient is unique. This equation admits a unique solution for the double-twist OPE coefficients $C_{\phi\phi(\phi\,\partial^l\phi)}$ at large spin.

large N or small ε expansions, the lightcone bootstrap applies universally to *any* CFT in Lorentzian signature. While the convergence properties of the large spin expansion were initially unclear, the work of Simmons-Duffin [40] in the $d = 3$ Ising model demonstrated surprisingly close agreement with numerical results down to spin two, strongly suggesting that the large spin expansion at fixed twist converges. This was later proven in Caron-Huot's landmark paper [41] with the inception of the Lorentzian inversion formula, an analog of the Froissart-Gribov formula for scattering amplitudes. For the many subsequent developments in the analytic bootstrap, we refer to [42] and references therein.

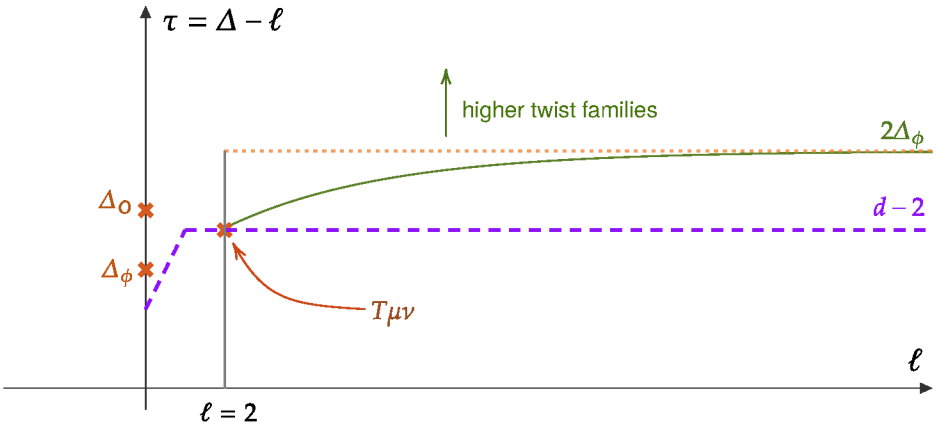

Figure 5: Schematic depiction of an allowed spectrum of twists (scaling dimension minus spin) as a function of spin in a generic unitary CFT. The dashed purple curve is the lower bound imposed by unitarity. Double-twist operators with spin $\ell \geq 2$ lie on smooth Regge trajectories, the lowest of which is represented above in green.

The state of the art. To summarize, the numerical and analytic bootstrap are complementary. The former is optimal in determining CFT data for low twist and low scaling dimension at high levels of precision, while the latter expands double-twist data at higher spin as a function of the low spin, single-twist input. The state of the art in the conformal bootstrap compares the outputs of both analyses for the most complete description of the CFT data, as in e.g. [40, 43]. Ideally, analytics and numerics could be combined into a "hybrid" bootstrap [44] for maximal efficiency, provided the analytic approximations are accompanied by rigorous error bars — see [45] for progress in this direction.

1.3 The conformal bootstrap at higher points

Higher point crossing symmetry equations. Despite its numerous achievements, the current formulation of the conformal bootstrap is limited to finite sets of four-point functions of low twist and low spin fields. On the other hand, associativity of the OPE is encoded in the crossing symmetry of *all* four-point functions, even for external fields of arbitrarily large spin and conformal dimension. In this regard, a promising approach to efficiently encode infinite sets of four-point CSEs is the analysis of higher point functions. Indeed, any higher point function generates an infinite set of four-point functions with the OPE, as one may for example intuit from Fig. 6. At the current time, it is not clear how many higher point CSEs are needed to reproduce the full set of associativity constraints. For example, this can depend on how the external fields transform under the symmetries of the theory. However, a single one already contains more dynamical information than any finite set of four-point functions could ever capture — that much is clear.

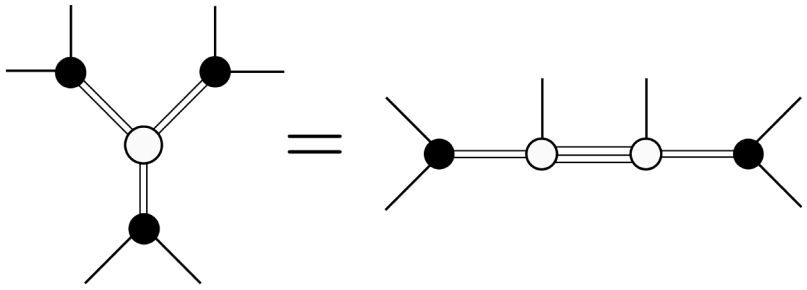

Figure 6: Example of a scalar six-point crossing symmetry equation from a "snowflake" channel to a "comb" channel. Each side involves a sum over products of four OPE coefficients. Internal legs are associated to operators appearing in the OPE, while white vertices are associated to tensor structures that distinguish between multiple appearances of the same operator in an OPE.

The integrability based approach to higher point blocks. The higher point bootstrap suffers from the same bottleneck as the four-point bootstrap did in the 70s: insufficient knowledge of the blocks. While there has been recent progress in computing these higher point blocks [46–56], particularly for the exchange of scalar fields, efficient methods tantamount to Dolan and Osborn's for $N = 4$ are still lacking. The search for a more systematic approach to higher point conformal blocks thereby constituted a major motivation for this thesis. Inspired by previous work [57–61] on the integrable structure of four-point blocks, we developed the formulation of multipoint blocks as a basis of wavefunctions of a many body quantum integrable system in [62–65]. In a conformal blocks integrable system, the eigenvalue equations of the Hamiltonians are expressed as differential equations that fully determine the blocks up to boundary conditions fixed by the OPE. While a full solution

theory of the blocks is not yet developed, the results presented in this thesis already demonstrate concrete applications to five- and six-point functions.

Higher point lightcone bootstrap. One important motivation for the analysis of higher point functions is the determination of multi-twist CFT data. Indeed, the four-point analytic bootstrap has been mostly limited to the study of double-twist operators[9]. To study triple-twists or higher (corresponding to multi-particle states in AdS), it is natural to consider higher point functions involving multiple OPEs in their crossing symmetry equations (see also [40, Sec. 7.2]). Even in four-point functions, contributions from multi-twist composites of lighter[10] operators can play in important role in the analysis of heavier double-twist composites, see e.g. [43, Sec. 5.2]. At a conceptual level, the analyticity properties of multi-twist Regge trajectories is also an open problem that must be addressed in any complete description of the CFT spectrum.

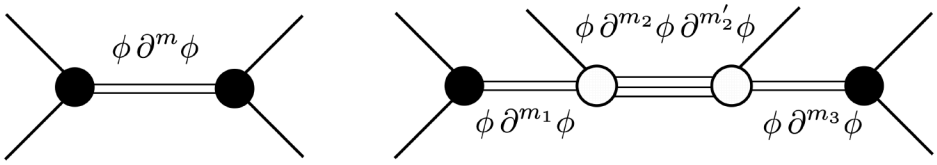

Figure 7: Appearance of double-twist and triple-twist operators in the OPE decomposition of the four-, respectively six-point function of a scalar field ϕ.

Recently, the lightcone bootstrap of five- and six-point functions was initiated by Bercini et al. [66] for conformal gauge theories and later by Antunes et al. [67] for CFTs with a twist gap. Their results already include large spin, double-twist CFT data that cannot be accessed by any four-point function of finite spin fields. However, they rely crucially on the integral formula for lightcone OPE of two scalars in [37–39], which limits the range of applicability. In particular, the aformentioned formula does not apply to iterated OPEs, like in the six-point "comb channel" diagram of Fig. 7, where multi-twist data is most readily accessed.
In this work, we will use the integrability based theory of higher point blocks to put the results of [66, 67] on a more rigorous footing and derive some new results as well. Ultimately, the technology developed in this thesis goes far beyond these first applications, opening the door to computations of triple-twist CFT data and higher in the near future.

1.4 Plan of the thesis

This thesis is divided into three parts. The first two chapters are a review of the conformal field theory and bootstrap methods that will be used for the study of higher point functions. The next three chapters then develop the integrability based theory of multipoint blocks for scalar N-point functions. Finally, the last chapter presents applications to the multipoint lightcone bootstrap.
Chapter 2 is a review of the foundations of conformal field theory and of the bootstrap program, with a stronger emphasis on the bookkeeping of three-point tensor structures compared to more standard references. Its practical use is mainly to establish conventions and notation in a self-contained manner, most importantly the notation (2.3.20) for OPE coefficients. At the end of this chapter, we are left

[9] While multi-twist operators already appear in the OPE of two single-twist operators, their contributions are typically suppressed in the large spin expansion, as explained in [40, Sec. 3.1.1].
[10] Here, the light/heavy distinction refers to lower/higher twist.

with unwieldy expressions for conformal blocks, whose simplification will be the subject of the next chapter.

Chapter 3 is an overview of conformal kinematics and efficient methods for computing conformal blocks. Using embedding space methods, we systematize the reduction of space(time) and spin degrees of freedom of correlators with conformal symmetry to a small set of cross ratios. We then review efficient methods to compute and analyze conformal blocks based on differential equations and integral representations. While a large part of the material is standard in the four-point bootstrap literature, it is explicitly set up for generalizations to higher point functions. Most importantly, some non standard notation and terminology will be introduced there and reused throughout the thesis. This includes the definition of "seed", "prefactor" and (generalized) "cross ratios" in section 3.2, the expansion (3.2.16) of spinning three-point functions into a basis of tensor structures and the conformal block expansion (3.3.1) of a generic N-point function.

Chapter 4 follows the work of [63], where we proved that all scalar N-point blocks in any OPE channel are eigenfunctions of a complete set of commuting differential operators. The latter form a quantum integrable system given by the Gaudin model for the conformal algebra on the N-punctured sphere, in a specific limit adapted to the OPE channel. The complete set divides into two families. On the one hand, Casimir operators control the scaling dimensions and spins of operators appearing in the OPE. On the other hand, vertex operators account for multiple occurrences of the same operator in an OPE, distinguished by different types of three-point tensor structures. Subsequently, we mainly restrict our focus to comb channel N-point blocks.

Chapter 5, based on [64], determines the explicit basis of tensor structures that diagonalizes the vertex operators by reducing them to an integrable subsystem acting on three-point functions. The vertex integrable systems with one degree of freedom are found to be elliptic $\mathbb{Z}_4$ Calogero-Moser-Sutherland integrable models [68]. Their eigenfunctions thereby specify all three-point tensor structures appearing in five and comb channel six-point blocks.

Chapter 6 expounds on the work of [65], where the Gaudin differential operators are used to determine efficient choices of cross ratios for comb channel blocks. This includes cross ratios for which all differential operators have polynomial coefficients, and cross ratios adapted to OPE limits. In particular, the OPE cross ratios highlight a factorization limit of higher point blocks into a product of lower point blocks. In a correlation function, this is equivalent to a refinement of the cluster decomposition property. In particular, the limiting behavior of blocks in OPE cross ratios determine explicit boundary conditions for blocks in terms of three-point tensor structures.

Finally, chapter 7 applies the integrability based theory of multipoint blocks to the lightcone bootstrap. After reviewing a lesser known approach to the four-point CSE based on lightcone limits of differential operators, the same method is generalized to five points and independently reproduces some results of [67]. On top of this, we derive novel results for the OPE coefficients of two double-twist operators at subleading order in the large spin limit. Finally, we explain how we will generalize our methods to the six-point bootstrap in our upcoming work [69].

Part I

Conformal Field Theory Review

Chapter 2

Foundations of Conformal Field Theory

The modern conformal bootstrap program for statistical or quantum field theories is founded upon three fundamental properties.

Pr1. *Conformal symmetry*: Physical states and operators organize themselves into irreducible representations of the conformal algebra, each labeled by a scaling dimension and a set of spin labels.

Pr2. *Unitarity:* States and operators undergo unitary time evolution in Lorentzian signature, or inversion-symmetric radial evolution in Euclidean signature.

Pr3. *Convergent operator product expansion (OPE):* At finite distance and away from the lightcone, the product of two operators admits a convergent expansion into a linear combination thereof.

Pr1 and Pr2 ensure that operators and states organize into conformal families, each made up of one primary and of its descendants. Next, Pr3 provides an algorithm to determine all N-point functions in terms of two- and three-point functions of primaries. Finally, Pr2 implies that OPE coefficients are real and that scaling dimension are bounded below by a positive function of their spin labels. These bounds imply a natural ordering of states and operators according to the distance of their scaling dimension away from the lower bounds.

2.1 Conformal symmetry

In this section, we will be studying $\mathbb{R}^d$ in coordinates $(x^\mu)_{\mu=0,\dots,d-1}$, equipped with a flat metric $\mathrm{d}x^2 := \eta_{\mu\nu}\mathrm{d}x^\mu \mathrm{d}x^\nu$. Depending on the signature of η, $(\mathbb{R}^d, \mathrm{d}x^2)$ corresponds to either Euclidean space or Minkowski space, which we will denote as

$$\mathbb{R}^{p,d-p} := \left(\mathbb{R}^d, -\sum_{\mu=0}^{p-1}(\mathrm{d}x^\mu)^2 + \sum_{\mu=p}^{d-1}(\mathrm{d}x^\mu)^2\right), \quad p = 0, 1. \tag{2.1.1}$$

Later on, we will also consider $\mathbb{R}^{d+2}$ in coordinates $(X^A)_{A=-1,\dots,d}$, equipped with the flat metric $\mathrm{d}X^2 := \eta_{AB}\mathrm{d}X^A\mathrm{d}X^B$ in two possible signatures, which we denote by

$$\mathbb{R}^{p+1,d-p+1} := \left(\mathbb{R}^{d+2}, -\sum_{A=-1}^{p-1}(\mathrm{d}X^A)^2 + \sum_{A=p}^{d}(\mathrm{d}X^A)^2\right), \quad p = 0, 1. \tag{2.1.2}$$

2.1.1 The conformal group

Conformal transformations of $(\mathbb{R}^d, \mathrm{d}x^2)$ are defined by

$$x^\mu \to x'^\mu, \quad \mathrm{d}x'^2 = \Omega(x)^2\mathrm{d}x^2, \tag{2.1.3}$$

where $x \to x'$ must be non-singular on some open set of $\mathbb{R}^d$, and $x \mapsto \Omega(x)$ is called the conformal factor. The three most important subsets of conformal transformations are given by

- isometries: $x \to x', \quad \mathrm{d}x'^2 = \mathrm{d}x^2,$
- dilations: $x \to \lambda x, \quad \mathrm{d}(\lambda x)^2 = \lambda^2\mathrm{d}x^2, \quad \lambda \in \mathbb{R}_{>0},$
- inversion: $x \to x^{-1} := (x^2)^{-1}x, \quad \mathrm{d}\left(x^{-1}\right)^2 = (x^2)^{-2}\mathrm{d}x^2.$

In fact, all sufficiently smooth conformal transformations can be expressed in terms of these three subsets:

Theorem. *If $d > 2$ and $x \mapsto x'$ is at least of class C^3 on an open set of $\mathbb{R}^d$, then $x \mapsto x'$ can be expressed as a finite composition of isometries, dilations and inversions.*

Proof. For Euclidean signature and $d = 3$, this theorem was first proven by Liouville in 1850 [70] and therefore goes under his name. Since then, several generalizations have appeared in the literature, including $d > 3$, Lorentzian signature, and weaker smoothness constraints on $x \mapsto x'$. Here, we will repeat the core steps of Liouville's proof (going from "2" to "5" in [70]), but in our more general setting, all the while simplifying some intermediate derivations in step 5.
2. First of all, in the $\Omega = 1$ case, isometries $\mathrm{d}x'^2 = \mathrm{d}x^2$ are known to to form the semi-direct group

$$\mathrm{ISO}(p, d-p) := \left\{x \mapsto \Lambda x + a \,|\, (\Lambda, a) \in \mathrm{O}(p, d-p) \times \mathbb{R}^d\right\}, \tag{2.1.4}$$

where the simple subgroup

$$\mathrm{O}(p, d-p) =: \left\{\Lambda \in \mathrm{Mat}(\mathbb{R}^d) \,|\, \Lambda^\mu{}_\rho\eta_{\mu\nu}\Lambda^\nu{}_\sigma = \eta_{\rho\sigma}\right\} \tag{2.1.5}$$

consists of rotations in Euclidean space or Lorentz transformations in Minkowski space.
3. Second of all, given a certain $\Omega^2 \neq 1$, any two conformal transformations $x \mapsto x'$ and $x \mapsto x''$ will be related by an isometry because $\mathrm{d}x''^2 = \mathrm{d}x'^2$. It follows that each Ω^2 defines an equivalence class $[x \mapsto x'] := \{x \mapsto \Lambda x' + a\}$ of conformal transformations [1]. Therefore, the classification of all conformal transformations reduces to the classification of all possible conformal factors Ω^2.
4. In the third step, we recall the equivalence classes

$$\Omega^2(x) = \left(\frac{\lambda}{(x+a)^2}\right)^2, \quad \left[x \to \lambda(x+a)^{-1}\right], \tag{2.1.6}$$

[1] in group theory language, these equivalence classes form the left coset space of the conformal group with respect to the isometry subgroup.

where the representative conformal transformation used by Liouville is the composition of a translation by a, an inversion and a dilation by λ.

5. As the final and most difficult step, we will prove that the most general Ω^2 takes the form of (2.1.6). In [70], Liouville used the differential equations [71, Eq. (16*bis*), (17)] for $h := \Omega^{-1}$, derived by Lamé from second and third derivatives of the Jacobian matrix $\frac{\partial x'^\mu}{\partial x^\nu}$. To avoid Lamé's lengthy derivation, we can instead use a well known trick based on Weyl transformations of the flat metric $\eta_{\mu\nu}$,

$$\eta_{\mu\nu} \mapsto g_{\mu\nu}(x) := \Omega^2(x)\eta_{\mu\nu}, \quad g_{\mu\nu}(x)\mathrm{d}x^\mu \mathrm{d}x^\nu = \mathrm{d}x'^2. \tag{2.1.7}$$

If Ω^2 in the above Weyl transformation is the conformal factor of a conformal transformation $x \mapsto x'$, then the curvature of $g_{\mu\nu}(x)$ must vanish. It is now a standard exercise to compute the Ricci curvature tensor of these so called conformally flat metrics, which takes the form

$$\begin{aligned} R_{\mu\nu} =& (d-2)\left(\partial_\mu \log\Omega\, \partial_\nu \log\Omega - \partial_\mu\partial_\nu \log\Omega\right) \\ &- \left(\partial^2 \log\Omega + (d-2)\left(\partial \log\Omega\right)^2\right)\eta_{\mu\nu}. \end{aligned}$$

In particular, the scalar curvature takes the form

$$R = R^\mu_\mu = -(d-1)\Omega^{-2}\left(2\partial^2 \log\Omega + (d-2)\left(\partial \log\Omega\right)^2\right).$$

Solving first $R = 0$ for $\partial^2 \log\Omega$, we can simplify the Ricci tensor to

$$\begin{aligned} R_{\mu\nu}|_{R=0} &= (d-2)\left(\partial_\mu\partial_\nu \log\Omega^{-1} + \partial_\mu \log\Omega^{-1}\, \partial_\nu \log\Omega^{-1} - \frac{1}{2}(\partial \log\Omega^{-1})^2\eta_{\mu\nu}\right) \\ &= \frac{d-2}{\Omega^{-1}}\left(\partial_\mu\partial_\nu\Omega^{-1} - \frac{1}{2}\frac{(\partial\Omega^{-1})^2}{\Omega^{-1}}\eta_{\mu\nu}\right). \end{aligned} \tag{2.1.8}$$

For $d = 3$ and Euclidean signature, setting $\mu = \nu$ in the first line reproduces [71, Eq. (17)], while setting $\mu \neq \nu$ in the second line yields [71, Eq. (16*bis*)]. We can now reproduce the same steps of Liouville's proof: starting with $\mu \neq \nu$, we obtain

$$\partial_\mu\partial_\nu\Omega^{-1} = 0 \Longrightarrow \Omega^{-1}(x) = f_0(x^0) + \cdots + f_{d-1}(x^{d-1}). \tag{2.1.9}$$

Next, plugging in this variable-separated form of Ω^{-1} into the $\mu = \nu$ equations yields

$$f''_\nu(x^b) = \frac{1}{2}\eta_{\nu\nu}\frac{\eta_{00}f'_0(x^0)^2 + \cdots + f'_{d-1}(x^{d-1})^2}{f_0(x^0) + \cdots + f_{d-1}(x^{d-1})}, \quad \nu = 0, \ldots, d-1. \tag{2.1.10}$$

This implies in particular $\eta_{00}f''_0 = f''_1 = \cdots = f''_{d-1} = \text{const}$, such that Ω^{-1} is a second order polynomial in x of the form

$$\Omega^{-1} = h_0 + h_1^\mu x_\mu + \frac{1}{2}h_2 x^2. \tag{2.1.11}$$

Plugging this form back into (2.1.8) yields the extra condition $h_1^\mu h_{1\mu} = 2h_0h_2$, such that

$$\Omega^{-1} = \frac{h_2}{2}\left(x^\mu + \frac{h_1^\mu}{h_2}\right)\left(x_\mu + \frac{h_{1\mu}}{h_2}\right) \equiv \lambda^{-1}(x+a)^2. \tag{2.1.12}$$

This conformal factor takes the same form as (2.1.6) for the $\mathrm{ISO}(p, d-p)$ equivalence class of a translation composed with an inversion and then a dilation. □

Symmetry enhancement in $d = 2$. In two dimensions, Liouville's theorem fails at stage 5 of the proof, where the conformally flat Ricci curvature tensor simplifies drastically to

$$R_{\mu\nu} = -\partial^2 \log \Omega \, \eta_{\mu\nu}. \tag{2.1.13}$$

Since there always exists a linear change of variables $(x^0, x^1) \to (z, \bar{z})$ for which $\partial^2 = 4\partial_z \partial_{\bar{z}}$ (complex coordinates in Euclidean space and lightcone coordinates in Minkowski space), the most general conformal factor is of the form

$$\Omega(x)^2 = f(z)\bar{f}(\bar{z}), \tag{2.1.14}$$

and the most general conformal transformation is of the form

$$(z, \bar{z}) \to (z'(z), \bar{z}'(\bar{z})), \quad \left(\frac{\mathrm{d}z'}{\mathrm{d}z}, \frac{\mathrm{d}\bar{z}'}{\mathrm{d}\bar{z}}\right) = \left(f, \bar{f}\right). \tag{2.1.15}$$

We thus obtain an infinite-dimensional group of conformal transformations — in Euclidean space, these correspond to holomorphic maps on open sets of the complex plane. If, however, we require these transformations to be non-singular everywhere on $\mathbb{R}^2 \cup \{\infty\} \cong S^2$, we retrieve a finite-dimensional group generated by inversions, dilations and isometries.

2.1.2 The conformal algebra

Liouville's theorem, along with step 2 of its proof, provides us with an efficient presentation of the conformal group:

$$\mathrm{Conf}(p, d-p) \cong \left\{\mathcal{P}_{(\Lambda,b)}\, g_{\lambda,a} \,|\, \lambda \in \mathbb{R}^\times, a, b \in \mathbb{R}^d, \Lambda \in \mathrm{O}(p, d-p)\right\}, \tag{2.1.16}$$

where $\mathcal{P}_{(\Lambda,b)}$ is an isometry and $g_{\lambda,a}$ is any conformal transformation that satisfies

$$\mathrm{d}(g_{\lambda,a} \cdot x)^2 = \left(\frac{\lambda}{(x+a)^2}\right)^2 \mathrm{d}x^2. \tag{2.1.17}$$

While the representative used in Liouville's proof took the form $g_{\lambda,a} = \mathcal{D}_\lambda \mathcal{I} \mathcal{P}_{(1,a)}$, we will make a different choice to describe the conformal algebra,

$$g_{\lambda=b^{-2}\omega, a=b^{-1}} = \mathcal{D}_\omega \mathcal{I} \mathcal{P}_{(1,b)} \mathcal{I}, \quad g_{b^{-2}\omega, b^{-1}} \cdot x = \omega(x^{-1} + b)^{-1}. \tag{2.1.18}$$

Here, $x \mapsto (x^{-1} + b)^{-1}$ is known as a *special conformal transformation* (SCT). This choice of representative comes from rewriting the conformal factor as

$$\frac{\lambda}{(x+a)^2} = \frac{a^{-2}\lambda}{1 + 2a^{-1} \cdot x + a^{-2}x^2} \equiv \frac{\omega}{1 + 2b \cdot x + b^2 x^2}, \tag{2.1.19}$$

which is the well known conformal factor of a SCT, followed by a dilation. The advantage of this parameterization is that it connects explicitly to the identity at $b^a = 0 = \omega$. As a result, we can recast any element of the conformal group in the form

$$g_{\Lambda,a,\lambda,b} = \mathcal{P}_{(\Lambda,0)} \mathcal{P}_{(1,a)} \mathcal{D}_\lambda \left(\mathcal{I} \mathcal{P}_{(1,b)} \mathcal{I}\right) \in \mathrm{Conf}(p, d-p), \tag{2.1.20}$$

and parameterize the expansion of group elements near the identity as

$$(\Lambda^\mu{}_\nu, a^\mu, \lambda, b^\mu) = (\delta^\mu_\nu, 0, 0, 0) + \epsilon\, (\omega^\mu{}_\nu, \omega^\mu, \omega, \tilde{\omega}^\mu) + \mathrm{O}(\epsilon^2), \tag{2.1.21}$$

for a small parameter ϵ. The coefficients at $\mathrm{O}(\epsilon)$ then constitute the elements of the conformal algebra.

Theorem. *The conformal algebra is a Lie algebra isomorphic to* $\mathfrak{so}(1, d+1)$ *in Euclidean signature, and* $\mathfrak{so}(2, d)$ *in Lorentzian signature.*

Proof. An early proof of this isomorphism is given by Dirac in [72], where he also introduces an embedding of $\mathbb{R}^{p,d-p}$ into the lightcone of $\mathbb{R}^{p+1,d-p+1}$ — we will review this construction in section 2.1.3. Here, we will check the isomorphism directly, fixing conventions for the Lie algebra generators in the process. First, a count of the free parameters in the expansion (2.1.21) shows that the dimensions match,

$$\dim \mathfrak{so}(p, d-p) + d + 1 + d = \frac{(d+1)(d+2)}{2} = \dim \mathfrak{so}(p+1, d-p+1). \tag{2.1.22}$$

Next, we represent elements of the conformal algebra by vector fields $\xi = \xi^\mu(x)\partial_\mu$ on $\mathbb{R}^d$, such that the commutation relations correspond to the Lie bracket of vector fields,

$$[\xi_1, \xi_2] = (\xi_1[\xi_2^\mu] - \xi_2[\xi_1^\mu])\,\partial_\mu. \tag{2.1.23}$$

Following the decomposition (2.1.20) of conformal group elements and the expansion (2.1.21) of its parameters, an infinitesimal conformal transformation will take the form

$$\begin{aligned} g_{\Lambda,a,\lambda,b} \cdot x &= x + \epsilon\, \xi[x] + \mathrm{O}(\epsilon^2), \\ \xi &= \omega^{\mu\nu} L_{\mu\nu} + \omega^\mu P_\mu + \omega\, D + \tilde{\omega}^\mu K_\mu, \end{aligned}$$

where the four vector fields in the sum are generators of

$$\text{rotations/Lorentz} : L_{\mu\nu} = x_\nu \partial_\mu - x_\mu \partial_\nu, \tag{2.1.24}$$

$$\text{translations} : P_\mu = \partial_\mu, \tag{2.1.25}$$

$$\text{dilations} : D = x^\nu \partial_\nu, \tag{2.1.26}$$

$$\text{SCTs} : K_\mu = \partial_{x^{-1\mu}} = x^2 \partial_\mu - 2x_\mu (x^\nu \partial_\nu). \tag{2.1.27}$$

The Lie brackets of the $\mathfrak{so}(p, d-p)$ vector fields are given by

$$[L_{\nu_1\nu_2}, L_{\nu_3\nu_4}] = \eta_{\nu_1\nu_3} L_{\nu_2\nu_4} - \eta_{\nu_2\nu_3} L_{\nu_1\nu_4} - \eta_{\nu_1\nu_4} L_{\nu_2\nu_3} + \eta_{\nu_2\nu_4} L_{\nu_1\nu_3}.$$

Then L and D commute amongst themselves and act as a linear map on P, K,

$$[L_{\mu\nu}, P_\rho] = \delta_{\mu\rho} P_\nu - \delta_{\nu\rho} P_\mu, \qquad [D, P_\rho] = -P_\rho, \tag{2.1.28}$$

$$[L_{\mu\nu}, K_\rho] = \delta_{\mu\rho} K_\nu - \delta_{\nu\rho} K_\mu, \qquad [D, K_\rho] = K_\rho. \tag{2.1.29}$$

Finally, the commutation relations between translations and SCTs close into rotations and dilations,

$$[K_\mu, P_\nu] = 2\left(\eta_{\mu\nu}\, D - L_{\mu\nu}\right). \tag{2.1.30}$$

Now, to establish the isomorphism of the conformal algebra with $\mathfrak{so}(p+1, d-p+1)$, we introduce the orthogonal vector fields

$$L_{\mu\nu} := X_\nu \partial_\mu - X_\mu \partial_\nu, \quad (X^A) = (X^{-1}, X^\mu, X^d) \in \mathbb{R}^{d+2}, \tag{2.1.31}$$

where $\mathbb{R}^{d+2}$ is equipped with an indefinite metric

$$\eta_{AB} \mathrm{d}X^A \mathrm{d}X^B = -\,\mathrm{d}\big(X^{-1}\big)^2 + \eta_{\mu\nu} \mathrm{d}X^\mu \mathrm{d}X^\nu + \mathrm{d}\big(X^d\big)^2, \tag{2.1.32}$$

and, just like in (2.1.28), commutation relations are given by

$$[L_{A_1A_2}, L_{A_3A_4}] = \eta_{A_1A_3}L_{A_2A_4} \pm \text{perms}. \tag{2.1.33}$$

We now reconstruct the commutation relations of the conformal algebra from $[L, L]$ in three steps:

1. for $A_i = \nu_i = 0, \ldots, d-1$, we retrieve the $\mathfrak{so}(p, d-p)$ relations.

2. For $(A_1, A_2, A_3, A_4) = (d, -1, \mu, \nu)$ we obtain a vector field commuting with $\mathfrak{so}(p, d-p)$, such that
$$D = c_D L_{d(-1)}, \tag{2.1.34}$$
for some constant c_D.

3. For $(A_1, A_2, A_3, A_4) = (d, -1, \alpha, \mu)$, $\alpha = -1, d$, we observe that $[D, -]$ acts linearly on $L_{\alpha\mu}$. This motivates the ansatz
$$K_\mu = k^\alpha L_{\alpha\mu}, \quad P_\nu = p^\beta L_{\beta\nu}, \quad k, p \in \mathbb{R}^{1,1}, \tag{2.1.35}$$
which leads to the commutation relations
$$[D, K_\mu] = -c_D(\omega k)^\alpha L_{\alpha\mu}, \quad [D, P_\mu] = -c_D(\omega p)^\alpha L_{\alpha\mu}, \tag{2.1.36}$$
where $\omega x = (-x^d, -x^{-1})$. We must therefore set $c_D^2 = 1$ and $k, p \propto (1, 1)$ or $(1, -1)$ to retrieve (2.1.29). By leveraging inner automorphisms generated by dilations, k, p are fixed up to a constant $c_P \in \mathbb{R}^\times$ and a sign $s \in \{+, -\}$, such that
$$K_\mu = sc_P \left(L_{(-1)\mu} + c_D L_{d\mu}\right), \quad P_\mu = c_P \left(L_{(-1)\mu} - c_D L_{d\mu}\right). \tag{2.1.37}$$

4. For the remaining case $(A_1, A_2, A_3, A_4) = (\alpha, \mu, \beta, \nu)$, we are left with
$$[K_\mu, P_\nu] = 2sc_P^2 \left(\eta_{\mu\nu} D - L_{\mu\nu}\right),$$
To retrieve (2.1.30), we must therefore impose $(c_P, s) = (1, 1)$.

The remaining freedom in $c_D = \pm 1$ is equivalent to the freedom in redefining generators by conjugation w.r.t. conformal inversion — the latter is defined by replacing $x \to x^{-1}$ in the expressions (2.1.24)—(2.1.27) of the generators,

$$\mathcal{I} L_{\mu\nu} \mathcal{I} = L_{\mu\nu}, \quad \mathcal{I} P_\mu \mathcal{I} = K_\mu, \quad \mathcal{I} D \mathcal{I} = -D, \quad \mathcal{I} K_\mu \mathcal{I} = P_\mu, \tag{2.1.38}$$

and constitutes an outer isomorphism of the conformal algebra. In accordance with the standard convention in the CFT literature, we fix the sign by imposing

$$D \cdot \frac{X^\mu}{X^{-1} + X^d} = \frac{X^\mu}{X^{-1} + X^d} \Longrightarrow c_D = 1. \tag{2.1.39}$$

□

In summary, the isomorphism between the *conformal* algebra of $\mathbb{R}^{p,d-p}$ and the *orthogonal* algebra of $\mathbb{R}^{p+1,d+1-p}$ dimensions is realized by

$$\mathfrak{so}(p, d-p) = \text{Span}(L_{\mu\nu}), \tag{2.1.40}$$
$$P_\mu = L_{(-1)\mu} - L_{d\mu}, \tag{2.1.41}$$
$$D = L_{d(-1)}, \tag{2.1.42}$$
$$K_\mu = L_{(-1)\mu} + L_{d\mu}. \tag{2.1.43}$$

2.1.3 Conformal completions and embedding space

Since inversions are singular at points where $x^2 = 0$, global conformal transformations composed of inversions do not necessarily preserve $\mathbb{R}^{p,d-p}$. However, inversions can be defined globally on conformally flat manifolds

$$(\mathcal{M}, \mathrm{d}s^2), \quad \mathrm{d}s^2 = \Omega(x)^2 \mathrm{d}x^2, \tag{2.1.44}$$

where $x \mapsto x^{-1}$ is a transition map between two coordinate patches of $\mathcal{M}$.
To construct explicit conformal completions, we can exploit the local isomorphism between the conformal group and the indefinite orthogonal group $\mathrm{O}(p+1, d-p+1)$. Starting from the $d+2$ dimensional lightcone

$$(X^A) \in \mathbb{R}^{p+1,d-p+1}, \quad \eta_{AB} X^A X^B = 0, \tag{2.1.45}$$

the change of variables first found by Dirac [72],

$$X^{-1} = X^+ \frac{1+x^2}{2}, \quad X^d = X^+ \frac{1-x^2}{2}, \quad X^\mu = X^+ x^\mu, \tag{2.1.46}$$

defines a foliation into $\mathbb{R}^{p+1,d-p+1}$ submanifolds for any $X^+ = X^{-1} + X^d \in \mathbb{R}^\times$. The leaf at $X^+ = 1$ is commonly denoted the *flat patch* or *Poincaré patch*. It's easy to verify that this foliation is conformally covariant,

$$(X_\nu \partial_\mu - X_\mu \partial_\nu) \frac{X^\rho}{X^+} = L_{\mu\nu} \cdot x^\rho. \tag{2.1.47}$$

Moreover, the metric induced from $\mathrm{d}X^2$ on the lightcone is given by

$$\mathrm{d}X^2 = (X^+)^2 \mathrm{d}x^2. \tag{2.1.48}$$

As a result, any orthogonal transformation $X \mapsto \Lambda X$, $\Lambda \in \mathrm{O}(p+1, d-p+1)$ induces a conformal transformation $x \mapsto x'$ with a conformal factor given by

$$(\Lambda X)^+ = \Omega^{-1}(x) X^+. \tag{2.1.49}$$

In particular, a reflection $s_d : X^d \mapsto -X^d$ induces an inversion $\mathcal{I} : x \mapsto x^{-1}$ with[2]

$$X^{-1} - X^d = x^2 X^+ = (s_d X)^+. \tag{2.1.50}$$

Thus, any submanifold of the $d+2$ dimensional lightcone that is preserved under s_d defines a conformal completion. The topology of the conformal completions depends significantly on the signature of $\mathrm{d}x^2$.

Euclidean signature: There are two standard embeddings of Euclidean space into conformal completions.

1. If we reexpress the lightcone condition as

$$\sum_{a=0}^{d-1} \left(\frac{X^\mu}{X^{-1}} \right)^2 + \left(\frac{X^d}{X^{-1}} \right)^2 = 1, \tag{2.1.51}$$

we obtain an embedding of the sphere for any $X^{-1} \neq 0$ that contains the flat patch

$$\left(\frac{X^\mu}{X^{-1}}, \frac{X^d}{X^{-1}} \right) = \left(\frac{2x^\mu}{1+x^2}, \frac{1-x^2}{1+x^2} \right), \quad \mathrm{d}X^2 = \left(\frac{2X^{-1}}{1+x^2} \right)^2 \mathrm{d}x^2, \tag{2.1.52}$$

[2]It is important not to confuse inversion $x^{-1} := (x^2)^{-1} x$ in position space with the component X^A, $A = -1$ in embedding space. The two notations are mutually exclusive because $\mu \neq -1$ in position space and $(X^2)^{-1} X^A = \infty$ is divergent in embedding space.

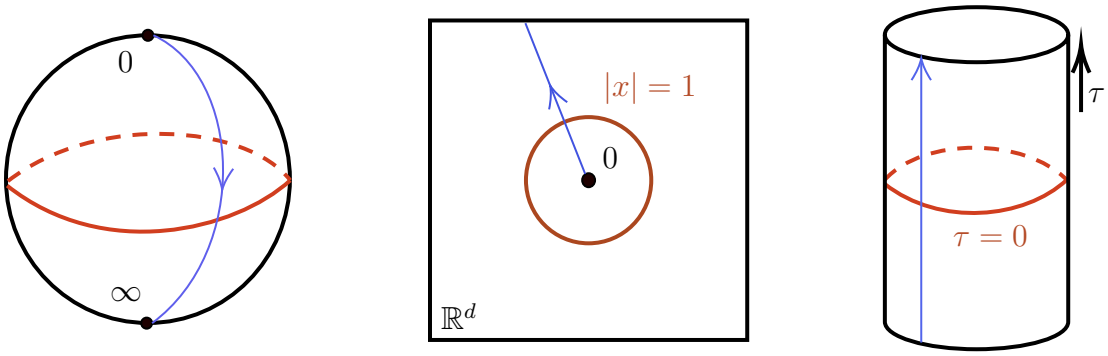

Figure 8: Conformal completions of Euclidean space to the sphere (left) and the cylinder (right). An example of radial evolution $e^{-\tau D}$ at a fixed angle is represented by a blue line.

proving that S^d is a conformal completion of $\mathbb{R}^d$. There, inversion corresponds to the antipodal map, going from the north pole $X^d = 1$ ($x = 0$) to the south pole $X^d = -1$ ($x = \infty$).

2. Rewriting the lightcone condition as

$$(X^{-1})^2 - (X^d)^2 = R^2 = \eta_{\mu\nu} X^\mu X^\nu, \tag{2.1.53}$$

we obtain an embedding of the cylinder for any $|X^{-1}| > |X^d|$. It can be explicitly parameterized by

$$(X^{-1}, X^\mu, X^d) = R\,(\cosh\tau, n^a, \sinh\tau), \quad \mathrm{d}X^2 = R^2 e^{2\tau}\left(\mathrm{d}\tau^2 + \mathrm{d}s^2_{S^{d-1}}\right), \tag{2.1.54}$$

for $(\tau, n^a) \in \mathbb{R} \times S^{d-1}$, with the flat patch given by $x^\mu = e^{-\tau} n^\mu$. In this case, the dilation generator $D = -\frac{\partial}{\partial\tau}$ generates imaginary time translation on the cylinder, and inversion acts as time reversal $\tau \mapsto -\tau$. An equivalent parameterization of (2.1.53) is obtained by replacing X^d with X^0, such that

$$(X^{-1}, X^0, X^i, X^d) = R(\cosh\tau, \sinh\tau, \cos\theta\, n^i, \sin\theta), \tag{2.1.55}$$

with $(\tau, \theta, n^i) \in \mathbb{R} \times [0, \pi) \times S^{d-2}$. Then the flat patch is becomes

$$(x^0, x^i) = \left(\frac{\sinh\tau}{\cosh\tau + \sin\theta}, \frac{\sin\theta\, n^i}{\cosh\tau + \sin\theta}\right). \tag{2.1.56}$$

In this case, imaginary time translation is generated by L_{-10}, also called the Euclidean conformal Hamiltonian.

Lorentzian signature: In Lorentzian signature, we can express the lightcone condition in terms of a Wick rotated version of the Euclidean cylinder (2.1.53), i.e.

$$(X^{-1})^2 + (X^0)^2 = R^2 = \sum_{i=1}^{d-1} (X^i)^2 + (X^d)^2. \tag{2.1.57}$$

This condition now defines an embedding of $S^1 \times S^{d-1}$ with parameterization

$$(X^{-1}, X^0, X^i, X^d) = R(\cos t, \sin t, \sin\theta\, n^i, \cos\theta), \tag{2.1.58}$$

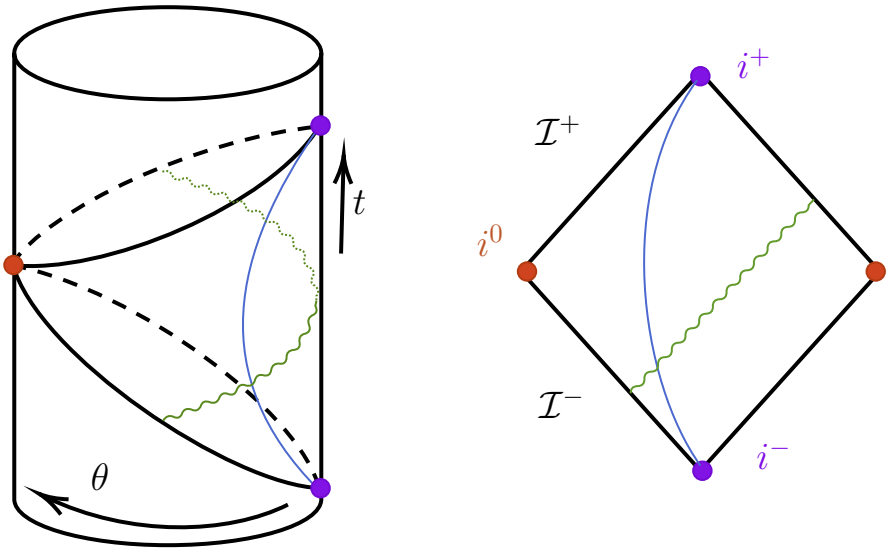

Figure 9: Left: conformal completion of Minkowski space, identified as a Poincaré patch of the Lorentzian cylinder. Right: Penrose diagram of the Minkowski space. The blue and green lines represent the worldlines of a massive and massless particle respectively.

for $t \sim t + 2\pi$ and $(\theta, n^i) \in [0, \pi] \times S^{d-2}$. As depicted in Fig. 9, Minkowski space is embedded as a diamond,

$$(x^0, x^i) = \left(\frac{\sin t}{\cos t + \cos\theta}, \frac{\sin\theta\, n^i}{\cos t + \cos\theta} \right), \quad |t| + \theta < \pi, \tag{2.1.59}$$

with an induced metric

$$\mathrm{d}X^2 = R^2(\cos t + \cos\theta)^2 \left(-\mathrm{d}t^2 + \mathrm{d}\theta^2 + \sin^2\theta\, \mathrm{d}s^2_{S^{d-2}} \right). \tag{2.1.60}$$

The boundary of the diamond at $|t| + \theta = \pi$ constitutes the image of the lightcone under inversion. Following Penrose [73, Sec. 8], this conformal boundary divides into five parts, describing the asymptotics of lightlike, spacelike and timelike curves.

$\mathcal{I}^{\pm}$: Future/past null infinity: $\theta = \pi \mp t$.

$\imath^0$: Spatial infinity: $t = 0$, $\theta = \pi$.

$\imath^{\pm}$: Future/past timelike infinity: $t = \pm\pi$, $\theta = 0$.

Causality: Global conformal transformations need not preserve causality in Minkowski space (see e.g. [74, Sec. 8]). In particular, the conformal generator

$$L_{-10} = \frac{P_0 + K_0}{2} = -\frac{\partial}{\partial t} \tag{2.1.61}$$

generates closed timelike curves that can bring $\imath^+$ to $\imath^-$. These acausalities are eliminated after decompactifying to the Lorentzian cylinder,

$$\mathbb{R} \times S^{d-1} := \bigsqcup_{n \in \mathbb{Z}} e^{2\pi n L_{-10}} \cdot S^1 \times S^{d-1}. \tag{2.1.62}$$

It is known (see e.g. [11, Eq. (7.10)] and references therein) that this Lorentzian cylinder admits a conformal invariant causal ordering. In terms of representation theory, the compact conformal completion is homogeneous for $\mathrm{SO}(2,d)$, with an infinite fundamental group

$$\pi_1(\mathrm{SO}(2,d)) = \mathbb{Z}\times\mathbb{Z}_2 = \langle e^{2\pi L_{-10}}\rangle \times \langle e^{2\pi L_{12}} \,|\, e^{4\pi L_{12}} = 1\rangle. \tag{2.1.63}$$

Conversely, the Lorentzian cylinder is homogeneous for $\widetilde{\mathrm{SO}}(2,d)/\mathbb{Z}_2$, with an infinite center

$$Z\left(\widetilde{\mathrm{SO}}(2,d)/\mathbb{Z}_2\right) = \mathbb{Z} = \langle e^{2\pi L_{-10}}\rangle. \tag{2.1.64}$$

While these global considerations may be avoided in classical field theory by restricting to local conformal transformations, they can play an important role in quantum field theory. Indeed, Wigner's theorem states that the Hilbert space is a *projective* unitary representation of the symmetry group, which is in turn a *true* unitary representation of the universal cover. For $\mathrm{SO}(2,d)$, this means that the generators of the $\mathrm{SO}(d)$ subgroup can admit half-integer eigenvalues and L_{-10} can admit real eigenvalues in a projective representation.

2.1.4 Primaries and descendants

Isometry invariance: In isometry invariant field theories, local observables $\mathcal{O}_\rho(x)$ are tensor valued fields obeying the covariance law

$$\left(\mathcal{P}_{(\Lambda,a)}\cdot\mathcal{O}_\rho\right)_I(\Lambda x+a) = \rho(\Lambda)_{IJ}\,\mathcal{O}_{\rho,J}(x), \tag{2.1.65}$$

where $(\rho,\mathbb{V})$ is a finite dimensional representation of $\mathfrak{so}(p,d-p)$ and $I,J=1,\ldots,\dim\mathbb{V}$ labels components of $\mathcal{O}_\rho$ in a basis. We will replace the component notation with implicit vectors $\mathcal{O}_\rho$ and matrices $\rho(\Lambda)$ whenever this is clear from context. Infinitesimally, the covariance law (2.1.65) is equivalent to

$$P_\mu\cdot\mathcal{O}_\rho = -\partial_\mu\mathcal{O}_\rho, \quad L_{\mu\nu}\cdot\mathcal{O}_\rho = \left(x_\mu\partial_\nu - x_\nu\partial_\mu + \rho(L_{\mu\nu})\right)\mathcal{O}_\rho. \tag{2.1.66}$$

To take full advantage of translation invariance, one typically decomposes the fields in the momentum eigenbasis $\mathcal{O}_{k,\rho}$, $k\in\mathbb{R}^d$. For a given momentum, $\mathrm{O}(p,d-p)$ transformations divide into rotations that map k to a distinct momentum Λk, and elements $\Lambda\in\mathrm{Stab}(k)$ that leave k invariant. It follows that irreducible representations take the form

$$\mathcal{O}_{\Lambda k_0,\rho}, \quad \Lambda\in\mathrm{SO}(p,d-p)/\mathrm{Stab}(k_0), \tag{2.1.67}$$

for some reference momentum k_0. In summary, local observables naturally organize into plane waves $\mathcal{O}_{\Lambda k_0,\rho}(x)$, labeled by a momentum $k_{0\mu}$ and one or more spin labels for the stabilizer subgroup $\rho|_{\mathrm{Stab}(k_0)}$.

Conformal invariance: In a conformal invariant theory, the most relevant observables transform by local rescalings and $\mathrm{O}(p,d-p)$ rotations under the action of the conformal group — examples include the order parameter $\phi(x)$ of a continuous phase transition or the energy-momentum tensor $T_{\mu\nu}(x)$. These so called *primary* fields were first defined in full generality by Mack and Salam [75][3], and their covariance law can be stated as follows:

$$\text{if} \quad \frac{\partial(g\cdot x)^\mu}{\partial x^\nu} = \Omega(x)\Lambda^\mu{}_\nu(x), \quad \Lambda(x)\in\mathrm{O}(p,d-p), \tag{2.1.68}$$

$$\text{then} \quad \left(g\cdot\mathcal{O}_{\Delta,\rho}\right)(g\cdot x) = \Omega(x)^{-\Delta}\rho(\Lambda(x))\mathcal{O}_{\Delta,\rho}(x), \tag{2.1.69}$$

[3]Mack and Salam were studying Lorentzian conformal symmetry in a particle physics context, where they called primaries "interpolating fields" for particles transforming in an irreducible representations of the conformal algebra.

where Δ is called the *scaling dimension* of the primary, and ρ is once again a representation of $\mathfrak{so}(p, d-p)$. In addition to isometries, we now have

$$\text{dilations}: \quad \Omega = \lambda, \quad \Lambda^{\mu}{}_{\nu} = \delta^{\mu}_{\nu}, \tag{2.1.70}$$

$$\text{inversion}: \quad \Omega(x) = (x^2)^{-1}, \quad \Lambda^{\mu}{}_{\nu}(x) = \delta^{\mu}_{\nu} - 2\frac{x^{\mu}x_{\nu}}{x^2} =: I^{\mu}_{\nu}(x), \tag{2.1.71}$$

and all other conformal transformations obtained by composition. Expanding translations, rotations, dilations and SCTs near the identity, we derive from (2.1.69) the following covariance laws of primaries with respect to the conformal algebra,

$$P_{\mu} \cdot \mathcal{O}_{\Delta,\rho} = -\partial_{\mu}\mathcal{O}_{\Delta,\rho}, \tag{2.1.72}$$

$$L_{\mu\nu} \cdot \mathcal{O}_{\Delta,\rho} = \left(x_{\mu}\partial_{\nu} - x_{\nu}\partial_{\mu} + \rho(L_{\mu\nu})\right)\mathcal{O}_{\Delta,\rho}, \tag{2.1.73}$$

$$D \cdot \mathcal{O}_{\Delta,\rho} = -\left(x^{\sigma}\partial_{\sigma} + \Delta\right)\mathcal{O}_{\Delta,\rho}, \tag{2.1.74}$$

$$K_{\mu} \cdot \mathcal{O}_{\Delta,\rho} = \left\{x^{\nu}\left(x_{\mu}\partial_{\nu} - x_{\nu}\partial_{\mu} + 2\rho(L_{\mu\nu})\right) + x_{\mu}(x^{\sigma}\partial_{\sigma} + 2\Delta)\right\}\mathcal{O}_{\Delta,\rho}. \tag{2.1.75}$$

Primaries as lowest weight states: The infinitesimal covariance laws of $\mathcal{O}_{\Delta,\rho}$ lead to an alternative but equivalent definition of a primary, based on conformal generators acting at $x = 0$,

$$K_{\mu} \cdot \mathcal{O}_{\Delta,\rho}(0) = 0, \quad D \cdot \mathcal{O}_{\Delta,\rho}(0) = -\Delta\mathcal{O}_{\Delta,\rho}, \quad L_{\mu\nu} \cdot \mathcal{O}_{\Delta,\rho}(0) = \rho(L_{\mu\nu})\mathcal{O}_{\Delta,\rho}(0).$$

In analogy with the irreducible representations (2.1.67) of the isometry group reviewed above, the origin $x = 0$ is the equivalent of the reference momentum, and the stabilizer subgroup is generated by K, D, L. Since the primary field diagonalizes D with eigenvalue $-\Delta$, the commutation relation $[D, P] = -P$ implies

$$D \cdot P_{\mu_1} \dots P_{\mu_m}\mathcal{O}_{\Delta,\rho}(0) = -(\Delta + n)P_{\mu_1} \dots P_{\mu_m}\mathcal{O}_{\Delta,\rho}(0). \tag{2.1.76}$$

These states are called *descendants* at level m — together, they form an irreducible representation of the conformal algebra called a conformal family[4]. In this construction, the fundamental property of a primary is $K \cdot \mathcal{O}_{\Delta,\rho}(0) = 0$. When ρ is a finite dimensional representation of $\mathfrak{so}_{\mathbb{C}}(d)$, this condition defines a parabolic Verma module, see [76, Sec. 6.2].
At this stage, we have not yet specified what domains of the scaling dimension Δ and which $\mathfrak{so}(p, d-p)$ representations ρ are allowed for CFT primaries. In the next section, we will review how unitarity implies that ρ is a finite-dimensional representation, while Δ is positive and bounded below by the spin labels of ρ.

2.2 Unitarity

2.2.1 Positive energy representations

The importance of unitarity is best appreciated in Lorentzian signature, in the framework of a relativistic conformal quantum field theory. There, the Hilbert space of states $\mathcal{H}$ must form a unitary, positive energy representation of the Poincaré algebra. In our conventions (2.1.24),(2.1.25), this means

$$L^{\dagger}_{\mu\nu} = -L_{\mu\nu}, \quad P^{\dagger}_{\mu} = -P_{\mu}, \quad \langle\Psi|\left(-\mathrm{i}P_0\right)|\Psi\rangle \geq 0, \quad \forall\,|\Psi\rangle \in \mathcal{H}, \tag{2.2.1}$$

[4]The terminology of primary, descendant and conformal family actually originated from Belavin, Polyakov and Zamolodchikov's famous paper [28] on two dimensional CFT to describe irreducible representations of the infinite dimensional conformal algebra of the plane.

with $P_0 |\Psi\rangle = 0$ if and only if $|\Psi\rangle = |0\rangle$ is the Poincaré invariant vacuum state. When Poincaré symmetry is enhanced to conformal symmetry, the Hilbert space $\mathcal{H}$ must be a unitary representation of the full conformal algebra $\mathfrak{so}(2,d)$,

$$D^\dagger = -D, \quad K_\mu^\dagger = -K_\mu. \tag{2.2.2}$$

In [77], G. Mack classified all unitary, positive energy, irreducible representations of the conformal algebra in $d = 4$. His first result relates these representations to primaries and descendants.

Theorem. *Unitary, irreducible, positive energy representations of* $\mathfrak{so}(2,d)$ *are isomorphic to*

$$\bigoplus_{m=0}^{\infty} \text{Span}\left\{P_{\mu_1} \dots P_{\mu_m} \mathcal{O}_{\Delta,\rho,I}(0) |0\rangle\right\}_{(I,\mu_i)}, \tag{2.2.3}$$

where $\Delta \in \mathbb{R}_+$ *and* ρ *is a finite-dimensional representation of* $\mathfrak{so}_{\mathbb{C}}(d)$.

Proof. Mack's derivation can be straightforwardly generalized to any $d > 2$ and summarized in four steps.
1. First, define the *conformal Hamiltonian*,

$$H_0 := -\mathrm{i}L_{-10} = \frac{P_0 + K_0}{2\mathrm{i}} = \frac{P_0 + \mathcal{I}P_0\mathcal{I}^{-1}}{2\mathrm{i}}. \tag{2.2.4}$$

If inversions $\mathcal{I}$ act irreducibly on $\mathcal{H}$, then the last equality makes the positivity of H_0 manifest. If $\mathcal{I}$ does not act irreducibly, we can instead introduce a so called Weyl reflection

$$w_1 := \mathcal{I}s_1 \in \mathrm{SO}(2,d), \quad s_1 : x^\mu \mapsto (-)^{\delta_{\mu 1}} x^\mu \in \mathrm{O}(1,d-1),$$

such that $K_0 = w_1 P_0 w_1^{-1}$. Defining $|\Psi'\rangle := w_1 |\Psi\rangle$, we obtain

$$\langle\Psi| H_0 |\Psi\rangle = \frac{\langle\Psi| (-\mathrm{i}P_0) |\Psi\rangle + \langle\Psi'| (-\mathrm{i}P_0) |\Psi'\rangle}{2} \geq 0, \quad H_0 |\Psi\rangle = 0 \iff |\Psi\rangle = |0\rangle, \tag{2.2.5}$$

where $|0\rangle$ is the conformal invariant vacuum state. At the same time, $H_0 = -\mathrm{i}L_{-10}$ is a compact rotation generator in the Euclidean (X^{-1}, X^0) plane, so its eigenvalues must be quantized. More specifically, $e^{2\pi \mathrm{i} H_0}$ generates the center of the universal cover of $\mathrm{SO}(2,d)$ and must therefore be represented by a constant. It follows that

$$\mathrm{Spec}(H_0) = \{E_0 + n \,|\, n \in \mathbb{Z}_{\geq} 0\}, \tag{2.2.6}$$

for some $E_0 \in \mathbb{R}_+$.
2. Next, H_0 commutes with all generators L_{AB}, $A, B > 0$, which generate the maximal compact subgroup $\mathrm{SO}(d)$. As a result, in an eigenbasis of H_0, the Hilbert space admits a direct sum decomposition

$$\mathcal{H} = \bigoplus_{n=0}^{\infty} \mathcal{H}_n, \tag{2.2.7}$$

where each $\mathcal{H}_n$ is a unitary representation of $\mathfrak{so}(d)$, and therefore a direct sum of finite dimensional irreducible representations.
3. Now, a primary field $\mathcal{O}_{\Delta,\rho}$ transforming in a representation $(\rho, \mathbb{V})$ of $\mathfrak{so}(1,d-1)$ defines a unique representation of the complexified conformal algebra $\mathfrak{so}_{\mathbb{C}}(d+2)$, where states are (complex) linear superpositions of

$$P_{\mu_1} \dots P_{\mu_m} \mathcal{O}_{\Delta,\rho,I}(0) |0\rangle, \quad I = 1, \dots, \dim \mathbb{V}. \tag{2.2.8}$$

In $\mathfrak{so}_{\mathbb{C}}(d+2)$, the dilation generator $D = L_{d(-1)}$ is conjugate to the conformal Hamiltonian by means of a complexified boost in the (X^0, X^d) plane, i.e. $e^{\frac{i\pi}{2}L_{d0}} D\, e^{-\frac{i\pi}{2}L_{d0}} = H_0$. It follows that the Hilbert space spanned by

$$e^{\frac{i\pi}{2}L_{d0}} P_{\mu_1} \dots P_{\mu_m} \mathcal{O}_{\Delta,\rho,I}(0)\,|0\rangle \tag{2.2.9}$$

is a unitary, positive energy representation of $\mathfrak{so}(2,d)$ if ρ is finite dimensional and $\Delta = E_0$.
4. The remaining step is to show that all admissible representations are isomorphic to (2.2.9). In [77], Mack argued that this holds because complexifications of the former and the latter are highest weight modules of $\mathfrak{so}_{\mathbb{C}}(d+2)$ with the same highest weight vector. □

2.2.2 Reflection positivity

Consider the slicing of Minkowski space by the spacelike hypersurfaces $t = \text{const}$ of the parameterization $x^\mu(t,\theta,n)$ in (2.1.59). If we insert a Hermitian primary $\mathcal{O}_{\Delta,\rho}(x)$ at the $t = 0$ slice, then the conformal Hamiltonian generates unitary evolution along a timelike curve,

$$\text{Lorentzian}: \quad H_0 = -\mathrm{i}\frac{\partial}{\partial t}, \quad \mathcal{O}_{\Delta,\rho}(x(t,\theta,n)) = e^{\mathrm{i}tH_0}\mathcal{O}_{\Delta,\rho}(x(0,\theta,n))\, e^{-\mathrm{i}tH_0}. \tag{2.2.10}$$

The same parameterization $x^\mu(t,\theta,n)$ for imaginary time $t \in \mathrm{i}\mathbb{R}$ is equivalent to that of the Euclidean cylinder (2.1.56). Then the conformal Hamiltonian generates imaginary time evolution in Euclidean signature as

$$\text{Euclidean}: \quad H_0 = \frac{\partial}{\partial(\mathrm{i}t)}, \quad \mathcal{O}_{\Delta,\rho}(x(t,\theta,n)) = e^{(\mathrm{i}t)H_0}\mathcal{O}_{\Delta,\rho}(x(0,\theta,n))\, e^{-(\mathrm{i}t)H_0}. \tag{2.2.11}$$

It follows that Hermitian primaries in Euclidean signature satisfy *reflection positivity*,

$$\text{RP}: \quad \mathcal{O}_{\Delta,\rho}(x)^\dagger = s_0\mathcal{O}_{\Delta,\rho}(x)s_0^{-1} = \rho(s_0)\,\mathcal{O}_{\Delta,\rho}(s_0 x). \tag{2.2.12}$$

Equivalently, after rotating $H_0 = L_{-10}$ to $-D = L_{-1d}$ in Euclidean signature, we retrieve the slicing by spheres of constant radius in the parameterization $x^\mu(\tau,n) = e^{-\tau}n^a$ of the cylinder, with imaginary time evolution given by

$$\text{Euclidean}: \quad D = -\frac{\partial}{\partial\tau}, \quad \mathcal{O}_{\Delta,\rho}(x(\tau,n)) = e^{-\tau D}\mathcal{O}_{\Delta,\rho}(x(0,n))\, e^{\tau D}. \tag{2.2.13}$$

With this choice of Hamiltonian, the operator satisfies *inversion positivity*,

$$\text{IP}: \quad \mathcal{O}_{\Delta,\rho}(x)^\dagger = s_d\mathcal{O}_{\Delta,\rho}(x)s_d^{-1} = x^{2\Delta}\rho(I(x))\,\mathcal{O}_{\Delta,\rho}(x^{-1}). \tag{2.2.14}$$

2.2.3 Unitarity bounds

The norm squared of any non-trivial state in a Hilbert space must be positive and non-zero — imposing this requirement on primaries and descendants constrains Δ and ρ to satisfy *unitarity bounds*. In Euclidean signature with inversion positivity $P^\dagger = -K$, these constraints concretely take the form

$$\bar{\xi}^{I\mu_1\dots\mu_m} A_{I\mu_1\dots\mu_m\nu_1\dots\nu_m J}\, \xi^{J\nu_1\dots\nu_m} \geq 0, \quad \forall\, \xi \in \mathbb{V}\otimes(\mathbb{C}^d)^{\otimes m}, \tag{2.2.15}$$

where A is a matrix of scalar products of primaries and descendants in Hilbert space,

$$A_{I\mu_1\dots\mu_m\nu_1\dots\nu_m J} = (-1)^m \langle 0|\, \mathcal{O}_{\Delta,\rho,I}(0)^\dagger K_{\mu_1}\dots K_{\mu_m} P_{\nu_1}\dots P_{\nu_m}\mathcal{O}_{\Delta,\rho,J}(0)\,|0\rangle\,. \tag{2.2.16}$$

After repeated commutation of K_{μ_i} to the right and P_{ν_j} to the left, we obtain a polynomial of the generators $D\,\delta_{\mu_i\nu_j}, L_{\mu_i\nu_j}$. Acting on the primary $\mathcal{O}_{\Delta,\rho,I}\,|0\rangle$, this evaluates to a matrix with entries depending on Δ and the spin labels of ρ. Here we will review the two most important unitarity bounds: scalar fields at $m = 2$ and symmetric traceless tensor (STT) fields at $m = 1$.

(S) If $\rho(L_{\mu\nu}) = 0$, we can easily evaluate

$$K^2 P^2 = 4dD\,(2D + 2 - d) + \mathrm{O}(L, P(-), (-)K), \tag{2.2.17}$$

Whenever $\Delta \neq 0$, the conformal dimension is then bounded below by $\frac{d-2}{2}$. The bound is saturated for a free, massless scalar field satisfying $P^2\varphi(x) = 0$.

(STT) When ρ is the symmetric traceless representation of spin $l \in \mathbb{Z}_{>0}$, the bounds arising from (2.2.15) at $m = 1$ in any d were first derived in [78, Sec. 2.5]. Here, we will present an alternative derivation that emphasizes analogies with the conformal crossing equation. The matrix (2.2.16) of scalar products is an invariant in the tensor product of four representations of $\mathrm{SO}(d)$,

$$A_{I\mu\nu J} \in (\rho_l \otimes \rho_1 \otimes \rho_1 \otimes \rho_l)^{\mathrm{SO}(d)}. \tag{2.2.18}$$

By (anti-)symmetrizing indices and subtracting traces, tensor products decompose into direct sums of irreducibles $\rho_{(l_1,l_2,\ldots,l_L)}$ labeled by Young tableaux with columns of length $l_1, l_2, \ldots, l_L$. This yields three different bases of invariant tensors $\{A^{(ij)}_{(l_1,l_2,\ldots,l_L)}\}$ that are computed using standard CFT methods in appendix 2.A. Commuting K_μ to the right of P_ν, we obtain the coefficients of A in the (23) channel,

$$\rho_1 \otimes \rho_2 = \rho_0 \oplus \rho_{(1,1)} \oplus \rho_2, \quad A = \Delta A^{(23)}_0 - l A^{(23)}_{(1,0)}. \tag{2.2.19}$$

After a linear change of basis to the (12) channel, we obtain the decomposition

$$\rho_l \otimes \rho_1 = \rho_{l-1} \oplus \rho_{(l,1)} \oplus \rho_{l+1}, \tag{2.2.20}$$

$$A = \frac{l(2l+d-4)(\Delta - l - d + 2)}{(l+d-3)(2l+d-2)} A^{(12)}_{l-1} + \frac{l(\Delta-1)}{l+1} A^{(12)}_{(l,1)} + (\Delta + l) A^{(12)}_{l+1}.$$

At the same time, the (12) channel is *reflection positive*,

$$A^{(12)}_\rho \in (\rho^\dagger \otimes \rho)^{\mathrm{SO}(d)} \Longrightarrow \bar{\xi}^{I\mu} \left(A^{(12)}_\rho\right)_{I\mu\nu J} \xi^{J\nu} \geq 0. \tag{2.2.21}$$

Thus, the inequality (2.2.15) is satisfied if and only if each coefficient of A in the (12) channel is positive,

$$\Delta \geq l + d - 2 \geq 1. \tag{2.2.22}$$

The bound is saturated at $\Delta - l = d - 2$, which corresponds to a spin l STT field satisfying a conservation equation $P^{\mu_1} \mathcal{J}_{\mu_1 \ldots \mu_l}(x) = 0$.

Similar bounds for more general spinning representations of $\mathrm{SO}(d)$ can be found in [77] for $d = 4$ and in [76] for general d. While the realization of the lower bounds by free massless scalars (respectively conserved STTs) suggest that there are no sharper bounds for $m > 2$ (respectively $m > 1$), an actual proof of sufficiency is more involved. Apart from Mack's proof in [77] for $d = 4$, a general proof follows from Jantzen's criterion in the theory of parabolic Verma modules (see [76] and references therein).

2.3 The operator product expansion

2.3.1 State operator correspondence and OPE

The combination of Mack's classification of unitary positive energy representations of $\mathfrak{so}(2, d)$ reviewed in section 2.2.1, with the Euclidean formulation of unitarity reviewed in section 2.2.2, yields the *state*

operator correspondence,

$$\prod_i P_{\mu_i}\mathcal{O}_{\Delta,\rho,I}(x) \longleftrightarrow \prod_i P_{\mu_i}\mathcal{O}_{\Delta,\rho,I}(0)\,|0\rangle \in \mathcal{H}, \tag{2.3.1}$$

where $I = 1, \ldots, \dim \mathbb{V}$ labels components of $\mathcal{O}_{\Delta,\rho}$ in a basis of the representation $(\rho, \mathbb{V})$ of $\mathrm{SO}(d)$. In other words, the full set of primaries in a CFT is equivalent to a complete basis of states for its Hilbert space. Now, denoting irreducible representations of the conformal algebra by $\pi = (\Delta, \rho)$, consider a state made out of two primaries $\mathcal{O}_{\pi_1,I_1}$, $\mathcal{O}_{\pi_2,I_2}$ inserted at distinct points and acting on the vacuum,

$$|\Psi\rangle := \mathcal{O}_{\pi_1,I_1}(x)\mathcal{O}_{\pi_2,I_2}(0)\,|0\rangle \in \mathcal{H}.$$

If the state operator correspondence holds, then $|\Psi\rangle$ can be expanded in the basis of states given by (2.3.1), such that

$$|\Psi\rangle = \sum_{\pi_3}\sum_{m=0}^{\infty}\sum_{\mu_1,\ldots,\mu_m}\sum_{\alpha_3=1}^{\dim \mathbb{V}_3} c_{\pi_3,I_3,\{\mu_i\}}(x)\prod_i P_{\mu_i}\mathcal{O}_{\pi_3,I_3}(0)\,|0\rangle\,. \tag{2.3.2}$$

Equating both expressions of $|\Psi\rangle$ yields an expansion of the operator product $\mathcal{O}_1(x)\mathcal{O}_2(0)$ into a linear combination of primaries and descendants $P^m\mathcal{O}_3(0)$ that converges for any $x \in \mathbb{R}^d$. This expansion can be more efficiently organized using the covariance of both sides under conformal transformations. More specifically, the operator product transforms as a tensor product $\pi_1 \otimes \pi_2$, while the expansion transforms as a direct sum $\bigoplus \pi_3$. It follows from group theory that the OPE can be recast in the form

$$\mathcal{O}_{\pi_1,I_1}(x)\mathcal{O}_{\pi_2,I_2}(0) = \sum_{\pi_3 \subset \pi_1\otimes\pi_2}\sum_{I_3=1}^{\dim \mathbb{V}_3} F_{\pi_i;I_1I_2I_3}(x,\partial)\cdot\mathcal{O}_{\pi_3,I_3}(0), \tag{2.3.3}$$

where the tensor valued differential operator F_{π_i} must be covariant with respect to conformal transformations in the stabilizer subgroup $\{g \in \mathrm{O}(1,d+1)\,|\,g\cdot 0 = 0\}$. This subgroup is generated by dilations, rotations and SCTs, which lead to three independent sets of covariance conditions:

$$\lambda^{\Delta_1+\Delta_2}F_{\pi_i;I_1I_2J_3}(\lambda x,\partial) = F_{\pi_i;I_1I_2J_3}(x,\lambda^{-1}\partial)\lambda^{\Delta_3}, \tag{2.3.4}$$

$$\rho_1(\Lambda)_{I_1J_1}\rho_2(\Lambda)_{I_2J_2}F_{\pi_i;J_1J_2J_3}(\Lambda^{-1}x,\partial) = F_{\pi_i;I_1I_2I_3}(x,\Lambda\partial)\rho_3(\Lambda)_{I_3J_3}, \tag{2.3.5}$$

$$\Omega_b(x)^{-\Delta_1}\rho_1(\Lambda_b(x))_{I_1J_1}F_{\pi_i;J_1I_2J_3}((x^{-1}-b)^{-1},\partial) = F_{\pi_i;I_1I_2J_3}(x,\Omega_b(x)^{-1}\Lambda_b(x)\partial), \tag{2.3.6}$$

where $(\lambda,\Lambda,b) \in \mathbb{R}^\times \times \mathrm{SO}(d) \times \mathbb{R}^d$ and for SCTs,

$$\Omega_b(x) = \left(1 + 2b\cdot x + b^2x^2\right)^{-1}, \quad \Lambda_b(x) = I(x+b^{-1})I(b). \tag{2.3.7}$$

2.3.2 Three-point functions and OPE coefficients

The conformal covariance conditions for the differential operators F_{π_i} of the OPE (2.3.3) are difficult to solve directly. Instead, they are more readily analyzed via the amplitudes of $\mathcal{O}_{\pi_1,I_1}(x)\mathcal{O}_{\pi_2,I_2}(0)\,|0\rangle$ with other primary states.

Vacuum amplitude and two-point functions: First of all, the vacuum state cannot have any overlap with any other state, because it forms an invariant subspace of $\mathcal{H}$ with respect to the conformal group action,

$$\langle 0|\,\mathcal{O}_\pi(0)\,|0\rangle = \langle\mathcal{O}_\pi(0)\rangle = \delta_{\pi,\mathbb{1}}\,\langle 0|0\rangle = \delta_{\pi,\mathbb{1}}. \tag{2.3.8}$$

This yields the vacuum amplitude,

$$\langle \mathcal{O}_{\pi_1,I_1}(x)\mathcal{O}_{\pi_2,I_2}(0)\rangle = F_{\pi_1\pi_2\mathbb{1};I_1I_2}(x). \tag{2.3.9}$$

To compute this amplitude, consider instead its inversion positive analogue,

$$\langle \mathcal{O}_{\pi_1,I_1}(x)^\dagger\mathcal{O}_{\pi_2,I_2}(0)\rangle = x^{-2\Delta_1}\rho(I(x))_{I_1J_1}\langle \mathcal{O}_{\pi_1,J_1}(x^{-1})\mathcal{O}_{\pi_2,I_2}(0)\rangle. \tag{2.3.10}$$

The latter is a constant because $x = 0$ is a fixed point of SCTs $K^\dagger = -P$,

$$\langle \mathcal{O}_1(x)^\dagger\mathcal{O}_2(0)\rangle = \langle e^{-x_1\cdot K}\mathcal{O}_1(0)^\dagger e^{x_1\cdot K}\mathcal{O}_2(0)\rangle = \langle \mathcal{O}_1(0)^\dagger\mathcal{O}_2(0)\rangle.$$

At $x = 0$, this two-point function is the overlap between two different primary states, which is non-vanishing if and only if $\pi_1 \cong \pi_2$. In this case, the reflection positive two-point function reduces to the matrix elements of an orthonormal basis,

$$\langle \mathcal{O}_{\pi,I}(0)^\dagger\mathcal{O}_{\pi,J}(0)\rangle = \delta_{IJ}. \tag{2.3.11}$$

In conclusion, the coefficient of the identity operator in the OPE of two primaries is entirely fixed by conformal symmetry,

$$F_{\pi_1\pi_2\mathbb{1};I_1I_2}(x) = \delta_{\pi_1\pi_2}\frac{\rho(I(x))_{I_1I_2}}{x^{2\Delta_1}}. \tag{2.3.12}$$

Primary amplitudes and three-point functions: Using the previous result on two-point functions, the three-point functions take the form

$$\langle \mathcal{O}_{\pi_3,I_3}(x_3)\mathcal{O}_{\pi_1,I_1}(x_1)\mathcal{O}_{\pi_2,I_2}(x_2)\rangle = F_{\pi_1\pi_2\pi_3;I_1I_2J_3}(x_{12},\partial_{x_2})\frac{\rho_3(I(x_{32}))_{J_3I_3}}{x_{32}^{2\Delta_3}}. \tag{2.3.13}$$

In principle, combining this equation with the covariance laws for $F_{\pi_i;\alpha_i}$ in an expansion around $x_{12} = 0$ entirely determines the OPE in terms of three-point functions. In conformal bootstrap applications, it is particularly useful to compute the leading term in a radial expansion $|x_{12}| \to 0$. This limits suppresses the contribution of descendants, because the $\partial_{x_2}^m$ term scales like $|x_{12}|^{\Delta_3-\Delta_1-\Delta_2+m}$ as a consequence of (2.3.4). Comparing both sides gives

$$\frac{F_{\pi_i;I_i}(x_{12},\partial)|_{\mathrm{O}(\partial^0)}}{|x_{12}|^{\Delta_3-\Delta_1-\Delta_2}} = \lim_{|x_{12}|\to 0} x_{23}^{2\Delta_3}\rho_3(I(x_{23}))_{I_3J_3}\frac{\langle \mathcal{O}_{\pi_3,J_3}(x_3)\mathcal{O}_{\pi_1,I_1}(x_1)\mathcal{O}_{\pi_2,I_2}(x_2)\rangle}{|x_{12}|^{\Delta_3-\Delta_1-\Delta_2}}. \tag{2.3.14}$$

Now, using the conformal transformation

$$g_{x_i} := \Lambda_n^{-1}\, e^{-|x|D}e^{x_{23}^{-1}\cdot K}e^{-x_2\cdot P} : (x_3,x_1,x_2) \mapsto (\infty,e_1,0), \tag{2.3.15}$$

where $x^\mu := (x_{12}^{-1}+x_{23}^{-1})^{-1a} = |x|n^a$ and $(\Lambda_n)^\mu{}_1 = n^a$, the three-point function can always be mapped to the Hilbert space amplitude

$$A_{\pi_i\pi_2\pi_3;I_1I_2I_3} := \langle \mathcal{O}_{\pi_3,I_3}(0)^\dagger\mathcal{O}_{\pi_1,I_2}(e_0)\mathcal{O}_{\pi_2,I_2}(0)\rangle, \tag{2.3.16}$$

which corresponds to an invariant rank three tensor with respect to the $\mathrm{O}(d-1)$ subgroup of rotations and reflections that stabilize e_1,

$$\prod_{j=1}^{3}\rho_j(\Lambda)_{I_jJ_j}\,A_{\pi_i\pi_2\pi_3;J_1J_2J_3} = A_{\pi_i\pi_2\pi_3;I_1I_2I_3}, \quad \forall\,\Lambda\in\mathrm{O}(d-1). \tag{2.3.17}$$

The invariance condition defines a finite dimensional space of tensors in which the amplitude can be expanded,

$$A_{\pi_i;I_i} = \sum_{n=0}^{N_{123}} C^{(t_n)}_{\pi_1\pi_2\pi_3}(t_n)_{I_i}. \tag{2.3.18}$$

OPE coefficients: Plugging the expansion (2.3.18) back into the formula (2.3.13) for the three-point function in generic configuration, the OPE takes the form

$$\mathcal{O}_{\pi_1,I_1}(x_1)\mathcal{O}_{\pi_2,I_2}(x_2) = \sum_{\pi_3 \subset \pi_1 \otimes \pi_2} \sum_{n=1}^{N_{123}} C^{(t_n)}_{\pi_1\pi_2\pi_3} f^{(t_n)}_{\pi_1\pi_2\pi_3;I_1I_2I_3}(x_{12},\partial_{x_2}) \cdot \mathcal{O}_{\pi_3,I_3}(x_2). \tag{2.3.19}$$

The operators $f^{(t_n)}_{\pi_1\pi_2\pi_3}(x_{12},\partial_{x_2})$ are entirely determined by the expansion of the amplitude $A_{\pi_i;I_i}$ in (2.3.16), such that the only remaining freedom is in the constants $\{C^{(t_n)}_{\pi_1\pi_2\pi_3}\}$ — these are called the *OPE coefficients* or *structure constants*. Since a primary is specified by its conformal group representation, it is standard to relabel these coefficients by the operators themselves, i.e.

$$C^{(t_n)}_{\pi_1\pi_2\pi_3} \longleftrightarrow C^{(t_n)}_{\mathcal{O}_1\mathcal{O}_2\mathcal{O}_3}. \tag{2.3.20}$$

Both notations will be used interchangeably.

2.3.3 Higher point functions from the OPE

In principle, any N-point correlation function is determined algorithmically by the repeated application of the OPE (2.3.19) to pairs of primaries in the correlator. For example, a four-point correlator can be expanded into the sum

$$\langle \mathcal{O}_{\pi_1,I_1}(x_1)\dots\mathcal{O}_{\pi_4,I_4}(x_4)\rangle = \sum_{\pi,n_1,n_2} C^{(t_{n_1})}_{\pi_1\pi_2\pi} C^{(t_{n_2})}_{\pi_3\pi_4\pi}\, \mathcal{G}^{(12)}_{\pi;n_1n_2;I_1I_2I_3I_4}(x_i), \tag{2.3.21}$$

where the tensor valued functions $\mathcal{G}$ multiplying the OPE coefficients are given by

$$\mathcal{G}^{(12)}_{\pi;n_1n_2;I_1I_2I_3I_4}(x_i) = f^{(t_{n_1})}_{\pi_1\pi_2\pi;I_1I_2J}(x_{12},\partial_{x_2}) f^{(t_{n_2})}_{\pi_3\pi_4\pi;I_3I_4K}(x_{34},\partial_{x_4}) \frac{\rho(I(x_{24}))_{JK}}{x_{24}^{2\Delta_\pi}}. \tag{2.3.22}$$

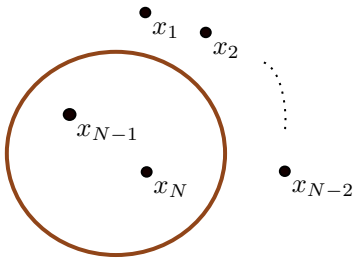

Figure 10: Illustration of the radius of convergence of the OPE $\mathcal{O}_{N-1}(x_{N-1})\mathcal{O}_N(x_N)$ in a N-point correlator.

Radius of convergence: In radial quantization, correlators are only well defined if the operators are *radially ordered*. Otherwise, its expansion in a basis of primaries and descendants will involve matrix elements of $e^{-|\tau|D}$ with unbounded spectrum $\{e^{|\tau|(\Delta+n)}\}_{n\geq 0}$. As a result, the $\mathcal{O}_{N-1}(x_{N-1})\mathcal{O}_N(x_N)$ OPE yields a convergent expansion of a N-point correlator only if

$$\exists\, y \in \mathbb{R}^d : \quad |x_{N-1}-y|, |x_N - y| < \min_{i\in\{1,\dots,N-2\}} |x_i - y|. \tag{2.3.23}$$

In the case of $N=4$ points, there always exists a conformal transformation[5] $x_i \mapsto x_i'$ such that

$$x_1' = \infty, \quad x_2' = e_1, \quad x_3' = \frac{z+\bar z}{2} e_1 + \frac{z-\bar z}{2\mathrm{i}} e_0, \quad x_4' = 0. \tag{2.3.24}$$

[5]take the conformal transformation that fixes three points to $(0, e_1, \infty)$, and use a $\mathrm{SO}(d-1)$ rotation stabilizing e_1 to put the last point in the (e_0, e_1) plane.

This configuration of points is called the conformal frame. In this frame, the (34) OPE converges for $(z, \bar{z}) \in \mathbb{C}\backslash\{1 \leq z = \bar{z} \leq \infty\}$, as can be seen from figure 11.

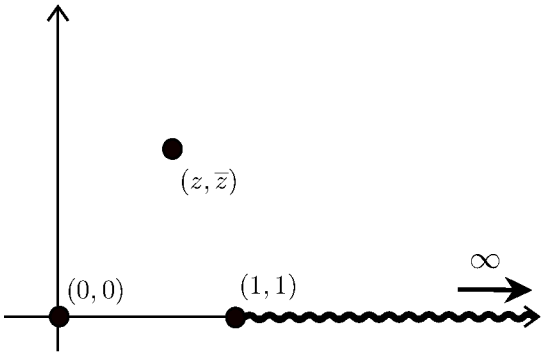

Figure 11: Conformal frame of the four-point function. If $(z, \bar{z}) \in [1, \infty)$, then there is no ball that contains $(0,0)$ and $(z, \bar{z})$ in its interior without also containing $(1,1)$. This defines the radius of convergence of the OPE for the four-point function.

Lorentzian signature: Since the standard derivation of a convergent OPE relies on quantization[6] (2.2.11) or (2.2.13) in Euclidean space, its convergence properties in Minkowski space are more difficult to access. Heuristically, one expects to obtain Lorentzian correlators from Euclidean correlators via the iϵ prescription: for a time ordered Euclidean correlator with points $x_i(\tau_i, \theta_i, n_i)$ parameterized as in (2.1.56), one assumes the existence of an analytic continuation to $\tau_i = \epsilon_i + it_i$, $\epsilon_1 > \epsilon_2 > \cdots > \epsilon_N$. Then taking the limits $\epsilon_i \to 0$ in the appropriate order, one recovers a correlation function with points $x_i(t_i, \theta_i, n_i)$ in the slicing (2.1.59) of Minkowski space. However, it is important to note that correlators and OPEs in Lorentzian signature have a much more intricate singularity structure, arising from configurations of points at lightlike separations, $(x_i - x_j)^2 = 0$. For example, if the conformal frame (11) contains a timelike direction e_0, then $z, \bar{z}$ are real and independent lightcone coordinates, such that $z \to 0$ does not imply $\bar{z} \to 0$. Unsurprisingly, the statement that Lorentzian correlators are obtainable from analytic continuation of Euclidean correlators is highly non-trivial to prove rigorously. The recent work of Kravchuk, Qiao and Rychkov [80] provides a comprehensive review of the literature on the subject, and a proof in the case of $N \leq 4$ points. The generalization to $N > 4$ points remains an interesting open problem, and the work on multipoint conformal blocks presented in this thesis may help make progress in this direction. Finally, Mack and Lüscher [11] (see also [80, footnote 68]) provided substantial evidence that CFT correlators in Minkowski space can be continued to the whole Lorentzian cylinder (see Fig. 9), which can be seen as the most conclusive formulation of Lorentzian correlators. Indeed, the cylinder is transitive for the (infinite sheeted cover of) the conformal group, has a conformal invariant causal structure, and provides the natural arena for the AdS/CFT correspondence [81, Sec. 2.2.1]. This extension is addressed in Jiaxin Qiao's doctoral dissertation [82] for the scalar four-point function. In the meantime, for the purposes of this thesis, we will adopt the widespread and well founded assumption that N-point CFT correlators and OPEs can be continued from Euclidean space to Minkowski space, based on the plethora of comparisons and checks scattered throughout the conformal bootstrap literature.

[6]The choice of H_0 as a Hamiltonian is referred to "North-South quantization" in [79, Sec. 3.1.5], while the choice of D as a Hamiltonian is commonly referred to as radial quantization in the CFT literature. In both cases, the OPE is based on the Hamiltonian operator having a positive, integer spaced spectrum and two fixed points on $\mathbb{R}^d \cup \{\infty\}$.

2.4 The conformal bootstrap

Associativity and crossing symmetry The state $\mathcal{O}_{\pi_1,I_1}(x_1)\mathcal{O}_{\pi_2,I_2}(x_2)\mathcal{O}_{\pi_3,I_3}(x_3)\,|0\rangle$ has a unique expansion in the basis (2.3.1) of primary and descendant states. As a result, any sequence of operator products must yield the same result — this is equivalent to the *associativity* property of the OPE,

$$\Big(\mathcal{O}_{\pi_1,I_1}(x_1)\mathcal{O}_{\pi_2,I_2}(x_2)\Big)\mathcal{O}_{\pi_3,I_3}(x_3) = \mathcal{O}_{\pi_1,I_1}(x_1)\Big(\mathcal{O}_{\pi_2,I_2}(x_2)\mathcal{O}_{\pi_3,I_3}(x_3)\Big). \tag{2.4.1}$$

Plugging this equality into a four-point function yields the crossing symmetry equation (CSE),

$$\sum_{\pi,n_1,n_2} C^{(t_{n_1})}_{\pi_1\pi_2\pi}C^{(t_{n_2})}_{\pi_3\bar{\pi}_4\pi}\,\mathcal{G}^{(12)}_{\pi;n_1n_2;I_1I_2I_3I_4}(x_i) = \sum_{\pi,n} C^{(t_{n_1})}_{\pi_2\pi_3\pi}C^{(t_{n_2})}_{\pi_1\bar{\pi}_4\pi}\,\mathcal{G}^{(23)}_{\pi;n_1n_2;I_2I_3I_1I_4}(x_i). \tag{2.4.2}$$

The CSE is often represented graphically in terms of OPE diagrams, as in Fig. 12.

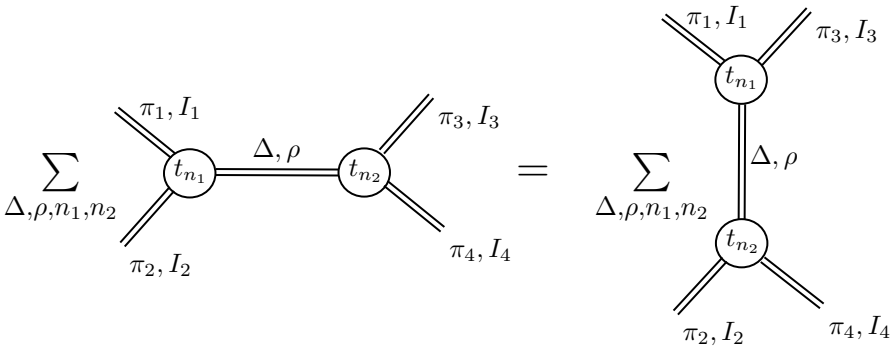

Figure 12: Graphical representation of the spinning four-point crossing symmetry equation with OPE diagrams. Internal legs are labeled by the scaling dimensions and spin labels of the primaries appearing in the OPE, while vertices are labeled by three-point tensor structures.

Four-point bootstrap review: In section 2.3, we reviewed how all correlation functions are fixed by the CFT data $\{\pi_i = (\Delta_i, \rho_i), C^{(t_n)}_{\pi_i\pi_j\pi_k}\}$. In this context, the goal of the conformal bootstrap is to constrain this data with as little extra assumptions as possible about the microscopic details of the underlying physical system. The most important sources of constraints are the CSEs (2.4.2). However, a CSE is an infinite system of linear equations for products of OPE coefficients that is untractable without further input. This is where unitarity plays a crucial role, ensuring both bounds on scaling dimensions,

$$\Delta \geq \frac{d-2}{2} \quad \text{(scalar)}, \qquad \Delta \geq l + d - 2 \quad \text{(STT)}, \tag{2.4.3}$$

and reality conditions for the OPE coefficients[7]. The last crucial ingredient is a precise understanding of the kinematically determined functions $\mathcal{G}^{(ij)}_{\pi_i;n_s;I_i}$ in (2.3.22), allowing for systematic truncations and expansions of the CSE controlled by the distance of (Δ, ρ) away from the unitarity bounds. These analyses of the CSE in the modern bootstrap literature separate into two types.

[7]Following [32, p. 12], reality conditions for OPE coefficients can be derived from six-point functions in reflection positive configurations. From the cluster decomposition principle, the latter reduces to a reflection positive product of three-point functions in a limit where the first three points are very far away from the last three points.

1. *Numerical bootstrap.* A set of CSEs can always be recast as a vanishing quadratic form in the OPE coefficients,

$$\sum_{\{\pi,n\}}\sum_{\{\pi',n'\}} C^{(t_n)}_{\{\pi\}} C^{(t_{n'})}_{\{\pi'\}} V_{\{\pi,n\}\{\pi',n'\}}(z,\bar{z};I_1I_2I_3I_4) = 0. \tag{2.4.4}$$

   If there exists a linear functional ω[8] such that $\omega\left[V_{\{\pi,n\}\{\pi',n'\}}\right]$ is a positive definite matrix for a putative spectrum of $\pi = (\Delta,\rho)$, then this putative spectrum is excluded. Similarly, if ω produces a negative semi-definite matrix on a finite subset and a positive-definite matrix on its complement, then OPE coefficients of the latter are bounded by the former. After numerical implementation, a subspace of non-excluded CFT data can be carved out in this manner, the most precise constraints involving primaries of low scaling dimension and spin. In the simplest and most studied case of a single CSE for four identical scalars ϕ, the quadratic form is proportional to the sum of $C^2_{\phi\phi\mathcal{O}}\left(\mathcal{G}^{(12)}_{\phi\phi\mathcal{O}} - \mathcal{G}^{(23)}_{\phi\phi\mathcal{O}}\right)$ over $(\Delta_{\mathcal{O}}, l_{\mathcal{O}})$. Then positive functionals are typically of the form $\partial_z^n\partial_{\bar{z}}^{\bar{n}}|_{z=\bar{z}=1/2}$, corresponding to expansions of the CSE around the crossing symmetric point $z=\bar{z}=1/2$ in the conformal frame of Fig. (11). Since no numerical bootstrap computations are present in this thesis, we will not discuss it further and refer to [32] for further details and references.

2. *Analytic bootstrap:* In Lorentzian signature, it is possible to study the CSE near kinematical configurations where *both* $x_1 - x_2$ *and* $x_2 - x_3$ are near-to-lightlike separations. As we will see in chapter 7, these lightcone limits make the contributions of primaries $\mathcal{O}_i$ closest to the unitarity bound dominate the LHS of the CSE, while families of composite primaries $[\mathcal{O}_i\mathcal{O}_j] := \mathcal{O}_i\partial\ldots\partial\mathcal{O}_j$, called double-twist, at large spin but fixed distance from the unitarity bound dominate the RHS. The expansion near one lightcone limit yields corrections in the large spin limit, while the other accesses the CFT data of double-twist operators further away from the unitarity bounds. Beyond large spin limits, the Lorentzian inversion formula of Caron-Huot establishes that this CFT data is analytic in the spin, converging at least down to spin two, and systematizes the lightcone expansion of the CSE sketched above. At the same time, depending on the theory, it is also possible to expand the CSE in a small parameter (e.g. weak coupling, ϵ-expansion, or $1/N$ expansions in holographic CFTs). These perturbative expansions are often compatible with, and enhanced by, the reorganization of the CSE into the Lorentzian inversion formula.

2.A Derivation of unitarity bounds

For any STT representation $\rho = \rho_l$ of $\mathrm{SO}(d)$, the tensor $A_{I\mu\nu J} \equiv A_{(\lambda_1\ldots\lambda_l)\mu\nu(\tau_1\ldots\tau_l)}$ defined by (2.2.16) is composed of four groups of symmetrized indices. To study its decomposition into irreducibles, we contract the indices of each group with a polarization vector $z_i \in \mathbb{C}^d$, $i = 1,2,3,4$, and define the polynomial

$$F(z_1,z_2,z_3,z_4) := A_{(\lambda_1\ldots\lambda_l)\mu\nu(\tau_1\ldots\tau_l)} z_1^{\lambda_1}\ldots z_1^{\lambda_l} z_2^{\mu} z_3^{\nu} z_4^{\tau_1}\ldots z_4^{\tau_l}, \tag{2.A.1}$$

which is manifestly homogeneous of degree $(l,1,1,l)$ in (z_1,z_2,z_3,z_4). Acting with a $\mathrm{SO}(d)$ generator $(L_i)^{\mu}{}_{\nu}$ on the i-th index group is equivalent to acting with $-(L_i)^{\mu}{}_{\nu}$ on z_i. Thus, the invariance

[8] this is any tensor valued operator that turns V into a matrix in $\{\pi,n\}$ space and satisfies $\omega[\lambda V_1+V_2] = \lambda\omega[V_1]+\omega[V_2]$.

condition for A translates to Ward identities for F,

$$\sum_{i=1}^{4}(z_{i\mu}\partial_{z_i^\nu} - z_{i\nu}\partial_{z_i^\mu})F(z_1,z_2,z_3,z_4) = 0. \tag{2.A.2}$$

Combining the Ward identities with homogeneity, F is restricted to a three-dimensional space of polynomials

$$F \in \text{Span}\left(f_0 := z_{12}z_{34}z_{14}^{l-1}, f_1 := z_{13}z_{24}z_{14}^{l-1}, f_2 := z_{23}z_{14}^{l}\right), \quad z_{ij} := z_i \cdot z_j. \tag{2.A.3}$$

The tensor structures $A^{(ij)}_{(l_1,\ldots,l_L)}$ are given by a solution to the Casimir equation

$$-\frac{1}{2}\sum_{i,j=1}^{2}(z_{i\mu}\partial_{z_i^\nu} - z_{i\nu}\partial_{z_i^\mu})(z_j^\mu\partial_{z_{j\nu}} - z_j^\nu\partial_{z_{j\mu}})f^{(ij)}_{(l_1,\ldots,l_L)} = \sum_{b=1}^{L} l_\nu(l_\nu + d - 2b)f^{(ij)}_\rho. \tag{2.A.4}$$

In the basis (f_0, f_1, f_2) of (2.A.3), the Casimir differential operators act as 3×3 matrices that are straightforward to diagonalize. Finally, in analogy to CFT four-point blocks continued to negative integer conformal dimensions, we fix the normalization of the Casimir eigenfunctions by requiring

$$f^{(23)}_{(J,\kappa)} \overset{z_2\to z_3, z_4\to z_1}{\sim} (z_{23}z_{14})^{\frac{2-J-\kappa}{2}} z_{34}^{J-\kappa}\left(z_2 \wedge z_3 \cdot z_1 \wedge z_4\right)^\kappa, \tag{2.A.5}$$

$$f^{(12)}_{(J,\kappa)} \overset{z_1\to z_2, z_3\to z_4}{\sim} (z_{12}z_{34})^{\frac{l+1-J-\kappa}{2}} z_{24}^{J-\kappa}\left(z_1 \wedge z_2 \cdot z_4 \wedge z_3\right)^\kappa. \tag{2.A.6}$$

In this case, we obtain

$$f_0^{(23)} = f_2, \quad f^{(23)}_{(1,1)} = f_1 - f_0, \quad f_2^{(23)} = \frac{f_1 + f_0 - \frac{2}{d}f_2}{2}, \tag{2.A.7}$$

$$f^{(12)}_{l-1} = f_0, \quad f^{(12)}_{(l,1)} = f_2 - f_1 - \frac{l-1}{l+d-3}f_0, \quad f^{(12)}_{l+2} = \frac{f_2 + l f_1 - \frac{2l}{2l+d-2}f_0}{l+1}. \tag{2.A.8}$$

Note that in $d = 3$, representations of SO(3) have one single spin label and the eigenvalue of the Casimir for $\rho_{(l,1)}$ is $l(l+d-2) + 1(1+d-4) = l(l+1)$, such that $\rho_{(l,1)} = \rho_l$.

Chapter 3

Conformal Correlators and Blocks

The modern incarnation of the conformal bootstrap, briefly reviewed in section 2.4, relies on a detailed knowledge of the kinematically determined functions in the OPE decomposition of correlators — see (2.3.21) for $N = 4$. In this chapter, we will review some approaches to simplifying conformal kinematics that are now widespread in the conformal bootstrap literature. First, using the embedding space formalism, we will write down the most general solution to the conformal Ward identities of a N-point function in the form of (3.2.9). By applying sequences of OPEs to this formula, the kinematically determined functions are then related to conformal blocks by the formula (3.3.1). Finally, we will review several efficient methods to compute conformal blocks for scalar four-point functions, in anticipation of their higher point generalizations in subsequent chapters.

3.1 The embedding space formalism

In section 2.1.3, the standard conformal completions of $\mathbb{R}^d$ were constructed by embedding them in the $d+2$ dimensional lightcone $\{X \in \mathbb{R}^{d+2} \,|\, X^2 = 0\}$. In the foliation of the lightcone by $\mathbb{R}^d$, the metric is given by $\mathrm{d}X^2 = (X^+)^2 \mathrm{d}x^2$. For a scalar primary, this implies

$$(X'^+)^{-\Delta} \mathcal{O}'_\Delta(x') = (X^+)^{-\Delta} \mathcal{O}_\Delta(x), \tag{3.1.1}$$

for any conformal transformations $x \mapsto x'$. This transformation law is equivalent to a scalar field on the lightcone satisfying

$$\phi_\Delta(\Lambda X) = \lambda^{-\Delta} \phi_\Delta(X), \quad \phi'_\Delta(\Lambda X) = \phi_\Delta(X), \tag{3.1.2}$$

with the identification

$$\phi_\Delta\left(\frac{1+x^2}{2}, x, \frac{1-x^2}{2}\right) = \mathcal{O}_\Delta(x). \tag{3.1.3}$$

In the next section, we will describe the lift to embedding space for primaries that transform in mixed symmetry tensor representations of $\mathrm{SO}(d)$[1].

3.1.1 Tensor representations of the conformal algebra

Primary fields in d-dimensional CFT are irreducible representations of the $\mathfrak{so}(1, d+1)$ algebra labeled by an $\mathfrak{so}(1,1)$ weight Δ, the scaling dimension, and an ordered set of $\mathfrak{so}(d)$ weights $l_1 \geq l_2 \geq \cdots \geq l_L$

[1] All integer spin representations of $\mathrm{SO}(d)$ are isomorphic to mixed symmetry tensors.

which we refer to as the *spins* of the representation[2]. Focusing on bosonic representations, we associate representations of $\mathfrak{so}(d)$ with Young diagrams, where the integers l_ν represent the length of the ν-th row of the diagram as in Figure 13.

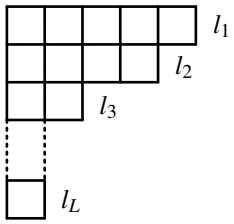

Figure 13: Young diagram associated with the representation labeled by integers $l_1 \geq l_2 \geq \cdots \geq l_L$ where l_ν represents the length of the ν-th row of the diagram.

More explicitly, these representations correspond to traceless tensors whose indices can be grouped following the rows of the Young diagram, thereby making the symmetry of permuting indices within those groups manifest

$$\mathbf{F}^{\Delta}_{l_1,\ldots,l_L}(x) \equiv \left(F_{\left(a_1^{(1)}\ldots a_{l_1}^{(1)}\right)\ldots\left(a_1^{(L)}\ldots a_{l_L}^{(L)}\right)}(x)\right) . \tag{3.1.4}$$

Note that one could equivalently focus, instead, on the columns of the Young diagram and therefore make the antisymmetries of such indices manifest, as detailed in [83].
We denote a Mixed-Symmetry Tensor like (3.1.4) with $L \geq 2$ groups of symmetric indices as MST_L, while for the single spin case $L = 1$ we use the standard terminology of Symmetric Traceless Tensor (STT). For scalar five- and six-point functions, that is to say the main examples for bootstrap applications in this thesis, we need only to consider the STT and MST_2 cases. Finally, with this notation, it is important to note that tensors of the form (3.1.4) do *not* form irreducible representations when the dimension is even and the depth is maximal, i.e. $d = 2L$. The first non-trivial case, $d = 2L = 4$ and $l_1 = l_2 = 1$, corresponds to a field strength $F_{ab} = -F_{ba}$ with dual field strength $\star F_{ab} := \frac{1}{2}\epsilon_{abcd}F^{cd}$. The latter are known to decompose into two irreducible representations of SO(4): the self-dual part, $\star F = F$, and the anti-self-dual part, $\star F = -F$. The duality map $\star$ that distinguishes irreducible representations at $L = d/2$ can be generalized to any spins $l_1, \ldots, l_L$, and we will explain below how we project to the irreducible self-dual and anti-self-dual subrepresentations in our formalism.

The main purpose of this subsection is to re-express the rather conventional description of tensor fields and the associated representations in a way that simplifies explicit computations and makes results more compact. This is achieved using the so-called embedding space formalism and a generalized index-free notation using polarization variables.
The *embedding space formalism* realizes points on $\mathbb{R}^d$ with a non-linear action of the conformal group in terms of projective null rays that live in a $(d+2)$-dimensional Minkowski space and admit a linear action of $\mathrm{SO}(1, d+1)$. Given any field of conformal weight Δ, one can use this relation to define the uplift

$$\mathbf{F}^{\Delta}_{\mathbf{l}}(x) \to \mathbf{F}^{\Delta}_{\mathbf{l}}(X) , \qquad \left\{X \in \mathbb{R}^{1,d+1} \,|\, X^2 = 0\right\} , \tag{3.1.5}$$

to a function on light-like vectors that is homogeneous of degree $-\Delta$ with respect to rescalings of X,

$$\mathbf{F}^{\Delta}_{\mathbf{l}}(\lambda X) = \lambda^{-\Delta}\mathbf{F}^{\Delta}_{\mathbf{l}}(X) . \tag{3.1.6}$$

[2] As discussed section 2.2, these are equivalent to unitary, positive energy representations of $\mathfrak{so}(2, d)$.

For fields with spin, all physical space indices a get promoted to embedding space indices A. The tensor (3.1.4) in physical space can be recovered from the tensor in embedding space by contracting each index with a copy of the Jacobian $\frac{\partial X^A}{\partial x^a}$. In order to transform irreducibly under the action of the conformal group, the uplifted fields possess a number of additional properties. In particular, they are required to be transverse with respect to any index of the tensor in embedding space,

$$X^{A_i^{(\nu)}} F^{\Delta}_{\left(A_1^{(1)}\ldots A_{l_1}^{(1)}\right)\ldots A_i^{(\nu)}\ldots\left(A_1^{(L)}\ldots A_{l_L}^{(L)}\right)}(X) = 0\,, \tag{3.1.7}$$

and traceless with respect to any pair of indices

$$\eta^{A_i^{(\mu)}A_j^{(\nu)}} F^{\Delta}_{A_1^{(1)}\ldots A_i^{(\mu)}\ldots A_j^{(\nu)}\ldots A_{l_L}^{(L)}}(X) = 0\,. \tag{3.1.8}$$

Here, the capital letters A are vector indices in embedding space and (η_{AB}) is the $(d+2)$-dimensional Minkowski metric. The embedding space formalism relates conformal transformations of d-dimensional space to Lorentz transformations of the embedding space coordinates,

$$\mathcal{T}_{AB} = X_A \frac{\partial}{\partial X^B} - X_B \frac{\partial}{\partial X^A}\,. \tag{3.1.9}$$

When transforming tensor fields one needs to add additional terms that act on the tensor indices. Instead of detailing these terms, however, we now want to explain how to get rid of all the tensor indices. The idea is to encode the tensor components of the field as coefficients of some polynomial in several variables. This has been known for a long time, at least for STTs , see e.g. [84, 85]. The extension to more general mixed-symmetry tensors of depth $L > 1$ comes in two variants, one that encodes the antisymmetrization between different rows of a Young diagram with fermionic coordinates, see [83], and another that instead encodes the symmetrization between different columns of a Young diagram with bosonic coordinates, see [86]. Here we shall adopt the bosonic approach and introduce one auxiliary polarization vector $Z_\nu \in \mathbb{C}^{d+2}$ for every spin quantum number l_ν of the MST; these polarization vectors are contracted with the MST to form a polynomial in all of the polarizations

$$F^{\Delta}_{l_1,\ldots,l_L}(X, Z_1, \ldots, Z_L) \equiv F^{\Delta}_{\left(A_1^{(1)}\ldots A_{l_1}^{(1)}\right)\ldots\left(A_1^{(L)}\ldots A_{l_L}^{(L)}\right)}(X) \left(Z_1^{A_1^{(1)}}\cdots Z_1^{A_{l_1}^{(1)}}\right)\cdots\left(Z_L^{A_1^{(L)}}\cdots Z_L^{A_{l_L}^{(L)}}\right). \tag{3.1.10}$$

The properties of tracelessness and transversality of the tensor $F_{\{A_i^{(\nu)}\}}(X)$ are translated into the conditions

$$X^2 = X\cdot Z_\nu = Z_\nu \cdot Z_\mu = 0 \tag{3.1.11}$$

for the coordinates. In addition, these new objects obey the following multiple homogeneity condition for a field of conformal weight Δ and with spin labels l_ν,

$$F^{\Delta}_{\{l_\nu\}}(\lambda_0 X, \{\lambda_\nu Z_\nu\}) = \lambda_0^{-\Delta}\lambda_1^{l_1}\cdots\lambda_L^{l_L} F^{\Delta}_{\{l_\nu\}}(X, \{Z_\nu\})\,. \tag{3.1.12}$$

This extends the condition (3.1.6) and rephrases that fields with spin l_ν have a polynomial dependence on Z_ν with homogeneous degree l_ν. Finally, the dependence on the polarizations respects the following set of gauge invariance conditions

$$F^{\Delta}_{\{l_\nu\}}\left(X, \left\{Z_\nu + \beta_{\nu,0}X + \sum_{\mu<\nu}\beta_{\nu,\mu}Z_\mu\right\}\right) = F^{\Delta}_{\{l_\nu\}}(X, \{Z_\nu\})\,, \qquad \forall\beta_{\nu,\mu}\in\mathbb{C}\,. \tag{3.1.13}$$

In this formulation, the generators act on fields as derivations that include terms involving polarizations next to the spacetime part (3.1.9),

$$\mathcal{T}_{AB} = X_A \frac{\partial}{\partial X^B} + \sum_\nu Z_{\nu\, A} \frac{\partial}{\partial Z_\nu^B} - (A \leftrightarrow B)\,. \tag{3.1.14}$$

Before we conclude this brief presentation of embedding space for tensor fields, we want to add a couple of comments. First, note that functions in the variables X, Z_ν can be assigned a multi-degree that has $L+1$ components, one for the variable X and then one for each of the L polarizations Z_ν. The assignment is such that a field F with weight Δ and spins l_ν has degree $[-\Delta, l_1, \ldots, l_L]$. This degree is measured by the independent rescalings of the variables that we have introduced.

At this point, we have rephrased the concept of a tensor field of weight Δ and spin l_ν in terms of functions F of the variables (X, Z_ν) subject to the conditions (3.1.11). These functions must satisfy the homogeneity conditions (3.1.12), as well as the gauge invariance conditions (3.1.13). These two conditions ensure that the differential operators (3.1.14) give rise to an irreducible representation of the conformal algebra. From now on, we will think of tensor fields in terms of functions $F(X, Z_\nu)$. Let us note in passing that the homogeneity conditions (3.1.12) can be continued to non-integer values of l_ν.

It is also important to notice how the gauge invariance conditions (3.1.13) constrain the way in which the variables Z_ν can appear in expressions that involve the field $F_{\Delta,\{l_\nu\}}$. In fact, the only gauge invariant tensors that can be formed from (X, Z_ν) are linear combinations or contractions of the wedge products (see also [86, eq. 27]):

$$C^{(0)}_A = X_A\,, \qquad C^{(\nu)}_{A_1\ldots A_{\nu+1}} = \left(X \wedge \bigwedge_{\mu=1}^{\nu} Z_\mu\right)_{A_1\ldots A_{\nu+1}}\,. \tag{3.1.15}$$

Let us point out that the projective light ray contains d degrees of freedom. After imposing transversality $X \cdot Z_1 = 0$ and the gauge invariance (3.1.13), there remain $d-2$ degrees of freedom in the polarization Z_1. Similarly, Z_2 contains $d-4$ degrees of freedom, etc. This implies that the variable Z_L for tensor fields of maximal depth $L = \text{rank}_d - 1 = d/2$ in even dimensions has no continuous physical degrees of freedom. In the reduction from embedding space variables to gauge-invariant tensors, all $C^{(0)}, \ldots, C^{(L-1)}$ are fixed by $X, \ldots, Z_{L-1}$, while $C^{(L)} = C^{(L-1)} \wedge Z_L$. Up to gauge equivalence, this implies that $\text{Span}(Z_L)$ is fixed to be one of two unique null directions in the complex plane orthogonal to $\text{Span}(X, \ldots, Z_{L-1})$. To distinguish these two null directions, we can use the fact that $C^{(L)}$ is a $(L+1)$-form in $\mathbb{C}^{2(L+1)}$ given by the wedge product of $L+1$ mutually orthogonal null vectors, and must therefore be either self-dual or anti-self-dual with respect to the Hodge star,

$$\star\, C^{(L)}{}_{A_1\ldots A_{L+1}} = \frac{1}{(L+1)!}\epsilon_{A_1\ldots A_{2L+2}} C^{(L)A_{L+2}\ldots A_{2L+2}} = \pm \mathrm{i}^L\, C^{(L)}_{A_1\ldots A_{L+1}}. \tag{3.1.16}$$

The above condition separates the space of gauge equivalence classes of $(X, Z_1, \ldots, Z_L)$ into two distinct $\text{SO}(1, d+1)$ orbits: the *self-dual* and the *anti-self-dual* one, according to the eigenvalue in (3.1.16). Contracting a tensor with null vectors in the (anti-)self-dual orbit projects said tensor to its (anti-)self-dual part, such that the restriction of $F^{\Delta}_{l_1,\ldots,l_L}(X, Z_1, \ldots, Z_L)$ to one of these orbits defines an irreducible representation of $\mathfrak{so}(1, d+1)$. In subsection 5.2.2, we find a concrete parameterization of the two orbits for $d = 4$ in a gauge given by two iterated Poincaré patches. To the best of our knowledge, our publication [64] was the first to construct these irreducible representations directly in $d = 4$ embedding space.

3.1.2 Back to tensor representations in position space

Denote a MST field in embedding space by $F^{\Delta}_{\{l_\nu\}}(X,\{Z_\nu\}) \equiv F(X,\{Z_\nu\})$. The covariance properties of F under a conformal transformation $X'^A = \Lambda^A{}_B X^B$ are encoded in the invariance of the differential

$$\Phi_F := F(X,\{\mathrm{d}X\}), \quad \Phi'_F = \Phi_F. \tag{3.1.17}$$

This differential admits a pullback to the Poincaré patch (2.1.46) given by the pullback of the coordinate one-forms,

$$\mathrm{d}X^A = \frac{\partial X^A}{\partial x^a}\mathrm{d}x^a. \tag{3.1.18}$$

The pullback produces an invariant differential on $\mathbb{R}^d$ that encodes the MST field in position space,

$$F\left(X(x),\left\{\frac{\partial X(x)}{\partial x^a}\mathrm{d}x^a\right\}\right) = (X^+)^{|l|-\Delta}\mathcal{O}(x,\{\mathrm{d}x\}), \quad |l| := \sum_{\nu=1}^{L} l_\nu. \tag{3.1.19}$$

After introducing L position space polarization vectors,

$$z_1,\dots,z_L \in \mathbb{C}^d, \quad z_\nu \cdot z_{\nu'} = 0, \tag{3.1.20}$$

the substitution $\mathrm{d}x \wedge \cdots \wedge \mathrm{d}x \leftrightarrow z_1 \wedge \cdots \wedge z_\nu$ yields the explicit relation between MST primary fields in position space and in embedding space,

$$\mathcal{O}_{\Delta,\{l_\nu\}}(x,\{z_\nu\}) = (X^+)^{\Delta-|l|}\, F^{\Delta}_{\{l_\nu\}}\left(X(x),\left\{\frac{\partial X(x)}{\partial x^a}z^a_\nu\right\}\right). \tag{3.1.21}$$

3.2 Conformal invariance of correlation functions

Correlation functions of primaries $F^{\Delta_i}_{\{l_{i\nu}\}}(X_i,\{Z_{i\nu}\})$ satisfy conformal Ward identities, that is to say they are invariant under the diagonal action of the conformal algebra,

$$\sum_{i=1}^{N}\mathcal{T}_{iAB}(X_i,\partial_{X_i},\{Z_{i\nu},\partial_{Z_{i\nu}}\})\left\langle\prod_{i=1}^{N}F^{\Delta_i}_{\{l_{i\nu}\}}(X_i,\{Z_{i\nu}\})\right\rangle = 0. \tag{3.2.1}$$

The number of degrees of freedom depends on the dimension d, the number of points N, the spin depths $(L_i)_{i=1}^N$, and most importantly the *critical dimension*

$$d_c := N + |L| - 2, \quad |L| = L_1 + \cdots + L_N. \tag{3.2.2}$$

- If $d \le d_c$, the conformal group acts transitively on the embedding space vectors and the number of degrees of freedom is

$$n_{cr}(d,N,L_i) = \sum_{i=1}^{N}(L_i+1)(d-L_i) - \frac{(d+1)(d+2)}{2}. \tag{3.2.3}$$

- If $d+2 > d_c$, the conformal group does not act transitively and a $\mathrm{O}(d+2-N-|L|)$ subgroup of conformal transformations leaves the N-point configuration invariant. Thus, the number of degrees of freedom no longer varies with the dimension and

$$n_{cr}(d > d_c,N,L_i) = n_{cr}(d_c,N,|L|). \tag{3.2.4}$$

As is well known from the invariant theory of Lie groups, this space of functions is generated by semi-invariants[3] of $(\mathbb{C}^\times)^{N+|L|} \times \mathrm{O}(1,d+1)$, namely contractions of the gauge invariant tensors $C^{(\nu)}_{iA_1\dots A_\nu}$ with the metric $\eta_{A_1A_2}$ and the Levi-Civita symbol $\epsilon_{A_1\dots A_{d+2}}$. To classify these semi-invariants, we introduce a space of multi-degrees

$$\sigma := [(\sigma_{i\nu})_{i,\nu}; \sigma_\star] \in \mathbb{C}^{N+|L|} \times \mathbb{Z}_2, \tag{3.2.5}$$

where the weight $\sigma_\star = 0, 1 \bmod 2$ is known as the $\mathrm{O}(d)$ parity. In this case, a semi-invariant of degree σ is a function satisfying

$$f_\sigma\left(\lambda_{i0}\dots\lambda_{i\nu}\,\Lambda\cdot C^{(\nu)}_i\right) = (\det\Lambda)^{\sigma_\star}\prod_{i=1}^{N}\prod_{\nu=0}^{L_i}\lambda_{i\nu}^{\sigma_{i\nu}} f_\sigma(C^{(\nu)}_i). \tag{3.2.6}$$

In particular, correlation functions (3.2.1) in a parity preserving theory are semi-invariants of weight $\sigma_{\Delta,l} = [-\Delta_i, l_{i\nu}; \sigma_\star]$[4]. We will often drop the component $\sigma_\star$ from the multi-degree once its parity is made clear.

Define $n_s(d,N,L_i) := n_{cr}(d,N,L_i) + N + |L|$. We call a set $\{e_1,\dots,e_{n_s}\}$ of semi-invariants a *seed* if its elements are linearly independent polynomials of the embedding space vectors and if any other semi-invariant with positive integer degrees $\sigma_{i\nu} \in \mathbb{Z}_{\geq 0}$ can be expanded as

$$f_\sigma = \sum_{k\in\mathbb{L}_\sigma} c_{\sigma;k_1\dots k_{n_s}}\, e_1^{k_1}\dots e_{n_s}^{k_{n_s}}, \quad \mathbb{L}_\sigma := \left\{k\in\mathbb{Z}^{n_s}_{\geq 0}\,|\,\sum_{i=1}^{n_s} k_i\sigma_i^e = \sigma\right\}. \tag{3.2.7}$$

Finally, we call *cross ratios* any linearly independent set of functions of the seed generators $\{u_1(e_i),\dots$ $\dots,u_{n_{cr}}(e_i)\}$, such that

$$\frac{f_\sigma(e_1,\dots,e_{n_s})}{f'_\sigma(e_1,\dots,e_{n_s})} = g_\sigma(u_1,\dots,u_{n_{cr}}), \tag{3.2.8}$$

for any two semi-invariants of degree σ. Given a seed and a set of cross ratios, a conformal correlator can then be explicitly parameterized as

$$\left\langle\prod_{i=1}^{N} F^{\Delta_i}_{\{l_{i\nu}\}}(X_i,\{Z_{i\nu}\})\right\rangle = e_1^{\omega_1}\dots e_{n_s}^{\omega_{n_s}}\, G^{(\Delta_i,\{l_{i\nu}\})}(u_1,\dots,u_{n_s}), \tag{3.2.9}$$

where $\Omega := e_1^{\omega_1}\dots e_{n_s}^{\omega_{n_s}}$ is called a prefactor, specified by any decomposition $\sigma_{\Delta,l} = \omega_1\sigma_1^e + \dots + \omega_{n_s}\sigma^e_{n_s}$ of the N-point multi-degree in the seed basis. There is no algorithm to determine a seed for correlation functions of primaries with arbitrary spin depths $0 \leq L_i \leq r_d$. There is, however, a significant amount of results near both extremeties of the spin depth range.

- For $L_1 = \dots = L_N = 0$, semi-invariants are generated by scalar products and determinants, with relations below the critical dimension given by the vanishing minors of the Gram matrix.
- For $L_1 = \dots = L_N = r_d$, Fock-Goncharov "$\mathcal{A}$-coordinates" [87, 88] constitute seeds both by the definition provided above, and in the sense of cluster algebras. In this case, cluster mutation

[3] Here, semi-invariant is a synoynm for (multiplicative) character. All semi-invariants in N-point functions are strictly invariant under the action of conformal transformations connected to the identity.

[4] In a parity violating theory, a correlation function can be a non-trivial linear combination of semi-invariants with even parity $\sigma_\star = 0$ and odd parity $\sigma_\star = 1$, but otherwise equal degrees. We will not be distinguishing between parity preserving and parity violating theories in this thesis.

is a birational map that generates new seeds related to an initial seed by so called exchange relations. Moreover, in any seed, the Fock-Goncharov "$\mathcal{X}$-coordinates" give specific ratios of the $\mathcal{A}$-coordinates that constitute an independent set of generalized cross ratios for the N-point function. In $d = 1$, Fock-Goncharov coordinates are equivalent to a subset of $\left\{X_{ij}^{1/2}\right\}$, while in $d = 2$ there always exists a seed made out of $\left\{\left(C_i^{(1)} \cdot C_j^{(1)}\right)^{1/2}, \left(\bar{C}_{\bar{i}}^{(1)} \cdot \bar{C}_{\bar{j}}^{(1)}\right)^{1/2}\right\}$. These constructions are both based on the isomorphism $\mathfrak{so}_{\mathbb{C}}(3) \cong \mathfrak{sl}_{\mathbb{C}}(2)$.

In the representation theory of $\mathfrak{sl}(n)$, there is strong evidence that all seeds carry the structure of a cluster algebra via generalizations of Fock and Goncharov's construction. It is therefore worthwhile to investigate their $\mathfrak{so}(d+2)$ analogues. In the meantime, within the confines of this thesis, we will restrict our analysis to general two- or three-point functions and scalar N-point functions.

3.2.1 Two-point functions

In section 2.3.2, two-point functions were shown to be non-vanishing only if $(\Delta_1, \rho_1^\dagger) = (\Delta_2, \rho_2)$, and uniquely fixed by the scalar product on the spinning representation $\rho_1^\dagger = \rho_2$, leading to the formula (2.3.12) when $\rho_1^\dagger \cong \rho_1$. In the embedding space formalism, this translates to all two-point semi-invariants being generated by contractions $C_1^{(\nu)} \cdot C_2^{(\nu)}$. Thus, fixing the homogeneity singles out a unique semi-invariant up to a multiplicative constant, that is fixed in turn by the normalization of the scalar product of two MSTs. From now on, the normalization will be fixed by imposing

$$\left\langle F^{\Delta}_{\{l_\nu\}}(X_1, \{Z_{1\nu}\}) F^{\Delta}_{\{l_\nu\}}(X_2, \{Z_{2\nu}\}) \right\rangle = X_{12}^{-2h} \prod_{\nu=1}^{L} \left(H_{12}^{(\nu)}\right)^{l_\nu - l_{\nu+1}}, \tag{3.2.10}$$

$$h := \frac{\Delta - |l|}{2}, \quad X_{12} := -2X_1 \cdot X_2, \quad H_{12}^{(\nu)} := \frac{1}{\nu!} C_1^{(\nu)} \cdot C_2^{(\nu+1)}. \tag{3.2.11}$$

The corresponding normalization for the scalar product of STTs can be worked out explicitly using the map (3.1.21). In particular,

$$\frac{X_{12}}{X_1^+ X_2^+} = x_{12}^2, \quad \frac{H_{12}}{X_1^+ X_2^+} = -\frac{1}{4} x_{12}^2 I_{a_1 a_2}(x_{12})\, z_1^{a_1} z_2^{a_2}, \tag{3.2.12}$$

where $H_{12} \equiv H_{12}^{(1)}$.

(Anti-)self dual representations: In even dimensions, where the maximal spin depth is $L = d/2$, the maximally antisymmetric tensor $C^{(d/2)}$ splits into two orbits of the conformal group, labeled by

$$\star\, C^{(d/2)} = \mathrm{i}^{d/2} C^{(d/2)}, \quad \star \bar{C}^{(d/2)} = -\mathrm{i}^{d/2} \bar{C}^{(d/2)}. \tag{3.2.13}$$

Each orbit projects a tensor to a self-dual (respectively anti-self-dual) representation which we denote by ρ_+ (respectively ρ_-). At the same time, for any rank $\frac{d+2}{2}$ forms F_1, F_2 in $\mathbb{R}^{1,d+1}$, the scalar product is given by $F_1 \wedge \star F_2 = -(F_1 \cdot F_2)\mathrm{d}^{d+2}X$. Using the property $\star^2 = (-1)^{\frac{d}{2}}$, we deduce that

$$\star\, F_1 \cdot \star F_2 = -F_1 \cdot F_2. \tag{3.2.14}$$

Depending on whether $\mathrm{i}^{d/2}$ squares to 1 or -1, this forces some contractions of self-dual and anti-self-dual forms to vanish identically.

- If $d/2$ is odd, then the Hodge star has real eigenvalues and $C_i^{(d/2)} \cdot \bar{C}_j^{(d/2)} = 0$. This implies $\rho_\pm^\dagger \cong \rho_\pm$.

- If $d/2$ is even, then the Hodge star has pure imaginary eigenvalues and $C_i^{(d/2)} \cdot C_j^{(d/2)} = 0$. This implies $\rho_\pm^\dagger \cong \rho_\mp$.

In this case, the semi-invariant $H_{12}^{(d/2)}$ reduces to one of the four pairings, depending on the dimension and the self-duality type,

$$H_{12}^{(d/2)} \longrightarrow H_{12}^{(d/2)}, H_{1\bar{2}}^{(d/2)}, H_{\bar{1}2}^{(d/2)}, H_{\bar{1}\bar{2}}^{(d/2)}. \tag{3.2.15}$$

3.2.2 Three-point functions and tensor structures

The conformal bootstrap program relies on one fundamental property of three-point functions: they are fixed by conformal symmetry up to a finite number of dynamical coefficients. In section (2.3.13), this property was demonstrated by mapping the three points to $(x_1, x_2, x_3) = (\infty, e_1, 0)$, in which case the correlator is a linear combination (2.3.18) of three-point tensor structures in $(\rho_1 \otimes \rho_2 \otimes \rho_3)^{\mathrm{O}(d-1)}$. In the embedding space formalism, the space of three-point functions is finite-dimensional because there are only three semi-invariants X_{12}, X_{13}, X_{23} with zero support on the polarization vectors $Z_{i\nu}$. Consequently, any three-point function takes the form

$$\left\langle \prod_{i=1}^{3} F^{\Delta_i}_{\{l_{i\nu}\}}(X_i, \{Z_{i\nu}\}) \right\rangle = \left(\frac{X_{12}}{X_{13}X_{23}}\right)^{\frac{\Delta_3}{2}} \left(\frac{X_{23}}{X_{31}X_{12}}\right)^{\frac{\Delta_1}{2}} \left(\frac{X_{31}}{X_{23}X_{12}}\right)^{\frac{\Delta_2}{2}} \times$$
$$\text{polynomial}\left(\sqrt{\frac{X_{12}}{X_{13}X_{23}}}C_3^{(\nu)}, \sqrt{\frac{X_{23}}{X_{31}X_{12}}}C_1^{(\nu)}, \sqrt{\frac{X_{31}}{X_{23}X_{12}}}C_2^{(\nu)}\right).$$

In the frame where $(x_1, x_2, x_3) = (\infty, e_1, 0)$, the scalar semi-invariants reduce to $X_{12} = X_{23} = X_{13} = 1$, and the $\mathrm{SO}(1, d+1)$ invariant polynomial is equal to a tensor structure (2.3.18) after applying the relation (3.1.21). Therefore, expanding three-point tensor structures into a basis is the same as expanding the embedding space three-point function into a basis of polynomials of the (generalized) cross ratios,

$$\left\langle \prod_{i=1}^{3} F^{\Delta_i}_{\{l_{i\nu}\}} \right\rangle = e_1^{\omega_1} \dots e_{n_s}^{\omega_s} \sum_{n=1}^{N_{123}} C^{(t_n)}_{\pi_1\pi_2\pi_3} t_n(u_1, \dots, u_{n_{cr}}). \tag{3.2.16}$$

In general, there is no canonical choice of basis $(t_n)_{n=1}^{N_{123}}$. However, in the lowest depth cases where $n_{cr} = 0$, there is only one constant tensor structure that can be normalized to $t_1 \equiv 1$. This only occurs for two scalars and one STT $\langle \phi_1(X_1)\phi_2(X_2)F_3(X_3, Z_3)\rangle$, for which we can choose the seed

$$\{e_1, e_2, e_3, e_4\} = \{X_{12}, X_{23}, X_{13}, J_{3,12}\}, \quad J_{3,12} := (X_3 \wedge Z_3)_{AB} X_1^A X_2^B, \tag{3.2.17}$$

with a decomposition

$$e_1^{\omega_1} \dots e_{n_s}^{\omega_{n_s}} = X_{12}^{-\frac{\Delta_{12;3}-l_3}{2}} X_{23}^{-\frac{\Delta_{23;1}+l_3}{2}} X_{31}^{-\frac{\Delta_{31;2}+l_3}{2}} J_{3,12}^{l_3}. \tag{3.2.18}$$

In position space,

$$\frac{J_{3,12}}{X_1^+ X_2^+ X_3^+} = -\frac{1}{2}\left(x_{31}^2 x_{32}^a - x_{32}^2 x_{31}^a\right) z_a. \tag{3.2.19}$$

This can be used to determine the leading contribution of $\mathcal{O}_3$ in the $|x_{12}| \to 0$ of the $\phi_1(x_1)\phi_2(x_2)$ OPE. Following the expression (2.3.14), if $\langle \phi_1\phi_2\mathcal{O}_3\rangle = C_{\phi_1\phi_2\mathcal{O}}\, e_1^{\omega_1} \dots e_{n_s}^{\omega_{n_s}}$, then

$$\phi_1(x_1)\phi_2(x_2) \overset{|x_{12}|\to 0}{\sim} C_{\phi_1\phi_2\mathcal{O}_3} |x_{12}|^{\Delta_3 - \Delta_1 - \Delta_2 - l_3} \mathcal{O}_3(x_2, x_{12}). \tag{3.2.20}$$

After this, all three-point functions with $n_{cr} = 1$ are described in detail in Chapter 5 — the latter appear in the comb channel OPE decomposition of scalar five- and six-point correlators. There is no systematic method to determine seeds and bases for $n_{cr} > 1$. However, we can review a significant mass of results from the literature in two particularly important cases.

- A comprehensive approach for three STTs above or at the critical dimension $d_c = 4$ can be found in [89]. In this case, there are $n_{cr} = 3$ spinning cross ratios and $n_s = 9$ seed generators. The results found in their work can be translated into the language of section 3.2 as follows. For parity even semi-invariants, the authors constructed a set of generators[5]

$$\{e_1, \dots, e_9\} = \{X_{ij}, H_{ij}, J_{k,ij}\}, \tag{3.2.21}$$

  and proved that this constitutes a seed. Then with the choice of prefactors and cross ratios

$$\Omega = \prod_{i<j} X_{ij}^{\omega_{ij}} J_{k,ij}^{l_k}, \quad \{u_1, u_2, u_3\} = \left\{ \frac{H_{ij} X_{ki} X_{jk}}{J_{i,jk} J_{j,ki}} \right\}, \tag{3.2.22}$$

  they constructed a monomial basis of tensor structures $t_n = u_1^{n_1} u_2^{n_2} u_3^{n_3}$ with exponents bounded by [90, Eq. (4.19)]. In $d = 4$, there exists a parity-odd generator

$$e_{10} = \epsilon_{ABCDEF} C_1^{AB} C_2^{CD} C_3^{EF}, \tag{3.2.23}$$

  which is used to expand any parity-odd three-point function just like in (3.2.22) with $\Omega \to \Omega e_{10}$.

- There is a large body of literature concerning three-point functions of three maximal depth primaries in $d = 3$ (e.g. [91]) and $d = 4$ (e.g. [92]). Many of these results exploit the fact that $\mathrm{Sp}(4)$ is the double cover of $\mathrm{SO}(2,3)$, and $\mathrm{SU}(2,2)$ is the double cover of $\mathrm{SO}(2,4)$. In the cluster algebra literature, their seeds have also been constructed explicitly, and correspond to cluster algebras of finite type $B_2 \cong C_2$ and A_3 respectively.

3.2.3 Scalar N-point functions

In the case of N scalars $F_{\{0\}}^{\Delta_i}(X_i) := \phi_i(X_i)$, the seed is constructed as a dimension dependent subset of the $\frac{N(N-1)}{2}$ scalar products $(X_{ij})_{1 \le i < j \le N}$.

- For $d \ge d_c = N - 2$, we have $n_{cr} = n_s - N = \frac{N(N-3)}{2}$, such that all of the X_{ij} are independent and form a seed.

- For $d < d_c$, we have

$$n_{cr}(d_c, N) - n_{cr}(d, N) = \frac{(d_c - d)(d_c - d + 1)}{2}. \tag{3.2.24}$$

  The corresponding relations between the scalar products stem from the linear dependencies between $N > d + 2$ vectors in a $d + 2$ dimensional space. More specifically, for any subset $I \subset \{1, \dots, N\}$, $|I| > d + 2$,

$$\mathrm{Span}(X_i)_{i \in I} \subset \mathbb{R}^{d+2} \iff p_I = \det (X_{ij})_{i,j \in I} = 0. \tag{3.2.25}$$

  To solve these constraints and obtain a seed, we can proceed by iteration in $n := d_c - d = 1, 2, \dots, N - 3$.

[5] $J_{k,ij} = X_{ij} V_{k,ij}$ in their conventions.

1. For $n_{cr}(d_c-1,N)=n_{cr}(d_c,N)-1$, there is one single relation $p_{\{1,\dots,N\}}=0$. Without loss of generality, the relation can be solved for X_{1N}, such that the seed is given by
$$\{e_1,\dots,e_{n_{cr}+N}\}=\{X_{ij}\}_{|i-j|\leq N-2}. \tag{3.2.26}$$

2. For $n_{cr}(d_c-2,N)=n_{cr}(d_c-1,N)-2$, the seed is a subset of (3.2.26). There exist only two relations without any explicit dependence on X_{1N}, and therefore, polynomial in the seed variables of (3.2.26),
$$p_{\{1,\dots,N-1\}}=0=p_{\{2,\dots,N\}}. \tag{3.2.27}$$
These can be solved for separately for $X_{1(N-1)}$ and X_{2N} respectively, such that
$$\{e_1,\dots,e_{n_{cr}+N}\}=\{X_{ij}\}_{|i-j|\leq N-3}. \tag{3.2.28}$$

n. For $n_{cr}(d_c-n-1,N)=n_{cr}(d_c-1,N)-n-1$, the result of the iteration is
$$\{e_1,\dots,e_{n_{cr}+N}\}=\{X_{ij}\}_{|i-j|\leq d+1}. \tag{3.2.29}$$

Of course, any permutation of the points defines an equivalent seed to (3.2.29). This choice of labeling is particularly well adapted to the comb channel conformal blocks, which we will return to in chapter 6.

Given the seed (3.2.29) and an associated set of cross ratios $\{u_1,\dots,u_{n_{cr}}\}$, the most natural choice of prefactor to parameterize the correlator is independent of the dimension — this requires setting $\Omega=\prod_{|i-j|\leq 2}X_{ij}^{\omega_{ij}}$. The remaining $2N-3$ exponents $\omega_{i(i+1)},\omega_{i(i+2)}$ are constrained by N homogeneity constraints
$$\omega_{i(i+1)}+\omega_{(i-1)i}+\omega_{i(i+2)}+\omega_{(i-2)i}=-\Delta_i, \tag{3.2.30}$$
leaving $N-3$ unconstrained exponents that affect the leading terms in the various OPE decompositions of the correlator. In particular, when studying a channel involving the OPE $\phi_i\times\phi_j$, it is standard to set $\omega_{ij}=-\frac{\Delta_i+\Delta_j}{2}$ because it cancels with the equal and opposite exponent in the first contribution to the OPE, given in (3.2.20). For future reference, we will list here the $N=4,5,6$ prefactors adapted to the comb channel OPE decomposition with $\phi_1\times\phi_2$ and $\phi_{N-1}\times\phi_N$,
$$\Omega_4^{(\Delta_1,\dots,\Delta_4)}=X_{12}^{-\frac{\Delta_1+\Delta_2}{2}}\left(X_{13}^{-1}X_{23}\right)^{\frac{\Delta_{12}}{2}}\left(X_{23}^{-1}X_{24}\right)^{\frac{\Delta_{34}}{2}}X_{34}^{-\frac{\Delta_3+\Delta_4}{2}}, \tag{3.2.31}$$
$$\Omega_5^{(\Delta_1,\dots,\Delta_5)}=X_{12}^{-\frac{\Delta_1+\Delta_2}{2}}\left(X_{13}^{-1}X_{23}\right)^{\frac{\Delta_{12}}{2}}\left(X_{23}^{-1}X_{24}X_{34}^{-1}\right)^{\frac{\Delta_3}{2}}\left(X_{34}^{-1}X_{35}\right)^{\frac{\Delta_{45}}{2}}X_{45}^{-\frac{\Delta_4+\Delta_5}{2}}, \tag{3.2.32}$$
$$\begin{aligned}\Omega_6^{(\Delta_1,\dots,\Delta_6)}=&X_{12}^{-\frac{\Delta_1+\Delta_2}{2}}\left(X_{13}^{-1}X_{23}\right)^{\frac{\Delta_{12}}{2}}\times\\&\left(X_{23}^{-1}X_{24}\right)^{\frac{\Delta_3}{2}}X_{34}^{-\frac{\Delta_3+\Delta_4}{2}}\left(X_{45}^{-1}X_{35}\right)^{\frac{\Delta_4}{2}}\left(X_{45}^{-1}X_{46}\right)^{\frac{\Delta_{56}}{2}}.\end{aligned} \tag{3.2.33}$$

3.3 The conformal block decomposition

An *OPE channel* is a sequence of $N-3$ operator products that reduces a N-point function to three-point functions. These channels can be represented as (plane) tree diagrams $\mathcal{C}$ with enumerated leaves, and we will treat the diagram and the channel itself synonymously. Figure 14 shows one such example for the scalar ten point function. Given a fixed enumeration of the external fields, the number of OPE channels is $(2N-5)!!$. The internal lines of the OPE diagram are enumerated by Latin indices $r=1,\dots,N-3$, while its vertices are enumerated by Greek indices $\rho=1,\dots,N-2$. Then we can

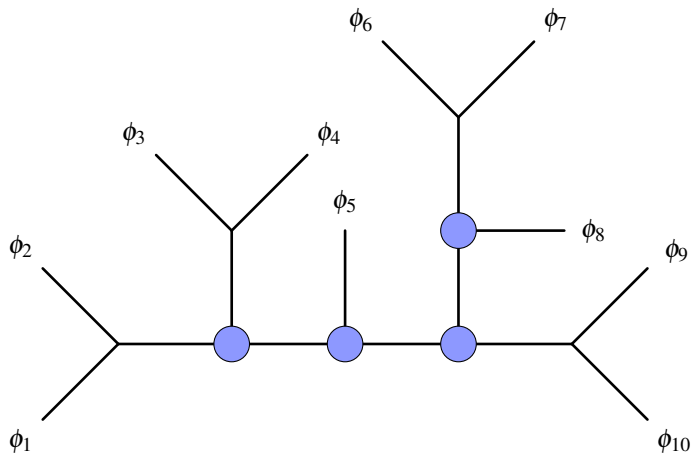

Figure 14: Choice of an OPE channel for a 10-point function. Vertices highlighted in blue are associated with non-trivial tensor structures.

associate to any internal line the quantum numbers $\pi_r = (\Delta_r, \{l_{r\nu}\})$ of the primaries appearing in the corresponding OPE, and to any vertex an element t_{n_ρ} of a basis of tensor structures[6]. The latter specifies an expansion (3.2.16) of the three-point function $\langle F_{\pi_{r_{1\rho}}} F_{\pi_{r_{2\rho}}} F_{\pi_{r_{3\rho}}} \rangle$, where $r_{i\rho}$ are the internal and/or external legs attached to ρ. In this case, the conformal block decomposition in the channel $\mathcal{C}$ takes the form

$$\left\langle \prod_{i=1}^{N} F^{\Delta_i}_{\{l_{i\nu}\}} \right\rangle = e_1^{\omega_1} \dots e_{n_s}^{\omega_{n_s}} \sum_{\{\pi_r\},\{n_\rho\}} \left(\prod_{\rho=1}^{N-2} C^{(t_{n_\rho})}_{\pi_{r_{1\rho}} \pi_{r_{2\rho}} \pi_{r_{3\rho}}} \right) \psi^{\mathcal{C}}_{\{\pi_r\},\{t_{n_\rho}\}}(u_1, \dots, u_{n_{cr}}), \tag{3.3.1}$$

where $\psi^{\mathcal{C}}_{\{\pi_r\},\{t_{n_\rho}\}}(u_1, \dots, u_{n_{cr}})$ is a basis of kinematically determined functions of the cross ratios, the *conformal blocks*. It will often be convenient to repackage the product of OPE coefficients next to the conformal block into a single symbol,

$$P^{(t_{n_1},\dots,t_{n_\rho})}_{\pi_1 \dots \pi_{N-3}} := \prod_{\rho=1}^{N-2} C^{(t_{n_\rho})}_{\pi_{r_{1\rho}} \pi_{r_{2\rho}} \pi_{r_{3\rho}}}. \tag{3.3.2}$$

In most cases, it is very difficult to compute and/or analyze conformal blocks directly from the OPE. Already at $N = 4$, blocks are given by the unwieldy expression (2.3.22). In this section, we will review some more efficient methods to compute conformal blocks, falling into two categories: differential equations and integral representations. These methods are illustrated in the case of four scalars, and will be generalized to comb channel five- and six-point blocks in later chapters.

3.3.1 Casimir differential equations

Casimir operators correspond to invariant powers of the conformal generators L_{AB}. There are as many independent Casimirs as there are scaling dimensions plus spin labels, and their orders $p =$

[6]Technically, a bijective numeration of all tensor structures at all vertices requires a base ($\rho = 1, \dots, N-2, n_\rho = 1, \dots, N_{r_{1\rho} r_{2\rho} r_{3\rho}}$) specifying both the choice of vertex and the choice of basis element at the vertex. However, in all cases where the basis element label n_ρ is unspecified, we will use it simultaneously to denote the choice of vertex ρ and simply write $t_{\rho,n_\rho} \equiv t_{n_\rho}$ as a means to streamline notation.

$2, 4, \ldots, 2r_d - 2, 2r_d$ (or r_d when d is even) are classified. Starting from their representation as differential operators $\mathcal{T}_{AB}$, the action of a Casimir on a primary field evaluates to a polynomial of the scaling dimensions and spin labels. In the case of the second order Casimir,

$$\frac{1}{2}\mathcal{T}^A{}_B\,\mathcal{T}^B{}_A\,F^{\Delta}_{\{l_\nu\}} = \left\{\Delta(d-\Delta) + \sum_{\nu=1}^{L} l_\nu(l_\nu + d - 2\nu)\right\} F^{\Delta}_{\{l_\nu\}}. \tag{3.3.3}$$

Clearly, the eigenvalue of the Casimir operator is invariant under certain discrete transformations of the quantum numbers, such as $\Delta \leftrightarrow d - \Delta$, $l_\nu \leftrightarrow 2\nu - d - l_\nu$. More generally the Harish-Chandra isomorphism [93] implies that Casimirs generate the space of W-invariant polynomials of (Δ, l_ν), where W is the Weyl group of $\mathfrak{so}(d+2)$. For finite dimensional representations of $\mathfrak{so}(d+2)$ (where Δ is a negative integer), it is known from highest weight theory that there is no Weyl reflection under which all $-\Delta, l_\nu$ remain positive integers. Similarly, for reflection positive representations of $\mathfrak{so}(1, d+1)$, the only Weyl transformation preserving integer spins l_ν is $\Delta \leftrightarrow d - \Delta$, which can only preserve unitarity bounds if $l_\nu = 0$ and $\frac{d-2}{2} \leq \Delta \leq \frac{d+2}{2}$ [7]. Apart from this exceptional occurrence of a two-fold degeneracy, the Casimir eigenvalues single out a unique set of quantum numbers (Δ, l_ν).
Since the OPE intertwines $\pi_1 \otimes \pi_2$ with $\bigoplus \pi_3$, conformal blocks (i.e. the direct summands in the OPE) must diagonalize the Casimir of the diagonal generators $(L_1 + L_2)_{AB}$. Acting on a correlator (3.2.1) expressed in terms of a prefactor $\Omega = \prod_i e_i^{\omega_i}$ and a function $G(u_i)$, the Casimir operator reduces to a p^{th} order differential operator on G in the cross ratios $u_1, \ldots, u_{n_{cr}}$. In the case of a scalar four-point function, there are two independent cross ratios u, v, two independent Casimir operators of orders $p = 2, 4$, and two labels (Δ, l) for the STT propagating in the $\phi_1 \times \phi_2$ OPE. This translates into a system of two independent differential equations in two variables

$$\Omega^{-1}\frac{1}{p!}\mathrm{tr}\,(\mathcal{T}_1 + \mathcal{T}_2)^p \Omega\; \psi^{(12)}_{\Delta,l}(u,v) = \mathcal{D}^p_{12}(u, v, \partial_u, \partial_v)\psi^{(12)}_{\Delta,l}(u,v) = C^p(\Delta, l)\psi^{(12)}_{\Delta,l}(u,v). \tag{3.3.4}$$

To completely fix the normalization of blocks, the leading contributions in a certain limit of the OPE can serve as a boundary condition. In the limit $|x_{12}| \to 0$ with OPE asymptotics of the form (3.2.20), the limit of the blocks can be derived as in [89, Eq. (2.22)], and is proportional to $u^{\frac{\Delta}{2}} C_l^{(d/2-1)}\left(\frac{v-1}{2\sqrt{u}}\right)$ (see [56, Tab. 1] for a list of normalization conventions of the OPE and the blocks that can appear in the literature). These equations were first written by Dolan and Osborn in [29, 30], and have since become one the most efficient tools for the analysis of blocks in view of applications to the bootstrap.

Integrability of four-point blocks: In [57], it was shown that the second order Casimir equations of scalar four-point blocks are equivalent to the Schrödinger equation for the BC_2 Calogero-Sutherland integrable model, where the potential depends parametrically on $a := \Delta_{12}/2$, $b := \Delta_{43}/2$ [8] and d. After the change of variables $(u, v) \to (z, \bar{z}) \to (x, \bar{x})$ in [57, Eq. (2),(3),(14)] and the gauge transformation $\psi \to \Theta\,\psi$ in [57, Eq. (13)], the Casimir operator (times one half) becomes up to a constant the CS Hamiltonian,

$$H_{CS} = \partial_x^2 - V_{PT}^{(a,b)}(x) + \partial_{\bar{x}}^2 - V_{PT}^{(a,b)}(\bar{x}) - \frac{(d-2)(d-4)}{32}\left(\frac{1}{\sinh^2\frac{x-\bar{x}}{2}} + \frac{1}{\sinh^2\frac{x+\bar{x}}{2}}\right),$$

[7] In [94], scalar primaries related by $\Delta \leftrightarrow d - \Delta$ are explicitly realized as scalar fields in AdS with the same mass, but different boundary conditions.

[8] Notice the difference $(a, b)_{\text{here}} = (-a, -b)_{\text{there}}$ in comparison with [57, 95]. This comes from the convention (3.2.31) for the prefactor $\Omega^{(\Delta_1,\ldots,\Delta_4)}$, different from [95, Eq. (2.1)], but related to it by [95, Eq. (2.13)].

where V_{PT} is the one-particle Pöschl-Teller Hamiltonian [96]

$$V_{PT}^{(a,b)}(x) := -\frac{ab}{\sinh^2\frac{x}{2}} + \frac{(a+b)^2-\frac{1}{4}}{\sinh^2 x}, \tag{3.3.5}$$

with integrable wavefunctions given by Gauss hypergeometric functions in $z := -\sinh^{-2}\frac{x}{2}$. This formulation of the differential equation efficiently repackages many results in the CFT literature. For example, the vanishing of the last term in the potential implies Dolan and Osborn's famous exact result [29, Eq. (3.11)] for conformal blocks in $d = 4$ in terms of products of two Gauss hypergeometric functions. Another example is the expression for blocks in the lightcone limit

$$\bar{x} \to \infty \Rightarrow \bar{z} \to 0 \Rightarrow u \to 0 \Rightarrow (x_1 - x_2)^2 \to 0, \tag{3.3.6}$$

first derived by Ferrara et al. in [97, Eq. (54)]. In this limit, the last term in the potential is subleading and the dependence on $\bar{x}$ of the wavefunction factorizes to a plane wave $\psi(x,\bar{x}) \sim e^{-h\bar{x}}\psi_{\text{PT}}^{(a,b)}(x)$. After absorbing the resulting shift in the half-Casimir eigenvalue, the Hamiltonian becomes independent of the dimension d at leading order and reduces to Pöschl and Teller's, $\partial_x^2 - V_{PT}^{(a,b)}(x,\partial_x)$. This Schrödinger equation is solved by the well known formula for lightcone blocks $e^{-h\bar{x}}{}_2F_1\left(\bar{h}+a,\bar{h}+b;2\bar{h};-\sinh^{-2}(x/2)\right)$, where $(h,\bar{h}) := \frac{1}{2}(\Delta-l,\Delta+l)$. Finally, the large spin limit of blocks relevant for the lightcone bootstrap can be obtained by imposing

$$x := \frac{y}{J} + \mathrm{i}\pi, \quad \bar{h} = h + J \to \infty. \tag{3.3.7}$$

This large J limit of the Hamiltonian yields a rational degeneration of Pöschl-Teller at leading order,

$$\partial_x^2 - V_{PT}^{(a,b)}(x) = J^2\left(\partial_y^2 - \frac{(a+b)^2-\frac{1}{4}}{y^2}\right) + \mathrm{O}(J^0). \tag{3.3.8}$$

Eigenfunctions of this Hamiltonian are known in terms of Bessel functions $K_{a+b}(y)$, in concomitance with [35, Eq. (77)] for $a+b=0$ and [98, Eq. (A.4)] for $a+b\neq 0$.

The integrability of scalar four-point blocks was later generalized to several types of spinning external fields in [58, 59, 61]. Based on the harmonic analysis of the conformal group, these authors derived that the second order Casimirs are Hamiltonians of matrix BC_2 Calogero-Sutherland models. Finally, for external fields in arbitrary representations of $\mathrm{SO}(d)$, Harish-Chandra's radial component map [99] provides a way to construct a universal, spinning, two particle Calogero-Sutherland model, as will be discussed in [100]. We refer to [101] for a more detailed overview of this subject.

3.3.2 Integral representations

Consider any three primary fields $\mathcal{O}_1, \mathcal{O}_2, \mathcal{O}_3$ and their three-point function. Any integral representation of the form

$$\left\langle \prod_{i=1}^{3} \mathcal{O}_i(x_i,\{z_{i\nu}\}) \right\rangle = \int_{\mathcal{M}} \mathrm{d}\mu(s) \left\langle \mathcal{O}_3(x(s),\{z_\nu(s)\})\mathcal{O}_3(x_3,\{z_{3\nu}\})\right\rangle, \tag{3.3.9}$$

defines an analogous integral representation for the contribution of $\mathcal{O}_3$ to the $\mathcal{O}_1\mathcal{O}_2$ OPE, provided that $\mathrm{d}\mu$ is independent of $(x_3,\Delta_3,\{z_{3\nu},l_{3\nu}\})$. The latter can then be inserted in correlators to obtain integral representations of blocks with $\mathcal{O}_3$ exchange.

Shadow integral: In the case of three scalar fields ϕ_1, ϕ_2, ϕ_3, the star-triangle relation (e.g. in [102, Eq. (7a)] for $n = 3$) realizes (3.3.9) with

$$\mathcal{M} = \mathbb{R}^d, \quad \mathrm{d}\mu = \mathcal{N}_{\Delta_i,d}\, \mathrm{d}^d x\, \langle \phi_1(x_1)\phi_2(x_2)\phi_3(x)\rangle|_{\Delta_3 \to d-\Delta_3}, \tag{3.3.10}$$

where the normalization is given by

$$\mathcal{N}_{\Delta_i,d} = \pi^{-\frac{d}{2}} \prod_{i=1}^{3} \frac{\Gamma(\delta_i)}{\Gamma(\frac{d}{2}-\delta_i)}, \quad (\delta_1,\delta_2,\delta_3) := \left(\frac{d+\Delta_{12}-\Delta_3}{2}, \frac{d-\Delta_{12}-\Delta_3}{2}, \Delta_3\right). \tag{3.3.11}$$

This formula is at the basis of the shadow operator formalism of Ferrara, Parisi, Gatto and Grillo [103]. To generalize this construction to spinning fields, one defines an operator $\tilde{\mathcal{O}}_3$ with scaling dimension $\tilde{\Delta}_3 := d - \Delta_3$ as an integral transform of $\mathcal{O}_3$,

$$\begin{aligned} \tilde{\mathcal{O}}_3(x,\{z_\nu\}) &= \mathbf{S}_\Delta[\mathcal{O}_3](x,\{z_\nu\}) \\ &:= K_{\Delta_3,\{l_{3\nu}\}} \int_{\mathbb{R}^d} \frac{\mathrm{d}^d\tilde{x}}{(x-\tilde{x})^{2\tilde{\Delta}_3}} \mathcal{O}_3\left(\tilde{x}, \{I(x-\tilde{x})\cdot z_\nu\}\right), \end{aligned} \tag{3.3.12}$$

where $K_{\Delta,\{l_\nu\}}$ is fixed by requiring $\mathbf{S}_\Delta$ to be an involution. In representation theory, the integral transform (3.3.12) is known as an intertwining operator, see [104] for its group theoretic derivation and references to the mathematics literature. In general, integral representations of blocks are obtained by inserting the projector

$$|\mathcal{O}| := \int_{\mathcal{M}} \mathrm{d}^d x\, \tilde{\mathcal{O}}^{\{a\}}(x)\, |0\rangle\langle 0|\, \mathcal{O}_{\{a\}}(x), \tag{3.3.13}$$

In the case of the scalar four-point function,the projector insertion yields the formula

$$\langle \phi_1(x_1)\phi_2(x_2)|\mathcal{O}|\phi_3(x_3)\phi_4(x_4)\rangle = \int_{\mathcal{M}} \mathrm{d}^d x\, \langle \phi_1(x_1)\phi_2(x_2)\tilde{\mathcal{O}}^{a_1\ldots a_l}(x)\rangle\langle \mathcal{O}_{a_1\ldots a_l}(x)\phi_3(x_3)\phi_4(x_4)\rangle. \tag{3.3.14}$$

It follows from the covariance properties of the shadow operator that (3.3.14) transforms irreducibly under the diagonal action $L_1 + L_2$ and thus diagonalizes the Casimirs. However, contrary to the conformal blocks, the integrand of (3.3.14) is manifestly invariant under $\Delta \leftrightarrow d - \Delta$. Consequently, the integral must be a linear combination of the actual block $\psi^{(12)}_{\Delta,l}$ and its shadow $\psi^{(12)}_{d-\Delta,l}$, with the precise linear combination depending on the choice of integration contour $\mathcal{M}$. In [105], an efficient method to disentangle the block from its shadow was developed based on the action of the operator $e^{2\pi\mathrm{i}(D_1+D_2)}$. Indeed, this operator will act by a constant $e^{2\pi\mathrm{i}\Delta}$ in any irreducible representation. It follows that the block must transform like $x_{1,2} \to e^{2\pi\mathrm{i}} x_{1,2}$, $\psi^{(12)}_{\Delta,l} \to e^{2\pi\mathrm{i}\Delta}\psi^{(12)}_{\Delta,l}$. This determines an appropriate choice of contour in (3.3.14) to obtain a function proportional to the conformal block.

The lightcone OPE: We would like to compare the two-point function of a STT $\mathcal{O}_3$ on the one hand,

$$\langle \mathcal{O}_3(X,Z)\mathcal{O}_3(X',Z')\rangle = \left(-\frac{1}{2}X\cdot X'\right)^{-2\bar{h}_3}\left(\frac{1}{2}X\wedge Z\cdot X'\wedge Z'\right)^{l_3}, \tag{3.3.15}$$

and its three-point function with two scalars ϕ_1, ϕ_2 on the other hand,

$$\frac{\langle \phi_1(X_1)\phi_2(X_2)\mathcal{O}_3(X_3,Z_3)\rangle}{C_{\phi_1\phi_2\mathcal{O}_3} X_{12}^{\frac{h_3-\Delta_1-\Delta_2}{2}}} = X_{23}^{a-\bar{h}_3} X_{13}^{-a-\bar{h}_3}\left(\frac{1}{2}X_1\wedge X_2\cdot X_3\wedge Z_3\right)^{l_3}. \tag{3.3.16}$$

Here again, $h := \frac{\Delta - l}{2}$, $\bar{h} := \frac{\Delta + l}{2}$ and $a := \frac{\Delta_1 - \Delta_2}{2}$. Using a Feyman parameterization, we can re-express the three-point tensor structures as an integral of two-point tensor structures,

$$X_{23}^{a-\bar{h}_3} X_{13}^{-a-\bar{h}_3} = \frac{1}{\mathrm{B}_{\bar{h}_3-a,\bar{h}_3+a}|\mathbb{R}^\times|} \int_{\mathbb{R}_+^2} \frac{\mathrm{d}s_1 \mathrm{d}s_2}{s_1 s_2} s_1^{\bar{h}_3-a} s_2^{\bar{h}_3+a} \left(s_1 X_{13} + s_2 X_{23}\right)^{-2\bar{h}_3},$$

where $\mathrm{B}_{a,b} := \Gamma(a)\Gamma(b)/\Gamma(a+b)$ is the Euler Beta function, and $|\mathbb{R}^\times| = \int_0^\infty \frac{\mathrm{d}s}{s}$ is the volume of the dilation group $(s_1, s_2) \to (\lambda s_1, \lambda s_2)$. Plugging the Feynman parameterization back into the three-point function yields an integral formula,

$$\frac{\langle \phi_1 \phi_2 \mathcal{O}_3 \rangle}{C_{\phi_1\phi_2\mathcal{O}_3} X_{12}^{\frac{h_3-\Delta_1-\Delta_2}{2}}} = \int_{\mathbb{R}_+^2} \mathrm{d}\mu(s_1, s_2) \langle \mathcal{O}_3(s_1 X_1 + s_2 X_2, X_1 - X_2) \mathcal{O}_3(X_3, Z_3) \rangle. \tag{3.3.17}$$

In general, the identity cannot be extrapolated to an OPE because the embedding space vectors $X := s_1 X_1 + s_2 X_2$, $Z := X_1 - X_2$ are not null and orthogonal if $X_{12} \neq 0$. On the other hand, in Lorentzian signature, this integral formula can be precisely interpreted as the leading contribution of the OPE in the limit where x_1 and x_2 become lightlike separated.

$$\phi_1(X_1)\phi_2(X_2) \overset{X_{12}\to 0}{\sim} X_{12}^{h-\frac{\Delta_1+\Delta_2}{2}} \sum_{\mathcal{O}: h_\mathcal{O} = h} C_{\phi_1\phi_2\mathcal{O}} \int_{\mathbb{R}_+^2} \mathrm{d}\mu(s_1, s_2) \mathcal{O}(s_1 X_1 + s_2 X_2, X_1 - X_2). \tag{3.3.18}$$

In particular, we obtain the important result that the lightcone limit suppresses the *twist* $2h = \Delta - l$ of primaries and descendants appearing in the OPE. If we restrict X_1, X_2 to the Poincaré patch (2.1.46) and set

$$s_1 = st, \quad s_2 = s(1-t), \quad \frac{\mathrm{d}s_1 \mathrm{d}s_2}{s_1 s_2} = \frac{\mathrm{d}s}{s} \frac{\mathrm{d}t}{t(1-t)}, \tag{3.3.19}$$

then the integral over s factorizes to $|\mathbb{R}^\times|$, and we retrieve the result of Ferrara et. al. [37–39], with its first appearance in [37, Eq. (3.22)]. Note that these authors derive the result in a different way, starting from an expression for the OPE in terms of differential operators in embedding space, viz. [106, Eq. (1)—(5)]. While their starting point is more general in scope, the method presented here in terms of Feynman parameterization is much simpler to use directly within the lightcone limit. This method also generalizes to OPEs of spinning fields, as we will see in chapter 7.

Part II

The Integrability Based Theory of Multipoint Blocks

Chapter 4

Multipoint Conformal Blocks from Gaudin Integrable Models

Section 3.3 provided a general description of the multipoint conformal block decomposition (3.3.1), followed by a review of Dolan and Osborn's computation of four-point blocks via diagonalization of the Casimir operators. For higher point blocks, the same principle applies: the diagonalization of Casimir operators fixes the scaling dimensions and spins of the primaries propagating in the OPE channel. However, this no longer specifies a unique basis of conformal blocks, since the three-point tensor structures remain undetermined. Consequently, the Casimirs must be supplemented by operators that singles out an unambiguous expansion into tensor structures at each vertex of the OPE channel. The most general ansatz for such an operator is a linear combination of invariant powers of conformal generators at different points,

$$H_V = \sum_{p\geq 0} \sum_{i_1,\ldots,i_p=1}^{N} c_{i_1\ldots i_p} \mathrm{tr}\, \mathcal{T}_{i_1} \ldots \mathcal{T}_{i_p},$$

with the requirement that H_V commutes with all of the Casimirs. In [63], we solve this problem by virtue of one central observation: these differential operators (along with the Casimirs) act on the same Hilbert space as that of the Gaudin integrable model for the conformal algebra on the N-punctured sphere. With this starting point, we construct for any scalar N-point function in any OPE channel a complete set of commuting operators — as many as the number of cross ratios — that fully characterizes the basis of blocks. Each complete set of commuting operators defines a conformal block integrable system that is embedded in the Gaudin model via a limit of colliding punctures on the N-punctured sphere.

4.1 Summary of Results

In this chapter, we denote the action of the conformal algebra on scalar primary fields $\phi_i(x_i)$ by

$$[T_\alpha, \phi_i(x_i)] = \mathcal{T}_\alpha^{(i)} \phi_i(x_i), \tag{4.1.1}$$

where $(\mathcal{T}_\alpha) = (\mathcal{T}_{AB})$ are the usual first order differential operators and α runs through the set of conformal generators. Recall the number of independent cross ratios of a scalar N-point function,

$$n_{cr}(N,d) = \begin{cases} \frac{1}{2}N(N-3) & N \leq d+2 \\ Nd - \frac{1}{2}(d+2)(d+1) & N > d+2 \end{cases} \tag{4.1.2}$$

For example, in the case of a 4-point function in $d > 1$ one has two cross ratios. The associated blocks are famously labeled by the conformal weight Δ and the spin l of the field that is exchanged in the intermediate channel. Since the latter transforms in a symmetric traceless tensor representation of the rotation subgroup, a single number l is sufficient to characterize the spin. The precise number of such intermediate field labels does depend on the channel topology, at least for $N > 5$, but it is always strictly smaller than the number n_{cr} of cross ratios. As an example let us consider $N = 5$. In this case

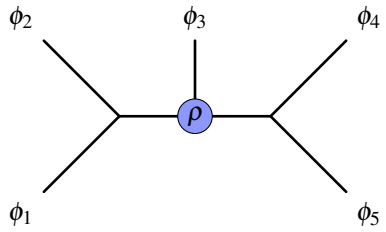

Figure 15: Choice of OPE diagram for 5-point correlator.

there exist 15 OPE channels but they all possess the same topology. In Figure 15 we have displayed one of the 15 OPE channels. All other 14 channels are related to this one by a permutation of the leaves, modulo symmetries of the bare OPE diagram that has been stripped of its leaves. As one can readily see, the OPE evaluation involves two intermediate fields. Since these appear in the operator product of scalar fields, they are symmetric traceless tensors and hence characterized by two quantum numbers each. The intermediate fields thus carry four quantum numbers in total. We think of these as being attached to the (internal) links of the OPE diagram. The remaining quantum number is attached to the central vertex of the 5-point OPE diagram. Note that two legs of this central vertex are associated with a symmetric traceless tensor while only one is scalar. For $d \geq 3$, such 3-point functions are not determined by conformal symmetry. They require the choice of a so-called tensor structure. For a very particular basis in the space of tensor structures it becomes possible to assign a fifth quantum number that can be measured simultaneously with the four independent eigenvalues of the Casimir operators. Measuring a complete set of quantum numbers simultaneously through a sufficiently large set of commuting differential operators is the main goal of this work. We want to do so in any d, for any number N of external points and for all OPE channels. Quantum numbers are measured by acting with differential operators in the cross ratios. The latter divide into two families. First, differential operators that measure the quantum numbers of intermediate fields are associated with the links of the OPE diagram and are referred to as *Casimir differential operators*, since they are straightforward generalizations of the Casimir differential operators constructed for $N = 4$ by Dolan and Osborn. Second, differential operators that measure choices of tensor structure, the first example of which was introduced recently in [62], are referred to as *vertex differential operators*. Let us note that for scalar blocks, the choice of tensor structures and hence the vertex differential operators are relevant as soon as multiple non-scalar exchanges are involved. These types of blocks have only been

considered very recently in [56] and [54, Appendix E] for five-point blocks, and in a certain limit in [66] for five or six scalar legs.

Before we can describe our results on both types of differential operators we need to set up some notation. Given an OPE channel, recall the enumeratation of internal lines by Latin indices $r = 1, \ldots, N-3$ and vertices by Greek indices $\rho = 1, \ldots, N-2$. There are no rules on how to order these two sets of objects. OPE diagrams are (plane) trees and hence by cutting any internal line with label r we separate the diagram into two disconnected pieces. Hence, r is associated with a partition of the external fields into two disjoint sets,

$$\underline{N} = \{1, \ldots, N\} = I_{r,1} \uplus I_{r,2} \ . \tag{4.1.3}$$

Similarly, any vertex ρ gives rise to a partition of $\underline{N}$ into three disjoint sets

$$\underline{N} = I_{\rho,1} \uplus I_{\rho,2} \uplus I_{\rho,3} \ . \tag{4.1.4}$$

Given any subset $I \subset \underline{N}$ we can define the following set of first order differential operators in the insertion points x_i,

$$\mathcal{T}_\alpha^{(I)} = \sum_{i \in I} \mathcal{T}_\alpha^{(i)} \ . \tag{4.1.5}$$

Let us note that for two disjoint sets $I_1, I_2 \subset \underline{N}$ we have

$$\mathcal{T}_\alpha^{(I_1 \uplus I_2)} = \mathcal{T}_\alpha^{(I_1)} + \mathcal{T}_\alpha^{(I_2)} \ , \quad [\, \mathcal{T}_\alpha^{(I_1)} \, , \, \mathcal{T}_\beta^{(I_2)} \,] = 0 \ . \tag{4.1.6}$$

Casimir differential operators. With this notation it is very easy to construct the differential operators that measure the quantum numbers of the intermediate fields,

$$\mathcal{C}as_r^{\,p} = \mathcal{D}_{r,1}^p = \kappa_p^{\alpha_1, \ldots, \alpha_p} \left[\mathcal{T}_{\alpha_1}^{(I_{r,1})} \cdots \mathcal{T}_{\alpha_p}^{(I_{r,1})} \right]_{|\mathcal{G}} = \mathcal{D}_{r,2}^p \ . \tag{4.1.7}$$

Here κ_p denotes *symmetric* conformally invariant tensors of order p and the superscript p runs through

$$p = 2, 4, \ldots \begin{cases} d + 1 = 2r_d \ \textit{for } d \ \textit{odd} \\ d = 2r_d - 2 \ \textit{for } d \ \textit{even} \end{cases} \tag{4.1.8}$$

The number $r_d = [(d+2)/2]$ denotes the rank of the conformal Lie algebra. In even dimensions d, the symmetric invariant tensor κ_p of order $p = 2r_d = d+2$ actually possesses a square root of order $p = r_d$ that also commutes with all generators of the conformal algebra. This so-called *Pfaffian* differential operator has the same form as in (4.1.7), but with a symmetric invariant tensor κ_p of order $p = d/2+1$,

$$\mathcal{P}f_r = \mathcal{D}_{r,1}^{d/2+1} = \kappa_{d/2+1}^{\alpha_1, \ldots, \alpha_{d/2+1}} \left[\mathcal{T}_{\alpha_1}^{(I_{r,1})} \cdots \mathcal{T}_{\alpha_{d/2+1}}^{(I_{r,1})} \right]_{|\mathcal{G}} = -(-1)^{d/2} \mathcal{D}_{r,2}^{d/2+1} \ . \tag{4.1.9}$$

When $d = 4k+2$, the symmetric invariants of order $p = d/2+1$ are twofold degenerate and we should use two different symbols for these two invariants of order $d/2+1$. In order not to clutter notation too much, we decided to ignore this distinction. In other words, we will consider $\kappa_{d/2+1}$ as a pair of symmetric invariants when $d = 4k+2$.

In our formulas for the differential operators we have placed a subscript $|\mathcal{G}$ to stress that they are defined as operators acting on correlations functions, i.e. on functions $\mathcal{G}$ that satisfy the conformal Ward identities

$$\mathcal{T}_\alpha^{(\underline{N})} \mathcal{G}_N(x_i, \Delta_i) = 0 \ . \tag{4.1.10}$$

In our construction of the differential operators we have favored the set $I_{r,1}$ over $I_{r,2}$. But from the conformal Ward identities we can conclude that

$$\mathcal{T}_\alpha^{(I_{r,1})}\mathcal{G}_N(x_i,\Delta_i) = -\mathcal{T}_\alpha^{(I_{r,2})}\mathcal{G}_N(x_i,\Delta_i)\ .$$

Though some caution is needed when we apply this relation to the evaluation of the Casimir differential operator, see Subsection 4.2.1 for details, it is not difficult to see that all differential operators of even order come out the same if we pick $I_{r,2}$ rather than $I_{r,1}$. There is only one family for which the set matters, namely for the Pfaffian operators when d is a multiple of four. In that case the operator flips sign when we change the set. Of course, overall factors are a matter of convention and hence of no concern. Therefore, we shall drop the reference to the set we use in the construction of Casimir differential operators, writing $\mathcal{D}_r^p$ instead of $\mathcal{D}_{r,1}^p$.

An important point to note is that the Casimir differential operators need not all be independent. For example, for $N = 4$ and $d > 1$, the single intermediate field is a symmetric traceless tensor and is hence characterized by two numbers only, its weight Δ and spin l, which are encoded in the eigenvalues of the first and second Casimirs $\mathcal{D}^2$ and $\mathcal{D}^4$. But starting from $d = 4$, the conformal algebra possesses Casimir elements of higher order which are independent in general, but become dependent on the lower order ones when evaluated on symmetric traceless tensors. More generally, the number of independent Casimir differential operators at a given internal line r is given by

$$\mathfrak{d}_r(\mathcal{C}^N_{OPE},d) = \mathfrak{d}(I_{r,1},d), \quad \textit{where} \quad \mathfrak{d}(I,d) = min(|I|, N-|I|, r_d), \tag{4.1.11}$$

and $|I|$ denotes the order of the set I.[1] We shall refer to the number $\mathfrak{d}(I,d)$ as the *depth* of the index set I and to $\mathfrak{d}_r$ as the depth of the link r. Note that $\mathfrak{d}_r = \mathfrak{d}(I_{r,1},d) = \mathfrak{d}(I_{r,2},d)$ is independent of which of the two index sets we choose to compute it with. By summing the depths of all internal links, we can determine the total number of independent Casimir differential operators to be

$$n_{cdo}(\mathcal{C}^N_{OPE},d) = \sum_{r=1}^{N-3} \mathfrak{d}_r(\mathcal{C}^N_{OPE},d)\ . \tag{4.1.12}$$

It is thus clear that the total number of Casimir differential operators depends on the topology of the OPE channel, not just on the number N of points. In the case of $N = 6$ and $d \geq 4$, for example, there are $n_{cdo}(\mathcal{C}^{N=6}_{comb},d) = 7$ Casimir differential operators in the comb channel, while the snowflake channel admits only $n_{cdo}(\mathcal{C}^{N=6}_{snowflake},d) = 6$ of such operators.

Vertex differential operators. What we have described so far is nothing new, and can be established by elementary means. But as we have explained, starting from $N = 5$ the Casimir differential operators do not suffice to resolve all quantum numbers of the conformal blocks, i.e. n_{cdo} is strictly smaller that n_{cr} for all OPE channels. Our main task is to construct additional differential operators that can measure the choice of tensor structures at the vertices independently of the weights and spins of the intermediate fields, i.e. we need to find a complete set of vertex differential operators that commute with the Casimir differential operators and among themselves. In this work we describe how to accomplish this task, for any number N of external scalar fields and any OPE topology. One central claim is that these vertex differential operators take the form

$$\mathcal{D}^{p,\nu}_{\rho,12} = \kappa_p^{\alpha_1,\ldots,\alpha_\nu,\alpha_{\nu+1},\ldots,\alpha_p}\left[\mathcal{T}^{(I_{\rho,1})}_{\alpha_1}\ldots\mathcal{T}^{(I_{\rho,1})}_{\alpha_\nu}\mathcal{T}^{(I_{\rho,2})}_{\alpha_{\nu+1}}\ldots\mathcal{T}^{(I_{\rho,2})}_{\alpha_p}\right]_{|\mathcal{G}} \tag{4.1.13}$$

[1] See the appendix B, where we collect some elements of $SO(1,d+1)$ representation theory.

where $\nu = 1, \dots, p-1$ and $p = 2, 4, \dots, 2r_d = d+1$ when d is odd. For even d, we let p run through even integers until we reach d and add a set of Pfaffian vertex operators $\mathcal{P}f^{\nu}_{\rho,12}, \nu = 1, 2, \dots d/2$ which are constructed with a symmetric invariant tensor κ_p of order $p = d/2+1$. Let us note that the definition of all these vertex differential operators also makes sense for $\nu = 0$ and $\nu = p$. The corresponding objects coincide with Casimir differential operators for the links that enter the first and second leg of the vertex. This is why we have excluded them from our list. The remaining operators still allow us to reconstruct the Casimir operators for the link that enters the third leg. Therefore, there is one linear relation for each value that p can assume, i.e. we have r_d linear relations in total. One may use these relations to eliminate e.g. the operator with $\nu = p/2$.

Let us note that the definition of the vertex operators $\mathcal{D}^{p,\nu}_{\rho,ij}$ depends on the choice of labeling of the subsets $I_{\rho,j}$ forming the partition $\underline{N} = I_{\rho,1} \cup I_{\rho,2} \cup I_{\rho,3}$ associated with the vertex ρ, which is arbitrary. However, the algebra generated by the vertex operators $\mathcal{D}^{p,\nu}_{\rho}$ is in fact independent of this choice: more precisely, the vertex operators constructed from another choice of labeling of the $I_{\rho,j}$'s are linear combinations of the operators $\mathcal{D}^{p,\nu}_{\rho,12}$, modulo the use of the conformal Ward identities (4.1.10), see Section 4.2.2.

The number of vertex differential operators at a given vertex is now easy to count. Taking into account that one additional linear relation among the operators listed in eq. (4.1.13), one finds

$$n_v(d) = \begin{cases} \frac{1}{4}(d^2-4) \ \textit{for } d \textit{ even} \\ \frac{1}{4}(d^2-1) \ \textit{for } d \textit{ odd} \end{cases} \tag{4.1.14}$$

The first key result of this work is that these vertex differential operators commute among themselves and with the Casimir differential operators. Commutation between Casimir and vertex differential operators is obvious. Similarly, it is easy to show that two vertex operators commute if they are associated with different vertices $\rho \neq \rho'$. The deepest part of our claim concerns the fact that also vertex operators associated with the same vertex commute. It does not seem straightforward to prove this statement by elementary manipulations. Below we shall use an indirect strategy in which we identify these vertex differential operators with Hamiltonians of some Gaudin integrable system defined on a 3-punctured sphere. For the latter, commutativity has already been established.

Of course the vertex differential operators we listed may not all be independent, as for the Casimir operators, see discussion above. In order to count the number of independent vertex differential operators, we shall employ the depth function $\mathfrak{d}(I,d)$ we introduced in eq. (5.1.1). For a given vertex ρ inside an OPE channel $\mathcal{C}^N_{OPE}$, the number of independent vertex differential operators is expected to be equal to the degrees of freedom associated to this vertex

$$n_{vdo,\rho}(\mathcal{C}^N_{OPE}, d) = n_{cr}(\sum_{i=1}^{3} \mathfrak{d}_{\rho,i}, d) - \sum_{i=1}^{3} \mathfrak{d}_{\rho,i}(\mathfrak{d}_{\rho,i} - 1) \leq n_v(d) \tag{4.1.15}$$

where $\mathfrak{d}_{\rho,i} = \mathfrak{d}(I_{\rho,i}, d)$ with $i = 1, 2, 3$. The inequality is saturated for vertices ρ with $\mathfrak{d}_{\rho,i} = r_d$. For the special vertices that can appear in the comb channel and in which one of the legs is scalar, the formula becomes

$$n_{vdo,\rho_m} = m - 1 \ , \quad n_{vdo,\rho_{r_d}} = r_d - 1 - \delta_{d,even}$$

for $m = 1, \dots, r_d - 1$. Here ρ_m is a vertex with $\mathfrak{d}_{\rho_m,1} = m, \mathfrak{d}_{\rho_m,2} = 1$ and $\mathfrak{d}_{\rho_m,3} = m+1$, see Figure 16, and ρ_d is the maximal comb channel vertex with $\mathfrak{d}_{\rho_{r_d},1} = r_d = \mathfrak{d}_{\rho_{r_d},3}$. The total number $n_{vdo}(\mathcal{C}^N_{OPE}, d)$ of vertex differential operators is obtained by summing over all $N-2$ vertices, i.e.

$$n_{vdo}(\mathcal{C}^N_{OPE}, d) = \sum_{\rho=1}^{N-2} n_{vdo,\rho}(\mathcal{C}^N_{OPE}, d) \ .$$

At least for the comb channel, it is easy to verify that the number of independent Casimir and vertex differential operators coincides with the number of cross ratios,

$$n_{cdo}(\mathcal{C}^N_{OPE}, d) + n_{vdo}(\mathcal{C}^N_{OPE}, d) = n_{cr}(N, d) \ .$$

The formula holds of course for all OPE channels. Below we shall exhibit the relations among

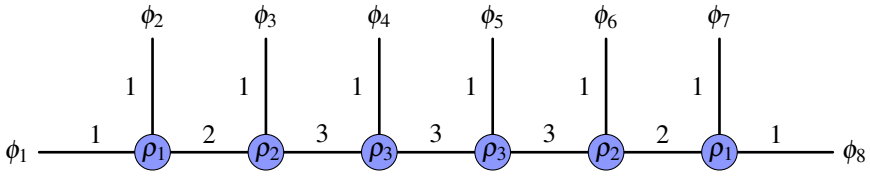

Figure 16: OPE diagram in the comb channel for a scalar eight-point function in $d = 4$. The edge labels correspond to the depth $\mathfrak{d}$ of the associated links. When taking an OPE with a scalar field, the depth always increases by one until the maximal allowed depth $\mathfrak{d} = r_d$ is reached.

vertex differential operators that are responsible for the reduction from the $n_v(d)$ operators in our list (4.1.13) (with $\nu = p/2$ removed) to the $n_{vdo,\rho}(\mathcal{C}^N_{OPE}, d)$ independent vertex differential operators that are needed to characterize the vertex ρ. This is the second key result of this work. It will allow us in particular to determine the precise order of each independent vertex differential operator.

While Gaudin models for the 3-punctured sphere only enter the discussion as a convenient tool to construct commuting vertex differential operators at the individual vertices, the relation between conformal blocks and Gaudin models turns out to reach much further. In fact, is is possible to embed the whole set of Casimir and vertex differential operators for arbitrary scalar N-point functions into Gaudin models on the N-punctured sphere. The latter contains N additional complex parameters that are not present in correlation functions. In the Gaudin integrable model these parameters correspond to the poles of the Lax matrix and they enter all Gaudin Hamiltonians. By considering different limiting configurations of these parameters is is possible to recover the full set of Casimir and vertex differential operators for scalar N-point functions in all the OPE channels. This construction not only embeds our differential operators into a unique Gaudin integrable model, but also shows that operators in different channels are related by a smooth deformation.

Let us finally outline the content of the following sections. Section 4.2 is mostly devoted to the study of the individual vertices. After a brief discussion of commutativity for Casimir differential operators and also vertex differential operators assigned to different vertices, we shall zoom into the individual vertices for most of Section 4.2. In Section 4.2.2 we construct the vertex differential operators in terms of the commuting Hamiltonians of a 3-site Gaudin integrable system. Section 4.2.3 addresses the relations between these operators for restricted vertices. The main purpose of Section 4.3 is to embed the whole set of Casimir and vertex differential operators for arbitrary scalar N-point functions into Gaudin models on the N-punctured sphere. In Section 4.4 we discuss one concrete example, namely we construct all five differential operators that characterize the blocks of a scalar 5-point function in any $d \geq 3$. Two of these operators are of order two while the other three are of fourth order. The paper concludes with a summary, outlook to further results and a list of interesting open problems to be addressed.

4.2 The Vertex Integrable System

The aim of this section is to address the key new element in the construction of multi-point conformal blocks for $d \geq 3$: the vertices themselves. In the first subsection we shall show that the construction of commuting differential operators for scalar N-point blocks can be reduced by rather elementary arguments to the construction of commuting differential operators for 3-point functions of spinning fields. Recall that the dependence on spin degrees of freedom can be encoded in auxiliary variables from which one is often able to construct non-trivial cross ratios,[2] even in the case of a 3-point function. Constructing sufficiently many commuting vertex differential operators that act on such cross ratios of the 3-point function requires more powerful technology from integrability which we shall turn to in the second subsection. There we construct commuting differential operators for vertices from the Gaudin integrable model for the 3-punctured sphere. The basic construction provides $n_v(d)$ of such commuting operators and hence sufficiently many even for the most generic vertices. For special vertices, such as those appearing in the comb channel with external scalars, there exist linear relations between these operators. These are the subject of the third subsection.

4.2.1 Reduction to the vertex systems

Our goal here is to prove that Casimir and vertex operators constructed around different vertices of an OPE diagram commute. More precisely we shall show that

$$[\,\mathcal{D}^p_r\,,\,\mathcal{D}^q_{r'}\,]=0 \quad , \quad [\,\mathcal{D}^p_r\,,\,\mathcal{D}^{q,\nu}_{\rho,a}\,]=0 \tag{4.2.1}$$

for every pair $(r,p),(r',q)$ of Casimir operators and any choice (ρ,q,ν) of a vertex operator, including the Pfaffian Casimir and vertex operators that appear at order $p,q=d/2+1$ when the dimension d is even. Note that the individual vertex differential operators also depend on the choice $a\in\{12,23,13\}$ of a pair of legs. In addition, we shall also establish that vertex operators associated with different vertices commute,

$$[\,\mathcal{D}^{p,\nu}_{\rho,a}\,,\,\mathcal{D}^{q,\mu}_{\rho',b}\,]=0 \quad \textit{for } \rho\neq\rho' \tag{4.2.2}$$

and all triples (p,ν,a) and (q,μ,b). This leaves only the commutativity of operators attached to the same vertex which is deferred to the next subsection.

The properties (4.2.1) and (4.2.2) are in fact elementary. They require global conformal invariance, the tree structure of OPE diagrams and the commutativity property (4.1.6). To begin with, let us recall that we associated two disjoint sets $I_{r,1}$ and $I_{r,2}$ to every link. As we pointed out before, the Casimir differential operators (4.1.7) do not depend on whether we used the generators $\mathcal{T}^{(I_{r,1})}_\alpha$ or $\mathcal{T}^{(I_{r,2})}_\alpha$ to construct them. Let us briefly discuss the details of the proof. Note that we think of $\mathcal{D}$ as an operator acting on correlation functions $\mathcal{G}$. This is signaled by the subscript $|\mathcal{G}$ in the definition of the Casimir differential operators. In evaluating products of first order differential operators, one can only apply the Ward identity (4.1.10) to the rightmost operator, which acts directly on the correlation function, and not on some derivative thereof. But once we have converted the rightmost operators $\mathcal{T}^{(I_{r,1})}$ into $-\mathcal{T}^{(I_{r,2})}$, they will commute with all operators to their left, such that we can freely move them all the way to the left and proceed to apply the Ward identity to the next set of first order operators, and so on. If we finally take into account that the invariants κ of the conformal Lie algebra are symmetric, we arrive at an expression for the Casimir differential operators in terms of $\mathcal{T}^{(I_{r,2})}$.

[2] Here and throughout the entire text we use the term 'cross ratio' rather loosely to refer to all conformally invariant combinations of the positions and auxiliary variables at each point.

A similar analysis can be carried out for vertex operators, see also Subsection 4.2.2. Without loss of generality we can assume that we have constructed our vertex operators in terms of the generators $\mathcal{T}^{(I_{\rho,1})}$ and $\mathcal{T}^{(I_{\rho,2})}$ and want to switch to constructing them from $\mathcal{T}^{(I_{\rho,1})}$ and $\mathcal{T}^{(I_{\rho,3})}$ instead. To do so we make use of the invariance condition

$$\left[\mathcal{T}_{\alpha}^{(I_{\rho,2})}\right]_{|\mathcal{G}} = -\left[\mathcal{T}_{\alpha}^{(I_{\rho,1})} - \mathcal{T}_{\alpha}^{(I_{\rho,3})}\right]_{|\mathcal{G}} \tag{4.2.3}$$

that follows from relations (4.1.4) and (4.1.10). After we apply this to the rightmost operator in the vertex differential operator, we use the commutativity property (4.1.6) to move the generators $\mathcal{T}^{(I_{\rho,1})}$ and $\mathcal{T}^{(I_{\rho,3})}$ to the left of $\mathcal{T}^{(I_{\rho,2})}$. We continue this replacement process until all the generators $\mathcal{T}^{(I_{\rho,2})}$ are removed and using symmetry of the tensor κ we find

$$\mathcal{D}_{\rho,12}^{p,\nu} = (-1)^{p-\nu} \sum_{\mu=0}^{p-\nu} \binom{p-\nu}{\mu} \mathcal{D}_{\rho,13}^{p,\nu+\mu} \tag{4.2.4}$$

along with a similar relation for the Pfaffian vertex operators for $p = d/2+1$ and d even. Since the last term in this sum with $\mu = p-\nu$ is just a Casimir operator, we have managed to express all vertex differential operators that are constructed from the generators associated with $I_{\rho,1}$ and $I_{\rho,2}$ as a linear combination of the vertex operators associated with the pair $I_{\rho,1}$ and $I_{\rho,3}$ and a Casimir operator. This is the main input in proving the commutativity statements (4.2.1) and (4.2.2).

Let us start with a pair of links r, r'. Each of these links divides the set of external points into the two disjoint sets $I_{r,1}, I_{r,2}$ and $I_{r',1}, I_{r',2}$ respectively. Since the OPE diagram is a tree, it is always possible to find a pair $i,j = 1,2$ such that $I_{r,i} \cap I_{r',j} = \emptyset$. For this choice

$$[\,\mathcal{D}_{r}^{p}\,,\,\mathcal{D}_{r'}^{q}\,] = [\,\mathcal{D}_{r,i}^{p}\,,\,\mathcal{D}_{r',j}^{q}\,] = 0 \tag{4.2.5}$$

because of the commutativity property (4.1.6). This proves our first claim. Note that the same arguments also apply to the case in which $r = r'$ and also if one or both operators are Pfaffian, i.e. if d is even and $p, q = d/2+1$.

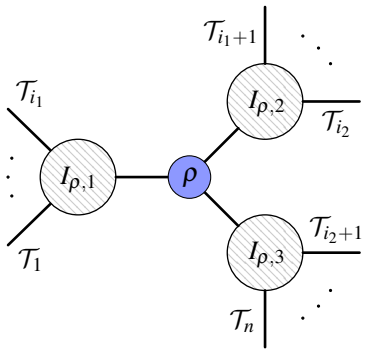

Figure 17: Schematic representation of a generic OPE diagram with focus on one vertex. The choice of a vertex automatically divides the diagram into three branches.

Let us now extend this argument to include vertex differential operators. In order to prove that the Casimir operators associated to a link r commute with the vertex operators associated to any vertex ρ we recall that any choice of a vertex ρ on an OPE diagram divides the diagram into the three

distinct branches that are glued to the vertex, and we denote these by $I_{\rho,j}$ as in Figure 17. A quick glance at Figure 17 suffices to conclude that given r and ρ it is possible to find a pair $i \in 1,2$ and $j \in 1,2,3$ such that $I_{r,i} \subset I_{\rho,j}$, since the link r must be in one of the three branches. It follows that $I_{r,i} \cap (I_{\rho,j_1} \cup I_{\rho,j_2}) = \emptyset$ for $j_1 \neq j \neq j_2$. Commutativity of Casimir and vertex differential operators then follows since we can construct the Casimir differential operators in terms of the generators for $I_{r,i}$ while using the generators for I_{ρ,j_1} and I_{ρ,j_2} for the vertex differential operators.

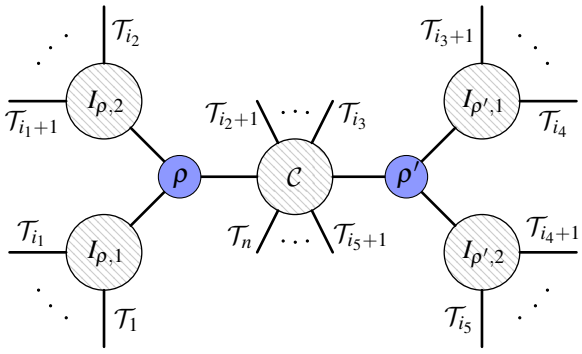

Figure 18: Schematic representation of a generic OPE diagram with focus on two internal vertices. Operators supported around distinct vertices trivially commute, as they can be written in terms of generators that belong to different branches.

Let us finally consider any two distinct vertices ρ and ρ' on an OPE diagram. As we highlight in Figure 18, any configuration of two vertices divides the diagram into five parts: four external branches $I_{\rho,j}$, $I_{\rho',j}$, $j = 1,2$, attached to only one vertex, and the central part $\mathcal{C}$ of the diagram that is attached to both vertices ρ and ρ'. Following what we just claimed with focus on one vertex, we can use diagonal conformal symmetry to rewrite the operators around ρ and ρ' to depend on disjoint sets of legs $I_{\rho,j}$, $I_{\rho',j}$ with $j = 1,2$. Since generators associated to these sets commute (4.1.6), it follows automatically that operators constructed around different vertices must commute as well.
This implies that to prove commutativity of our set of operators, we can just focus on operators that live around one single vertex. To prove the commutativity of these vertex operators we will now make use of the integrability technology that is provided by Gaudin models.

4.2.2 The vertex system and Gaudin models

In this section, we will explain how the operators (4.1.13) associated with a vertex ρ in the OPE diagram naturally arise from a specific Gaudin model, which in particular will provide us with a proof of their commutativity. Let us start by reviewing briefly how Gaudin models are defined [107, 108]. They are integrable systems naturally constructed from a choice of a simple Lie algebra $\mathfrak{g}$. Having in mind applications of these systems to conformal field theories, we will choose $\mathfrak{g}$ to be the conformal Lie algebra $\mathfrak{so}(d+1,1)$ of the Euclidean space $\mathbb{R}^d$, with basis T_α as in the previous section. The Gaudin model depends in general on M complex numbers w_j, called its sites, to which are attached M independent representations of the algebra $\mathfrak{g}$. To obtain the vertex system we address in this section, we restrict our attention here to the case $M = 3$ and associate with these three sites the representations of $\mathfrak{g}$ corresponding to the three fields attached to the vertex ρ. More precisely, using the notation defined in Section 4.1 and in particular the partition $\underline{N} = I_{\rho,1} \cup I_{\rho,2} \cup I_{\rho,3}$ constructed from the vertex ρ, we will attach to the three sites w_j, $j = 1,2,3$, of the Gaudin model the generators

$\mathcal{T}_\alpha^{(I_{\rho,j})}$ which define representations of $\mathfrak{g}$ in terms of first-order differential operators in the insertion points x_i.

A key ingredient in the construction of the Gaudin model is its so-called Lax matrix, whose components in the basis T^α are defined here as

$$\mathcal{L}_\alpha^\rho(z) = \sum_{j=1}^{3} \frac{\mathcal{T}_\alpha^{(I_{\rho,j})}}{z - w_j}, \tag{4.2.6}$$

where z is an auxiliary complex variable called the spectral parameter. In the above equation, we have denoted the Lax matrix as $\mathcal{L}_\alpha^\rho(z)$ to emphasize that this is the matrix corresponding to the vertex ρ. For any elementary symmetric invariant tensor κ_p of degree p on $\mathfrak{g}$, there is a corresponding z-dependent Gaudin Hamiltonian of the form

$$\mathcal{H}_\rho^{(p)}(z) \;=\; \kappa_p^{\alpha_1\cdots\alpha_p} \mathcal{L}_{\alpha_1}^\rho(z)\cdots\mathcal{L}_{\alpha_p}^\rho(z) + \ldots, \tag{4.2.7}$$

where $\ldots$ represent quantum corrections, involving a smaller number of components of the Lax matrix $\mathcal{L}_\alpha^\rho$ and their derivatives with respect to z. These corrections are chosen specifically to ensure that the Gaudin Hamiltonians commute for all values of the spectral parameter and all degrees:

$$\big[\mathcal{H}_\rho^{(p)}(z), \mathcal{H}_\rho^{(q)}(w)\big] = 0, \qquad \forall\, z, w \in \mathbb{C}, \quad \forall\, p, q\ . \tag{4.2.8}$$

The existence of such commuting Hamiltonians was first proven in [109], using some previously established results [110] on the so-called Feigin-Frenkel center of affine algebras at the critical level. The explicit expression for the quantum corrections was obtained in [111, 112] for Lie algebras of type A and in [113] for types B, C, D, which is the case we are concerned with here (indeed, $\mathfrak{g} = \mathfrak{so}(d+1,1)$ is of type B for d odd and of type D for d even). We refer to [114] for a summary of these results. The properties of the Feigin-Frenkel center were further studied in the recent work [115], the results of which imply that the quantum corrections in $\mathcal{H}_\rho^{(p)}(z)$ are sums of terms of the form

$$\tau^{\alpha_1\cdots\alpha_q}\, \partial_z^{r_1-1}\mathcal{L}_{\alpha_1}^\rho(z)\cdots\partial_z^{r_q-1}\mathcal{L}_{\alpha_q}^\rho(z), \tag{4.2.9}$$

where $q < p$, $\tau^{\alpha_1\cdots\alpha_q}$ is a completely symmetric invariant tensor of degree q on $\mathfrak{g}$ and $r_1, \cdots, r_q$ are positive integers such that $r_1 + \cdots + r_q = p$. For what follows, it will be useful to consider the leading part of the Hamiltonian (5.1.11) alone, without quantum corrections, which we will denote as

$$\widehat{\mathcal{H}}_\rho^{(p)}(z) = \kappa^{\alpha_1\cdots\alpha_p}\mathcal{L}_{\alpha_1}^\rho(z)\cdots\mathcal{L}_{\alpha_p}^\rho(z)\ . \tag{4.2.10}$$

Let us finally note that the quantum corrections are absent for both the quadratic Hamiltonian $\mathcal{H}_\rho^{(2)}(z)$ and the Pfaffian Hamiltonian $\mathcal{H}_\rho^{(d/2+1)}(z)$ that exists for d even, such that these two Hamiltonians coincide with their leading parts.

To make the link with the vertex operators defined in Section 4.1, we will make a specific choice of the parameters w_j of the Gaudin model. More precisely, we set

$$w_1 = 0, \qquad w_2 = 1 \qquad \text{and} \qquad w_3 = \infty\ . \tag{4.2.11}$$

In particular, the Lax matrix (5.1.10) reduces to

$$\mathcal{L}_\alpha^\rho(z) = \frac{\mathcal{T}_\alpha^{(I_{\rho,1})}}{z} + \frac{\mathcal{T}_\alpha^{(I_{\rho,2})}}{z-1}\ . \tag{4.2.12}$$

Let us now study the Gaudin Hamiltonians $\mathcal{H}_\rho^{(p)}(z)$ for this particular choice of parameters. We will first focus on their leading part $\widehat{\mathcal{H}}_\rho^{(p)}(z)$. Reinserting the above expression of the Lax matrix in eq. (4.2.10), we simply find

$$\widehat{\mathcal{H}}_\rho^{(p)}(z) = \sum_{\nu=0}^{p} \binom{p}{\nu} \frac{\mathcal{D}_{\rho,12}^{p,\nu}}{z^\nu (z-1)^{p-\nu}}, \tag{4.2.13}$$

where $\mathcal{D}_{\rho,12}^{p,\nu}$ is the vertex operator defined in eq. (4.1.13). To obtain this expression, we have used the fact that $\mathcal{T}_\alpha^{(I_{\rho,1})}$ and $\mathcal{T}_\beta^{(I_{\rho,2})}$ commute to bring all $\mathcal{T}_\alpha^{(I_{\rho,1})}$'s to the left, as well as the symmetry of the tensor $\kappa_p^{\alpha_1\cdots\alpha_p}$ to relabel the Lie algebra indices as in eq. (4.1.13). Noting that the fractions $z^{-\nu}(z-1)^{\nu-p}$ for $\nu = 0, \cdots, p$ are linearly independent functions of z, it is then clear that one can extract all the vertex operators $\mathcal{D}_{\rho,12}^{p,\nu}$ from $\widehat{\mathcal{H}}_\rho^{(p)}(z)$. Note that the "extremal" operators $\mathcal{D}_{\rho,12}^{p,0}$ and $\mathcal{D}_{\rho,12}^{p,p}$ coincide with the Casimir operators of the fields at the branches $I_{\rho,1}$ and $I_{\rho,2}$ of the vertex. The same equation also holds for the Pfaffian operators $\mathcal{H}_\rho^{(d/2+1)}(z)$.

Our goal in this section is to prove the commutativity of the vertex operators $\mathcal{D}_{\rho,12}^{p,\nu}$ using known results on Gaudin models. This would follow automatically from the commutativity (4.2.8) of the Gaudin Hamiltonians $\mathcal{H}_\rho^{(p)}(z)$ if these Hamiltonians contained the operators $\mathcal{D}_{\rho,12}^{p,\nu}$. But we have already proven above that the latter are naturally extracted from the leading parts $\widehat{\mathcal{H}}_\rho^{(p)}(z)$ of the Gaudin Hamiltonians, without the quantum corrections. These quantum corrections are in general crucial for the commutativity of the Hamiltonians. However, we shall prove below that the quantum corrections of the specific Gaudin model considered here can always be expressed in terms of lower-degree Hamiltonians, and can thus be discarded without breaking the commutativity property. In this case, the non-corrected Hamiltonians $\widehat{\mathcal{H}}_\rho^{(p)}(z)$ pairwise commute for all values of the spectral parameter and all degrees, thus demonstrating the desired commutativity of the vertex operators $\mathcal{D}_{\rho,12}^{p,\nu}$.

Let us then analyze these quantum corrections. Recall that they are composed of terms of the form (4.2.9). Reinserting the expression (4.2.12) of the Lax matrix for the present choice of parameters w_j in this equation, we find that the quantum corrections contain only terms of the form

$$\tau^{\alpha_1\cdots\alpha_q}\, \mathcal{T}_{\alpha_1}^{(I_{\rho,1})} \cdots \mathcal{T}_{\alpha_\nu}^{(I_{\rho,1})} \mathcal{T}_{\alpha_{\nu+1}}^{(I_{\rho,2})} \cdots \mathcal{T}_{\alpha_q}^{(I_{\rho,2})}, \tag{4.2.14}$$

with prefactors composed of powers of z and $z-1$, and where $\tau^{\alpha_1\cdots\alpha_q}$ is a completely symmetric invariant tensor on $\mathfrak{g}$ of degree $q < p$, as in eq. (4.2.9). In particular, $\tau^{\alpha_1\cdots\alpha_q}$ decomposes as a product of elementary symmetric invariant tensors κ_k, symmetrized over the indices α_i, with $k \leq q < p$. The correction in the above equation can thus be re-expressed as an algebraic combination of lower-degree vertex operators $\mathcal{D}_{\rho,12}^{k,\nu}$. Since these are the coefficients of the non-corrected Hamiltonian $\widehat{\mathcal{H}}_\rho^{(k)}(z)$, recursion on the degrees shows that the quantum corrections can indeed be expressed in terms of lower-degree Hamiltonians, as anticipated.

Let us end this subsection with a brief discussion on the role played by the choice of labeling of the branches $I_{\rho,1}$, $I_{\rho,2}$ and $I_{\rho,3}$ attached to the vertex ρ. As mentioned in Section 4.1, this choice is arbitrary but enters the definition (4.1.13) of the vertex operators $\mathcal{D}_{\rho,12}^{p,\nu}$, which in this case contain only the generators $\mathcal{T}_\alpha^{(I_{\rho,1})}$ and $\mathcal{T}_\alpha^{(I_{\rho,2})}$. In the context of the 3-sites Gaudin model considered in this subsection, this is related to the choice of positions w_j of the sites made in eq. (4.2.11). In particular, the absence of generators $\mathcal{T}_\alpha^{(I_{\rho,3})}$ in the Gaudin Hamiltonians $\mathcal{H}^{(p)}(z)$ is due to the fact that we sent the site w_3 to infinity. One could have made another choice of labeling and constructed vertex operators $\mathcal{D}_{\rho,23}^{p,\nu}$ from the generators $\mathcal{T}_\alpha^{(I_{\rho,3})}$ and $\mathcal{T}_\alpha^{(I_{\rho,2})}$, for instance. The corresponding choice of positions of the sites would then be related to the initial one by the Möbius transformation that exchanges 0 and ∞ and fixes 1, i.e. the inversion $z \mapsto \frac{1}{z}$. More precisely, under such a transformation of the spectral

parameter, the Lax matrix of the Gaudin model behaves as a 1-form on the Riemann sphere and satisfies

$$-\frac{1}{z^2}\mathcal{L}^{\rho}_{\alpha}\left(\frac{1}{z}\right) = -\frac{\mathcal{T}^{(I_{\rho,1})}_{\alpha}+\mathcal{T}^{(I_{\rho,2})}_{\alpha}}{z}+\frac{\mathcal{T}^{(I_{\rho,2})}_{\alpha}}{z-1}\ . \tag{4.2.15}$$

Acting on the correlation function $\mathcal{G}_N$, which satisfies the Ward identities (4.1.10), this Lax matrix then becomes

$$-\frac{1}{z^2}\mathcal{L}^{\rho}_{\alpha}\left(\frac{1}{z}\right)_{|\mathcal{G}} = \left[\frac{\mathcal{T}^{(I_{\rho,3})}_{\alpha}}{z}+\frac{\mathcal{T}^{(I_{\rho,2})}_{\alpha}}{z-1}\right]_{|\mathcal{G}}\ , \tag{4.2.16}$$

and thus coincides with the Lax matrix from which one would build the vertex operators $\mathcal{D}^{p,\nu}_{\rho,23}$ with generators $\mathcal{T}^{(I_{\rho,3})}_{\alpha}$ and $\mathcal{T}^{(I_{\rho,2})}_{\alpha}$. This proves that the operators $\mathcal{D}^{p,\nu}_{\rho,23}$ can naturally be extracted from the generating functions

$$\frac{(-1)^p}{z^{2p}}\widehat{\mathcal{H}}^{(p)}_{\rho}\left(\frac{1}{z}\right)_{|\mathcal{G}}\ . \tag{4.2.17}$$

Using the expression (4.2.13) of $\widehat{\mathcal{H}}^{(p)}_{\rho}(z)$ in terms of the initial vertex operators $\mathcal{D}^{p,\nu}_{\rho,12}$, we thus get that the $\mathcal{D}^{p,\nu}_{\rho,23}$'s are linear combinations of the $\mathcal{D}^{p,\nu}_{\rho,12}$'s, as was demonstrated by direct computation in the previous subsection. Let us note that the use of the Ward identities was a crucial step in the above reasoning, as highlighted for instance by the subscript $\mathcal{G}$ in eq. (4.2.17). This step should be performed with care, in particular when using the Ward identities to replace $-\mathcal{T}^{(I_{\rho,1})}_{\alpha}-\mathcal{T}^{(I_{\rho,2})}_{\alpha}$ by $\mathcal{T}^{(I_{\rho,3})}_{\alpha}$ in the Hamiltonians (4.2.17). Indeed, one can use the Ward identities only for generators on the right. In order to do so, one thus has to commute generators to bring them to the right, replace them through the Ward identities and commute them back to their original place. Although this procedure can in general create non-trivial corrections, it can in fact be done freely in the case at hand: indeed, commuting operators $\mathcal{T}^{(I_{\rho,j})}_{\alpha_k}$ and $\mathcal{T}^{(I_{\rho,j})}_{\alpha_l}$ within the Hamiltonian $\widehat{\mathcal{H}}^{(p)}_{\rho}$ creates a term proportional to the structure constant $f_{\alpha_k\alpha_l}{}^{\beta}$, which vanishes when contracted with the symmetric tensor $\kappa_p^{\alpha_1\cdots\alpha_p}$. This ensures that the Hamiltonian (4.2.17) indeed serves as a generating function of the operators $\mathcal{D}^{p,\nu}_{\rho,23}$ built from $\mathcal{T}^{(I_{\rho,3})}_{\alpha}$ and $\mathcal{T}^{(I_{\rho,2})}_{\alpha}$. A similar reasoning applies for the other choices of labeling, by considering the appropriate Möbius transformations that permute the sites 0, 1 and ∞ of our 3-site Gaudin model.

4.2.3 Restricted vertices and relations between vertex operators

In the previous subsection we have shown that all of the operators listed in eq. (4.1.13) commute with each other. As we have pointed out before, we did not include operators with $\nu = 0$ and $\nu = p$ in the list since these coincide with Casimir differential operators,

$$\mathcal{D}^{p,0}_{\rho,12} = \mathcal{D}^{p}_{r_1} \quad , \quad \mathcal{D}^{p,p}_{\rho,12} = \mathcal{D}^{p}_{r_2}\ . \tag{4.2.18}$$

Here r_i denotes the link that is attached to the i^{th} leg of the vertex ρ, i.e. for which $I_{r_i,j} = I_{\rho,i}$ with either $j = 1$ or $j = 2$. The remaining $p-1$ operators satisfy one more linear relation since

$$\sum_{\nu=0}^{p}\binom{p}{\nu}\mathcal{D}^{p,\nu}_{\rho} = \mathcal{D}^{p}_{r_3}\ . \tag{4.2.19}$$

Let us note that this relation also applies to the Pfaffian vertex operators that exist for $p = d/2+1$ when d is even. We have used this relation to drop one of the vertex differential operators. Once these obvious relations are taken care of, the total number of commuting vertex differential operators is given

by eq. (4.1.14) and matches precisely the maximal number of cross ratios that can be associated to a single (generic) vertex, see upper bound of eq. (5.1.2) in the introduction. But restricted vertices carry fewer variables, so their corresponding differential operators (constructed in the previous section) must obey further relations. It is the main goal of this subsection to discuss these relations. We will also check that, once these are taken into account, the number of remaining vertex differential operators matches the number (5.1.2) of cross ratios at restricted vertices.

Our arguments are based on an important auxiliary result concerning the differential operators $\mathcal{T}_\alpha^{(I)}$ that are associated to some subset $I \subset \underline{N}$ of order $|I| \leq N/2$. To present this requires a bit of preparation. Up to this point there was no need to spell out the precise form of the symmetric invariant tensors κ_p that we used to construct our differential operators. Now we need to be a bit more specific. As is well known, such tensors can be realized as symmetrized traces,

$$\kappa_p^{\alpha_1\cdots\alpha_p} = tr\Big(T^{(\,\alpha_1}\cdots T^{\alpha_p\,)}\Big) = str(T^{\alpha_1}\cdots T^{\alpha_p}) \ . \tag{4.2.20}$$

Here T^α denote the generators of the conformal Lie algebra and $(\dots)$ signal symmetrization with respect to the indices. In the following we shall use the symbol *str* to denote this symmetrized trace. The trace can be taken in any faithful representation. The simplest of such choices is to use the fundamental representation. In order to construct the associated symmetric invariants more explicitly, we shall replace the index α that enumerates the basis of the conformal algebra by a pair $\alpha = [AB]$ where A, B run through $A, B = -1, 0, \dots, d$ with $T^{[AB]} = -T^{[BA]}$. In the fundamental representation, the matrix elements of these generators take the form

$$\big(T_f^{[AB]}\big)^C{}_D = \eta^{AC}\,\delta^B{}_D - \eta^{BC}\,\delta^A{}_D \ ,$$

where η_{AB} is the Minkowski metric with signature $(d+1,1)$ and η^{AB} is its inverse. This makes it now easy to compute κ_p explicitly. The only issue arises in even d. In this case the symmetrized traces in the fundamental representation do not generate all the invariants. In order to obtain the missing invariant, one has to include the trace in a chiral representation. The standard construction employs the spinor representation in which generators $T^{[AB]}$ are represented as

$$\big(T_s^{[AB]}\big)^\sigma{}_\tau = \frac{1}{4}\,[\,\gamma^A\,,\,\gamma^B\,]^\sigma{}_\tau \ ,$$

where γ^A are the $d+2$-dimensional γ matrices and the matrix indices are $\sigma, \tau = 1, \dots, 2^{d/2+1}$. One can then project to a chiral spinor representation with the help of $\gamma_c \sim \gamma^0 \cdots \gamma^{d+1}$.

Let us now introduce the symbol $\mathcal{T}^{(I)}$ to denote the following Lie-algebra valued differential operators

$$\mathcal{T}^{(I)} = T^\alpha \cdot \mathcal{T}_\alpha^{(I)} = \frac{1}{2} T^{[AB]} \cdot \mathcal{T}_{[AB]}^{(I)} \ .$$

Upon evaluation in some finite-dimensional representation, such as the fundamental or the spinor representation, these become matrix valued differential operators. With this notation we write our set (4.1.13) as

$$\mathcal{D}_{\rho,12}^{p,\nu} = str_f\left(\underbrace{\mathcal{T}^{(I_{\rho,1})}\dots\mathcal{T}^{(I_{\rho,1})}}_{\nu}\underbrace{\mathcal{T}^{(I_{\rho,2})}\dots\mathcal{T}^{(I_{\rho,2})}}_{p-\nu}\right)_{|\mathcal{G}} \tag{4.2.21}$$

when d is odd and the parameters p and ν assume the values $p = 2, 4, \dots, d+1$ and $\nu = 1, \dots, p-1$, as usual. For even dimension d, on the other hand, we use the symmetrized trace in the fundamental

representation for $p = 2, 4, \ldots, d$ and construct the missing Pfaffian vertex differential operators as

$$\mathcal{D}^{d/2+1,\nu}_{\rho,12} = str_s \left(\underbrace{\mathcal{T}^{(I_{\rho,1})} \ldots \mathcal{T}^{(I_{\rho,1})}}_{\nu} \underbrace{\mathcal{T}^{(I_{\rho,2})} \ldots \mathcal{T}^{(I_{\rho,2})}}_{d/2+1-\nu} \gamma_c \right)_{|\mathcal{G}} \tag{4.2.22}$$

where we take the trace in the spinor representation and include the factor γ_c in the argument.

In finding relations between the vertex differential operators for restricted vertices we actually work with the total symbols of the differential operators rather than the operators themselves. This means that we replace the partial derivatives $\partial^{(i)}_\mu$ with commuting coordinates p^i_μ. The associated matrices of functions of x^μ_i and p^i_μ will be denoted by $\bar{\mathcal{T}}^{(I)}$. As before we shall add a subscript f, s to denote the matrices in the fundamental and the spinor representation. After passing to the total symbol the entries of the matrices commute and we can drop the symmetrization prescription when taking traces. As a result, the total symbols of the vertex differential operators are simply traces of powers of the matrices $\bar{\mathcal{T}}^{(I)}$.

We are now ready to state the main result needed to elucidate the relations between vertex differential operators. It concerns the matrix elements of the n^{th} power of the matrices $\bar{\mathcal{T}}^{(I)}_{f,s}$ for the fundamental and the spinor representations. In both cases, these matrix elements are functions of x^μ_i and p^i_μ with $i \in I$. Our main claim is that these matrix elements can be expressed in terms of lower order ones of the same form whenever $n > 2\mathfrak{d}_I$, where $\mathfrak{d}_I = \mathfrak{d}(I, d)$ is the integer defined in eq. (5.1.1). More precisely, for each matrix element AB there exist coefficients $\varrho^{(n,m)}_{AB}$ such that

$$\big(\bar{\mathcal{T}}^{(I)\,n}_f\big)^A{}_B = \sum_{m=0}^{2\mathfrak{d}_I} \varrho^{(n,m)}_{f;AB} \big(\bar{\mathcal{T}}^{(I)\,m}_f\big)^A{}_B \ . \tag{4.2.23}$$

Note that there is no summation over A, B on the right hand side. The coefficients ϱ_{AB} depend only on the external conformal weights Δ_i and the total symbols $\bar{\mathcal{D}}^p_{(I)}$ of the Casimir operators associated with the index set I. If the index set I has depth $\mathfrak{d}_I = 1$, for example, i.e. if the $\bar{\mathcal{T}}^{(I)}$ describe the action of the conformal algebra on a single scalar primary, then starting from $n = 3$ all matrix elements can be expressed in terms of lower order ones. In the case of the spinor representation one has a very similar relation

$$\big(\bar{\mathcal{T}}^{(I)\,n}_s\big)^\sigma{}_\tau = \sum_{m=0}^{\mathfrak{d}_I} \varrho^{(n,m)}_{s;\sigma,\tau} \big(\bar{\mathcal{T}}^{(I)\,m}_s\big)^\sigma{}_\tau \ . \tag{4.2.24}$$

which now applies for $n > \mathfrak{d}_I$ and involves a summation over m that ends at $\mathfrak{d}_I = \mathfrak{d}(I, d)$, see definition (5.1.1). So if $\mathfrak{d}_I = 1$, for example, the matrix elements of the square are expressible in terms of the matrix elements of $\bar{\mathcal{T}}^{(I)}_s$. We verify both statements (4.2.23) and (4.2.24) in Appendix 4.C using embedding space formalism, see Appendix 4.B.

We are now prepared to discuss relations between vertex differential operators. Let us consider a vertex ρ inside our OPE diagram. As we have explained before, ρ splits the set $\underline{N}$ into three subsets $I_{\rho,i}$ with $i = 1, 2, 3$. Each of these sets determines an integer $\mathfrak{d}_i = \mathfrak{d}(I_{\rho,i}, d)$. Let us suppose that we construct the vertex differential operators using $\mathcal{T}^{(I_{\rho,i})}$ for $i = 1, 2$ as in eq. (4.2.21). If one of the integers $\mathfrak{d}_1$ or $\mathfrak{d}_2$ is smaller than r_d we immediately obtain relations among the vertex differential operators. In fact, when applied to the matrices $\bar{\mathcal{T}}^{(I_\rho,1)}$, our claim (4.2.23) implies that all operators we obtain when $\nu > 2\mathfrak{d}_1$ can be expressed in terms of Casimir and vertex differential operators of lower order. The same is true when $p - \nu > 2\mathfrak{d}_2$, as follows again from eq. (4.2.23), but this time

applied to $\bar{\mathcal{T}}^{(I_\rho,2)}$. Consequently, for any $p \geq 2\mathfrak{d}_1, 2\mathfrak{d}_2$, we can restrict the range of the index ν to be $p - 2\mathfrak{d}_2 \leq \nu \leq 2\mathfrak{d}_1$, with $\nu = 0, p$ excluded as before.
But this does not yet include the full set of relations that appears whenever $\mathfrak{d}_3$ is smaller than $min(\mathfrak{d}_1 + \mathfrak{d}_2, r_d)$. One of the simplest examples of this occurs in the 6-point snowflake channel in $d > 3$, see Figure 19, where two symmetric traceless tensor operators on two branches are combined at the central vertex ρ to form another symmetric traceless tensor on the third branch.

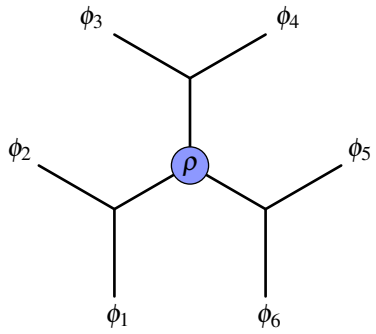

Figure 19: Snowflake OPE diagram. Here the tensor product of any two branches around the vertex ρ would allow a mixed symmetry tensor of depth $\mathfrak{d} = 4$ to appear in $d \geq 7$, but diagonal conformal symmetry constrains this to match with the symmetric traceless tensor produced on the third branch.

To take restrictions from the third branch I_3 into account, it is sufficient to use the total symbol of eq. (4.2.3) and impose once more our dependence statement (4.2.23) for product matrices, this time for $\mathcal{T}^{(I_\rho,3)}$. This tells us that the matrix elements of powers

$$\left(\bar{\mathcal{T}}^{(I_\rho,1)} + \bar{\mathcal{T}}^{(I_\rho,2)}\right)^{n\ A}_{\quad B} \tag{4.2.25}$$

with $n > 2\mathfrak{d}_3$ can be written in terms of lower order terms. In order to convert this observation into relations among the vertex differential operators of order p, we can multiply the expression (4.2.25) with some appropriate powers of $\bar{\mathcal{T}}^{(I_\rho,i)}$, $i = 1, 2$, and consider the matrix elements of the products

$$\left(\bar{\mathcal{T}}^{(I_\rho,1)} + \bar{\mathcal{T}}^{(I_\rho,2)}\right)^{n} \left(\bar{\mathcal{T}}^{(I_\rho,2)}\right)^{\nu} \left(\bar{\mathcal{T}}^{(I_\rho,1)}\right)^{p-n-\nu} \tag{4.2.26}$$

for $n > 2\mathfrak{d}_3$, any allowed value of $p > n$ and $\nu = 0, \ldots, p - n$. By binomial expansion, we can write the expression (4.2.26) as a linear combination of our basic vertex differential operators. After taking relations on the branches $I_{\rho,1}$ and $I_{\rho,2}$ into account, we obtain an additional nontrivial relation from the third branch $I_{\rho,3}$. For example, in the cases where n is odd, contracting (4.2.25) with $\left(\mathcal{T}^{(I_\rho,2)}\right)^{B}_{\ A}$ leads to a relation between vertex and Casimir operators of order $n + 1$ and further lower order operators. This effectively reduces the amount of vertex operators at order p by up to $p - 2\mathfrak{d}_3 - 1$, though the actual number can be lower in case there are less than $p - 2\mathfrak{d}_3 - 1$ vertex operators at order p left after imposing the constraints from the first two branches. If we are interested in counting the number of vertex operators at a given even order p, the procedure we just outlined is summarized in the following counting formula

$$n^{(p)}_{vdo,\rho} = max\left[\left((p-2) - \sum_{i=1}^{3} \Theta_0(p - 2\mathfrak{d}_i)(p - 2\mathfrak{d}_i - 1)\right), 0\right], \tag{4.2.27}$$

where Θ_0 is the Heaviside step function with $\Theta_0(0) = 0$, the factor $(p-2)$ gives the maximal amount of vertex operators at order p, the factor $(p - 2\mathfrak{d}_i - 1)$ corresponds to the number of relations introduced for every $\mathfrak{d}_i < p/2$, and the maximum enforces the number to be 0 if there are more than $(p-2)$ relations in total.
Our description of relations between vertex differential operators exploited the auxiliary statement (4.2.23) and did not include the Pfaffian vertex differential operators. It is clear, however, that precisely the same reasoning also applies to the latter using eq. (4.2.24) instead of eq. (4.2.23). The counting formula (4.2.27) gets also slightly modified for this Pfaffian case

$$n_{vdo,\rho}^{(p=d/2+1)} = max\left[\left((p-2) - \sum_{i=1}^{3} \Theta_0(p-\mathfrak{d}_i)(p-\mathfrak{d}_i-1)\right), 0\right] . \tag{4.2.28}$$

Note that the arguments we have outlined here exhibit relations between vertex operators, but we have not shown that these relations are complete, i.e. that the remaining vertex differential operators are in fact independent. A priori, it could in fact happen that the exceeding relations we get from here, or additional relations obtained from a different reasoning, could provide additional dependencies. We checked however that summing the counting formulas (4.2.27) and (4.2.28) for all allowed orders p in a given dimension d, gives rise to a number of vertex differential operators equal to the number of cross ratios (5.1.2) associated with every allowed vertex. This provides strong evidence in favor of the independence of our vertex differential operators. In some particularly relevant cases in lower dimensions we can also prove independence.

Example: The $N = 6$ snowflake channel for $d = 7$. Let us see how all of this works in the example of a snowflake channel in $d = 7$, presented in Figure 19. We enumerate the internal links by $r = 1, 2, 3$. The associated index sets $I_{r,i}$ are $I_{1,1} = \{1, 2\}, I_{2,1} = \{3, 4\}, \ldots$. Here we have two symmetric traceless tensors associated with $r = 1, 2$. In a more general OPE diagram these could produce a mixed symmetry tensor with maximal depth $\mathfrak{d} = r_d = 4$, but in the snowflake diagram the field on the third link must also be a symmetric traceless tensor of depth $\mathfrak{d}(I_3, d = 7) = 2$. Our prescription tells us to consider operators (4.2.21) up to $p = 8$. Eliminating powers of $\mathcal{T}_1 = \mathcal{T}^{(12)}$ and $\mathcal{T}_2 = \mathcal{T}^{(34)}$ higher than 4, it immediately follows that there are no vertex operators of order 8

$$\cancel{\mathcal{T}_1^7\mathcal{T}_2}\,, \quad \cancel{\mathcal{T}_1^6\mathcal{T}_2^2}\,, \quad \cancel{\mathcal{T}_1^5\mathcal{T}_2^3}\,, \quad \cancel{\mathcal{T}_1^3\mathcal{T}_2^5}\,, \quad \cancel{\mathcal{T}_1^2\mathcal{T}_2^6}\,, \quad \cancel{\mathcal{T}_1\mathcal{T}_2^7}\,, \tag{4.2.29}$$

while there could be up to two operators of order 6

$$\cancel{\mathcal{T}_1^5\mathcal{T}_2}\,, \quad \mathcal{T}_1^4\mathcal{T}_2^2\,, \quad \mathcal{T}_1^2\mathcal{T}_2^4\,, \quad \cancel{\mathcal{T}_1\mathcal{T}_2^5}\,, \tag{4.2.30}$$

and two operators of order 4

$$\mathcal{T}_1^3\mathcal{T}_2\,, \quad \mathcal{T}_1\mathcal{T}_2^3\,. \tag{4.2.31}$$

Here and in the following steps we are using notation for which stroked terms are dependent on lower order operators. Let us also recall that the operators with $\nu = p/2$ have been omitted to account for the relation between the vertex and Casimir differential operators for the third leg. The reduction of $\mathcal{T}_3 = \mathcal{T}^{(56)}$ to a symmetric traceless tensor implies the existence of $p - 2\mathfrak{d}_3 - 1$ relations between p order monomials. The only useful relation in this case is the one produced for $p = 6$, coming from the expansion

$$\cancel{(\mathcal{T}_1 + \mathcal{T}_2)^5} = \mathcal{T}_1^5 + 5\mathcal{T}_1^4\mathcal{T}_2 + 10\mathcal{T}_1^3\mathcal{T}_2^2 + 10\mathcal{T}_1^2\mathcal{T}_2^3 + 5\mathcal{T}_1\mathcal{T}_2^4 + \mathcal{T}_2^5\,, \tag{4.2.32}$$

which can be contracted with either $\mathcal{T}_1$ or $\mathcal{T}_2$ and traced over to get a relation between the sixth order monomials (including the one associated to the Casimir of the third leg):

$$\cancel{(\mathcal{T}_1+\mathcal{T}_2)^5\mathcal{T}_2} = \cancel{\mathcal{T}_1^5\mathcal{T}_2} + 5\mathcal{T}_1^4\mathcal{T}_2^2 + 10\mathcal{T}_1^3\mathcal{T}_2^3 + 10\mathcal{T}_1^2\mathcal{T}_2^4 + 5\cancel{\mathcal{T}_1\mathcal{T}_2^5} + \cancel{\mathcal{T}_2^6}\,. \tag{4.2.33}$$

This reduces the amount of independent vertex operators by one, bringing us to a total of three independent operators, which matches with the number of associated cross ratios.

4.3 OPE channels and limits of Gaudin models

At this point we have defined a set of differential operators associated with the intermediate fields and the individual vertices of a given OPE diagram with N external fields. The new vertex operators were constructed in Subsection 4.2.2 from a Gaudin model with three sites, which was crucial in proving their commutativity. Our construction of the vertex operators has been *local* in its focus on a particular building block, namely a single vertex that is associated to a local element of the OPE diagram. The purpose of this section is to adopt a more *global* perspective by showing that the whole set of Casimir and vertex differential operators for any N-point OPE channel can be obtained by taking an appropriate limit of an N-site Gaudin model. The N-site Gaudin model itself makes no reference to the choice of OPE channel. The latter enters only through the choice of limit. We will therefore refer to these limits as OPE limits of the N-site Gaudin model. These OPE limits are generalizations of the so-called bending flow and caterpillar limits that have been considered in the mathematical literature, see e.g. [116–118]. The same limit of a 4-site Gaudin model - which may be identified with the elliptic Inozemtsev model [119] - has also appeared in the physics literature recently [120]. Eberhardt, Komatsu and Mizera have shown that the limit theory coincides with the hyperbolic Calogero-Sutherland model, which is known to describe the Casimir equations of 4-point conformal blocks.

4.3.1 N sites Gaudin model and OPE limits

Let us first define the Gaudin model that we will use in this section. Since this construction is similar to the one of the 3-sites Gaudin model considered in Section 4.2.2, we refer to that section for details and references. As before, we consider a Gaudin model based on the conformal Lie algebra $\mathfrak{g} = \mathfrak{so}(d+1,1)$ but now with N sites, whose positions $w_1, \cdots, w_N \in \mathbb{C}$ are for the moment arbitrary. We naturally associate these sites with the N external fields in the correlation function under consideration and more precisely attach to each site $i \in \{1, \cdots, N\}$ the representation of $\mathfrak{g}$ defined by the generators $\mathcal{T}_\alpha^{(i)}$, which describe the action of the conformal transformations on the scalar field $\phi_i(x_i)$ in terms of first-order differential operators. Then we define the (components of the) Lax matrix of the model as

$$\mathcal{L}_\alpha(z, w_i) = \sum_{i=1}^{N} \frac{\mathcal{T}_\alpha^{(i)}}{z - w_i}\,. \tag{4.3.1}$$

The associated Gaudin Hamiltonians $\mathcal{H}^{(p)}(z, w_i)$ of degree p are given by the same equation (5.1.11) that we used for the 3-site case. Recall that κ_p denotes the conformally invariant symmetric tensor of degree p and $\ldots$ represent quantum corrections. The latter have the same form as in the 3-site case, see eq. (4.2.9). It is well known that these N-site Gaudin Hamiltonians commute, just as their three site analogues, i.e. they satisfy eq. (4.2.8). At the same time, it is easy to verify that they are invariant under diagonal conformal transformations,

$$\big[\mathcal{H}^{(p)}(z, w_i), \mathcal{T}_\alpha^{(N)}\big] = 0, \qquad \forall\, z \in \mathbb{C}, \quad \forall\, p, \tag{4.3.2}$$

where $\mathcal{T}_\alpha^{(\underline{N})} = \sum_{i=1}^N \mathcal{T}_\alpha^{(i)}$ are the diagonal conformal generators that also appear in the Ward identities (4.1.10). This means that Gaudin Hamiltonians descend to correlation functions $\mathcal{G}$.
The Hamiltonian $\mathcal{H}^{(p)}(z, w_i)$ of the N-site Gaudin model depends on the N complex parameters w_i that specify the poles of the Lax matrix. These parameters have no a priori interpretation in the context of correlation functions. Note that we can always apply Möbius transformations on the z-variable to fix three of the w_i. This is what allowed us in the previous section to set the parameters of the 3-site Gaudin model to the specific values (4.2.11), in which case the Lax matrix (4.2.12) and its corresponding differential operators contain no extra parameters. Our main claim is that we can reconstruct the entire set of 3-site Lax matrices $\mathcal{L}_\alpha^\rho(z)$, as well as the associated vertex Hamiltonians $\mathcal{H}_\rho^{(p)}(z)$, one set for each vertex ρ, from the N-site Lax matrix and the associated Gaudin Hamiltonians $\mathcal{H}^{(p)}(z) = \mathcal{H}^{(p)}(z, w_i)$ by taking appropriate scaled limits of the complex parameters w_i.

In order to make a precise statement, we need a bit of preparation. The limits we are about to discuss must depend on the choice of the OPE channel. So let us assume we are given such a channel $\mathcal{C}$. In order to define the limits we pick an (arbitrary) external edge in the diagram, which will serve as a reference point and which, up to reordering, we can suppose to have label N. As this edge is external, it is attached to a unique vertex, which we will denote by ρ_*. Such a choice of reference vertex defines a so-called rooted tree representation of the diagram. We then draw the OPE diagram on a plane, with the vertex ρ_* situated at the top and with each vertex having two downward edges attached. Such a representation on a plane forces us to make a choice of which edges are pointing towards the left and which edges are pointing towards the right: this choice is arbitrary, and gives rise to what is called a plane (or ordered) representation of the underlying rooted tree. We give an example of such a plane rooted tree representation for an 8-point OPE diagram in Figure 20 below. Recall from

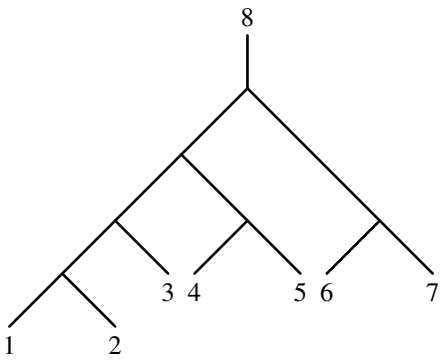

Figure 20: Plane rooted tree representation of an OPE diagram with 8 external fields.

Section 4.1 that each vertex ρ of the OPE diagram defines a partition $\underline{N} = I_{\rho,1} \cup I_{\rho,2} \cup I_{\rho,3}$, with the sets $I_{\rho,j}$ formed by the labels of the external fields attached to the three branches of the vertex. Although the choice of labeling of these branches was arbitrary in Section 4.1, we will now fix it using the plane rooted tree representation of the diagram picked above: choose the branch $I_{\rho,1}$ to be the one pointing to the bottom left and the branch $I_{\rho,2}$ to be the one pointing to the bottom right. By construction, the last branch $I_{\rho,3}$ then always points to the top and contains the reference point N.

Each vertex ρ in the diagram is thereby associated with a sequence $s^\rho = (s_1^\rho, s_2^\rho, \ldots, s_{n_\rho}^\rho)$ of elements $s_a^\rho \in \{1, 2\}$. This sequence s^ρ encodes the path from ρ_* to ρ. It tells us whether we have to move to

the left (for $s_a^\rho = 1$) or right (for $s_a^\rho = 2$) every time we reach a new vertex until we arrive at ρ after n_ρ steps. We shall also refer to the length n_ρ of the sequence as the depth of the vertex and to s^ρ as the *binary sequence* of ρ. Note that the top vertex ρ_* has depth $n_{\rho_*} = 0$. Let us point out that the notion of depth used in this section refers to the distance from the root ρ_* and is very different from the depth $\mathfrak{d}$ introduced in eq. (5.1.1) of the introduction.
In order to construct the limit of the Gaudin model that we are interested in, we will need to assign a polynomial $g_\rho(\varpi)$ to each vertex ρ. If s^ρ is the binary sequence associated with the vertex ρ, the polynomial g_ρ is defined as

$$g_\rho(\varpi) = \sum_{a=1}^{n_\rho} \varpi^{a-1} \delta_{s_a^\rho,2} \ . \tag{4.3.3}$$

Obviously the top vertex ρ_* is assigned to $g_{\rho_*}(\varpi) = 0$. The vertices of depth $n_\rho = 1$ are associated with $g_{\rho_1}(\varpi) = 0$ or $g_{\rho_2}(\varpi) = 1$, depending on whether they are reached from ρ_* by going down to the left (ρ_1) or to the right (ρ_2).
Similarly, we can assign polynomials $f_i(\varpi)$ to each external edge $1 \leq i < N$ at the bottom of the plane rooted tree. Once again, we can encode the path from ρ_* down to the edge i by a binary sequence $s^i = (s_1^i, s_2^i, \ldots, s_{n_i}^i)$. The length n_i of the sequence s^i is also referred to as the depth of the edge i. Now we introduce

$$f_i(\varpi) = \sum_{a=1}^{n_i} \varpi^{a-1} \delta_{s_a^i,2} + \varpi^{n_i} \delta_{s_{n_i}^i,1} \ . \tag{4.3.4}$$

and set

$$f_N(\varpi) = \varpi^{-1} \tag{4.3.5}$$

for the external edge of the reference field at the top of the plane rooted tree. Thereby we have now set up all the necessary notation that is needed to construct the relevant scaling limits of the N-site Gaudin model.

We can now move on to the main result of this section, namely how to reconstruct the vertex Hamiltonians $\mathcal{H}_\rho^{(p)}(z)$ of the 3-site Gaudin model of the previous section from the N-site Hamiltonians $\mathcal{H}^{(p)}(z) = \mathcal{H}^{(p)}(z, w_i)$. To this end, we will first construct the vertex Lax matrices (4.2.12) from the Lax matrix (4.3.1) before studying the associated Hamiltonians (5.1.11) in the limit. As it turns out, we can recover the parameter free Lax matrix $\mathcal{L}^\rho$ that is associated with the vertex ρ as

$$\mathcal{L}_\alpha^\rho(z) = \frac{\mathcal{T}_\alpha^{(I_{\rho,1})}}{z} + \frac{\mathcal{T}_\alpha^{(I_{\rho,2})}}{z-1} = \lim_{\varpi \to 0} \ \varpi^{n_\rho} \mathcal{L}_\alpha\big(\varpi^{n_\rho} z + g_\rho(\varpi), w_i = f_i(\varpi)\big) \ . \tag{4.3.6}$$

Let us note that in the limit, the site $w_N = \varpi^{-1}$ associated with the reference field N goes to infinity, while the sites of the other external fields approach $z = 0$ or $z = 1$ depending on whether they are located at the right or left branch of the the plane rooted tree, i.e. whether their binary sequence s^ρ starts with $s_1^\rho = 1$ or $s_1^\rho = 2$. We shall prove eq. (4.3.6) in the third Subsection 4.3.3 through a recursive procedure that will also offer insight into the construction of the polynomials g_ρ and f_i.

Let us now turn to the limit construction for the Gaudin Hamiltonians. We claim that the Hamiltonians $\mathcal{H}^{(p)}(z, w_i)$ of the N-sites Gaudin model give rise to the Hamiltonians $\mathcal{H}_\rho^{(p)}(z)$ of the different 3-sites vertex Gaudin models defined in Section 4.2.2 as

$$\mathcal{H}_\rho^{(p)}(z) = \lim_{\varpi \to 0} \varpi^{p n_\rho} \mathcal{H}^{(p)}\big(\varpi^{n_\rho} z + g_\rho(\varpi), w_i = f_i(\varpi)\big) \ . \tag{4.3.7}$$

The fact that this statement holds for the leading part of the Hamiltonians, without quantum corrections, follows directly from the corresponding limit (4.3.6) of the Lax matrix

$$\varpi^{pn_\rho}\kappa_p^{\alpha_1\cdots\alpha_p}\mathcal{L}_{\alpha_1}\big(\varpi^{n_\rho}z+g_\rho(\varpi)\big)\cdots\mathcal{L}_{\alpha_p}\big(\varpi^{n_\rho}z+g_\rho(\varpi)\big)\xrightarrow{\varpi\to 0}\kappa^{\alpha_1\cdots\alpha_p}\mathcal{L}^\rho_{\alpha_1}(z)\cdots\mathcal{L}^\rho_{\alpha_p}(z)\ .$$

But it requires a bit of work to argue that the quantum corrections also have the required behaviour under the limit. Consider a term of the form (4.2.9) in the correction: by appropriately distributing the powers ϖ^{pn_ρ}, using the fact that $r_1+\cdots+r_q=p$, and performing the change of spectral parameter $z\mapsto z'_\rho(\varpi)=\varpi^{n_\rho}z+g_\rho(\varpi)$ in the derivatives, we find that

$$\begin{aligned}
&\varpi^{pn_\rho}\tau^{\alpha_1\cdots\alpha_q}\,\partial^{r_1-1}_{z'_\rho(\varpi)}\mathcal{L}_{\alpha_1}\big(z'_\rho(\varpi)\big)\cdots\partial^{r_q-1}_{z'_\rho(\varpi)}\mathcal{L}_{\alpha_q}\big(z'_\rho(\varpi)\big)\\
&\quad=\quad\tau^{\alpha_1\cdots\alpha_q}\partial_z^{r_1-1}\Big(\omega^{n_\rho}\mathcal{L}_{\alpha_1}\big(\varpi^{n_\rho}z+g_\rho(\varpi)\big)\Big)\cdots\partial_z^{r_q-1}\Big(\omega^{n_\rho}\mathcal{L}_{\alpha_q}\big(\varpi^{n_\rho}z+g_\rho(\varpi)\big)\Big)\\
&\xrightarrow{\varpi\to 0}\quad\tau^{\alpha_1\cdots\alpha_q}\,\partial_z^{r_1-1}\mathcal{L}^\rho_{\alpha_1}(z)\cdots\partial_z^{r_q-1}\mathcal{L}^\rho_{\alpha_q}(z),
\end{aligned}$$

such that this correction term reduces in the OPE limit to the corresponding correction in $\mathcal{H}^{(p)}_\rho(z)$. As the vertex operators $\mathcal{D}^{p,\nu}_\rho$ and the Casimir operators $\mathcal{D}^p_r$ of the intermediate fields attached to the vertex ρ are naturally extracted from the Hamiltonian $\mathcal{H}^{(p)}_\rho(z)$, the property (4.3.7) shows that the full set of operators defined in Section 4.1 can be obtained from the limit of the N-sites Gaudin model considered here. Before the limit $\varpi\to 0$, The commutativity property (4.2.8) of the N-site Gaudin Hamiltonians can be written as

$$\Big[\mathcal{H}^{(p)}\big(\varpi^{n_\rho}z+g_\rho(\varpi)\big),\mathcal{H}^{(q)}\big(\varpi^{n_\rho}w+g_\rho(\varpi)\big)\Big]=0,\qquad\forall\, z,w\in\mathbb{C},\quad\forall\, p,q,\quad\forall\,\rho,\rho'.\tag{4.3.8}$$

for arbitrary ϖ, and is therefore preserved in the limit $\varpi\to 0$,

$$\big[\mathcal{H}^{(p)}_\rho(z),\mathcal{H}^{(q)}_{\rho'}(w)\big]=0,\qquad\forall\, z,w\in\mathbb{C},\quad\forall\, p,q,\quad\forall\,\rho,\rho'.\tag{4.3.9}$$

This provides an alternative proof of the commutativity of all Casimir operators $\mathcal{D}^p_r$ and vertex operators $\mathcal{D}^{p,\nu}_\rho$. Moreover, this statement now holds without needing to use conformal Ward identities. The proof relies on a specific choice of labeling of the edges at vertices, given by a plane rooted tree representation of the OPE diagram. Different such representations of the diagram correspond to different limits of the same underlying N-sites Gaudin model and give rise to different sets of commuting operators, which however generate the same algebra when acting on solutions of the conformal Ward identities. Finally, let us note that the above construction automatically ensures the compatibility of these operators with the conformal Ward identities, since taking appropriate limits of eq. (4.3.2) demonstrates that they commute with the diagonal conformal generators $\mathcal{T}^{(N)}_\alpha$.

4.3.2 Examples

Before we prove our main result, let us illustrate the construction of the operators from limits of Gaudin models with two examples. The first one addresses the so-called comb channel OPE diagrams for which we have already outlined the limit in [62]. The second example deals with the snowflake OPE channel of the $N=6$-point function.

Comb channel. Let us consider the comb channel OPE diagram with N external fields. To apply the construction of the present section, we first need to pick a plane rooted tree representation of this diagram. We will choose to represent it with all internal edges pointing towards the bottom left. We

then label the external edges of the tree as follows: we let N be the top edge of the tree, 1 be edge furthest to the left and label by $2, \cdots, N-1$ the external edges pointing to the bottom right at each vertex, from the bottom to the top. Moreover, following our conventions in [62], we enumerate the vertices $\rho = [r]$ by an integer $r = 1, \ldots, N-2$, from bottom to top. We represent this plane rooted tree in Figure 21 below, with external edges indicated in black and vertices in blue. One can compute

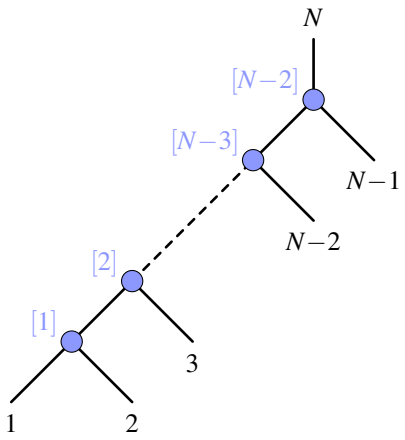

Figure 21: Choice of plane rooted tree representation of the comb channel OPE diagram with N points.

the limit of the Gaudin model associated with this tree using the construction outlined in the previous subsection. For the polynomials f_i that determine the parameters w_i of the Gaudin model, one finds from eq. (4.3.4) that

$$w_i = f_i(\varpi) = \varpi^{N-1-i}, \qquad \forall\, i \in \{1, \cdots, N\}\ . \tag{4.3.10}$$

Let us now consider the vertices $\rho = [r]$, with $r = 1, \ldots, N-2$. From the general construction, and formula (4.3.3) in particular, we find

$$n_{[r]} = N - 2 - r \qquad \text{and} \qquad g_{[r]}(\varpi) = 0, \qquad \forall\, r \in \{1, \cdots, N-2\}\ . \tag{4.3.11}$$

Note in particular that for this choice of plane rooted tree, the polynomial functions g_ρ are all zero, since all vertices $\rho = [r]$ sit on the most left branch of the tree. The limit of the Gaudin Lax matrix

$$\mathcal{L}_\alpha(z, w_i = f_i(\varpi)) = \sum_{i=1}^{N} \frac{\mathcal{T}_\alpha^{(i)}}{z - \varpi^{N-1-i}} \tag{4.3.12}$$

associated with the vertex $[r]$ then reads

$$\varpi^{N-2-r}\mathcal{L}_\alpha\big(\varpi^{N-2-r} z\big) \xrightarrow{\varpi \to 0} \mathcal{L}_\alpha^{[r]}(z) = \frac{\mathcal{T}_\alpha^{(1)} + \cdots + \mathcal{T}_\alpha^{(r)}}{z} + \frac{\mathcal{T}^{(r+1)}}{z-1}. \tag{4.3.13}$$

In sum, the vertex Gaudin Hamiltonians of the comb channel OPE limit are

$$\varpi^{p(N-2-r)}\mathcal{H}^{(p)}\big(\varpi^{N-2-r} z\big) \xrightarrow{\varpi \to 0} \mathcal{H}_{[r]}^{(p)}(z). \tag{4.3.14}$$

The above limit coincides exactly with the one introduced in [62] to describe the comb channel, thus showing that the results of [62] are contained in the more general construction discussed here.

Snowflake channel. The results of the present article allow us to discuss more general topologies of OPE diagrams than the comb channel. The first example of such a topology is the snowflake channel of 6-point functions. We represent this OPE diagram as a plane rooted tree following the conventions of Figure 22, where the external edges are labeled in black from 1 to 6 and the vertices are labeled in blue from [1] to [4]. Note in particular that the internal vertex of the diagram corresponds here to the label [3]. We can immediately read off the depth of the four vertices as

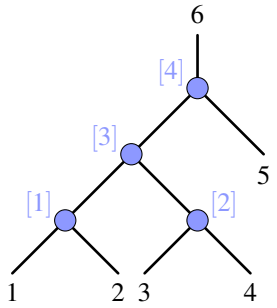

Figure 22: Choice of plane rooted tree representation of the snowflake OPE diagram.

$$n_{[1]} = n_{[2]} = 2, \qquad n_{[3]} = 1, \qquad n_{[4]} = 0. \tag{4.3.15}$$

We can now encode the positions of all four vertices in a binary sequence and apply the formulas (4.3.3) to construct the polynomials g_ρ, yielding

$$g_{[1]}(\varpi) = g_{[3]}(\varpi) = g_{[4]}(\varpi) = 0 \qquad \text{and} \qquad g_{[2]}(\varpi) = \varpi. \tag{4.3.16}$$

Similarly, one can encode the five external edges at the bottom of the diagram in binary sequences and apply eq. (4.3.4) to determine the positions of the $N = 6$ sites,

$$w_1 = \varpi^3, \qquad w_2 = \varpi^2, \qquad w_3 = \varpi + \varpi^3, \qquad w_4 = \varpi + \varpi^2, \qquad w_5 = 1, \qquad w_6 = \frac{1}{\varpi}. \tag{4.3.17}$$

Inserting this parameterization of the complex parameters w_i in terms of ϖ back into the Lax matrix of the 6-sites Gaudin model, we obtain

$$\mathcal{L}_\alpha(z) = \frac{\mathcal{T}_\alpha^{(1)}}{z-\varpi^3} + \frac{\mathcal{T}_\alpha^{(2)}}{z-\varpi^2} + \frac{\mathcal{T}_\alpha^{(3)}}{z-\varpi-\varpi^3} + \frac{\mathcal{T}_\alpha^{(4)}}{z-\varpi-\varpi^2} + \frac{\mathcal{T}_\alpha^{(5)}}{z-1} + \frac{\varpi\,\mathcal{T}_\alpha^{(6)}}{\varpi\,z-1}. \tag{4.3.18}$$

Given this expression and our formulas for n_ρ and g_ρ, it is now straightforward to check the limits (4.3.6) for all four vertices,

$$\varpi^2\mathcal{L}_\alpha(\varpi^2 z) \xrightarrow{\varpi\to 0} \frac{\mathcal{T}_\alpha^{(1)}}{z} + \frac{\mathcal{T}_\alpha^{(2)}}{z-1}, \qquad \varpi^2\mathcal{L}_\alpha(\varpi^2 z+\varpi) \xrightarrow{\varpi\to 0} \frac{\mathcal{T}_\alpha^{(3)}}{z} + \frac{\mathcal{T}_\alpha^{(4)}}{z-1}, \tag{4.3.19}$$

$$\varpi\mathcal{L}_\alpha(\varpi z) \xrightarrow{\varpi\to 0} \frac{\mathcal{T}_\alpha^{(1)}+\mathcal{T}_\alpha^{(2)}}{z} + \frac{\mathcal{T}_\alpha^{(3)}+\mathcal{T}_\alpha^{(4)}}{z-1}, \qquad \mathcal{L}_\alpha(z) \xrightarrow{\varpi\to 0} \frac{\mathcal{T}_\alpha^{(1)}+\mathcal{T}_\alpha^{(2)}+\mathcal{T}_\alpha^{(3)}+\mathcal{T}_\alpha^{(4)}}{z} + \frac{\mathcal{T}_\alpha^{(5)}}{z-1}.$$

These indeed give the expected vertex Lax matrices $\mathcal{L}_\alpha^\rho = \mathcal{L}_\alpha^{[r]}$ for the vertices labeled by $r = 1, 2, 3, 4$. These two examples suffice to gain a first intuition into how we take limits of Gaudin models and thereby manage to embed the vertex Lax matrices into the full N-sites model. We will now explain the derivation of our results for general OPE diagrams.

4.3.3 Recursive proof of the limits

Subtrees. Our goal in this subsection is to prove that our limit construction is indeed able to recover all vertex Lax matrices, as we have claimed. Let us consider some OPE channel $\mathcal{C}$ represented by a plane rooted tree T. The approach that we follow is recursive. Let us consider the top vertex ρ_* of the tree, which is by construction attached to the external edge N. We denote by e' and e'' the left and right downward edges attached to ρ_* (which can correspond to either external or intermediate fields depending on the topology of the diagram). We can then see the tree T as being composed of the vertex ρ_* and of two (plane rooted) subtrees with reference edges e' and e'', which we will call T' and T'' respectively. In Figure 23 below, we illustrate the two subtrees obtained in the example of Figure 20. We will now prove that if the limit construction of Subsection 4.3.1 holds for the subtrees T' and

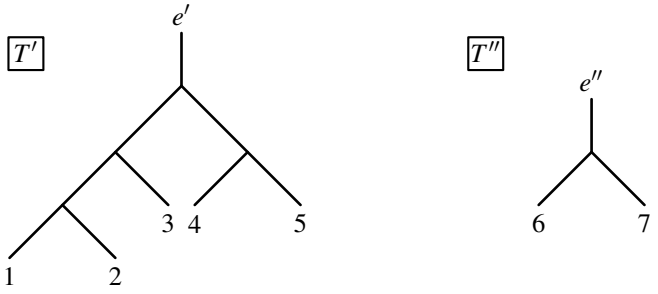

Figure 23: Subtrees of the tree 20.

T'', then it also holds for the initial tree T, thus proving that it holds for any tree by induction. Let us first introduce some useful notation. We will denote by E' and E'' the external edges of T that belong to the subtrees T' and T'' respectively. Note that if T' is not trivial, i.e. if e' is not an external edge of the initial tree T, then the full set of external edges of T' is $E' \cup \{e'\}$ (since e' is external in T' but not in T). On the other hand, if e' is external in T, then we simply have $E' = \{e'\}$ and the subtree T' is trivial. Let us also denote by V, V' and V'' the set of vertices of T, T' and T'', such that $V = V' \cup V'' \cup \{\rho_*\}$.

Recursion relations. Recall the polynomial $g_\rho(\varpi)$ defined in eq. (4.3.3) for any vertex $\rho \in V$ of T in terms of the binary sequence $s^\rho = (s^\rho_1, \cdots, s^\rho_{n_\rho})$. Let us suppose that this vertex is contained in the subtree T' and thus belongs to V': it is then associated with a binary sequence $s'^{\,\rho} = (s'^{\,\rho}_1, \cdots, s'^{\,\rho}_{n'_\rho})$ in T'. By construction, the depth n'_ρ of ρ in T' is given by $n_\rho - 1$. Moreover, it is clear that the binary sequence of ρ in T is related to that in T' by $s^\rho = (1, s'^{\,\rho}_1, \cdots, s'^{\,\rho}_{n_\rho - 1})$. Indeed, since ρ belongs to T', the path from ρ_* to ρ starts by going to the bottom left ($s^\rho_1 = 1$), and is then given by the path from e' to ρ, encoded by $s'^{\,\rho}$. It is then clear that the polynomial $g_\rho(\varpi)$ defined by eq. (4.3.3) is related to the corresponding polynomial $g'_\rho(\varpi)$ defined for T' by $g_\rho(\varpi) = \varpi\, g'_\rho(\varpi)$. Similarly, if ρ belongs to V'', we have $s^\rho = (2, s''^{\,\rho}_1, \cdots, s''^{\,\rho}_{n_\rho - 1})$ and thus $g_\rho(\varpi) = 1 + \varpi\, g''_\rho(\varpi)$. In conclusion, the polynomials $g_\rho(\varpi)$ satisfy the recursion relation

$$g_\rho(\varpi) = \begin{cases} \varpi g'_\rho(\varpi) & \text{if } \rho \in V', \\ 1 + \varpi g''_\rho(\varpi) & \text{if } \rho \in V'', \\ 0 & \text{if } \rho = \rho_*. \end{cases} \tag{4.3.20}$$

A similar analysis can be performed for the sites $w_i = f_i(\varpi)$ associated with the external edges $i \in \underline{N}$ through eq. (4.3.4), distinguishing three cases. If $i = N$ is the top reference edge, then we recall that $w_N = f_N(\varpi) = \varpi^{-1}$. If $i \in E'$ is an edge belonging to the subtree T', then one can relate the binary sequences s^i and s'^i describing i in T and T' in a similar way as for the vertices in the paragraph above. We then find that the polynomial $f_i(\varpi)$ satisfy the recursion relation

$$f_i(\varpi) = \begin{cases} \varpi & \text{if } e' \text{ is external in } T, \\ \varpi f'_i(\varpi) & \text{else.} \end{cases} \tag{4.3.21}$$

Note that in the first case, the subtree T' is trivial and the index i is then necessarily equal to e', while in the second case i is different from e' and the subtree T' is therefore non-trivial. Finally, if $i \in E''$ belongs to the subtree T'', then we similarly find

$$f_i(\varpi) = \begin{cases} 1 & \text{if } e'' \text{ is external in } T, \\ 1 + \varpi f''_i(\varpi) & \text{else.} \end{cases} \tag{4.3.22}$$

Here, $i = e''$ in the first case and $i \neq e''$ in the second one.

Induction hypotheses. We will now suppose that the limit procedure defined in Subsection 4.3.1 holds for the subtrees T' and T''. To phrase these induction hypotheses more precisely, let us focus first on the subtree T'. If it is non-trivial, i.e. if e' is not external in T, the external edges of T' are $E' \cup \{e'\}$. We then introduce the Gaudin Lax matrix associated with T' as

$$\mathcal{L}'_\alpha(z) = \sum_{i \in E' \cup \{e'\}} \frac{\mathcal{T}_\alpha^{(i)}}{z - f'_i(\varpi)}, \tag{4.3.23}$$

where the sites associated with the external edges $E' \cup \{e'\}$ are set to the positions $f'_i(\varpi)$ prescribed by the limit procedure of Subsection 4.3.1. Here, the generators $\mathcal{T}_\alpha^{(i)}$ associated with external fields $i \in E'$ are defined by their expression in the initial tree T, while the generators associated with e' are defined by $\mathcal{T}_\alpha^{(e')} = \mathcal{T}_\alpha^{(\underline{N} \setminus E')}$. By construction, the latter satisfy the commutation relations of $\mathfrak{g}$ and commute with the other generators $\mathcal{T}_\alpha^{(i)}$, $i \in E'$, as required. Moreover, this definition ensures that the diagonal conformal generators $\sum_{i \in \underline{N}} \mathcal{T}_\alpha^{(i)}$ of the tree T coincides with the ones $\sum_{i \in E' \cup \{e'\}} \mathcal{T}_\alpha^{(i)}$ of T' (however, as we will see, the definition of $\mathcal{T}_\alpha^{(e')}$ is in fact irrelevant for the recursive proof).
As T' is assumed to be non-trivial here, its vertex set V' is non-empty. The induction hypothesis that we make in this subsection is then that eq. (4.3.6) holds for the subtree T', that is to say

$$\mathcal{L}^\rho_\alpha(z) = \frac{\mathcal{T}_\alpha^{(I_{\rho,1})}}{z} + \frac{\mathcal{T}_\alpha^{(I_{\rho,2})}}{z-1} = \lim_{\varpi \to 0} \varpi^{n'_\rho} \mathcal{L}'_\alpha\big(\varpi^{n'_\rho} z + g'_\rho(\varpi)\big), \qquad \forall \rho \in V'. \tag{4.3.24}$$

In this equation, we used the Lax matrix $\mathcal{L}^\rho_\alpha(z)$ associated with the vertex ρ as defined in the initial tree T: indeed, it is clear that this vertex Lax matrix coincides with the one associated with ρ in the subtree T' (in particular, the subsets of external edges $I_{\rho,1}$ and $I_{\rho,2}$ associated with the left and right branches of ρ are the same when defined for T as when defined for T').
Similarly, if T'' is non-trivial, we consider the associated Lax matrix

$$\mathcal{L}''_\alpha(z) = \sum_{i \in E'' \cup \{e''\}} \frac{\mathcal{T}_\alpha^{(i)}}{z - f''_i(\varpi)}, \tag{4.3.25}$$

and suppose that it satisfies the induction hypothesis

$$\mathcal{L}^\rho_\alpha(z) = \frac{\mathcal{T}_\alpha^{(I_{\rho,1})}}{z} + \frac{\mathcal{T}_\alpha^{(I_{\rho,2})}}{z-1} = \lim_{\varpi \to 0} \varpi^{n''_\rho} \mathcal{L}''_\alpha\big(\varpi^{n''_\rho} z + g''_\rho(\varpi)\big), \qquad \forall \rho \in V''. \tag{4.3.26}$$

Proof of the induction. We are now in a position to prove that the induction carries from the subtrees T' and T'' to T. For that, we will show that the limit (4.3.6) holds for every vertex $\rho \in V$, with three cases to distinguish. If $\rho \in V'$ belongs to the subtree T', we will use the induction hypothesis (4.3.24) and the recursion relations (4.3.20), first case, and (4.3.21). Similarly, if $\rho \in V''$ belongs to T'', we will use the induction hypothesis (4.3.26) and the recursion relations (4.3.20), second case, and (4.3.22). Finally, if ρ is the reference vertex ρ_*, then the limit will follow without having to use any induction hypothesis. As these proofs are rather technical, we gather them in Appendix 4.A.

4.4 Example: five-point conformal blocks

As an example of our construction of commuting differential operators, let us consider a correlator of five scalar fields

$$\langle \phi_1 \phi_2 \phi_3 \phi_4 \phi_5 \rangle \tag{4.4.1}$$

and fix the OPE decomposition as in Figure 15. This correlator can be be written schematically as

$$\langle \phi_1 \phi_2 \phi_3 \phi_4 \phi_5 \rangle = \Omega_5^{(\Delta_i)}(x_i) \psi^{(\Delta_i)}(u_1, \dots, u_5) \tag{4.4.2}$$

where $\Omega_5^{(\Delta_i)}(x_i)$ is a prefactor that takes into account the covariance of the correlator with respect to conformal transformations, while $\psi^{(\Delta_i)}(u_1, \dots, u_5)$ is a conformally invariant function which depends on five cross ratios and admits a conformal block decomposition. In order to obtain differential equations for 5-point conformal blocks, one first needs to determine which Casimir and vertex operators characterize these blocks, and then compute their action on the space of cross ratios u_i.
For the OPE decomposition of Figure 15, the recipe of Section 4.2 instructs us to construct four Casimir operators, two for each internal leg

$$\mathcal{D}^2_{(12)} = (\mathcal{T}_1 + \mathcal{T}_2)_{[AB]} (\mathcal{T}_1 + \mathcal{T}_2)^{[BA]} , \tag{4.4.3}$$

$$\mathcal{D}^2_{(45)} = (\mathcal{T}_4 + \mathcal{T}_5)_{[AB]} (\mathcal{T}_4 + \mathcal{T}_5)^{[BA]} , \tag{4.4.4}$$

$$\mathcal{D}^4_{(12)} = (\mathcal{T}_1 + \mathcal{T}_2)_{[AB]} (\mathcal{T}_1 + \mathcal{T}_2)^{[BC]} (\mathcal{T}_1 + \mathcal{T}_2)_{[CD]} (\mathcal{T}_1 + \mathcal{T}_2)^{[DA]} , \tag{4.4.5}$$

$$\mathcal{D}^4_{(45)} = (\mathcal{T}_4 + \mathcal{T}_5)_{[AB]} (\mathcal{T}_4 + \mathcal{T}_5)^{[BC]} (\mathcal{T}_4 + \mathcal{T}_5)_{[CD]} (\mathcal{T}_4 + \mathcal{T}_5)^{[DA]} , \tag{4.4.6}$$

and one vertex operator

$$\mathcal{D}^{4,3}_{\rho,(12)3} = (\mathcal{T}_1 + \mathcal{T}_2)_{[AB]} (\mathcal{T}_1 + \mathcal{T}_2)^{[BC]} (\mathcal{T}_1 + \mathcal{T}_2)_{[CD]} (\mathcal{T}_3)^{[DA]} . \tag{4.4.7}$$

Note that – in agreement with the general recipe – the vertex operator is not uniquely defined and (5.3.17) can be shifted by terms proportional to $(\mathcal{T}_1 + \mathcal{T}_2)^2 (\mathcal{T}_3)^2$ or to the Casimir operators.[3]
To make explicit computations, we will use the embedding space formalism of [89], with which one can efficiently compute the action of the differential operators in cross ratio space; we briefly review this formalism in Appendix 4.B. Note here that the dimension of spacetime only appears in our computations as a parameter when contracting Kronecker deltas $\delta^A_A = d + 2$, and can be therefore kept generic. The first step is the choice of prefactor $\Omega_5^{(\Delta_i)}$ and cross ratios u_i. We chose to use the same conventions as [46], where the author computed 5-point blocks in the case of scalar exchange;

[3] In [62], we had picked the more symmetric expression $(\mathcal{T}_1 + \mathcal{T}_2 - \mathcal{T}_3)^4$ for the vertex operator, which leads to an equivalent set of operators.

the expression for $\Omega_5^{(\Delta_i)}$ in physical space coordinates can be easily translated into one in embedding space through the simple relation

$$-2X_i \cdot X_j = (x_i - x_j)^2 \,, \tag{4.4.8}$$

and one obtains (up to an overall normalization) the prefactor

$$\Omega_5^{(\Delta_i)} = \frac{\left(\frac{X_2\cdot X_3}{X_1\cdot X_3}\right)^{\frac{\Delta_1-\Delta_2}{2}} \left(\frac{X_2\cdot X_4}{X_2\cdot X_3}\right)^{\frac{\Delta_3}{2}} \left(\frac{X_3\cdot X_5}{X_3\cdot X_4}\right)^{\frac{\Delta_4-\Delta_5}{2}}}{(X_1\cdot X_2)^{\frac{\Delta_1+\Delta_2}{2}} (X_3\cdot X_4)^{\frac{\Delta_3}{2}} (X_4\cdot X_5)^{\frac{\Delta_4+\Delta_5}{2}}} \,. \tag{4.4.9}$$

Regarding the cross ratios, it is natural to build four of these using the same construction of the standard 4-point cross ratios (u, v) introduced in [29], but supported on two different sets of points

$$\begin{aligned} u_1 &= \frac{(X_1\cdot X_2)\,(X_3\cdot X_4)}{(X_1\cdot X_3)\,(X_2\cdot X_4)} \,, & u_2 &= \frac{(X_1\cdot X_4)\,(X_2\cdot X_3)}{(X_1\cdot X_3)\,(X_2\cdot X_4)} \,, \\ u_3 &= \frac{(X_2\cdot X_3)\,(X_4\cdot X_5)}{(X_2\cdot X_4)\,(X_3\cdot X_5)} \,, & u_4 &= \frac{(X_2\cdot X_5)\,(X_3\cdot X_4)}{(X_2\cdot X_4)\,(X_3\cdot X_5)} \,, \end{aligned} \tag{4.4.10}$$

while an interesting choice for the fifth cross ratio is

$$u_5 = \frac{(X_1\cdot X_5)\,(X_2\cdot X_3)\,(X_3\cdot X_4)}{(X_2\cdot X_4)\,(X_1\cdot X_3)\,(X_3\cdot X_5)} \,. \tag{4.4.11}$$

In comparison with a potentially more natural parameterization using five independent 4-point cross ratios, as in e.g. [49, 66], this parameterization of cross ratio space has the advantage of presenting all of our differential operators with polynomial coefficients in the u_i.
Using the scalar representation (3.1.9) for generators in the embedding space, the operators (5.3.13)–(5.3.17) can be easily expressed as objects $D_{(X_i)}$ acting on the coordinates X_i^A. To obtain their action on the space of cross ratios $\mathcal{D}_{(u_i)}$, one simply conjugates the $D_{(X_i)}$ by the prefactor as follows

$$\mathcal{D}_{(u_i)} F(u_1, \ldots, u_5) = \frac{1}{\Omega_5^{(\Delta_i)}} D_{(X_i)} \left(\Omega_5^{(\Delta_i)} F(u_1, \ldots, u_5)\right) \,. \tag{4.4.12}$$

In practical terms, the RHS above is expressed in terms of the generators (3.1.9), the expressions (5.3.9)–(4.4.11) of $\Omega_5^{(\Delta_i)}$, and the u_i's in terms of scalar products. The LHS is then obtained by solving (4.4.10–4.4.11) for five different scalar products and substituting them in the RHS after the conjugation has been done; the remaining scalar products will drop out and the final answer for the LHS will be expressed only in terms of the cross ratios.
To implement this procedure more concretely, we attach to this publication a Mathematica notebook[4], where we present the explicit computation of the quadratic Casimirs, as well as the final expressions one gets for the fourth-order Casimirs and the vertex operator (5.3.17) by trivially extending the same algorithm.

As an attempt to simplify the analytic expressions for the differential equations, it is natural to try to extend the 4-point change of coordinates of Dolan and Osborn [30, 95]

$$u = z\bar{z} \,, \qquad v = (1-z)(1-\bar{z}) \tag{4.4.13}$$

[4]part of this Mathematica code is based on the one written by J. Penedones for the 2013 edition of the Mathematica Summer School in Theoretical Physics: http://msstp.org/?q=node/285.

to the 5-point case. A very good candidate for this purpose is the change of coordinates

$$\begin{aligned} u_1 &= z_1\bar{z}_1\,, \qquad u_2 = (1-z_1)(1-\bar{z}_1)\,, \\ u_3 &= z_2\bar{z}_2\,, \qquad u_4 = (1-z_2)(1-\bar{z}_2)\,, \\ u_5 &= w(z_1-\bar{z}_1)(z_2-\bar{z}_2) + (1-z_1-z_2)(1-\bar{z}_1-\bar{z}_2)\,, \end{aligned} \tag{4.4.14}$$

which leads to the simplest expressions for the quadratic Casimirs that we could find. Indeed, by introducing the notation

$$\epsilon = \frac{d-2}{2}\,, \tag{4.4.15}$$

$$a = \frac{\Delta_1-\Delta_2}{2}\,, \qquad \tilde{a} = \frac{\Delta_5-\Delta_4}{2}\,, \qquad b = -\frac{\Delta_3}{2}\,, \tag{4.4.16}$$

$$U_i^{(k)} = z_i^k\partial_{z_i} - \bar{z}_i^k\partial_{\bar{z}_i} \tag{4.4.17}$$

$$V_{i,j} = \frac{z_i\bar{z}_i}{z_i-\bar{z}_i}\left(U_i^{(0)} - U_i^{(1)} + \frac{1}{z_i-\bar{z}_i}\left(1 + w(z_i+\bar{z}_i-2) + \frac{z_i\bar{z}_j - z_j\bar{z}_i}{z_j-\bar{z}_j}\right)\partial_w\right) \tag{4.4.18}$$

$$W_{i,j} = \frac{z_j+\bar{z}_j}{z_j-\bar{z}_j}U_i^{(2)} + \frac{2z_i\bar{z}_i}{z_i-\bar{z}_i}U_j^{(1)} + \frac{2z_i\bar{z}_i}{z_i-\bar{z}_i}\left(\frac{1}{z_i-\bar{z}_i} - w\frac{z_j+\bar{z}_j}{z_j-\bar{z}_j} + \frac{z_i\bar{z}_j - z_j\bar{z}_i}{(z_i-\bar{z}_i)(z_j-\bar{z}_j)}\right)\partial_w \tag{4.4.19}$$

and the expression for the $d=1$ quadratic Casimirs

$$D^{(a,b)}_{z_1,z_2} = z_1^2(1-z_1)\partial_{z_1}^2 - (a+b+1)z_1^2\partial_{z_1} - abz_1 - z_1^2z_2\partial_{z_1}\partial_{z_2} - az_1z_2\partial_{z_2} \tag{4.4.20}$$

one obtains the following compact expressions for the quadratic Casimirs in arbitrary dimension[5]

$$\mathcal{D}^2_{(12)} = D^{(a,b)}_{z_1,z_2} + D^{(a,b)}_{\bar{z}_1,\bar{z}_2} + 2\epsilon V_{1,2} + w(1-w)\frac{(z_2-\bar{z}_2)^{1+a}}{(z_1-\bar{z}_1)^a}W_{1,2}\frac{(z_1-\bar{z}_1)^a}{(z_2-\bar{z}_2)^{1+a}}\partial_w + \frac{w}{(z_1\bar{z}_1)^a}U_1^{(2)}(z_1\bar{z}_1)^aU_2^{(1)}\,, \tag{4.4.21}$$

$$\mathcal{D}^2_{(45)} = D^{(\tilde{a},b)}_{z_2,z_1} + D^{(\tilde{a},b)}_{\bar{z}_2,\bar{z}_1} + 2\epsilon V_{2,1} + w(1-w)\frac{(z_1-\bar{z}_1)^{1+\tilde{a}}}{(z_2-\bar{z}_2)^{\tilde{a}}}W_{2,1}\frac{(z_2-\bar{z}_2)^{\tilde{a}}}{(z_1-\bar{z}_1)^{1+\tilde{a}}}\partial_w + \frac{w}{(z_2\bar{z}_2)^{\tilde{a}}}U_2^{(2)}(z_2\bar{z}_2)^{\tilde{a}}U_1^{(1)}\,. \tag{4.4.22}$$

We have also attempted similar types of factorizations for the quartic Casimirs and the vertex operator, in the spirit of the decomposition in equation (4.14) of [95]; so far to no great avail.

4.5 Outlook

In this work, we focused on correlation functions of N scalar representations of the conformal algebra $\mathfrak{so}(1,d+1)$, with applications to the higher point conformal bootstrap in mind. However, it is worth noting that this construction can be generalized in several directions, with applications both within and without of the conformal bootstrap

First off, the same methods apply to spinning representations of the conformal algebra. The counting of depths of representations at the internal legs and dependencies between vertex operators at vertices should follow an analysis similar to what we presented here for external scalars. In particular, for $N=4$, the corresponding vertex operators may provide a more systematic approach to organizing four-point and three-point tensor structures in the spinning conformal bootstrap.

[5] these expressions differ with what one would get from (5.3.13) and (5.3.14) by an overall factor of (-2).

More generally, these limits of Gaudin models apply in principle to any invariants in the tensor product of N unitary, irreducible representations $(\pi_i, \mathbb{V}_i)_{i=1}^N$ of a Lie algebra $\mathfrak{g} = \mathrm{Lie}(G)$, where the generators act as linear operators $\mathcal{T}_\alpha^{(i)}$ at each point. In this broader context, two-point invariants are also fixed up to a constant normalization, owing to an orthogonality result from group theory,

$$(\mathbb{V}_1 \otimes \mathbb{V}_2)^G \cong \begin{cases} \mathbb{C} & \text{if} \quad \rho_1^\dagger \cong \rho_2, \\ 0 & \text{otherwise.} \end{cases} \tag{4.5.1}$$

Thus, the conformal block decomposition generalizes to a decomposition of the space of N-point invariants $(\mathbb{V}_1 \otimes \cdots \otimes \mathbb{V}_N)^G$ into a direct sum of spaces of three-point invariants $(\mathbb{V}_{r_{\rho 1}} \otimes \mathbb{V}_{r_{\rho 2}} \otimes \mathbb{V}_{r_{\rho 3}})^G$, depicted by a binary rooted trees with vertices ρ and internal legs r. Then Casimir operators measure the representations π_r appearing in direct sum decompositions of the tensor products, while the vertex operators measure a basis of three-point invariants at each vertex.
In theories with a continuous global symmetry group $\mathfrak{g}$, it is common to consider N-point correlators of fields transforming in finite dimensional representations π_r of $\mathfrak{g}$. By contracting spin indices with polarization vectors, these representations can always be realized as homogeneous polynomials on which generators $\mathcal{T}_\alpha$ of $\mathfrak{g}$ act as first order differential operators[6] One can then decompose these N-point correlators into global symmetry channels by diagonalizing the corresponding Casimir and vertex operators of that channel.

4.A Proof of the induction in the limits of Gaudin models

In this appendix, we detail the induction in the proof of the limit procedure of Section 4.3. We thus refer to this section for notation and definitions. Our main goal is to show that for every vertex $\rho \in V$, the Lax matrix of the N-sites Gaudin model satisfies the limit (4.3.6). For the purposes of this appendix, it will be useful to rewrite this limit as

$$\varpi^{n_\rho} \mathcal{L}_\alpha\big(h_\rho(z,\varpi)\big) \xrightarrow{\varpi \to 0} \mathcal{L}_\alpha^\rho(z) = \frac{\mathcal{T}_\alpha^{(I_{\rho,1})}}{z} + \frac{\mathcal{T}_\alpha^{(I_{\rho,2})}}{z-1}, \tag{4.A.1}$$

where we introduced

$$h_\rho(z,\varpi) = \varpi^{n_\rho} z + g_\rho(\varpi). \tag{4.A.2}$$

In the left-hand side of (4.A.1), and in all this appendix, we fix the sites w_i of the Gaudin model to their value $w_i = f_i(\varpi)$ prescribed by the limit procedure of Subsection 4.3.1. Recall that ρ is either the reference vertex ρ_*, in V' or in V''. We will treat these three cases separately.

4.A.1 Reference vertex

Let us first consider the reference vertex ρ_*. The definition of n_{ρ_*} and g_{ρ_*} made in Subsection 4.3.1 can be simply rewritten as

$$n_{\rho_*} = 0 \qquad \text{and} \qquad h_{\rho_*}(z,\varpi) = z. \tag{4.A.3}$$

We then have

$$\varpi^{n_{\rho_*}} \mathcal{L}_\alpha\big(h_{\rho_*}(z,\varpi)\big) = \mathcal{L}_\alpha(z) = \sum_{i=1}^N \frac{\mathcal{T}_\alpha^{(i)}}{z - w_i}. \tag{4.A.4}$$

To proceed further, we decompose this sum over external edges $i \in \{1, \cdots, N\}$ into three parts.

[6] See appendix 2.A for an example of this construction with $N = 4$ and $\mathfrak{g} = \mathfrak{so}(d)$.

Contribution of the reference edge. The first part is the contribution from the reference edge N, with corresponding site $w_N = f_N(\varpi) = \varpi^{-1}$, according to eq. (4.3.5). It simply reads

$$\frac{\mathcal{T}_\alpha^{(N)}}{z - w_N} = \frac{\varpi\, \mathcal{T}_\alpha^{(N)}}{\varpi\, z - 1} \xrightarrow{\varpi \to 0} 0 \tag{4.A.5}$$

and thus does not contribute to the limit of (4.A.4) when $\varpi \to 0$.

Contribution of the subtree T'. The second part is the contribution from the subtree T' attached to e', for which we should distinguish the cases where e' is external or not. If e' is external (in which case T' is trivial and e' is the only contribution from this subtree), recall from the first case of eq. (4.3.21) that we then have $w_{e'} = f_{e'}(\varpi) = \varpi$, so that the contribution to (4.A.4) simply is

$$\frac{\mathcal{T}_\alpha^{(e')}}{z - \varpi} \xrightarrow{\varpi \to 0} \frac{\mathcal{T}_\alpha^{(e')}}{z}. \tag{4.A.6}$$

Note that as e' is external, we have $E' = \{e'\}$ so that the generators $\mathcal{T}_\alpha^{(e')}$ coincide with $\mathcal{T}_\alpha^{(E')}$.
If e' is intermediate in the initial diagram then the contribution from the subtree T' comes from the edges $i \in E' \subset \underline{N}$, with corresponding sites $w_i = f_i(\varpi) = \varpi\, f_i'(\varpi)$ as in the second line of eq. (4.3.21). By construction, the functions $f_i'(\varpi)$ associated with the external edges $i \in E'$ stay finite when $\varpi \to 0$: indeed, as we supposed T' non-trivial, the edges $i \in E'$ are not the reference edge e' of T' and are thus associated with polynomial functions $f_i'(\varpi)$. Thus, we get that the corresponding sites $w_i = \varpi\, f_i'(\varpi)$ in the initial tree tend to 0 when $\varpi \to 0$. In this limit, the contribution of this subtree T' to the sum (4.A.4) then simply becomes

$$\sum_{i \in E'} \frac{\mathcal{T}_\alpha^{(i)}}{z - w_i} \xrightarrow{\varpi \to 0} \frac{1}{z} \sum_{i \in E'} \mathcal{T}_\alpha^{(i)}. \tag{4.A.7}$$

To conclude, let us observe that the sum in the right-hand side of the above equation is by definition $\mathcal{T}_\alpha^{(E')}$. Combined with the eq. (4.A.6) and the discussion that followed it for the case where e' is external, we thus observe that in both cases e' external and internal, the contribution of the subtree T' in the limit $\varpi \to 0$ of eq. (4.A.4) is simply

$$\sum_{i \in E'} \frac{\mathcal{T}_\alpha^{(i)}}{z - w_i} \xrightarrow{\varpi \to 0} \frac{\mathcal{T}_\alpha^{(E')}}{z}. \tag{4.A.8}$$

Contribution of the subtree T''. A similar argument applies to the contribution of the right subtree T'', attached to e''. If the latter is external, this contribution is simply equal to

$$\frac{\mathcal{T}_\alpha^{(e'')}}{z - 1}, \tag{4.A.9}$$

since we then have $w_{e''} = 1$ – see the first line of eq. (4.3.22). If e'' is intermediate, the corresponding sites w_i, $i \in E''$, are given by the second line of eq. (4.3.22) and read $w_i = f_i(\varpi) = 1 + \varpi\, f_i''(\varpi)$, which thus tend to 1 when $\varpi \to 0$. In both cases, we find that the contribution to (4.A.4) is given by

$$\sum_{i \in E''} \frac{\mathcal{T}_\alpha^{(i)}}{z - w_i} \xrightarrow{\varpi \to 0} \frac{\mathcal{T}_\alpha^{(E'')}}{z - 1}, \tag{4.A.10}$$

where in the first case $\mathcal{T}_\alpha^{(E'')} = \mathcal{T}_\alpha^{(e'')}$ while in the second case $\mathcal{T}_\alpha^{(E'')}$ is a composite operator formed by the sum of $\mathcal{T}_\alpha^{(i)}$ for $i \in E''$.

Conclusion. Summing the contributions (4.A.5), (4.A.8) and (4.A.10) in the limit of eq. (4.A.4) when $\varpi \to 0$, we then find

$$\varpi^{n_{\rho_*}} \mathcal{L}_\alpha\big(h_{\rho_*}(z,\varpi)\big) \xrightarrow{\varpi\to 0} \frac{\mathcal{T}_\alpha^{(E')}}{z} + \frac{\mathcal{T}_\alpha^{(E'')}}{z-1}. \tag{4.A.11}$$

To conclude, we observe that the labeling of branches at vertices made in Subsection 4.3.1 using the plane rooted tree representation T of the diagram implies that $E' = I_{\rho_*,1}$ and $E'' = I_{\rho_*,2}$. This shows that the limit (4.A.1) is satisfied for the reference vertex ρ_*.

4.A.2 Vertices in V'.

Let us now consider the case of a vertex $\rho \in V'$ in the subtree attached to e'. Note that the existence of this vertex requires the subtree T' to be non-trivial and thus the edge e' to be intermediate in the initial diagram. The definition of n_ρ and the recursion relation for $g_\rho(\varpi)$ in the first line of eq. (4.3.20) can be rewritten as

$$n_\rho = n'_\rho + 1 \qquad \text{and} \qquad h_\rho(z,\varpi) = \varpi\, h'_\rho(z,\varpi), \tag{4.A.12}$$

where we have defined $h'_\rho(z,\varpi) = \varpi^{n'_\rho} z + g'_\rho(\varpi)$ as the equivalent of $h_\rho(z,\varpi)$ for the subtree T'. We thus have

$$\varpi^{n_\rho} \mathcal{L}_\alpha\big(h_\rho(z,\varpi)\big) = \varpi^{n'_\rho+1} \mathcal{L}_\alpha\big(\varpi\, h'_\rho(z,\varpi)\big) = \sum_{i=1}^{N} \frac{\varpi^{n'_\rho+1}\mathcal{T}_\alpha^{(i)}}{\varpi\, h'_\rho(z,\varpi) - w_i}. \tag{4.A.13}$$

We will once again separate this expression in three parts, coming from the contributions of the reference edge N and the two subtrees.

Contribution of the reference edge. Let us start with the edge N, with associated site $w_N = f_N(\varpi) = \varpi^{-1}$. Its contribution to (4.A.13) in the limit $\varpi \to 0$ is then given by

$$\frac{\varpi^{n'_\rho+1}\mathcal{T}_\alpha^{(N)}}{\varpi\, h'_\rho(z,\varpi) - w_N} = \frac{\varpi^{n'_\rho+2}\mathcal{T}_\alpha^{(N)}}{\varpi^2\, h'_\rho(z,\varpi) - 1} \xrightarrow{\varpi\to 0} 0. \tag{4.A.14}$$

Contribution of the subtree T''. Let us now consider the contribution coming from the subtree T'' attached to e''. If e'' is external in the initial tree T, then we simply have $w_{e''} = 1$ according to the first line of eq. (4.3.22) and the contribution to (4.A.13) is

$$\frac{\varpi^{n'_\rho+1}T_\alpha^{(e'')}}{\varpi\, h'_\rho(z,\varpi) - 1} \xrightarrow{\varpi\to 0} 0. \tag{4.A.15}$$

If e'' is initially intermediate, then the contribution comes from the external edges $i \in E'' \subset \underline{N}$ whose corresponding sites are given by the second line of eq. (4.3.22) to be $w_i = f_i(\varpi) = 1 + \varpi\, f''_i(\varpi)$. In particular, these tend to 1 when $\varpi \to 0$. Thus, in this case, the contribution of the subtree T'' to (4.A.13) also vanishes:

$$\sum_{i\in E''} \frac{\varpi^{n'_\rho+1}\mathcal{T}_\alpha^{(i)}}{\varpi\, h'_\rho(z,\varpi) - w_i} \xrightarrow{\varpi\to 0} 0. \tag{4.A.16}$$

Contribution of the subtree T'. Thus, the only non-vanishing contribution to (4.A.13) in the limit $\varpi \to 0$ comes from the subtree T' attached to e'. Recall that T' is non-trivial since it possesses a vertex ρ: the external edges $i \in E' \subset \underline{N}$ are thus different from e' and are associated with the sites

$w_i = f_i(\varpi) = \varpi f_i'(\varpi)$, according to the second line of eq. (4.3.21). The contribution of T' to (4.A.13) then reads

$$\sum_{i\in E'} \frac{\varpi^{n'_\rho+1}\mathcal{T}_\alpha^{(i)}}{\varpi\, h'_\rho(z,\varpi) - w_i} = \sum_{i\in E'} \frac{\varpi^{n'_\rho}\mathcal{T}_\alpha^{(i)}}{h'_\rho(z,\varpi) - f_i'(\varpi)}. \tag{4.A.17}$$

The Gaudin Lax matrix of the subtree T' (the one of the full tree, not the ones associated with vertices) is given by eq. (4.3.23) and thus can be rewritten as

$$\mathcal{L}'_\alpha(z) = \sum_{i\in E'} \frac{\mathcal{T}_\alpha^{(i)}}{z - f_i'(\varpi)} + \frac{\varpi\,\mathcal{T}_\alpha^{(e')}}{\varpi\, z - 1}, \tag{4.A.18}$$

where we used the fact that $f'_{e'}(\varpi) = \varpi^{-1}$ since e' is the reference edge of T'. Thus, we can rewrite the above contribution (4.A.17) as

$$\sum_{i\in E'} \frac{\varpi^{n'_\rho+1}\mathcal{T}_\alpha^{(i)}}{\varpi\, h'_\rho(z,\varpi) - w_i} = \varpi^{n'_\rho}\mathcal{L}'_\alpha\big(h'_\rho(z,\varpi)\big) - \frac{\varpi^{n'_\rho+1}\mathcal{T}_\alpha^{(e')}}{\varpi\, h'_\rho(z,\varpi) - 1}. \tag{4.A.19}$$

The second term vanishes in the limit $\varpi \to 0$. Moreover, by the induction hypothesis (4.3.24) for the subtree T', the first term tends to $\mathcal{L}^\rho_\alpha(z)$ in this limit. In conclusion, we thus get

$$\sum_{i\in E'} \frac{\varpi^{n'_\rho+1}\mathcal{T}_\alpha^{(i)}}{\varpi\, h'_\rho(z,\varpi) - w_i} \xrightarrow{\varpi\to 0} \mathcal{L}^\rho_\alpha(z). \tag{4.A.20}$$

Conclusion. Since the contribution (4.A.20) is the only non-vanishing term in the limit of eq. (4.A.13) when $\varpi \to 0$, we thus get in the end that

$$\varpi^{n_\rho}\mathcal{L}_\alpha\big(h_\rho(z,\varpi)\big) \xrightarrow{\varpi\to 0} \mathcal{L}^\rho_\alpha(z), \tag{4.A.21}$$

as required. This indeed shows that the limit (4.A.1) is satisfied for vertices $\rho \in V'$, using the induction hypothesis (4.3.24) that a similar property also holds in the subtree T'.

4.A.3 Vertices in V''

Let us finally consider a vertex $\rho \in V''$. The procedure here will resemble the one in the previous subsection so we will not describe it in detail. The definition of n_ρ and the recursion relation for $g_\rho(\varpi)$ in the second line of eq. (4.3.20) can be rewritten as

$$n_\rho = n''_\rho + 1 \qquad \text{and} \qquad h_\rho(z,\varpi) = 1 + \varpi\, h''_\rho(z,\varpi). \tag{4.A.22}$$

The main difference with the case of a vertex in V' is that we introduced a shift by 1 in the expression of $h_\rho(z,\varpi)$. The effect of this shift is that in the computation of the limit of $\varpi^{n_\rho}\mathcal{L}_\alpha\big(h_\rho(z,\varpi)\big)$ when $\varpi \to 0$, the only non-vanishing contribution now comes from the subtree T'' and not from T'. More precisely, using the fact that the shift by 1 cancels with the 1 in the recursive expression (4.3.22) of the sites w_i, $i \in E''$, we find in the end that

$$\lim_{\varpi\to 0} \varpi^{n_\rho}\mathcal{L}_\alpha\big(h_\rho(z,\varpi)\big) = \lim_{\varpi\to 0} \varpi^{n''_\rho}\mathcal{L}''_\alpha\big(h''_\rho(z,\varpi)\big) = \mathcal{L}^\rho_\alpha(z), \tag{4.A.23}$$

with $\mathcal{L}''_\alpha$ the Lax matrix (4.3.25) associated with the subtree T'', and where the last equality follows from the induction hypothesis (4.3.26) for the subtree T''. This then completes the proof of the induction.

4.B Proof of relations using embedding space formalism

4.B.1 Classical Embedding space

For the proof in appendix 4.C we are going to need a classical version of the embedding space formalism for the spinning fields introduced in section 3.1.1. For this purpose, we introduce P_A as the conjugate momentum to X^A, and Q^i_A as conjugate momenta of the auxiliary variables Z^A_i.
To see which constraints are imposed on these classical variables, one can check the action of the operators

$$X \cdot \frac{\partial}{\partial X}\,, \qquad X \cdot \frac{\partial}{\partial Z_i}\,, \qquad Z_i \cdot \frac{\partial}{\partial X}\,, \qquad Z_i \cdot \frac{\partial}{\partial Z_j} \tag{4.B.1}$$

on fields or correlation functions to get conditions that need to be satisfied by scalar products of coordinates and momenta. Some of the operators in (4.B.1) are in fact evaluated to constants on correlation functions. By imposing the same behavior when replacing derivatives with momenta, one obtains the following relations for phase space variables:

$$\begin{aligned} X^2 = Z_i^2 = Z_i \cdot Z_j = 0\,, \\ X \cdot Z_i = X \cdot Q_i = 0\,, \\ Z_i \cdot Q_j = 0 \quad \forall\, i < j\,, \\ X \cdot P = -\Delta\,, \quad Z_i \cdot Q_i = l_i\,. \end{aligned} \tag{4.B.2}$$

One can directly verify that the conditions (3.1.14), combined with the classical version

$$\bar{\mathcal{T}}_{[AB]} = X_A P_B + \sum_{i=1}^{L} Z_{i\,A} Q_{i\,B} - (A \leftrightarrow B) \tag{4.B.3}$$

of the generators (3.1.9), lead to the correct classical Casimirs associated to mixed-symmetry tensors:

$$\mathcal{C}as^{\,2p} = 2\Delta^{2p} + 2\sum_{i=1}^{L} l_i^{2p}\,. \tag{4.B.4}$$

4.C Relations among vertex differential operators

Our goal in this appendix is to justify the relations (4.2.23) and (4.2.24) for the total symbols of our vertex differential operators. There are many ways to derive these relations. Here we shall follow a more pedestrian approach that does not require much background from representation theory.
In order to derive the relations (4.2.23), (4.2.24) we first note that these were formulated in terms of the coordinates and momenta of the external scalar fields. The representation of the conformal algebra that is associated to the index set I decomposes into an infinite number of spinning representations. Each of the irreducible components can be prepared in embedding space formalism (see appendix 4.B). Here we shall study the relations (4.2.23) for a given irreducible component so that the coefficients $\varrho_{f,s}$ are functions of the associated weight and spins rather than functions of symbols of the Casimir differential operators.
After these introductory comments let us approach relation (4.2.23) by considering the simplest example in which the intermediate irreducible representation is scalar. We can construct explicitly the

first three matrices $(\bar{\mathcal{T}}^n)^A{}_B$[7] in the classical embedding space that we introduced in Appendix 4.B.1:

$$\begin{aligned}\left(\bar{\mathcal{T}}^1\right)^A{}_B &= X^A P_B - X_B P^A \\ \left(\bar{\mathcal{T}}^2\right)^A{}_B &= \Delta\left(X^A P_B + X_B P^A\right) - P^2 X^A X_B \\ \left(\bar{\mathcal{T}}^3\right)^A{}_B &= \Delta^2\left(X^A P_B - X_B P^A\right) = \Delta^2\left(\bar{\mathcal{T}}^1\right)^A{}_B .\end{aligned} \tag{4.C.1}$$

It is then clear that, when considering scalar representations, the powers of generators $\bar{\mathcal{T}}^n$ with $n \geq 3$ will be dependent on lower powers of the generators. This directly implies that any vertex operator of the type (4.2.21) that contains a power of a scalar generator higher than two will become dependent on operators of lower order, e.g.

$$\bar{\mathcal{T}}^3 \cdot \mathcal{B} \propto \bar{\mathcal{T}} \cdot \mathcal{B} . \tag{4.C.2}$$

We would now like to prove that something analogous to (4.C.1) is valid for representations of higher depth $\mathfrak{d}$ and higher powers, respectively. Let us then consider the generators for a mixed symmetry tensor of depth $\mathfrak{d}$,

$$\bar{\mathcal{T}}_{[AB]} = X_A P_B + \sum_{i=1}^{\mathfrak{d}-1} Z_{i\,A} Q_{i\,B} - (A \leftrightarrow B); \tag{4.C.3}$$

we expect the n-fold contractions of generators $\bar{\mathcal{T}}^n$ to be independent up to power $n = 2\mathfrak{d}$, with the first dependent object produced at power $n = 2\mathfrak{d}+1$. To prove this, let us focus on a specific matrix entry $(\bar{\mathcal{T}}^n)^A{}_B$ of the powers $\bar{\mathcal{T}}^n$ and construct the following submatrix of the Jacobian for fixed indices A, B and C:

$$\begin{pmatrix} \frac{\partial(\bar{\mathcal{T}}^1)^A{}_B}{\partial X^C} & \frac{\partial(\bar{\mathcal{T}}^1)^A{}_B}{\partial P^C} & \frac{\partial(\bar{\mathcal{T}}^1)^A{}_B}{\partial Z_1^C} & \frac{\partial(\bar{\mathcal{T}}^1)^A{}_B}{\partial Q_1^C} & \cdots & \frac{\partial(\bar{\mathcal{T}}^1)^A{}_B}{\partial Q_{\mathfrak{d}-1}^C} \\ \vdots & \vdots & \vdots & \vdots & & \vdots \\ \frac{\partial(\bar{\mathcal{T}}^{2\mathfrak{d}+1})^A{}_B}{\partial X^C} & \frac{\partial(\bar{\mathcal{T}}^{2\mathfrak{d}+1})^A{}_B}{\partial P^C} & \frac{\partial(\bar{\mathcal{T}}^{2\mathfrak{d}+1})^A{}_B}{\partial Z_1^C} & \frac{\partial(\bar{\mathcal{T}}^{2\mathfrak{d}+1})^A{}_B}{\partial Q_1^C} & \cdots & \frac{\partial(\bar{\mathcal{T}}^{2\mathfrak{d}+1})^A{}_B}{\partial Q_{\mathfrak{d}-1}^C} \end{pmatrix} . \tag{4.C.4}$$

If what we argued above holds, we should be able to see that some $2\mathfrak{d}$-minors of (4.C.4) are equal to zero, while the same matrix with the last row dropped out has all nonzero $2\mathfrak{d}$-minors. We checked this with Mathematica symbolically for the case of symmetric traceless tensors, and numerically for mixed symmetry tensors of depth $\mathfrak{d} \leq 6$, exhausting all tensorial representations that are allowed in the range of dimensions of known CFTs. One can use a similar reasoning to show eq. (4.2.24).

Let us finally comment on a more conceptual interpretation of the results of this appendix. We consider first the case of a scalar representation, whose generators can be gathered in the matrix $(\bar{\mathcal{T}}_f)^A{}_B = X^A P_B - X_B P^A$ in the fundamental representation. Using the relations $X^A X_A = 0$ and $X^A P_A = -\Delta$, one can show that the matrix $\bar{\mathcal{T}}_f$ is diagonalisable, with eigenvalues Δ, $-\Delta$ and 0 (with multiplicity d). It is a standard result of linear algebra that $\bar{\mathcal{T}}_f$ is then annihilated by the polynomial with simple roots equal to these eigenvalues, namely $T(T-\Delta)(T+\Delta) = T^3 - \Delta^2 T$: we recover this way that $\bar{\mathcal{T}}_f^3 = \Delta^2 \bar{\mathcal{T}}_f$.

A similar argument can be formulated for a representation with higher depth $\mathfrak{d} = L+1$, characterized by a weight Δ and L spins $l_1, \ldots, l_L$. The (symbols of the) generators of this representation are given by eq. (4.B.3) and can be gathered in a matrix $\bar{\mathcal{T}}_f$ valued in the fundamental representation. The traces of odd powers of $\bar{\mathcal{T}}_f$ vanish, while the traces of even powers are given by the classical Casimirs (4.B.4). These traces are the Newton sums $\sum_{i=1}^{d+2} \lambda_i^p$ of the eigenvalues $\lambda_1, \cdots, \lambda_{d+2}$ of $\bar{\mathcal{T}}_f$

[7] Here and in the discussion below we shall drop the subscript f.

and thus determine these eigenvalues uniquely (up to permutation). More precisely, we find that $\bar{\mathcal{T}}_f$ has eigenvalues $\Delta, -\Delta, l_1, -l_1, \dots, l_L, -l_L$ and 0 (with multiplicity $d-2L$). If we suppose that $\bar{\mathcal{T}}_f$ is diagonalizable, it is then annihilated by the polynomial with simple roots equal to these eigenvalues, hence

$$\bar{\mathcal{T}}_f\big(\bar{\mathcal{T}}_f^2-\Delta^2\big)\big(\bar{\mathcal{T}}_f^2-l_1^2\big)\cdots\big(\bar{\mathcal{T}}_f^2-l_L^2\big)=0. \tag{4.C.5}$$

This shows that the power $\bar{\mathcal{T}}_f^{2L+3}=\bar{\mathcal{T}}_f^{2\mathfrak{d}+1}$ is expressible in terms of lower power $\bar{\mathcal{T}}_f^n$, $n\leq 2\mathfrak{d}$, as expected. Let us finally note that the coefficients in the relation (4.C.5) are elementary symmetric polynomials in the variables $(\Delta^2, l_1^2, \dots, l_L^2)$: by the Newton identities, these coefficients are then also polynomials in the Newton sums $\Delta^{2p}+\sum_{i=1}^{L} l_i^{2p}$ and thus in the values (4.B.4) of the classical Casimirs. This ensures that the coefficients $\varrho_{f;AB}^{(n,m)}$ in eq. (4.2.23) are polynomials in the total symbols of the Casimir operators.

Chapter 5

Three-Point Vertex Integrable Systems

In chapter 4, we demonstrated that N-point blocks in (3.3.1) are eigenfunctions of a many-body quantum integrable system. The complete set of commuting differential operators splits into Casimir operators specifying the quantum numbers $(\Delta_r, \{l_{r\nu}\})_{r=1}^{N-3}$, and vertex operators specifying the tensor structures $(t_{n_\rho})_{\rho=1}^{N-2}$ in the OPE decomposition. The goal of this chapter is to determine explicitly which basis of tensor structures in the expansion (3.2.16) of the three-point functions is singled out by the vertex operators of the Gaudin model. More specifically, for scalar correlators, we will solve this problem in the case of five-point blocks, comb channel six-point blocks, and comb channel $N > 6$-point blocks when $d = 3, 4$. In all of these cases, the tensor structures are encoded in a compact way by one-variable polynomials $t_{n_\rho}(\mathcal{X}_\rho)$, where $\mathcal{X}_\rho$ is an example of the generalized cross ratios introduced in chapter 3. We can now state the main result of this chapter: the basis of tensor structures $t_n(\mathcal{X})$ measured by vertex operators are eigenfunctions of the elliptic $\mathbb{Z}_4$ Calogero-Moser integrable model, first written by Etingof, Felder, Ma and Veselov in [68, Eq. (4.3)].

5.1 Review and Summary of Results

The number of degrees of freedom a single vertex contributes depends on the spin of the three fields involved, as given in Eq. (3.2.3) and Eq. (3.2.4). In a scalar N-point function, the depth of the intermediate fields grows with the number of operator products that are required to construct them from scalars. More precisely, the spin depth of a link r in an OPE diagram is given by

$$L_r(\mathcal{C}^N_{OPE}, d) = L(I_{r,1}, d), \quad \textit{where} \quad L(I, d) = \textit{min}(|I|, N - |I|, \text{rank}_d) - 1 \ . \tag{5.1.1}$$

Here, rank_d denotes the rank of the d-dimensional conformal algebra, i.e. the dimension of its Cartan subalgebra. Let us now look at a particular vertex ρ in an OPE diagram in a d-dimensional conformal field theory. We call the ordered set $(L_{\rho,1}, L_{\rho,2}, L_{\rho,3})$ of depths $L_{\rho,k}$ of the three adjacent legs with $L_{\rho,1} \geq L_{\rho,2} \geq L_{\rho,3}$ the *type* of the vertex. This type determines the number of degrees of freedom that are associated with ρ according to the formula

$$n_{vdo,\rho}(\mathcal{C}^N_{OPE}, d) = n_{cr}(\sum_{k=1}^{3} L_{\rho,k} + 3, d) - \sum_{k=1}^{3} L_{\rho,k}(L_{\rho,k} + 1) \ . \tag{5.1.2}$$

Here, $n_{cr}(M,d)$ counts the total number of independent cross ratios of a scalar M-point function in d dimensions,

$$n_{cr}(M,d) = \begin{cases} \frac{1}{2}M(M-3) & M \leq d+2 \\ Md - \frac{1}{2}(d+2)(d+1) & M > d+2 \end{cases} . \tag{5.1.3}$$

As is well known, vertices ρ with two scalar legs do not contribute any degree of freedom, i.e. $n_{vdo,\rho} = 0$ for $L_{\rho,1} = 0 = L_{\rho,2}$. Vertices for which none of the legs are scalar are easily seen to have at least two degrees of freedom. Hence, vertices that possess a single degree of freedom must necessarily have one scalar leg. Namely,

$$(L_{\rho,1}, L_{\rho,2}, L_{\rho,3}) = \begin{cases} \text{I}: (1,1,0) & \textit{for } d \geq 3 \\ \text{II}: (2,1,0) & \textit{for } d \geq 4 \\ \text{III}: (2,2,0) & \textit{for } d = 4 \end{cases} . \tag{5.1.4}$$

Let us note that in $d \geq d_c = 5$ the vertex of type III possesses two degrees of freedom in supracritical

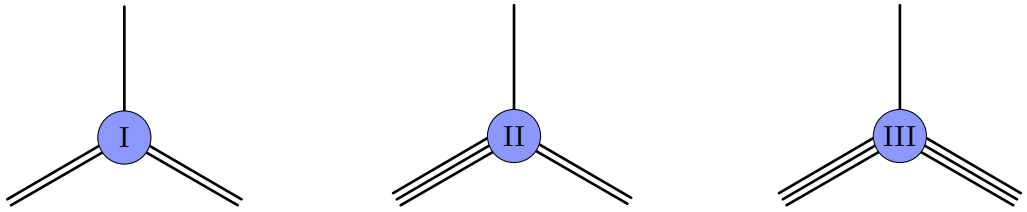

(a) STT-STT-scalar (b) MST_2-STT-scalar (c) MST_2-MST_2-scalar

Figure 24: Vertices with an associated one-dimensional space of tensor structures. Single-lined legs are scalars; double or triple lines correspond respectively to STT and MST_2 representations. For the type III vertex in Figure 24c, the space is two-dimensional and reduces to one dimension only in $d = 4$.

dimensions. The reduction to a single degree of freedom in $d = 4$ is therefore exceptional. In standard terms, type I vertices involve one scalar and two STTs, type II occur for one scalar, one STT and one Mixed-Symmetry Tensor (MST) of depth $L = 2$ while type III contain one scalar and two MSTs of depth $L = 2$. These three different types, depicted in Figure 24, exhaust all those vertices that can appear in the comb channel of scalar N-point functions in $d = 3$ and $d = 4$ dimensions. By definition, all vertices in the comb channel have at least one external leg which is scalar, i.e. has $L = 0$. Let us also note that for 5-point functions in any d the only non-trivial vertex is of type I, which is included in our list. Similarly, for 6-point functions in the comb channel one only needs vertices of type II. In this sense, the theory we are about to describe addresses some of the vertices that are most relevant for applications.

5.1.1 Reduction to vertex systems via shadow integrals

Higher point blocks can be explicitly related to the three-point functions at the vertices of their OPE diagram via the projectors (3.3.13) of the shadow formalism reviewed in Section 3.3.
Let us illustrate the procedure of shadow integral reduction in the case of five-point blocks, containing type I vertices. This example is simpler than the others, because the projectors only involve STT representations. However, a similar procedure can be carried out for more general spinning field propagating in the OPE. Now, in concomitance with the index-free approach used in (3.2.16) for

spinning three-point functions, we can rewrite the contraction of STT indices as the integral over polarization vectors given by the Bargmann-Todorov scalar product [84],

$$\mathcal{O}^{a_1\ldots a_l}(x)\mathcal{O}'_{a_1\ldots a_l}(x') = \int_{\mathbb{C}^d} \mathrm{d}^{2d}z\, \delta(z^2)\rho(\bar{z}\cdot z)\, \mathcal{O}(x,\bar{z})\mathcal{O}'(x',z), \tag{5.1.5}$$

$$\rho(t) = \left(\frac{2}{\pi}\right)^{d-1} \frac{(16t)^{1-d/4}}{\Gamma(d/2-1)} K_{(d/2-2)}(2\sqrt{t}), \tag{5.1.6}$$

where K is the modified Bessel function of the second kind. Inserting two projectors (3.3.13) in the five-point function, we then obtain

$$\begin{aligned}&\langle\phi_1(x_1)\phi_2(x_2)|\mathcal{O}_a|\phi_3(x_3)|\mathcal{O}_b|\phi_4(x_4)\phi_5(x_5)\rangle = \\ &\prod_{r=a,b}\int_{\mathcal{M}}\mathrm{d}^d x_r \int_{\mathbb{C}^d}\mathrm{d}^{2d}z_r\delta(z_s^2)\rho(\bar{z}_r\cdot z_r)\langle\phi_1(x_1)\phi_2(x_2)\tilde{\mathcal{O}}_a(x_a,\bar{z}_a)\rangle \\ &\qquad\times\langle\mathcal{O}_a(x_a,z_a)\phi_3(x_3)\mathcal{O}_b(x_b,z_b)\rangle\langle\tilde{\mathcal{O}}_b(x_b,\bar{z}_b)\phi_4(x_4)\phi_5(x_5)\rangle\ .\end{aligned} \tag{5.1.7}$$

Due to the conformal Ward identities of the three-point function, acting on the shadow integral with $\mathcal{T}_1(x_1,\partial_{x_1})+\mathcal{T}_2(x_2,\partial_{x_2})$ is equivalent to acting on the shadow integrand with $\mathcal{T}_a(x_a,\partial_{x_a},z_a,\partial_{z_a})$. The five-point vertex operator thus reduces to a three-point vertex operator

$$\begin{aligned}&\mathrm{tr}\,(\mathcal{T}_1+\mathcal{T}_2)^3\mathcal{T}_3\cdot\langle\phi_1(x_1)\phi_2(x_2)|\mathcal{O}_a|\phi_3(x_3)|\mathcal{O}_b|\phi_4(x_4)\phi_5(x_5)\rangle = \\ &\prod_{r=a,b}\int_{\mathcal{M}}\mathrm{d}^d x_r \int_{\mathbb{C}^d}\mathrm{d}^{2d}z_r\delta(z_r^2)\rho(\bar{z}_r\cdot z_r)\langle\phi_1(x_1)\phi_2(x_2)\tilde{\mathcal{O}}_a(x_a,\bar{z}_a)\rangle \\ &\qquad\times\mathrm{tr}\,\mathcal{T}_a^3\mathcal{T}_3\cdot\langle\mathcal{O}_a(x_a,z_a)\phi_3(x_3)\mathcal{O}_b(x_b,z_b)\rangle\langle\tilde{\mathcal{O}}_b(x_b,\bar{z}_b)\phi_4(x_4)\phi_5(x_5)\rangle.\end{aligned} \tag{5.1.8}$$

Once we descend to the level of three-point functions, we can realize the expansion (3.2.16) explicitly. We will thus construct a seed $\{e_1,\ldots,e_{n_s}\}$ with $n_s = 6,7,8$ in types I, II, III respectively, and with the same unique cross ratio $u_1 := \mathcal{X}$, in section 5.2. For example, in the case of type I vertices shown above,

$$\{e_1,\ldots,e_6\} = \{X_{12},X_{23},X_{13},J_{1,23},J_{2,31},H_{12}\},\quad \{u_1\} = \left\{\mathcal{X} = \frac{H_{12}X_{13}X_{23}}{J_{1,23}J_{2,31}}\right\}, \tag{5.1.9}$$

In this parameterization, the reduced vertex operator $\mathrm{tr}\,\mathcal{T}_a^3\mathcal{T}_3$ acts as the fourth order differential operator $H(\mathcal{X},\partial_{\mathcal{X}})$ in (5.3.3). Remarkably, this operator coincides exactly with the Hamiltonian of a $\mathbb{Z}_4$ Calogero-Moser model.

5.1.2 From Gaudin Hamiltonians to Lemniscatic CMS models

The Gaudin Hamiltonians [107–109] provide a complete set of commuting higher order differential operators on $\mathcal{M}$. The construction of these operators has been reviewed in [62, 63]. Here we shall content ourselves with a very brief review of the vertex system, see section 2 of [63]. A key ingredient in the construction of the Gaudin model is its so-called Lax matrix, whose components in the basis T^α of the conformal Lie algebra are defined as

$$\mathcal{L}^\rho_\alpha(w) = \sum_{k=1}^{3}\frac{\mathcal{T}^{(k)}_\alpha}{w-w_k}\,, \tag{5.1.10}$$

where w is an auxiliary complex variable called the spectral parameter and we can fix the three complex parameters w_k to be $w_1 = 0$, $w_2 = 1$ and $w_3 = \infty$. The symbols $\mathcal{T}_\alpha^{(k)}$ denote the first order differential operators that describe the action of the conformal algebra on the three spinning primaries at the vertex. We have placed a superscript ρ on the Lax matrix to emphasize that this is the matrix corresponding to the vertex ρ.

For any elementary symmetric invariant tensor κ_p of degree p on the conformal Lie algebra, there is a corresponding w-dependent Gaudin Hamiltonian [107–109]. Here we choose κ_p such that the Hamiltonian takes the form

$$\mathcal{H}_\rho^{(p)}(w) \;=\; str\Big(\mathcal{L}_{\alpha_1}^\rho(w)\cdots\mathcal{L}_{\alpha_p}^\rho(z)\Big) + \ldots, \tag{5.1.11}$$

where $\ldots$ represent quantum corrections, involving a smaller number of components of the Lax matrix. The construction involves a symmetrized trace prescription in some appropriate representation, see [63] for details. The analysis in subsection 2.3 of [63] shows that for the vertex systems in our list (5.1.4) there is only one such independent Hamiltonian and it is of order $p = 4$. Indeed we have argued there that the lower order operators are trivial while the higher order ones can be rewritten in terms of lower order operators. A non-trivial operator can be extracted from the family (5.1.11) with $p = 4$ as

$$\mathcal{D}_\rho \equiv \mathcal{D}_{\rho,13}^{4,3} = \mathrm{str}\left(\mathcal{T}^{(1)}\mathcal{T}^{(1)}\mathcal{T}^{(1)}\mathcal{T}^{(3)}\right). \tag{5.1.12}$$

For the single variable vertices listed in (5.1.4) the Gaudin model provides the single differential operator of order four which depend on the conformal weights and spins of the three fields. We will work it out explicitly for all three cases, see section 5.3. Our results extend the formulas given in our earlier announcement [62] by including also the vertices of type II and III which we had not calculated before. The results are a bit cumbersome to spell out at first.

In section 5.4 we will massage the answer and thereby pass to a much more compact algebraic formulation where we construct the Hamiltonian from the generators of a deformation of some generalized Weyl algebra. The commutation relations of its three generators $A, A^\dagger$ and N depend on the spins of the fields, see eqs. (5.4.17) - (5.4.20). In the limit of $d = 3$ this algebra is actually well known in the literature on quiver varieties where it appears as a generalized Weyl algebra or deformed/quantized Kleinian singularity of affine type $\tilde{A}_3$. Our deformation to $d \neq 3$ can be seen to possess finite dimensional representations whenever the spin quantum numbers are integers, and the dimension of these representations coincides with the number of 3-point tensor structures. Once the algebra generated by $A, A^\dagger$ and N is introduced, the expression for the Hamiltonian can be stated in a single line, see eq. (5.4.22). Obviously, this Hamiltonian does depend on the choice of conformal weights, unlike the algebra it is a part of. In some sense, the formulas of section 5.4 provide the most compact formulation of our vertex operators and we believe that similar formulations are likely to exist for higher dimensional vertex systems. Nevertheless, for the main focus of the current paper, the material of section 5.4 may be considered supplementary.

Section 5.5 contains the main new result of this paper: there we show that the vertex operators for all three vertex systems listed in eq. (5.1.4) can be mapped to a CMS Hamiltonian, namely the Hamiltonian for a crystallographic elliptic model that was originally discovered by Etingof, Felder, Ma and Veselov about a decade ago, see [68]. This lemniscatic CMS Hamiltonian is spelled out in equation (5.5.16). It is a fourth-order differential operator in a single variable z. The relation between the cross ratio $\mathcal{X}$ of the vertex system and the new elliptic variable z is stated in eq. (5.5.30). The map involves Weierstrass' elliptic function $\wp(z)$. The lemniscatic Hamiltonian contains three non-trivial coefficient functions $g_p(z)$ which are defined in eqs. (5.5.17)-(5.5.19). These coefficient functions depend on 12

multiplicities $m_{i,\nu}$ with $i = 1, \ldots, 4$, and $\nu = 0, 1, 2$, subject to the five constraints given in eq. (5.5.9), such that there are only seven remaining independent parameters. These determine the coupling constants in the coefficient functions $g_p(z)$ through eq. (5.5.36) and eqs. (5.5.20)-(5.5.22). For each of the three single variable vertex systems we determine the parameters $m_{i,\nu}$ in equations (5.5.36) and (5.5.37)-(5.5.44) (type I, II; for type II one sets $\ell_2 = 0$) and (5.5.48)-(5.5.55) (type III). We note that in cases I and II, the vertex Hamiltonians do not exhaust the entire seven parameter family of lemniscatic models. In fact, for these two cases the multiplicities satisfy the additional constraint (5.5.47) that reduces the number of independent parameters to six. Only for vertices of type III are the parameters of the lemniscatic model unrestricted.

5.2 Three-Point Functions in Embedding Space

In our explicit construction of cross ratios and the calculation of the differential operators we employ the embedding space formalism. Our presentation follows mostly [89], which has advocated the usefulness of this formalism in the context of spinning correlators, though restricted to STTs. More recently, this analysis was extended to mixed symmetry tensors, see [83, 86]. Here, we discuss the structure of 3-point functions for the three cases listed in eq. (5.1.4). Vertices of type I and II which exist for all sufficiently high dimensions, are treated together in the second subsection. The case of type III which is restricted to $d = 4$ dimensions requires special treatment in the third subsection. Our construction of tensor structures and cross ratios for this case seems to be new even though the construction of 3-point tensor structures has a long history, see e.g. [121, 122]. The use of embedding space formalism and polarization variables gives rise to an elegant reformulation that allows us to construct 3-point correlators easily, up to a function t of conformal invariant variables [62] that is not determined by conformal symmetry.

5.2.1 Spinning 3-point functions in embedding space

We are now interested in those 3-point functions for which conformal symmetry leaves one free parameter, i.e. the three configurations of spinning fields listed in eq. (5.1.4). These correspond to the vertices for STT-STT-scalar in $d \geq 3$, MST_2-STT-scalar in $d \geq 4$, and MST_2-MST_2-scalar in $d = 4$, respectively. In the section 5.3 we will actually address the computation of the vertex operators for these three cases through a single computation by passing through the 3-point function for MST_2-MST_2-scalar in $d > 4$. From there, we can then descend to the three cases we are interested in. As one can easily see, the vertex of type $(2, 2, 0)$ in $d > 4$ comes with two cross ratios and carries seven quantum numbers: three conformal weights and four spin labels. In order to descend to the three types in the list (5.1.4), we need to specialize the quantum numbers and restrict to a single cross ratio, see below.

To simplify notation and avoid multiple indices, we will rename our variables from here on as

$$Z \equiv Z_1\,, \quad W \equiv Z_2\,, \quad l \equiv l_1\,, \quad \ell \equiv l_2\,, \tag{5.2.1}$$

and use Latin indices $i, j, k = 1, 2, 3$ to run over the three points. For instance, the first field $\phi_{\Delta_1, l_1, \ell_1}(X_1, Z_1, W_1)$ has spins $l_1 \geq \ell_1 \geq 0$ and depends on the coordinate X_1 and the two polarization vectors Z_1 and W_1, and similarly for the fields $\phi_{\Delta_2, l_2, \ell_2}(X_2, Z_2, W_2)$ and $\phi_{\Delta_3}(X_3)$.

The first task now is to find which non-vanishing independent tensor structures can be constructed from the gauge invariant quantities (3.1.15). This means building a set of conformal invariants from the position variables X_i and the polarizations Z_i, W_i that generate functions of any degree in all of

the seven variables, along with the two cross ratios. The latter are conformal invariants of vanishing degree. To begin with, we have the scalar products of position vectors

$$X_{12} = X_1 \cdot X_2 \,, \qquad X_{23} = X_2 \cdot X_3 \,, \qquad X_{31} = X_3 \cdot X_1 \,. \tag{5.2.2}$$

If we denote the multi-degree of a MST_2-MST_2-scalar vertex by $[-\Delta_1, l_1, \ell_1; -\Delta_2, l_2, \ell_2; -\Delta_3]$, these scalar products have degree $deg X_{12} = [1,0,0;1,0,0;0]$ etc. Next, it is customary to introduce the following contractions of the two-forms with two position vectors

$$V_1 = V_{1,32} = \frac{X_3 \cdot (X_1 \wedge Z_1) \cdot X_2}{X_{23}} \,, \qquad V_2 = V_{2,13} = \frac{X_1 \cdot (X_2 \wedge Z_2) \cdot X_3}{X_{31}} \,. \tag{5.2.3}$$

The two objects V_1 and V_2 have degree $deg\, V_1 = [1,1,0;0,0,0;0]$ and $deg\, V_2 = [0,0,0;1,1,0;0]$. Another simple tensor structure is given by the the contractions of the two-forms

$$H_{12} = \frac{1}{2}(X_1 \wedge Z_1) \cdot (X_2 \wedge Z_2) \,. \tag{5.2.4}$$

It has degree $deg\, H_{12} = [1,1,0;1,1,0;0]$. The tensor structures we have introduced so far do not depend on the polarizations W_i, in contrast to the remaining three variables that we will introduce now. These include the following contractions of a three-form with a two-form and a vector,

$$U_{123} = \frac{1}{2}(X_1 \wedge Z_1 \wedge W_1)_{ABC}(X_2 \wedge Z_2)^{AB} X_3^C \,, \qquad U_{213} = \frac{1}{2}(X_2 \wedge Z_2 \wedge W_2)_{ABC}(X_1 \wedge Z_1)^{AB} X_3^C \,, \tag{5.2.5}$$

and, finally, the contraction of the two three-forms

$$K_{12} = \frac{1}{3!}(X_1 \wedge Z_1 \wedge W_1) \cdot (X_2 \wedge Z_2 \wedge W_2) \,. \tag{5.2.6}$$

In the notation of [86], these MST_2 tensor structures correspond to $U_{ijk} = T^{3,21}_{i,jk}$ and $K_{ij} = T^{3,3}_{i,j}$. The degrees of these three tensor structures are $deg\, U_{123} = [1,1,1;1,1,0;1]$, $deg\, U_{213} = [1,1,0;1,1,1;1]$ and $deg\, K_{12} = [1,1,1;1,1,1;0]$. This concludes our list of building blocks of tensor structures for the MST_2-MST_2-scalar vertex in $d > 4$. For the reader's convenience we listed the tensor structures and their degrees in Tab. 5.1.

As one can easily count, we have written nine independent tensor structures, the degrees of which span the entire 7-dimensional space of multi-degrees. Since we know that the MST_2-MST_2-scalar vertex admits two cross ratios, the tensor structures we introduced indeed suffice to decompose the 3-point function in the following way

$$\Phi_{123}(X_i; Z_i, W_i) := \langle \phi_{\Delta_1, l_1, \ell_1}(X_1, Z_1, W_1) \phi_{\Delta_2, l_2, \ell_2}(X_2, Z_2, W_2) \phi_{\Delta_3}(X_3) \rangle = \Omega^{\Delta_1, \Delta_2, \Delta_3}_{l_1, l_2; \ell_1, \ell_2}\, t(\mathcal{X}, \mathcal{Y}) \,, \tag{5.2.7}$$

where $\Omega^{\Delta_1, \Delta_2, \Delta_3}_{l_1, l_2; \ell_1, \ell_2}$ is a prefactor that takes care of all homogeneity conditions (3.1.12), i.e. it is a product of powers of tensor structures that matches the degree of the correlation function on the left hand side. The function $t(\mathcal{X}, \mathcal{Y})$ is a conformal invariant that depends on two variables of vanishing degree,

$$\mathcal{X} = \frac{H_{12}}{V_1 V_2} \,, \qquad \mathcal{Y} = \frac{X_{13} X_{23} V_1 V_2 K_{12}}{X_{12} U_{123} U_{213}} \,. \tag{5.2.8}$$

Of course, the prefactor Ω is not uniquely fixed by the homogeneity condition simply because it is possible to form objects of vanishing degree from the nine tensor structures. The remaining freedom

can be fixed by choosing not to employ H_{12} and K_{12} in the construction of Ω. This leaves us with a unique prefactor satisfying all of the required homogeneities in (X_i, Z_i, W_i),

$$\Omega^{\Delta_1,\Delta_2,\Delta_3}_{l_1,l_2;\ell_1,\ell_2} = \frac{V_1^{l_1-\ell_1-\ell_2} V_2^{l_2-\ell_1-\ell_2} U_{123}^{\ell_1} U_{213}^{\ell_2}}{X_{12}^{\frac{\Delta_1+\Delta_2-\Delta_3+l_1+l_2-\ell_1-\ell_2}{2}} X_{23}^{\frac{\Delta_2+\Delta_3-\Delta_1-l_1+l_2+\ell_1+\ell_2}{2}} X_{31}^{\frac{\Delta_3+\Delta_1-\Delta_2+l_1-l_2+\ell_1+\ell_2}{2}}} \,. \tag{5.2.9}$$

After one has fixed Ω, the remaining freedom in the 3-point function is normally taken into account by expanding in a discrete set of 3-point tensor structures with vanishing multi-degree. These are then combined with OPE coefficients to make up the full correlator. The standard tensor structures, once homogenized, represent a basis for the space of $t(\mathcal{X}, \mathcal{Y})$, but this basis is of course not unique. As we have recalled in the introduction, it is one of the key observations in [62] that a distinguished basis arises naturally from the study of higher-point conformal blocks, as eigenfunctions of our new vertex differential operators.

Now that we have parametrized the MST_2-MST_2-scalar vertex in terms of the function $t(\mathcal{X}, \mathcal{Y})$ of two cross ratios, we need to explain how to descend to the three types of vertices we are interested in. We will postpone the reduction to type III to subsection 5.2.2, and we will address here types I and II that are the simplest to discuss. In these two cases, the variable W_2 does not appear because the spinning field $\phi_{\Delta_2,l_2,\ell_2}$ is in an STT representation. Therefore, we only have seven tensor structures whose degrees span a 6-dimensional space of degrees. Consequently, there can be only one non-trivial cross ratio which is $\mathcal{X}$. Since it is impossible to construct the cross ratio $\mathcal{Y}$, the function $t(\mathcal{X}, \mathcal{Y})$ cannot depend on it, and therefore reduces to $t(\mathcal{X})$.
Going to type I does not impose any further constraint on the remaining variable $\mathcal{X}$. Indeed, without a variable W_1 it is not possible to construct the tensor structure U_{123} so that we remain with six tensor structures whose degrees span a 5-dimensional space of degrees. The construction of $\mathcal{X}$ is not affected. The upshot of all this discussion is very simple: for vertices of type I and II in our list (5.1.4) the 3-point function assumes the form spelled out in eq. (5.2.7), but with a function t that depends only on $\mathcal{X}$ and not on $\mathcal{Y}$,

$$\langle \phi_{\Delta_1,l_1,\ell_1}(X_1, Z_1, W_1) \phi_{\Delta_2,l_2,\ell_2=0}(X_2, Z_2) \phi_{\Delta_3}(X_3) \rangle = \Omega^{\Delta_1,\Delta_2,\Delta_3}_{l_1,l_2;\ell_1,\ell_2=0} t(\mathcal{X}) \,, \tag{5.2.10}$$

where the prefactor Ω is given in eq. (5.2.9) and for vertices of type I one imposes $\ell_1 = 0$.

Before we conclude this section, we want to carry our discussion of the function $t(\mathcal{X})$ one step further. So far we have not enforced spin labels to be integers so that our general form (5.2.10) still applies to 3-point functions of objects with continuous spin. Now we would like to explore the additional conditions that arise from the restriction to spins with integer values. We already saw in subsection 3.1.1 that MSTs depend polynomially on the auxiliary variables Z_i. This rather basic fact constrains $t(\mathcal{X})$ to live in a finite-dimensional space, as one can infer from the definition (5.2.8) of the cross ratio $\mathcal{X}$. The tensor structures V_i that appear in its denominator each contain factors of Z_i. Therefore, the highest power of V_i from the denominators of $t(\mathcal{X})$ must not exceed the power of V_i that appears in the numerator of the prefactor (5.2.9) in order to ensure polynomial dependence on the Z variables. This provides an upper bound on the exponent M of $\mathcal{X}^M$ in a series expansion of $t(\mathcal{X})$. Negative powers of $\mathcal{X}$ are not possible either, as these would produce the tensor structure H_{12} in the denominator, which itself contains both Z_1 and Z_2 but cannot be compensated by the prefactor Ω that does not contain H_{12}. In conclusion, $t(\mathcal{X})$ must be a polynomial of order up to $n_t = \min(l_1 - \ell_1, l_2 - \ell_1)$ if $n_t \geq 0$, and it must vanish if $n_t < 0$. The set of all allowed functions $t(\mathcal{X})$ therefore spans an $(n_t + 1)$-dimensional space of tensor structures. For type III vertices, we will be able to write 3-point functions in the same

	$-\Delta_1$	$-\Delta_2$	$-\Delta_3$	l_1	l_2	ℓ_1	ℓ_2
H_{12}	1	1	0	1	1	0	0
K_{12}	1	1	0	1	1	1	1
V_1	1	0	0	1	0	0	0
V_2	0	1	0	0	1	0	0
U_{123}	1	1	1	1	1	1	0
U_{213}	1	1	1	1	1	0	1

Table 5.1: Degrees of tensor structures of the MST_2-MST_2-scalar 3-point function in $d > 4$.

form as (5.2.10) with $\ell_2 \neq 0$. However, this last discussion on the polynomiality of $t(\mathcal{X})$ and the space of tensor structures will be substantially different.
There is a slight twist to this story that is relevant for the STT-STT-scalar vertex in $d = 3$. Note that all the tensor structures we have introduced so far are even under parity. So all of the 3-point tensor structures that they generate are also parity even. But for the type I vertex in $d = 3$, it is also possible to construct a parity-odd tensor structure given by

$$O^{(3)}_{123} = \epsilon_{ABCDE} X_1^A X_2^B X_3^C Z_1^D Z_2^E \,. \tag{5.2.11}$$

Its degree in the 5-dimensional space of degrees for type I vertices is $deg\, O_{123} = [1, 1; 1, 1; 1]$. The square of this parity-odd tensor structure must be parity-even, and it can be expressed in terms of tensor structures constructed above as

$$\left(O^{(3)}_{123}\right)^2 \propto (1-\mathcal{X})\mathcal{X} V_1^2 V_2^2 \frac{X_{13}X_{23}}{X_{12}} \,. \tag{5.2.12}$$

We infer from this equation that parity-odd 3-point tensor structures contain factors of $\sqrt{(1-\mathcal{X})\mathcal{X}}$, generalizing the polynomial space of $t(\mathcal{X})$ to also include these half-integer powers. A similar analysis can be done for the type II vertex in $d = 4$. However one finds no extension of the space of polynomials; we will describe this in the following subsection.

5.2.2 Embedding space construction in $d = 4$ dimensions

We now address the restriction of the 3-point function (5.2.7) to $d = 4$, thereby describing vertices of type III. In going from $d > 4$ to $d = 4$, the number of independent cross-ratios reduces from two to just one. One may think of this reduction in terms of a constraint that is imposed on the variable $\mathcal{Y}$. The simplest way to understand the need of a reduction in cross-ratio space is by observing that the embedding space for a theory in $d = 4$ dimensions is 6-dimensional, while the MST_2-MST_2-scalar 3-point function described in the previous subsection depends on seven vectors $(X_1, Z_1, W_1, X_2, Z_2, W_2, X_3)$. Seven vectors in a six-dimensional space must be linearly dependent, which is equivalent to the vanishing of the determinant of their Gram matrix (matrix of scalar products). For the case at hand, the Gram determinant is easily computed in terms of our tensor structures, and the vanishing condition becomes

$$\frac{X_{12}}{X_{13}X_{23}} \frac{U_{213}U_{123}}{V_1 V_2} \frac{\mathcal{Y}^2(-1+\mathcal{X})+\mathcal{Y}}{\mathcal{X}} = 0 \,, \tag{5.2.13}$$

with two solutions in cross-ratio space: $\mathcal{Y} = 0$ and $\mathcal{Y} = 1/(1-\mathcal{X})$. To understand the reason why two different solutions appear and what each one means, we first need to explain in more detail some properties of the embedding space representation of mixed-symmetry tensors in $d = 4$.

As we already anticipated at the end of section 3.1.1, the representations labeled by Young diagrams that we considered so far are reducible in even dimensions when $L = d/2$, and further decompose into irreducible self-dual and anti-self-dual representations. To see this more concretely, let us write out the X and Z vectors in the following Poincaré patches,

$$\begin{aligned} X &= \left(1, x^2, x^a\right) \,, \\ Z = (0, 2x\cdot z, z^\mu) \qquad z^\mu &= (1, -\zeta_+\zeta_-, \zeta_+, \zeta_-) \,, \end{aligned} \tag{5.2.14}$$

where we use three pairs of coordinates $(X_{+1}, X_{-1}, X_{+2}, X_{-2}, X_{+3}, X_{-3})$ in which metric given by $ds^2 = -dX_{+1}dX_{-1} + dX_{+2}dX_{-2} + dX_{+3}dX_{-3}$. The variable W has been introduced to parameterize the space of solutions to $X\cdot W = Z\cdot W = W^2 = 0$, quotiented by the gauge and projective equivalence $W \sim \lambda W + \alpha Z + \beta X$. These conditions allow for two independent solutions in a six-dimensional embedding space, namely

$$W = (0, 2x\cdot w, w^a) \qquad (w^a) = (0, -\zeta_+, 0, 1) \quad \textit{or} \tag{5.2.15}$$

$$\overline{W} = (0, 2x\cdot \overline{w}, \overline{w}^a) \qquad (\overline{w}^a) = (0, -\zeta_-, 1, 0) \,. \tag{5.2.16}$$

It is easy to check that $\star(X\wedge Z\wedge W) = X\wedge Z\wedge W$, and $\star(X\wedge Z\wedge W) = -X\wedge Z\wedge \overline{W}$. As a result, W and $\overline{W}$ define two distinct orbits of the conformal group in embedding space, and the restriction to the W or $\overline{W}$ orbit projects a spinning representation to its self-dual or anti-self-dual part. To make the choice of orbit and duality explicit, we now slightly modify the homogeneity conditions of (3.1.12): we redefine W and $\overline{W}$ to have opposite homogeneity degree, such that $\ell > 0$ denotes self-dual representations encoded by polynomials of order $|\ell|$ in W, and $\ell < 0$ denotes anti-self-dual representations encoded by polynomials of order $|\ell|$ in $\overline{W}$. To motivate this prescription, recall that the double cover of the Lorentzian conformal group $\mathrm{SO}(2,4)$ by $\mathrm{SU}(2,2)$ defines a map from $\mathbb{C}^4$ twistor fields to $\mathbb{R}^{2,4}$ embedding space fields. In the twistor formalism, it is customary to label representations by the positive integers $(j, \bar{j})$ that respectively count the number of indices transforming in the chiral and anti-chiral representation of the $\mathrm{SL}_{\mathbb{C}}(2)$ Lorentz subgroup[1]. Using the explicit map from gauge invariant embedding space tensors to twistor space variables constructed in Appendix 5.A, our prescription to label self-dual and anti-self-dual representations is then equivalent to the identification

$$l = \frac{j+\bar{j}}{2} \,, \qquad \ell = \frac{j-\bar{j}}{2} \,, \tag{5.2.17}$$

which is standard in the CFT_4 literature.

With the introduction of these two vectors W and $\overline{W}$, the space of tensor structures that one can construct changes dramatically. To see this, we begin by evaluating our expression for the tensor structure K with W_i, respectively $\overline{W}_i$, $i = 1, 2$, taken from the same Poincaré patch (5.2.15), respectively (5.2.16),

$$K_{12} = \frac{1}{3!}\left(X_1\wedge Z_1\wedge W_1\right)\cdot\left(X_2\wedge Z_2\wedge W_2\right) = 0 = \frac{1}{3!}\left(X_1\wedge Z_1\wedge \overline{W}_1\right)\cdot\left(X_2\wedge Z_2\wedge \overline{W}_2\right) = K_{\bar{1}\bar{2}} \,. \tag{5.2.18}$$

On the right hand side, we introduced the notation that barred indices $\bar{\imath}$ in tensors correspond to occurrences of the variable $\overline{W}_i$, as opposed to W_i. The vanishing of the tensor structures K_{12} and $K_{\bar{1}\bar{2}}$ in $d = 4$ forces us to introduce new non-vanishing structures[2].

[1] More specifically the double cover of the Lorentz subgroup $\mathrm{SO}(1,3) \subset \mathrm{SO}(2,4)$.

[2] if for no other reason than to write the 2-point function of fields with $\ell \neq 0$.

It turns out that it is possible to construct two non-vanishing tensor structures by mixing the self-dual and anti-self-dual Poincaré patches in the expression of K_{12},

$$k_{1\bar{2}} = \sqrt{\frac{1}{3!}\left(X_1 \wedge Z_1 \wedge W_1\right) \cdot \left(X_2 \wedge Z_2 \wedge \overline{W}_2\right)}\,, \qquad k_{\bar{1}2} = \sqrt{\frac{1}{3!}\left(X_1 \wedge Z_1 \wedge \overline{W}_1\right) \cdot \left(X_2 \wedge Z_2 \wedge W_2\right)}\,. \tag{5.2.19}$$

We introduced square roots because it turns out that the arguments are perfect squares. Therefore, even with inclusion of the square roots in the definition, $k_{1\bar{2}}$ and $k_{\bar{1}2}$ are both polynomials in the d-dimensional variables x_i, z_i. These two structures satisfy the following relation

$$H_{12} = 2k_{1\bar{2}}k_{\bar{1}2}\,. \tag{5.2.20}$$

Let us also spell out the degrees of the two new tensor structures,

$$deg\, k_{1\bar{2}} = \left[\frac{1}{2},\frac{1}{2},\frac{1}{2};\frac{1}{2},\frac{1}{2},-\frac{1}{2};0\right], \qquad deg\, k_{\bar{1}2} = \left[\frac{1}{2},\frac{1}{2},-\frac{1}{2};\frac{1}{2},\frac{1}{2},\frac{1}{2};0\right]. \tag{5.2.21}$$

In conclusion, we have now replaced the two tensor structures K_{12} and H_{12} of the previous subsection by the two tensor structures $k_{1\bar{2}}$ and $k_{\bar{1}2}$. Furthermore, one can show that the objects U_{ij3} can be decomposed into

$$U_{123} = \mho\, k_{1\bar{2}}\,, \qquad U_{213} = \mho\, k_{\bar{1}2}\,, \tag{5.2.22}$$

with a new tensor structure $\mho$ defined as

$$\mho = \sqrt{X_3^A \left(X_1 \wedge Z_1 \wedge W_1\right)_{ABC} \left(X_2 \wedge Z_2 \wedge W_2\right)^{BCD} X_{3\,D}}\,. \tag{5.2.23}$$

The degree of $\mho$ is given by

$$deg\, \mho = \left[\frac{1}{2},\frac{1}{2},\frac{1}{2};\frac{1}{2},\frac{1}{2},\frac{1}{2};1\right]\,, \tag{5.2.24}$$

The tensor structure $\mho$ uses only W_i. Of course, it is also possible to construct a similar tensor structure $\overline{\mho}$ in terms of $\overline{W}_i$ as

$$\overline{\mho} = \sqrt{X_3^A \left(X_1 \wedge Z_1 \wedge \overline{W}_1\right)_{ABC} \left(X_2 \wedge Z_2 \wedge \overline{W}_2\right)^{BCD} X_{3\,D}}\,, \tag{5.2.25}$$

with

$$deg\, \overline{\mho} = \left[\frac{1}{2},\frac{1}{2},-\frac{1}{2};\frac{1}{2},\frac{1}{2},-\frac{1}{2};1\right]\,. \tag{5.2.26}$$

In direct analogy with eq. (5.2.22) we also find that

$$U_{\bar{1}23} = \overline{\mho}\, k_{\bar{1}2}\,, \qquad U_{\bar{2}13} = \overline{\mho}\, k_{1\bar{2}}\,. \tag{5.2.27}$$

At this point we have nine basic tensor structures at our disposal, namely $k_{\bar{1}2}, k_{1\bar{2}}, \mho$ and $\overline{\mho}$ in addition to $X_{12}, X_{23}, X_{13}, V_1$ and V_2. Their degrees certainly span the 7-dimensional space and in addition, we can construct the unique cross ratio $\mathcal{X}$ as

$$\mathcal{X} = 2\frac{k_{\bar{1}2}k_{1\bar{2}}}{V_1 V_2}\,. \tag{5.2.28}$$

Finally, the nine fundamental tensor structures that we introduced satisfy one relation,

$$(X_{23}V_1)(X_{13}V_2) = X_{12}\mho\,\overline{\mho} + 2k_{1\bar{2}}k_{\bar{1}2}X_{13}X_{23}\,. \tag{5.2.29}$$

	$-\Delta_1$	$-\Delta_2$	$-\Delta_3$	l_1	l_2	ℓ_1	ℓ_2
$k_{1\bar{2}}$	1/2	1/2	0	1/2	1/2	1/2	−1/2
$k_{\bar{1}2}$	1/2	1/2	0	1/2	1/2	−1/2	1/2
$\mho$	1/2	1/2	1	1/2	1/2	1/2	1/2
$\bar{\mho}$	1/2	1/2	1	1/2	1/2	−1/2	−1/2

Table 5.2: Degrees of additional tensor structures of the MST_2-MST_2-scalar 3-point function in $d = 4$.

For the reader's convenience we listed these additional tensor structures and their degrees in Tab. 5.2. Having introduced this new set of tensor structures for vertices of type III, we immediately see that the two solutions to the vanishing of the Gram determinant (5.2.13) in $d = 4$ arise very naturally when trying to construct a second $\mathcal{Y}$-like cross ratio. First, note that the cross ratio $\mathcal{Y}$ introduced in eq. (5.2.8) vanishes when ℓ_1 and ℓ_2 have the same sign,

$$\mathcal{Y}_{++} = \frac{X_{13}X_{23}V_1V_2K_{12}}{X_{12}U_{123}U_{213}} = 0 = \frac{X_{13}X_{23}V_1V_2K_{\bar{1}\bar{2}}}{X_{12}U_{\bar{1}23}U_{\bar{2}13}} = \mathcal{Y}_{--}\,, \tag{5.2.30}$$

because of the property (5.2.18). On the other hand, when the fields have opposite duality, one can only construct a cross ratio with the help of the non-vanishing tensor structures $k_{\bar{1}2}$ or $k_{1\bar{2}}$,

$$\mathcal{Y}_{-+} = \frac{X_{13}X_{23}V_1V_2k_{\bar{1}2}^2}{X_{12}U_{\bar{1}23}U_{213}} = \frac{1}{1-\mathcal{X}} = \frac{X_{13}X_{23}V_1V_2k_{1\bar{2}}^2}{X_{12}U_{123}U_{\bar{2}13}} = \mathcal{Y}_{+-}\,. \tag{5.2.31}$$

To compare with eq. (5.2.30), note that $K_{12} = k_{12}^2$. In evaluating the expressions for $\mathcal{Y}_{-+}$ and $\mathcal{Y}_{+-}$, we have used the relation (5.2.29) before inserting the definition (5.2.28) of the cross ratio $\mathcal{X}$. In this sense, the second zero of the Gram determinant can be associated with 3-point functions in which the spins ℓ_i of the MSTs have opposite sign.
Keeping in mind that we are also allowed to have negative values of the spin ℓ_i in $d = 4$, we can now write a generic 3-point function as in equation (5.2.10), but with the prefactor Ω given by

$$\Omega^{\Delta_1,\Delta_2,\Delta_3}_{l_1,l_2;\ell_1,\ell_2} = \frac{V_1^{l_1-|\ell_1|-|\ell_2|}V_2^{l_2-|\ell_1|-|\ell_2|}U_{s_123}^{|\ell_1|}U_{s_213}^{|\ell_2|}}{X_{12}^{\frac{\Delta_1+\Delta_2-\Delta_3+l_1+l_2-|\ell_1|-|\ell_2|}{2}}X_{23}^{\frac{\Delta_2+\Delta_3-\Delta_1-l_1+l_2+|\ell_1|+|\ell_2|}{2}}X_{31}^{\frac{\Delta_3+\Delta_1-\Delta_2+l_1-l_2+|\ell_1|+|\ell_2|}{2}}} \tag{5.2.32}$$

instead of (5.2.9). In spelling out the new prefactor that is defined for arbitrary integer values of ℓ_i, we have introduced the notation

$$s_i = \begin{cases} i & \ell_i \geq 0 \\ \bar{\imath} & \ell_i < 0 \end{cases}\,. \tag{5.2.33}$$

Note that, despite the presence of absolute values in (5.2.32), representations with any sign of ℓ_i are allowed, as the possible presence of $\overline{W}_i$ takes full care of negative homogeneity degrees. Formula (5.2.32) is the main result of this subsection.

As in the previous subsection, we can use our expression for the 3-point function to count the number of tensor structures when we impose spins to acquire integer values. In order to do so, we need to expand (5.2.32) in terms of the tensor structures specific to $d = 4$, in a form that depends specifically on the duality of the two MST_2 involved. To distinguish between those cases, we introduce the notation $\Omega_{\sigma_1\sigma_2}$, where $\sigma_i = +, -$ depending whether the field i is in a self-dual or anti-self-dual representation

respectively. Those prefactors satisfy the relations $\Omega_{++} = \overline{\Omega}_{--}$ and $\Omega_{+-} = \overline{\Omega}_{-+}$, where the bar operation exchanges $W_i \leftrightarrow \overline{W}_i$ for both $i = 1, 2$; we can therefore focus on only the Ω_{++} and Ω_{+-} cases, as the results in these cases can easily be translated to the other two cases.
In analyzing the first case, involving Ω_{++}, we can express the prefactor in terms of $\mho$, $k_{1\bar{2}}$ and $k_{\bar{1}2}$, leading to the 3-point function

$$\Omega_{++}t(\mathcal{X}) = \frac{V_1^{l_1-|\ell_1|-|\ell_2|}V_2^{l_2-|\ell_1|-|\ell_2|}\mho^{|\ell_1|+|\ell_2|}k_{1\bar{2}}^{|\ell_1|}k_{\bar{1}2}^{|\ell_2|}}{X_{12}^{\frac{\Delta_1+\Delta_2-\Delta_3+l_1+l_2-|\ell_1|-|\ell_2|}{2}}X_{23}^{\frac{\Delta_2+\Delta_3-\Delta_1-l_1+l_2+|\ell_1|+|\ell_2|}{2}}X_{31}^{\frac{\Delta_3+\Delta_1-\Delta_2+l_1-l_2+|\ell_1|+|\ell_2|}{2}}}t(\mathcal{X})\,. \tag{5.2.34}$$

By requiring polynomial dependence on the variables Z_i, W_i, $\overline{W}_i$ in this expression, it is easy to see that $t(\mathcal{X})$ must contain integer powers of the cross ratio (5.2.28), with exponents that are bounded from above by the minimum exponent of the V_i in the prefactor, and bounded from below by the minimum exponent of the k_{ij}. As a result, the function $t(\mathcal{X})$ must take the form

$$t(\mathcal{X}) = \sum_n c_n \mathcal{X}^n\,, \tag{5.2.35}$$

with the sum over exponents restricted by the inequalities

$$-\min(|\ell_1|,|\ell_2|) \leq n \leq \min(l_1,l_2) - |\ell_1| - |\ell_2|\,. \tag{5.2.36}$$

In cases where ℓ_1 and ℓ_2 have opposite sign, e.g. $\ell_1 > 0$, $\ell_2 < 0$ and the prefactor Ω_{+-} is used, the discussion is a bit different. Here we can use the relation (5.2.29) to eliminate one of the tensor structures $\mho$ or $\overline{\mho}$ from the prefactor and write the 3-point function as

$$\frac{V_1^{l_1-|\ell_1|-|\ell_2|}V_2^{l_2-|\ell_1|-|\ell_2|}\mho^{|\ell_1|-\min(|\ell_1|,|\ell_2|)}\overline{\mho}^{|\ell_2|-\min(|\ell_1|,|\ell_2|)}k_{1\bar{2}}^{|\ell_1|+|\ell_2|}\left(V_1V_2-2k_{1\bar{2}}k_{\bar{1}2}\right)^{\min(|\ell_1|,|\ell_2|)}}{X_{12}^{\frac{\Delta_1+\Delta_2-\Delta_3+l_1+l_2-|\ell_1|-|\ell_2|}{2}}X_{23}^{\frac{\Delta_2+\Delta_3-\Delta_1-l_1+l_2+|\ell_1|+|\ell_2|}{2}}X_{31}^{\frac{\Delta_3+\Delta_1-\Delta_2+l_1-l_2+|\ell_1|+|\ell_2|}{2}}\left(\frac{X_{12}}{X_{13}X_{23}}\right)^{\min(|\ell_1|,|\ell_2|)}}t(\mathcal{X})\,.$$

In order to analyze the resulting constraints on the function $t(\mathcal{X})$, we shall think of t as a function of

$$1-\mathcal{X} = \frac{V_1V_2-2k_{1\bar{2}}k_{\bar{1}2}}{V_1V_2}. \tag{5.2.37}$$

Requiring polynomial dependence on the polarization vectors, t is constrained to contain integer powers of $(1-\mathcal{X})$ that are bounded from above by the minimum power of the V_i as in the previous case, and are bounded from below by the power of the factor $(V_1V_2-2k_{1\bar{2}}k_{\bar{1}2})$. This can be written concretely as

$$t(\mathcal{X}) = \sum_n c'_n(1-\mathcal{X})^n\,, \tag{5.2.38}$$

with the same constraint on the sum over exponents n that was spelled out in eq. (5.2.36). Thus, in both cases, we have determined that the space of tensor structures $t(\mathcal{X})$ has dimension

$$\min(l_1,l_2) - \max(|\ell_1|,|\ell_2|) + 1\,, \tag{5.2.39}$$

which matches exactly the expected number from the representation theory of the conformal group.
For the computation of the vertex operator in section 5.3, it will prove useful to spell out an explicit relation between the prefactors Ω_{++} and Ω_{+-},

$$\Omega_{+-}\Big|_{|\ell_2|\to-|\ell_2|} = \left(\frac{\mathcal{X}(1-\mathcal{X})}{2}\right)^{-|\ell_2|}\Omega_{++}\,. \tag{5.2.40}$$

In other words, the prefactor for one self-dual and one anti-self-dual field is related to the one for two self-dual MSTs through a simple function of the cross ratio $\mathcal{X}$, plus a change of sign for the homogeneity of the field for which we are changing duality. This equation will allow us to relate the vertex operator computed in one case to the other one, see eq. (5.3.6).
We now address the tensor structures that can be constructed with the use of a six-dimensional Levi-Civita symbol for vertices of type II and III. Using only one W_i or $\overline{W}_i$ vector, it is possible to construct the structures

$$O^{(4)}_{ijk} = \epsilon_{ABCDEF} X_i^A X_j^B X_k^C Z_i^D Z_j^E W_i^F \,, \qquad O^{(4)}_{\bar{i}jk} = \epsilon_{ABCDEF} X_i^A X_j^B X_k^C Z_i^D Z_j^E \overline{W}_i^F \,. \tag{5.2.41}$$

These are however easily seen to be proportional to the U_{ijk} tensor structure

$$\left(O^{(4)}_{s_i jk}\right)^2 \propto \left(U_{s_i jk}\right)^2 \,, \tag{5.2.42}$$

so that the vertex function $t(\mathcal{X})$ is unaffected by the introduction of parity-odd tensor structures for vertices of type II in $d = 4$. For vertices of type III we can also construct parity odd tensors of the form

$$\widetilde{O}^{(4)}_{12} = \epsilon_{ABCDEF} X_1^A X_2^B Z_1^C Z_2^D W_1^E W_2^F \,, \qquad \widetilde{O}^{(4)}_{\bar{1}2} = \epsilon_{ABCDEF} X_1^A X_2^B Z_1^C Z_2^D \overline{W}_1^E W_2^F \,, \tag{5.2.43}$$

as well as their images under $1 \leftrightarrow \bar{1}$ and $2 \leftrightarrow \bar{2}$. However, these structures are once again proportional to tensors that we have already introduced:

$$\left(\widetilde{O}^{(4)}_{12}\right)^2 \propto (K_{12})^2 \overset{d=4}{=} 0 \,, \qquad \left(\widetilde{O}^{(4)}_{\bar{1}2}\right)^2 \propto (K_{\bar{1}2})^2 \,. \tag{5.2.44}$$

We can therefore conclude that structures of the type (5.2.41) or (5.2.43) do not extend the space of $t(\mathcal{X})$ for vertices of type II and III.
Before ending this section, we would like to point out that the construction of $d = 4$ 3-point tensor structures in this section is the embedding space version of the twistor based construction of tensor structures in [92, 105]. We describe in more detail in Appendix 5.A the dictionary from embedding space variables to twistor variables and vice versa.

5.3 The Single Variable Vertex Operator

Having assembled all of the required background, including in particular a detailed discussion of single variable 3-point functions of the form (5.2.10), we now move on to our central goal. In this section, we work out the explicit expression for the action of our vertex differential operators on the function $t(\mathcal{X})$ that multiplies the prefactors (5.2.9) or (5.2.32). Our strategy is to obtain the results for all three sub-cases listed in eq. (5.1.4) by studying the MST_2-MST_2-scalar vertex in $d \geq 4$. Note that passing through this 2-variable vertex is just a trick that allows us to shorten the discussion and avoid displaying multiple long expressions for all different cases; using the same procedure described in this section, one can compute the vertex operator in each individual case and easily verify that the answer is the same as what is obtained by reduction of the more general vertex. The results of this section should be seen as providing raw data that we will process in the subsequent sections. We will also comment on the relation between our formulas and the vertex differential operator of a 5-point function in $d \geq 3$, see [63]. To this end, we shall look at both shadow integrals and OPE limits in the second subsection.

5.3.1 Construction of the reduced vertex operator

As we had argued in [62, 63], see also the review in section 5.1, there is a distinguished basis for the vertex functions t that is selected by solving the eigenvalue equations of some commuting set of vertex differential operators. A full prescription of how to construct these operators for 3-point vertices with sites of arbitrary depth L_i, $i = 1, 2, 3$ was given in [63]. For the MST_2-MST_2-scalar vertex there are two such operators, one of order four and the other of order six. When we descend from there to the single variable vertices in the list (5.1.4) via the constraint $\mathcal{Y} = 0$, the sixth order operator becomes dependent. Hence to achieve our goals it is sufficient to work out the fourth order operator. The operator starts its existence as a differential operator on the space of coordinates and polarizations of three fields. We use the embedding space constructions that were reviewed in the previous section to write the operator

$$\mathcal{D}_\rho \equiv \mathcal{D}^{4,3}_{\rho,13} = \mathrm{str}\left(\mathcal{T}^{(1)}\mathcal{T}^{(1)}\mathcal{T}^{(1)}\mathcal{T}^{(3)}\right) \tag{5.3.1}$$

in terms of the simple first order differential operators (3.1.14) encoding the action of the conformal generators on the variables (X_i, Z_i, W_i). Let us also recall that str stands for symmetrized trace. The action of the differential operator (5.3.1) can be reduced to the cross-ratio space of $t(\mathcal{X})$ by conjugation with the prefactor $\Omega^{\Delta_1,\Delta_2,\Delta_3}_{l_1,l_2;\ell_1,\ell_2}$, as is the case for Casimir differential operators,

$$H^{(d,\Delta_i,l_i,\ell_i)}t(\mathcal{X}) = \frac{1}{\Omega^{\Delta_1,\Delta_2,\Delta_3}_{l_1,l_2;\ell_1,\ell_2}}\mathcal{D}_\rho\left(\Omega^{\Delta_1,\Delta_2,\Delta_3}_{l_1,l_2;\ell_1,\ell_2}t(\mathcal{X})\right). \tag{5.3.2}$$

By plugging eqs. (3.1.14) and (5.3.1) in eq. (5.3.2), it is then possible to compute the action of $\mathcal{D}^{\mathcal{X}}_\rho$ in cross ratio space. To do this, we implemented the action of generators (3.1.14) in `Mathematica`[3] and first obtained the conjugation with the prefactor expressed in terms of scalar products of X_i, Z_i, W_i. We then solved the expressions of the cross ratios (5.2.8) for two scalar products, set $\mathcal{Y} = 0$, and plugged these expressions in the conjugated differential operator; due to conformal invariance all of the remaining scalar products drop out, and one is left with a differential operator in one cross ratio of the form

$$H^{(d,\Delta_i,l_i,\ell_i)} = h_0(\mathcal{X}) + \sum_{q=1}^{4} h_q(\mathcal{X})\mathcal{X}^{q-1}(1-\mathcal{X})^{q-1}\partial^q_{\mathcal{X}}\,. \tag{5.3.3}$$

Apart from a constant piece in $h_0(\mathcal{X})$, all of the coefficients $h_q(\mathcal{X})$ are symmetric under exchange of fields $1 \leftrightarrow 2$, and we can therefore represent them as

$$h^{(d,\Delta_i,l_i,\ell_i)}_q(\mathcal{X}) = \chi^{(d,\Delta_i,l_i,\ell_i)}_q(\mathcal{X}) + (1 \leftrightarrow 2)\,. \tag{5.3.4}$$

Finally, we write h_0 as

$$h^{(d,\Delta_i,l_i,\ell_i)}_0(\mathcal{X}) = \left[\chi^{(d,\Delta_i,l_i,\ell_i)}_0(\mathcal{X}) + (1 \leftrightarrow 2)\right] + \tilde{\chi}^{(d,\Delta_i,l_i,\ell_i)}_0\,. \tag{5.3.5}$$

[3] for an implementation of the code used to compute the fourth-order operator, see the supplementary material attached to this publication.

These coefficients take the following form:

$$
\begin{aligned}
\chi_4(\mathcal{X}) &= -2\,,\\
\chi_3(\mathcal{X}) &= -8\mathcal{X}\left(l_1-2\left(\ell_1+1\right)\right)+2\Delta_3+4l_1-8\ell_1-d-8\,,\\
\chi_2(\mathcal{X}) &= -4\mathcal{X}^2\left(l_1\left(2l_2-6\ell_1-9\right)+6\ell_1\left(-l_2+\ell_1+\ell_2+3\right)+l_1^2+7\right)\\
&\quad+\mathcal{X}\big[-2l_1\left(d-2\Delta_3-2l_1-4l_2+12\ell_1+18\right)+2\ell_1\left(3d-6\Delta_3-12l_2+12\ell_1+13\ell_2+36\right)\\
&\qquad d^2-2d(\Delta_1-1)-\Delta_3(d+4)+2\Delta_1\Delta_2+28\big]\\
&\quad+l_1\left(-2\Delta_3-l_1-l_2+6\ell_1+2d+4\right)+\ell_1\left(-2d+6\Delta_3+6l_2-5\ell_1-7\ell_2-16\right)-3d+\Delta_1^2\\
&\quad-\Delta_1\Delta_2+\frac{\Delta_3}{2}(-\Delta_3+2d+4)-2\,,\\
\chi_1(\mathcal{X}) &= 8\mathcal{X}^3\big[-3l_1\ell_1^2-3l_2\ell_1^2+l_1^2\ell_1+l_2^2\ell_1-6l_1\ell_1+4l_1l_2\ell_1-6l_2\ell_1-6l_1\ell_2\ell_1+l_1^2-3l_1-l_1^2l_2+2l_1l_2\\
&\qquad+2\ell_1^3+6\ell_2\ell_1^2+6\ell_1^2+6\ell_2\ell_1+6\ell_1+1\big]\\
&\quad+\mathcal{X}^2\big[l_1\left(2d(d-\Delta_3-\Delta_1)+4\Delta_1\Delta_2-l_2\left(d-2\Delta_3+24\right)+4\ell_1\left(d-2\Delta_3+19\ell_2+18\right)+36\right)\\
&\qquad-2\ell_1\big(2d^2-2l_2\left(d+9\ell_1+18\right)+(3d+37)\ell_2+\ell_1(3d+40\ell_2+36)+d+6l_2^2+12\ell_1^2+36\big)\\
&\qquad-d^2+2d\Delta_1\left(-l_2+2\ell_1+2\ell_2+1\right)+\Delta_3\left(4\ell_1\left(d-2l_2+3\ell_1+3\ell_2+1\right)+d\right)-48l_1l_2\ell_1\\
&\qquad+36l_1\ell_1^2+12l_1^2\left(l_2-\ell_1-1\right)-2\Delta_1\Delta_2\left(4\ell_1+1\right)-12\big]\\
&\quad+\frac{1}{2}\mathcal{X}\big[-2l_1\big(-2\Delta_1(d-2\Delta_2)-2l_2(d+10\ell_1+3)+4\ell_1(d+10\ell_2+7)+d(d+6)+16\ell_1^2+4\big)\\
&\qquad+2\ell_1\left(-2\Delta_1\left(d+\Delta_1-4\Delta_2\right)-4(d+7)l_2+(5d+34)\ell_2+d(3d+4)+6l_2^2+24\right)\\
&\qquad+4\Delta_3l_1\left(d-l_2+4\ell_1\right)+2\Delta_1\left(-(d-2)\Delta_1+2dl_2-2\ell_2\left(d+\Delta_1\right)+(d-4)d+2\Delta_2\right)\\
&\qquad+2\ell_1^2\left(5(d+6)-16l_2+42\ell_2\right)+8d+20\ell_1^3+2l_1^2\left(d-4l_2+6\ell_1+2\right)+\Delta_3^2\left(d+4\ell_1-2\right)\\
&\qquad-\Delta_3\left(d^2+4\ell_1\left(3d-4l_2+6\ell_1+7\ell_2+2\right)\right)\big]\\
&\quad\frac{1}{4}\big[4\Delta_3\left(-l_1\left(d+2\ell_1-2\right)+\ell_1\left(d-2l_2+2\ell_1+4\ell_2+2\right)+d-2\right)-2\ell_1^2\left(d-4l_1-4l_2+6\right)\\
&\qquad+4\left(l_1+l_2-2\right)\ell_1\left(d-l_1-l_2\right)-2\ell_2\ell_1\left(d-16l_1+14\ell_1+10\right)-2(d-2)\left(l_1\left(l_1+l_2-4\right)+2\right)\\
&\qquad+2\Delta_1^2\left(d+2\ell_1+2\ell_2-2\right)-\Delta_3^2\left(d+4\ell_1-2\right)-2\Delta_1\Delta_2\left(d+4\ell_1-2\right)-4\ell_1^3\big]\,,\\
\tilde{\chi}_0 &= \frac{1}{6}\left(\Delta_1-\Delta_2\right)\left(d-\Delta_1-\Delta_2\right)\left(d^2-3d\left(\Delta_1+\Delta_2+\Delta_3+1\right)+3\left(\Delta_1^2+\Delta_2^2+\Delta_3^2\right)\right)\\
&\quad-\frac{1}{6}\left(l_1-l_2\right)\left(d+l_1+l_2-2\right)\left(d^2+3d\left(-\Delta_3+l_1+l_2-3\right)+3\left(\Delta_3^2+l_1^2-2l_1+l_2^2-2l_2+2\right)\right)\\
&\quad-\frac{1}{6}(\ell_1-\ell_2)\left(d+\ell_1+\ell_2-4\right)\left(d^2+3d\left(-\Delta_3+\ell_1+\ell_2-5\right)+3\left(\Delta_3^2+\ell_1^2-4\ell_1+\ell_2^2-4\ell_2+8\right)\right),
\end{aligned}
$$

$$
\begin{aligned}
\chi_0(\mathcal{X}) \;=\; & 2\mathcal{X}^2\big[l_1\left(-4l_2^2\ell_1+l_2\left(8\ell_1\left(\ell_1+\ell_2+1\right)+1\right)-2\ell_1\left(\ell_1+1\right)\left(2\ell_1+6\ell_2+1\right)\right)\\
&\quad +2\ell_1\left(\ell_2\left(2\ell_1\left(-3l_2+2\ell_1+3\right)+1\right)+\left(\ell_1+1\right)\left(\ell_1-l_2\right)\left(-l_2+\ell_1+1\right)+3\ell_1\ell_2^2\right)\\
&\quad +l_1^2\left(-2l_2\left(2\ell_1+1\right)+l_2^2+2\ell_1\left(\ell_1+2\ell_2+1\right)\right)\big]\\
&+\mathcal{X}\big[2\ell_1l_2\left(d^2-d\left(\Delta_1+\Delta_3+1\right)+2\left(\Delta_1\Delta_2+\Delta_3+1\right)+\ell_1\left(d-2\Delta_3+14\ell_2+6\right)+4\ell_1^2\right)\\
&\quad -d\Delta_1l_2\ell_2+2\ell_1^2\left(-d^2+\Delta_1\left(d-2\Delta_2\right)+(d-2)\Delta_3-3\ell_2\left(d-2\Delta_3+4\right)+d-8\ell_2^2-2\right)\\
&\quad +2\ell_1\ell_2\left(-d^2+2\Delta_1\left(d-\Delta_2\right)+(d-2)\Delta_3+d-2\right)-2\ell_1^3\left(d-2\Delta_3+10\ell_2+4\right)\\
&\quad +l_1\big(-l_2\left(2\Delta_1\left(\Delta_2-d\right)+2\ell_1\left(d+9\ell_2+8\right)+(d-1)d+16\ell_1^2+2\right)\\
&\qquad +2\ell_1\left(-\Delta_1\left(d-2\Delta_2\right)-(d-2)\Delta_3+2\ell_2\left(d-2\Delta_3+6\right)+(d-1)d+2\right)\\
&\qquad -2d\Delta_1\ell_2+8\ell_1^3+2\ell_1^2\left(d-2\Delta_3+14\ell_2+6\right)+\Delta_3l_2\left(d+4\ell_1-2\right)+8l_2^2\ell_1\big)\\
&\quad +2d\Delta_1\ell_2^2-4l_2^2\left(\ell_1+1\right)\ell_1-4\ell_1^4-2l_1^2\left(-2l_2\left(2\ell_1+1\right)+l_2^2+2\ell_1\left(\ell_1+2\ell_2+1\right)\right)\big]\\
&-\frac{\ell_1\ell_2}{2\mathcal{X}}\left(\Delta_3^2+4\Delta_3\left(l_1-\ell_1\right)+2\left(\Delta_1\left(\Delta_2-\Delta_1\right)+l_1\left(l_2-2\ell_1\right)+\ell_1\left(-2l_2+\ell_1+\ell_2\right)+l_1^2\right)\right)\\
&+\frac{1}{12}\big[6l_1\big(l_2\left(d^2+2\Delta_1\left(\Delta_2-d\right)-(d-2)\Delta_3+2\ell_1\left(d-2\Delta_3+7\ell_2+2\right)+8\ell_1^2-2\right)-(d-2)\Delta_3^2\\
&\qquad -2\left(\ell_1\left(d\left(d-\Delta_1-1\right)+(d+6)\ell_2+2\Delta_1\Delta_2\right)-d\Delta_1\ell_2+\ell_1^2\left(d+12\ell_2+2\right)+2\ell_1^3\right)\\
&\qquad +\Delta_3\left(2\ell_1\left(d+2\ell_1+6\ell_2-2\right)+(d-2)d\right)+2(d-2)(d-1)-4l_2^2\ell_1\big)\\
&\quad -\Delta_3^2\left(6\Delta_1\left(\Delta_1-d\right)+(d-3)d\right)+d\Delta_3\left(6\Delta_1\left(\Delta_1-d\right)+(d-3)d\right)\\
&\quad -6l_1^2\left(-d\Delta_3+(d-6)d+\Delta_3^2+4l_2\ell_1-l_2^2-2\ell_1\left(\ell_1+4\ell_2+1\right)+6\right)\\
&\quad -6\Delta_1\big(\left(\Delta_1-\Delta_2\right)\left(\left(d-\Delta_1\right)^2+\Delta_1\Delta_2\right)+2l_2^2\left(d-\Delta_1\right)+2l_2\left(\left(d-2\right)\left(d-\Delta_1\right)-d\ell_2\right)\\
&\qquad +2\ell_2\left(\Delta_1-d\right)+2d\ell_2^2\big)\\
&\quad +6\ell_1^2\big(\Delta_3\left(-3d+\Delta_3+4\right)+2\ell_2\left(3d-10\Delta_3+5\right)+(d-2)(d+8)-2\Delta_1\left(\Delta_1-2\Delta_2\right)\\
&\qquad +4l_2\left(\Delta_3-6\ell_2-2\right)+4l_2^2+15\ell_2^2\big)\\
&\quad +6\ell_1\big(2l_2\left(\Delta_1\left(d-2\Delta_2\right)+(d-2)\Delta_3-5d+8\right)+(d-2)\Delta_3^2+2(d-3)\Delta_1\left(d-\Delta_1\right)\\
&\qquad +\ell_2\left(-2\Delta_1\left(d-3\Delta_2\right)+\Delta_3\left(-5d+2\Delta_3+10\right)+3(d-2)d-4\Delta_1^2\right)\\
&\qquad -(d-2)d\Delta_3+2(d-3)l_2^2-4d+8\big)\\
&\quad -12(d-2)l_1^3+12\ell_1^3\left(-2\Delta_3-2l_2+8\ell_2+5\right)-6l_1^4+6\ell_1^4\big]\,.
\end{aligned}
$$

From the operator above, it is easy to reduce to the vertex operators of type I and II: one has simply to impose the corresponding $\ell_i = 0$. For vertices of type III, where representations labeled by Young diagrams are reducible, the reduction requires some further comments. Let us note that the prefactor (5.2.32) for two self-dual fields (respectively two anti-self-dual fields) acquires precisely the same form as the $d > 4$ one, modulo the replacement of both second polarizations with their $d = 4$ counterparts W_i (respectively $\overline{W}_i$), and the replacement of the ℓ_i with their absolute values $|\ell_i|$. This means that the computation of the vertex operator for these cases will proceed in exactly the same way as in $d > 4$ up to the replacements described above. Furthermore, we observed with equation (5.2.30) that the cross ratio $\mathcal{Y}$ vanishes in $d = 4$ when expressed only in terms of (anti-)self-dual variables. We can therefore conclude that the vertex operator for two (anti-)self-dual fields corresponds to (5.3.1) with $\ell_i \to |\ell_i|$, as we have already imposed $\mathcal{Y} = 0$ in the computation of the $d > 4$ vertex operator. If instead we wish to describe the type III vertex operator with one self-dual and one anti-self-dual field, we can use our observation (5.2.40) relating prefactors in the $\ell_1\ell_2 > 0$ case to the $\ell_1\ell_2 < 0$ case. In particular, labeling the operator with $\ell_1, \ell_2 > 0$ as $H = H_{++}$ and the operator for $\ell_1 > 0$, $\ell_2 < 0$ as

H_{+-}, we find that

$$H_{+-}^{(d=4;\Delta_i;l_i;|\ell_1|,-|\ell_2|)} = \left(\frac{\mathcal{X}(1-\mathcal{X})}{2}\right)^{|\ell_2|} H_{++}^{(d=4;\Delta_i;l_i;|\ell_1|,|\ell_2|)} \left(\frac{\mathcal{X}(1-\mathcal{X})}{2}\right)^{-|\ell_2|} . \tag{5.3.6}$$

and analogously for H_{-+} with $\ell_1 \leftrightarrow \ell_2$. This concludes our construction of the vertex differential operators for all three single variable cases listed in eq. (5.1.4)
Having written out the results of our computations, let us add a few quick remarks and observations. First of all, it is important to note that almost all terms have a polynomial dependence on the cross ratio $\mathcal{X}$. The only exception appears in our expression for $\chi_0(\mathcal{X})$, which contains one term proportional to $\ell_1\ell_2\mathcal{X}^{-1}$. For vertices of type I and II, where $\ell_2 = 0$, this non-polynomial term is absent, while it remains present for vertices of type III. For vertices of type I, the expression is equivalent to the one introduced in [62], up to normalization and a constant shift. Let us stress again that our derivation is valid for $\ell_2 \neq 0$ and for arbitrary dimension $d \geq 4$. As we shall show in section 5.5, the mapping of our operator (5.3.3) to the elliptic CMS model of [68] also works for all cases, including MST_2-MST_2-scalar vertices $d > 4$ with kinematics reduced to $\mathcal{Y} = 0$. Nevertheless, it turns out that the map has significantly different features when it is applied beyond the list (5.1.4) of single variable vertex systems, c.f. section 5.5 and appendix 5.C for a discussion. Our analysis of the results in the next section will be restricted to the cases with $\ell_2 = 0$ which possess polynomial coefficients.

5.3.2 Relation with vertex operator for 5-point functions

It is worth to pause our analysis of the single variable vertex operators for a moment and to explain how this differential operator is related to the vertex operator for a 5-point function in $d \geq 3$ that we worked out in [63]. As usual, we split the scalar 5-point function

$$\langle \phi_1(X_1)\phi_2(X_2)\phi_3(X_3)\phi_4(X_4)\phi_5(X_5)\rangle = \Omega_5^{(\Delta_i)}(X_i)\, G(u_i) \tag{5.3.7}$$

into a function G of cross ratios and a prefactor Ω that accounts for the nontrivial covariance law of the scalar fields under conformal transformations. The former can be further decomposed into conformal blocks,

$$G(u_i) = \sum_{\Delta_a, l_a, \Delta_b, l_b, t} C_{12a} C_{a3b;t} C_{b45} \psi^{(\Delta_{12},\Delta_3,\Delta_{45})}_{(\Delta_a,\Delta_b;l_a,l_b;t)}(u_i) , \tag{5.3.8}$$

while the latter is given by

$$\Omega_5^{(\Delta_i)}(X_i) = \frac{\left(\frac{X_2\cdot X_3}{X_1\cdot X_3}\right)^{\frac{\Delta_1-\Delta_2}{2}} \left(\frac{X_2\cdot X_4}{X_2\cdot X_3}\right)^{\frac{\Delta_3}{2}} \left(\frac{X_3\cdot X_5}{X_3\cdot X_4}\right)^{\frac{\Delta_4-\Delta_5}{2}}}{(X_1\cdot X_2)^{\frac{\Delta_1+\Delta_2}{2}} (X_3\cdot X_4)^{\frac{\Delta_3}{2}} (X_4\cdot X_5)^{\frac{\Delta_4+\Delta_5}{2}}} . \tag{5.3.9}$$

For $N = 5$ points in $d \geq 3$, one can construct five cross ratios. Two common sets of such conformal invariant coordinates are denoted by $z_1, \bar{z}_1, z_2, \bar{z}_2, w$ and u_i, respectively. These are obtained from the embedding space variables by the following relations

$$\begin{aligned}
u_1 &= \frac{(X_1\cdot X_2)(X_3\cdot X_4)}{(X_1\cdot X_3)(X_2\cdot X_4)} = z_1\bar{z}_1 , \qquad u_2 = \frac{(X_1\cdot X_4)(X_2\cdot X_3)}{(X_1\cdot X_3)(X_2\cdot X_4)} = (1-z_1)(1-\bar{z}_1) , \\
u_3 &= \frac{(X_2\cdot X_3)(X_4\cdot X_5)}{(X_2\cdot X_4)(X_3\cdot X_5)} = z_2\bar{z}_2 , \qquad u_4 = \frac{(X_2\cdot X_5)(X_3\cdot X_4)}{(X_2\cdot X_4)(X_3\cdot X_5)} = (1-z_2)(1-\bar{z}_2) , \\
u_5 &= \frac{(X_1\cdot X_5)(X_2\cdot X_3)(X_3\cdot X_4)}{(X_2\cdot X_4)(X_1\cdot X_3)(X_3\cdot X_5)} = w(z_1-\bar{z}_1)(z_2-\bar{z}_2) + (1-z_1-z_2)(1-\bar{z}_1-\bar{z}_2) .
\end{aligned} \tag{5.3.10}$$

Since the OPE diagram for a 5-point function contains two internal fields of depth $L = 1$, i.e. two STTs, its blocks are characterized by four Casimir and one vertex operator. The latter is of type I and it was constructed in [63] as a fourth order operator acting on the five cross ratios.

One way to express the relation between this full vertex operator and the reduced 3-point vertex operator we have of the previous subsection makes use of the shadow formalism [103]. Shadow integrals turn the graphical representation of a conformal block, such as that of Fig. 15, into an integral formula. Just as in the case of Feynman integrals, the 'shadow integrand' is built from relatively simple building blocks that are assigned to the links and 3-point vertices of the associated OPE diagram. For a scalar 5-point function, the only non-trivial vertex is of type I. Within this subsection we label the two internal STT lines that are attached to this vertex by a and b rather than 1 and 2, to distinguish them from the external lines. The basic building block for the integrand of the shadow integral is the 3-point function Φ that was introduced in eq. (5.2.7). In the context of the 5-point function, only two special cases of this formula appear. On the one hand, there are two 1-STT-2 scalar vertices Φ_{1a2} and Φ_{b54} that are completely fixed by conformal symmetry, i.e. where t is trivial. On the other hand, there is the central vertex Φ_{ab3} of type I. With these notations, the shadow integral for scalar 5-point blocks of weight $\Delta_i, i = 1, \dots, 5$ reads

$$\Psi^{(\Delta_1,\dots,\Delta_5)}_{(\Delta_a,\Delta_b;l_a,l_b;t)}(X_1,...,X_5) = \tag{5.3.11}$$
$$\prod_{s=a,b}\int \mathrm{d}\mu(X_a,X_b,Z_a,Z_b)\Phi_{1\tilde{a}2}(X_1,X_a,X_2;\bar{Z}_a)\,\Phi^t_{ab3}(X_a,X_b,X_3;Z_a,Z_b)\,\Phi_{\tilde{b}54}(X_b,X_5,X_4;\bar{Z}_b)\ .$$

Here the tilde on the indices of the first and third vertex means that we use eq. (5.2.7) for two scalar legs but with Δ_a and Δ_b replaced by $d-\Delta_a$ and $d-\Delta_b$, respectively. We have placed a superscript t on the vertex function of the central vertex to remind the reader that this depends on a function t of the 3-point cross ratio. Integration is performed with the conformal invariant measure $\mathrm{d}\mu$ of the embedding space variables (5.B.34). After splitting off the prefactor (5.3.9),

$$\Psi^{(\Delta_i)}_{(\Delta_a,\Delta_b;l_a,l_b;t)}(X_i) = \Omega^{(\Delta_i)}(X_i)\psi^{(\Delta_{12},\Delta_3,\Delta_{45})}_{(\Delta_a,\Delta_b;l_a,l_b;t)}(u_1,...,u_5) \tag{5.3.12}$$

the shadow integral (5.3.11) gives rise to a finite conformal integral that defines the conformal block ψ as a function of the five conformal invariant cross ratios u_i. These integrals depend on the choice of (Δ_a, l_a), (Δ_b, l_b) and the function $t(\mathcal{X})$.
In [63] we constructed five differential equations for these blocks. Four of these are given by the eigenvalue equations for the second and fourth order Casimir operators for the intermediate channels,

$$\mathcal{D}^2_{(12)} = (\mathcal{T}_1+\mathcal{T}_2)_{[AB]}\,(\mathcal{T}_1+\mathcal{T}_2)^{[BA]}\ , \tag{5.3.13}$$
$$\mathcal{D}^2_{(45)} = (\mathcal{T}_4+\mathcal{T}_5)_{[AB]}\,(\mathcal{T}_4+\mathcal{T}_5)^{[BA]}\ , \tag{5.3.14}$$
$$\mathcal{D}^4_{(12)} = (\mathcal{T}_1+\mathcal{T}_2)_{[AB]}\,(\mathcal{T}_1+\mathcal{T}_2)^{[BC]}\,(\mathcal{T}_1+\mathcal{T}_2)_{[CD]}\,(\mathcal{T}_1+\mathcal{T}_2)^{[DA]}\ , \tag{5.3.15}$$
$$\mathcal{D}^4_{(45)} = (\mathcal{T}_4+\mathcal{T}_5)_{[AB]}\,(\mathcal{T}_4+\mathcal{T}_5)^{[BC]}\,(\mathcal{T}_4+\mathcal{T}_5)_{[CD]}\,(\mathcal{T}_4+\mathcal{T}_5)^{[DA]}\ . \tag{5.3.16}$$

5-point conformal blocks are eigenfunctions of these four differential operators with eigenvalues determined by the conformal weights Δ_a, Δ_b and the spins l_a, l_b of the two internal fields $a = (12)$ and $b = (45)$ that appear in the operator products $\phi_1\phi_2$ and $\phi_4\phi_5$, respectively. The shadow integrals ψ for conformal 5-point blocks turn out to be eigenfunctions of the following fifth differential operator

$$\mathcal{D}^{4,3}_{\rho,(12)3} = (\mathcal{T}_1+\mathcal{T}_2)_{[AB]}\,(\mathcal{T}_1+\mathcal{T}_2)^{[BC]}\,(\mathcal{T}_1+\mathcal{T}_2)_{[CD]}\,(\mathcal{T}_3)^{[DA]} \tag{5.3.17}$$

if and only if the vertex functions $t(\mathcal{X})$ we use in the integrand to represent the central vertex of the OPE diagram is an eigenfunction of the reduced vertex operator of the previous subsection, specialized to vertices of type I. In this sense, the shadow integral intertwines the full 5-point vertex operator constructed explicitly in [63] with the reduced vertex operator above.

There is another way to relate the full 5-point operator with the reduced one for type I vertices that employs OPE limits. In order to work out the reduction, we make use of the OPE in the limit where fields (ϕ_1, ϕ_2) and (ϕ_4, ϕ_5) are taken to be colliding, and are replaced with fields ϕ_a and ϕ_b whose conformal dimension and spin belongs to the tensor product of their representations. The first step is to reduce the operators to act on a spinning 4-point function, as in Figure 25.

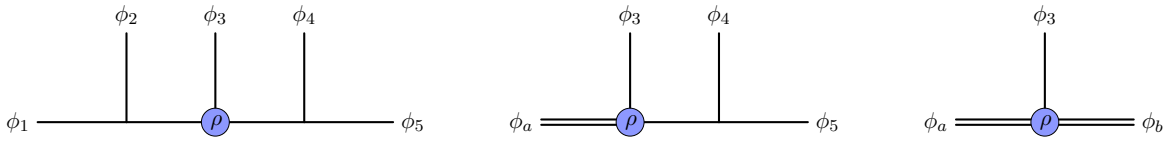

Figure 25: Scalar five-point function (left), which in the OPE limit of fields ϕ_1 and ϕ_2 gets reduced to the 4-point function with a spinning leg ϕ_a (center), and after a second OPE limit for fields ϕ_4 and ϕ_5 gets fully reduced to a type I vertex (right).

The OPE of the fields ϕ_1 and ϕ_2 acquires schematically the form

$$\phi_1(X_1)\phi_2(X_2) = \sum_{\Delta_a, l_a} \frac{1}{(X_1 \cdot X_2)^{\frac{\Delta_1+\Delta_2-\Delta_a+l_a}{2}}} C_{\phi_a}(X_1, X_2, Y, \partial_Y)\phi_a(Y)\,. \tag{5.3.18}$$

Plugging this into the left hand side of eq. (5.3.7) allows us to rewrite the equation as

$$\sum_{\Delta_a, l_a} \left(\frac{1}{(X_1 \cdot X_2)^{\frac{\Delta_1+\Delta_2-\Delta_a+l_a}{2}}} C_{\phi_a}(X_1, X_2, Y, \partial_Y) \langle \phi_a(Y)\phi_3(X_3)\phi_4(X_4)\phi_5(X_5)\rangle \right.$$
$$\left. - \Omega_5^{\Delta_i}(X_i) \sum_{\Delta_b, l_b, t} \lambda_{12a}\lambda_{a3b;t}\lambda_{b45}\psi^{(\Delta_{12},\Delta_3,\Delta_{45})}_{(\Delta_a,\Delta_b;l_a,l_b;t)}(z_1, \bar{z}_1, z_2, \bar{z}_2, w) \right) = 0\,. \tag{5.3.19}$$

The whole sum over weights Δ_a and spins l_a on the left hand side can only vanish if every term vanishes separately. By considering the $X_1 \cdot X_2 \to 0$ limit in this expression, we can reproduce the pole on the first term only by imposing a specific leading behavior of the conformal blocks in the second term. If by convention we pick $\bar{z}_1$ to be the cross ratio that vanishes for $X_1 \cdot X_2 \to 0$ (otherwise we can simply rename variables $z_1 \leftrightarrow \bar{z}_1$) and take into account that the prefactor $\Omega_5^{\Delta_i}(X_i)$ contains $(X_1 \cdot X_2)^{\frac{\Delta_1+\Delta_2}{2}}$, we can then deduce the following behavior of the conformal blocks:

$$\psi(z_1, \bar{z}_1, z_2, \bar{z}_2, w) \overset{\bar{z}_1 \to 0}{\sim} \bar{z}_1^{\frac{\Delta_a - l_a}{2}} \psi(z_1, z_2, \bar{z}_2, w)\,. \tag{5.3.20}$$

Imposing this leading behavior in the eigenvalue equations for the differential operators (5.3.13)–(5.3.17) allows to reduce the action of the differential operators to a 4-dimensional subspace of cross ratios in the following way:

$$\lim_{\bar{z}_1 \to 0} \left[\bar{z}_1^{-\frac{\Delta_a - l_a}{2}} \mathcal{D} \left(\bar{z}_1^{\frac{\Delta_a - l_a}{2}} \psi(z_1, z_2, \bar{z}_2, w) \right) \right] = \mathcal{E}\, \psi(z_1, z_2, \bar{z}_2, w). \tag{5.3.21}$$

To complete the OPE limit, one needs to impose $X_2 \to X_1$ which is of course stronger than the condition $X_1 \cdot X_2 = 0$ we discussed up to now. Doing so requirs a bit of caution. One subtlety is that the limit is quite sensitive to the set of cross ratios used to parameterize the 5-point function. For example, if we had decided to work with the cross ratios u_i, the complete OPE limit $X_1 = X_2$ would have implied both $u_2 = 1$ and $u_5 = u_4$, thereby overreducing the space of cross ratios. This issue is avoided in the $\{z_i, \bar{z}_i, w\}$ set of cross ratios, provided that the limit is taken in the appropriate way. The correct way to address this limit in coordinate space is to take $X_1 = X_a - \epsilon Z_a$, $X_2 = X_a + \epsilon Z_a$, and then take the $\epsilon \to 0$ limit. Note how this step requires either Lorentzian signature or an analytic continuation: given that we have already imposed the light-cone condition $X_1 \cdot X_2 = 0$, the variable Z_a must satisfy the constraints $Z_a \cdot X_a = Z_a \cdot Z_a = 0$. The latter are the same as the orthogonality and null constraints of an STT polarization vector, which explains why we used the symbol Z_a to parameterize the difference between X_2 and X_1. Following this prescription, the $\epsilon \to 0$ limit in cross ratio space corresponds to taking the sole limit $z_1 \to 0$, with $z_2, \bar{z}_2$ being unaffected and w acquiring a dependence on the newly introduced coordinate X_a and spin variable Z_a. In order to reproduce the correct eigenvalue for the quadratic Casimir $\mathcal{D}^2_{(12)}$ in the $z_1 \to 0$ limit, the Euclidean conformal blocks must exhibit leading behavior in z_1 of the type

$$\psi(z_1, z_2, \bar{z}_2, w) \overset{z_1 \to 0}{\sim} z_1^{\frac{\Delta_a + l_a}{2}} \psi(z_2, \bar{z}_2, w). \tag{5.3.22}$$

After these conjugations and limits, both the quadratic and quartic Casimirs associated to the internal leg $a = (12)$ are reduced to constants, and the remaining three operators

$$\mathcal{D}^2_{(45)}\,, \qquad \mathcal{D}^4_{(45)}\,, \qquad \mathcal{D}^{4,3}_{\rho,a3} \tag{5.3.23}$$

characterize the spinning 4-point function that is shown in Figure 25 (center). The latter depends only on three cross ratios $z_2, \bar{z}_2, w$, the spacetime dimension d, and the external data

$$\frac{\Delta_a - \Delta_3}{2}\,, \qquad \frac{\Delta_5 - \Delta_4}{2}\,, \qquad l_a\,. \tag{5.3.24}$$

It is straightforward to repeat the same procedure we just outlined for the leg $b = (45)$ in the remaining correlator, i.e. one can impose leading behaviors of the type

$$\psi(z_2, \bar{z}_2, w) \overset{\bar{z}_2 \to 0}{\sim} \bar{z}_2^{\frac{\Delta_b - l_b}{2}} \psi(z_2, w) \overset{z_2 \to 0}{\sim} z_2^{\frac{\Delta_b + l_b}{2}} \bar{z}_2^{\frac{\Delta_b - l_b}{2}} \psi(w) \tag{5.3.25}$$

to ensure that the quadratic and quartic Casimir of the internal leg $b = (45)$ assume constant values that are determined by the weight and spin of the intermediate field.

At the end of this procedure, one is left with a 3-point block of two STT's and one scalar, that is to say a vertex of type I, which is characterized by the sole vertex operator $\mathcal{D}^{4,3}_{\rho,a3}$ acting on the remaining cross ratio w. By replacing $X_5 = X_b - \epsilon' Z_b$, $X_4 = X_b + \epsilon' Z_b$ and taking $\epsilon' \to 0$, we find the following expression for w in terms of the external 3-point data,

$$w = 1 - \frac{(X_3 \cdot X_a)(X_3 \cdot X_b)\left[(X_a \cdot Z_b)(X_b \cdot Z_a) - (X_a \cdot X_b)(Z_a \cdot Z_b)\right]}{\left[(X_3 \cdot Z_b)(X_a \cdot X_b) - (X_3 \cdot X_b)(X_a \cdot Z_b)\right]\left[(X_3 \cdot Z_a)(X_a \cdot X_b) - (X_3 \cdot X_a)(X_b \cdot Z_a)\right]}\,. \tag{5.3.26}$$

After further inspection, this expression can be identified with

$$w = 1 - \frac{H_{ab}}{V_{a,3b} V_{b,a3}} = 1 - \mathcal{X}'\,, \tag{5.3.27}$$

where the cross ratio $\mathcal{X}'$ is equal to $\mathcal{X}$ with the replacement $(1, 2, 3) \to (a, b, 3)$. The resulting operator can be easily identified with the $\ell_1 = \ell_2 = 0$ case of our general expression (5.3.3).

5.4 Vertex Operator and Generalized Weyl algebras

The Hamiltonians we constructed in our letter [62] and the extension discussed in the previous section have nice properties, even though they may look a bit uninviting at first. In this section we exhibit some of their underlying algebraic structure. This allows us to recast the vertex operator into a one-line expression, somewhat analogous to the harmonic oscillator that possesses a particularly simple representation in terms of creation and annihilation operators. Here we define a generalized Weyl algebra with relatively simple commutation relations and then build our vertex operators directly in terms of its generators. An important role in our discussion is played by the scalar product of the vertex system.

5.4.1 Single variable vertices and the Gegenbauer scalar product

Functions on the configuration space $\mathcal{M}$ inherit a scalar product from the Haar measure on the conformal group. This is the case in general, but in particular for the 1-dimensional spaces we are dealing with in this paper. Working out this scalar product is straightforward in principle, but a bit cumbersome in practice. Since we have not found the answer in the literature, we included the full calculation in Appendix 5.B. The result is surprisingly simple: it turns out that, when written in the variable $s = 1 - 2\mathcal{X}$, the group theoretic scalar product on the configuration space $\mathcal{M}$ coincides with the Gegenbauer scalar product,

$$\langle f, g\rangle_{\alpha(d;\ell_i)} := \int_{-1}^{+1} \mathrm{d}s\, (1-s^2)^{\alpha(d;\ell_i)-\frac{1}{2}}\, \overline{f(s)}\, g(s)\,, \tag{5.4.1}$$

with the parameter α given by

$$\alpha(d;\ell_i) := \ell_1 + \ell_2 + \frac{d-3}{2}\,. \tag{5.4.2}$$

In the following we shall implicitly assume that the parameters assume only those values that appear in the context of our three single parameter vertices, i.e. for $d = 3$ we have $\ell_1 = 0 = \ell_2$ while for $d > 3$ only $\ell_2 = 0$. The only case for which ℓ_2 can also be non-zero is in $d = 4$. Gegenbauer polynomials $C_n^{(\alpha)}(s)$ provide an orthogonal basis for $\langle -, -\rangle_\alpha$:

$$\langle C_m^{(\alpha)}, C_n^{(\alpha)}\rangle_\alpha = \frac{\pi\, 2^{1-2\alpha}}{\Gamma(\alpha)^2}\, \frac{\Gamma(n+2\alpha)\Gamma(n+\alpha)}{\Gamma(n+\alpha+1)\Gamma(n+1)}\, \delta_{mn}\,. \tag{5.4.3}$$

As one may check by explicit computation, our vertex differential operators $H^{(d;\Delta_i;l_i)}(\mathcal{X}, \partial_{\mathcal{X}})$ are hermitian with respect to a Gegenbauer scalar product whenever the conformal weights Δ_i and the STT spins l_i are analytically continued to satisfy,

$$\bar{\Delta}_i = d - \Delta_i\,, \qquad \bar{l}_i = 2 - d - l_i\,, \tag{5.4.4}$$

i.e. $(\Delta_i; l_i) \in \left(\frac{d}{2} + \mathrm{i}\mathbb{R}\right) \times \left(\frac{2-d}{2} + \mathrm{i}\mathbb{R}\right)$, while $(d; \ell_i)$ are kept as real parameters. Our goal now is to compute the Hamiltonian in the basis of Gegenbauer polynomials. In doing so we shall restrict to the case with $d > 3$ and $\ell_2 = 0$, i.e. we exclude the somewhat special case of $d = 4$ with $\ell_1 \neq 0 \neq \ell_2$ for which our Hamiltonian contains a non-polynomial term, see comments at the end of the previous section. The computation of the Hamiltonian in the Gegenbauer basis relies on its expression as

$$H^{(d,\Delta_i,l_i,\ell_i)} = h_0^{(s)}(s) + \sum_{q=1}^{4} h_q^{(s)}(s)(1-s^2)^{q-1}\partial_s^q\,, \tag{5.4.5}$$

where all $h_q^{(s)}(s)$ are polynomials of order at most 3 in s whenever $\ell_2 = 0$. It proceeds with the help of three well-known identities:

(S) the recursion relation of Gegenbauer polynomials

$$s \cdot C_n^{(\alpha)} = \frac{(n+1)C_{n+1}^{(\alpha)} + (n+2\alpha-1)C_{n-1}^{(\alpha)}}{2(n+\alpha)}\,, \tag{5.4.6}$$

(D) the Gegenbauer differential equation in self-adjoint form,

$$\mathcal{D}_\alpha \cdot C_n^{(\alpha)} = (1-s^2)^{\frac{1}{2}-\alpha}\partial_s\,(1-s^2)^{\frac{1}{2}+\alpha}\partial_s \cdot C_n^{(\alpha)} = -n(n+2\alpha)C_n^{(\alpha)}\,, \tag{5.4.7}$$

(Θ) and the first order differentiation operator

$$\partial_\Theta \cdot C_n^{(\alpha)} = (1-s^2)\partial_s \cdot C_n^{(\alpha)} = \frac{(n+2\alpha-1)(n+2\alpha)C_{n-1}^{(\alpha)} - n(n+1)C_{n+1}^{(\alpha)}}{2(n+\alpha)}\,. \tag{5.4.8}$$

Using these building blocks (S),(D),(Θ), our Hamiltonians can be recast into the form

$$\begin{aligned} H^{(d,\Delta_i,l_i,\ell_i)} =& \mathcal{D}_\alpha\partial_\Theta^2 + (k_{3,1}s+k_{3,0})\,\mathcal{D}_\alpha\partial_\Theta + \left(k_{2,2}s^2+k_{2,1}s+k_{2,0}\right)\mathcal{D}_\alpha \\ &+ (k_{1,1}s+k_{1,0})\,\partial_\Theta + k_{0,2}s^2 + k_{0,1}s + k_{0,0}\,, \end{aligned} \tag{5.4.9}$$

where the coefficients $k_{i,j} = k_{i,j}(d,\Delta_i,l_i,\ell_i)$ are given by

$$\begin{aligned} &k_{3,0} = 2\mathrm{i}\gamma_3\,, \qquad k_{3,1} = 2(\nu_1+\nu_2+\alpha)+3\,, \\ &k_{2,0} = \gamma_1^2+\gamma_2^2-\gamma_3^2-2\nu_1\nu_2-2(\alpha-1)(\nu_1+\nu_2)-\alpha(1+3\alpha)+\frac{13}{4}\,, \\ &k_{2,1} = -2\gamma_1\gamma_2+\mathrm{i}\gamma_3\,(2(\nu_1+\nu_2+\alpha)+3)\,, \qquad k_{2,2} = \nu_1^2+\nu_2^2+4l\nu_1\nu_2+(4\alpha+1)(\nu_1+\nu_2)+4\alpha^2+3\,, \\ &k_{1,0} = 2(\nu_1+\nu_2+\alpha)\gamma_1\gamma_2+\mathrm{i}\gamma_3\left(-2\nu_1\nu_2+(2\alpha+1)(\nu_1+\nu_2)-4\alpha^2+2\alpha+2\right), \\ &k_{1,1} = -2(\nu_1^2\nu_2+\nu_2^2\nu_1)+(1-2\alpha)\left(\nu_1^2+\nu_2^2+4\nu_1\nu_2+(1+4\alpha)(\nu_1+\nu_2+\alpha+1)-\alpha-2\right), \\ &k_{0,1} = 2\nu_1\nu_2\left(\gamma_1\gamma_2+\mathrm{i}\gamma_3(\alpha+\frac{1}{2})\right), \qquad k_{0,2} = -\nu_1\nu_2(\nu_1-1)(\nu_2-1)\,. \end{aligned} \tag{5.4.10}$$

The parameters γ_k, ν_k are defined through

$$\Delta_k := \frac{d}{2}+\mathrm{i}\gamma_k\,, \qquad k=1,2,3\,, \qquad\qquad \nu_k := l_k-\ell_1\,, \qquad k=1,2\,, \tag{5.4.11}$$

and α was introduced in eq. (5.4.2). Let us stress once again that the solution we have displayed here applies to $\ell_2 = 0$ and $d \geq 3$. When $\ell_2 \neq 0$, the Hamiltonian contains a non-polynomial term in $h_0^{(s)}(s)$ which is proportional to $(1-s)^{-1}$. So, while it is in principle possible to compute the action of the MST_2-MST_2-scalar Hamiltonian in $d=4$ on Gegenbauer polynomials with $\alpha = (d-3)/2+\ell_1+\ell_2$, it does not directly fit our Ansatz (5.4.9).

Plugging the identities (5.4.6), (5.4.7), (5.4.8) back into (5.4.9) one can obtain simple explicit formulas for the matrix elements

$$H_{mn}^{(d;\Delta_i;l_i;\ell_i)} = \frac{\langle C_m^{(\alpha)}, H^{(d;\Delta_i;l_i;\ell_i)} \cdot C_n^{(\alpha)}\rangle_\alpha}{\langle C_m^{(\alpha)}, C_m^{(\alpha)}\rangle_\alpha}\,. \tag{5.4.12}$$

One observes that these vanish whenever $|n-m| > 2$, so our Hamiltonian in the Gegenbauer basis has non-vanishing matrix elements only close to the diagonal. In terms of the matrix elements, the hermiticity property of the vertex differential operators reads

$$H_{mn}^{(d;\Delta_i;l_i;\ell_i)} = \frac{\langle C_n^{(\alpha)}, C_n^{(\alpha)}\rangle_\alpha}{\langle C_m^{(\alpha)}, C_m^{(\alpha)}\rangle_\alpha} H_{nm}^{(d;d-\Delta_i;2-d-l_i;\ell_i)}\,. \tag{5.4.13}$$

With our formulas (5.4.9) and (5.4.10) we have fulfilled our first promise, namely to write the Hamiltonian in a much more compact form that fully replaces the two pages of formulas we spelled out in the previous section.

5.4.2 A generalized Weyl algebra acting on tensor structures

We want to go one step further and write the vertex Hamiltonians in terms of the generators of some Weyl-like algebraic structure that acts on Gegenbauer polynomials and hence on 3-point tensor structures. Our algebra contains three generators $A, A^\dagger$ and N and it depends on the parameters α, ν_1 and ν_2 which we introduced in eqs. (5.4.2) and (5.4.11). When acting on Gegenbauer polynomials, these three operators are given by

$$NC_n^{(\alpha)} := nC_n^{(\alpha)}, \tag{5.4.14}$$

$$AC_n^{(\alpha)} := (n+\nu_1+2\alpha)(n+\nu_2+2\alpha)\frac{n+2\alpha-1}{n+\alpha}C_{n-1}^{(\alpha)}\,, \tag{5.4.15}$$

$$A^\dagger C_n^{(\alpha)} := (n-\nu_1)(n-\nu_2)\frac{n+1}{n+\alpha}C_{n+1}^{(\alpha)}, \tag{5.4.16}$$

where eq. (5.4.15) applies to all $n>0$, and $AC_0^{(\alpha)}=0$ when $n=0$, i.e. the state $C_0^{(\alpha)}$ is annihilated by the lowering operator A. Similarly, the action of the raising operator $A^\dagger$ vanishes if $n=\nu_1$ or $n=\nu_2$. Consequently, one can restrict the action of $A, A^\dagger$ and N to the finite dimensional subspace that is spanned by $C_n^{(\alpha)}$ for $n=0,\ldots,\min(\nu_1,\nu_2)$. This should remind us of the space of 3-point tensor structures we discussed at the very end of section 5.2. There we argued that the space of 3-point tensor structures has dimension n_t+1 with $n_t = min(l_1-\ell_1, l_2-\ell_1) = min(\nu_1,\nu_2)$ in the case of $\ell_2=0$, using the definition (5.4.11) of ν_k. Therefore, the truncation of the action of $A, A^\dagger$ and N to a finite dimensional subspace of Gegenbauer polynomials we observe here is fully consistent with the finiteness of the space of 3-point tensor structures, at least for $d>3$. We will discuss the special case of $d=3$ below.

From the action on Gegenbauer polynomials it is possible to check that the operators $A, A^\dagger$ and N obey the following relations

$$[N, A^\dagger] = A^\dagger, \tag{5.4.17}$$

$$[N, A] = -A\,, \tag{5.4.18}$$

$$AA^\dagger = \frac{(N+1)(N+2\alpha)}{(N+\alpha)(N+\alpha+1)}(N-\nu_1)(N+2\alpha+\nu_1+1)(N-\nu_2)(N+2\alpha+\nu_2+1)\,, \tag{5.4.19}$$

$$A^\dagger A = \frac{N(N+2\alpha-1)}{(N+\alpha-1)(N+\alpha)}(N+\nu_1+2\alpha)(N-\nu_1-1)(N+\nu_2+2\alpha)(N-\nu_2-1)\,. \tag{5.4.20}$$

We can use these to define a family of abstract algebras that depends parametrically on $\alpha=\ell_1+(d-3)/2$ and $\nu_k = l_k-\ell_1$. This family comes equipped with an involutive antiautomorphism $(-)^*$ defined by $N^*=N$ and $A^*=A^\dagger$. It coincides with the adjoint whenever d is real and the spins l_i satisfy the relation (5.4.4) that is needed in order for our vertex operators to be hermitian or, equivalently,

$$\bar\alpha = \alpha\,, \qquad \bar\nu_1 = -(2\alpha+1+\nu_1)\,, \qquad \bar\nu_2 = -(2\alpha+1+\nu_2)\,. \tag{5.4.21}$$

Having introduced the algebra generated by $A, A^\dagger$ and N, the vertex operator H can now be written as a rational combination of the generators of this algebra:

$$H^{(d;\Delta_i;l_i;\ell_i)} = B^\dagger B - \Gamma(N+\alpha)^2 + \frac{\alpha(\alpha-1)\,K}{(N+\alpha)^2-1} + E^{(d;\Delta_i;l_i;\ell_i)}. \tag{5.4.22}$$

Here, we defined the operators

$$B^\dagger := \frac{A - A^\dagger}{2\mathrm{i}} - \mathrm{i}(2\gamma_1\gamma_2 + \mathrm{i}\gamma_3)(N+\alpha)\,, \tag{5.4.23}$$

$$B := \frac{A - A^\dagger}{2\mathrm{i}} + \mathrm{i}(2\gamma_1\gamma_2 - \mathrm{i}\gamma_3)(N+\alpha)\,, \tag{5.4.24}$$

and the two parameters

$$\Gamma := \frac{1}{4}(1+4\gamma_1^2)(1+4\gamma_2^2)\,, \tag{5.4.25}$$

$$K := (\nu_1+\alpha)(\nu_2+\alpha)(\nu_1+\alpha+1)(\nu_2+\alpha+1)\,. \tag{5.4.26}$$

The constant term $E^{(d;\Delta_i;l_i;\ell_i)}$ is obtained by relating $H^{(d;\Delta_i;l_i;\ell_i)}\cdot 1 = h_0^{(d;\Delta_i;l_i;\ell_i)}(0)$ to the action of $A, A^\dagger, N$ on $C_0^{(\alpha)}$. In this way we find

$$\begin{aligned} E^{(d;\Delta_i;l_i;\ell_i)} =& h_0^{(d;\Delta_i;l_i;\ell_i)}(0) - \alpha^4 - (1+2\nu_1+2\nu_2)\alpha^3 \\ &+ \alpha^2\left(\frac{1}{4} + \gamma_1^2 + \gamma_2^2 - \gamma_3^2 + \nu_1(\nu_1+1) + \nu_2(\nu_2+1) + 4\nu_1\nu_2\right) \\ &- 2\nu_1\nu_2\alpha - \nu_1\nu_2(1+\nu_1\nu_2). \end{aligned}$$

This concludes the algebraic reformulation of our vertex Hamiltonians. It is remarkable that the algebra only depends on the spins and dimension d, i.e. that all the dependence on the conformal weights of the three fields resides in the Hamiltonian.

The case of $d = 3$, which implies $\ell_1 = 0$, requires additional consideration since in this case one can also have odd-parity tensor structures, see our discussion at the end of subsection 5.2.1. As we saw there, the STT-STT-scalar vertex in $d = 3$ is unique in that it admits a total number

$$(\min(\nu_1,\nu_2)+1) + \min(\nu_1,\nu_2) = \min(2l_1+1, 2l_2+1) \tag{5.4.27}$$

of 3-point tensor structures. A complete and orthogonal basis can be obtained from the union of Chebyshev polynomials of the first and second kind,

$$\{C_n^{(0)}(s)\}_{n=0,\ldots,\min(l_1,l_2)} \quad , \quad \{\sqrt{1-s^2}C_n^{(1)}(s)\}_{n=1,\ldots,\min(l_1,l_2)}\,.$$

The action of $A, A^\dagger, N$ in $d = 3$, however, is more conveniently written in the Fourier basis $e^{\mathrm{i}n\theta}$, where $n = -\min(l_1,l_2),\ldots,+\min(l_1,l_2)$ and the new variable θ is related to our cross ratio $\mathcal{X}$ by $\mathcal{X} = \sin^2\frac{\theta}{2}$. In this case, the action of $A, A^\dagger$ and N on the Fourier basis is

$$N\,e^{\mathrm{i}n\theta} := n e^{\mathrm{i}n\theta}, \qquad A^\dagger e^{\mathrm{i}n\theta} := (n-l_1)(n-l_2)e^{\mathrm{i}(n+1)\theta}, \qquad A\,e^{\mathrm{i}n\theta} := (n+l_1)(n+l_2)e^{\mathrm{i}(n-1)\theta}.$$

It is easy to see that these operators satisfy the following polynomial relations

$$[N, A^\dagger] = A^\dagger, \tag{5.4.28}$$

$$[N, A] = -A\,, \tag{5.4.29}$$

$$AA^\dagger = (N-l_1)(N-l_2)(N+l_1+1)(N+l_2+1)\,, \tag{5.4.30}$$

$$A^\dagger A = (N-l_1-1)(N-l_2-1)(N+l_1)(N+l_2)\,. \tag{5.4.31}$$

These relations agree with those we found in eqs. (5.4.17)-(5.4.19) above for the special choice $\alpha = \ell_1 + (d-3)/2 = 0$ relevant for vertices in $d = 3$, where $\ell_1 = 0$. In other words, we have now shown

that for $d = 3$, the algebra we have introduced above possesses a finite dimensional representation on the space of Chebyshev polynomials of first and second kind.

For $\alpha = 0$ and $\alpha = 1$, the algebra of $A, A^\dagger$ and N is one special example of a larger family of algebras of the form $A^\dagger A = f(N)$, $AA^\dagger = f(N+1)$ that can be associated with a polynomial $f(N)$. Such families of algebras have been studied for a long time in the mathematics literature, going back at least as early as [123, §3]. The representation theory of these algebras was studied in [124] and in [125], where the latter author first used the term "generalized Weyl algebra". It was then in [126] that these algebras were first reformulated as non-commutative deformations of the Kleinian singularity of type $\tilde{A}_{n-1}$ when f is a polynomial of degree n. Finally, using quiver theory, the authors of [127] generalized this analysis to non-commutative deformations of the Kleinian singularities associated to any finite subgroup of $\mathrm{SL}_{\mathbb{C}}(2)$. In this context, the algebra with relations (5.4.28) — (5.4.31) is thus called a generalized Weyl algebra or deformed Kleinian singularity of type $\tilde{A}_3$.

For $\alpha \neq 0, 1$, the relations (5.4.19) and (5.4.20) are no longer polynomial, at least not in the way we wrote them. Nevertheless, they can be recast as an α-dependent family of generalized Weyl algebras if we are willing to sacrifice the property $A^* = A^\dagger$. Indeed, any rescaling of the operators A and $A^\dagger$ by a rational function of N defines a homomorphism of algebras[4]. In the case of eqs. (5.4.19) and (5.4.20), it is natural to take

$$U := \frac{(N+\alpha)(N+\alpha+1)}{(N+1)(N+2\alpha)} A\,, \qquad V := A^\dagger\,, \tag{5.4.32}$$

in which case the modified relations read

$$[N, V] = V\,, \tag{5.4.33}$$
$$[N, U] = -U\,, \tag{5.4.34}$$
$$UV = (N-\nu_1)(N+\nu_1+2\alpha+1)(N-\nu_2)(N+\nu_2+2\alpha+1)\,, \tag{5.4.35}$$
$$VU = (N-\nu_1-1)(N+\nu_1+2\alpha)(N-\nu_2-1)(N+\nu_2+2\alpha)\,, \tag{5.4.36}$$

and also define a generalized Weyl algebra of type $\tilde{A}_3$, but now with an extra deformation parameter α. In any given representation, the homomorphism $A \longleftrightarrow U$ in (5.4.32) is bijective if and only if $-1, -\alpha, -(\alpha+1), -2\alpha \notin \mathrm{Spec}(N)$. This condition is indeed satisfied in the Gegenbauer polynomial representations, where U is explicitly represented as

$$U \cdot C_n^{(\alpha)} = (n+\nu_1+2\alpha)(n+\nu_2+2\alpha)\frac{n+\alpha-1}{n} C_{n-1},\ \ \forall n > 0, \qquad U \cdot C_0^{(\alpha)} = 0. \tag{5.4.37}$$

As a result, $(A, A^\dagger, N) \mapsto (U, V, N)$ defines an isomorphism, and all vertex systems of type I and II are representations of the generalized $\tilde{A}_3$ Weyl algebra with relations (5.4.33) — (5.4.36).

Our final comment in this subsection concerns the fact that our expression (5.4.22) for the Hamiltonian depends on parameters only through the combinations α, ν_i, γ_i, at least up to the constant term. It follows that (see appendix 5.C for a further generalization)

$$H^{(d;\Delta_i;l_i;\ell_1,0)} = H^{(d+2\ell_1;\Delta_i+\ell_1;l_i-\ell_1;0,0)} + \Delta E^{(d;\Delta_i;l_i;\ell_1)}, \tag{5.4.38}$$

[4] We thank Pavel Etingof for pointing this out to us.

where

$$\begin{aligned}\ell_1^{-1}\Delta E^{(d;\Delta_i;l_i;\ell_1)} =& -\frac{2}{3}\ell_1^3+\frac{8\alpha+26}{3}\ell_1^2\\ &+\frac{4}{3}\left(-2\alpha^2+2(\nu_1-\nu_2-41/2)\alpha-\gamma_1^2+\gamma_2^2-\gamma_3^2+\nu_1(\nu_1+1)-\nu_2(\nu_2+1)-33\right)\ell_1\\ &+\frac{16}{3}\alpha^2(\nu_2-\nu_1+17/4)+\frac{8}{3}\alpha\left(\gamma_1^2-\gamma_2^2+\gamma_3^2-\nu_1(\nu_1+4)+\nu_2(\nu_2+5/2)+9\right)\\ &+2\left(2\gamma_1^2-\gamma_2^2+\gamma_3^2-2\nu_1(\nu_1+1)+\nu_2(\nu_2+1)+\frac{9}{2}\right).\end{aligned}$$

Now, the α-deformed relations (5.4.19) and (5.4.20) of the generalized Weyl algebra coincide with the $d=3$ relations (5.4.30), (5.4.31) whenever $\alpha=0$ or $\alpha=1$. In the former case, $\alpha=0 \iff (d,\ell_1)=(3,0)$. On the other hand, the latter case $\alpha=1$ can occur in two situations,

$$(d,\ell_1)=(5,0)\,,\qquad \text{or}\qquad (d,\ell_1)=(4,\frac{1}{2})\,, \tag{5.4.39}$$

in which case

$$\nu_i=l_i\,,\qquad \text{or}\qquad \nu_i=l_i-\frac{1}{2}\,, \tag{5.4.40}$$

and the two operators are the same up to a constant shift,

$$H^{(d=5;\Delta_i;l_i;0,0)}(\mathcal{X},\partial_{\mathcal{X}})=H^{(d=4;\Delta_i-\frac{1}{2};l_i+\frac{1}{2};\frac{1}{2},0)}(\mathcal{X},\partial_{\mathcal{X}})+\Delta E\,. \tag{5.4.41}$$

In both of these cases, the Gegenbauer polynomials become Chebyshev polynomials of the second kind $\{C_n^{(1)}(s)\}_{n=0,\dots,\min(l_1,l_2)}$, and the two vertex operators are related to the $d=3$ operator by a similarity transformation,

$$H^{(d=5;\Delta_i;l_i;0,0)}(\mathcal{X},\partial_{\mathcal{X}})=\frac{1}{\sqrt{\mathcal{X}(1-\mathcal{X})}}H^{(d=3;\Delta_i-1;l_i+1)}(\mathcal{X},\partial_{\mathcal{X}})\sqrt{\mathcal{X}(1-\mathcal{X})}+\Delta E\,. \tag{5.4.42}$$

In particular, the parity-even 3-point tensor structures of two STTs in $d=5$, are equivalent to the parity-odd 3-point tensor structures of two STTs in $d=3$.

5.5 Map to the Lemniscatic CMS model

In the previous section we have found quite an elegant reformulation of our vertex operators that makes it seem a bit more tractable than the original formulas we displayed in section 5.3. All this is somewhat similar to the Casimir operators of Dolan and Osborn, which appeared a bit uninviting at first, but were found to possess interesting algebraic structure that led to explicit solutions, in particular in even dimensions. In [57], it was discovered that the usual Casimir operator can be mapped to another well studied operator, namely the Hamiltonian of an integrable 2-particle CMS model. Here we establish a very similar statement for the vertex operators. By explicit computations, these operators can be mapped to the lemniscatic CMS model, a special case of the crystallographic elliptic CMS models found by Etingof, Felder, Ma and Veselov [68]. We review this model in the first subsection before constructing the map from our vertex differential operator. The third subsection contains a complete identification of parameters.

5.5.1 The elliptic $\mathbb{Z}/4\mathbb{Z}$ CMS model

While our vertex system examples have received little attention, there has been much discussion in similar cases of the relation between deformations of Kleinian singularities on the one hand, and CMS models for the corresponding complex reflection group on the other hand — see e.g. [128] for $\tilde{A}_{n-1}$, and [129] for the general case, both of which are based on [130]. Thus, the identification of our operator with a lemniscatic CMS model is less surprising in light of the $\tilde{A}_3$ singularity of §5.4.2. That said, apart from $\tilde{A}_1$, the only integrable models explicitly studied in this particular context have so far always been rational. And while the integrable systems in [131] include, amongst others, the compact $\mathfrak{so}_{\mathbb{R}}(6)$ analogue of our MST_2-MST_2-scalar vertex in $d = 4$, the authors do not make the connection with the elliptic integrable models of [68].

The elliptic CMS models associated with the complex reflection groups $\mathbb{Z}_m$ form a family of quantum mechanical integrable systems with (complexified) coordinate on an orbifold curve of the form

$$\mathcal{M} = \mathbb{C}/\left(\mathbb{Z}_m \ltimes (\mathbb{Z} \oplus \tau\mathbb{Z})\right), \tag{5.5.1}$$

where $\mathbb{Z} \oplus \tau\mathbb{Z} \subset \mathbb{C}$ is a 2-dimensional lattice with elliptic modulus τ in the upper half of the complex plane, and elements of the group $\mathbb{Z}_m \subset \mathrm{SO}(2)$ act on the lattice as a point group, i.e. through rotations by angles $\varphi_n = n/2m\pi$ where $n = 1, \dots, m$. It is well known that the only 2-dimensional lattices with a non-trivial point group $\mathbb{Z}_m$ appear for $m = 2, 3, 4, 6$. Apart from $m = 2$, the elliptic modulus τ is also fixed so that spaces $\mathcal{M}$ of the form (5.5.1) only appear for

$$(m, \tau) \in \{2\} \times \mathbb{C}_+\,, \qquad \text{or} \qquad (m, \tau) \in \{3, e^{2\pi\mathrm{i}/3}\} \cup \{4, \mathrm{i}\} \cup \{6, e^{\pi\mathrm{i}/3}\}\,. \tag{5.5.2}$$

In [68], the authors construct new integrable models on each of these curves, but only the case $\tau = \mathrm{i}$ with group action of $\mathbb{Z}_4$ turns out to be relevant for us. In order to proceed, let us write the associated curve (5.5.1) as the quotient of the so-called lemniscatic elliptic curve E_{i} by a $\mathbb{Z}_4$ action,

$$\mathcal{M} = E_{\mathrm{i}}/\mathbb{Z}_4\,, \quad \textit{where} \quad E_{\mathrm{i}} = \mathbb{C}/(\mathbb{Z} \oplus \mathrm{i}\mathbb{Z}) = \{z \in \mathbb{C} \,|\, z \sim z + 1 \sim z + \mathrm{i}\}\,. \tag{5.5.3}$$

Here, the $\mathbb{Z}_4$ action is the obvious one that is given by multiplication of $z \in E_{\mathrm{i}}$ with any fourth root of unity $\zeta^4 = 1$, i.e. $z \mapsto \zeta \cdot z$. Under this action, the lemniscatic curve E_{i} has four fixed points:

$$\omega_0 := 0\,, \qquad \zeta \cdot 0 = 0\,, \tag{5.5.4}$$

$$\omega_1 := \frac{1+\mathrm{i}}{2}\,, \qquad \zeta \cdot \frac{1+\mathrm{i}}{2} = \frac{-1+\mathrm{i}}{2} \sim \frac{1+\mathrm{i}}{2}\,, \tag{5.5.5}$$

$$\omega_2 := \frac{\mathrm{i}}{2}\,, \qquad \zeta^2 \cdot \frac{\mathrm{i}}{2} = -\frac{\mathrm{i}}{2} \sim \frac{\mathrm{i}}{2}\,, \tag{5.5.6}$$

$$\zeta^3 \cdot \omega_2 = \omega_3 := \frac{1}{2}\,, \qquad \zeta^2 \cdot \frac{1}{2} = -\frac{1}{2} \sim \frac{1}{2}\,, \tag{5.5.7}$$

where $\zeta \in \mathbb{Z}_4$ denotes the generating element $\zeta = \mathrm{i}$, and the equivalence relation $\sim$ identifies points that are obtained from one another by lattice shifts. From the short computation in the second column we conclude that ω_0, ω_1 are fixed points stabilized by the entire $\mathbb{Z}_4$, i.e. they are fixed points of order 4, while ω_2, ω_3 are fixed points of order 2 with a stabilizer subgroup $\mathbb{Z}_2 \subset \mathbb{Z}_4$. These last two fixed points are mapped to each other by the nontrivial $\mathbb{Z}_4$ transformation on E_{i}. They thus give rise to the same point in the quotient $\mathcal{M} = E_{\mathrm{i}}/\mathbb{Z}_4$. We conclude that $\mathcal{M}$ has three (singular) orbifold points which we denote as

$$z_0 := \omega_0\,, \quad z_1 := \omega_1\,, \quad z_2 := \omega_2 \sim \omega_3. \tag{5.5.8}$$

At these points, the orbifold singularities are of orders $4, 4, 2$, respectively. The elliptic CMS model associates to each of these singular points z_ν, $\nu = 0, 1, 2$, a family of multiplicities $m_{i,\nu}$, $i = 1, \dots, 4$ such that

$$\sum_{i=1}^{4} m_{i,\nu} := 6\,, \quad \nu = 0, 1, 2\,, \qquad m_{1,2} + m_{2,2} = 1\,, \qquad m_{3,2} + m_{4,2} = 5\,. \tag{5.5.9}$$

Note that there is one relation among the four multiplicities we associate with the fixed points of order four, while there are three relations among the four multiplicities that are associated with the fixed point of order two. Given that there are three relations that constrain the four multiplicities $m_{i,2}$, it is often convenient to parametrize the solutions in terms of a single parameter k which we define as

$$m_{1,2} := k + 1\,. \tag{5.5.10}$$

The Hamiltonian L_{EFMV} of the lemniscatic CMS model has a relatively complicated dependence on the multiplicities. On the other hand, it may be uniquely characterized by a rather simple set of conditions: if we require that that the $\mathbb{Z}_4$-invariant operator $L_{\text{EFMV}}(z, \partial_z)$ takes the normalized form

$$L_{\text{EFMV}} = \partial_z^4 + \mathcal{O}(\partial_z^2)\,, \tag{5.5.11}$$

then its dependence on the multiplicities is uniquely determined by the following set of conditions

$$L_{\text{EFMV}}(z, \partial_z) \cdot (z - z_0)^r = \prod_{i=1}^{4} (r - m_{i,0})\,(z - z_0)^{r-4} + \mathcal{O}((z - z_0)^r)\,, \tag{5.5.12}$$

$$L_{\text{EFMV}}(z, \partial_z) \cdot (z - z_1)^r = \prod_{i=1}^{4} (r - m_{i,1})\,(z - z_1)^{r-4} + \mathcal{O}((z - z_1)^r)\,, \tag{5.5.13}$$

$$\begin{aligned} L_{\text{EFMV}}(z, \partial_z) \cdot (z - z_2)^r = &\prod_{i=1}^{4} (r - m_{i,2})\,(z - z_2)^{r-4} \\ &+ \lambda (r - m_{1,2})(r - m_{2,2})(z - z_2)^{r-2} + \mathcal{O}((z - z_2)^r)\,, \end{aligned} \tag{5.5.14}$$

which we assume to hold for some constant $\lambda \in \mathbb{C}$, in the neighborhood of the singular points $z = z_\nu$. In order to write the Hamiltonian explicitly over the full orbifold $\mathcal{M}$, we first introduce the Weierstrass elliptic function

$$\wp(z) := \frac{1}{z^2} + \sum_{w \in (\mathbb{Z} \oplus i\mathbb{Z}) \setminus \{0\}} \left(\frac{1}{(z - w)^2} - \frac{1}{w^2} \right), \tag{5.5.15}$$

which is double-periodic by construction, $\wp(z) = \wp(z + 1) = \wp(z + \mathrm{i})$. Then the Hamiltonian of the lemniscatic $\mathbb{Z}/4\mathbb{Z}$ CMS model is given by [68, Eq. 4.3]

$$L_{\text{EFMV}}(z, \partial_z) = \partial_z^4 + \sum_{p=0}^{2} g_p^{(z)}(z) \partial_z^p\,, \tag{5.5.16}$$

where

$$g_2^{(z)}(z) = \sum_{\nu=0}^{3} a_\nu \, \wp(z-\omega_\nu)\,, \tag{5.5.17}$$

$$g_1^{(z)}(z) = \sum_{\nu=0}^{3} b_\nu \, \wp'(z-\omega_\nu)\,, \tag{5.5.18}$$

$$g_0^{(z)}(z) = \sum_{\nu=0}^{3} c_\nu \, \wp^2(z-\omega_\nu) + \wp(\omega_3)(a_0-a_1)k(k+1)\left(\wp(z-\omega_2)-\wp(z-\omega_3)\right). \tag{5.5.19}$$

The various coefficients (a_ν, b_ν, c_ν) for $\nu = 0,1,2$ are related to the multiplicities as [68, Example 7.7]

$$a_\nu := -11 + \sum_{1\le i<j\le 4} m_{i,\nu} m_{j,\nu}\,, \tag{5.5.20}$$

$$b_\nu := \frac{1}{2}\left(-a_\nu - 6 + \sum_{1\le i<j<k\le 4} m_{i,\nu} m_{j,\nu} m_{k,\nu}\right), \tag{5.5.21}$$

$$c_\nu := \prod_{i=1}^{4} m_{i,\nu}\,, \tag{5.5.22}$$

$(a_3,b_3,c_3) = (a_2,b_2,c_2)$ and the parameter k is $k = m_{1,2} - 1$. Note that in eq. (5.5.17)-(5.5.19) we are summing over the four fixed points $(\omega_0,\omega_1,\omega_2,\omega_3)$ of the elliptic curve $E_{\rm i}$, and that we need $(a_3,b_3,c_3) \equiv (a_2,b_2,c_2)$ to ensure the $\mathbb{Z}_4$-symmetry of the Hamiltonian.

5.5.2 Construction of the map

In order to recast our vertex operator H in the form (5.5.11) of the lemniscatic CMS Hamiltonian, we need to find a change of variables from our cross-ratio $\mathcal{X}$ to a new variable ϕ and a 'gauge transformation' $\Theta(\mathcal{X}(\phi))$ such that

$$\Theta^{-1} H \Theta = (\text{const})\partial_\phi^4 + \mathcal{O}(\partial_\phi^2)\,. \tag{5.5.23}$$

Looking at the terms of order $\partial_{\mathcal{X}}^4$ and $\partial_{\mathcal{X}}^3$, we see that ϕ can be taken to solve the differential equation

$$\frac{\mathrm{d}\phi}{\mathrm{d}\mathcal{X}} = \frac{(-)^{\frac{1}{4}}}{4}\mathcal{X}^{-\frac{3}{4}}(1-\mathcal{X})^{-\frac{3}{4}}, \qquad \phi(\mathcal{X}=0) = 0\,, \tag{5.5.24}$$

and Θ must be of the form

$$\Theta = \Theta_0\, \mathcal{X}^{\frac{l_1+l_2-2(\ell_1+\ell_2)+\Delta_3+(1-d)/2}{4}} (1-\mathcal{X})^{\frac{l_1+l_2-2(\ell_1+\ell_2)-\Delta_3+(1+d)/2}{4}}\,, \tag{5.5.25}$$

where $\Theta_0 \in \mathbb{C}\backslash\{0\}$ is an arbitrary multiplicative constant. The solution to eq. (5.5.24) is proportional to the incomplete Beta function, which has the known analytic expression (see [132, Eq. 8.17.7])

$$\phi(\mathcal{X}) = \frac{(-)^{\frac{1}{4}}}{4}\int_0^{\mathcal{X}} \mathrm{d}\mathcal{X}'\, \mathcal{X}'^{-\frac{3}{4}}(1-\mathcal{X}')^{-\frac{3}{4}} = (-\mathcal{X})^{\frac{1}{4}}\, {}_2F_1\left(\frac{1}{4},\frac{3}{4};\frac{5}{4};\mathcal{X}\right). \tag{5.5.26}$$

If we now apply the Pfaff transformation of the Gauss hypergeometric function,

$${}_2F_1\left(a,b;c;\mathcal{X}\right) = (1-\mathcal{X})^{-a}\, {}_2F_1\left(a,c-b;c;\frac{\mathcal{X}}{\mathcal{X}-1}\right), \tag{5.5.27}$$

the above function can be expressed in terms of the inverse arc length function for the lemniscate curve (see [133, Eq. 5]),

$$\phi(\mathcal{X}) = \left(\frac{\mathcal{X}}{\mathcal{X}-1}\right)^{\frac{1}{4}} {}_2F_1\left(\frac{1}{4},\frac{1}{2};\frac{5}{4};\frac{\mathcal{X}}{\mathcal{X}-1}\right) \equiv \text{arcsinlemn}\left(\frac{\mathcal{X}}{\mathcal{X}-1}\right)^{\frac{1}{4}}. \tag{5.5.28}$$

Using [133, Eq. 21], the change of variables can be inverted to

$$\sqrt{\frac{\mathcal{X}}{\mathcal{X}-1}} = \frac{\text{sd}^2\left(\phi\sqrt{2},\frac{1}{\sqrt{2}}\right)}{2}, \tag{5.5.29}$$

where $\text{sd}(u,k)$ is one of the Jacobi elliptic functions. This can be equivalently expressed in terms of the Weierstrass function $\wp(z)$ defined in eq. (5.5.15),

$$\mathcal{X} = \frac{\wp(\omega_3)^2}{\wp(\omega_3)^2-\wp(z)^2}, \qquad \phi = \wp(\omega_3)\, z, \tag{5.5.30}$$

To re-express the corresponding operator in the form (5.5.16) and solve the parameters k, a_ν, b_ν, c_ν in eqs. (5.5.17), (5.5.18), (5.5.19) for Δ_i, l_i, ℓ_i, d, we made a symbolic computation in `Mathematica`[5]. This symbolic computation specifically avoids the use of the special functions `JacobiSD` and `WeierstrassP` that appear in eqs. (5.5.29) and (5.5.30), because `Mathematica` does not efficiently make use of the derivative and addition formulas of these special functions. Instead, we only use the `Hypergeometric2F1` in eq. (5.5.28) to compute the coefficients $g_0^{(z)}, g_1^{(z)}, g_2^{(z)}$ as functions of $\mathcal{X}$. More specifically, we start by determining the three functions

$$\begin{aligned}
h_0^{(\phi)}(\phi(\mathcal{X})) &= H(\mathcal{X},\partial_{\mathcal{X}})\cdot 1\,,\\
h_1^{(\phi)}(\phi(\mathcal{X})) &= H(\mathcal{X},\partial_{\mathcal{X}})\cdot \phi(\mathcal{X}) - \phi(\mathcal{X}) h_0^{(\phi)}(\phi(\mathcal{X}))\,,\\
h_2^{(\phi)}(\phi(\mathcal{X})) &= H(\mathcal{X},\partial_{\mathcal{X}})\cdot \frac{\phi(\mathcal{X})^2}{2} - \phi(\mathcal{X}) h_1^{(\phi)}(\mathcal{X}) - \frac{\phi(\mathcal{X})^2}{2} h_0^{(\phi)}(\mathcal{X})\,,
\end{aligned}$$

that are related to the g-coefficients by

$$g_p^{(z)}(z(\mathcal{X})) = 4^3\wp(\omega_3)^{2-\frac{p}{2}}\left(h_p^{(\phi)}\left(\phi\left(\mathcal{X}\right)\right) - \delta_{p,0}\, E_{\text{EFMV}}\right), \qquad p=0,1,2\,, \tag{5.5.31}$$

where $E_{\text{EFMV}}^{(d;\Delta_i;l_i;\ell_i)}$ is the constant shift of the Hamiltonian given in appendix 5.C.2. Following eq. (5.5.30), it is easy to show that the $g_p^{(z)}$ computed from $H(\mathcal{X},\partial_{\mathcal{X}})$ are algebraic functions of $\wp(z)$. Similarly, we can express each term in eqs. (5.5.17), (5.5.18), (5.5.19) as a rational function of $\wp(z)$ using the addition formulas

$$\wp\left(z-\omega_1\right) = -\frac{\wp(\omega_3)^2}{\wp(z)}, \tag{5.5.32}$$

$$\wp(z-\omega_2) = -\wp(\omega_3)\frac{\wp(z)-\wp(\omega_3)}{\wp(z)+\wp(\omega_3)}, \tag{5.5.33}$$

$$\wp(z-\omega_3) = \wp(\omega_3)\frac{\wp(z)+\wp(\omega_3)}{\wp(z)-\wp(\omega_3)}, \tag{5.5.34}$$

and the derivative formula

$$\wp'(z)^2 = 4\wp(z)\left(\wp(z)^2-\wp(\omega_3)^2\right), \tag{5.5.35}$$

[5]The corresponding notebook can be found in the supplementary material of this publication.

for the lemniscatic Weierstrass elliptic function. Following these identities, each of the coefficient functions $g_p^{(z)}$ in the Hamiltonian is the product of $\wp^{\frac{p}{2}-2}\left(\wp(\omega_3)^2-\wp^2\right)^{\frac{p}{2}-2}$ with a polynomial function in $\wp$. We can then identify each polynomial coefficient expressed as a function of k, a_ν, b_ν, c_ν with its expression in terms of Δ_i, l_i, ℓ_i, d to obtain the map from spins and conformal dimensions to multiplicities.

5.5.3 CMS multiplicities from weights and spins

In all cases, the multiplicity associated to z_2 (see eq. (5.5.10)) can be computed from the spin quantum numbers l_1, l_2 as

$$k = l_1 - l_2 - \frac{1}{2} \qquad \text{or} \qquad k = l_2 - l_1 - \frac{1}{2}\,. \tag{5.5.36}$$

Going from one choice to the other in eq. (5.5.36) is equivalent to the change of parameters $k \to -(k+1)$, which leaves the CMS Hamiltonian invariant. For the MST_2-STT-scalar (type II) vertex in all $d \geq 3$ we have

$$m_{1,0} = 3\,\frac{5-d}{2} - (l_1+l_2) - \Delta_3 - 2\ell_1\,, \tag{5.5.37}$$

$$m_{2,0} = \frac{d-1}{2} - (l_1+l_2) - \Delta_3 + 2\ell_1\,, \tag{5.5.38}$$

$$m_{3,0} = \frac{d-1}{2} + (l_1+l_2) + \Delta_3 + 2(\Delta_1-\Delta_2)\,, \tag{5.5.39}$$

$$m_{4,0} = \frac{d-1}{2} + (l_1+l_2) + \Delta_3 - 2(\Delta_1-\Delta_2)\,, \tag{5.5.40}$$

and

$$m_{1,1} = -5\,\frac{d-3}{2} - (l_1+l_2) + \Delta_3 - 2\ell_1\,, \tag{5.5.41}$$

$$m_{2,1} = -\frac{d+1}{2} - (l_1+l_2) + \Delta_3 + 2\ell_1\,, \tag{5.5.42}$$

$$m_{3,1} = -\frac{d+1}{2} + (l_1+l_2) - \Delta_3 + 2(\Delta_1+\Delta_2)\,, \tag{5.5.43}$$

$$m_{4,1} = \frac{7d-1}{2} + (l_1+l_2) - \Delta_3 - 2(\Delta_1+\Delta_2)\,, \tag{5.5.44}$$

which also contains the particular case of type I with two spinning fields in $d \geq 3$ simply by setting $\ell_1 = 0$. It is easy to observe from eqs. (5.5.37)—(5.5.44) that

$$m_{i,\nu}(d;\Delta_i,l_i;\ell_1) = m_{i,\nu}\left(d+\delta d;\Delta_i+\frac{\delta d}{2};l_i-\frac{\delta d}{2};\ell_1-\frac{\delta d}{2}\right), \tag{5.5.45}$$

or equivalently

$$m_{i,\nu}(2\alpha+3-2\ell_1;\alpha-\ell_1+\frac{3}{2}+\mathrm{i}\gamma_i,l_i;\nu_i+\ell_1;\ell_1) = \text{function}\,(\alpha;\gamma_i;\nu_i)\,. \tag{5.5.46}$$

This is a direct consequence of the observation made in eq. (5.4.38). We conclude that the three weight and three spin labels along with the dimension d of the MST_2-STT-scalar vertices do not exhaust the full 7-dimensional parameter space of the elliptic $\mathbb{Z}_4$ CMS model. In fact, it is easy to see that the parameters are constrained by

$$m_{1,0} - m_{2,0} = m_{1,1} - m_{2,1}\,. \tag{5.5.47}$$

When specializing to $d = 4$, this last constraint defines the restriction of the generic MST_2-MST_2-scalar (type III) vertex to the MST_2-STT-scalar case. We have determined that the full MST_2-MST_2-scalar vertex in $d = 4$ yields the CMS multiplicities

$$m_{1,0} = \frac{3}{2} - (l_1 + l_2) - \Delta_3 - 2(\ell_1 - \ell_2)\,, \tag{5.5.48}$$

$$m_{2,0} = \frac{3}{2} - (l_1 + l_2) - \Delta_3 + 2(\ell_1 - \ell_2)\,, \tag{5.5.49}$$

$$m_{3,0} = \frac{3}{2} + (l_1 + l_2) + \Delta_3 + 2(\Delta_1 - \Delta_2)\,, \tag{5.5.50}$$

$$m_{4,0} = \frac{3}{2} + (l_1 + l_2) + \Delta_3 - 2(\Delta_1 - \Delta_2)\,, \tag{5.5.51}$$

$$m_{1,1} = -\frac{5}{2} - (l_1 + l_2) + \Delta_3 - 2(\ell_1 + \ell_2)\,, \tag{5.5.52}$$

$$m_{2,1} = -\frac{5}{2} - (l_1 + l_2) + \Delta_3 + 2(\ell_1 + \ell_2)\,, \tag{5.5.53}$$

$$m_{3,1} = -\frac{5}{2} + (l_1 + l_2) - \Delta_3 + 2(\Delta_1 + \Delta_2)\,, \tag{5.5.54}$$

$$m_{4,1} = \frac{27}{2} + (l_1 + l_2) - \Delta_3 - 2(\Delta_1 + \Delta_2)\,. \tag{5.5.55}$$

Let us note that this set of multiplicities does not satisfy any additional constraints. This concludes our description of the precise relation between the vertex differential operators for single variable vertices and the lemniscatic CMS model of [68]. We would like to finish this section off with two additional comments.

Comments on algebraic integrability: The CMS operator is said to be algebraically integrable if the multiplicities $m_{i,\nu}$ defined by eqs. (5.5.12), (5.5.13), (5.5.14) are integers (see [134, Corollary 2.4]). In this case, according to [134, Theorem 2.5], a generic eigenfunction of L_{EFMV} will take the form

$$\psi_\lambda(z) = e^{\beta z} \prod_{i=1}^{4} \frac{\theta(z - \alpha_i)}{\theta(z - \beta_i)}, \tag{5.5.56}$$

where $\theta(z)$ is the first Jacobi theta-function of the lemniscatic elliptic curve, and $\beta, \beta_1, \alpha_1, \ldots, \beta_4, \alpha_4$ are certain parameters that can be solved in terms for the multiplicities and eigenvalue λ by writing the eigenvalue equation $L_{\mathrm{EFMV}}\psi_\lambda = \lambda\psi_\lambda$ for (5.5.56) near the singular points $z = z_0, z_1, z_2$. We have determined above that all multiplicities are linear combinations of the quantum numbers $(\Delta_i; l_i; \ell_i)$ and the dimension d, with coefficients in $\frac{1}{2}\mathbb{Z}$. Therefore, depending on whether d is odd or even, the vertex operator is algebraically integrable when the quantum numbers $[-\Delta_i; l_i; \ell_i]$ that define the representation at each point are either integers or half-integers. This setup is equivalent to placing unitary irreducible representations of the compact real form $\mathrm{SO}_{\mathbb{R}}(d + 2)$ at each point (or the double cover thereof). It would be interesting to explore the generalization of this result to non-integer conformal weights.

CMS multiplicities for all vertex systems: As a final comment we want to rewrite the relations between the CMS multiplicities and the weight and spin quantum numbers in terms of the parameters that appeared in our discussion of the generalized Weyl algebra, see previous section. Recall the parameters of the generalized Weyl algebra,

$$\alpha := \frac{d-3}{2} + \ell_1 + \ell_2\,, \qquad \nu_1 = l_1 - \ell_1 - \ell_2\,, \qquad \nu_2 = l_2 - \ell_1 - \ell_2\,. \tag{5.5.57}$$

To determine a universal formula for the CMS multiplicities of all 1-dimensional vertex systems, we use the four extra parameters

$$\beta := \ell_1 - \ell_2 + \frac{d-5}{2}\,, \qquad \gamma_i := -\mathrm{i}\left(\Delta_i - \frac{d}{2}\right)\,. \tag{5.5.58}$$

The parameters γ_i had appeared in our construction of the Hamiltonian already, see eq. (5.4.11). Only the parameter β is new. Of course, the map from spin quantum numbers $(l_i;\ell_i)$ to α,β,ν_1,ν_2 can be inverted as

$$l_1 = \nu_1 + \alpha + \frac{3-d}{2}\,, \qquad l_2 = \nu_2 + \alpha + \frac{3-d}{2}\,, \tag{5.5.59}$$

$$\ell_1 = \frac{\alpha+\beta+4-d}{2}\,, \qquad \ell_2 = \frac{\alpha-\beta-1}{2}\,. \tag{5.5.60}$$

If we insert these formulas into the expressions for multiplicities we listed above, these become completely universal to all 1-dimensional vertex systems, i.e. they no longer depend on type of the vertex (I, II, or III). Explicitly one finds

$$k = \nu_1 - \nu_2 - \frac{1}{2}\,, \qquad \text{or} \qquad k = \nu_2 - \nu_1 - \frac{1}{2}\,, \tag{5.5.61}$$

and

$$m_{1,0} = -\frac{1}{2} - (\nu_1+\nu_2) - \mathrm{i}\gamma_3 - 2\alpha - 2\beta\,, \tag{5.5.62}$$

$$m_{2,0} = \frac{3}{2} + (\nu_1+\nu_2) - \mathrm{i}\gamma_3 - 2\alpha + 2\beta\,, \tag{5.5.63}$$

$$m_{3,0} = \frac{5}{2} + (\nu_1+\nu_2) + \mathrm{i}\gamma_3 + 2\alpha + 2\mathrm{i}(\gamma_1-\gamma_2)\,, \tag{5.5.64}$$

$$m_{4,0} = \frac{5}{2} + (\nu_1+\nu_2) + \mathrm{i}\gamma_3 + 2\alpha - 2\mathrm{i}(\gamma_1-\gamma_2)\,, \tag{5.5.65}$$

$$m_{1,1} = \frac{3}{2} - (\nu_1+\nu_2) + \mathrm{i}\gamma_3 - 4\alpha\,, \tag{5.5.66}$$

$$m_{2,1} = -\frac{1}{2} - (\nu_1+\nu_2) + \mathrm{i}\gamma_3\,, \tag{5.5.67}$$

$$m_{3,1} = \frac{5}{2} + (\nu_1+\nu_2) - \mathrm{i}\gamma_3 + 2\alpha + 2\mathrm{i}(\gamma_1+\gamma_2)\,, \tag{5.5.68}$$

$$m_{4,1} = \frac{5}{2} + (\nu_1+\nu_2) - \mathrm{i}\gamma_3 + 2\alpha - 2\mathrm{i}(\gamma_1+\gamma_2)\,. \tag{5.5.69}$$

In particular, the MST_2-STT-scalar (type II) case in all $d \geq 3$ is obtained by imposing the additional relation $\beta = \alpha - 1$, equivalent to $\ell_2 = 0$.

5.6 Outlook

The most natural vertex integrable system to analyze next is that of three STTs, with $n_{cr} = 2$ cross ratios in $d = 3$ and $n_{cr} = 3$ cross ratios in $d \geq 4$. These vertices are reductions of the integrable systems for six-point snowflake channel blocks, which have already started to be analyzed in the six-point lightcone bootstrap [66, 67]. In $d = 3$, an efficient choice of seed and cross ratios is given in [88, Sec. 4.1], with the structure of a $B_2 \cong C_2$ cluster algebra. In $d \geq 4$, the relevant results were derived in [89] and reviewed in section 3.2.2, with the seed datum of Eq. (3.2.21),(3.2.22). This gives

us all the information we need to expand the three-point function as in (3.2.16). We established in section 4.2.3 that the snowflake vertex integrable system in $d \geq 4$ has two Hamiltonians of order four, and one Hamiltonian of order six. In $d = 3$, one further relation should make the sixth order operator dependent on the fourth order operators. It is not clear whether the corresponding integrable systems have already been identified and/or studied in the literature.

Finally, for type I and type II vertex systems, we saw that the second order differential operators in (5.4.14),(5.4.15),(5.4.16) satisfy the commutation relations of a generalized Weyl algebra of type $\tilde{A}_3$. The orthogonal basis of Gegenbauer polynomials $C_n^{((d-3)/2)}(1-2\mathcal{X})$ form an irreducible representation of this algebra, and define an alternative basis of tensor structures for conformal block decompositions that is easier to compute and manipulate. However, unlike the vertex operator eigenbasis, a putative lift of the generalized Weyl algebra to higher point functions is not known. In fact, if such a generalized Weyl algebra *were* to lift to higher points, it would make higher point comb channel blocks *superintegrable* (see [135] for a definition of superintegrable systems).

In summary, it would be very useful to replace eigenfunctions of the higher order vertex operators with representations of an algebra generated by lower order superintegrable differential operators. For five-point lightcone blocks, we can demonstrate superintegrability directly using the integral representation obtained from the lightcone OPE in (3.3.18). Beyond this, the superintegrability of higher point blocks remains an open question.

5.A Map from $\mathfrak{so}_{\mathbb{C}}(6)$ embedding space to $\mathfrak{sl}_{\mathbb{C}}(4)$ twistors

We use indices $A, B, C = 0, \ldots, 5$ to label an orthonormal basis in the fundamental representation of $\mathfrak{so}_{\mathbb{C}}(6)$, and $a, b, c = 1, 2, 3, 4$ to label a basis in the fundamental representation of $\mathfrak{sl}_{\mathbb{C}}(4)$. We saw that irreducible representations of $\mathfrak{so}_{\mathbb{C}}(6)$ are sections of a line bundle over the space of isotropic flags in $\mathbb{C}^6$

$$\mathrm{Span}(X) \subset \mathrm{Span}(X,Z) \subset \mathrm{Span}(X,Z,W) = \mathrm{Span}(X,Z,W)^{\perp} \subset \mathrm{Span}(X,Z)^{\perp} \subset \mathrm{Span}(X)^{\perp} \subset \mathbb{C}^6, \tag{5.A.1}$$

where $\mathbb{V}^{\perp}$ is the orthogonal complement of the vector subspace $\mathbb{V} \subset \mathbb{C}^6$ with respect to the 6-dimensional metric (η_{AB}). These sections are equivalent to certain functions $F(X,Z,W)$ of three vectors in $\mathbb{C}^6$ that are null and mutually orthogonal with respect to the Minkowski metric,

$$X^2 = Z^2 = W^2 = X \cdot Z = X \cdot W = Z \cdot W = 0\,. \tag{5.A.2}$$

Said functions must be homogeneous of fixed multi-degree, and invariant under the gauge transformations that preserve the isotropic flag,

$$F(X, Z + \beta_{10}X, W + \beta_{20}X + \beta_{21}Z) = F(X,Z,W)\,. \tag{5.A.3}$$

Depending on the choice of real form of $\mathfrak{so}_{\mathbb{C}}(6)$ (or equivalently the signature of (η_{AB})), as well as the choice of representation, one must either apply reality conditions on some of the X, Z, W or impose that F is holomorphic in some of the X, Z, W variables. For the reflection positive and integer spin representations of CFT_4, X is real and F is holomorphic in $Z, W \in \mathbb{C}^6$. In this case, the space of vectors $(X, Z, W) \in \mathbb{R}^6 \times (\mathbb{C}^6)^2$ satisfying (5.A.2) is informally known as embedding space. The gauge constraints can be explicitly solved by a change of variables

$$C^{(0)}_A := X_A, \qquad C^{(1)}_{AB} := (X \wedge Z)_{AB}, \qquad C^{(2)}_{ABC} := (X \wedge Z \wedge W)_{ABC}, \tag{5.A.4}$$

such that $F(X,Z,W) = F'(C^{(0)},C^{(1)},C^{(2)})$ for some function F'.
Similarly, irreducible representations of $\mathfrak{sl}_{\mathbb{C}}(4)$ are sections of a line bundle over the space of flags in $\mathbb{C}^4$,

$$\mathrm{Span}(Y_1) \subset \mathrm{Span}(Y_1,Y_2) \subset \mathrm{Span}(Y_1,Y_2,Y_3) \subset \mathbb{C}^4\,. \tag{5.A.5}$$

This is equivalent to functions $\Psi(Y_1,Y_2,Y_3)$ of three (arbitrary) vectors in $\mathbb{C}^4$. Said functions must also be homogeneous of fixed multi-degree, and invariant under the gauge transformations that preserve the flag,

$$\Psi(Y_1,Y_2+c_{21}Y_1,W+c_{31}Y_1+c_{32}Y_2) = \Psi(Y_1,Y_2,Y_3)\,. \tag{5.A.6}$$

Once again, the gauge constraints can be explicitly solved by the change of variables to gauge-invariant tensors

$$S_a := Y_{1a}, \qquad X_{ab} := (Y_1 \wedge Y_2)_{ab}, \qquad \bar{S}_{abc} := (Y_1 \wedge Y_2 \wedge Y_3)_{abc}\,, \tag{5.A.7}$$

such that $\Psi(Y_1,Y_2,Y_3) = \Psi'(S,X,\bar{S})$ for some function Ψ'. The gauge invariant, anti-symmetric, and $\mathfrak{su}(2,2)$-covariant tensors $(S,X,\bar{S})$ are known as *twistor* variables in the physics literature. Similarly to the previous case, reality conditions on Y_1,Y_2,Y_3 or holomorphicity conditions on Ψ are required to realize irreducible representations of real forms of $\mathfrak{sl}_{\mathbb{C}}(4)$. In particular, the reflection positive and half-integer spin representations of CFT_4 are realized by imposing that X_{ab} is real and Ψ' is a holomorphic function of S and $\bar{S}$. This follows from the fact that $\mathrm{SU}(2,2)$ is the double cover of the Lorentzian conformal group $\mathrm{SO}(2,4)$.
More generally, as $\mathfrak{so}_{\mathbb{C}}(6) \cong \mathfrak{sl}_{\mathbb{C}}(4)$, representations of the latter can be mapped to representations of the former. As a result, there exists a map from homogeneous, gauge-invariant functions on $\mathfrak{so}_{\mathbb{C}}(6)$ embedding space to homogeneous functions of the twistor variables (5.A.7). This translates into a map from the gauge-invariant tensors (5.A.4) in $\mathbb{C}^6$ to the gauge-invariant tensors (5.A.7) in $\mathbb{C}^4$. To determine explicit expressions, we make use of the chiral Γ-matrices Γ^A_{ab} defined for example in [105, Appendix B]. If $M^A{}_B \in \mathfrak{so}_{\mathbb{C}}(6)$, then there exists $L_a{}^b \in \mathfrak{sl}_{\mathbb{C}}(4)$ such that

$$M^A{}_B\,\Gamma^B_{ab} = L_a{}^c\,\Gamma^A_{cb} + L_b{}^d\,\Gamma^A_{ad}\,. \tag{5.A.8}$$

These Γ-matrices are anti-symmetric, such that we can define their duals with respect to the 4-dimensional ϵ-tensor,

$$\bar{\Gamma}^{Aab} := \frac{1}{2}\epsilon^{abcd}\Gamma^A_{ab}\,. \tag{5.A.9}$$

The fundamental identities of the Γ-matrices can also be found in [105, Appendix B]. The Clifford relations are

$$\bar{\Gamma}^{Aab}\Gamma^B_{bc} + \bar{\Gamma}^{Bab}\Gamma^A_{bc} = -2\eta^{AB}\delta^a_c\,, \tag{5.A.10}$$

while the contraction identity is

$$\eta_{AB}\Gamma^A_{ab}\Gamma^B_{cd} = 2\epsilon_{abcd}\,. \tag{5.A.11}$$

The map from gauge-invariant tensors in $\mathfrak{so}(1,5)$ embedding space to twistor variables is then given by

$$C^{(0)}_A = X_A = \frac{1}{4}X_{ab}\bar{\Gamma}^{ab}_A\,, \tag{5.A.12}$$

$$C^{(1)}_{AB} = (X \wedge Z)_{AB} = \frac{1}{\sqrt{2}}\bar{S}^a\Gamma_{Aab}\bar{\Gamma}^{bc}_B S_c\,, \tag{5.A.13}$$

$$C^{(2)}_{ABC} = (X \wedge Z \wedge W)_{ABC} = \frac{1}{2\sqrt{2}}S_a\bar{\Gamma}^{ab}_A\Gamma_{Bbc}\bar{\Gamma}^{cd}_B S_d\,, \tag{5.A.14}$$

$$\bar{C}^{(2)}_{ABC} = (X \wedge Z \wedge \bar{W})_{ABC} = \frac{1}{2\sqrt{2}}\bar{S}^a\Gamma_{Aab}\bar{\Gamma}^{bc}_B\Gamma_{Ccd}\bar{S}^d\,. \tag{5.A.15}$$

Here, we defined the dual tensors

$$\bar{S}^a := \frac{1}{3!}\epsilon^{abcd}\bar{S}_{bcd}, \qquad \bar{X}^{ab} := \frac{1}{2}\epsilon^{abcd}X_{cd}. \tag{5.A.16}$$

We can now summarize our nomenclature for various spinning representations of maximal spin depth in $d = 4$:

- we call a self-dual (respectively anti-self-dual) representation any function on embedding space that is a homogeneous polynomial of order $\ell \in \mathbb{Z}_+$ in W (respectively a polynomial of order $-\ell \in \mathbb{Z}_+$ in $\overline{W}$). In twistor space, we see that these representations correspond to homogeneous polynomials of order $j \in 2\mathbb{Z}_+$ in S and $\bar{\jmath} \in 2\mathbb{Z}_+$ with $j > \bar{\jmath}$ (respectively $j < \bar{\jmath}$).
- We call a chiral (respectively anti-chiral) representation any function on twistor space that is a polynomial of order $j \in \mathbb{Z}_+$ in S (respectively $\bar{\jmath} \in \mathbb{Z}_+$ in $\bar{S}$) with $\bar{\jmath} = 0$ (respectively $j = 0$). In cases where j (respectively $\bar{\jmath}$) is an even integer, these coincide with the self-dual (respectively anti-self-dual) parts of $\mathfrak{so}(4)$ representations with rectangular Young tableaux of height $h_1 = \cdots = h_l = 2$ and length $l = \ell = j/2$ (respectively $l = -\ell = \bar{\jmath}/2$).

With this map, it is easy to directly relate the MST_2-MST_2-scalar tensor structures in $\mathfrak{so}(1,5)$ embedding space with those of twistor space:

$$X_i \cdot X_j = \frac{1}{4}\bar{X}_i^{ab}X_{jab} = -\frac{1}{4}\mathrm{tr}\,\bar{X}_i X_j, \tag{5.A.17}$$

$$X_{jk}V_{i,jk} = \bar{S}_i X_j \bar{X}_k S_i \tag{5.A.18}$$

$$(k_{\bar{\imath}j})^2 = (\bar{S}_i S_j)^2 \tag{5.A.19}$$

$$\mho^2_{ij,k} = (S_i \bar{X}_k S_j)^2 \tag{5.A.20}$$

$$\bar{\mho}^2_{ij,k} = (\bar{S}_i X_k \bar{S}_j)^2. \tag{5.A.21}$$

It is important to note that the squared tensor structures on the left hand side of (5.A.19), (5.A.20), (5.A.21) are also perfect squares of $\mathfrak{so}_{\mathbb{C}}(6)$ embedding space variables. This means that we can compute 3-point functions of any half-integer spin fields in our formalism.

5.B Comments on scalar products and unitarity

5.B.1 Integral formula for the $\mathrm{SO}(d+2)$-invariant scalar product

Consider an arbitrary finite-dimensional and irreducible representation of $\mathfrak{so}(d+2)$, labeled by a Young tableau with row lengths $-\Delta \geq l_1 \geq \cdots \geq l_L$, $L := \mathrm{rank}(\mathfrak{so}(d))$. The latter can be represented as a tensor on $\mathbb{C}^{d+2}$,

$$F_{A_1^{(0)}\ldots A_{-\Delta}^{(0)}A_1^{(1)}\ldots A_{l_1}^{(1)}\ldots A_1^{(L)}\ldots A_{l_L}^{(L)}} := F_{\{A\}_{L+1}}, \quad A_i^{(j)} = -1, \ldots, d\,, \tag{5.B.1}$$

satisfying the same (anti)-symmetry and tracelessness conditions as in subsection 3.1.1. By contracting the first family of indices with a null polarization vector $X \in \mathbb{C}^{d+2}, X^2 = 0$,

$$F_{\Delta,\{A\}_L}(X) := X^{A_1^{(0)}} \ldots X^{A_{-\Delta}^{(0)}} F_{A_1^{(0)}\ldots A_{-\Delta}^{(0)}A_1^{(1)}\ldots A_{l_1}^{(1)}\ldots A_1^{(L)}\ldots A_{l_L}^{(L)}}\,, \tag{5.B.2}$$

these $[-\Delta, l_1, \ldots, l_L]$ tensors are equivalent to transverse $[l_1, \ldots, l_L]$ tensor-valued homogeneous functions on the complex light-cone in $\mathbb{C}^{d+2}$:

$$F_{\Delta,\{A\}_L}(\lambda_0 X) = \lambda_0^{-\Delta}F_{\Delta,\{A\}_L}(X)\,, \qquad X^{A_i^{(j)}}F_{\Delta,\{A\}_L}(X) = 0\,, \tag{5.B.3}$$

with the gauge equivalence relation

$$F_{\Delta,\{A\}_L}(X) \sim F_{\Delta,\{A\}_L}(X) + C_{\{A\}_L\setminus\{A_i^{(j)}\}}(X)\, X_{A_i^{(j)}}\,, \tag{5.B.4}$$

valid for any transverse $[l_1,\dots,l_j-1,\dots,l_L]$- tensor valued function $X \mapsto \mathbf{C}(X)$ of homogeneity $-\Delta-1$. The $\mathrm{SO}(d+2)$-invariant scalar product of two irreducible tensors is given by the contraction of indices,

$$\langle F, G\rangle = \bar{F}_{\{A\}_{L+1}}\delta^{\{AA'\}_{L+1}}G_{\{A'\}_{L+1}}\,, \qquad \delta^{\{BB'\}_{L+1}} := \prod_{j=0}^{L}\prod_{i=1}^{l_j}\delta^{B_i^{(j)}B'^{(j)}_i}\,. \tag{5.B.5}$$

A result of Bargmann and Todorov (c.f. [84], Proposition 4.1) recasts this scalar product as an integral over $\mathbb{C}^{d+2}$:

$$\langle F_\Delta, G_\Delta\rangle = \int_{\mathbb{C}^{d+2}} \mathrm{d}^{d+2}X\delta(X^2)\mathrm{d}^{d+2}\bar{X}\delta(\bar{X}^2)\rho_{d+2}(\bar{X}\cdot X)\overline{F_\Delta^{\{A\}_L}}(\bar{X})\, W^{\bar{X},X}_{\{AB\}_L}G_\Delta^{\{B\}_L}(X)\,. \tag{5.B.6}$$

The measure is given by

$$\rho_{d+2}(t) := \frac{8}{\pi^{d+1}\Gamma(d/2)}t^{-(d-2)/4}K_{(d-2)/2}(2\sqrt{t})\,, \tag{5.B.7}$$

where $K_\epsilon(s)$ is the modified Bessel function of the second kind, while to ensure gauge invariance, the indices are contracted with the tensor

$$W^{\bar{X},X}_{\{AB\}_L} := \prod_{j=0}^{L}\prod_{i=1}^{l_j}W^{\bar{X},X}_{A_i^{(j)}B_i^{(j)}}\,, \qquad W^{\bar{X},X}_{AB} := \delta_{AB} - \frac{X_A\bar{X}_B}{\bar{X}\cdot X}\,, \tag{5.B.8}$$

satisfying

$$\bar{X}^A W^{\bar{X},X}_{AB} = 0 = W^{\bar{X},X}_{AB}X^B\,. \tag{5.B.9}$$

While there are other integral formulas for $\mathrm{SO}(d+2)$-invariant scalar products (e.g. in [105]), the Bargmann-Todorov scalar product ensures that the adjoint of the X_A operator is the so-called Thomas-Todorov operator,

$$X_A^\dagger = D_A = \left(X^B\frac{\partial}{\partial X^B} + \frac{d}{2}\right)\frac{\partial}{\partial X^A} - \frac{1}{2}X_A\frac{\partial^2}{\partial X^B\partial X_B}\,. \tag{5.B.10}$$

We would now like to reduce the integral formula (5.B.6) to the Poincaré patch,

$$X^A(X^+,x) = X^+\chi^A(x)\,, \qquad X^+ := X^{d+1}+\mathrm{i}X^{d+2}\,, \qquad \chi(x) := \left(\frac{x^2-1}{2},\mathrm{i}\frac{x^2+1}{2},-x^a\right)\,. \tag{5.B.11}$$

First, the measure is modified as

$$\mathrm{d}^{d+2}X = \frac{\mathrm{i}}{2}\,\mathrm{d}\big(X^2\big)\,\mathrm{d}X^+(X^+)^{d-1}\mathrm{d}^dx\,, \qquad \mathrm{d}^{d+2}\bar{X} = -\frac{\mathrm{i}}{2}\,\mathrm{d}\big(\bar{X}^2\big)\,\mathrm{d}\bar{X}^+(\bar{X}^+)^{d-1}\frac{\mathrm{d}^d\tilde{x}}{\tilde{x}^{2d}}\,, \tag{5.B.12}$$

where $\tilde{x}^a := -\bar{x}^a/\bar{x}^2$ is the generalized antipode of x^a on $\mathbb{C}^d\cup\{\infty\}$. Next, the scalar product in the measure is expressible as

$$\bar{X}\cdot X = \frac{1}{2}\big|X^+\big|^2\frac{(x-\tilde{x})^2}{\tilde{x}^2}\,. \tag{5.B.13}$$

Finally, the fields can be rewritten as

$$G_\Delta^{\{B\}_L}(X) = (X^+)^{-\Delta}g_\Delta^{\{b\}_L}(x)e^{\{B\}_L}_{\{b\}_L}(x)\,, \qquad e^B_b(x) := \frac{\partial\chi^A}{\partial x^b}(x)\,, \tag{5.B.14}$$

and

$$\overline{F_\Delta^{\{A\}_L}}(\bar{X}) = (\bar{X}^+)^{-\Delta}\overline{f_\Delta^{\{a\}_L}}\left(\frac{\tilde{x}}{\tilde{x}^2}\right) e_{\{a\}_L}^{\{A\}_L}\left(\frac{\tilde{x}}{\tilde{x}^2}\right) \sim (\bar{X}^+)^{-\Delta}\overline{f_\Delta^{\{c\}_L}}\left(\frac{\tilde{x}}{\tilde{x}^2}\right) I_{\{c\}_L}^{\{a\}_L}(\tilde{x})\, e_{\{a\}_L}^{\{A\}_L}(\tilde{x})\,, \quad (5.B.15)$$

where "$\sim$" denotes gauge equivalence, $I_b^a(x) := \delta_b^a - 2x^a x_b/x^2$, and the $\mathbb{C}^{d+2}$ contraction of the e-tensors with the W-tensors yields

$$e_a^A(\tilde{x}) W_{AB}^{\bar{X},X} e_b^B(x) = I_{ab}(\tilde{x}-x)\,. \quad (5.B.16)$$

Putting all of these changes of variables together yields

$$\langle F_\Delta, G_\Delta\rangle = \frac{1}{4}\int_{\mathbb{C}\times\mathbb{C}^d} \mathrm{d}^2X^+ \left|X^+\right|^{2(d-\Delta-1)} \mathrm{d}^d x \frac{\mathrm{d}^d\tilde{x}}{\tilde{x}^{2d}}\, \rho_{d+2}\left(\frac{|X^+|^2(x-\tilde{x})^2}{2\tilde{x}^2}\right) \overline{f_\Delta^{\{c\}_L}}\left(\frac{\tilde{x}}{\tilde{x}^2}\right) I_{\{c\}_L}^{\{a\}_L}(\tilde{x})\, I_{\{ab\}_L}(x-\tilde{x}) g_\Delta^{\{b\}_L}(x)\,.$$

The integral over X^+ is factorized by the change of variables

$$t := \bar{X}\cdot X = \frac{|X^+|^2(x-\tilde{x})^2}{2\tilde{x}^2}\,, \qquad \mathrm{d}\left(\left|X^+\right|^2\right) = \frac{2\tilde{x}^2}{(x-\tilde{x})^2}\mathrm{d}t\,, \quad (5.B.17)$$

and the adjoint naturally appears as

$$(f_\Delta^\dagger)^{\{a\}_L}(x) := x^{-2\Delta} I_{\{b\}_L}^{\{a\}_L}(x) f_\Delta^{\{b\}_L}\left(\frac{x}{x^2}\right), \quad (5.B.18)$$

such that

$$\langle F_\Delta, G_\Delta\rangle = \left\{\frac{2^{d-\Delta}\pi}{4}\int_0^\infty \mathrm{d}t\, t^{d-\Delta-1}\rho_{d+2}(t)\right\}\int_{\mathbb{C}^d}\frac{\mathrm{d}^d x\,\mathrm{d}^d\tilde{x}}{(x-\tilde{x})^{2(d-\Delta)}}(f_\Delta^\dagger)^{\{a\}_L}(\tilde{x}) I_{\{ab\}_L}(\tilde{x}-x) g_\Delta^{\{b\}_L}(x)\,.$$

The t-integral is computed using [132, Eq. 10.43.19],

$$\int_0^\infty \mathrm{d}s\, s^{\mu-1}K_\nu(s) = 2^{\mu-1}\Gamma\left(\frac{\mu-\nu}{2}\right)\Gamma\left(\frac{\mu+\nu}{2}\right), \quad \forall\,\mathrm{Re}(\mu) > |\mathrm{Re}(\nu)|\,. \quad (5.B.19)$$

and the final result can be concisely written as

$$\langle F_\Delta, G_\Delta\rangle = \mathcal{N}_{-\Delta}^{(d+2)}\int_{\mathbb{C}^d}\mathrm{d}^d x\,\mathrm{d}^d\tilde{x}\,(f_\Delta^\dagger)^{\{a\}_L}(\tilde{x})\frac{I_{\{ab\}_L}(\tilde{x}-x)}{(\tilde{x}-x)^{2(d-\Delta)}} g_\Delta^{\{b\}_L}(x)\,, \quad (5.B.20)$$

where the normalization is

$$\mathcal{N}_{-\Delta}^{(d+2)} := \frac{2^{d-\Delta}}{\pi^d}\frac{\Gamma(d+2-2\Delta)\Gamma(d+1-\Delta)}{\Gamma(d/2)}\,. \quad (5.B.21)$$

5.B.2 Generalizations to different real forms of $\mathfrak{so}_\mathbb{C}(d+2)$

In contrast with standard tensor contraction, formula (5.B.20) has the advantage of generalizing to infinite-dimensional unitary representations of $\mathrm{SO}(1,d+1)$ and $\mathrm{SO}(2,d)$ by changing the domain of integration of x and re-applying the same algebraic manipulations of section 5.B.1. We distinguish three cases:

$(2,d)$: if $X \mapsto F_{\Delta,\{A\}_L}(X)$, $\Delta \in \mathbb{R}_{\geq 0}$ denotes a reflection-positive representation of $\mathrm{SO}(1,d+1)$ (i.e. a unitary representation of $\mathrm{SO}(2,d)$), then we replace (5.B.20) by an integral over two independent variables $x^a, \tilde{x}^a \in \mathbb{R}^{1,d-1}$ in d-dimensional Minkowski space. In this context, the scalar product is conventionally recast as

$$\langle F_\Delta, G_\Delta \rangle = \mathcal{N}_{-\Delta}^{(d+2)} \int_{\mathbb{R}^{1,d-1}} \mathrm{d}^d x \, \mathbf{S}_{-\Delta}^{(2,d)}[f_\Delta^\dagger]^{\{a\}_L}(\tilde{x}) \delta_{\{ab\}_L} g_\Delta^{\{b\}_L}(x)\,, \tag{5.B.22}$$

where $\mathbf{S}_{-\Delta}^{(2,d)}$ is the well-known (non-normalized) shadow transform,

$$\mathbf{S}_{-\Delta}^{(2,d)}[f]^{\{a\}_L}(x) := \int_{\mathbb{R}^{1,d-1}} \mathrm{d}^d \tilde{x} \, \frac{I_{\{ab\}_L}(x-\tilde{x})}{(x-\tilde{x})^{2(d-\Delta)}} f_\Delta^{\{b\}_L}(\tilde{x})\,, \tag{5.B.23}$$

consisting of a non-local integral transform mapping a primary of conformal dimension Δ to a primary of conformal dimension $d-\Delta$.

$(1,d+1)$: If $X \mapsto F_{\Delta,\{A\}_L}(X)$, $\Delta \in \frac{d}{2} + \mathrm{i}\mathbb{R}_+$ denotes principal series representations of $\mathrm{SO}(1,d+1)$, then we replace (5.B.20) by an integral over two independent variables $x^a, \tilde{x}^a \in \mathbb{R}^d$ in d-dimensional Euclidean space. Once again, we can re-express the analytic continuation of (5.B.20) in terms of the Euclidean shadow transform

$$\mathbf{S}_{-\Delta}^{(1,d+1)}[f]^{\{a\}_L}(x) := \int_{\mathbb{R}^d} \mathrm{d}^d \tilde{x} \, \frac{I_{\{ab\}_L}(x-\tilde{x})}{(x-\tilde{x})^{2(d-\Delta)}} f_\Delta^{\{b\}_L}(\tilde{x}). \tag{5.B.24}$$

This integral transform is known as a Knapp-Stein intertwining operator [85] between the principal series representation of weight Δ, and the principal series representation of weight $\bar{\Delta} = d-\Delta$. On the other hand, if f_Δ transforms in a principal series representation of weight Δ, then $\overline{f_\Delta}$ will transform in a principal series representation of weight $\bar{\Delta}$. We can thus obtain the scalar product between principal series representations by replacing the shadow transform with complex conjugation, i.e.

$$\langle F_\Delta, G_\Delta \rangle = \mathcal{N}_{-\Delta}^{(d+2)} c_\Delta^{(d+2)} \int_{\mathbb{R}^d} \mathrm{d}^d x \, \overline{f_\Delta^{\{a\}_L}(x)} \, \delta_{\{ab\}_L} \, g_\Delta^{\{b\}_L}(x), \tag{5.B.25}$$

where $c_\Delta^{(d+2)}$ is some normalization.

$(0,d+2)$: Back to unitary representations of the compact real form, where $-\Delta \in \mathbb{Z}_{\geq 0}$, we can make the change of coordinates from antipode $\tilde{x}$ back complex conjugate $\bar{x}$ and rewrite (5.B.20) as

$$\langle F_\Delta, G_\Delta \rangle = \mathcal{N}_{-\Delta}^{(d+2)} \int_{\mathbb{C}^d} \mathrm{d}^d x \, \mathrm{d}^d \bar{x} \, \frac{\bar{f}^{\{a\}_L}(\bar{x}) I_{\{ab\}_L}(x + x^2\bar{x}) I_{\{c\}_L}^{\{b\}_L}(x) g^{\{c\}_L}(x)}{(1+2x\cdot\bar{x}+x^2\bar{x}^2)^{d-\Delta}} \tag{5.B.26}$$

It is known (see e.g. [136, Eq. 2.48]), that the denominator in (5.B.26) appears in the Kähler potential

$$\mathcal{K}(x,\bar{x}) := \log\bigl(1+2x\cdot\bar{x}+x^2\bar{x}^2\bigr) \tag{5.B.27}$$

of the Grassmannian

$$\mathrm{Gr}(2,d+2) := \mathrm{SO}_{\mathbb{R}}(d+2)/H_{\mathbb{R}}, \qquad H_{\mathbb{R}} := \mathrm{SO}_{\mathbb{R}}(2) \times \mathrm{SO}_{\mathbb{R}}(d), \tag{5.B.28}$$

which is not only a Kähler manifold, but also a Hermitian symmetric space. A more succinct formula for this scalar product is then given by

$$\langle F_\Delta, G_\Delta \rangle = \mathcal{N}_{-\Delta}^{(d+2)} \int_{\mathrm{Gr}(2,d+2)} (\partial\bar{\partial}\mathcal{K})^{\wedge d} \, e^{\mathcal{K}\Delta} \bar{f}_\Delta^{\{a\}_L}(\bar{x}) I_{\{ab\}_L}(\partial_{\bar{x}}\mathcal{K}) I_{\{c\}_L}^{\{b\}_L}(x) g_\Delta^{\{c\}_L}(x), \tag{5.B.29}$$

where $\partial, \bar{\partial}$ denote the holomorphic and anti-holomorphic exterior derivatives on the complex manifold $\mathrm{Gr}(2, d+2)$. The above formula does not lend itself well to direct computation. Instead, for practical purposes, we will introduce a compact analogue of the shadow transform, defined as

$$\mathrm{d}^d x\, \mathbf{S}^{(0,d+2)}_{-\Delta}[f^\dagger]_{\{c\}_L}(x) := \int_{\bar{x}} (\partial\bar{\partial}\mathcal{K})^{\wedge d}\, e^{\mathcal{K}\Delta}\, \bar{f}^{\{a\}_L}(\bar{x}) I_{\{ab\}_L}(\partial_{\bar{x}}\mathcal{K}) I^{\{b\}_L}_{\{c\}_L}(x), \tag{5.B.30}$$

where $\int_{\bar{x}}$ denotes integration of anti-holomorphic top forms in the Dolbeault cohomology of $\mathrm{Gr}(2, d+2)$, such that $\mathrm{d}^n x\, \mathbf{S}^{(0,d+2)}_{-\Delta}[f^\dagger]^{\{c\}_L}(x)$ is a holomorphic top form. We will now determine the image of the finite-dimensional representation $[-\Delta, l_1, \ldots, l_L]$ of $\mathrm{SO}_{\mathbb{R}}(d+2)$ under the compact shadow transform. First, if we denote the action of the conformal generators on a $[l_1, \ldots, l_L]$ tensor-valued field $\mathbf{f}_\Delta(x)$ as $\mathcal{T}^{(\Delta)}_\alpha(x^a, \partial_a)$, then the highest and lowest weight vectors of the representation $[-\Delta, l_1, \ldots, l_L]$ with respect to the first Cartan element are given by

$$\begin{aligned} &\mathbf{K}^{(\Delta)}_\mu \mathbf{f}_\Delta = 0 \iff \mathbf{f}_\Delta(x) = x^{-2\Delta}\mathbf{I}(x)\mathbf{v}\,, && \forall \mathbf{v} \in [l_1, \ldots, l_L]\,, \\ &\mathbf{P}^{(\Delta)}_\mu \mathbf{f}_\Delta = 0 \iff \mathbf{f}_\Delta(x) = \mathbf{v}\,, && \forall \mathbf{v} \in [l_1, \ldots, l_L]\,. \end{aligned}$$

Inserting both of these expressions for $f^{\{a\}_L}_\Delta$ in (5.B.30), it is easy to deduce how $\mathrm{d}^d x\, \mathbf{S}^{(0,d+2)}_{-\Delta}[f^\dagger](x)$ transforms under the left action of $H_{\mathbb{R}}$ on $\mathrm{Gr}(2, d+2)$ (the latter are defined in (5.B.28)). Combining these $H_{\mathbb{R}}$-covariance properties with the holomorphicity constraint is enough to determine, up to normalization, the image of the highest and lowest weights under the compact shadow transform:

$$\mathbf{S}^{(0,d+2)}_{-\Delta}[\mathbf{v}^\dagger](x) \propto (x^2)^{-\frac{d}{2}} \bar{\mathbf{v}}^{\mathsf{T}} \mathbf{I}(x)\,, \qquad \mathbf{S}^{(0,d+2)}_{-\Delta}[\big(x^{-2\Delta}\mathbf{I}(x)\mathbf{v}\big)^\dagger](x) \propto (x^2)^{-\frac{d}{2}+\Delta} \bar{\mathbf{v}}^{\mathsf{T}}\,.$$

Next, we know that all other states in the representation $[-\Delta, l_1, \ldots, l_L]$ are given by the repeated action of either $\mathbf{P}^{(\Delta)}_\mu$ or $\mathbf{K}^{(\Delta)}_\mu$ on either the highest weight vectors $x^{-2\Delta}\mathbf{I}(x)\mathbf{v}$ or the lowest weight vectors $\mathbf{v}$ respectively, until the opposite weights are reached. Integrating by parts the action of conformal generators in (5.B.30), we can deduce that the compact shadow transform continues to satisfy the interwining property,

$$\begin{aligned} \mathbf{S}^{(0,d+2)}_{-\Delta}[(\mathbf{K}^{(\Delta)}_\mu \mathbf{f}_\Delta)^\dagger](x) &= -\mathbf{S}^{(d+2)}_{-\Delta}[\mathbf{f}^\dagger_\Delta](x)\mathbf{P}^{(d-\Delta)}_\mu, \\ \mathbf{S}^{(d+2)}_{-\Delta}[(\mathbf{P}^{(\Delta)}_\mu \mathbf{f}_\Delta)^\dagger](x) &= -\mathbf{S}^{(0,d+2)}_{-\Delta}[\mathbf{f}^\dagger_\Delta](x)\mathbf{K}^{(d-\Delta)}_\mu. \end{aligned}$$

This allows us to compute the compact shadow transform of any vector in $[-\Delta, l_1, \ldots, l_L]$ from the shadow transform of the highest/lowest weights determined above. The compact shadow transform thus maps the space of $[l_1, \ldots, l_L]$-tensor valued polynomials in x with $x^a\partial_a = \mathrm{diag}(-d, \ldots, -d + 2\Delta)$ to a finite dimensional space of $[l_1, \ldots, l_L]$-tensor valued rational functions of x with $x^a\partial_a = \mathrm{diag}(-d, \ldots, -d + 2\Delta)$. Both spaces are meromorphic functions in x^a, and they are paired together with scalar product

$$\langle F_\Delta, G_\Delta \rangle = \mathcal{N}^{(d+2)}_{-\Delta} \int_{S^1 \times S^{d-2}} \mathrm{d}^d x\, \mathbf{S}^{(0,d+2)}_{-\Delta}[f^\dagger]_{\{a\}_L}(x)\, g^{\{a\}_L}_\Delta(x). \tag{5.B.31}$$

Note that the integration domain, $S^1 \times S^{d-2}$, is isomorphic to the $H_{\mathbb{R}}$-orbit of any non-zero point in $\mathrm{Gr}(2, d+2)$.

5.B.3 Iterated integration over Poincaré patches

For each of the L remaining Cartan generators in $\mathfrak{so}_{\mathbb{C}}(d+2)$, we can repeat the procedure in section 5.B.1 to write the scalar product of the representation $[-\Delta, l_1, \ldots, l_L]$ as iterated integrals over coordinates $x, y_1, \ldots, y_{\nu_{\max}}$, $\nu_{\max} \leq L$. Having discussed the analytic continuations of the integral formula

for all relevant real forms of $\mathfrak{so}_{\mathbb{C}}(d+2)$, we will make the representative choice

$$(x, y_1, \dots, y_{\nu_{\max}}) \in \mathbb{R}^d \times \mathbb{C}^{d-2} \times \cdots \times \mathbb{C}^{d-2\nu_{\max}}, \tag{5.B.32}$$

which are local coordinates on the flag manifolds

$$\mathrm{SO}(1,d+1)/(\mathrm{SO}(1,1)\times\mathrm{SO}(d)) \ltimes \mathbb{R}^d \quad , \quad \mathrm{SO}_{\mathbb{C}}(d+2-2\nu)/(\mathrm{SO}_{\mathbb{C}}(2)\times\mathrm{SO}_{\mathbb{C}}(d-2\nu)) \ltimes \mathbb{C}^{d-2\nu}\,,$$

for $\nu = 1, \dots, \nu_{\max}$. At the STT level ($\nu_{\max} = 1$) we introduce null polarization vectors in $\mathbb{C}^d$ and write

$$f_{\Delta,l_1,\{a\}_{L-1}}(x,z_1) := f_{\Delta,a_1^{(1)}\dots a_{l_1}^{(1)} a_1^{(2)}\dots a_{l_L}^{(L)}}(x) z_1^{a_1^{(1)}} \dots z_1^{a_{l_1}^{(1)}}. \tag{5.B.33}$$

Then, applying the reduction to the $\mathbb{C}^{d-2}$ Poincaré patch of $z \in \mathbb{C}^d$,

$$z^a(z^+, y_1) = z^+ \psi_1^a(y_1)\,, \quad z^+ := z^d + \mathrm{i}z^0, \quad \psi_1(x) := \left(\mathrm{i}\frac{y_1^2+1}{2}, -y_1^\alpha, \frac{y_1^2-1}{2}\right),$$

such that

$$f_{\Delta,l_1,\{a\}_{L-1}}(x,z_1) = (z_1^+)^{l_1} f_{\Delta,l_1,\{\alpha\}_{L-1}}(x,y_1) e^{\{a\}_{L-1}}_{\{\alpha\}_{L-1}}(y_1)\,, \quad e^a_\alpha(y_1) := \frac{\partial \psi_1^a}{\partial y_1^\alpha}(y_1)\,,$$

yields

$$\begin{aligned}\langle F_\Delta, G_\Delta\rangle = \mathcal{N}_{-\Delta}^{(d+2)} \mathcal{N}_{l_1}^{(d)} \int_{\mathbb{R}^d\times(S^1\times S^{d-3})} & \mathrm{d}^d x\, \mathrm{d}^{d-2} y_1 \\ & \mathbf{S}_{l_1}^{(0,d)} \circ \mathbf{S}_{-\Delta}^{(1,d+1)} [f^\dagger_{\Delta,l_1}]_{\{\alpha\}_{L-1}}(x,y_1)\, g_\Delta^{\{\alpha\}_{L-1}}(x,y_1)\,.\end{aligned} \tag{5.B.34}$$

The above choice of domain then corresponds to a principal series representation of $\mathrm{SO}(1,d+1)$. Another choice relevant for CFT corresponds to representations where $l_1 \in \frac{2-d}{2} + i\mathbb{R}$ is on the principal series of the $\mathrm{SO}(1,d-1)$ subgroup of $\mathrm{SO}(2,d)$. Such representations are known as *light-ray operators* in the CFT literature [137]. The scalar product for such representations can then be obtained by replacing $\mathbf{S}_{l_1}^{(0,d)} \to \mathbf{S}_{l_1}^{(1,d-1)}$, $S^1 \times S^{d-3} \to \mathbb{R}^{d-2}$ in (5.B.34).

For the remaining spins $l_2, \dots, l_L$, the only physically relevant reality condition is $l_2, \dots l_L \in \mathbb{Z}_{\geq 0}$ and $y_2, \dots, y_L$ as in (5.B.32). Omitting the domain of integration over $\mathbb{R}^d \times \prod_{\nu=1}^L (S^1 \times S^{d-2\nu-1})$, the integral formula of the scalar product at maximal depth is given by

$$\langle F_\Delta, G_\Delta\rangle = \mathcal{N}^{(d+2)}_{[-\Delta,\{l_\nu\}]} \int \mathrm{d}^d x \prod_{\nu=1}^L \mathrm{d}^{d-2\nu} y_\nu\, \mathbf{S}_{[-\Delta,\{l_\nu\}]}[f^\dagger_{\Delta,\{l_\nu\}}](x,\{y_\nu\})\, g_{\Delta,\{l_\nu\}}(x,\{y_\nu\})\,, \tag{5.B.35}$$

where

$$\mathcal{N}^{(d+2)}_{[-\Delta,\{l_\nu\}]} := \mathcal{N}^{(d+2)}_{-\Delta} \mathcal{N}^{(d)}_{l_1} \dots \mathcal{N}^{(d+2-2L)}_{l_L}, \quad \mathbf{S}_{[-\Delta,\{l_\nu\}]} := \mathbf{S}^{(0,d+2-2L)}_{l_L} \circ \cdots \circ \mathbf{S}^{(0,d)}_{l_1} \circ \mathbf{S}^{(1,d+1)}_{-\Delta}. \tag{5.B.36}$$

5.B.4 Application to the scalar products of 3-point vertex systems

3-point functions are invariants in the tensor product of three irreducible unitary representations of $\mathrm{SO}(2,d)$, from which they naturally inherit a $\mathrm{SO}(2,d)$-invariant scalar product. In the notation of section 5.1, this takes the form

$$\begin{aligned}\langle t, t'\rangle_{\mathrm{H}} = \prod_{i=1}^3 \mathcal{N}_{[-\Delta_i;l_i;\ell_i]} \int & \mathrm{d}^d x \mathrm{d}^{d-2} y_{1i} \mathrm{d}^{d-4} y_{2i} \\ & \bigotimes_{i=1}^3 \mathbf{S}^{(d+2)}_{[-\Delta_i;l_i;\ell_i]} \left[(\Omega t)^\dagger\right]\, \Omega t',\end{aligned}$$

where we have suppressed the dependence of Ω and t on the quantum numbers $[-\Delta_i; l_i; \ell_i]$ for convenience. The subscript "H" in $\langle -, - \rangle_{\mathrm{H}}$ stands for "Haar", because this formula for the scalar product can be understood as descending from the scalar product on $G \times G \times G$ defined by the Haar measure. In the conformal partial wave literature, it has now become common practice to analytically continue the conformal weights Δ from the physical region $\Delta \in \mathbb{R}_{\geq 0}$ to the domain of the $\mathrm{SO}(1, d+1)$ principal series representations, $\Delta \in \frac{d}{2} + \mathrm{i}\mathbb{R}$. For similar reasons, it will be useful to analytically continue the STT spins from the physical region $l_i \in \mathbb{Z}_{\geq 0}$ to the domain of the $\mathrm{SO}(1, d-1)$ principal series representations, $l_i \in \frac{2-d}{2} + \mathrm{i}\mathbb{R}$. In these regions, we can replace the shadow transforms in the scalar product with complex conjugation. In particular, for the STT-STT-scalar system (vertices of type I), this allows us to write the scalar product as

$$\langle t, t' \rangle_{\mathrm{H}} = \mathcal{N}_{[-\Delta_i; l_i]} \int_{(\mathbb{R}^d)^3 \times (\mathbb{R}^{d-2})^2} \mathrm{d}^d x_1 \, \mathrm{d}^d x_2 \, \mathrm{d}^d x_3 \, \mathrm{d}^{d-2} y_1 \, \mathrm{d}^{d-2} y_2 \, (\omega^\dagger \omega) \, t^\dagger t' \,, \tag{5.B.37}$$

where we defined

$$\Omega^{(\Delta_i; l_i)}(X_i; Z_i) =: \prod_{i=1}^{3} (X_i^+)^{-\Delta_i} \prod_{i=1}^{2} (z_i^+)^{l_i} \omega^{(\Delta_i; l_i)}(x_i; y_i) \,, \tag{5.B.38}$$

and

$$f^\dagger_{\Delta, l}(x, y) = x^{-2\bar{\Delta}} y^{2\bar{l}} \, \overline{f_{\Delta, l}} \, (x/x^2, I(x) \cdot y / y^2) \,. \tag{5.B.39}$$

Note that $t^\dagger = \bar{t}$ because of the conformal invariance of $\mathcal{X}$. To reduce $\langle -, - \rangle_{\mathrm{H}}$ to an integral over cross-ratio space, we need to factorize the global $\mathrm{SO}(1, d+1)$ symmetry acting on the integration variables $x_1, x_2, x_3 \in \mathbb{R}^d$ and $y_1, y_2 \in S^1 \times S^{d-3}$. This can be achieved either by applying the Faddeev-Popov method to a given conformal frame (passive picture), or by directly reducing the integration variables to the cross-ratio via conformally covariant changes of variables (active picture). We will adopt the latter approach.

First, let us decompose the prefactor $\omega^{(\Delta_i; l_i)}$ as

$$\omega^{(\Delta_i; l_i)}(x_i, y_i) := \omega_{\mathrm{sc}}^{(\Delta_i)}(x_i) \omega_{\mathrm{sp}}^{(l_i)}(x_i, y_i) \,, \tag{5.B.40}$$

$$\omega_{\mathrm{sc}}^{(\Delta_i)}(x_i) := |X_{23;1}|^{\Delta_1} |X_{31;2}|^{\Delta_2} |X_{12;3}|^{\Delta_3}, \tag{5.B.41}$$

$$\omega_{\mathrm{sp}}^{(l_i)}(x_i, y_i) = (N_{23;1} \cdot \psi_1)^{l_1} \, (N_{23;1} \cdot I(x_{12}) \psi_2)^{l_2} \,, \tag{5.B.42}$$

where

$$X_{ij;k} := x_{ik}/x_{ik}^2 - x_{jk}/x_{jk}^2 \,, \qquad X_{ij;k}^2 = \frac{x_{ij}^2}{x_{ik}^2 x_{jk}^2} \,, \qquad N_{ij;k} := \frac{X_{ij;k}}{|X_{ij;k}|} \,, \tag{5.B.43}$$

and $\psi_i = \psi_1(y_i) = \left(\frac{y_i^2 - 1}{2}, \mathrm{i} \frac{y_i^2 + 1}{2}, -y_i^\alpha \right)$ is the projective null vector in $\mathbb{C}^{d-2}$ defined above. Now, because $\bar{\Delta}_i = d - \Delta_i$ on the principal series, the prefactors in the integral simplify to

$$\omega_{\mathrm{sc}}^{(\Delta_i)} (\omega_{\mathrm{sc}}^{(\Delta_i)})^\dagger = \omega_{\mathrm{sc}}^{(\Delta_i)} \omega_{\mathrm{sc}}^{(d - \Delta_i)} = |x_{12}|^{-d} |x_{23}|^{-d} |x_{31}|^{-d}, \tag{5.B.44}$$

$$\omega_{\mathrm{sp}}^{(l_i)} (\omega_{\mathrm{sp}}^{(l_i)})^\dagger = \omega_{\mathrm{sp}}^{(l_i)} \omega_{\mathrm{sp}}^{(2-d-l_i)} = (N_{23;1} \cdot \psi_1)^{2-d} (N_{23;1} \cdot I(x_{12}) \psi_2)^{2-d}. \tag{5.B.45}$$

In the second line, we used the transformation properties of (x_i, y_i) under simultaneous $\mathrm{SO}(2, d)$ and $\mathrm{SO}(1, d-1)$ inversion,

$$\begin{aligned}
&(x_i, y_i) \mapsto (x_i / x_i^2, -I(x_i) \cdot y_i / y_i^2) \,, \\
&I_b^a(x_{ij}) \mapsto I_c^a(x_i) I_d^c(x_{ij}) I_b^d(x_j) \,, \\
&N_{ij;k}^a \mapsto I_b^a(x_k) N_{ij;k}^b \,, \\
&\psi_i^a \mapsto -y_i^2 I_b^a(x_i) \psi_i^b \,.
\end{aligned}$$

We can then re-express the measure coming from the $x_i \in \mathbb{R}^d$ as

$$\begin{aligned}\prod_{i=1}^{3} \mathrm{d}^d x_i \, (\omega_{\mathrm{sc}}\omega_{\mathrm{sc}}^{\dagger}) =& \frac{\mathrm{d}^d x_1 \mathrm{d}^d x_2 \mathrm{d}^d x_3}{|x_{12}|^d |x_{23}|^d |x_{31}|^d} \\ =& \mathrm{d}^d x_1 \mathrm{d}^d x_{21}^{-1} \frac{\mathrm{d}^d X_{23;1}}{|X_{23;1}|^d} \\ =& \mathrm{d}^d x_1 \mathrm{d}^d x_{21}^{-1} \mathrm{d}\log|X_{23;1}| \mathrm{d}^{d-1} N_{23;1}\,,\end{aligned}$$

where $\mathrm{d}^{d-1}N$ denotes the measure of the $(d-1)$-sphere in $\mathbb{R}^d$. Recall that in x^a, y^α-variables, the cross-ratio takes the form

$$\mathcal{X} = \frac{1}{2} \frac{\psi_1 \cdot I(x_{21}^{-1})\psi_2}{(N_{23;1}\cdot\psi_1)(N_{23;1}\cdot I(x_{21}^{-1})\psi_2)}\,. \tag{5.B.46}$$

Since $I(x)$ is independent of $|x|$, the non-compact moduli of the x_i-integrals fully factorize to

$$\int_{\mathbb{R}^d\times\mathbb{R}^d\times\mathbb{R}_+} \mathrm{d}^d x_1 \mathrm{d}^d x_{21}^{-1} \mathrm{d}\log|X_{23;1}| = \frac{|\mathrm{SO}(1,d+1)|}{|\mathrm{SO}(d)|}\,, \tag{5.B.47}$$

where $|G|$ denotes the volume of G. Here, we understand $\mathrm{d}^d x_1 \mathrm{d}^d x_{21}^{-1} \mathrm{d}\log|X_{23;1}|$ as integrals over translations, SCTs, and dilations respectively. Next, we change isospin variables to

$$\mathrm{d}^{d-2} y_1 \mathrm{d}^{d-2} y_2 \, (\omega_{\mathrm{sp}}\omega_{\mathrm{sp}}^{\dagger}) = \mathrm{d}^{d-2} y_1 \mathrm{d}^{d-2} y_{2;1} \, (N_{23;1}\cdot\psi_1)^{2-d} (N_{23;1}\cdot\psi_{2;1})^{2-d},$$

where $y_{2;1} := I(x_{21}^{-1})\cdot y_2$ and $\psi_{2;1}^a := \psi_1^a(y_{2;1})$, such that

$$\mathcal{X} = \frac{1}{2} \frac{\psi_1 \cdot \psi_{2;1}}{(N_{23;1}\cdot\psi_1)(N_{23;1}\cdot\psi_{2;1})}\,. \tag{5.B.48}$$

As we have now eliminated all ambiguity, let us denote $N_{23;1}^a \equiv N^a \in S^{d-1}$. We can always find a rotation matrix $\Lambda_N \in \mathrm{SO}(d)$ such that $N^a = (\Lambda_N)^a{}_b \delta_1^b$, where if $\psi(y) = \left(\frac{y^2-1}{2}, \mathrm{i}\frac{y^2+1}{2}, -y^\alpha\right)$, then $e_1 := (0,0,\delta_1^\alpha)$. We can thereby absorb any appearance of N in the integrand as the action of Λ_N^{-1} on ψ_1, $\psi_{2;1}$, i.e.

$$\begin{aligned}(N_{23;1}\cdot\psi_1)^{2-d}(N_{23;1}\cdot\psi_{2;1})^{2-d} &= (e_1\cdot\Lambda_N^{-1}\psi_1)^{2-d}(e_1\cdot\Lambda_N^{-1}\psi_{2;1})^{2-d}, \\ \mathcal{X} &= \frac{1}{2}\frac{(\Lambda_N^{-1}\psi_1)\cdot(\Lambda_N^{-1}\psi_{2;1})}{(e_1\cdot\Lambda_N^{-1}\psi_1)(e_1\cdot\Lambda_N^{-1}\psi_{2;1})}\,.\end{aligned}$$

Now, recall that $\psi^a(y) = \frac{z^a}{z^+}$, for some null vector $z \in \mathbb{C}^d$, so that

$$\Lambda_N^{-1}\cdot\psi(y) = \frac{(\Lambda_N^{-1}z)^+}{z^+}\psi(\Lambda_N^{-1}\cdot y)\,. \tag{5.B.49}$$

As we know from CFT, linearity of the Λ-action in $\mathbb{C}^d$ embedding space ensures that $\frac{(\Lambda_N^{-1}z)^+}{z^+}$ is a function of y, and it is determined by the Jacobian of the action of Λ_N^{-1} on $y \in \mathbb{C}^{d-2}$,

$$\frac{(\Lambda_N^{-1}z)^+}{z^+} = \left|\det\frac{\partial(\Lambda_N^{-1}\cdot y)}{\partial y}\right|^{\frac{1}{d-2}}. \tag{5.B.50}$$

It is precisely for this reason that we can write

$$\mathrm{d}^{d-2}y \left(\frac{(\Lambda_N^{-1}z)^+}{z^+}\right)^{2-d} = \mathrm{d}^{d-2}y \left|\det\frac{\partial(\Lambda_N^{-1}\cdot y)}{\partial y}\right| = \mathrm{d}^{d-2}(\Lambda_N^{-1}\cdot y)\,. \tag{5.B.51}$$

If we define $y_1' := \Lambda_N^{-1} \cdot y_1$, $y_2' := \Lambda_N^{-1} \cdot y_2$, and

$$e_1 \cdot y_i' := y_i'^{\parallel}, \qquad y_i - y_i'^{\parallel} e_1 := y_i^{\perp}, \tag{5.B.52}$$

this yields

$$\mathrm{d}^{d-2}y_1 \mathrm{d}^{d-2}y_2 \, (\omega_{\mathrm{sp}}\omega_{\mathrm{sp}}^{\dagger}) = \frac{\mathrm{d}^{d-2}y_1' \mathrm{d}^{d-2}y_2'}{(y_1'^{\parallel})^{d-2}(y_2'^{\parallel})^{d-2}}\,, \qquad \mathcal{X} = -\frac{(y_1'-y_2')^{\alpha}\delta_{\alpha\beta}(y_1'-y_2')^{\beta}}{4(y_1'^{\parallel})(y_2'^{\parallel})}\,. \tag{5.B.53}$$

Having eliminated the dependence on $N = N_{23;1}$, we can then factorize the integral over S^{d-1} as

$$\int_{S^{d-1}} \mathrm{d}^{d-1}N = \left|S^{d-1}\right| = \frac{|\mathrm{SO}(d)|}{|\mathrm{SO}(d-1)|}\,. \tag{5.B.54}$$

To reach this point, we have exclusively made changes of variables given by conformal transformations. In summary, we have simplified the scalar product to

$$\langle t, t' \rangle = \prod_{i=1}^{3} \mathcal{N}_{[-\Delta_i;l_i]}^{(d+2)} \frac{|\mathrm{SO}(1,d+1)|}{|\mathrm{SO}(d-1)|} \tag{5.B.55}$$

$$\int_{(\mathbb{R}^{d-2})^2} \frac{\mathrm{d}^{d-2}y_1 \mathrm{d}^{d-2}y_2}{(y_1^{\parallel})^{d-2}(y_2^{\parallel})^{d-2}} \bar{t}\left(\mathcal{X}(y_i)\right) t'\left(\mathcal{X}(y_i)\right). \tag{5.B.56}$$

From the Faddeev-Popov perspective, this expression is equivalent to the partial gauge fixing

$$(x_1^{\star a}, x_2^{\star a}, x_3^{\star a}) = (0, \delta_1^a, \infty)\,, \tag{5.B.57}$$

with a residual $\mathrm{SO}(1,d-2)$ symmetry on the $a = 2, \ldots, d$ plane remaining. To get a better intuition of the kinematics at hand, it is worth noting that (5.B.56) is equivalent to the conformal invariant pairing of scalar 2-point functions in $(d-2)$-dimensional Euclidean boundary CFT, with boundary at $y^{\parallel} = 0$ (see section 5.B.5 for further details). To obtain a scalar product with discrete orthonormal basis, we will restrict the domain of (y_1, y_2) from $(\mathbb{R}_+ \times \mathbb{R}^{d-3})^2$, to a $\mathrm{SO}(1,d-2)$-invariant submanifold for which the image of $(y_1, y_2) \mapsto \mathcal{X}(y_1, y_2)$ is a compact domain. To find this restriction, we can write the cross-ratio in manifestly $\mathrm{SO}(1,d-2)$-invariant form as

$$s = 1 - 2\mathcal{X} = \frac{(y_2 - \mathcal{P}y_1)^2 + (y_2 - y_1)^2}{(y_2 - \mathcal{P}y_1)^2 - (y_2 - y_1)^2}, \tag{5.B.58}$$

where $\mathcal{P}y := -y^{\parallel}e_1 + y^{\perp}$ maps a point in half-space to its mirror image. Since $\mathcal{P}$ commutes with conformal transformations that preserve the boundary, both $(y_2 - y_1)^2$ and $(y_2 - \mathcal{P}y_1)^2$ are $\mathrm{SO}(1,d-2)$-invariant. Thus, the restriction of these conformal invariants to

$$(y_2 - y_1)^2 \leq 0, \quad (y_2 - \mathcal{P}y_1)^2 \geq 0 \Longrightarrow |s| \leq 1, \tag{5.B.59}$$

defines an invariant submanifold where s is bounded. Note that this requires a continuation to the $(d-2)$-dimensional Minkowski metric, with respect to which y_2 and y_1 are then timelike separated. To proceed further, we act with $\mathrm{SO}(1,d-2)$ transformations on y_i:

$$y_i \to y_i - y_1^{\perp} \to \frac{y_i - y_1^{\perp}}{y_1^{\parallel}} \equiv y_i^{\star}, \tag{5.B.60}$$

which maps a generic pair of isospins to the gauge

$$y_1^{\star\alpha} = \delta_1^\alpha, \qquad y_2^{\star\alpha} = \frac{y_2^\alpha - (y_1^\perp)^\alpha}{y_1^\parallel} \in \mathbb{R}^{d-2}. \tag{5.B.61}$$

On the domain (5.B.59), $y_2^\star$ is a spacelike vector and can be parameterized as

$$y_2^\star = e^\psi \left(\cosh\phi\, e_1 + \sinh\phi\, n^\perp\right), \tag{5.B.62}$$

where $n^\perp \in \mathcal{H}^{n-1}$ is the two-sheeted hyperboloid of unit timelike vectors in $\mathbb{R}^{1,n-1}$. With these variables, we can write the cross-ratio as

$$s = 1 - 2\mathcal{X} = \frac{\cosh\psi}{\cosh\phi}, \qquad 1 \le \cosh^2\psi \le \cosh^2\phi. \tag{5.B.63}$$

Now, it's easy to transform the measure to

$$\begin{aligned}\frac{\mathrm{d}^{d-2}y_1\mathrm{d}^{d-2}y_2}{(y_1^\parallel)^{d-2}(y_2^\parallel)^{d-2}} =& \frac{\mathrm{d}^{d-2}y_1\mathrm{d}y_2^\parallel\mathrm{d}^{d-3}y_{21}^\perp}{(y_1^\parallel)^{d-2}(y_2^\parallel)^{d-2}}\\ =& \frac{\mathrm{d}^{d-2}y_1}{(y_1^\parallel)^{d-2}}\frac{\mathrm{d}\left(y_2^\parallel/y_1^\parallel\right)\mathrm{d}^{d-3}(y_{21}^\perp/y_1^\parallel)}{(y_2^\parallel/y_1^\parallel)^{d-2}}\\ =& \frac{\mathrm{d}^{d-2}y_1}{(y_1^\parallel)^{d-2}}\frac{\mathrm{d}^{d-2}y_2^\star}{(y_2^{\star\parallel})^{d-2}}.\end{aligned}$$

This factorizes the y_1 measure, leading to another normalization that corresponds to the volume of half-space,

$$\mathcal{V}_{\mathrm{hs}} = \int_0^\infty \mathrm{d}x\, x^{2-d}\int_{\mathbb{R}^{d-3}}\mathrm{d}^{d-3}y.$$

Next, applying the parameterization (5.B.61) to $y_2^\star$, we get

$$\begin{aligned}\frac{\mathrm{d}^{d-2}y_2^\star}{(y_2^{\star\parallel})^{d-2}} =& \frac{\mathrm{d}\left(e^\psi\right)(e^\psi)^{d-3}\mathrm{d}\phi\sinh^{d-4}\phi\,\mathrm{d}^{d-4}n^\perp}{(e^\phi)^{d-2}\cosh^{d-2}\phi}\\ =& \mathrm{d}\psi\,\mathrm{d}(\cosh\phi)\cosh^{2-d}\phi\,\sinh^{d-5}\phi\,\mathrm{d}^{d-4}n^\perp\\ =& \frac{\mathrm{d}(s\cosh\phi)}{\sqrt{s^2\cosh^2\phi-1}}\frac{\mathrm{d}\left(\cosh^2\phi\right)}{2\cosh\phi}(\cosh^2\phi)^{\frac{2-d}{2}}(\cosh^2\phi-1)^{\frac{d-5}{2}}\mathrm{d}^{d-4}n^\perp\\ =& \frac{1}{2}\mathrm{d}^{d-4}n^\perp\,\mathrm{d}t\,t^{\alpha-\frac{3}{2}}(1-t)^{-\frac{1}{2}}\,\mathrm{d}s\,(1-s^2)^{\alpha-\frac{1}{2}}, \qquad t := \frac{\cosh^2\phi-\cosh^2\psi}{\cosh^2\phi-1} \in [0,1].\end{aligned}$$

The t-integral yields

$$\int_0^1 \mathrm{d}t\, t^{\alpha-\frac{3}{2}}(1-t)^{-\frac{1}{2}} = \frac{\Gamma(\alpha-1/2)}{\Gamma(\alpha)}\sqrt{\pi}, \tag{5.B.64}$$

and the unit vector $\mathrm{d}^{d-4}n^\perp$ integrates to an extra $\left|H^{d-4}\right|$ volume. Putting everything back together, we obtain

$$\begin{aligned}\langle t, t'\rangle_{\mathrm{H}} = \frac{\sqrt{\pi}}{2}\prod_{i=1}^4 \mathcal{N}_{[-\Delta_i;l_i]}^{(d+2)}\,\mathcal{V}_{\mathrm{hs}}\,\frac{|\mathrm{SO}(1,d+1)|\,|\mathrm{SO}(1,d-5)|}{|\mathrm{SO}(d-1)||\mathrm{SO}(d-5)|}\frac{\Gamma(\alpha-1/2)}{\Gamma(\alpha)}\\ \int_{-1}^{+1}\mathrm{d}s\,(1-s^2)^{\alpha-\frac{1}{2}}\,\bar{t}\left(\frac{1-s}{2}\right)t'\left(\frac{1-s}{2}\right).\end{aligned} \tag{5.B.65}$$

We have thus proven that for the STT-STT-scalar vertex, the scalar product descending from the Haar measure coincides, up to normalization, with the Gegenbauer scalar product,

$$\langle t, t' \rangle_{\mathrm{H}} \propto \langle t, t' \rangle_{\alpha}. \tag{5.B.66}$$

For a space of functions with the appropriate boundary conditions at $\mathcal{X} = 0, 1 \iff s = -1, +1$, the hermiticity constraint of the 2-STT vertex operator (5.3.3) relative to this scalar product is then given by

$$\begin{aligned} H^{(d;\Delta_i;l_i)}(\mathcal{X}, \partial_{\mathcal{X}}) = & h_0^{(d;d-\Delta_i;2-d-l_i)}(\mathcal{X}) + \\ & \sum_{q=1}^{4} (-)^q [\mathcal{X}(1-\mathcal{X})]^{\frac{1}{2}-\alpha} \partial_{\mathcal{X}}^q [\mathcal{X}(1-\mathcal{X})]^{\alpha+1-\frac{3}{2}} h_q^{(d;d-\Delta_i;2-d-l_i)}(\mathcal{X}), \end{aligned} \tag{5.B.67}$$

where $\alpha = \frac{d-3}{2}$ in this case. In principle, one could obtain the generalization of this scalar product to MST_2-STT-scalar, and MST_2-MST_2-scalar in $d = 4$ by direct computation, using the scalar product on arbitrary spinning primaries that was derived in the previous section. However, given the full expression of the vertex Hamiltonian, we can instead make a simple self-adjointness ansatz for a modified Gegenbauer scalar product,

$$\begin{aligned} H^{(d;\Delta_i;l_i;\ell_i)}(\mathcal{X}, \partial_{\mathcal{X}}) \overset{!}{=} & h_0^{(d;d-\Delta_i;2-d-l_i;\ell_i)}(\mathcal{X}) + \\ & \sum_{q=1}^{4} (-)^q [\mathcal{X}(1-\mathcal{X})]^{\frac{1}{2}-\alpha} \partial_{\mathcal{X}}^q [\mathcal{X}(1-\mathcal{X})]^{\alpha+1-\frac{3}{2}} h_q^{(d;d-\Delta_i;2-d-l_i;\ell_i)}(\mathcal{X}). \end{aligned} \tag{5.B.68}$$

For the values of $(d; \Delta_i; l_i; \ell_i)$ where the vertex system is 1-dimensional, this ansatz is valid if and only if $\alpha = \ell_1 + \ell_2 + \frac{d-3}{2}$.

5.B.5 Relationship with boundary and projective space in CFT_{d-2}:

Consider once again two STTs and one scalar field in d dimensions, and define

$$\mathcal{O}_{\Delta_i, l_i}(X_i, Z_i) := (X_i^+)^{-\Delta_i} \Phi_{\Delta_i, l_i}(x_i, z_i), \tag{5.B.69}$$

as well as

$$\Omega_{\mathrm{sc}}(x_1, x_2, x_3) := |X_{23;1}|^{-\Delta_1} |X_{31;2}|^{-\Delta_2} \left|X^a_{23;1}\right|^{-\Delta_3}, \qquad N^a := \frac{X_{23;1}}{|X_{23;1}|}. \tag{5.B.70}$$

Then a general 3-point function of such representations is given by

$$\Omega_{\mathrm{sc}}^{-1} \langle \Phi_{\Delta_1, l_1}(x_1, z_1) \Phi_{\Delta_2, l_2}(x_2, z_2) \Phi_{\Delta_3}(x_3) \rangle = (N \cdot z_1)^{l_1} (N \cdot z_{2;1})^{l_2}\, t(\mathcal{X}), \tag{5.B.71}$$

where

$$\mathcal{X} = \frac{z_1 \cdot z_{2;1}}{2(N \cdot z_1)(N \cdot z_{2;1})}. \tag{5.B.72}$$

The right hand side of eq. (5.B.71) takes the exact same form as the 2-point function of two scalars with conformal dimensions $(-l_1, -l_2)$ in $(d-2)$-dimensional boundary CFT with $\mathcal{X} = -\xi$ when $N^2 = 1$, or $(d-2)$-dimensional projective space CFT with $\mathcal{X} = \eta$ when $N^2 = -1$. Using this kinematic equivalence, we could have directly obtained the Gegenbauer formula for the scalar product from [138, Eq. 4.10], by continuing $\xi = -\mathcal{X} \in [0, \infty)$ to $\xi \in [-1, 0]$. However, in this correspondence, the

CFT_{d-2} embedding space vectors $P \in \mathbb{R}^{1,d-1}$ are replaced with complex null vectors $z \in \mathbb{C}^d$, and there is no reality condition to distinguish projective space kinematics and bCFT kinematics in the case of finite dimensional representations of the rotation/Lorentz group. That being said, in Lorentzian signature, we expect our setup to coincide with the kinematics of Euclidean projective space CFT after analytically continuing to principal series representations of the $\text{SO}(1, d-1)$ subgroup.

5.C The d-deformation of the MST_2-MST_2-scalar vertex operator

5.C.1 Comparison with one-dimensional vertex systems

For all combinations of $(d; \Delta_i; l_i; \ell_i)$ that yield one-dimensional vertex systems, the Hamiltonian can be written as

$$H^{(d;\Delta_i;l_i;\ell_i)} = \tilde{H}^{(\gamma_i;\nu_i;\alpha;\beta)} + \Delta\tilde{E}^{(\gamma_i;\nu_i;\alpha;\beta;d)}\,, \tag{5.C.1}$$

where $(\Delta_i; l_i; \ell_i) \leftrightarrow (\gamma_i; \nu_i; \alpha; \beta)$ is the d-dependent bijection of seven parameters defined in subsection 5.5.3, and $\Delta\tilde{E}^{(\gamma_i;\nu_i;\alpha;\beta;d)}$ is a constant energy shift determined by

$$\Delta\tilde{E} - E_{\text{EFMV}} = L_{\text{EFMV}} - \tilde{H}, \tag{5.C.2}$$

with $E_{\text{EFMV}}^{(\Delta_i;l_i;\ell_i;d)}$ given in 5.C.2. Even for the two-dimensional vertex systems $d > 4, \ell_1, \ell_2 \neq 0$, we can obtain a d-dependent, MST_2-MST_2-scalar Hamiltonian for a one-dimensional system by restricting to the $\mathcal{Y} = 0$ plane:

$$H^{(d>4;\Delta_i;l_i;\ell_1,\ell_2)}(\mathcal{X}, \partial_{\mathcal{X}}) := H^{(d>4;\Delta_i;l_i;\ell_1,\ell_2)}(\mathcal{X}, \mathcal{Y} = 0, \partial_{\mathcal{X}}, \partial_{\mathcal{Y}} = 0)\,. \tag{5.C.3}$$

This d-deformation of the MST_2-MST_2-scalar operator is qualitatively different from the $d = 4$ or $\ell_2 = 0$ cases for several reasons:

1) First, while we can still write the whole operator $H^{(d>4;\Delta_i;l_i;\ell_1,\ell_2)}$ in (5.C.5) as an elliptic CMS Hamiltonian, two of its multiplicities will no longer be linear in the quantum numbers — instead

$$m_{1,0} = \frac{7-d}{2} - (l_1 + l_2) - \Delta_3 - 2\sqrt{\left(\ell_1 + \frac{d-4}{2}\right)^2 + 2\ell_2\left(\frac{d-4}{2} - \ell_1\right) + \ell_2^2}\,,$$
$$m_{2,0} = \frac{7-d}{2} - (l_1 + l_2) - \Delta_3 + 2\sqrt{\left(\ell_1 + \frac{d-4}{2}\right)^2 + 2\ell_2\left(\frac{d-4}{2} - \ell_1\right) + \ell_2^2}\,,$$

and the remaining multiplicities are

$$k(d; \Delta_i; l_i; \ell_1, \ell_2) = k(d; \Delta_i; l_i; \ell_1, 0)\,,$$
$$m_{i,\nu}(d; \Delta_i; l_i; \ell_1, \ell_2) = m_{i,\nu}(d; \Delta_i; l_i; \ell_1 + \ell_2, 0)\,, \qquad (i, \nu) \in \{3, 4\} \times \{0\} \cup \{1, 2, 3, 4\} \times \{1\}\,.$$

2) Second, there is no choice of α such that $H^{(d>4;\Delta_i;l_i;\ell_1,\ell_2)}$ is hermitian with respect to the Gegenbauer scalar product $\langle -, - \rangle_\alpha$, nor any scalar product with a measure of the form $\mathcal{X}^a(1 - \mathcal{X})^b$, $\mathcal{X} \in [0, 1]$.

3) It goes hand in hand with reason (1) that $H^{(d>4;\Delta_i;l_i;\ell_1,\ell_2\neq 0)}$ will now exhibit an explicit dependence on dimension after the reparametrization $(\Delta_i; l_i; \ell_i) \leftrightarrow (\gamma_i; \nu_i; \alpha; \beta)$, i.e.

$$H^{(d>4;\Delta_i;l_i;\ell_1,\ell_2\neq 0)} = \tilde{H}^{(d>4;\gamma_i;\nu_i;\alpha;\beta)}. \tag{5.C.4}$$

In fact, the generalization of (5.C.1) to $H^{(d>4;\Delta_i;l_i;\ell_1,\ell_2\neq 0)}$ is given by

$$H^{(d;\Delta_i;l_i;\ell_i)} = \tilde{H}^{(\gamma_i;\nu_i;\alpha;\beta)} + (d-4)(\alpha-\beta-1)H_{\text{def}}^{(\gamma_i;\nu_i;\alpha;\beta)}(\mathcal{X},\partial_{\mathcal{X}}) + \Delta\tilde{E}^{(\gamma_i;\nu_i;\alpha;\beta;d)}\,, \tag{5.C.5}$$

where

$$\begin{aligned} H_{\text{def}}^{(\gamma_i;\nu_i;\alpha;\beta)}(\mathcal{X},\partial_{\mathcal{X}}) =& 4\mathcal{X}(1-\mathcal{X})^2\partial_{\mathcal{X}}^2 \\ &+ 2(1-\mathcal{X})\left[(\nu_1+\nu_2-1)\mathcal{X} - (\nu_1+\nu_2+1) - 2\alpha - 2\mathrm{i}\gamma_3\right]\partial_{\mathcal{X}} + 4\nu_1\nu_2\mathcal{X} \\ &+ \frac{1}{4\mathcal{X}}\left(4\left(\gamma_1-\gamma_2\right)^2 + \left(2\alpha+2\mathrm{i}\gamma_3+2\nu_1+2\nu_2+3\right)^2\right), \end{aligned}$$

is the $d\neq 4$ deformation, and $\Delta\tilde{E}^{(\gamma_i;\nu_i;\alpha;\beta;d>4)}$ is also a constant obtained from

$$\Delta\tilde{E} - E_{\text{EFMV}} = L_{\text{EFMV}} - \tilde{H} - (d-4)(\alpha-\beta-1)H_{\text{def}}. \tag{5.C.6}$$

5.C.2 The constant shift for the CMS Operator

In section 5.5 (more specifically Eq. (5.5.31)), we determined the Hamiltonian of all one-dimensional vertex systems in terms of the CMS operator L_{EFMV} up to a constant shift E_{EFMV}. This was generalized in the previous section to $H^{(d\neq 4;\Delta_i;l_i;\ell_i\neq 0)}(\mathcal{X},\mathcal{Y}=0,\partial_{\mathcal{X}},\partial_{\mathcal{Y}}=0)$ with generalized CMS multiplities that are no longer linear in the dimension and quantum numbers. In all of these cases, the constant shift in the Hamiltonian is given by

$$H^{(d;\Delta_i;l_i;\ell_i)}(\mathcal{X},\partial_{\mathcal{X}}) = L_{\text{EFMV}}(\mathcal{X},\partial_{\mathcal{X}}) + E_{\text{EFMV}}^{(d;\Delta_i;l_i;\ell_i)}. \tag{5.C.7}$$

To write out E_{EFMV} explicitly, we make use of the previous change of variables to $(\gamma_i;\nu_i;\alpha,\beta)$ and expand the dimension around $d=4$, $\beta=0$, and $\alpha=0$, i.e.

$$d := 4+2\varepsilon,\;\; E_{\text{EFMV}} := \sum_{m=0}^{4}\varepsilon^m E_{\text{EFMV}}^{(m)}, \qquad E_{\text{EFMV}}^{(m)} := \sum_{n=0}^{3}\beta^n E_{\text{EFMV}}^{(m,n)}, \qquad E_{\text{EFMV}}^{(m,n)} := \sum_{p=0}^{4}\alpha^p E_{\text{EFMV}}^{(m,n,p)}.$$

The simplest coefficients are at the highest order in each of the three expansion parameters,

$$\begin{aligned} &E_{\text{EFMV}}^{(4)} = -128/3, \qquad E_{\text{EFMV}}^{(3)} = \frac{64(\beta-\alpha)-1856}{3}, \qquad E_{\text{EFMV}}^{(2,2)} = 32, \\ &E_{\text{EFMV}}^{(1,3)} = E_{\text{EFMV}}^{(0,0,4)} = -16, \qquad E_{\text{EFMV}}^{(0,3)} = 8(1-2\alpha). \end{aligned}$$

The next highest order terms are also relatively simple,

$$\begin{aligned} &E_{\text{EFMV}}^{(2,1)} = \frac{64(\alpha-3\mathrm{i}\gamma_3)+896}{3}, \qquad E_{\text{EFMV}}^{(1,2)} = 16(2\mathrm{i}\gamma_3+\alpha-2), \qquad E_{\text{EFMV}}^{(1,0,2)} = 16(15+6\nu_1-2\nu_2), \\ &E_{\text{EFMV}}^{(0,1,2)} = 8(1+8\nu_1-8\nu_2), \qquad E_{\text{EFMV}}^{(0,0,3)} = 80\nu_2-176\nu_1-16\mathrm{i}\gamma_3-64. \end{aligned}$$

We can then write all terms at $\mathcal{O}(\varepsilon,\beta)$ as

$$\begin{aligned} E_{\text{EFMV}}^{(1,1)} =& 56\nu_1(\nu_1-\frac{12}{7}\alpha-1) + 8\nu_2(\nu_2+4\alpha+1) + 16\nu_1\nu_2 + 8(4\gamma_1^2-4\gamma_2^2+\gamma_3^2) \\ &- 16\mathrm{i}\gamma_3(\nu_1+\nu_2-2\alpha) + \frac{688}{3}\alpha - 16\alpha^2 + \frac{230}{3}. \end{aligned}$$

The remaining terms that fit on one line are

$$E^{(0,1,1)}_{\mathrm{EFMV}} = -16\nu_1(2\nu_1-1)+16\nu_2(2\nu_2+1)+16\mathrm{i}\gamma_3+32(\gamma_1^2-\gamma_2^2+\gamma_3^2)+\frac{1120}{3},$$
$$E^{(0,1,0)}_{\mathrm{EFMV}} = 28\nu_1(\nu_1+1)-4\nu_2(\nu_2+1)-8\nu_1\nu_2+8\mathrm{i}\gamma_3(\nu_1+\nu_2+\frac{3}{2})-4\gamma_3^2+16(\gamma_2^2-\gamma_1^2)-\frac{347}{3}$$
$$E^{(0,0,2)}_{\mathrm{EFMV}} = 60\nu_2(\nu_2+\frac{31}{15})-124\nu_1(\nu_1+1)+88\nu_1\nu_2+4\mathrm{i}\gamma_3(1-2\nu_1-2\nu_2)+60\gamma_3^2-32(\gamma_1^2+\gamma_2^2)+183.$$

Finally, we have

$$\begin{aligned}
E^{(1,0,1)}_{\mathrm{EFMV}} =&56\nu_1^2-8\nu_2^2-16\nu_1\nu_2-\frac{1208}{3}\nu_2-\frac{1928}{3}\nu_1\\
&+16\mathrm{i}\gamma_3(\nu_1+\nu_2+\frac{3}{2})-8\gamma_3^2+32(\gamma_2^2-\gamma_1^2)-\frac{278}{3},\\
E^{(1,0,0)}_{\mathrm{EFMV}} =&\frac{856}{3}\nu_1(\nu_1+1)-\frac{616}{3}\nu_2(\nu_2+1)+16\nu_1\nu_2\\
&+16\mathrm{i}\gamma_3(\nu_1+\nu_2-\frac{3}{2})-\frac{616}{3}\gamma_3^2+\frac{544}{3}\gamma_2^2-\frac{928}{3}\gamma_1^2-\frac{4874}{3},\\
E^{(0,2)}_{\mathrm{EFMV}} =&16\alpha\left(-\alpha+\nu_1+\nu_2+\mathrm{i}\gamma_3+2\right)+12\nu_1(\nu_1+1)+12\nu_2(\nu_2+1)+8\nu_1\nu_2\\
&+4\mathrm{i}\gamma_3(2\nu_1+2\nu_2+3)+59,
\end{aligned}$$

along with

$$\begin{aligned}
E^{(0,0,1)}_{\mathrm{EFMV}} =&16\nu_2^3-240\nu_1^3+52\nu_2^2-364\nu_1^2\\
&+48\nu_1\nu_2(\nu_1+\nu_2+104)+\frac{2168}{3}\nu_1-\frac{1352}{3}\nu_2+4\mathrm{i}\gamma_3(3+2\nu_1+2\nu_2)\\
&+4\gamma_3^2(13+28\nu_1-4\nu_2)+\gamma_1^2(32\nu_1-96\nu_2)-32\gamma_2^2(1+3\nu_1-\nu_2)+64\mathrm{i}\gamma_1\gamma_2\gamma_3+\frac{899}{3},
\end{aligned}$$

and

$$\begin{aligned}
E^{(0,0,0)}_{\mathrm{EFMV}} =&4\nu_2^4-60\nu_1^4+8\nu_2^3-120\nu_1^3+24\nu_1^2\nu_2^2+\frac{1084}{3}\nu_1^2-\frac{724}{3}\nu_2(\nu_2+1)+28\nu_1\nu_2+\frac{1276}{3}\nu_1\\
&+16\mathrm{i}\gamma_1\gamma_2\gamma_3(1+2\nu_1+2\nu_2)-2\gamma_3^4-64\gamma_1^2(\gamma_1^2-\gamma_2^2)\\
&-\gamma_3^2\left(\frac{751}{3}+56\gamma_1^2-8\gamma_2^2-52\nu_1^2-56\nu_1+8\nu_1-8\nu_1\nu_2+12\nu_2^2\right)\\
&-\gamma_1^2\left(\frac{1330}{3}+56\nu_2^2-8\nu_1^2+40\nu_2-24\nu_1-16\nu_1\nu_2\right)\\
&+\gamma_2^2\left(\frac{766}{3}+8\nu_2^2-56\nu_1^2+24\nu_2-40\nu_1+16\nu_1\nu_2\right).
\end{aligned}$$

Chapter 6

OPE Limits and Cluster Decomposition

For scalar five-point and comb channel six-point blocks, we identified in chapter 5 the basis of tensor structures that diagonalize the vertex operators of the conformal block integrable system: they are polynomial eigenfunctions of an elliptic $\mathbb{Z}_4$ Calogero-Moser integrable model. We can now begin generalizing Dolan and Osborn's influential approach to conformal blocks, reviewed in section 3.3.1, to the N-point comb. In our work [65], which will be the subject of this chapter, we made important steps in this direction by generalizing the u, v cross ratios to *polynomial* cross ratios $u_i, v_i, U_i^{(m)}$, and generalizing the $z, \bar{z}$ variables to *OPE* cross ratios $z_i, \bar{z}_i, \Upsilon_i, w_s$. This judicious choice of variables substantially simplifies the form of the differential operators, which are then used to derive some fundamental properties of the blocks. Case in point: all differential operators have polynomial coefficients in the $u_i, v_i, U_i^{(m)}$ variables, and the higher point Gaudin Hamiltonians separate into lower point Hamiltonians in the limits $z_i, , \bar{z}_i, \Upsilon_i \to 0$. This last property can be understood as a refinement of the cluster decomposition principle in quantum field theory. For example, the cluster decomposition of a Euclidean six-point function into two triplets takes the form

$$\big\langle \phi_1(x_1)\phi_2(x_2)\phi_3(x_3)\phi_4(y_1)\phi_5(y_2)\phi_6(y_3)\big\rangle \overset{|x_i-y_j|\gg|x_i-x_j|,|y_i-y_j|}{\sim} \big\langle \phi_1(x_1)\phi_2(x_2)\phi_3(x_3)\big\rangle\big\langle \phi_4(y_1)\phi_5(y_2)\phi_6(y_3)\big\rangle.$$

In the presence of conformal symmetry, any such kinematical regime reduces in cross ratio space to what we call the middle leg OPE limit: $z_2, \bar{z}_2, \Upsilon_2 \to 0$. Now, if one of the two OPE coefficients C_{123} or C_{456} vanishes, then the leading contribution must involve a primary with non-zero scaling dimension. By computing the Gaudin differential operators in this limit, we find

$$\frac{\big\langle \phi_1\phi_2\phi_3\phi_4\phi_5\phi_6\big\rangle}{\Omega^{(\Delta_1,\dots,\Delta_6)}} \sim G_{\phi_1\phi_2\phi_3\mathcal{O}}(z_1,\bar{z}_1,w_1)\, z_2^{\frac{\Delta_{\mathcal{O}}-l_{\mathcal{O}}-\ell_{\mathcal{O}}}{2}} \bar{z}_2^{\frac{\Delta_{\mathcal{O}}+l_{\mathcal{O}}+\ell_{\mathcal{O}}}{2}} \Upsilon^{\kappa}\, G_{\mathcal{O}\phi_4\phi_5\phi_6}(z_3,\bar{z}_3,w_3),$$

where $\mathcal{O}$ is the operator with the lowest scaling dimension and spin in the composition of two OPEs $\phi_4 \times (\phi_5 \times \phi_6)$. This is one of the major results of this chapter. At a further stage, the additional OPE limits $z_{1,3}, \bar{z}_{1,3} \to 0$ entirely reduce the six-point block to a product of three-point vertex systems in $w_1 = 1 - \mathcal{X}_1$ and $w_2 = 1 - \mathcal{X}_2$ respectively. This general limiting behavior, summarized in equation (6.1.6), defines boundary conditions for multipoint conformal blocks.

6.1 Summary of results

Figure 26: Schematic representation of an M-point comb channel OPE diagram in $d = 4$. All the external legs at the interior of the comb are scalars, while we allow fields ϕ_1 and ϕ_M to sit in a generic representation.

Let us now describe the main new results of this work in some detail. To set up some notation, we consider the comb channel for M fields in $d = 4$, see Figure 26.[1] In general, we can insert arbitrary spinning fields at the external legs, but we shall assume that the fields ϕ_j on the external legs $j = 2, \ldots, M-1$ in the interior of the comb are scalar fields of conformal weight Δ_j. The two fields ϕ_1 and ϕ_M at the two sides of the comb are allowed to carry any spin, i.e. they can be symmetric traceless tensors (STTs) or even mixed symmetry tensors (MSTs). We denote the quantum numbers of these fields by $\varphi_1 = [\Delta_L, l_L, \ell_L]$ and $\varphi_M = [\Delta_R, l_R, \ell_R]$. Here, the subscripts L and R stand for 'left' and 'right', respectively, in accordance with their position in the OPE diagram. Note that STTs correspond to fields with $\ell = 0$ and scalar fields are obtained if we also set $l = 0$. The intermediate fields that appear along the horizontal lines of the comb are labeled by $[s]$ with $s = 1, \ldots, M-3$. We may think of $[s] = \{s+1, s+2\}$ as a pair of consecutive integers that enumerate the two external scalar fields attached to the two sides of the internal link. The associated intermediate fields $\Phi_{[s]}$ possess quantum numbers $\varphi_{[s]} = [\Delta_s, l_s, \ell_s]$ with non-vanishing ℓ_s in generic cases. Only ϕ_1 being scalar enforces $\ell_1 = 0$ at the first internal leg, and similarly $\ell_{M-3} = 0$ in case ϕ_M is scalar. When $M > 4$, the total number of cross ratios for M-point functions with $M-2$ scalar and two spinning insertions is given by

$$n_{cr}^{M} = 4(M-3) + 1 - 2\delta_{l_L=0=\ell_L} - 2\delta_{l_R=0=\ell_R} \ . \tag{6.1.1}$$

The subtractions correspond to the cases in which either one or both of the fields ϕ_1, ϕ_M are scalar. An $M = 3$-point function (vertex) with one scalar external field has no cross ratios unless the other two fields are both spinning, in which case there is a unique cross ratio, see [64]. For $M = 4$ points with at least two scalar insertions, one has

$$n_{cr}^{M=4} = 5 - 2\delta_{l_L=0=\ell_L} - 2\delta_{l_R=0=\ell_R} + \delta_{l_L=0=\ell_L}\delta_{l_R=0=\ell_R} \ . \tag{6.1.2}$$

Note that the application to a four-point function of four scalar fields gives $n_{cr}^{M=4} = 5-4+1 = 2$, i.e. there are two cross ratios in this case, as is well known.

The comb channel Hamiltonians are relatively easy to construct, at least in principle. In order to do so, we employ the first order differential operators $\mathcal{T}_{j,\alpha}, j = 1, \ldots M$, that correspond to the action of the conformal generators T_a on primary fields $\phi_j(x_j)$. In addition, let us also define

$$\mathcal{T}_{[s],\alpha} = \sum_{k=1}^{s+1} \mathcal{T}_{k,\alpha} \ . \tag{6.1.3}$$

[1] The following discussion is later applied to subdiagrams of an N-point comb channel OPE diagram, which is why we do not set $M = N$ and also allow for two of the external fields to carry spin.

The Casimir differential operators $\mathcal{D}_p^s, s = 1, \ldots, M-3$, are given by the p^{th}-order Casimir element for the generators $\mathcal{T}_{[s],\alpha}$. For generic comb channel links in $d = 4$, the integer p assumes the values $p = 2, 3, 4$. In cases where the field ϕ_1 is a scalar, the first link only carries two quantum numbers. There must hence be one relation between the three Casimir elements, such that one can restrict to $p = 2, 4$. A similar statement holds when the field ϕ_M is scalar. In addition, we have fourth order vertex differential operators of the form

$$\mathcal{V}_s^4 = \kappa_4^{\alpha_1 \cdots \alpha_4} \mathcal{S}_{s,\alpha_1} \cdots \mathcal{S}_{s,\alpha_4}, \qquad \mathcal{S}_{s,\alpha} = \mathcal{T}_{s+1,\alpha} - \mathcal{T}_{[s-1],\alpha} \tag{6.1.4}$$

for $s = 1, \ldots, M-2$. The operators $\mathcal{V}_1^4$ and $\mathcal{V}_{M-2}^4$ can be expressed in terms of the Casimir differential operators whenever ϕ_1 and ϕ_M are both scalar. So the number of differential operators we have constructed here coincides with the number n_{cr}^M of cross ratios. As we have shown in [63], these operators are all independent and they are mutually commuting. Let us note that the set of operators satisfying these properties is of course not unique. In our discussion of the six-point function, we will work with a set that is slightly different from the one we described here.

The joint eigenfunctions of these operators depend on the weights $\Delta_j, j = 2, \ldots, M-1$ of the external scalar fields, as well as the quantum numbers $\varphi_1 = [\Delta_L, l_L, \ell_L]$ and $\varphi_M = [\Delta_R, l_R, \ell_R]$ of the two fields ϕ_1 and ϕ_M, respectively. Of course, they also depend on the eigenvalues of the differential operators. We parameterize the eigenvalues of the Casimir differential operators through the quantum numbers $\varphi_{[s]} = [\Delta_s, l_s, \ell_s], s = 1, \ldots, M-3$ of the internal primaries, and we define $\tau_s, s = 1, \ldots, M-2$, to be the eigenvalues of the vertex differential operators $\mathcal{V}_4^s$. The latter correspond to a choice of tensor structures at the vertices. These wave functions are denoted by

$$\Psi^{\varphi_1, \Delta_j, \varphi_M}_{[\Delta_s, l_s, \ell_s; \tau_s]} = \Psi^{\varphi_1, \Delta_j, \varphi_M}_{[\Delta_s, l_s, \ell_s; \tau_s]}(u) \tag{6.1.5}$$

where u denotes any set of n_{cr}^M independent cross ratios. While the construction of the n_{cr} differential equations that these functions satisfy is fully algorithmic, see previous paragraph, the resulting expressions are rather lengthy in general, see e.g. [63] for some examples. Nevertheless, there are a few cases for which one obtains well-known differential operators. For $M = 3$ with two spinning fields ϕ_1, ϕ_3, the unique vertex differential operator was shown in [64] to coincide with the lemniscatic elliptic Calogero-Moser-Sutherland Hamiltonian discovered by Etingof, Felder, Ma and Veselov in [68]. The most well-known system appears for $M = 4$ when all the fields ϕ_i are scalar. In this case the resulting Hamiltonians famously coincide with those of a 2-particle hyperbolic Calogero-Sutherland model of type BC_2, [57]. The associated eigenvalue equations turn out to be equivalent to the Casimir equations for scalar four-point blocks that were calculated and analyzed by Dolan and Osborn [30]. The corresponding eigenfunctions have been studied extensively. In mathematics, this was initiated by the work of Heckman and Opdam [139]. The most relevant mathematical results were later re-derived independently in physics, starting with the work of Dolan and Osborn [29, 30, 95]. Continuing with $M = 4$, the next step is to include cases in which one or both of the fields ϕ_1 and ϕ_4 carry spin. Systems of this type have been studied in the physics literature by [89, 90, 140]. In particular, so-called seed conformal blocks in $d = 4$ dimensions have been characterized through a set of Casimir differential equations. The solution for these special blocks was developed in the same papers, and extensions to more general blocks in [141]. Alternatively, it is also possible to derive Casimir differential equations within the context of harmonic analysis of the conformal group [58, 59, 61]. In this context, the generalization to a universal spinning 2-particle Calogero-Sutherland Hamiltonian for any choice of spin representations of ϕ_1 and ϕ_4 can be constructed from Harish-Chandra's radial component map [99],

as will be discussed in [100]. The radial component map provides Casimir equations for spinning four-point blocks with external fields of arbitrary spin and in any dimension, thereby vastly generalizing its current status in the physics literature. In spite of being so general, the resulting expressions for the universal spinning Casimir operators turn out to be surprisingly compact. Nevertheless, a universal solution theory has not yet been developed.

After this preparation we are now able to state the main results of this work. They concern conformal blocks for correlation functions of N scalar fields. Obviously, the explicit form of the differential operators depends very much on the coordinates/cross ratios that are being used. Below, we shall start with one relatively simple choice that consists of $2(N-3)$ four-point cross ratios, $N-4$ five-point cross ratios and $N-5$ six-point cross ratios. The total number is $4N-15$ which coincides with the number of cross ratios of a scalar N-point function in $d=4$ when $N>4$. These initial cross ratios are depicted in Figures 27a and 28. They turn out to be well adapted to performing explicit computations. In particular, one can verify that all the coefficients of the differential operators are polynomials in these cross ratios. For this reason we shall refer to them as 'polynomial' cross ratios.
The key to this work is contained in subsection 6.2.4, where we introduce a new set of independent conformal invariants, first for $N=6$ and then more generally for any number N of insertions. The $2(N-3)$ four-point cross ratios mentioned above give rise to $N-3$ pairs $(z_r,\bar{z}_r), r=1,\dots,N-3$, of invariants, one for each internal edge. These are direct generalizations of the usual invariants $z,\bar{z}$ that are used to parameterize four-point cross ratios. The five-point cross ratios are then employed to build $N-4$ invariants $w_r, r=2,\dots,N-3$, one for each non-trivial vertex. The construction of the w_r is an immediate extension of the variable w that we introduced in the study of five-point blocks in our previous work [63], to complement the variables $z_1,\bar{z}_1,z_2,\bar{z}_2$. But starting with $N=6$, there exists $N-5$ additional independent invariants that involve the six-point cross ratios we described above. From these we define new conformal invariants $\Upsilon_r, r=2,\dots,N-4$, one for each internal edge in which an MST can propagate. This invariant is first constructed for the unique intermediate MST exchange in a six-point comb channel diagram for scalar external fields, see eq. (6.2.24), and then extended to higher numbers $N\geq 6$ of insertions at the end of section 6.2.4. In the same subsection, we also provide a nice geometrical interpretation of the new conformal invariants, which we shall refer to as comb channel OPE coordinates.
The association of these invariants with specific links and vertices is much more than mere counting. Consider a link $r\in\{2,\dots,N-4\}$ in which an MST propagates. This link comes with a set of three invariants $z_r,\bar{z}_r,\Upsilon_r$. Our central claim concerning OPE factorization of multipoint blocks can now be formulated after rewriting the blocks Ψ in terms of the OPE coordinates $\Psi=\Psi(z_r,\bar{z}_r,\Upsilon_r;w_s)$. When these functions are expanded around $z_b=\bar{z}_b=0=\Upsilon_b$[2] for one particular value of $b\in\{2,\dots,N-4\}$ the leading term is claimed to be of the form

$$\Psi^{\Delta_i}_{[\Delta_r,l_r,\ell_r;\tau_r]}(z_r,\bar{z}_r,\Upsilon_r;w_s)=z_b^{\frac{1}{2}(\Delta_b+l_b+\ell_b)}\bar{z}_b^{\frac{1}{2}(\Delta_b-l_b-\ell_b)}\Upsilon_b^{\ell_b}\times \tag{6.1.6}$$
$$\times\left(\Psi^{\Delta_{i\leq b+1},[\Delta_b,l_b,\ell_b]}_{[\Delta_r,l_r,\ell_r;\tau_s]}(z_r,\bar{z}_r,\Upsilon_r;w_s)^{r<b}_{s<b}\times\Psi^{[\Delta_b,l_b,\ell_b],\Delta_{i>b+1}}_{[\Delta_r,l_r,\ell_r;\tau_s]}(z_r,\bar{z}_r,\Upsilon_r;w_s)^{r>b}_{s\geq b}+O(z_b,\bar{z}_b,\Upsilon_b)\right)\,.$$

In the first line we have displayed the leading exponents in any of the three variables. Note that these are determined by the quantum numbers of the exchanged intermediate field $\phi_{[b]}$. In case the latter is an STT, that is if and only if $\ell_b=0$, this leading term is familiar from the theory of blocks for four-point functions of scalars. Once this term in the first line of the expression is factored out, the

[2]Note that the three limits do not commute. We take the limit $\bar{z}_b\to 0$ first before taking z_b and Υ_b to zero. For these last two variables the order of limits does not matter.

remaining function admits a power series expansion in the three variables $z_b, \bar{z}_b$ and Υ_b. The constant term in this power series expansion turns out to factorize into a product of two eigenfunctions of Gaudin Hamiltonians with $M_1 = b+2$ and $M_2 = N-b$ sites, respectively. The sub- and superscripts we have placed on the eigenfunctions restrict the dependence on both the quantum numbers and the conformal invariants. Let us note that this OPE factorization also holds for $b = 1$ and $b = N-3$, except that in these two cases, the prefactor in the first line only contains powers of z_b and $\bar{z}_b$ because $\ell_b = 0$. In both such cases, one of the two blocks in the second line is simply a constant. One can directly verify such factorization formulas whenever explicit formulas for the blocks are available, e.g. for $d = 1$ comb-channel blocks, which have been constructed in [46]. We have included one such explicit check for the six-point function in Appendix 6.C.

To prove the remarkable result (6.1.6) beyond those cases in which the blocks are known, the differential operators play a decisive role. Strictly speaking, our central claim remains conjectural for $N > 6$. But in the case of $N = 6$ we are able to establish it rigorously. A scalar six-point function in $d = 4$ dimensions depends on nine cross ratios. We parameterize these through the variables $z_r, \bar{z}_r, r = 1, 2, 3$, $\Upsilon = \Upsilon_2$ and $w_s, s = 1, 2$. When we perform the limit on the variables $(z_2, \bar{z}_2, \Upsilon)$ that are associated with the internal MST exchange along the central link, the block factorizes into a product of two spinning $M = 4$-point blocks with a single spinning field and three scalars in each of them. Such spinning four-point blocks depend on three variables each. In our special parameterization, these are given by $(z_1, \bar{z}_1; w_1)$ and $(z_3, \bar{z}_3; w_2)$, respectively. As we recalled above, spinning four-point blocks may be characterized as solutions of a specific set of differential equations that has been worked out at least for some examples in the CFT literature, see in particular [140]. As we will announce in this paper, the full set of these differential equations can been obtained with the help of Harish-Chandra's radial component map [100]. The strategy to prove our factorization result is to evaluate the limit of the six-site Gaudin Hamiltonians as $z_2, \bar{z}_2, \Upsilon$ are sent to zero and to map the resulting operators to the differential operators for spinning four-point blocks through an appropriate change of variables. Similarly, one can also consider the limit in which the pairs $(z_1, \bar{z}_1)$ and $(z_3, \bar{z}_3)$ are both sent to zero. Our OPE factorization states that the leading term in the resulting expansion is given by a spinning four-point block for two scalar and two spinning fields. Once again, it is possible to verify this claim by mapping the relevant differential operators onto each other.

Let us now briefly outline the content of each section. The next section is entirely devoted to a discussion of cross ratios. After a brief review of the two most commonly used sets of cross ratios for four-point functions, we will extend both of them to multipoint functions. The usual cross ratios u, v can be generalized to higher numbers N of insertion points in such a way that the Casimir differential operators for comb channel blocks have polynomial coefficients, at least for $N \leq 10$. These *polynomial cross ratios* for multipoint functions are defined in section 6.2.2. While the latter have some nice features, they are not well adapted to taking OPE limits. For this reason we shall introduce a second set of conformal invariants which we dub *OPE cross ratios*. We do so for $N = 5$ and $N = 6$ points first before discussing the case $N > 6$, based on a geometric/group theoretic interpretation of these variables. Section 6.3 is devoted to OPE limits, and the discussion focuses on $N = 6$-point functions. After a brief review of the Gaudin Hamiltonians that characterize comb channel blocks, we derive the asymptotic behaviour in the first line of eq. (6.1.6) and show that the leading term indeed factorizes into a product of functions of the respective variables. These functions may be characterized through certain differential operators which can be obtained by studying the limiting behaviour of the original Gaudin Hamiltonians. In particular, it turns out that the Gaudin Hamiltonians split into two sets of operators that act on a disjoint subset of cross ratios. These can be identified with the Casimir

operators of spinning four-point blocks, thus establishing our result (6.1.6).

6.2 Cross ratios for multipoint correlation functions

As we have explained in the introduction, there is much freedom in introducing sets of independent conformally invariant variables. In this section, we introduce two such sets for multipoint correlation functions. The first one is referred to as polynomial cross ratios and it is a direct generalization of the common four-point cross ratios u and v to scalar correlators with $N > 4$ field insertions. When written in these cross ratios, all of the $N-3$ quadratic Casimir differential operators that characterize the comb channel multipoint blocks in sufficiently large dimension d turn out to possess polynomial coefficients, at least for $N \leq 10$. The second set of conformal invariants we introduce in this section is fundamental to all of our subsequent discussion. These new coordinates are akin to the variables z and $\bar{z}$ that are widely used for four-point functions. They possess a large number of remarkable properties. Most importantly for us, they behave well under dimensional reductions and when taking OPE limits, which is why we shall also refer to them as *OPE cross ratios*. In addition, these variables possess a nice geometric interpretation.
In the first subsection, the case of $N = 4$ will be briefly reviewed to highlight some of the properties of the cross ratios u, v and $z, \bar{z}$ that make them so useful and are desirable to maintain as we go to a higher number N of insertions. The polynomial cross ratios are then introduced in the second subsection. Next, in the third subsection, we discuss the OPE coordinates for $N = 5$, where there is a single qualitatively new invariant that was already introduced in [63]. The fourth subsection contains the construction of yet another new invariant that is now attached to the central link of the six-point comb channel diagram. We introduce this invariant and provide a geometrical interpretation. The latter is then used to extend the construction of comb channel invariants in $d = 4$ to $N > 6$ insertion points.

6.2.1 Prologue: Cross ratios for four-point blocks

In order to enter the discussion of cross ratios for correlation functions of scalar fields, we will begin with the well known case of $N = 4$ operators. Famously, there exist two independent cross ratios one can build from their four insertions points $x_i, i = 1, \ldots, 4$,

$$u = \frac{x_{12}^2 x_{34}^2}{x_{13}^2 x_{24}^2}\,, \qquad v = \frac{x_{14}^2 x_{23}^2}{x_{13}^2 x_{24}^2}\,. \tag{6.2.1}$$

These cross ratios can be represented schematically as in Figure 27a, where we disposed the four points along a square and every colored edge corresponds to a scalar product present in the associated cross ratio, with intersecting lines being present in the denominator. When written in these four-point cross ratios u, v, the second order Casimir operator takes the form, see eq. (2.10) in [95],

$$\frac{1}{2}\mathcal{D}_{(12)}^2 = (1-u-v)\partial_v\left(v\partial_v + a + b\right) + u\partial_u\left(2u\partial_u - d\right) - (1+u-v)\left(u\partial_u + v\partial_v + a\right)\left(u\partial_u + v\partial_v + b\right), \tag{6.2.2}$$

with the two parameters $2a = \Delta_2 - \Delta_1$ and $2b = \Delta_3 - \Delta_4$ determined by the conformal weights Δ_i of the four external scalar fields. We observe that in these coordinates, the Casimir operator takes a relatively simple form in which all coefficient functions are polynomials in the two cross ratios u and v. But it also has some less pleasant features. In particular, it is not directly amenable to a power series solution in the variables u, v. In order to formalize this a bit more, let us introduce the

notion of a *grade* in some variable w. We say that a differential operator of the form $cw^n\partial_w^m$ has w-grade $\mathrm{gr}_w(cw^n\partial_w^m) = n - m$. When the grade is applied to some linear combination of such simple 'monomial' differential operators, it returns a set of grades, one element for each term. For the grades of the Casimir operator (7.2.7), we find

$$\mathrm{gr}_u\left(\mathcal{D}^2_{(12)}\right) = \{0, 1\} \quad , \quad \mathrm{gr}_v\left(\mathcal{D}^2_{(12)}\right) = \{-1, 0, 1\} \ . \tag{6.2.3}$$

While the u-grade of the individual terms is non-negative, this is not the case for the v-grade. In other words, when written in the variables u, v, the quadratic Casimir operator contains simultaneously terms that lower and terms that raise the degree of a polynomial in v.
In order to analyze the eigenfunctions of four-point Casimir operators, Dolan and Osborn switched to another parameterization of the cross ratios through the complex variables z and $\bar{z}$,

$$u = z\bar{z} \quad , \quad v = (1 - z)(1 - \bar{z}) \ . \tag{6.2.4}$$

We point out that the change of variables is not one-to-one since u and v are invariant under the action of the $\mathbb{Z}_2$ whose non-trivial element exchanges z with $\bar{z}$. Hence, functions of the cross ratios u and v correspond to $\mathbb{Z}_2$ invariant functions of $z, \bar{z}$. The invariants $z, \bar{z}$ possess a nice geometric interpretation. As is well known, conformal transformations can be used to move the insertion points to the special positions $x_2 = 0$, $x_4 = \vec{e}_1$, $x_3 = \infty\vec{e}_1$, where $\vec{e}_1$ denotes the unit vector along the first coordinate direction of the d-dimensional Euclidean space. This choice of a conformal frame is stabilized by a subgroup $SO(d-1) \subset SO(d)$ of the rotation group that describes rotations around the first coordinate axis. These rotations can be used to move x_1 into the plane spanned by $\vec{e}_1$ and $\vec{e}_2$. The invariants $z, \bar{z}$ are the complex coordinates of x_1 in this plane. Let us note that in these coordinates, it is very easy to implement the restriction to $d = 1$ for which there exists only one cross ratio, namely $z = \bar{z}$.
The geometric interpretation of the $z, \bar{z}$ coordinates, and in particular their simple reduction to $d = 1$, also manifests itself in another property. Indeed, the so-called Gram determinant of the N insertion points takes a particularly simple form when written in terms of $z, \bar{z}$. Before stating the concrete formula, we need to briefly review the concepts of embedding space and Gram determinants. The embedding space formalism associates a light-like vector $X \in \mathbb{R}^{1,d+1}$ of the form

$$X = \left(\frac{1 + x^2}{2}, \frac{1 - x^2}{2}, x\right) \in \mathbb{R}^{1,d+1}$$

to any point $x \in \mathbb{R}^d$. The associated light rays are in one-to-one correspondence with points in $\mathbb{R}$. Note that we have chosen a particular representative X of the light ray by fixing the sum of the first two components to $X_{-1} + X_0 = 1$. Given N insertion points x_i, we construct N light-like vectors $X_i \in \mathbb{R}^{1,d+1}$. These vectors are linearly dependent if and only if the associated Gram matrix, that is to say the matrix of scalar products $X_{ij} = \langle X_i, X_j\rangle$, has vanishing determinant. For $N = 4$ points $x_i \in \mathbb{R}^d$, the associated Gram determinant takes the form

$$\det(X_{ij})\big|_4 = (z - \bar{z})^2 X_{13}^2 X_{24}^2 \, . \tag{6.2.5}$$

We see that this expression is rather simple when written in terms of the cross ratios $z, \bar{z}$, much simpler than its expression in terms of u, v. Since any four vectors $X_i \in \mathbb{R}^{1,2}$ are linearly dependent, the four-point Gram determinant must vanish in $d = 1$. This is achieved by setting $z = \bar{z}$ so that all four points lie on a single line, in agreement with our discussion in the previous paragraph. The simplicity of the Gram determinant in the $z, \bar{z}$ coordinates means that these are very well suited to implement the dimensional reduction.

Next we turn to a discussion of the Casimir operator. When the expression we spelled out in eq. (7.2.7) is rewritten in terms of z and $\bar{z}$ it acquires the form, see eq. (2.19) in [95],

$$\frac{1}{2}\mathcal{D}_{(12)}^2 = z^2(1-z)\frac{\partial^2}{\partial z^2} + \bar{z}^2(1-\bar{z})\frac{\partial^2}{\partial \bar{z}^2} - (a+b+1)\left(z^2\frac{\partial}{\partial z} + \bar{z}^2\frac{\partial}{\partial \bar{z}}\right) - 2ab(z+\bar{z}) + \varepsilon\frac{z\bar{z}}{z-\bar{z}}\left((1-z)\frac{\partial}{\partial z} - (1-\bar{z})\frac{\partial}{\partial \bar{z}}\right), \quad (6.2.6)$$

with $\varepsilon = d-2$. We note that the resulting expression is only slightly longer than for the original set u, v of four-point cross ratios. On the other hand, its coefficients are no longer polynomial. The main advantage of the $z, \bar{z}$ coordinates is that they admit a rather simple implementation of the OPE limit in which we send $\bar{z} \to 0$ first, followed by the limit $z \to 0$. When $|\bar{z}| < |z|$, we can actually expand the last term in the expression for $\mathcal{D}_{(12)}^2$ in a power series. In the resulting expression, all terms possess non-negative $\bar{z}$ grade, i.e.

$$\mathrm{gr}_{\bar{z}}\left(\mathcal{D}_{(12)}^2\right) \in \{0, 1, 2, \dots\} . \quad (6.2.7)$$

This means that there is no term in which the derivatives with respect to $\partial_{\bar{z}}$ outnumber the multiplications with $\bar{z}$. Keeping only terms of vanishing $\bar{z}$-grade, we have

$$\mathcal{D}_{(12)}^2 \sim 2z^2(1-z)\frac{\partial^2}{\partial z^2} + 2\bar{z}^2\frac{\partial^2}{\partial \bar{z}^2} - 2(a+b+1)z^2\frac{\partial}{\partial z} - 2abz - 2\varepsilon\bar{z}\frac{\partial}{\partial \bar{z}} + \dots \quad (6.2.8)$$

In turn, one observes that the terms above all have non-negative z-grade, among which the terms of vanishing grade are given by

$$\mathcal{D}_{(12)}^2 \sim 2z^2\frac{\partial^2}{\partial z^2} + 2\bar{z}^2\frac{\partial^2}{\partial \bar{z}^2} - 2\varepsilon\bar{z}\frac{\partial}{\partial \bar{z}} + \dots , \quad (6.2.9)$$

where now the $\dots$ contain terms of both positive $\bar{z}$- and positive z-grade. Let us now apply this discussion to the problem of finding eigenfunctions of the Casimir operator,

$$\mathcal{D}_{(12)}^2\psi_{\Delta,l}(z,\bar{z}) = \left[\Delta(\Delta-d) + l(l+d-2)\right]\psi_{\Delta,l}(z,\bar{z}) . \quad (6.2.10)$$

For the limiting regime in which we replace the Casimir operator by the expression in eq. (6.2.9), the eigenvalue problem is very easy to solve:

$$\psi_{\Delta,l}(z,\bar{z}) \sim z^{\frac{\Delta+l}{2}}\bar{z}^{\frac{\Delta-l}{2}}c_{\Delta,l} + \dots , \quad (6.2.11)$$

where $c_{\Delta,l}$ is a non-vanishing constant factor that is not determined by the eigenvalue equation and depends on the normalization. Since all of the terms omitted from our original Casimir operator have positive grade, we conclude that it possesses an eigenfunction of the form

$$\psi_{\Delta,l}(z,\bar{z}) \;=\; z^{\frac{\Delta+l}{2}}\bar{z}^{\frac{\Delta-l}{2}}F_{\Delta,l}(z,\bar{z}) = z^{\frac{\Delta+l}{2}}\bar{z}^{\frac{\Delta-l}{2}}\left(c_{\Delta,l} + O(z,\bar{z})\right), \quad (6.2.12)$$

i.e. the function F possesses a power series expansion in z and $\bar{z}$ with non-vanishing constant term $c_{\Delta,l}$.

Before we turn to a higher number $N > 4$ of insertion points, we want to summarize a few of the desirable properties of the coordinates $z, \bar{z}$ that are relevant to the rest of the paper. To begin with, when working with multipoint correlators, it is certainly very desirable to have simple expressions for the Gram determinant. Note that N points $X_i \in \mathbb{R}^{1,d+1}$ are linearly dependent whenever $N > d+2$.

So if we keep the dimension d fixed, going to larger values of N will inevitably lead to vanishing Gram determinants. Consequently, an N-point function in dimension $d < N-2$ lives on a subspace within the larger space of cross ratios for $d \geq N-2$. The explicit description of this subspace is easiest when working with coordinates in which the Gram determinant factorizes into simple functions of the cross ratios. More importantly, we would like to find coordinates that are well adapted to the OPE limit in the sense we outlined above. For higher point functions, this means finding coordinates, subsets of which are associated with the internal links of the OPE diagram, such that eigenfunctions admit a power series expansion in all of the link variables. For $N > 4$, the leading term of these expansions will no longer be constant, of course, but should rather factorize into a product of functions that are associated with the two subdiagrams connected by the link. We will indeed be able to construct such variables for all N-point comb channel diagrams, at least in $d = 4$ dimensions.

6.2.2 Polynomial cross ratios for comb channel multipoint blocks

In this subsection we address the construction of sets of cross ratios which make all coefficients of comb channel differential operators polynomial. Because of this property, we dub this set *polynomial cross ratios*. We have seen this feature before when writing the Casimir operator for four-point functions in the coordinates u, v, see eq. (7.2.7). In this sense, the polynomial cross ratios we are about to construct are natural extensions of the four-point cross ratios u, v.

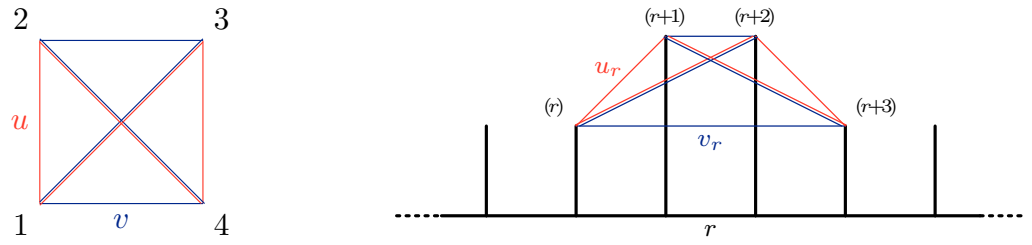

(a) Four-point cross ratios (b) Construction of four-point cross ratios around internal leg r

Figure 27: Schematic representation of the four-point cross ratios u and v, where intersecting lines correspond to terms in the denominator. The same type of cross ratios can be constructed around every internal leg by focusing on the closest four points.

We start be constructing the four-point cross ratios of the same type for each internal link of the comb channel OPE diagram. Consider the link with label $r = 1, \ldots, N-3$. Then the four nearest neighbor insertion points are x_i with $i = r, r+1, r+2, r+3$, see Figure 27b. From these we can build two four-point cross ratios u_r, v_r using the same expressions as in the case of four-point functions, i.e. for an N-point comb channel diagram we can construct $(N-3)$ sets of u, v type cross ratios through

$$u_r = \frac{X_{r(r+1)}X_{(r+2)(r+3)}}{X_{r(r+2)}X_{(r+1)(r+3)}}\,, \qquad v_r = \frac{X_{r(r+3)}X_{(r+1)(r+2)}}{X_{r(r+2)}X_{(r+1)(r+3)}}\,, \qquad r = 1, \ldots, N-3\,. \tag{6.2.13}$$

Here we have used the construction in terms of the embedding space variables X_i, see previous subsection. The $2(N-3)$ cross ratios we have introduced so far do not suffice to generate all conformal invariants as soon as $d > 2$ and $N > 4$. We conjecture that a set of cross ratios making all coefficients of the N-point comb channel Casimir operators polynomial in $d \geq N-2$ is obtained if we complement

the four-point cross ratios (u_r, v_r) introduced above by the following set of m-point cross ratios

$$U_s^{(m)} = \frac{X_{s(s+m-1)} \prod_{j=1}^{m-3} X_{(s+j)(s+j+1)}}{\prod_{j=0}^{m-3} X_{(s+j)(s+j+2)}}, \qquad s = 1, \ldots, (N-m+1), \qquad m = 5, \ldots, N. \quad (6.2.14)$$

The total number of cross ratios we have introduced is $N(N-3)/2$, which coincides with the number of independent cross ratios as long as $d \geq N-2$. We checked our claim of polynomial dependence explicitly by verifying that all comb channel quadratic Casimir operators that appear for up to $N = 10$ external scalar fields indeed have polynomial coefficients in these cross ratios. In addition, we also verified the claim for vertex differential operators with $N \leq 6$. We shall often refer to the variables (6.2.14) as the *m-point polynomial cross ratios*, since they are constructed around every set of m adjacent points in an N-point function. The first few examples of these type of cross ratios with low values of m are represented schematically in Figure 28.

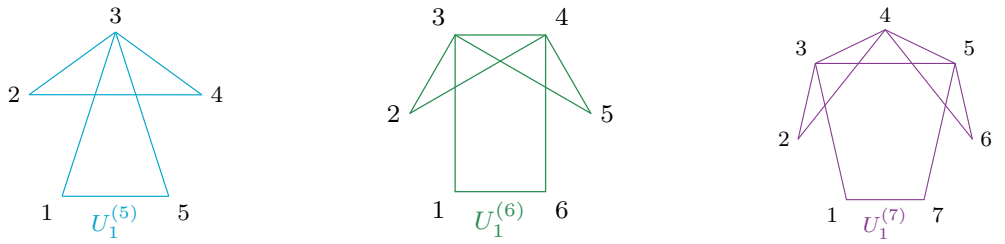

(a) Five-point cross ratio (b) Six-point cross ratio (c) Seven-point cross ratio

Figure 28: Polynomial cross ratios for five, six, and seven point functions. The colored lines correspond to scalar products present in the expression of the cross ratio, with lines that intersect outside vertices corresponding to terms in the denominator.

If the dimension d drops below its lower bound or alternatively, if for fixed dimension d the number N of insertion points satisfies $N > d+2$, then there are additional relations between the cross ratios that we have introduced. These can be found by computing the Gram determinant for the scalar products X_{ij}. Given d, the relations allow us to express our m-point cross ratios $U^{(m)}$ with $m > d+2$ in terms of cross ratios involving a lower number of insertion points. In other words, in dimension d, the space of N-point conformal invariants is generated by the cross ratios $U_s^{(m)}$ with $m \leq d+2$. It is easy to verify that the number of such cross ratios indeed coincides with the expected number n_{cr}, see eq. (6.1.1).

In d dimensions, there are $N-d-1$ of these m-point cross ratios with maximal value $m = d+2$. In particular, the first time one of the latter cross ratios is needed is for $(d+2)$-point functions. For example, to construct the conformal invariants of an N-point function in $d = 3$, we need m-point cross ratios with $m = 4, 5$ only, and the five-point cross ratios first appear for $N = 5$. Similarly, in $d = 4$ dimensions, we work with m-point cross ratios for $m = 4, 5, 6$, and all these invariants appear together starting with $N = 6$ insertion points. Since we are mostly interested in $d = 3, 4$, it will be sufficient for us to analyze Casimir operators for correlation functions of $N = 5$ and $N = 6$ scalar fields.

The set of polynomial cross ratios we have introduced in this subsection leads to relatively simple expressions of Casimir operators, but it does not behave nicely when taking OPE limits of fields, i.e. the OPE limit cannot simply be obtained by taking a limit for a subset of cross ratios to specific values. We will now turn to the construction of new variables that are more suitable for OPE limits.

6.2.3 Five-point OPE cross ratios

We begin our discussion of the new OPE cross ratios with $N = 5$. As we reviewed above, five insertion points give rise to five independent cross whenever $d \geq 3$. Our recipe for the construction of polynomial cross ratios in the previous subsection provides us with the following set,

$$u_1 = \frac{X_{12}X_{34}}{X_{13}X_{24}}\,, \qquad v_1 = \frac{X_{14}X_{23}}{X_{13}X_{24}}\,, \qquad U_1^{(5)} = \frac{X_{15}X_{23}X_{34}}{X_{24}X_{13}X_{35}}\,. \tag{6.2.15}$$
$$u_2 = \frac{X_{23}X_{45}}{X_{24}X_{35}}\,, \qquad v_2 = \frac{X_{25}X_{34}}{X_{24}X_{35}}\,,$$

For this case, we already introduced a new parameterization in [63] through the following set of relations,

$$u_1 = z_1\bar{z}_1\,, \qquad v_1 = (1-z_1)(1-\bar{z}_1)\,,$$
$$u_2 = z_2\bar{z}_2\,, \qquad v_2 = (1-z_2)(1-\bar{z}_2)\,, \tag{6.2.16}$$
$$U_1^{(5)} = w_1(z_1-\bar{z}_1)(z_2-\bar{z}_2) + (1-z_1-z_2)(1-\bar{z}_1-\bar{z}_2)\,.$$

Note that the $\mathbb{Z}_2$ symmetry one introduces when passing from u, v to $z, \bar{z}$ for four points is now enhanced to $\mathbb{Z}_2 \times \mathbb{Z}_2$. In the case of five-point functions, the two non-trivial generators of this symmetry act by $z_r \leftrightarrow \bar{z}_r, w_1 \to (1-w_1)$ for $r = 1, 2$. When written in the conformal invariant coordinates $z_r, \bar{z}_r$ and $w = w_1$, the complexity of the differential operators remains roughly on the same level as for the polynomial cross ratios, in the same way as the quadratic Casimir operators for $N = 4$ which have similar complexity in the two sets of variables, c.f. eqs. (7.2.7) and (6.2.6). But our OPE coordinates for five-point functions have a number of additional properties that are worth pointing out.
To begin with, they possess a rather nice geometric interpretation in a certain conformal frame.[3] Using conformal transformations, it is possible to move three points, let's say x_2, x_3 and x_4, onto a single line with positions $0, 1, \infty$. Then we can use the remaining rotations transverse to that line in order to move x_1 into a plane, and finally rotations transverse to that plane in order to move x_5 into some 3-dimensional subspace. Thus, there exists a conformal transformation $g^{(5)}$ such that

$$g^{(5)}(x_1) = \varrho_1(\cos\theta_1, \sin\theta_1, 0, \vec{0})\,, \qquad g^{(5)}(x_2) = (0,0,0,\vec{0})\,,$$
$$g^{(5)}(x_3) = (\infty, 0, 0, \vec{0})\,, \qquad g^{(5)}(x_4) = \vec{e}_1 = (1,0,0,\vec{0})\,, \tag{6.2.17}$$
$$g^{(5)}(x_5) = e_1 - \varrho_2(\cos\theta_2, \sin\theta_2\cos\phi, \sin\theta_2\sin\phi, \vec{0})\,.$$

Here we have parameterized the image point $g^{(5)}(x_1)$ in the plane through an angle θ_1 and a distance ϱ_1, as usual. Similarly, we have also parameterized the point $g^{(5)}(x_5)$ in a 3-dimensional space through two angles θ_2, ϕ and one distance ϱ_2, using $g^{(5)}(x_4) = \vec{e}_1$ as reference point. In all of these expressions, $\vec{0}$ denotes a vector with $d-3$ vanishing components. We note that in $d = 4$ dimensions, the conformal transformation $g^{(5)}$ is uniquely fixed by our choice of frame. It is now easy to compute our new variables $z_r, \bar{z}_r$ and w_1 in terms of θ_r, ϱ_r and ϕ,

$$z_1 = \varrho_1 e^{\mathrm{i}\theta_1}\,, \qquad \bar{z}_1 = \varrho_1 e^{-\mathrm{i}\theta_1}\,, \qquad z_2 = \varrho_2 e^{\mathrm{i}\theta_2}\,, \qquad \bar{z}_2 = \varrho_2 e^{-\mathrm{i}\theta_2}\,, \qquad w_1 = \sin^2\frac{\phi}{2}\,. \tag{6.2.18}$$

This is illustrated in Figure 29. In particular we see that z_1, $\bar{z}_1$ and z_2, $\bar{z}_2$ describe the two planes $x_1x_2x_3x_4$ and $x_2x_3x_4x_5$ respectively, while w_1 is a function of the angle ϕ between those planes. As

[3] We thank Luke Corcoran for pointing out this frame to us.

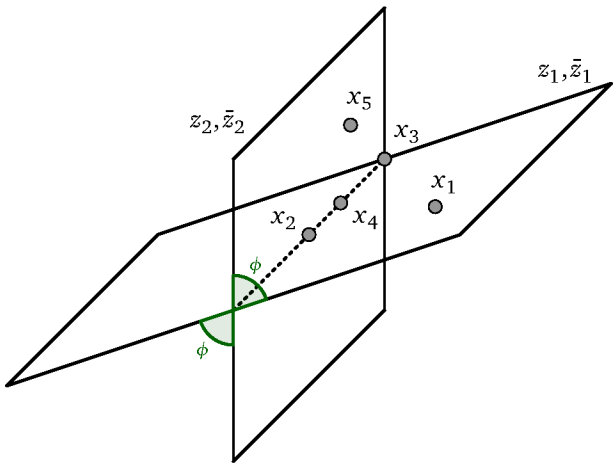

Figure 29: Conformal frame for five points

can be read off from this picture, the domain of w_1 in Euclidean signature is

$$w_1 \in [0, 1] \,. \tag{6.2.19}$$

The description we provided is valid for $d \geq 3$. As we go down to $d = 2$, there are no longer enough dimensions in order to have a non-vanishing angle ϕ between two 2-planes, i.e. we must set $\phi = 0$ or $\phi = \pi$ and hence $w_1 = 0$ or $w_1 = 1$. As in our review of four-point functions, we expect to recover these values of w_1 as zeroes of the Gram determinant. And indeed, the Gram determinant for the five coordinates X_i acquires the following form,

$$\det(X_{ij})\big|_5 = 2\frac{w_1\,(1-w_1)\,(z_1-\bar{z}_1)^2\,(z_2-\bar{z}_2)^2\,X_{13}^2 X_{24}^2 X_{35}^2}{X_{23}X_{34}} \,. \tag{6.2.20}$$

In addition to the two factors w_1 and $w_1 - 1$, we also notice the zeros that appear for $z_r = \bar{z}_r$, i.e. when the four points $x_1x_2x_3x_4$ or $x_2x_3x_4x_5$ lie on a line.
In section 4.2 of [64], we also used these coordinates to analyze the OPE limit of our Gaudin differential operators. This analysis showed clearly how the variable w_1 is naturally associated with the degree of freedom describing the choice of tensor structures at the internal vertex of a five-point OPE diagram. More specifically, we took the OPE limit for the two sets $z_1, \bar{z}_1$ and $z_2, \bar{z}_2$ of variables associated with the two internal links of the OPE diagram. In the limit where we take $\bar{z}_r \to 0$ first, followed by $z_r \to 0$, the joint eigenfunctions of the five differential operators behave as

$$\psi_{\Delta_r, l_r;\kappa}(z_r, \bar{z}_r, w_1) \sim \prod_{r=1}^{2} z_r^{\frac{\Delta_r + l_r}{2}} \bar{z}_r^{\frac{\Delta_r - l_r}{2}} \left(\gamma_{\Delta_r, l_r;\kappa}(w_1) + O(z_r, \bar{z}_r)\right) \,. \tag{6.2.21}$$

The derivation follows the same steps outlined in the discussion of four-point blocks in the first subsection. But in contrast to the case of $N = 4$, the leading term γ of the power series expansion in $z_r, \bar{z}_r$ is no longer constant, but rather an eigenfunction of a single variable vertex differential operator for an STT-STT-scalar three-point function, which we constructed and analyzed in [64]. The latter was shown to arise in the OPE limit of the five-point vertex operator, which acts on all the five cross ratios before taking the limit. The STT-STT-scalar three-point function is determined by conformal

symmetry up to a function of a single variable. The latter can be constructed in terms of the standard $2,3$-point tensor structures H_{ij} and $V_{i,jk}$ of [89]. The detailed comparison of the 3-point with the OPE limit of the five-point vertex operators gives

$$w_1 \to 1 - \frac{H_{ab}}{V_{a,3b}V_{b,a3}}\,, \tag{6.2.22}$$

where a and b are the internal legs on which the OPE limit projects, see [64] for a detailed discussion.

6.2.4 Six-point OPE cross ratios

Having reviewed our parameterization of five-point cross ratios, we now turn to a discussion of $N = 6$. As long as $d \geq 4$, our set of independent polynomial cross ratios consists of

$$u_3 = \frac{X_{34}X_{56}}{X_{35}X_{46}}\,, \qquad v_3 = \frac{X_{45}X_{36}}{X_{35}X_{46}}\,, \qquad U_2^{(5)} = \frac{X_{26}X_{34}X_{45}}{X_{35}X_{24}X_{46}}\,, \tag{6.2.23}$$

$$U_1^{(6)} = \frac{X_{16}X_{23}X_{34}X_{45}}{X_{13}X_{24}X_{35}X_{46}}\,, \tag{6.2.24}$$

in addition to the five cross ratios already introduced in eq. (7.3.1). While the three cross ratios in the first line are of the same type as those we met in our discussion of $N = 5$, the six-point cross ratio in the second line is fundamentally new. In passing to our OPE coordinates, it is natural to make use of the map (6.2.16) for those cross ratios shared with the previously discussed five-point function, while analogously mapping the cross ratios in eq. (6.2.23) to

$$\begin{aligned} u_3 = z_3\bar{z}_3\,, \qquad v_3 = (1-z_3)(1-\bar{z}_3)\,, \\ U_2^{(5)} = w_2(z_2-\bar{z}_2)(z_3-\bar{z}_3) + (1-z_2-z_3)(1-\bar{z}_2-\bar{z}_3)\,. \end{aligned} \tag{6.2.25}$$

For the six-point variable (6.2.24), a new type of mapping is necessary. In the same way that the variables z_r, $\bar{z}_r$ are associated with exchanges of STTs, and the w_s variables are associated with specific non-trivial tensor structures sitting at internal vertices of OPE diagrams, the new variable we want to introduce should be associated with exchanges of Mixed-Symmetry Tensors with two spins, and it should naturally combine with the z_2, $\bar{z}_2$ cross ratios to make up the three exchanged degrees of freedom of the middle link. We propose to introduce this conformal invariant $\Upsilon = \Upsilon_2$ via the relation

$$\begin{aligned} U_1^{(6)} = \Upsilon\,(z_1-\bar{z}_1)\,(z_2-\bar{z}_2)\,(z_3-\bar{z}_3)\,\sqrt{w_1(1-w_1)w_2(1-w_2)} - w_1w_2\,(z_1-\bar{z}_1)\,(\bar{z}_2+z_2)\,(z_3-\bar{z}_3) \\ + w_1\,(z_1-\bar{z}_1)\,[z_2\,(1-\bar{z}_3) - \bar{z}_2(1-z_3)] + w_2\,(z_3-\bar{z}_3)\,[z_2\,(1-\bar{z}_1) - \bar{z}_2(1-z_1)] \\ + [z_2-(1-z_1)(1-z_3)]\,[\bar{z}_2-(1-\bar{z}_1)(1-\bar{z}_3)]\,. \end{aligned} \tag{6.2.26}$$

The new variables $z_r, \bar{z}_r, w_s$ and Υ admit an action of $\mathbb{Z}_2^3$ that leaves the original cross ratios invariant. The nontrivial elements σ_r of the three $\mathbb{Z}_2$ factors each exchange one of the pairs $z_r \leftrightarrow \bar{z}_r$, map $w_s \to (1-w_s)$ for $r = s, s+1$ and send Υ to $-\Upsilon$.

As a first quick test of our proposal, we can compute the six-point Gram determinant. When expressed in the OPE coordinates, it reads

$$\frac{X_{34}^2\det(X_{ij})\big|_6}{\prod_{i=1}^4 X_{i,i+1}^2} = \frac{(1-w_1)\,w_1(1-w_2)\,w_2\,(z_1-\bar{z}_1)^2(z_2-\bar{z}_2)^2(z_3-\bar{z}_3)^2\big(4z_2\bar{z}_2 - \Upsilon^2\,(z_2-\bar{z}_2)^{\,2}\big)}{z_2^2\bar{z}_2^2}. \tag{6.2.27}$$

Given the lengthy relation between the six-point cross ratio $U^{(6)}$ and Υ it is very reassuring to see that the Gram determinant now fits into a single line. In addition, the new conformal invariant Υ appears in a single factor, combined only with the cross ratios $z_2, \bar{z}_2$. If we reduce the dimension to $d = 3$, the number of cross ratios drops by one. In our new set of conformal invariants, we see that Υ can then be expressed in terms of $z_2, \bar{z}_2$ as

$$\Upsilon^2 = \frac{4 z_2 \bar{z}_2}{(z_2 - \bar{z}_2)^2} \quad \textit{for} \quad d = 3. \tag{6.2.28}$$

All these simple relations are quite remarkable. On the other hand, they are not yet sufficient to fully appreciate our definition of Υ. For example, given what we have seen, one may still wonder why we did not rescale Υ to make the last bracket in the Gram determinant equal to $(\Upsilon^2 - 1)$. While that is certainly possible, and leads to a nicer geometrical interpretation, the rescaled variable would result in more complicated expressions for the asymptotics of comb channel blocks in OPE limits, see our discussion in the next section.

The interpretation of our coordinates proceeds as in the previous subsection. In that case, each of the two internal links was associated with a complex plane. We used the coordinates $z_1, \bar{z}_1$ and $z_2, \bar{z}_2$ to specify two positions on these two planes and related the variable w_1 to the relative angle between the two planes within a 3-dimensional subspace. As we go to $N = 6$, the same picture applies, but with dimensions raised by one. Instead of the 2-planes in 3-space, we now have two 3-spaces that are associated with the points $x_1, \ldots, x_5$ and $x_2, \ldots, x_6$, respectively. These are embedded in a 4-dimensional subspace with the relative angle being measured by a new angle φ. Each of the two 3-spaces contains the configuration of two planes depicted in Figure 29. For the first five points $x_1, \ldots, x_5$, this defines the coordinates $\varrho_1, \theta_1, \varrho_2, \theta_2$ and ϕ as before. We obtain a similar set of coordinates for the second set $x_2, \ldots, x_6$. Now it is easy to see that one pair of coordinates coincides with the ones from the first quintuple of insertion points, so that in total we need eight coordinates $\varrho_r, \theta_r, \phi_1, \phi_2$ with $r = 1, 2, 3$ to parameterize the configurations within each of the 3-spaces. With these coordinates, one finds that

$$z_r := \varrho_r e^{\mathrm{i}\theta_r}, \quad w_s := \sin^2 \frac{\phi_s}{2}, \quad \Upsilon := \pm \mathrm{i} \frac{\cos \varphi}{\sin \theta_2}, \tag{6.2.29}$$

where $r = 1, 2, 3$ and $s = 1, 2$. The sign in Υ is conventional, and can be absorbed in a shift of the angle φ. A more formal definition of the various geometric parameters on the right hand side will be given in the next subsection as part of a more general construction that applies to any number N of points in $d = 4$ dimensions.

6.2.5 Generalization to higher number of points

In order to extend our choice of coordinates to higher number N of insertion points in $d = 4$ dimensions, it is useful to formalize the construction we have described at the end of the previous subsection. As described in subsection 6.2.3, each quintuple of consecutive points $x_s, x_{s+1}, \ldots, x_{s+4}$ defines a conformal transformation $g_s^{(5)}$ as in eq. (6.2.17),

$$\begin{aligned} &g_s^{(5)}(x_s) =: \varrho_s \vec{n}(\theta_s, 0) \ , \quad g_s^{(5)}(x_{s+1}) =: (0,0,0,0), \\ &g_s^{(5)}(x_{s+2}) =: (\infty,0,0,0) \ , \quad g_s^{(5)}(x_{s+3}) =: \vec{e}_1 = (1,0,0,0), \\ &g_s^{(5)}(x_{s+4}) =: \vec{e}_1 - \varrho_{s+1} \vec{n}(\theta_{s+1}, \phi_s), \end{aligned} \tag{6.2.30}$$

where $s = 1, \ldots, N-4$ and we defined the unit vectors $\vec{n}$ as

$$\vec{n}(\theta, \phi) := (\cos\theta, \sin\theta\cos\phi, \sin\theta\sin\phi, 0). \tag{6.2.31}$$

Thus, to compute x_6 in the conformal frame where $g_1^{(5)}(x_1), \dots, g_1^{(5)}(x_5)$ are of the form (6.2.17), we express the sixth point as

$$g_1^{(5)}(x_6) = g_1^{(5)} \circ g_2^{(5)-1}(\vec{e}_1 - \varrho_3 \vec{n}(\theta_3, \phi_2)) \equiv h_{12}^{(5)}(\vec{e}_1 - \varrho_3 \vec{n}(\theta_3, \phi_2)). \tag{6.2.32}$$

By construction, $h_{12}^{(5)}$ is a conformal group element parameterized by the cross ratios of the six-point function. In appendix 6.A, we compute this conformal transformation and find

$$h_{12}^{(5)-1} = \varrho_2^{-D} \mathcal{I} \sigma_1 e^{-\varphi M_{34}} e^{-\theta_2 M_{12}} e^{-\phi_1 M_{23}} e^{P_1}, \tag{6.2.33}$$

where $\mathcal{I}$ is conformal inversion and $\sigma_1 : (x^1, x^2, x^3, x^4) \mapsto (-x^1, x^2, x^3, x^4)$ is a reflection along the hyperplane orthogonal to the first coordinate direction. The explicit action of the element (6.2.33) on spacetime points x is given by

$$h_{12}^{(5)-1}(x) = \varrho_2 \sigma_1 e^{-\varphi M_{34}} e^{-\theta_2 M_{12}} e^{-\phi_1 M_{23}} \frac{x - \vec{e}_1}{(x - \vec{e}_1)^2}. \tag{6.2.34}$$

In particular, we read off from there that the angle φ describes the relative angle between two 3-spaces. It is obvious how to continue these constructions beyond $N = 6$ points in $d = 4$. We continue to introduce comb channel cross ratios $z_r, \bar{z}_r$ and w_s in terms of the polynomial cross ratios through relations (6.2.16) with indices running over $r = 1, \dots, N-3$ and $s = 1, \dots N-4$, respectively. Similarly, we introduce Υ_r with $r = 2, \dots N-4$ through relations of the form (6.2.26). After extending our relations (6.2.29) to a higher number of comb channel OPE coordinates we introduce the geometric coordinates as

$$z_r := \varrho_r e^{\mathrm{i}\theta_r}, \quad w_s := \sin^2 \frac{\phi_s}{2}, \quad \Upsilon_r := \pm \mathrm{i} \frac{\cos \varphi_r}{\sin \theta_{r+1}}, \tag{6.2.35}$$

and define in direct analogy to eq. (6.2.33) the conformal transformations

$$h_{s(s+1)}^{(5)} := g_s^{(5)} \circ g_{s+1}^{(5)-1} = \varrho_{s+1}^{-D} \mathcal{I} \sigma_1 e^{-\varphi_s M_{34}} e^{-\theta_{s+1} M_{12}} e^{-\phi_s M_{23}} e^{-\varphi_{s-1} M_{34}} e^{P_1}, \tag{6.2.36}$$

for $s = 1, \dots, N-4$. We can thus supplement eqs. (6.2.30) by the relations

$$\begin{aligned}
&g_1^{(5)}(x_6) = h_{12}^{(5)}(\vec{e}_1 - \varrho_3 \vec{n}(\theta_3, \phi_2)) \ , \qquad g_1^{(5)}(x_7) = h_{23}^{(5)} \circ h_{12}^{(5)}(\vec{e}_1 - \varrho_4 \vec{n}(\theta_4, \phi_3)) \\
&\dots \\
&g_1^{(5)}(x_N) = h_{(N-5)(N-4)}^{(5)} \circ h_{(N-6)(N-5)}^{(5)} \circ \dots \circ h_{23}^{(5)} \circ h_{12}^{(5)}(\vec{e}_1 - \varrho_{N-3} \vec{n}(\theta_{N-3}, \phi_{N-4})).
\end{aligned}$$

These formulas allow us to compute the location of the insertion points in the conformal frame defined by the first five points $x_1, \dots, x_5$, see eq. (6.2.30), in terms of the geometric parameters $\varrho_r, \theta_r, \phi_s$ and φ_r. The latter possess a very simple relation with the OPE cross ratios that we spelled out in eq. (6.2.35).

6.3 OPE limits and factorization for six-point blocks

In the previous section, we introduced new conformally invariant coordinates for multipoint blocks in $d = 4$ dimensions that were naturally attached to the links and vertices of a comb channel OPE diagram, see e.g. Figure 30 for the example of $N = 6$. To support our choice, we provided a nice geometric interpretation and, closely related, showed that the Gram determinant for $N = 6$ points admits a simple factorized expression, see eq. (6.2.27). Recall that the six-point function in $d \leq 4$ is

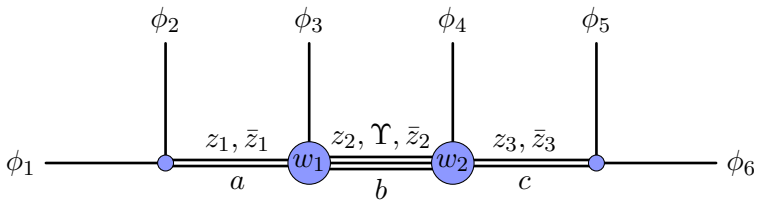

Figure 30: Six-point function with external scalars in the comb channel. The z_i, $\bar{z}_i$, w_i and Υ type of cross ratios are naturally associated with one particular internal leg or vertex of the OPE diagram.

the first correlator for which the new link variable Υ appears. This makes $N = 6$ the decisive case when it comes to testing our cross ratios for comb channel blocks in $d = 4$. The next two sections are devoted to the most important test.

As we have reviewed in subsection 6.2.1, what makes the cross ratios $z, \bar{z}$ for 4-point function so useful is the fact that they provide power series expansions in the OPE limit where $z, \bar{z}$ go to zero. One can deduce this important feature from the expressions of the Casimir differential operators. Here we want to extend this type of analysis to the OPE limits of six-point functions and in particular, to the limit in which the coordinates $z_2, \bar{z}_2$ and Υ attached to the central link of the comb channel diagram are sent to zero. Our goal is to show that in this limit, the six-point comb channel blocks possess a power series expansion, and that the leading term of this expansion factorizes into a product of two functions, one depending on $z_1, \bar{z}_1, w_1$, the other on $z_3, \bar{z}_3, w_2$.

In our approach, we characterize multipoint blocks as eigenfunctions of a complete set of commuting differential operators. For $N = 6$ comb channel blocks, these operators are briefly reviewed in the first subsection. Then we show that the OPE limit we are interested in does indeed correspond to sending $z_2, \bar{z}_2$ and Υ to zero. In the final subsection, we then perform the OPE limit on the differential operators, and show that these operators decouple into two independent sets associated with the left and right side of the diagram. We also provide concrete expressions for the limiting differential operators. These will be further analyzed in the next section.

6.3.1 Preliminaries on comb channel six-point blocks

In this subsection, we shall specify all of our conventions concerning six-point blocks and the differential operators we use to characterize them. As usual, any six-point correlation function of scalar fields can be split into a product of some homogeneous prefactor Ω, which depends on the scaling weights Δ_i and insertion points x_i of the external scalar fields, and a function F of the nine cross ratios,

$$\langle \phi_1 \phi_2 \phi_3 \phi_4 \phi_5 \phi_6 \rangle = \Omega_6^{(\Delta_i)}(X_i)\, F^{(\Delta_i)}\Big(u_1, v_1, u_2, v_2, u_3, v_3, U_1^{(5)}, U_2^{(5)}, U_1^{(6)}\Big)\,. \tag{6.3.1}$$

The prefactor is not unique[4]. Here we shall adopt the following choice:

$$\Omega_6^{(\Delta_i)}(X_i) = \frac{1}{X_{12}^{\frac{\Delta_1+\Delta_2}{2}} X_{34}^{\frac{\Delta_3+\Delta_4}{2}} X_{56}^{\frac{\Delta_5+\Delta_6}{2}}} \left(\frac{X_{23}}{X_{13}}\right)^{\frac{\Delta_1-\Delta_2}{2}} \left(\frac{X_{24}}{X_{23}}\right)^{\frac{\Delta_3}{2}} \left(\frac{X_{35}}{X_{45}}\right)^{\frac{\Delta_4}{2}} \left(\frac{X_{45}}{X_{46}}\right)^{\frac{\Delta_6-\Delta_5}{2}}\,. \tag{6.3.2}$$

[4]This liberty is $\Omega \mapsto \Omega\Theta^{-1}$, $\psi \mapsto \Theta\psi$, where Θ is a non-singular function of the cross ratios. However, after imposing the specific power law asymptotics (6.1.6) for the blocks in the OPE limit at each internal leg, our prefactor is a natural choice.

The function $F^{(\Delta_i)}$ admits a conformal block decomposition of the form

$$F^{(\Delta_i)} = \sum_{\Xi} \Lambda_\Xi \, \psi_\Xi^{(\Delta_i)} \left(u_r, v_r, U_1^{(5)}, U_2^{(5)}, U_1^{(6)}\right) , \quad \textit{where} \quad \Xi = \{\Delta_a, l_a, \Delta_b, l_b, \ell_b, \Delta_c, l_c, \tau_L, \tau_R\} \tag{6.3.3}$$

is a complete set of quantum numbers that includes the weights $\Delta_a, \Delta_b, \Delta_c$ and spins l_a, l_b, ℓ_b, l_c of the internal fields in the comb channel decomposition, as well as two quantum numbers τ_L and τ_R that label the choice of tensor structure at the two central vertices of the diagram in Figure 30. We have also split each summand into a product of OPE coefficients $\Lambda = \Lambda_\Xi$ and a conformal block ψ_Ξ. From now on, we will drop the labels on ψ, unless they are not clear from the context in which ψ appears. The six-point comb channel conformal blocks in eq. (6.3.3) are joint eigenfunctions of nine differential operators, as was shown in [63]. These include three quadratic Casimir operators, which are constructed for each of the three internal links of the OPE diagram as

$$\mathcal{D}^2_{(12)} = (\mathcal{T}_1 + \mathcal{T}_2)_{[AB]} (\mathcal{T}_1 + \mathcal{T}_2)^{[BA]} = \mathcal{D}^2_{(3456)} , \tag{6.3.4}$$

$$\mathcal{D}^2_{(123)} = (\mathcal{T}_1 + \mathcal{T}_2 + \mathcal{T}_3)_{[AB]} (\mathcal{T}_1 + \mathcal{T}_2 + \mathcal{T}_3)^{[BA]} = \mathcal{D}^2_{(456)} , \tag{6.3.5}$$

$$\mathcal{D}^2_{(56)} = (\mathcal{T}_5 + \mathcal{T}_6)_{[AB]} (\mathcal{T}_5 + \mathcal{T}_6)^{[BA]} = \mathcal{D}^2_{(1234)} . \tag{6.3.6}$$

Here we have adopted the standard convention to label the generators $\mathcal{T}_\alpha$ of the conformal algebra through pairs AB with $A, B = 1, \ldots, d+2$ such that $\mathcal{T}_{AB} = -\mathcal{T}_{BA}$. The three quadratic Casimir operators are joined by three quartic ones that take the following form,

$$\mathcal{D}^4_{(12)} = (\mathcal{T}_1 + \mathcal{T}_2)_{[AB]} (\mathcal{T}_1 + \mathcal{T}_2)^{[BC]} (\mathcal{T}_1 + \mathcal{T}_2)_{[CD]} (\mathcal{T}_1 + \mathcal{T}_2)^{[DA]} = \mathcal{D}^4_{(3456)} , \tag{6.3.7}$$

$$\mathcal{D}^4_{(123)} = (\mathcal{T}_1 + \mathcal{T}_2 + \mathcal{T}_3)_{[AB]} (\mathcal{T}_1 + \mathcal{T}_2 + \mathcal{T}_3)^{[BC]} (\mathcal{T}_1 + \mathcal{T}_2 + \mathcal{T}_3)_{[CD]} (\mathcal{T}_1 + \mathcal{T}_2 + \mathcal{T}_3)^{[DA]} = \mathcal{D}^4_{(456)} , \tag{6.3.8}$$

$$\mathcal{D}^4_{(56)} = (\mathcal{T}_5 + \mathcal{T}_6)_{[AB]} (\mathcal{T}_5 + \mathcal{T}_6)^{[BC]} (\mathcal{T}_5 + \mathcal{T}_6)_{[CD]} (\mathcal{T}_5 + \mathcal{T}_6)^{[DA]} = \mathcal{D}^4_{(1234)} . \tag{6.3.9}$$

In addition, there is one third-order Pfaffian operator that is assigned to the central link,

$$\mathcal{D}^3_{(123)} = \epsilon^{ABCDEF} (\mathcal{T}_1 + \mathcal{T}_2 + \mathcal{T}_3)_{[AB]} (\mathcal{T}_1 + \mathcal{T}_2 + \mathcal{T}_3)_{[CD]} (\mathcal{T}_1 + \mathcal{T}_2 + \mathcal{T}_3)_{[EF]} . \tag{6.3.10}$$

To complete the list of differential operators, we finally spell out the two fourth order vertex operators,

$$\mathcal{D}^{4,3}_{L,(12)3} = (\mathcal{T}_1 + \mathcal{T}_2)_{[AB]} (\mathcal{T}_1 + \mathcal{T}_2)^{[BC]} (\mathcal{T}_1 + \mathcal{T}_2)_{[CD]} (\mathcal{T}_3)^{[DA]} , \tag{6.3.11}$$

$$\mathcal{D}^{4,3}_{R,(56)4} = (\mathcal{T}_5 + \mathcal{T}_6)_{[AB]} (\mathcal{T}_5 + \mathcal{T}_6)^{[BC]} (\mathcal{T}_5 + \mathcal{T}_6)_{[CD]} (\mathcal{T}_4)^{[DA]} . \tag{6.3.12}$$

In the following, we will mostly focus on the quadratic Casimir operators. It is rather easy to compute the expression of these Casimir operators in the polynomial cross ratios with the aid of computer algebra software and verify that of all their coefficients are indeed polynomial, as we had claimed in the previous section. The resulting expressions for Casimir operators are actually the simplest we have been able to find, simpler than for any other set of coordinates. On the other hand, the polynomial cross ratios are not well adapted to taking OPE limits, as we will argue in section 6.3.3. Taking the OPE limit will require passing to the new OPE coordinates introduced in the previous section.

6.3.2 The OPE limit from embedding space

Our goal now is to motivate why we expect the sum over descendants in the central intermediate link to be encoded in a power series expansion in the variables $z_2, \bar{z}_2, \Upsilon$. The idea here is to prepare the

intermediate fields through an operator product expansion of either the three fields on the left, or the three fields on the right of the central link. For the left hand side, this amounts to making x_1, x_2 and x_3 collide.
It is a little more tricky to understand how the OPE limit is performed once we pass to the cross ratios. As an example, let us briefly look at the limit in which x_1 and x_2 come together. In the process, we expect to go from a six-point function of scalar fields to a five-point function with one STT insertion and four scalars. While the former has nine cross ratios, the latter has only seven, i.e. we expect that two cross ratios are fixed in the OPE limit. On the other hand, if we apply the limit to the nine polynomial cross ratios we find

$$u_1 \to 0\,, \qquad v_1 \to 1\,, \qquad U_1^{(5)} \to v_2\,, \qquad U_1^{(6)} \to U_2^{(5)}\,. \tag{6.3.13}$$

Of course, this simply means that one needs to consider subleading terms in the limiting behaviour of the cross ratios in order to parameterize the seven cross ratios of the resulting five-point function. But it does illustrate how subtle OPE limits are in the space of cross ratios.

In order to analyze the triple OPE limits of our new cross ratios, it is advantageous to work in embedding space. In the next few paragraphs, we will review how to take double limits into STTs and triple limits into MSTs. When dealing with computations in embedding space, we will work in a Poincaré patch in which the sum $X_{-1} + X_0$ of the first two entries is nonzero. We can then associate the following lightlike vector $X \in \mathbb{R}^{1,d+1}$ with the usual Minkowski metric to any insertion point $x \in \mathbb{R}^d$,

$$X = \left(\frac{1+x^2}{2}, \frac{1-x^2}{2}, x\right), \tag{6.3.14}$$

where we use rescalings to set $X_{-1}+X_0 = 1$. This amounts to working with a particular representative of the projective lightray defined by x. To describe STTs, we additionally need polarization vectors Z that take the form

$$Z = (x \cdot z, -x \cdot z, z)\,, \qquad z = (\frac{1-\zeta^2}{2}, \mathrm{i}\frac{1+\zeta^2}{2}, \zeta) \in \mathbb{C}^d \tag{6.3.15}$$

Here $\zeta \in \mathbb{C}^{d-2}$ describes the physical degrees of freedom of the polarization. These are first mapped to a vector $z \in \mathbb{C}^d$ that satisfies $z^2 = 0$. We think of z as describing a direction in $\mathbb{C}^d$ and use rescalings to set $z_1 + \mathrm{i}z_2 \equiv 1$. In the last step, we complement z into a vector Z with $d+2$ components. As one can easily verify, the vector Z satisfies light cone and transversality conditions of the form $Z^2 = 0 = X \cdot Z$. When dealing with MST fields, finally, we need a second polarization W. It has $d-4$ physical degrees of freedom, which we describe through a null vector $\omega \in \mathbb{C}^{d-2}$, $\omega^2 = 0$, normalized to $\omega_1 + \mathrm{i}\omega_2 \equiv 1$,

$$W = (x \cdot w, -x \cdot w, w)\,, \qquad w = (\zeta \cdot \omega, -i\zeta \cdot \omega, \omega) \in \mathbb{C}^d\,. \tag{6.3.16}$$

By construction, W is lightlike and transversal to both X and Z, i.e. $W^2 = 0 = X \cdot W = Z \cdot W$. With this notation in place, we spell out below the procedure to follow when taking OPE limits in embedding space, for each of the relevant cases.

To discuss the OPE limit of a pair of scalars inserted at x_1 and x_2, we use their embedding space coordinates X_1 and X_2. Projecting to the STTs that are produced by the OPE of those two scalar fields requires us to construct the embedding space coordinate X_{STT} and polarization Z_{STT} of said fields from the coordinates of the two scalars. This can be achieved by first taking a lightcone limit $X_1 \cdot X_2 = 0$. Once the lightcone condition is satisfied, we introduce

$$X_{\mathrm{STT}} = \frac{1}{2}(X_1 + X_2)\,, \qquad Z_{\mathrm{STT}} = \frac{1}{(X_2 - X_1)_1 + \mathrm{i}(X_2 - X_1)_2}(X_2 - X_1)\,. \tag{6.3.17}$$

Note that the prefactor in the definition of Z_{STT} ensures that the polarization is normalized such that $z_1 + \mathrm{i}z_2 = 1$. Thanks to the condition $X_1 \cdot X_2 = 0$, the two vectors we have built from X_1 and X_2 satisfy the usual relations for STT variables, namely $X_{\text{STT}}^2 = 0 = Z_{\text{STT}}^2$ and $X_{\text{STT}} \cdot Z_{\text{STT}} = 0$. So far, we have only assumed that the two insertion points of scalar fields are light-like separated, so that $X_1 \cdot X_2 = 0$. To complete the OPE limit, we can now set $X_2 = X_1 + \epsilon\, Z_{\text{STT}}$ and compute the $\epsilon \to 0$ limit.

In order to address the triple OPE limit, it remains to discuss the operator product of an STT with a scalar field. Let us consider an STT with associated coordinates X_1, Z_1 and a scalar at position X_2. If we want to project to the exchange of an MST_2 produced by their OPE, we need to construct embedding space coordinates X_{MST_2} and polarizations $Z_{\text{MST}_2}, W_{\text{MST}_2}$ starting from the degrees of freedom of the two initial fields. To this end, we will follow a nested procedure with two limits of the type described above. As before, we start by taking the lightcone limit $X_1 \cdot X_2 = 0$ and construct the expressions

$$X_{\text{MST}_2} = \frac{1}{2}(X_1 + X_2)\,, \qquad Z' = \frac{1}{(X_2 - X_1)_1 + \mathrm{i}(X_2 - X_1)_2}(X_2 - X_1)\,. \tag{6.3.18}$$

From here, one can take $X_2 = X_1 + \epsilon\, Z'$ and compute the $\epsilon \to 0$ limit. This leads temporarily to something described by one coordinate X_{MST_2} and two auxiliary vectors of STT type Z_1 and Z'. Finally, to make this set suitable to describe an MST_2, we take the lightcone limit $Z' \cdot Z_1 = X_2 \cdot Z_1 = 0$ and construct

$$Z_{\text{MST}_2} = \frac{1}{2}(Z' + Z_1)\,, \qquad W_{\text{MST}_2} = \frac{1}{(Z' - Z_1)_3 + \mathrm{i}(Z' - Z_1)_4}(Z' - Z_1)\,. \tag{6.3.19}$$

These two vectors indeed satisfy the appropriate conditions for polarizations associated with an MST_2 and the normalization matches that of the introduction. At this point, we can complete the OPE limit by writing $Z' = Z + \epsilon W$ and taking $\epsilon \to 0$.

Let us now come back to the cross ratios and analyze their behaviour when in the OPE limit. This is particularly simple for the OPE of two scalar fields ϕ_1 and ϕ_2, in which case one finds that $\bar{z}_1$ and z_1 both tend to zero while all other cross ratios remain finite. A similar statement holds for the OPE limit of the two scalar field ϕ_5 and ϕ_6. It is less straightforward to understand the leading behaviour for exchanges of an MST_2 at the internal leg in the middle. To study this, let us start by taking the OPE limit on the left side of the OPE diagram and reducing to a five-point function of fields $\mathcal{O}_a$, $\phi_3, \ldots, \phi_6$. Here, the OPE limit for leg b can simply be cast as a limit for one STT with coordinates X_a, Z_a and one scalar with coordinate X_3, of the form described in section 6.3.2. Following that procedure, it is possible to check that

$$w_1 \xrightarrow{((12)3)\text{ OPE}} \begin{cases} 1 & \text{if} \quad (X_a \wedge X_3) \cdot (X_4 \wedge X_5) > 0\,, \\ 0 & \text{else}\,, \end{cases} \tag{6.3.20}$$

while the cross ratios z_2, $\bar{z}_2$ and Υ all tend to zero. On the other hand, if we were to take the limit from the right side in the ((65)4) order, we would end up with

$$w_2 \xrightarrow{((65)4)\text{ OPE}} \begin{cases} 1 & \text{if} \quad (X_2 \wedge X_3) \cdot (X_4 \wedge X_c) > 0\,, \\ 0 & \text{else}\,, \end{cases} \tag{6.3.21}$$

while, once again, $z_2, \bar{z}_2$ and Υ vanish in the limit. This instructs us on the fact that the relevant regime to study the projection on exchanges of specific operators in the leg b of the six-point function

is the part that is common to both OPE limits taken above, namely $(z_2, \bar{z}_2, \Upsilon) \to 0$. Taking only these three cross ratios to zero, while leaving all others finite, corresponds to a regime in which the two triples (x_1, x_2, x_3) and (x_4, x_5, x_6) can each be enclosed in a sphere of radius r which is parametrically smaller than the distance R between any two points of the two triples. In this limiting regime, we need the six remaining cross ratios to parameterize the configuration of points in the two small spheres, see appendix 6.B for some more details.

6.3.3 OPE limits of six-point blocks

Our main goal in this subsection is to analyze the asymptotics of the six-point comb channel blocks in the limit where we send $\bar{z}_2, z_2$ and Υ to zero. We will first study the limiting behaviour of the Casimir equation for $\mathcal{D}^2_{(123)}$ under the assumption that eigenfunctions obey a leading power law behaviour

$$\Psi(z_s, \bar{z}_s, w_r, \Upsilon) \sim \bar{z}_2^{p_1} z_2^{p_2} \Upsilon^{p_3} \left(\psi(z_1, \bar{z}_1, z_3, \bar{z}_3, w_1, w_2) + O(z_2, \bar{z}_2, \Upsilon)\right) \tag{6.3.22}$$

in the three variables for the middle leg. Similarly to exchanges of STTs, see our review in subsection 6.3.1, the precise powers depend on the order in which the limits are taken. Taking the limit $\Upsilon \to 0$ first turns out to be inconsistent, as it produces divergences in the Casimir equation. Instead, we first take the $\bar{z}_2 \to 0$ limit followed by the one in z_2, in direct analogy to the $N = 4, 5$-point functions. Alternatively, we could also send z_2 to zero first, but this is a mere issue of convention given the symmetry of the cross ratios under $z \leftrightarrow \bar{z}$ and $w \leftrightarrow (1 - w)$. Once this limit is performed, the order of the remaining two limits is irrelevant and one finds

$$\bar{z}_2^{-p_1} z_2^{-p_2} \Upsilon^{-p_3} \mathcal{D}^2_{(123)} \bar{z}_2^{p_1} z_2^{p_2} \Upsilon^{p_3} \underset{z_2, \Upsilon \to 0}{\overset{\bar{z}_2 \to 0}{\longrightarrow}} -2\left(d\, p_1 - p_1^2 - p_2^2 + (p_3 + 1)(p_2 - p_1) - p_3(p_3 - 1)\right) + \ldots, \tag{6.3.23}$$

where we indicated the order of limits by placing the first one above the arrow and the remaining two below. As before, the $\ldots$ correspond to higher order terms in $z_2, \bar{z}_2$ and Υ. This behaviour, in which the leading term of the second order Casimir differential operator for the central link is a constant, was what we were aiming for when we introduced the OPE coordinates.
Of course, the constant term must be equal to the eigenvalue of the quadratic Casimir element in the MST_2 representation of the exchanged intermediate field. The latter is related to the weight and spin labels of said fields as

$$C^2(\Delta_b, l_b, \ell_b) = \Delta_b(\Delta_b - d) + l_b(l_b + d - 2) + \ell_b(\ell_b + d - 4)\,. \tag{6.3.24}$$

Equating this with eq. (6.3.23), we can only match the coefficients in front of the dimension d provided that

$$p_1 = \frac{\Delta_b - l_b - \ell_b}{2}\,.$$

Then to ensure that Ψ is single-valued in the $(z_2, \bar{z}_2)$ plane, we must set the exponent p_2 of the variable z_2 to be

$$p_2 = \frac{\Delta_b + l_b + \ell_b}{2}\,. \tag{6.3.25}$$

This also ensures that for $\ell_b = 0$, one recovers the usual leading behaviour for intermediate STT exchange, see subsection 6.3.1. Requiring finally a full match with the Casimir eigenvalue leaves us with two possible solutions for the leading behaviour in Υ

$$p_3 = \ell_b \qquad \text{or} \qquad p_3 = l_b + 1\,. \tag{6.3.26}$$

This freedom, which cannot be eliminated by considering higher Casimir differential operators, is associated with the invariance of the Casimir elements under the action of Weyl transformations. Let us note that the two possible solutions correspond to the two possible behaviours in $(1-v)$ for the four-point s-channel OPE that distinguish between Euclidean and Minkowski conformal blocks [142],

$$(1-v)^{l}\,, \qquad \text{or} \qquad (1-v)^{1-\Delta}\,, \tag{6.3.27}$$

modulo an exchange of $-\Delta \leftrightarrow l$ and $l \leftrightarrow \ell$. Following the interpretation of Υ as a degree of freedom associated with MST_2 fields, the first solution with $p_3 = \ell_b$ is the most natural. This choice will later be validated when we compare the limiting behaviour of the remaining non-trivial Casimir operators to those of spinning four-point blocks.

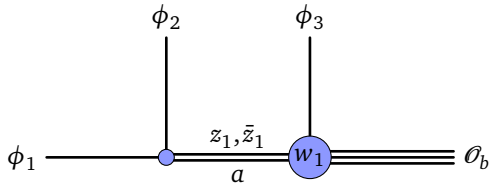

Figure 31: One of the four-point functions obtained in the OPE limit for the middle leg in a six-point function in comb channel. The rightmost field is a Mixed-Symmetry Tensor with two spin indices and the exchanged field is a Symmetric Traceless Tensor.

Now let us address the second part of our claim. As stated in the introduction, we want to show that expansion of the conformal block (6.3.22) takes the more specific form

$$\Psi(z_r, \bar{z}_r, w_1, w_2, \Upsilon) \overset{\bar{z}_2, z_2, \Upsilon \to 0}{\sim} \bar{z}_2^{\frac{\Delta_b - l_b - \ell_b}{2}} z_2^{\frac{\Delta_b + l_b + \ell_b}{2}} \Upsilon^{\ell_b} \left(\psi_a(z_1, \bar{z}_1, w_1)\psi_c(z_3, \bar{z}_3, w_2) + \dots\right)\,, \tag{6.3.28}$$

in which the leading term splits into a product of two functions of three variables each. Furthermore, we want to prove that each of these two factors is a spinning four-point conformal block, one corresponding to the left side of the OPE diagram, see Figure 31, the other for the right. The proof is a nice application of Gaudin integrability, i.e. our characterization of multipoint conformal blocks through differential equations. Having seen that the differential operators $\mathcal{D}^{p}_{(123)}, p = 2, 3, 4$, simply act as multiplication with the value of the associated Casimir elements, we now need to study the limiting behaviour of the remaining six differential operators. These include two quadratic and two fourth order Casimir operators, as well as two vertex operators. We will focus our discussion on the quadratic Casimir operators. Crucially, we find that the two quadratic Casimirs $\mathcal{D}^2_{(12)}$ and $\mathcal{D}^2_{(56)}$ decouple completely upon taking the OPE limit in the central link,

$$\mathcal{D}^2_{(12)} \xrightarrow{b\,\text{OPE}} \mathcal{D}^2_a(z_1, \bar{z}_1, w_1)\,, \qquad \mathcal{D}^2_{(123)} \xrightarrow{b\,\text{OPE}} C^2(\Delta_b, l_b, \ell_b)\,, \qquad \mathcal{D}^2_{(56)} \xrightarrow{b\,\text{OPE}} \mathcal{D}^2_c(z_3, \bar{z}_3, w_2)\,. \tag{6.3.29}$$

Here, b OPE denotes the limit in which we take $\bar{z}_2$ to zero followed by z_2 and Υ, as discussed before.

It suffices to spell out an expression for $\mathcal{D}_a^2$, which takes the relatively simple form

$$\begin{aligned}\mathcal{D}_a^2 = &-2\left(z_1-1\right)z_1^2\partial_{z_1}^2 - 2\left(\bar{z}_1-1\right)\bar{z}_1^2\partial_{\bar{z}_1}^2 + \frac{4\left(w_1-1\right)w_1 z_1\bar{z}_1\left(w_1\left(z_1-\bar{z}_1\right)+\bar{z}_1-1\right)}{\left(z_1-\bar{z}_1\right)^2}\partial_{w_1}^2 \\ &+2\left(1-w_1\right)w_1 z_1^2\partial_{z_1}\partial_{w_1} - 2\left(1-w_1\right)w_1\bar{z}_1^2\partial_{\bar{z}_1}\partial_{w_1} \\ &+2\left[z_1^2\left(a+b-1+\left(w_1-\frac{1}{2}\right)l_b\right)+\frac{z_1\bar{z}_1}{z_1-\bar{z}_1}(1-z_1)(d-2)\right]\partial_{z_1} \\ &+2\left[\bar{z}_1^2\left(a+b-1-\left(w_1-\frac{1}{2}\right)l_b\right)-\frac{z_1\bar{z}_1}{z_1-\bar{z}_1}\left(1-\bar{z}_1\right)(d-2)\right]\partial_{\bar{z}_1} \\ &+2\Bigg[a\left(w_1-1\right)w_1\left(z_1-\bar{z}_1\right)-\frac{2\left(w_1-1\right)w_1 z_1\bar{z}_1\left(l_b-1\right)}{z_1-\bar{z}_1} \\ &\qquad+\frac{z_1\bar{z}_1(d-2)\left(w_1\left(\bar{z}_1+z_1-2\right)-\bar{z}_1+1\right)}{\left(z_1-\bar{z}_1\right)^2}\Bigg]\partial_{w_1} \\ &-a\left[\left(2w_1-1\right)\left(z_1-\bar{z}_1\right)l_b+2b\left(\bar{z}_1+z_1\right)\right]-\frac{z_1\bar{z}_1\left(w_1\left(z_1-\bar{z}_1\right)+\bar{z}_1-1\right)}{\left(w_1-1\right)w_1\left(z_1-\bar{z}_1\right)^2}\ell_b\left(\ell_b+d-4\right)\ ,\end{aligned} \tag{6.3.30}$$

where the constants a, b are determined by the conformal weights of the external scalars and Δ_b through $2a = \Delta_2 - \Delta_1$ and $2b = \Delta_3 - \Delta_b$. Then the expression for $\mathcal{D}_c^2$ is the same, but with variables $z_3, \bar{z}_3, w_2$ instead of $z_1, \bar{z}_2, w_1$, along with the parameters $2a = \Delta_4 - \Delta_b$ and $2b = \Delta_3 - \Delta_4$. We have also analyzed the fourth order Casimir operators, as well as the vertex operators, and have found that they display the same decoupling. We refrain from spelling out explicit expressions here.
For the time being, all we can do with the explicit expression for $\mathcal{D}_a^2$ is appreciate that the formula looks relatively simple. In the next section, we will analyze it further and show that it can be mapped to the quadratic Casimir operator for a spinning four-point function with three scalar and one MST_2 external field. Let us note that the blocks for such spinning four-point functions indeed depend on three variables, the two 4-point cross ratios and one additional variable associated with the choice of tensor structure at the scalar-STT-MST_2 vertex. In particular, our analysis implies that conformal partial waves in this limit are polynomials of a bounded degree in a variable closely related to w_1, given in [65, eq. (4.40)], a fact that is already non-trivial from the mere definition of OPE cross ratios.

Before concluding this section, we briefly want to discuss a second OPE limit that we have also worked out explicitly. It concerns a setup where two OPE limits are taken on the links a and c, leaving a four-point function of two STT fields and two scalars, see Figure 32. We perform this limit by first sending $\bar{z}_1$ and $\bar{z}_2$ to zero before taking the limits $z_1, z_2 \to 0$. In this limit, five of the nine cross ratios survive and one finds

$$\psi(z_1,\bar{z}_1,z_2,\bar{z}_2,z_3,\bar{z}_3,w_1,w_2,\Upsilon) \overset{\bar{z}_1,z_1,\bar{z}_3,z_3\to 0}{\sim} \bar{z}_1^{\frac{\Delta_a-l_a}{2}} z_1^{\frac{\Delta_a+l_a}{2}} \bar{z}_3^{\frac{\Delta_c-l_c}{2}} z_3^{\frac{\Delta_c+l_c}{2}} \left(\psi_b(z_2,\bar{z}_2,w_1,w_2,\Upsilon)+\dots\right). \tag{6.3.31}$$

The derivation of this limit follows the same steps we carried out in the discussion of the OPE limit on the link b above. In particular, upon taking the combined a and c OPE limit, one can show that the second order Casimir operators behave as

$$\mathcal{D}^2_{(12)}, \mathcal{D}^2_{(56)} \xrightarrow{(a+c)\,\text{OPE}} C^2(\Delta_a, l_c), C^2(\Delta_c, l_c)\,, \qquad \mathcal{D}^2_{(123)} \xrightarrow{(a+c)\,\text{OPE}} \mathcal{D}_b^2(z_2,\bar{z}_2,w_1,w_2,\Upsilon)\,. \tag{6.3.32}$$

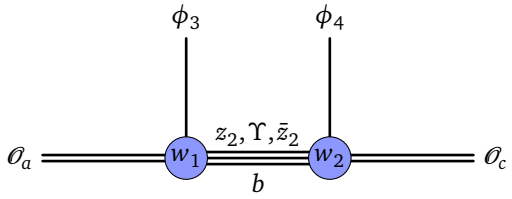

Figure 32: Four-point function obtained from OPE limit on legs a and c of a six-point function in comb channel. Fields at legs a and c are Symmetric Traceless Tensors, while the exchanged field is a Mixed-Symmetry Tensor with two spin indices.

The second order Casimir element for the link b reduces to an operator in the five remaining variables that can be worked out explicitly, even though the expression is a bit longer than in our discussion above. It can be found in the Mathematica notebook we include with this publication.

6.A Construction of a six-point conformal frame

In this section, we construct a conformal frame for the six-point function by appending x_6 to the conformal frame of the (12345) five-point function, namely:

$$x_1 = \varrho_1 \vec{n}(\theta_1, 0, 0), \quad x_2 = 0, \quad x_3 = \infty, \quad x_4 = \vec{e}_1, \quad x_5 = \vec{e}_1 - \varrho_2 \vec{n}(\theta_2, \phi_1, 0), \tag{6.A.1}$$

where we parameterize unit vectors in S^4 as

$$\vec{n}(\theta, \phi, \varphi) := \cos\theta\, \vec{e}_1 + \sin\theta \big\{ \cos\phi\, \vec{e}_2 + \sin\phi\, (\cos\varphi\, \vec{e}_3 + \sin\varphi\, \vec{e}_4) \big\} = e^{\varphi M_{34}} e^{\phi M_{23}} e^{\theta M_{12}} \vec{e}_1. \tag{6.A.2}$$

It will also be useful to define the rotation matrices

$$R(\theta, \phi, \varphi) := e^{-\theta M_{12}} e^{-\phi M_{23}} e^{-\varphi M_{31}} \Longrightarrow \vec{n}(\theta, \phi, \varphi) = R(\theta, \phi, \varphi)^{-1} \vec{e}_1. \tag{6.A.3}$$

Finally, we parameterize cross ratios as in (6.2.29),

$$z_r := \varrho_r e^{\mathrm{i}\theta_r}, \quad \bar{z}_r := \varrho_r e^{-\mathrm{i}\theta_r}, \quad w_s := \sin^2 \frac{\phi_s}{2}, \quad \Upsilon := \pm \mathrm{i} \frac{\cos\varphi}{\sin\theta_2}. \tag{6.A.4}$$

To understand how x_6 depends on the cross ratios, we compute a distinguished vector in this frame:

$$\psi_{56} := (x_{45}^{-1} - x_{46}^{-1})^{-1} \in \mathbb{R}^4_{1234}, \tag{6.A.5}$$

where $x^{-1} := x/x^2$ denotes the image of the vector x under conformal inversion. Note that we implicitly used the residual $\mathrm{SO}(d-4)$ symmetry preserving (6.A.1) to fix a gauge where $x_6 \in \mathrm{Span}(\vec{e}_1, \vec{e}_2, \vec{e}_3, \vec{e}_4)$. In Euclidean signature, we can parameterize the latter by its norm and its unit vector on the S^4, which we write as

$$\psi_{56} = |\psi_{56}|\, \hat{\psi}_{56}, \quad |\psi_{56}| = \varrho_2 \varrho_3^{-1}, \tag{6.A.6}$$

Then the unit vector $\hat{\psi}_{56}$ is determined by three equations:

$$\hat{\psi}_{56} \cdot \hat{x}_{45} = \frac{1 + u_2 - v_2}{2\varrho_2}, \quad \hat{\psi}_{56} \cdot x_4 = \frac{\mathcal{U}_2^{(5)}}{2\varrho_2\varrho_3}, \quad \hat{\psi}_{56} \cdot \hat{x}_1 = \frac{\mathcal{U}_1^{(6)}}{2\varrho_1\varrho_2\varrho_3}, \tag{6.A.7}$$

where the $\mathcal{U}_r^{(m)}$ are polynomials in the polynomial cross ratios:

$$\mathcal{U}_r^{(5)} := 1 - v_r - v_{r+1} + U_r^{(5)}, \quad \mathcal{U}_1^{(6)} := (1-v_1)(1-v_3) - v_2 + U_1^{(5)} + U_2^{(5)} - U_1^{(6)}. \tag{6.A.8}$$

Using the change of variables (6.2.25) and (6.2.26), we can express the scalar products of (6.A.7) in terms of the angle cross ratios $(\theta_s, \phi_r, \varphi)$:

$$\frac{\mathcal{U}_1^{(5)}}{2\varrho_2\varrho_3} = \cos\theta_2\cos\theta_3 + \sin\theta_2\sin\theta_3\cos\phi_2 \tag{6.A.9}$$

$$\begin{aligned}\frac{\mathcal{U}_1^{(6)}}{2\varrho_1\varrho_2\varrho_3} &= \cos\theta_1\cos\theta_2\cos\theta_3 + \cos\theta_1\sin\theta_2\cos\phi_2\sin\theta_3 + \sin\theta_1\sin\theta_2\cos\phi_1\cos\theta_3 \\ &\quad - \sin\theta_1\left(\cos\theta_2\cos\phi_1\cos\phi_2 + \sin\phi_1\sin\phi_2\cos\varphi\right)\sin\theta_3.\end{aligned} \tag{6.A.10}$$

Given that $x_4 = \vec{e}_1$, $\hat{x}_1 \in \mathrm{Span}(\vec{e}_1, \vec{e}_2)$, $\hat{x}_{45} \in \mathrm{Span}(\vec{e}_1, \vec{e}_2, \vec{e}_3)$, we can recursively compute the components of $\hat{\psi}_{56}$ as

$$\begin{aligned}&\hat{\psi}_{56}\cdot x_4 = \hat{\psi}_{56}\cdot\vec{e}_1 \Longrightarrow \hat{\psi}_{56}^1, \\ &\hat{\psi}_{56}\cdot\hat{x}_1 = \hat{\psi}_{56}\cdot\vec{n}(\theta_1,0,0) \Longrightarrow \hat{\psi}_{56}^2, \\ &\hat{\psi}_{56}\cdot\hat{x}_{45} = \hat{\psi}_{56}\cdot\vec{n}(\theta_2,\phi_1,0) \Longrightarrow \pm\hat{\psi}_{56}^3, \\ &(\hat{\psi}_{56}^1)^2 + (\hat{\psi}_{56}^2)^2 + (\hat{\psi}_{56}^3)^2 + (\hat{\psi}_{56}^4)^2 = 1 \Longrightarrow \pm\hat{\psi}_{56}^4.\end{aligned}$$

There is a sign indeterminacy in the third step coming from the convention for $\Upsilon \propto \pm\cos\varphi$, and there is also a sign indeterminacy in the last step coming from the two solutions to the quadratic equation. We compute the solution to each of these equations and find

$$\hat{\psi}_{56} = R(\theta_2,\phi_1,0)^{-1}\vec{n}(-\theta_3,\pm\phi_2,\pm\varphi) \overset{\text{choice}}{=} R(\theta_2,\phi_1,0)^{-1}\vec{n}(-\theta_3,\phi_2,\varphi). \tag{6.A.11}$$

Now, we can obtain x_6 in the conformal frame by a conformal transformation of ψ_{56},

$$\psi_{56} = (x_{64}^{-1} - x_{54}^{-1})^{-1} = e^{-x_{45}^{-1}\cdot K} e^{x_4\cdot P}\cdot x_6 = e^{-\varrho_2^{-1}\vec{n}(\theta_2,\phi_1,0)\cdot K} e^{P_1} x_6. \tag{6.A.12}$$

After simplifying and inverting the conformal transformation in (6.A.12), we then obtain

$$x_6 = e^{-P_1}\varrho_2^{-D} R(\theta_2,\phi_1,0)^{-1}\mathcal{I}\, e^{P_1}\cdot\varrho_3 n(-\theta_3,\phi_2,\varphi), \tag{6.A.13}$$

where $\mathcal{I} : x \mapsto x^{-1}$ is conformal inversion. To better understand the meaning of these conformal transformations, let's take a closer look at the conformal group element

$$g \equiv g(\varrho_2,\theta_2,\phi_1) = e^{-P_1}\varrho_2^{-D} R(\theta_2,\phi_1,0)^{-1}\mathcal{I}\, e^{P_1}. \tag{6.A.14}$$

Its inverse acts as

$$g^{-1} : x \mapsto \varrho_2^{-1} R(\theta_2,\phi_1)(x-\vec{e}_1)^{-1} + \vec{e}_1, \tag{6.A.15}$$

such that when g^{-1} acts on the points of the original conformal frame, the images are given by

$$g^{-1}(x_6) = \varrho_3\vec{n}(-\theta_3,\phi_2,\varphi), \quad g^{-1}(x_5) = 0, \quad g^{-1}(x_4) = \infty, \quad g^{-1}(x_3) = \vec{e}_1. \tag{6.A.16}$$

This suggests a general method to characterize the comb channel conformal frame of $N > 6$ points in $d = 4$, which depends on the cross ratios $(\varrho_r, \theta_r)_{r=1}^{N-3}$, $(\phi_s)_{s=1}^{N-4}$ and $(\varphi_r)_{r=2}^{N-4}$ defined in (6.2.35). First, define the conformal transformation

$$h^{-1}(\varrho_2, \theta_2, \phi_1, 0, \varphi_2) := e^{-\varphi_2 M_{34}} \sigma_1 \, e^{P_1} g^{-1}(\varrho_2, \theta_2, \phi_1) = \varrho_2^{-D} \mathcal{I} \sigma_1 e^{-\varphi_2 M_{zt}} R(\theta_2, \phi_1) e^{P_1}, \tag{6.A.17}$$

where $\sigma_1 : (x^1, x^2, x^3, x^4) \mapsto (-x^1, x^2, x^3, x^4)$ is a reflection along the hyperplane orthogonal to $\vec{e}_1$. Its action on a point is given by

$$h^{-1}(x) = \varrho_2 \sigma_1 e^{-\varphi_2 M_{34}} R(\theta_2, \phi_1)(x - \vec{e}_1)^{-1}. \tag{6.A.18}$$

From the previous discussion, we determined that this conformal transformation acts on the six-point conformal frame as follows:

$$h^{-1}(x_2) = \varrho_2 \vec{n}(\theta_2, 0, 0), \;\; h^{-1}(x_3) = 0, \;\; h^{-1}(x_4) = \infty, \;\; h^{-1}(x_5) = \vec{e}_1, \;\; h^{-1}(x_6) = \vec{e}_1 - \varrho_3 \vec{n}(\theta_3, \phi_2, 0).$$

Thus, h^{-1} shifts the framing from the constraints (6.A.1) on x_i, to the same constraints on x_{i+1}, $i = 1, \ldots, 5$. We can similarly express the seventh point as

$$h^{-1}(x_7) = h' \left(\vec{e}_1 - \varrho_4 \vec{n}(\theta_4, \phi_3, 0) \right), \tag{6.A.19}$$

where $h' \equiv h(\varrho_3, \theta_3, \phi_2, \varphi_2, \varphi_3)$ is now uniquely defined by

$$h'^{-1}(0) = \varrho_3 \vec{n}(\theta_3, 0, 0), \quad h'^{-1}(\infty) = 0, \quad h'^{-1}(e_x) = \infty,$$

$$h'^{-1}(h^{-1}(x_6)) = \vec{e}_1, \quad h'^{-1}(h^{-1}(x_7)) = \vec{e}_1 - \varrho_4 \vec{n}(\theta_4, \phi_3, 0).$$

A quick comparison with the action of h^{-1} on $x_2, \ldots, x_6$ implies that

$$h'^{-1} := \varrho_3^{-D} \mathcal{I} \sigma_1 e^{-\varphi_3 M_{34}} R(\theta_3, \phi_2, \varphi_2)^{-1} e^{P_1}. \tag{6.A.20}$$

We can then iterate this procedure until reaching x_N. More specifically, the frame will be given by

$$\begin{aligned}
x_1 &= \varrho_1 \vec{n}(\theta_1, 0, 0), \\
x_2 &= 0, \\
x_3 &= \infty, \\
x_4 &= \vec{e}_1, \\
x_5 &= \vec{e}_1 - \varrho_2 \vec{n}(\theta_2, \phi_1, 0), \\
x_6 &= h(\varrho_2, \theta_2, \phi_1, \varphi_1, 0)(\vec{e}_1 - \varrho_3 \vec{n}(\theta_3, \phi_2, 0)) \\
x_7 &= h(\varrho_2, \theta_2, \phi_1, \varphi_1, 0) \circ h(\varrho_3, \theta_3, \phi_2, \varphi_1, \varphi_2)(\vec{e}_1 - \varrho_4 \vec{n}(\theta_4, \phi_3, 0)), \\
&\cdots\cdots\cdots \\
x_N &= h(\varrho_2, \theta_2, \phi_1, \varphi_1, 0) \circ \prod_{r=3}^{N-4} h(\varrho_r, \theta_r, \phi_{r-1}, \varphi_{r-1}, \varphi_r) \left(\vec{e}_1 - \varrho_N \vec{n}(\theta_N, \phi_{N-1}, \varphi_{N-2}, 0) \right),
\end{aligned}$$

where

$$h^{-1}(\varrho_r, \theta_r, \phi_{r-1}, \varphi_{r-1}, \varphi_r) := \varrho_r^{-D} \mathcal{I} \sigma_1 e^{-\varphi_r M_{34}} R(\theta_r, \phi_{r-1}, \varphi_{r-1})^{-1} e^{P_1}. \tag{6.A.21}$$

The action of this conformal group element on points is then given by

$$h^{-1}(\varrho_r, \theta_r, \phi_{r-1}, \varphi_{r-1}, \varphi_r) : x \mapsto \varrho_r \sigma_1 e^{-\varphi_r M_{34}} R(\theta_r, \phi_{r-1}, \varphi_{r-1})^{-1} (x - \vec{e}_1)^{-1}. \tag{6.A.22}$$

6.B Middle leg OPE limit in embedding space

In the six-point function, the limit $\bar{z}_2 \to 0$ at the middle leg b can be lifted to embedding space as

$$X_{45}, X_{46}, X_{56} \to 0, \quad \frac{X_{45}}{X_{46}}, \frac{X_{56}}{X_{46}} = \text{finite}. \tag{6.B.1}$$

In other words, all distances between the three points x_4, x_5 and x_6 vanish at the same rate in spacetime. By first quantizing around x_6 and then mapping to the cylinder, a triplet satisfying (6.B.1) is mapped to past timelike infinity. The infinite distance between (x_4, x_5, x_6) and (x_1, x_2, x_3) in this limit factorizes the six-point function into a product of two four-point functions, in a manner reminiscent of the cluster decomposition principle.
To compute this limit in embedding space, it will be useful to define the vector

$$Y_5 := (X_4 - X_5) - \frac{X_{45}}{X_{46}}(X_4 - X_6). \tag{6.B.2}$$

In particular, $X_4 \wedge Y_5$ is a homogeneous tensor in both X_4 and X_5. For a spacetime interpretation of this vectors, recall the reduction $X, Z \mapsto x, z$ of a STT to the Poincare patch:

$$X_x = \left(\frac{1+x^2}{2}, \frac{1-x^2}{2}, x\right), \quad Z_{x,z} = (x \cdot z, -x \cdot z, z). \tag{6.B.3}$$

If we put all embedding space vectors in this patch, $X_i := X_{x_i}$, we obtain

$$Y_5 = \frac{x_{56}^2}{x_{46}^2} Z_{x_4, \psi_{56}}, \quad \psi_{56} := (x_{45}^{-1} - x_{46}^{-1})^{-1}. \tag{6.B.4}$$

Note also that $Y_5^2 = -2\frac{X_{45}X_{56}}{X_{46}} \to 0$ in the limit (6.B.1). We now define the full b OPE limit $z_2, \Upsilon \to 0$ in embedding space as

$$X_5 = X_4 + \epsilon Z_4, \quad Y_5 = \epsilon\epsilon' W_4, \quad \epsilon, \epsilon' \to 0. \tag{6.B.5}$$

where Z_4 and W_4 are MST_2 polarization vectors for X_4. To make the connection with the prescription of section 6.3.2 more explicit, we can rewrite the second equation in (6.B.5) as

$$\epsilon' W_4 = Z_4' - Z_4, \quad \epsilon Z_4' := \frac{X_{45}}{X_{46}}(X_6 - X_4). \tag{6.B.6}$$

We thereby obtain the same prescription as eq. (6.3.19) up to projective equivalence, with a rescaling of Z_4' outside of the conventional Poincare patch to simplify computations. Note that the permutation $(4,5,6) \leftrightarrow (3,2,1)$ leads to an identical parameterization of the b OPE limit. Thus, to make expressions more symmetric, we also define

$$Y_2 := Y_5|_{(4,5,6)\leftrightarrow(3,2,1)}. \tag{6.B.7}$$

Now, to understand how Υ encodes MST_2 transfer along the internal leg b, we would like to compute the b OPE limit of

$$\frac{X_{34}(X_3 \wedge X_2 \wedge Y_2) \cdot (X_4 \wedge X_5 \wedge Y_5)}{X_{24}^2 X_{35}^2} = \mathcal{U}_1^{(5)}\mathcal{U}_2^{(5)} - (1 - v_2)\mathcal{U}_1^{(6)}, \tag{6.B.8}$$

where $\mathcal{U}_r^{(m)}$ are the same functions of the polynomial cross-ratios defined in (6.A.8). To relate them to the left hand side of (6.B.8), we expressed them in embedding space as follows:

$$\mathcal{U}_1^{(5)} = \frac{(X_3 \wedge Y_2) \cdot (X_4 \wedge X_5)}{X_{24}X_{35}}, \quad \mathcal{U}_2^{(5)} = \frac{(X_3 \wedge X_2) \cdot (X_4 \wedge Y_5)}{X_{24}X_{35}}, \quad \mathcal{U}_1^{(6)} = \frac{(X_3 \wedge Y_2) \cdot (X_4 \wedge Y_5)}{X_{24}X_{35}}. \tag{6.B.9}$$

On the left hand side of (6.B.8), the OPE limit (6.B.5) is simple to compute:

$$\text{LHS} = \epsilon^2\epsilon' \frac{X_{23}U_{4,123}}{X_{13}X_{24}^2X_{34}} + \mathcal{O}(\epsilon^3\epsilon'), \quad U_{4,123} := (X_4 \wedge Z_4 \wedge W_4)_{ABC}X_1^A X_2^B X_3^C.$$

Note that $U_{4,123}$ is the unique independent MST_2 tensor structure of the four-point function of three scalars and one MST_2 field. On the other hand, the right hand side of (6.B.8) can be written in cross ratio space using

$$\mathcal{U}_1^{(5)} = z_1'z_2 + \bar{z}_1'\bar{z}_2, \tag{6.B.10}$$

$$\mathcal{U}_2^{(5)} = z_2z_3' + \bar{z}_2\bar{z}_3', \tag{6.B.11}$$

$$\mathcal{U}_1^{(6)} = z_1'z_2z_3' + \bar{z}_1'\bar{z}_2\bar{z}_3' - \left[(z_1-\bar{z}_1)\sqrt{w_1(1-w_1)}\right](z_2-\bar{z}_2)\Upsilon\left[(z_3-\bar{z}_3)\sqrt{w_2(1-w_2)}\right], \tag{6.B.12}$$

where we defined

$$z_1' := w_1z_1 + (1-w_1)\bar{z}_1, \quad \bar{z}_1' := w_1\bar{z}_1 + (1-w_1)z_1, \tag{6.B.13}$$

$$z_3' := w_2z_3 + (1-w_2)\bar{z}_3, \quad \bar{z}_3' := w_2\bar{z}_3 + (1-w_2)z_3. \tag{6.B.14}$$

Taking $\bar{z}_2 = 0$, we then find

$$\mathcal{U}_1^{(5)}\mathcal{U}_2^{(5)} - (1-v_2)\mathcal{U}_1^{(6)} = \frac{1}{4}\left[(z_1-\bar{z}_1)\sqrt{w_1(1-w_1)}\right]z_2^2\Upsilon\left[(z_3-\bar{z}_3)\sqrt{w_2(1-w_2)}\right]. \tag{6.B.15}$$

At the same time, using

$$1 - v_2 = z_2 = \epsilon\frac{J_{4,23}}{X_{24}X_{34}} + \mathcal{O}(\epsilon^2), \quad J_{4,23} := (X_4 \wedge Z_4)_{BC}X_2^B X_3^C, \tag{6.B.16}$$

we find that $\Upsilon = \mathcal{O}(\epsilon')$ in the b OPE limit (6.B.5) with leading behaviour

$$\Upsilon = \epsilon'\frac{U_{4,123}X_{23}X_{34}}{X_{13}J_{4,23}^2}\left[\frac{z_1-\bar{z}_1}{2}\frac{z_3-\bar{z}_3}{2}\sqrt{w_1(1-w_1)}\sqrt{w_2(1-w_2)}\right]^{-1} + \mathcal{O}(\epsilon\epsilon'). \tag{6.B.17}$$

In particular, if we define

$$\deg X_4^{-\Delta}Z_4^lW_4^\ell := [\Delta, l, \ell] \Longrightarrow \deg J_{4,23} = [-1,1,0], \quad \deg U_{4,123} = [-1,1,1], \tag{6.B.18}$$

then we find from (6.B.16) and (6.B.17) that

$$\deg z_2 = [1,1,0], \quad \deg \bar{z}_2 = [1,-1,0],, \quad \deg \Upsilon = [0,-1,1]. \tag{6.B.19}$$

This fits directly with the asymptotic behaviour (6.3.28) of conformal blocks in the b OPE limit.

6.C OPE limit factorization of six-point blocks in one-dimensional CFT

Let us consider the case of six-point conformal blocks in the comb channel for the $d = 1$ case. In this case, the conformal blocks have already been computed in [46]. To match the conventions of that paper, we introduce the three cross ratios

$$\chi_1 = \frac{x_{12}x_{34}}{x_{13}x_{24}}, \qquad \chi_2 = \frac{x_{23}x_{45}}{x_{24}x_{35}}, \qquad \chi_3 = \frac{x_{34}x_{56}}{x_{35}x_{46}}, \tag{6.C.1}$$

which make a complete set of independent cross ratios in $d = 1$, and we rename conformal dimensions as

$$\Delta_i = h_i\,, \qquad \Delta_a = \mathbb{h}_1\,, \qquad \Delta_b = \mathbb{h}_2\,, \qquad \Delta_c = \mathbb{h}_3\,. \tag{6.C.2}$$

Note that when reducing to $d = 1$, the Gram determinant relations impose $z_i = \bar{z}_i$, and that

$$\chi_i = z_i = \bar{z}_i\,. \tag{6.C.3}$$

The one-dimensional six-point conformal blocks can then be written as in [46, equation 2.11],

$$g^{h_1,\ldots,h_6}_{\mathbb{h}_1,\mathbb{h}_2,\mathbb{h}_3} = \chi_1^{\mathbb{h}_1}\chi_2^{\mathbb{h}_2}\chi_3^{\mathbb{h}_3} F_K\left[\begin{matrix} h_{12}+\mathbb{h}_1,\, \mathbb{h}_1+\mathbb{h}_2-h_3,\, \mathbb{h}_2+\mathbb{h}_3-h_4,\, \mathbb{h}_3+h_{65} \\ 2\mathbb{h}_1,\, 2\mathbb{h}_2,\, 2\mathbb{h}_3 \end{matrix}; \chi_1, \chi_2, \chi_3\right], \tag{6.C.4}$$

where the comb function F_K can be expressed as

$$F_K\left[\begin{matrix} a_1,\, b_1,\, b_2,\, a_2 \\ c_1,\, c_2,\, c_3 \end{matrix}; \chi_1, \chi_2, \chi_3\right] = \sum_{n=0}^{\infty} \frac{(b_1)_n (b_2)_n}{(c_2)_n} \frac{\chi_2^n}{n!} {}_2F_1\left[\begin{matrix} b_1+n,\, a_1 \\ c_1 \end{matrix}; \chi_1\right] {}_2F_1\left[\begin{matrix} b_2+n,\, a_2 \\ c_3 \end{matrix}; \chi_3\right]. \tag{6.C.5}$$

It is immediate to see that the leading behaviour with respect to the cross ratio χ_2, which is the one-dimensional analogue of $\bar{z}_2$, corresponds simply to $n = 0$ in eq. (6.C.5), leading to the factorized expression

$$g^{h_1,\ldots,h_6}_{\mathbb{h}_1,\mathbb{h}_2,\mathbb{h}_3} \overset{\chi_2\to 0}{\sim} \chi_2^{\mathbb{h}_2} \tag{6.C.6}$$

$$\left(\chi_1^{\mathbb{h}_1} {}_2F_1\left[\begin{matrix} \mathbb{h}_1+\mathbb{h}_2-h_3,\, h_{12}+\mathbb{h}_1 \\ 2\mathbb{h}_1 \end{matrix}; \chi_1\right]\right)\left(\chi_3^{\mathbb{h}_3} {}_2F_1\left[\begin{matrix} \mathbb{h}_2+\mathbb{h}_3-h_4,\, \mathbb{h}_3+h_{65} \\ 2\mathbb{h}_3 \end{matrix}; \chi_3\right]\right).$$

Expression (6.C.6) is an explicit factorization of six-point conformal blocks into the product of two four-point blocks, providing an explicit example of equation (6.3.28) for the one-dimensional case.

Part III

Applications to the Multipoint Lightcone Bootstrap

Chapter 7

Multipoint Comb Channel Lightcone Bootstrap

In the previous chapter, we used Gaudin differential operators to derive polynomial and OPE cross ratios for scalar comb channel N-point blocks. The defining properties of these two sets of variables play an instrumental role in applying the integrability based theory of multipoint blocks to the lightcone bootstrap, as we will review in the first section. After revisiting the four-point lightcone bootstrap with differential operators, we will then apply our methods to a detailed study of a planar five-point crossing symmetry equation (CSE). In addition to rederiving some results of Antunes et al. [67] in an independent way, we go one step further and derive the first result for large spin CFT data at finite tensor structure in (7.3.112). Finally, the outlook provides an overview of how our methods generalize to six points, and how we can apply them to compute double- and triple-twist OPE coefficients. This will be the subject of a forthcoming publication.

7.1 Applications of OPE and Polynomial Cross Ratios

Using the OPE coordinates $(z_r, \bar{z}_r, \Upsilon_r; w_\rho)$, we derived the factorization and reduction to lower point blocks in the OPE/cluster decomposition limit $z_r, \bar{z}_r, \Upsilon_r \to 0$. In particular, taking all OPE limits at all internal legs reduces the comb channel block to a product of three-point tensor structures, thereby defining boundary conditions for the blocks, see Fig. 33. These boundary conditions, along with the complete set of commuting operators, specify the blocks entirely. In this chapter, we will leverage this description of blocks to derive their explicit behavior in lightcone limits, where the Gaudin differential operators simplify drastically. These simplifications are actually best understood in terms of polynomial cross ratios $\{u_{I,\text{pol}}\}_{I=1}^{N(N-3)/2} := \{u_r, v_r, U_s^{(m)}\}$ defined in Eq. (6.2.13),(6.2.14) of section 6.2.2. Each polynomial cross ratio can be expressed as a product of powers of semi-invariants,

$$u_{I,\text{pol}} = \prod_{i<j} X_{ij}^{s_{Iij}}, \quad s_{Iij} \in \{-1, 0, +1\}. \tag{7.1.1}$$

More specifically, the only semi-invariants appearing with negative powers are $X_{i(i+2)}$ for $1 \leq i < N-1$. A Gaudin Hamiltonian $\mathcal{D}$ is a p^{th} order differential operator in $u_{I,\text{pol}}$ with polynomial coefficients. In other words, $\mathcal{D}$ is a polynomial of $N(N-3)$ non-commuting variables $(u_{I,\text{pol}}, \partial_{u_{I,\text{pol}}})$. In this case, we can define a notion of *degree* with respect to X_{ij} on the space of Gaudin differential operators, by

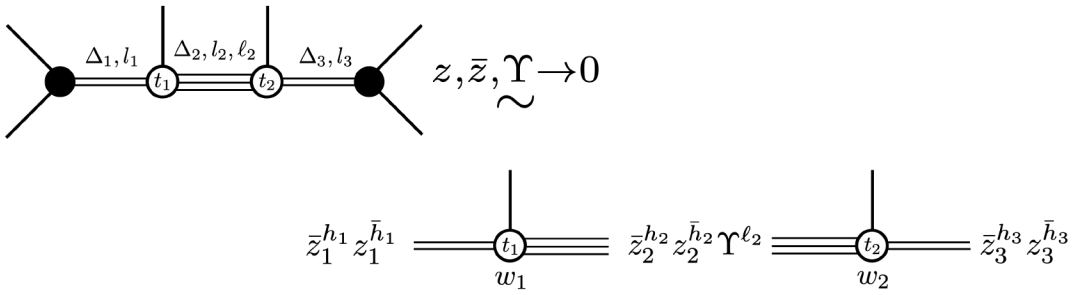

Figure 33: Graphical representation of the OPE boundary condition. Setting $w_s = 1 - \mathcal{X}_s$, $s = 1, 2$, the function $t_s(\mathcal{X}_s)$ in the boundary condition are identical to the polynomials that encode three-point tensor structures in the decompositon (3.2.16) of three-point functions. In this case, the polynomials correspond to vertex systems of type I,II, which were extensively studied in chapter 5. A basis $(t_{n_1}(\mathcal{X}_1), t_{n_2}(\mathcal{X}_2))$ of tensor structures specifies in turn a basis of six-point blocks.

associating the degrees s_{Iij} and $-s_{Iij}$ to $u_{I,\text{pol}}$ and $\partial_{u_{I,\text{pol}}}$ respectively[1]. Then $\mathcal{D}$ can be decomposed into a finite sum of homogeneous monomials using a scaling factor ϵ_{ij} for bookkeeping,

$$X_{ij} \to \epsilon_{ij} X_{ij}, \quad \mathcal{D} \to \sum_s \epsilon_{ij}^s \mathcal{D}^s. \tag{7.1.2}$$

In particular, the leading operator $\mathcal{D}^{s_{\min}}$ in the lightcone limit $\epsilon_{ij} \to 0$ is a homogeneous monomial of degree $s_{\min}$ in X_{ij}. This brings us to the main mechanism underlying the lightcone bootstrap from the point of view of differential operators: the existence of lightcone limits where $s_{\min} < 0$. We can then distinguish two cases:

1. If the eigenvalue is chosen *not* to scale with the lightcone limit, then the conformal block will have to lie in the kernel of $\mathcal{D}^{s_{\min}}$, thereby defining universal asymptotics as $X_{ij} \to 0$.

2. Otherwise, choosing the eigenvalue to scale is tantamount to coupling the small X_{ij} limit with the large eigenvalue limit of $\mathcal{D}$ in the conformal block decomposition. In this case, specific asymptotics in X_{ij} for the correlator can be imposed by tuning the asymptotics of the OPE coefficients.

In practice, the asymptotics are obtained by computing the kernel of $\mathcal{D}^{s_{\min}} - \lambda$, where the eigenvalue λ vanishes in the first case and is arbitrary in the second. To illustrate how far these limits can go in simplifying the behavior of blocks, consider the second order comb channel Casimirs $\mathcal{D} = \mathcal{D}^2_{(1\ldots k)}$ in the lightcone limit $X_{1N} \to 0$. On the one hand, they all have minimal degree $s_{\min} = -1$. On the other hand, there is only one polynomial cross ratio $U_1^{(N)} \equiv U^{(N)}$ with non-vanishing degree. It follows immediately that all monomials of degree $s_{\min} = -1$ must be proportional to ∂_{U^N}, such that the Casimir operator *factorizes* at leading order,

$$\mathcal{D}^{s_{\min}=-1} = \partial_{U^{(N)}} \mathcal{L}\left(U^{(N)}\partial_{U^{(N)}}; \left\{u_r, v_r, U_s^{(m)}, \partial_{u_r}, \partial_{v_r}, \partial_{U_s^{(m)}}\right\}_{m<N}\right), \tag{7.1.3}$$

where $\mathcal{L}$ is a first order differential operator when $\mathcal{D}$ is a second order Casimir.

[1]Note that the degree of a monomial does not depend on the ordering of the non-commuting variables u, ∂_u.

7.2 Lightcone Bootstrap for Four Points

The purpose of this section is to provide a smooth introduction to the multipoint lightcone bootstrap. To this end, we shall begin with a review of the standard analysis for scalar four-point functions. In general, the lightcone bootstrap is predicated on a good knowledge of conformal blocks in certain limits. While this limiting behavior is already well known for four-point blocks, our discussion here will deviate from the norm by emphasizing how most of these properties can be derived from Casimir differential equations only. We explain the usefulness of polynomial cross ratios, the way we take (scaled) limits, and the resulting expressions for lightcone blocks. Special attention will be paid to the normalization of the blocks in the relevant limit.

7.2.1 Preliminaries on blocks and lightcone limits

There are many ways to parameterize conformal invariants of four points. The most basic choice is given by the polynomial cross ratios (u, v) that are defined by

$$u = \frac{X_{12}X_{34}}{X_{13}X_{24}} = z\bar{z}, \quad v = \frac{X_{14}X_{23}}{X_{13}X_{24}} = (1-z)(1-\bar{z}). \tag{7.2.1}$$

Here, X_i denote the embedding space insertion points of the four scalar fields and $X_{ij} = -\frac{1}{2}X_i \cdot X_j = X_i^+ X_j^+ (x_i - x_j)^2$, as usual. Note that we have also introduced the OPE cross ratioss, $(z, \bar{z})$.
The usual conformal partial wave or conformal block expansions for correlation functions of four identical scalar fields ϕ with weight $\Delta_\phi = 2h_\phi$[2] are given by

$$\langle \phi(X_1) \dots \phi(X_4) \rangle = (X_{14}X_{23})^{-\Delta_\phi} \sum_{\mathcal{O}} C^2_{\phi\phi\mathcal{O}} \psi^{(14)(23)}_{\mathcal{O}}(u, v) \tag{7.2.2}$$

$$= (X_{12}X_{34})^{-\Delta_\phi} \sum_{\mathcal{O}} C^2_{\phi\phi\mathcal{O}} \psi^{(12)(34)}_{\mathcal{O}}(u, v) \tag{7.2.3}$$

The central objects in these equations are the conformal blocks ψ. The second line is an expansion in terms of s-channel blocks $\psi^{(12)(34)}$, while in the first line we expanded the same correlator in terms of t-channel blocks $\psi^{(14)(23)}$. The two sets of blocks are related by a simple exchange of the two cross ratios, $\psi^{(14)(23)}(u, v) = \psi^{(12)(34)}(v, u)$. The famous crossing symmetry equation for scalar four-point functions,

$$\sum_{\mathcal{O}} C^2_{\phi\phi\mathcal{O}} \psi^{(14)(23)}_{\mathcal{O}}(u, v) = v^{\Delta_\phi} u^{-\Delta_\phi} \sum_{\mathcal{O}} C^2_{\phi\phi\mathcal{O}} \psi^{(12)(34)}_{\mathcal{O}}(u, v) \ , \tag{7.2.4}$$

is obtained by equating the two expansions in terms of s- and t-channel blocks, respectively. As emphasized by Dolan and Osborn, the conformal blocks are best characterized through the differential equations they satisfy. For s-channel blocks, these are

$$\mathcal{D}^2_{12} \psi^{(12)(34)}_{\mathcal{O}} = \left\{ h_{\mathcal{O}}(h_{\mathcal{O}} - d + 1) + \bar{h}_{\mathcal{O}}(\bar{h}_{\mathcal{O}} - 1) \right\} \psi^{(12)}_{\mathcal{O}} =: \lambda_{\mathcal{O}} \psi^{(12)}_{\mathcal{O}}, \tag{7.2.5}$$

$$\mathcal{D}^2_{12} := (X_{12}X_{34})^{\Delta_\phi} \frac{1}{4} \mathrm{tr} \left(\mathcal{T}_1 + \mathcal{T}_2 \right)^2 (X_{12}X_{34})^{-\Delta_\phi}, \tag{7.2.6}$$

To write the eigenvalue $\lambda_{\mathcal{O}}$ on the right hand side we defined the half-twist $h := \frac{\Delta - J}{2}$ and the half-anti-twist $\bar{h} := \frac{\Delta + J}{2}$ in terms of the weight Δ and the spin J of the intermediate field $\mathcal{O}$. In the second line, we have introduced $\mathcal{T}_i$ to denote the usual action of the generators of the conformal Lie algebra on

[2] We will use both notations throughout this chapter.

the primary field $\phi(X_i)$. The operator $\mathcal{D}_{12}^2$ was first computed by Dolan and Osborn. When expressed in terms of the cross ratios u, v, it takes the form

$$\mathcal{D}_{12}^2 = (1-u-v)\partial_v v\partial_v + u\partial_u\left(2u\partial_u - d\right) - (1+u-v)\left(u\partial_u + v\partial_v\right)^2. \tag{7.2.7}$$

We note that the coefficients of this second order differential operator are polynomial in the cross ratios u, v. This is why we refer to them as polynomial cross ratios. Clearly, a similar discussion applies to the t-channel blocks, only that u and v are exchanged in passing from one channel to the other.

While the crossing symmetry equations of d-dimensional conformal field theories are difficult to solve analytically, at least when $d > 2$, there exist certain limits in which they simplify drastically. The most interesting of these is the lightcone limit that is reached after continuation to Lorentzian signature, when x_4 is lightlike separated from x_1, i.e. $X_{14} \sim 0$. Contrary to Euclidean kinematics, this Lorentzian limit $v \to 0$ does not force the two points two coincide and therefore $u \neq 1$ in general[3]. To perform the relevant limit, we shall assign appropriate orders to the cross ratios. Let us note that all the cross ratios depend on the insertion points only through X_{ij}. We can keep track of how a given cross ratio behaves as we make a pair of points x_i and x_j lightlike separated by introducing a parameter ϵ_{ij} and performing the substitution $X_{ij} \to \epsilon_{ij} X_{ij}$. In the case at hand, we want to make x_1 and x_4 lightlike separated and therefore introduce a parameter ϵ_{14}. Upon substitution $X_{14} \to \epsilon_{14} X_{14}$, the cross ratio v behaves as $v \to \epsilon_{14} v$ while the second cross ratio u is invariant. We can therefore think of v as a quantity of ϵ_{14}-order $\mathrm{O}(\epsilon_{14})$ while the cross ratio u has order $\mathrm{O}(\epsilon_{14}^0)$. Later in the analysis we will also make x_1 and x_2 lightlike separated. In this case, it is easy to see that u is of ϵ_{12}-order $\mathrm{O}(\epsilon_{12}^1)$ while v is $\mathrm{O}(\epsilon_{12}^0)$. We note that the order extends from the polynomial cross ratios to the Casimir differential operators. The operator (7.2.7), for example, has terms of ϵ_{12}-order $\mathrm{O}(\epsilon_{12}^n)$ with $n = 0, 1$. With respect to the ϵ_{14}-order, on the other hand, there are terms of order $\mathrm{O}(\epsilon_{14}^m)$ with $m = -1, 0, 1$, i.e. it contains ϵ_{14}-singular terms. We will often want to keep track of orders in several independent lightcone limits at the same time. In the case at hand, we introduce $\vec{\epsilon} = (\epsilon_{14}, \epsilon_{12})$ and then denote the $\vec{\epsilon}$-order by $\mathrm{O}(\epsilon_{14}^n \epsilon_{12}^m)$ or simply (n, m). With this notation, our cross ratios u and v have order $(0, 1)$ and $(1, 0)$ respectively. This implies that $\vec{\epsilon}$ is associated with the regime

$$LCL_{\vec{\epsilon}}: \; v \ll u \ll 1$$

in the space of cross ratios. We also define the vector $\vec{\epsilon}\,' = (\epsilon_{12}, \epsilon_{14})$ associated to a different regime in which we take u and v to zero in the opposite order, i.e. $u \ll v \ll 1$.

7.2.2 Lightcone blocks in the direct channel

In order to study the behaviour of the t-channel blocks in the lightcone regime $LCL_{\vec{\epsilon}}$, we shall study the limit of the Casimir eigenvalue equation. Let us note that the t-channel Casimir operator $\mathcal{D}_{14}^2$ is obtained from the s-channel operator we have displayed in eq. (7.2.7) by exchanging the cross ratios u and v, i.e.

$$\mathcal{D}_{14}^2 = (1-u-v)\partial_u u\partial_u + v\partial_v\left(2v\partial_v - d\right) - (1+u-v)\left(u\partial_u + v\partial_v\right)^2. \tag{7.2.8}$$

The dependence of the Casimir operator $\mathcal{D}_{14}^2$ on ϵ_{14} gives rise to a split into a sum of two terms,

$$\mathcal{D}_{14}^2 = \epsilon_{14}^0 \mathcal{D}_{14}^{(0)} + \epsilon_{14}\mathcal{D}_{14}^{(1)} \tag{7.2.9}$$

[3] *Caution.* Contrary to the usual conventions of the four-point bootstrap and of [67], we will take the channel containing the (12) OPE as the *crossed channel*. This will later simplify computations in the cross channel in terms of polynomial and OPE cross ratios.

where the first terms is given by

$$\mathcal{D}_{14}^{(0)} = {}_2\mathcal{D}_1(v\partial_v, v\partial_v; 2v\partial_v; 1-u; -\partial_u) + v\partial_v(2v\partial_v - d) \tag{7.2.10}$$

Here, we find it useful to introduce the symbol ${}_2\mathcal{D}_1(a,b;c;z,\partial)$ that will be used throughout the discussion,

$${}_2\mathcal{D}_1(a,b;c;w,\partial) := w\partial(w\partial + c - 1) - w(w\partial + a)(w\partial + b). \tag{7.2.11}$$

In general, the parameters a, b, c and the argument ∂ can be first order differential operators while w is some function of the cross ratios. Since only v scales with ϵ_{14}, it follows that $\mathcal{D}_{14}^{(0)}$ is homogeneous of degree zero in v, and therefore commutes with the Euler operator $\vartheta_v \equiv v\partial_v$.
Conformal blocks are eigenfunctions of the Casimir differential operator. If we assume the eigenvalues not to scale with ϵ_{14}, their limits as $\epsilon_{14} \to 0$ must thereby solve the differential equation

$$\mathcal{D}_{14}^{(0)}\psi_{\mathcal{O}}^{(14)(23);(0)}(u,v) = \left\{h_{\mathcal{O}}(h_{\mathcal{O}} - d + 1) + \bar{h}_{\mathcal{O}}(\bar{h}_{\mathcal{O}} - 1)\right\}\psi_{\mathcal{O}}^{(14)(23);(0)}(u,v)\ . \tag{7.2.12}$$

Since $\mathcal{D}_{14}^{(0)}$ commutes with the Euler operator $v\partial_v$, we can make the following ansatz for a complete set of solutions,

$$\psi_{(h,\bar{h})}^{(14)(23);(0)}(u,v) = v^h g_{h,\bar{h}}(u)\ . \tag{7.2.13}$$

Inserting this expression into the leading order eigenvalue equation and using the identity

$$v^{-h}\left(\mathcal{D}_{14}^{(0)} - h(h-d+1)\right)v^h = {}_2\mathcal{D}_1(h,h;2h;1-u,-\partial_u), \tag{7.2.14}$$

it is now easy to find an eigenfunction of the form

$$\psi_{(h,\bar{h})}^{(14)(23);(0)}(u,v) = v^h(1-u)^J {}_2F_1\left(\bar{h},\bar{h};2\bar{h};1-u\right). \tag{7.2.15}$$

with $J = \bar{h} - h$, as before. Let us note that the most general solution is a linear combination $c_1\psi_{(h,\bar{h})} + c_2\psi_{(h,1-\bar{h})}$. This linear combination is fixed to $(c_1, c_2) = (1, 0)$ by the OPE. Since this is a very important aspect of our discussion, we will provide more details below.
Before we get there, however, let us perform the remaining limit $\epsilon_{12} \ll 1$, where x_1 and x_2 become lightlike separated in addition to x_1 and x_4. As in the case of X_{14}, we control the value of X_{12} by a small parameter ϵ_{12}, i.e. we replace X_{12} by $\epsilon_{12}X_{12}$ and think of ϵ_{12} as a small parameter. As we send ϵ_{12} to zero the cross ratio $v \to \epsilon_{12}v$ is sent to zero while u is not affected. Having expanded the Casimir differential operator in ϵ_{14}, we can now expand each of the two terms in ϵ_{12} and find

$$\mathcal{D}_{14}^{(0)} = \epsilon_{12}^{-1}\mathcal{D}_{14}^{(0,-1)} + \mathrm{O}(\epsilon_{12}^0), \tag{7.2.16}$$

where the superscript reminds us that the leading term of the quadratic Casimir operator is of order $\mathrm{O}(\epsilon_{14}^0\epsilon_{12}^{-1})$. Explicitly, one finds that

$$\mathcal{D}_{14}^{(0,-1)} = \partial_u u\partial_u. \tag{7.2.17}$$

Let us also note that $\mathrm{O}(\epsilon_{12}^0)$ consists of two terms, one that is constant in ϵ_{12} and one that is linear. Their precise form is easily found but irrelevant for us. If we now assume that the eigenvalue $\bar{h}(\bar{h}-1) + h(h-d+1)$ of the Casimir operator does not depend on ϵ_{12}, we conclude that the leading contribution of our conformal blocks in the limit where ϵ_{12} is sent to zero must be in the kernel of the operator $\mathcal{D}_{14}^{(0,-1)}$,

$$\ker(\mathcal{D}_{14}^{(0,-1)}) = \mathrm{Span}(v^h, v^h\log u). \tag{7.2.18}$$

Here, the eigenvalue h of the Euler operator ϑ_v can assume any non-negative real value. This behavior of the lightcone blocks is indeed consistent with our previous equation (7.2.15) for the normalized lightcone blocks. As one can verify using standard results on hypergeometric functions, e.g. in [132, §15.4(ii)], lightcone asymptote to

$$\psi^{(14)(23)}_{(h,\bar{h})}(u,v) \overset{LCL_{\bar{e}}}{\sim} \begin{cases} 1 \quad \text{if } \bar{h}=0, \\ -\Gamma(\bar{h})^{-2}\Gamma(2\bar{h})\, v^h \log u + \mathrm{O}(1) \quad \text{if } \bar{h}>0. \end{cases} \tag{7.2.19}$$

In the first line, we have also used that $\bar{h}=0$ implies $h=0$. This concludes our discussion of the lightcone limit for the conformal blocks $\psi^{(14)(23)}$ in the direct channel.

After this detailed discussion of the direct channel blocks in the lightcone regime $LCL_{\bar{e}}$, we now return to the issue of normalization. In the case of four-point blocks, there are two different ways to determine it.

1. Let us first recall that conformal blocks are normalized by their behavior in the OPE limit. More precisely, in the limit where $v\sim 0$ and $u\sim 1$,[4]

$$\psi^{(14)(23)}_{(h,\bar{h})}(u,v) = v^h(1-u)^J\left(1+\mathrm{O}(v,1-u)\right)\ . \tag{7.2.20}$$

With this normalization condition for the blocks stated, we now take note of a very lucky fact: for four-point functions, we were able to solve the Casimir differential equations in the regime $v\ll 1$ that contains *both* the OPE limit point at $u=1$ *and* the lightcone limit point at $u=0$. As a result, we need only verify that the solution (7.2.15) is correctly normalized by matching the limiting behavior of eq. (7.2.15) near $u=1$ with the normalization condition (7.2.20). With the choice of the normalization in eq. (7.2.15), this is obviously the case. Once the correct normalization is ensured for (7.2.15), we can take the limit $u\to 0$ to obtain our results in eq. (7.2.19) with the correct normalization. This follows from standard limiting formulas for hypergeometric functions.

2. There is another way to determine the normalization of lightcone blocks that does not depend on our explicit knowledge of the solution (7.2.15) in the regime $v\ll 1$, but uses rather an integral formula for the lightcone limit of the $\phi(X_1)\phi(X_4)$ OPE. This formula, first derived by Ferrara et al. [37–39], was rederived in chapter 3 with an embedding space Feynman parameterization and is given by (3.3.18). Since we were able to infer the functional dependence of blocks in the lightcone regime from the differential operator (7.2.17), we only make use of this integral representation to determine the overall numerical factor. In the case of $N=4$ external points, plugging the lightcone OPE (3.3.18) into the four-point function gives the following expression for blocks in the $X_{14}\ll 1$ limit,

$$\psi^{(14)(23)}_{(h,\bar{h})}(u,v) = (X_{14}X_{23})^h(X_4{\wedge}X_1{\cdot}X_2{\wedge}X_3)^J\int_{\mathbb{R}^2_+}\frac{\mathrm{d}s_1\mathrm{d}s_4(s_1s_4)^{\bar{h}-1}}{\mathrm{B}_{\bar{h}}|\mathbb{R}^\times|}X_{a2}^{-\bar{h}}X_{a3}^{-\bar{h}}\left(1+\mathrm{O}(X_{14})\right). \tag{7.2.21}$$

In this expression, recall that $X_a := s_1X_1+s_4X_4$ is a point on the projective lightcone when $X_{14}=0$, $\mathrm{B}_{\bar{h}} := \Gamma(\bar{h})^2\Gamma(2\bar{h})^{-1}$ is the diagonal of the Euler Beta function, and $|\mathbb{R}^\times| := \int_0^\infty \lambda^{-1}\mathrm{d}\lambda$ is the volume of the dilation group $\{(s_1,s_2)\to(\lambda s_1,\lambda s_2)\}$. Since the integral is manifestly $\mathrm{SO}(1,d+1)$ invariant and homogeneous of degree zero in X_1,X_2,X_3,X_4, it can be written as a function of the cross ratios (u,v). After the change of variables $(s_1,s_4)=(\lambda s,\lambda)$, it takes the form

$$\psi^{(14)(23)}_{(h,\bar{h})}(u,v) \overset{v\ll 1}{\sim} \frac{v^h(1-u)^J}{\mathrm{B}_{\bar{h}}}\int_0^\infty\frac{\mathrm{d}s}{s}(1+su)^{-\bar{h}}(1+s)^{-\bar{h}}\ . \tag{7.2.22}$$

[4] Recall that our direct channel is what is often referred to as t-channel and hence the cross ratios u and v are exchanged with respect to the usual s-channel discussion.

It is easy to see that the integral in the last expression has a logarithmic divergence for $u \sim 0$ which stems from the integration near $s = 0$. In order to determine the leading term of the integral as we send u to zero, we can write

$$\int_0^\infty \frac{\mathrm{d}s}{s}(1+su)^{-\bar{h}}(1+s)^{-\bar{h}} \overset{u\ll 1}{\sim} \int_u^1 \frac{\mathrm{d}s}{s}\,(1+\mathrm{O}(s)) + \mathrm{O}(1) = -\log u + \mathrm{O}(1)\ . \tag{7.2.23}$$

In the first equality, the "O(1)" denotes the integral restricted to the region $(1,\infty)$, while the "O(s)" denotes higher powers in an expansion of the integrand around $s = 0$, which integrate over $(u, 1)$ to a finite result. In sum, we indeed reproduce the expected $\log u$ divergence with a coefficient $\mathrm{B}_{\bar{h}}^{-1}$ in eq. (7.2.22). This matches our result in eq. (7.2.19).

7.2.3 Lightcone blocks in the crossed channel

Let us now discuss the lightcone limit of conformal blocks in the crossed s-channel. The Casimir differential operator $\mathcal{D}_{12}^2$ for the crossed channel is displayed in eq. (7.2.7). We begin by implementing the $\epsilon_{14} \to 0$ limit. To this end, we expand the Casimir operator $\mathcal{D}_{12}^2$ in a Laurent series of ϵ_{14} after making the replacement $v \mapsto \epsilon_{14} v$. The leading term at order ϵ_{14}^{-1} then takes the form

$$\mathcal{D}_{12}^2 = \epsilon_{14}^{-1}\left(\partial_v v\partial_v - \epsilon_{12} u\partial_v v\partial_v\right) + \mathrm{O}(\epsilon_{14}^0). \tag{7.2.24}$$

In anticipation of the second limit $\epsilon_{12} \to 0$, we have already made the substitution $u \mapsto \epsilon_{12} u$. Since the leading contribution commutes with $u\partial_u$, we can without loss of generality choose a basis of functions with leading behavior of the form

$$\psi_{(h,\bar{h})}^{(12)(34)}(u,v) = u^h g_{(h,\bar{h})}(v)(1+\mathrm{O}(u^{h+1})) \tag{7.2.25}$$

as we send the cross ratio u to zero. The eigenvalue equation then reduces to

$$\epsilon_{14}^{-1}\partial_v v\partial_v g_{(h,\bar{h})}(v) = \lambda_{(h,\bar{h})} g_{(h,\bar{h})}(v), \quad \lambda_{(h,\bar{h})} = h(h-d+1) + \bar{h}(\bar{h}-1)\ . \tag{7.2.26}$$

Contrary to the direct t-channel, the $\epsilon_{14} \to 0$ limit does not restrict the twist of operators appearing in the (12) OPE of the s-channel. Thus, the Casimir eigenvalue can vary over all positive numbers, and we can distinguish three regimes

$$g(v) \overset{v\ll 1}{\sim} \mathcal{N} \begin{cases} 1 \text{ or } \log v & \text{if } \lambda = \mathrm{O}(\epsilon_{14}^0), \\ K_0(2\sqrt{\lambda v}) & \text{if } \lambda = \mathrm{O}(\epsilon_{14}^{-1}), \\ 0 & \text{otherwise.} \end{cases} \tag{7.2.27}$$

In the first case, the eigenfunctions must be in the kernel of $\partial_v v\partial_v$. If the eigenvalue $\lambda \to \epsilon^{-1}\lambda$ scales with ϵ_{14} as stated in the second line, the right hand side of the eigenvalue equation contributes and we obtain the equation

$$\left(\partial_v v\partial_v - \lambda\right) g = 0 \tag{7.2.28}$$

which can be transformed into Bessel's differential equation by a simple change of variables. The main issue is again to determine the normalization $\mathcal{N}$. To find the latter, we exploit the fact that the leading term $\partial_v v\partial_v$ in the Casimir operator $\mathcal{D}_{12}^2$ at order $\mathrm{O}(\epsilon_{14}^{-1}\epsilon_{12}^0)$ is the same regardless of whether we take ϵ_{14} or ϵ_{12} to zero first. We can thus retrieve these asymptotics of the crossed channel lightcone blocks in the order of limits $\vec{\epsilon}\,' = (\epsilon_{12}, \epsilon_{14})$. In this case, the analysis is identical to the one we described in

our discussion of the direct channel. That is, in the limit $\epsilon_{12} \to 0$ (with v kept finite) our blocks take the exact form of (7.2.15) with $u \leftrightarrow v$ and with h corresponding to a fixed half-twist,

$$\psi^{(12)(34)}_{(h,\bar{h})}(u,v) \overset{u\ll 1}{\sim} u^h (1-v)^J {}_2F_1(\bar{h},\bar{h};2\bar{h};v) \ , \tag{7.2.29}$$

and this limiting form is now normalized. Now, given that the eigenvalue is $\lambda = h(h-d+1)+\bar{h}(\bar{h}-1)$ and h is fixed, our three regimes correspond to

$$\psi^{(12)(34)}_{(h,\bar{h})}(u,v) \overset{LCL_{\vec{c}}}{\sim} \begin{cases} 1 \text{ or } \mathrm{B}_{\bar{h}}^{-1} \log v & \text{if } \bar{h} = \mathrm{O}(\epsilon_{14}^0) \\ \mathcal{N}^{\mathrm{LS}}_{(h,\bar{h})} u^h K_0(2\bar{h}\sqrt{v}), & \text{if } \bar{h} = \mathrm{O}(\epsilon_{14}^{-1/2}) \\ 0 \quad \text{otherwise.} \end{cases} \tag{7.2.30}$$

In order to determine the normalization $\mathcal{N}$ in the second case, we take the further limit

$$K_0(2\bar{h}\sqrt{v}) \overset{v\ll \bar{h}^{-2}}{\sim} -\frac{1}{2}\log v + \mathrm{O}(1). \tag{7.2.31}$$

Matching these asymptotics with (7.2.19), we obtain

$$\mathcal{N}^{\mathrm{LS}}_{(h,\bar{h})} = 2 \lim_{\bar{h}\to\infty} \Gamma(\bar{h})^{-2}\Gamma(2\bar{h}) = 4^{\bar{h}} \pi^{\frac{1}{2}} \bar{h}^{-\frac{1}{2}}. \tag{7.2.32}$$

In the second equality, we used the Stirling formula to evaluate $\mathrm{B}_{\bar{h}}^{-1}$ at leading order in $\bar{h}^{-1}$ as $\bar{h}$ tends to infinity, discarding any further $\mathrm{O}(\bar{h}^{-1})$ corrections — this is the meaning of our notation "lim" on the right hand side of the first equality. This concludes our discussion of the lightcone limit of four-point blocks for identical scalars in the direct and the crossed channel. We stress once again that in order to obtain the two key results (7.2.19), respectively (7.2.30) for the lightcone limits of blocks in the direct and crossed channel, we only needed the Casimir differential equations. This applies in particular to the dependence of the lightcone blocks on the cross ratios. The normalizations could also be determined from the Casimir equations, though for this purpose we had to solve them outside the lightcone limit and connect them to the OPE limit. Alternatively, one can also use integral representations to find the normalization. The latter procedure appears a bit easier to extend to higher points at the current stage.

7.2.4 Review of the four-point lightcone bootstrap

We can now exploit the results on lightcone blocks to analyse the crossing symmetry equation (7.2.4). Here, our discussion will closely follow the original literature [35, 36], while also reapplying some of Simmons-Duffin's insights from [40]. Let us first evaluate the direct channel, i.e. the left hand side of the crossing equation, in the regime $v \ll u \ll 1$. Using the result (7.2.19) for the limit of the blocks one finds

$$\sum_{\mathcal{O}} C_{\phi\phi\mathcal{O}} \psi^{(14)(23)}_{\mathcal{O}}(u,v) \sim 1 + C^2_{\phi\phi\mathcal{O}_\star} \frac{\Gamma(2\bar{h}_\star)}{\Gamma(\bar{h}_\star)^2} \left[v^{h_\star} \left(\log u + \mathrm{O}(u^0) \right) + \mathrm{O}(v^{h_\star+1}) \right] + \mathrm{O}(v^{h>h_\star}). \tag{7.2.33}$$

Here, we denote the leading twist operator in the operator product of ϕ with itself by $\mathcal{O}_\star$, and we assume it is unique. Note that uniqueness does not apply to free field theory, where the leading twist is infinitely degenerate and the operator product takes the form

$$\phi(X_1)\phi(X_4) = 1 + \sum_{n=0}^{\infty} X_{14}^n \sum_{J\in 2\mathbb{Z}_+}^{\infty} C_{\phi\phi[\phi\phi]_{n,J}} f_{\phi\phi[\phi\phi]_{n,J}}(X_1 - X_4, \partial_{X_4}) [\phi\phi]_{n,J}(X_4). \tag{7.2.34}$$

The standard notation $[\phi\phi]_{n,J}$ denotes double-twist operators of the form

$$[\phi\phi]_{n,J}(x,z) := \phi(x)\,\Box^n (z\cdot\partial)^J \phi(x)\ , \tag{7.2.35}$$

where the label J denotes the spin of the field and $\tau_{n,J} = 2\Delta_\phi + 2n$ is the twist in free field theory. In terms of our parameters h and $\bar{h}$ this means

$$h_{[\phi\phi]_{n,J}} = \tau_{n,j}/2 = \Delta_\phi + n \quad , \quad \bar{h}_{[\phi\phi]_{n,J}} = \Delta_\phi + n + J\ . \tag{7.2.36}$$

Note that if $\phi^\dagger = \phi$ is a real field, then only *even* spins are allowed [36, Eq. (2.2)]. As one can read off from these formulas, the operator product (7.2.34) contains an infinite tower of operators $\{[\phi\phi]_{0,J}\}_{J\in 2\mathbb{Z}_+}$ at leading twist. The degeneracy is lifted by interactions and the main goal of the analytic bootstrap is to find precise expressions for the correction terms. Note also that $C^2_{\phi\phi\mathcal{O}_\star}\mathrm{O}(v^{h_\star+1})$ corresponds to the contributions of descendants of the leading twist operator, whereas the next-to-leading-twist operator $\mathcal{O}'$ would give $C^2_{\phi\phi\mathcal{O}'}\mathrm{O}(v^{h'})$. In many cases of interest, we can expect several $h' > h_\star + 1$ primaries to dominate over the first descendants. In the $d = 3$ Ising model, for example, ϵ and $T_{\mu\nu}$ give important contributions.

Given the results (7.2.30) on the lightcone limit of crossed channel blocks, we can write the s-channel sum on the right hand side of the crossing symmetry equation (7.2.4) in the $v \ll u \ll 1$ limit as

$$\sum_{\mathcal{O}} C^2_{\phi\phi\mathcal{O}}\psi^{(12)(34)}(u,v) = \tag{7.2.37}$$

$$1 + \int_{\mathrm{O}(\epsilon_{14}^0)}^{\infty} \frac{\mathrm{d}\lambda_{\mathcal{O}}}{4\sqrt{\lambda_{\mathcal{O}}}} \mathcal{N}^{\mathrm{LS}} C^2_{\phi\phi\mathcal{O}} u^{h^{\min}_{\mathcal{O}}} K_0(2\sqrt{\lambda_{\mathcal{O}} v})\left(1 + \mathrm{O}(v^{\frac{\tau}{2}})\right) + \sum_{\lambda_{\mathcal{O}} = \mathrm{O}(\epsilon_{14}^0)} \mathrm{B}(\bar{h})^{-1} \log v \left(1 + \mathrm{O}(v^0)\right).$$

In the integral over large Casimir eigenvalues, $h^{\min}_{\mathcal{O}}$ is the minimal twist for which the Casimir $\lambda_{\mathcal{O}}$ is not bounded above. If this $h^{\min}_{\mathcal{O}}$ is finite[5], then this implies that $\mathcal{O}$ has large spin

$$\bar{h}_{\mathcal{O}} = J_{\mathcal{O}} + h^{\min}_{\mathcal{O}} = \sqrt{\lambda_{\mathcal{O}}} + \mathrm{O}(\epsilon_{12}^0). \tag{7.2.38}$$

In the next section, we will review how the crossing equation implies that

$$h^{\min}_{\mathcal{O}} = 2h_\phi = h_{[\phi\phi]_{J,0}} + \mathrm{O}(\lambda_{\mathcal{O}}^{-\frac{\tau}{2}}), \quad \tau = \tau_{\mathcal{O}_\star}, \tag{7.2.39}$$

where $\mathcal{O}_\star$ is the minimal twist operator in the operator product of ϕ with itself. The first major success of the lightcone bootstrap was the computation of the OPE coefficients $C_{\phi\phi[\phi\phi]_{0,J}}$ and anomalous dimensions $h_{[\phi\phi]_{J,0}} - 2h_\phi$ to leading order in the large $J_{\mathcal{O}}$ limit.

Comparing the two expressions (7.2.33) and (7.2.2) for the limiting behaviors the two sides of the crossing equation (7.2.4), we deduce to leading order

$$1 + \mathrm{O}(v^{h_\star}) = v^{\Delta_\phi} u^{-\Delta_\phi} \sum_{\mathcal{O}} C^2_{\phi\phi\mathcal{O}}\psi^{(12)(34)}(u,v). \tag{7.2.40}$$

One immediately observes that the s-channel sum must yield a divergent power law $v^{-\Delta_\phi}$ to leading order — this eliminates the finite sum over primaries with $\lambda_{\mathcal{O}} = \mathrm{O}(v^0)$, since these contributions diverge logarithmically at most. We thus need to solve

$$1 + \cdots = v^{\Delta_\phi} \int_{\mathrm{O}(1)}^{\infty} \frac{\mathrm{d}\lambda_{\mathcal{O}}}{4\sqrt{\lambda_{\mathcal{O}}}} C^2_{\phi\phi\mathcal{O}} u^{h^{\min}_{\mathcal{O}} - \Delta_\phi} K_0(2\sqrt{\lambda_{\mathcal{O}} v}) + \ldots \tag{7.2.41}$$

[5] Which it should be, since double-twist operators can have unbounded spin.

Imposing $h_{\mathcal{O}}^{\min} = \Delta_\phi$, we deduce that the left hand side of the crossing symmetry equation is reconstructed from a sum over double twist operators $[\phi\phi]_{0,J}$ with spins that scale as

$$\sqrt{\lambda} = J + \mathrm{O}(1) = \mathrm{O}(v^{-1/2}) \ .$$

After plugging in a power law ansatz for the OPE coefficients of the form

$$\mathcal{N}^{\mathrm{LS}} C^2_{\phi\phi\mathcal{O}} = c_0 \frac{4J^{\beta-1}}{\Gamma(\beta/2)^2} \left(1 + \mathrm{O}(J^{-\tau})\right), \tag{7.2.42}$$

and using the auxiliary formula

$$\int_{\mathrm{O}(\sqrt{v})}^{\infty} \frac{\mathrm{d}y}{y} \left(\frac{y}{2}\right)^{\beta} K_\alpha(y) = \frac{1}{4}\Gamma\left(\frac{\beta+\alpha}{2}\right)\Gamma\left(\frac{\beta-\alpha}{2}\right) + \mathrm{O}(v^{\frac{\beta-\alpha}{2}}), \quad \beta > \alpha, \tag{7.2.43}$$

we reduce the leading order terms of the crossing symmetry equation to

$$1 + \cdots = c_0 v^{\Delta_\phi - \frac{\beta}{2}} + \ldots \Longrightarrow \mathcal{N}^{\mathrm{LS}} C^2_{\phi\phi\mathcal{O}} = \frac{4J^{2\Delta_\phi - 1}}{\Gamma(\Delta_\phi)^2} \left(1 + \mathrm{O}(J^{-\tau})\right). \tag{7.2.44}$$

Moving on to the next-to-leading order in the crossing equation, we have

$$1 + \frac{C^2_{\phi\phi\mathcal{O}}}{\mathrm{B}(\bar{h}_\star)} v^{h_\star} \left(\log u + \mathrm{O}(u^0)\right) + \mathrm{O}(v^{h>h_\star}) = v^{\Delta_\phi} \int_{\mathrm{O}(1)}^{\infty} \frac{\mathrm{d}J}{J} \frac{2J^{2\Delta_\phi}}{\Gamma(\Delta_\phi)^2} u^{h_{[\phi\phi]_{0,J}} - \Delta_\phi} K_0(2J\sqrt{v})(1 + \mathrm{O}(J^{-\tau})),$$

having once again discarded the finite spin contributions with $\mathrm{O}(\log v)$ divergence at most. To reproduce $v^{h_\star} \log u$ asymptotics, one makes the following ansatz for leading anomalous dimension corrections to double twist operators at large spin,

$$h_{[\phi\phi]_{0,J}} = \Delta_\phi + \frac{\gamma}{2J^{2h_\star}} + \mathrm{O}\left(J^{-\tau}\right), \quad \tau > 2h_\star. \tag{7.2.45}$$

Expanding v^h in the t-channel, we obtain

$$\frac{C^2_{\phi\phi\mathcal{O}_\star}}{\mathrm{B}(\bar{h}_\star)} = \frac{\gamma}{2} \frac{\Gamma(\Delta_\phi - h_\star)^2}{\Gamma(\Delta_\phi)^2}. \tag{7.2.46}$$

Note that the anomalous dimension correction vanishes when $h_\star = \Delta_\phi$. This is the signature of free field theory: the leading twist operators are $[\phi\phi]_{0,J}$, and their scaling dimensions are not anomalous. The above analysis shows that we can only reproduce the leading terms on the left hand side of the crossing symmetry equations by summing over large spin double twist operators on the right hand side, i.e. with the help of crossed channel lightcone blocks (7.2.30) for which the Casimir eigenvalue λ scales as $\lambda \sim \epsilon_{14}^{-1}$. In [40, Sec. 4.1], Simmons-Duffin gave a simple proof of this fact. The argument is based on the observation that the Casimir operator $\mathcal{D}^2_{12}$ has a stable action on any finite spin subspace in the (12) channel, whereas $v^{-\Delta_\phi}$ does not. First, define the vector space

$$\mathbb{V}_L := \mathrm{Span}\left\{ \psi^{(12)(34)}_{\mathcal{O}} : h_{\mathcal{O}} = \Delta_\phi, \bar{h}_{\mathcal{O}} < L \right\}, \quad L < \infty. \tag{7.2.47}$$

We rewrite the crossing equation as

$$u^{\Delta_\phi} v^{-\Delta_\phi} + \cdots = \sum_{\mathcal{O}} C^2_{\phi\phi\mathcal{O}} \psi^{(12)(34)}_{\mathcal{O}}(u, v). \tag{7.2.48}$$

Acting repeatedly with $\mathcal{D}_{12}^2$ on the identity contribution, we find

$$\begin{aligned}
&\mathcal{D}_{12}^2 u^{\Delta_\phi} v^{-\Delta_\phi} = \Delta_\phi(\Delta_\phi+1) u^{\Delta_\phi} v^{-(\Delta_\phi+1)} + \mathrm{O}(v^{-\Delta_\phi}) \\
\longrightarrow\ &\mathcal{D}_{12}^2 u^{\Delta_\phi} v^{-(\Delta_\phi+1)} = (\Delta_\phi+1)(\Delta_\phi+2) u^{\Delta_\phi} v^{-(\Delta_\phi+1)} + \mathrm{O}(v^{-(\Delta_\phi+1)}) \\
\longrightarrow\ &\ldots
\end{aligned}$$

As long as $\Delta_\phi \notin \mathbb{Z}_{<0}$, this series never truncates and $\mathcal{D}_{14}^2$ stabilizes only on an infinite dimensional vector space $\mathrm{Span}(u^{\Delta_\phi} v^{-(\Delta_\phi+n)})_{n\in\mathbb{Z}_+}$. It follows that the expansion of $(v^{-1}u)^{\Delta_\phi}$ in eigenvectors of $\mathcal{D}_{12}^2$ has *infinite* support — we say that $(v^{-1}u)^{\Delta_\phi}$ is $\mathcal{D}_{12}^2$-singular. In short,

$$(v^{-1}u)^{\Delta_\phi} \notin \mathbb{V}_L, \quad \forall L < \infty. \tag{7.2.49}$$

In general, a direct channel contribution is reproduced by large spin operators in the cross channel if and only if it is $\mathcal{D}$-singular, for some Casimir differential operator $\mathcal{D}$ in the crossed channel. In five- and six-point crossing equations, where we obtain more unconventional asymptotics in the lightcone limit of the direct channel, we will demonstrate that they yield large spin CFT data using this precise criterion.

7.3 Lightcone Bootstrap for Five Points

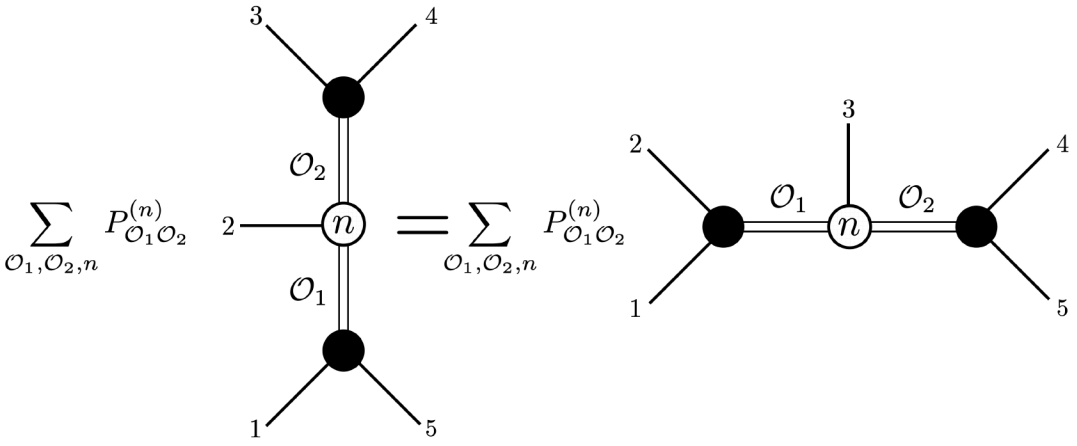

Figure 34: Graphical representation of the planar five-point crossing symmetry equation studied in this paper. The crossed channel is obtained from the direct channel by cyclic permutation of points, $i \to i+1 \bmod 5$.

In this section we extend the analysis of crossing symmetry in the lightcone limit to correlation functions of five identical scalar fields.

7.3.1 Preliminaries on blocks and lightcone limits

Five-point functions in $d \geq 3$ are parameterized by five cross ratios. The following polynomial cross ratios for five-point functions were first constructed in [65],

$$u_1 = \frac{X_{12}X_{34}}{X_{13}X_{24}}, \qquad v_1 = \frac{X_{14}X_{23}}{X_{13}X_{24}}, \qquad U_1^{(5)} = \frac{X_{15}X_{23}X_{34}}{X_{24}X_{13}X_{35}}. \tag{7.3.1}$$
$$u_2 = \frac{X_{23}X_{45}}{X_{24}X_{35}}, \qquad v_2 = \frac{X_{25}X_{34}}{X_{24}X_{35}},$$

It will often be convenient to use the "snowflake" cross ratios $u_{si}, i = 1, \ldots, 5$ used in [66, 67]. In terms of our polynomial cross ratios, they are be expressed as

$$u_{s1} = u_1/v_2 = \frac{X_{12}X_{35}}{X_{13}X_{25}}, \quad u_{s2} = v_1 = \frac{X_{14}X_{23}}{X_{13}X_{24}}, \tag{7.3.2}$$

$$u_{s3} = v_2 = \frac{X_{25}X_{34}}{X_{24}X_{35}}, \quad u_{s4} = u_2/v_1 = \frac{X_{45}X_{13}}{X_{35}X_{14}}, \tag{7.3.3}$$

$$u_{s5} = \frac{U^5}{v_1 v_2} = \frac{X_{15}X_{24}}{X_{14}X_{25}}. \tag{7.3.4}$$

These cross ratios have the simple shift properties $u_{s(i+1)} = u_{si}|_{X_i \to X_{i+1}}$ as we shift the label i of the external scalar fields by one unit. While we mostly work with the snowflake cross ratios, there is one more set of the OPE coordinates $z_1, z_2, \bar{z}_1, \bar{z}_2$ and $\mathcal{X} := 1 - w$ introduced in [65] will also play an important role. In the case of five-point functions, our definition of the OPE limit is

$$\text{OPE}_{12,45} : \bar{z}_1, \bar{z}_2 \ll z_1, z_2 \ll 1, \tag{7.3.5}$$

For the purposes of this paper, it suffices to record the map from snowflake cross ratios to OPE cross ratios near the lightcone limits $\bar{z}_{1,2} \to 0$,

$$u_{s1} = \bar{z}_1 z_1, \quad u_{s4} = \bar{z}_2 z_2, \quad u_{s2} = 1 - z_1 + \mathrm{O}(\bar{z}_1), \quad u_{s3} = 1 - z_2 + \mathrm{O}(\bar{z}_2), \tag{7.3.6}$$

$$u_{s5} = 1 - \frac{z_1 z_2 \mathcal{X}}{(1 - z_1)(1 - z_2)} + \mathrm{O}(\bar{z}_1, \bar{z}_2). \tag{7.3.7}$$

The behavior of conformal blocks in this OPE limit provides boundary conditions which are used to select a particular solution of the differential equations.

At five points, there exists a total number of 15 different channels that are all of the same (comb channel) topology. Here we shall look at one particular pair of channels that is obtained by cyclically shifting the label of the external fields as $i \mapsto i + 1 \mod 5$, see Figure 34. Our convention for the conformal block expansion is

$$\langle \phi(X_1) \ldots \phi(X_5) \rangle = \left(X_{12} X_{45} \sqrt{\frac{X_{23}X_{34}}{X_{24}}} \right)^{-\Delta_\phi} \sum_{\mathcal{O}_1, \mathcal{O}_2, n} P^{(n)}_{\mathcal{O}_1 \mathcal{O}_2} \psi^{(12)3(45)}_{\mathcal{O}_1 \mathcal{O}_2; n}(u_i, v_i, U^5), \tag{7.3.8}$$

where

$$P^{(n)}_{\mathcal{O}_1 \mathcal{O}_2} := C_{\phi\phi\mathcal{O}_1} C^{(n)}_{\mathcal{O}_1 \phi \mathcal{O}_2} C_{\phi\phi\mathcal{O}_2}. \tag{7.3.9}$$

Here $(\mathcal{O}_a)_{a=1,2}$ denote two STT primary fields of weight $\Delta_a = h_a + \bar{h}_a$ and spin $J_a = \bar{h}_a - h_a$. Given the two spin labels J_1 and J_2, the parameter $n = 0, \ldots, \min(J_1, J_2)$ labels the basis of tensor structures of the three-point function in the expansion

$$\langle \mathcal{O}_1(X_1, Z_1)\phi(X_3)\mathcal{O}_2(X_2, Z_2)\rangle = \sum_{n=0}^{\min(J_1,J_2)} C^{(n)}_{\mathcal{O}_1\phi\mathcal{O}_2} \prod_{i<j} X_{ij}^{n_{ij}} J_{1,32}^{J_1} J_{2,31}^{J_2} \mathcal{X}^n, \quad \mathcal{X} := \frac{H_{12}X_{13}X_{23}}{J_{1,32}J_{2,31}}. \tag{7.3.10}$$

This choice of basis is equivalent to fixing the following boundary condition for blocks in the OPE limit, derived in [65],

$$\lim_{z_1,z_2\to 0} \lim_{\bar{z}_1,\bar{z}_2\to 0} \frac{\psi^{(12),(45)}_{\mathcal{O}_1\mathcal{O}_2;n}(z_a, \bar{z}_1, \mathcal{X})}{\prod_{a=1}^2 \bar{z}_a^{h_a} z_a^{\bar{h}_a} \mathcal{X}^n} = 1. \tag{7.3.11}$$

The "1" on the right hand side of (7.3.11) is equivalent to the normalization of the three-point function in eq. (7.3.10), as shown in appendix 7.A.3. With all of our conventions set, the crossing equation we want to analyze takes the form

$$\sum_{\mathcal{O}_1,\mathcal{O}_2,n} P^{(n)}_{\mathcal{O}_1\mathcal{O}_2} \psi^{(51)2(34)}_{\mathcal{O}_1\mathcal{O}_2;n} = \left(\frac{u_{s5}\sqrt{u_{s3}}}{u_{s4}\sqrt{u_{s1}}}\right)^{\Delta_\phi} \sum_{\mathcal{O}_1,\mathcal{O}_2,n} P^{(n)}_{\mathcal{O}_1\mathcal{O}_2} \psi^{(12)3(45)}_{\mathcal{O}_1\mathcal{O}_2;n}. \tag{7.3.12}$$

Up to relabeling, this is the same planar crossing equation as in [67, Sec. 3.1]. To evaluate the constraints that arise from this CSE we shall consider a regime in which

$$X_{15} \ll X_{34} \ll X_{23} \ll X_{12} \ll X_{45} \ll 1, \tag{7.3.13}$$

i.e. we make pairs of points lightlike separated in the order that is given by reading the previous line from left to right. As we discussed in the previous section, this amounts to introducing an order

$$\vec{\epsilon} = (\epsilon_{15}, \epsilon_{34}, \epsilon_{23}, \epsilon_{12}, \epsilon_{45}).$$

With respect to this prescription, the cross ratios u_{si} are of order $\mathrm{O}(\epsilon_{i(i+1)})$. At the same time, the transition between direct and crossed channel is also easy to express in terms of these cross-ratios u_{si}.

$$\psi^{(12)3(45)}(u_{si}) = \psi^{(15)2(34)}(u_{s(i-1)}) \tag{7.3.14}$$

We conclude that, for the crossing equation we are about to study, the cross-ratios u_{si} are the perfect generalization of the cross ratios u, v we used in the discussion of four-point functions. Once again, the duality between the two channels corresponds to a cyclic permutation of the cross ratios and each of the cross ratios has unit order with respect to exactly one of the order parameters ϵ_{ij} we are taking to zero. On the other hand, the cross ratios u_{si} are simple rational functions of our polynomial cross ratios. Hence, when expressed in terms of the u_{si} all terms in the Casimir differential operators possess some definite $\vec{\epsilon}$-order.

7.3.2 Lightcone blocks: general strategy

This subsection will outline our general strategy in determining all relevant lightcone blocks. To a large extent, this mimics the strategy we outlined for four points. However, the additional degree of freedom arising from tensor structures at the middle vertex causes some new challenges, particularly when it comes to normalizing the blocks.

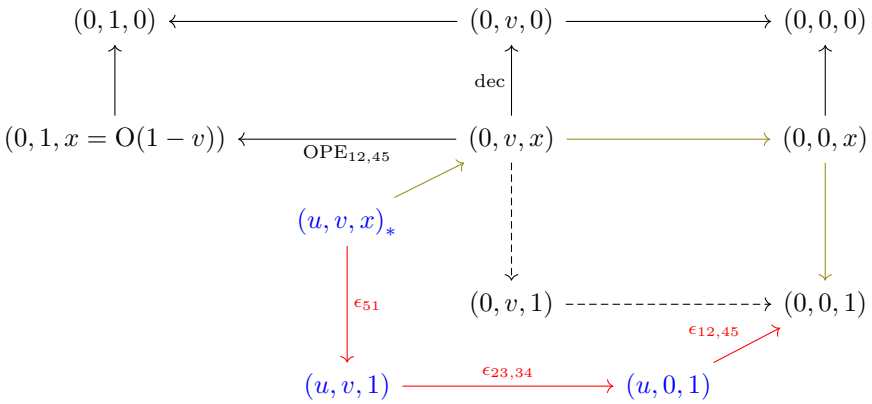

Figure 35: Diagrammatic representation of lightcone limits in five-point cross ratio space with $u \equiv u_{s1,4}$, $v \equiv u_{s2,3}$, $x = 1 - u_{s5}$. The cross ratios u_{s1}, u_{s4} (respectively u_{s2}, u_{s3}) are grouped together because they are mapped to one another under the $\mathbb{Z}_2$ symmetry of the (12)3(45) OPE diagram that exchanges its internal legs. Part of our approach hinges on the property that the same point $(0, 0, 1)$ can be reached from different paths, most importantly $\vec{\epsilon} := (\epsilon_{51}, \epsilon_{23,34}, \epsilon_{12,45})$ in red and $\vec{\epsilon}\,' := (\epsilon_{12,45}, \epsilon_{23,34}, \epsilon_{51})$ in green. We will also refer to this diagram for lightcone limits of the direct channel blocks (51)2(34), by exploiting the cyclic permutation (7.3.14) in snowflake cross ratios, mapping the order of limits $\vec{\epsilon}$ to the order of limits $\vec{\epsilon}\,'$.

In order to place all relevant limits of cross ratios on a single map, we shall group them as $u = \{u_{s1}, u_{s4}\}$, $v = \{u_{s2}, u_{s3}\}$ and also introduce $x = 1 - u_{s5}$. These three groups can be understood as orbits under the $\mathbb{Z}_2$ symmetry that exchanges the internal legs of the (12)3(45) OPE diagram. Once we have formed these three groups, we can draw a three-dimensional map for the space of cross ratios, see Fig. 35. The black vertices in this diagram label points in the $u = 0$ plane while the blue vertices have $u \neq 0$, with v varying along the horizonal while x varies along the vertical. We have marked the generic point with cross ratios (u, v, x) by an index $*$. The lightcone limit we explore below corresponds to the vertex $(0, 0, 1)$ in the figure. In the crossed channel we reach this point from generic cross ratios by going along the red arrows. In order to picture the direct channel limit within the same diagram we have shifted the entries in the order $\vec{\epsilon}$ by one unit, i.e. we defined $\vec{\epsilon}\,' = (\epsilon_{12}.\epsilon_{45}, \epsilon_{34}, \epsilon_{23}, \epsilon_{15}) = \vec{\epsilon}|_{i\to i+1}$ while keeping the cross ratios unaltered. This is of course equivalent to the direct channel limit in which we rotate the cross ratios while keeping the $\vec{\epsilon}$-order fixed.

In the next subsections we will compute the Casimir differential operators in the lightcone limit, i.e. near the point $(0, 0, 1)$, and find explicit solutions. As an illustration, we represent the successive

lightcone limits $H = \frac{1}{2}\mathcal{D}^2_{12,45} - \lambda_{1,2}$ in the diagram below.

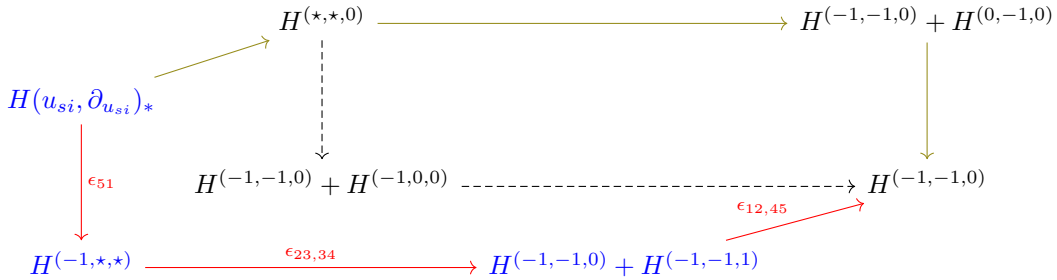

(7.3.15)

At this stage, in order to select the relevant linear combination of solutions and normalize it appropriately, we need to make contact with the OPE limit —the point $(0, 1, x)$ on the left side of Fig. 35. In the four-point case, where there is no analogue of the x variable, we showed two possible ways to achieve this: either by solving the differential equations for any $(0, v)$ and interpolating $v = 0$ with $v = 1$, or by direct evaluation of the already-normalized integral representation of lightcone blocks at $v = 0$. In the five-point case, we will combine both of these approaches to obtain control over the extra degree of freedom x. We start by computing differential operators in the *decoupling* limit, at the end of the arrow labeled "dec" in Fig. 35. There, the differential equations can be solved exactly in terms of a product of hypergeometric functions in the v variables, and normalized with the OPE limit. Next, we insert the $\phi \times \phi$ lightcone OPE formula (3.3.18) as $\langle(\phi\phi)\phi(\phi\phi)\rangle$ to deduce an integral representation for five-point blocks, valid in the whole $(0, v, x)$ region. Finally, to interpolate the OPE limit $(0, 1, x)$ with the lightcone limit $(0, 0, 1)$, we use the exact solution in the decoupling limit as a fulcrum, and the integral formula as a lever. This translates to an explicit power series expansion of blocks around the decoupling limit $x = 0$. While the expansion is difficult to evaluate at general points in the $(0, v, x)$ plane, comparing it with our knowledge of the asymptotics from limits of differential operators suffices to extract the desired normalization.

In order to state the results, it will be useful to make the redefinition

$$\psi^{(12)3(45)}_{\mathcal{O}_1\mathcal{O}_2;n}(u_{si}) = \omega^{(12)3(45)}_{\mathcal{O}_1\mathcal{O}_2;n}(u_{si})\, F^{(12)3(45)}_{\mathcal{O}_1\mathcal{O}_2;n}(u_{si}), \quad \text{where} \tag{7.3.16}$$

$$\omega^{(12)3(45)}_{\mathcal{O}_1\mathcal{O}_2;n}(u_{si}) = u_{s1}^{h_1} u_{s4}^{h_2} (u_{s2}u_{s3})^{h_\phi} (1-u_{s2})^{J_1-n} (1-u_{s3})^{J_2-n} (1-u_{s5})^n. \tag{7.3.17}$$

The function F now satisfies

$$\lim_{z_1,z_2\to 0} \lim_{\bar{z}_1,\bar{z}_2\to 0} F^{(12),(45)}(u_{si}) = 1, \qquad \lim_{u_{s1,4}\to 0} F^{(12),(45)} = f_1^{\text{dec}}(u_{s2}) f_2^{\text{dec}}(u_{s3}), \tag{7.3.18}$$

where

$$f_a^{\text{dec}}(v) = {}_2F_1\left[\begin{matrix}\bar{h}_a, \bar{h}_a - h_{b\phi} - n \\ 2\bar{h}_a\end{matrix}\right](1-v), \quad a \neq b = 1, 2. \tag{7.3.19}$$

The limit on the left of (7.3.18) is the OPE limit boundary condition "$\text{OPE}_{12,45}$" given in eq. (7.3.11), while the limit on the right is the decoupling limit "dec" in Fig. 35. In this latter case, the limits of the Casimir equations for $\mathcal{D}^2_{12}$ and $\mathcal{D}^2_{45}$ reduce to one-variable differential equations in u_{s2} and u_{s3} respectively, with solutions (7.3.19) normalized by the OPE limit. On the other hand, the integral representation derived from the lightcone OPE is given in eq. (7.A.8) of appendix 7.A. From there, we derive a power series expansion in x by expanding the integrand around $x = 1 - u_{s5} = 0$, leading to

the expression (7.A.19). This expression evaluates to the triple-sum power series expansion (7.A.20) in x, which is still quite complicated to manipulate in general. However, in all regimes of the direct and crossed channels where the cross ratios $v = (v_1, v_2)$ are small, solutions to the differential equations have *factorized* coefficients in their x-expansion, i.e.

$$F^{(12),(45)}_{\mathcal{O}_1\mathcal{O}_2;n} \sim \sum_{\eta\geq n}(1-u_{s\bar{5}})^{\eta-n}\,\langle\eta|n\rangle\, f_{1,\eta}(u_{s2})f_{2,\eta}(u_{s3}), \tag{7.3.20}$$

for some ranges of η and some functions $f_{a,\eta}(v)$ that will be derived below. Comparing with the exact integral formula (see appendix 7.A.2 for more details), we find this factorization of coefficients to coincide with a collapse of the triple-sum to a single sum in the x-expansion, resulting in the explicit expression

$$F^{(12)3(45)}_{(h_a,\bar{h}_a;n)}(u_{si}) \;\sim\; \mathcal{Q}\left((1-x\mathcal{S}_1(\vartheta_{u_{s2}})\mathcal{S}_2(\vartheta_{u_{s3}}))^{h_\phi-\bar{h}_1-\bar{h}_2}\right) f_1^{\text{dec}}(u_{s2})f_2^{\text{dec}}(u_{s3}), \tag{7.3.21}$$

$$\text{where}\quad \mathcal{Q}\left(\mathcal{S}_a(\vartheta)^k\right) := \frac{(h_{b\phi}+n+\vartheta)_k}{(h_{b\phi}+n+\bar{h}_a)_k}, \quad a\neq b=1,2, \quad k\in\mathbb{Z}_+, \tag{7.3.22}$$

and $\vartheta_u = u\partial_u$ is the Euler operator, as before. In order to evaluate the first line, we first expand the argument of $\mathcal{Q}$ as a power series in $x\mathcal{S}_1\mathcal{S}_2$ and then apply the 'quantization map' $\mathcal{Q}$ defined in the second line in order to express powers of the commuting objects $\mathcal{S}_1$ and $\mathcal{S}_2$ as differential operators that act on $v_1 = u_{s2}$ and $v_2 = u_{s3}$. In appendix 7.A.3, we go over all relevant regimes in which the approximation (7.3.21) holds, and verify that it includes the desired lightcone limit $(0,0,1)$ of direct and crossed channel blocks. Ultimately, the formula (7.3.21) is much more amenable to evaluations than the triple-sum expression of eq. (7.A.20) for generic values of v_1 and v_2.

Before we conclude this discussion, let us also recall that the limit of direct channel blocks (green path) passes through the $u = 0$ regime, while the limit of crossed channel blocks (red path) only enters this regime at the endpoint $(0,0,1)$. To normalize the crossed channel blocks, we will therefore make use of the Gaudin differential operators as a means to compare different orders of limits with the same leading behavior. This same feature already appeared in our discussion of four-point blocks.

7.3.3 Lightcone blocks in the direct channel

As in the four-point case that began this discussion, we shall perform the lightcone limit of the five-point blocks for the direct channel in two stages, starting with

$$X_{15} \ll X_{34} \ll X_{23} \ll X_{12} \ll 1\ . \tag{7.3.23}$$

The limit $X_{45}\to 0$ will be performed at the end. In terms of the cross ratios u_{si} this means that we will first study the partial light cone limit

$$LCL^{(1)}_{\vec{\epsilon}}: \quad u_{s5} \ll u_{s3} \ll u_{s2} \ll u_{s1} \ll 1$$

leaving the limit $u_{s4} \to 0$ for the second stage. Let us first display the leading terms of the two quadratic Casimir operators for direct channel blocks in the partial light cone limit $LCL^{(1)}_{\vec{\epsilon}}$,

$$\mathcal{D}^{2,\vec{\epsilon}}_{15} = \epsilon^0_{15}\left\{\epsilon^{-1}_{12}\mathcal{D}^{(0,0,0,-1)}_{15} + \mathrm{O}(\epsilon^0_{12})\right\} + \mathrm{O}(\epsilon_{15}) \tag{7.3.24}$$

$$\mathcal{D}^{(0,0,0,-1)}_{15} = \left(\partial_{u_{s1}} - \frac{u_{s3}}{u_{s1}}\partial_{u_{s3}} + \frac{1-u_{s4}}{u_{s1}}\partial_{u_{s4}}\right)(u_{s1}\partial_{u_{s1}} - h_\phi)\,, \tag{7.3.25}$$

$$\mathcal{D}^{2,\vec{\epsilon}}_{34} = \epsilon^0_{34}\left\{\epsilon^{-1}_{23}\mathcal{D}^{(0,0,-1,0)}_{34} + \mathrm{O}(\epsilon^0_{23})\right\} + \mathrm{O}(\epsilon_{34}), \tag{7.3.26}$$

$$\mathcal{D}^{(0,0,-1,0)}_{34} = \left(\partial_{u_{s2}} - \frac{u_{s5}}{u_{s2}}\partial_{u_{s5}} + \frac{1-u_{s4}}{u_{s2}}\partial_{u_{s4}}\right)(u_{s2}\partial_{u_{s2}} - h_\phi)\ . \tag{7.3.27}$$

At this stage, we can already observe that both differential operators at this order simultaneously commute with the three Euler operators

$$\vartheta_{u_{s5}}, \vartheta_{u_{s3}}, \vartheta_{1-u_{s4}} \in \mathcal{C}(\mathcal{D}^2_{15}, \mathcal{D}^2_{34}), \quad \vartheta_x := x\partial_x. \tag{7.3.28}$$

Working in a basis of eigenfunctions of these three operators, we know that $\psi^{(51),(34)}_{\mathcal{O}_1\mathcal{O}_2;n} \propto u^{h_1}_{s5}u^{h_2}_{s3}$ from the OPE limit boundary condition (7.3.11), where h_1, h_2 are the half-twists at the first and second internal leg. Furthermore, we can connect the $x = 1-u_{s4} \to 0$ limit to the decoupling limit in the $(0, v, x)$ plane of Fig. 35. This implies that the eigenvalues of $\vartheta_{1-u_{s4}}$ are bounded below by n. In summary, the two Casimirs can be diagonalized by functions of the form

$$F^{(15),(34)}_{(h_a,\bar{h}_a;n)}(u_{si}) \overset{LCL^{(1)}_{\vec{\epsilon}}}{\sim} \sum_{k=0}^{\infty}\langle n+k|n\rangle\,(1-u_{s4})^k g_{(h_a,\bar{h}_a;n),k}(u_{s1},u_{s2}), \tag{7.3.29}$$

where $F = \omega^{-1}\psi$ is defined by (7.3.16). Now, assuming the eigenvalues of the two second order Casimir operators do *not* scale with $\epsilon_{12}, \epsilon_{23}$, the functions g must lie in the kernel of $\mathcal{D}^{(0,0,0,-1)}_{15}$ and $\mathcal{D}^{(0,0,-1,0)}_{34}$, which is easily solved by

$$g_{(h_a,\bar{h}_a;n),k}(u_{s1},u_{s2}) \sim \left(1 \text{ or } \log u_{s1} \text{ or } u_{s1}^{h_{2\phi}+n+k}\right)\left(1 \text{ or } \log u_{s2} \text{ or } u_{s2}^{h_{1\phi}+n+k}\right). \tag{7.3.30}$$

More specifically, for $a \neq b = 1, 2$ and $h_{a\phi} := h_a - h_\phi$, the logarithm of u_{sb} is only allowed when $h_{a\phi} + n + k = 0$. Obviously, the constant function in the variable $u_{s1}[u_{s2}]$ dominates for small values of $u_{s1}[u_{s2}]$ whenever the exponent of $u_{s1}[u_{s2}]$ is positive. This motivates us to introduce the following family of functions

$$f_\beta(v) = \begin{cases} v^\beta, & \text{if} \quad \beta < 0, \\ \log v, & \text{if} \quad \beta = 0, \\ 1, & \text{if} \quad \beta > 0. \end{cases} \tag{7.3.31}$$

It is now easy to spell out the leading behavior of the eigenfunctions g as we send the two variables u_{s1} and u_{s2} to zero

$$g_{(h_a,\bar{h}_a;n),k}(u_{s1},u_{s2}) \sim f_{n+k+h_{2\phi}}(u_{s1})f_{n+k+h_{1\phi}}(u_{s2}). \tag{7.3.32}$$

Now, plugging this back into the expansion (7.3.29), we recognize two distinct cases

$(-,0)$ When $h_{b\phi} + n \leq 0$ for some $b \neq a = 1$ or 2, all higher powers $k \geq 0$ will be *subleading* in $u_{s(a+1)}$. In this case, $F \sim \langle n|n\rangle\, f_{n+h_{2\phi}}f_{n+h_{1\phi}}$.

(+) On the other hand, when $h_1, h_2 > h_\phi - n$, the leading asymptotics $g_{(h_a,\bar{h}_a;n),k}(u_{s1}, u_{s2}) \sim 1$ are independent of k and we obtain a power series in $1-u_{s4}$. In this case, $F \sim \sum_{k\geq 0} \langle n+k|n\rangle (1-u_{s4})^k$.

Later in the text, we may sometimes use the parameters

$$\alpha_1 = h_2 - h_\phi \quad , \quad \alpha_2 = h_1 - h_\phi \ . \tag{7.3.33}$$

Finally, in the full null polygonal limit (7.3.13) where $u_{s4} \sim X_{45} \to 0$,

$$\mathcal{D}_{15}^{(0,0,0,-1)} = \epsilon_{45}^{-1}\partial_{u_{s4}}\left(\partial_{u_{s1}} - \frac{h_\phi}{u_{s1}}\right) + \mathrm{O}(\epsilon_{45}^0),$$
$$\mathcal{D}_{34}^{(0,0,0,-1)} = \epsilon_{45}^{-1}\partial_{u_{s4}}\left(\partial_{u_{s3}} - \frac{h_\phi}{u_{s3}}\right) + \mathrm{O}(\epsilon_{45}^0).$$

Taking the u_{s4}^0 term in the expansion (7.3.29) puts F in the common kernel of these leading operators, so it suffices to evaluate the block at $u_{s4} = 0$. Ultimately, in all cases $(-,0,+)$ described above, the asymptotics of blocks in the direct channel then take the form

$$F^{(15),(34)}_{(h_a,\bar{h}_a;n)}(u_{si}) \overset{LCL_{\vec{\epsilon}}}{\sim} \mathcal{N}_{\mathcal{O}_1\mathcal{O}_2;n} f_{n+h_{2\phi}}(u_{s2}) f_{n+h_{1\phi}}(u_{s1}). \tag{7.3.34}$$

To obtain the normalization, we note that the functions $f_a^{\mathrm{dec}}(v)$ (see (7.3.19)) in the decoupling limit have the same asymptotics as (7.3.34). Comparing the $(0,0,1-u_{s5})$ asymptotics we derived in this subsection with the formula (7.3.21), we see that $\mathcal{S}_a(\vartheta_v) f_a^{\mathrm{dec}}(v)$ is subleading when $h_{a\phi} + n \leq 0$, and $\mathcal{S}_a^k(\vartheta_v) f_a^{\mathrm{dec}}(v) = \mathcal{S}_a^k(0) f_a^{\mathrm{dec}}(0)$ at leading order when $h_a > h_\phi - n$. As a result, we obtain

$$\mathcal{N}_{\mathcal{O}_1\mathcal{O}_2;n} = \begin{cases} \prod\limits_{a\neq b} \frac{\Gamma(2\bar{h}_a)}{\Gamma(\bar{h}_a)\Gamma(\bar{h}_a+|h_{b\phi}+n|)} \mathring{\Gamma}(|h_{a\phi}+n|), & \text{if} \quad \exists\, a = 1,2,\ h_{a\phi}+n \leq 0 \\ {}_3F_2\left[\begin{matrix} \bar{h}_{12;\phi} & h_{1\phi}+n, & h_{2\phi}+n \\ & \bar{h}_1+h_{2\phi}+n, & \bar{h}_2+h_{1\phi}+n \end{matrix}\right](1) \prod\limits_{a\neq b} \frac{\Gamma(2\bar{h}_a)\Gamma(h_{b\phi}+n)}{\Gamma(\bar{h}_a)\Gamma(\bar{h}_a+h_{b\phi}+n)} & \text{otherwise.} \end{cases} \tag{7.3.35}$$

For the first case, we define the function $\mathring{\Gamma} : \mathbb{R}_{\geq 0} \mapsto \mathbb{R}_{>0}$ by $\mathring{\Gamma}(x) := \Gamma(x)$ when $x > 0$ and $\mathring{\Gamma}(0) := 1$.

7.3.4 Lightcone blocks in the crossed channel

Let us now study the Casimir operators $\mathcal{D}_{12}^2$ and $\mathcal{D}_{45}^2$ for the crossed channel blocks. To leading $\vec{\epsilon}$-order these read

$$\mathcal{D}_{12}^{2,\vec{\epsilon}} = \frac{1}{\epsilon_{15}}\left(\epsilon_{34}^0\left(\frac{1}{\epsilon_{23}}\left(\epsilon_{12}^0\epsilon_{45}^0\mathcal{D}_{12}^{(-1,0,-1)} + \mathrm{O}(\epsilon_{12})\right) + \mathrm{O}(\epsilon_{23}^0)\right) + \mathrm{O}(\epsilon_{15}^0)\right), \tag{7.3.36}$$

$$\mathcal{D}_{12}^{(-1,0,-1)} = \left(\partial_{u_{s2}} - \frac{h_\phi}{u_{s2}}\right)\partial_{u_{s5}}, \tag{7.3.37}$$

$$\mathcal{D}_{45}^{2,\vec{\epsilon}} = \frac{1}{\epsilon_{15}}\left(\frac{1}{\epsilon_{34}}\epsilon_{23}^0\left(\epsilon_{12}^0\epsilon_{45}^0\mathcal{D}_{12}^{(-1,-1,0)} + \mathrm{O}(\epsilon_{56})\right) + \mathrm{O}(\epsilon_{34}^0)\right) + \mathrm{O}(\epsilon_{15}^0), \tag{7.3.38}$$

$$\mathcal{D}_{45}^{(-1,-1,0)} = \left(\partial_{u_{s3}} - \frac{h_\phi}{u_{s3}}\right)\partial_{u_{s5}}. \tag{7.3.39}$$

Since all the terms we spelled out have vanishing order with respect to $\epsilon_{12}, \epsilon_{45}$ we only displayed the valued of the three non-vanishing orders, i.e. the superscript on the right hand side only gives the values of $(\epsilon_{15}, \epsilon_{34}, \epsilon_{23})$. Let us also note that the leading terms of the two Casimir operators commute with the Euler operators $\vartheta_{si}, i = 1, 4, 5$ for the cross ratios u_{s1}, u_{s4} and with the derivative $\partial_{u_{s5}}$. In particular, just like in the direct channel, we may set the asymptotics $\psi^{(12),(45)}_{(\bar{h}_a, h_a; n)} \propto u_{s1}^{h_1} u_{s4}^{h_2}$ from the OPE boundary condition (7.3.11).

We now want to study solutions to the leading terms in the crossed channel Casimir differential equations

$$\mathcal{D}^2_{12}\psi^{(12)3(45)}_{(\mathcal{O}_1,\mathcal{O}_2;n)}(u_{si}) = 2\lambda_1\psi^{(12)3(45)}_{(\mathcal{O}_1,\mathcal{O}_2;n)}(u_{si}) \quad , \quad \mathcal{D}^2_{45}\psi^{(12)3(45)}_{(\mathcal{O}_1,\mathcal{O}_2;n)}(u_{si}) = 2\lambda_2\psi^{(12)3(45)}_{(\mathcal{O}_1,\mathcal{O}_2;n)}(u_{si}) \tag{7.3.40}$$

But as before we need to make some assumption about the scaling behavior of the eigenvalues. If we assume that the Casimirs eigenvalues are of vanishing $\vec{\epsilon}$-order, then we obtain the same asymptotics as in the discussion of the direct channel. For our analysis of the crossing equations, however, two other regimes turn out to be relevant.

Case (I). The eigenvalues λ_1 and λ_2 introduced in eqs. (7.3.40) behave as

$$\lambda_1 = \mathrm{O}(\epsilon_{15}^{-1}\epsilon_{23}^{-1}), \quad \lambda_2 = \mathrm{O}(\epsilon_{15}^{-1}\epsilon_{34}^{-1}). \tag{7.3.41}$$

Case (II). One Casimir eigenvalue, say λ_1 for definiteness, is only of subleading order,

$$\lambda_1 = \mathrm{O}(\epsilon_{15}^{-1}), \quad \lambda_2 = \mathrm{O}(\epsilon_{15}^{-1}\epsilon_{34}^{-1}). \tag{7.3.42}$$

Let us first deal with case (I). Having already established the asymptotics in u_{s1}, u_{s4}, we can further diagonalize both Casimirs in a basis of eigenfunctions of $\partial_{u_{s5}}$ with eigenvalues $-\eta$, along with a power law prefactor in u_{s2}, u_{s3} stripped off for later convenience,

$$\psi^{(12)3(45)}_{(h_a,\bar{h}_a;n)}(u_{si}) \sim u_{s1}^{h_1} u_{s4}^{h_2} (u_{s2}u_{s3})^{h_\phi} \sum_{\eta \geq n} \langle \eta | n \rangle \, e^{-\eta u_{s5}} g_{(h_a,\bar{h}_a;n)}(u_{s2}, u_{s3}). \tag{7.3.43}$$

For the argument ηu_{s5} of the exponential to be finite as ϵ_{15} goes to zero, the eigenvalue η must also scale as

$$\eta = \mathrm{O}(\epsilon_{15}^{-1}) \ . \tag{7.3.44}$$

Apart from this, we simply note for the moment that $\vartheta_{1-u_{s5}} = -\partial_{u_{s5}} + \mathrm{O}(\epsilon_{15}^0)$, such that the two eigenbases coincide in the (15) lightcone limit and $\eta \geq n$ in the expansion (7.3.43). In the meantime, let us turn to the non-trivial functions $g(u_{s2}, u_{s3})$ of the two remaining cross ratios $v_1 = u_{s2}$ and $v_2 = u_{s3}$. For these functions, the two Casimir equations reduce to the following set of linear differential equations

$$\eta\partial_{u_{s2,3}} g_{h_a,\bar{h}_a;\eta}(u_{s2}, u_{s3}) = -\lambda_{1,2} g_{h_a,\bar{h}_a;\eta}(u_{s2}, u_{s3}) \Longrightarrow g_{h_a,\bar{h}_a;\eta}(u_{s2}, u_{s3}) \sim e^{-\frac{\lambda_1 u_{s2} + \lambda_2 u_{s3}}{\eta}}. \tag{7.3.45}$$

Let us stress that the argument of the exponential function is finite as we send $\epsilon_{15}, \epsilon_{23}$ and ϵ_{34} to zero. Indeed, by assumption λ_1 is of order $\mathrm{O}(\epsilon_{15}^{-1}\epsilon_{23}^{-1})$ which is the same as for the ratio $u_{s2}^{-1}\eta$ and similarly for the term involving λ_2. All in all, with the most general hypothesis that n can scale with ϵ_{15}, the function $F = \omega^{-1}\psi$ in (7.3.16) takes the form

$$F^{(12),(45)}_{\mathcal{O}_1\mathcal{O}_2;n} \sim \sum_{\eta \geq n} \langle \eta | n \rangle \, e^{(n-\eta)u_{s5} - \frac{\lambda_1 u_{s2} + \lambda_2 u_{s3}}{\eta}}. \tag{7.3.46}$$

In the case of four-point functions, we pointed out that the leading terms of the crossed channel Casimir operators in the limit where $u \ll v$ coincide with the leading terms of the direct channel Casimir operators with u and v exchanged. Here, to determine the matrix elements $\langle\eta|n\rangle$ in the $\partial_{u_{s5}}$ eigenbasis, we can exploit the same property for five-point Casimirs. More specifically, the leading differential operators are the same in both the ordering $\vec{\epsilon} = (\epsilon_{15}, \epsilon_{23,34}, \epsilon_{12,45})$ and $\vec{\epsilon}\,' = (\epsilon_{12,45}, \epsilon_{23,34}, \epsilon_{15})$, of limits, i.e.

$$\lim_{\epsilon_{12,45}\to 0}\lim_{\epsilon_{23,34}\to 0}\lim_{\epsilon_{15}\to 0}\epsilon_{15}\epsilon_{23,34}\left(\mathcal{D}^{2,\vec{\epsilon}}_{12,45}-2\lambda_{1,2}\right)=\lim_{\epsilon_{15}\to 0}\lim_{\epsilon_{23,34}\to 0}\lim_{\epsilon_{12,45}\to 0}\epsilon_{15}\epsilon_{23,34}\left(\mathcal{D}^{2,\vec{\epsilon}}_{12,45}-2\lambda_{1,2}\right). \tag{7.3.47}$$

The left hand side is the red path $\vec{\epsilon}$ in the diagram (7.3.15), while the right hand side is the green path $\vec{\epsilon}\,'$ in (7.3.15), with the same scaling of λ_1, λ_2, n in both cases. On the right hand side, we can obtain the asymptotics (7.3.46) from the expansion of lightcone blocks ($u_{s1,4} \to 0$) around the decoupling limit, see (7.3.21). In the $u_{s2,3} \to 0$, we see that the x-dependent factor of that formula is subleading because $\mathcal{S}_a^k = \mathrm{O}(\bar{h}_a^{-k})$, so only the $\eta = n$ term survives. At the same time, the only way to retrieve non-trivial asymptotics in $\lambda_{1,2}u_{s2,3}$ from the formula (7.3.21) is to impose $n = \mathrm{O}(\epsilon_{15}^{-1})$. In this case,

$$\langle\eta|n\rangle = \delta_{\eta n}\mathcal{N}^{\mathrm{LS,I}}_{\mathcal{O}_1\mathcal{O}_2;n},\quad \mathcal{N}^{\mathrm{LS,I}}_{\mathcal{O}_1\mathcal{O}_2;n} = \frac{1}{2n}\left(\frac{n}{e}\right)^{2n} n^{h_1+h_2-2h_\phi}\prod_{a\neq b}4^{\bar{h}_a}\bar{h}_a^{\frac{1}{2}-(h_{b\phi}+n)}. \tag{7.3.48}$$

Note that we have written the normalization including terms of order $\mathrm{O}(1)$. To understand the normalization in a simple way, note that we retrieve the asymptotics $F \sim$ const of the direct channel blocks with $h_1, h_2 > h_\phi - n$ (7.3.34) in the limit $\bar{h}_1^2 u_{s2}, \bar{h}_2^2 u_{s3} \ll n \ll u_{s5}^{-1}$ after the replacement $u_{si} \to u_{s,i-1}$. Therefore, one can check that the above normalization is obtainable as

$$\mathcal{N}^{\mathrm{LS,I}}_{\mathcal{O}_1\mathcal{O}_2;n} = \lim_{n\to\infty}\lim_{\bar{h}_a\to\infty}\mathcal{N}_{\mathcal{O}_1\mathcal{O}_2;n} = \lim_{n\to\infty}\lim_{\bar{h}_a\to\infty}\prod_{a\neq b}\frac{\Gamma(2\bar{h}_a)\Gamma(h_{b\phi}+n)}{\Gamma(\bar{h}_a)\Gamma(\bar{h}_a+h_{b\phi}+n)}, \tag{7.3.49}$$

where $\mathcal{N}_{\mathcal{O}_1\mathcal{O}_2;n}$ is given in (7.3.35), and lim is a shorthand for taking the leading term in the Stirling formula for the Gamma functions[6]. In conclusion, the crossed channel blocks in the limiting regime $LCL_{\vec{\epsilon}}$ are given by

$$\psi^{(12)3(45)}_{(h_a,\bar{h}_a;n)}(u_{si}) \overset{LCL_{\vec{\epsilon}}}{\sim} \mathcal{N}^{\mathrm{LS,I}}_{(h_a,\bar{h}_a;n)}u_{s1}^{h_1}u_{s4}^{h_2}(u_{s2}u_{s3})^{h_\phi}e^{-nu_{s5}-\frac{\bar{h}_1^2u_{s2}+\bar{h}_2^2u_{s3}}{n}}. \tag{7.3.50}$$

In case (II), we must expand the Casimir operator $\mathcal{C}_{12}^2$ to the next-to-leading order in ϵ_{23}. The relevant additional term

$$\mathcal{D}_{12}^{(-1,0,0)} = \partial_{u_{s5}}\left(u_{s5}\partial_{us5} - u_{s2}\partial_{u_{s2}} - u_{s3}\partial_{u_{s3}}\right) \tag{7.3.51}$$

does still commute with the Euler operators ϑ_{s1} and ϑ_{s4} for the cross ratios u_{s1} and u_{s4}. On the other hand, it does not commute with the derivative $\partial_{u_{s5}}$. The dependence of the block on the variables u_{s1} and u_{s4} is determined by the eigenvalues h_1 and h_4 of the Euler operators ϑ_{s1} and ϑ_{s4}, i.e.

$$F^{(12)3(45)}_{\mathcal{O}_1\mathcal{O}_2;n}(u_{si}) \sim F_{(h_a,\bar{h}_a;n)}(u_{s2},u_{s3},u_{s5}). \tag{7.3.52}$$

To fix the dependence of the functions g on the remaining variables we need to consider the eigenvalue equations

$$\mathcal{D}_{12}^{(-1,0,*)} : \partial_{u_{s5}}\left(u_{s5}\partial_{us5} + (1-u_{s2})\partial_{u_{s2}} - u_{s3}\partial_{u_{s3}} + J_1 - n - h_\phi\right)F_{(h_a,\bar{h}_a;n)} = \lambda_1 F_{(h_a,\bar{h}_a;n)} \tag{7.3.53}$$

$$\mathcal{D}_{45}^{(-1,-1,0)} : \partial_{u_{s5}}\partial_{u_{s3}}F_{(h_a,\bar{h}_a;n)} = \lambda_2 F_{(h_a,\bar{h}_a;n)}. \tag{7.3.54}$$

[6] In particular, one can check that ${}_3F_2(1) \sim 1$ in the large $\bar{h}_1, \bar{h}_2$ limit of the normalization formula (7.3.35).

Note that we have written these terms as differential operators for the function F, i.e. after taking out a factor $u_{s3}^{h_\phi}(1-u_{s2})^{J_1-n}$. This is why the operator $\mathcal{D}_{45}^{(-1,-1,0)}$ in the previous expressions looks different from the expression we stated in eq. (7.3.39). We observe that the two operators commute with the Euler operator $\vartheta_{1-u_{s2}} = (1-u_{s2})\partial_{u_{s2}}$. This suggests to expand the functions g as

$$F_{(h_a,\bar{h}_a;n)}(u_{s2},u_{s3},u_{s5}) = \sum_\mu \langle \mu|n\rangle\,(1-u_{s2})^\mu F^\mu_{(h_a,\bar{h}_a;n)}(u_{s3},u_{s5})\ .$$

Inserting this ansatz into our eigenvalue equations and using the notation $J_1 - n := \delta n$ we obtain the following differential equations

$$\mathcal{D}_{12}^{(-1,0,*)} : \partial_{u_{s5}}\left(u_{s5}\partial_{us5} - u_{s3}\partial_{u_{s3}} + \mu + \delta n - h_\phi\right) F^\mu_{(h_a,\bar{h}_a;n)}(u_{s3},u_{s5}) = \lambda_1 F^\mu_{(h_a,\bar{h}_a;n)}(u_{s3},u_{s5}) \tag{7.3.55}$$

$$\mathcal{D}_{45}^{(-1,-1,0)} : \partial_{u_{s5}}\partial_{u_{s3}} F^\mu_{(h_a,\bar{h}_a;n)}(u_{s3},u_{s5})(u_{s3},u_{s5}) = \lambda_2 F^\mu_{(h_a,\bar{h}_a;n)}(u_{s3},u_{s5}). \tag{7.3.56}$$

We solve the first equation by making an ansatz as a power series in the variable u_{s3} of the form

$$F^\mu_{(h_a,\bar{h}_a;n)}(u_{s3},u_{s5}) \propto g_{(h_a,\bar{h}_a;\mu)}(u_{s3},u_{s5}) = \sum_{\nu=0}^\infty f_\nu u_{s3}^\nu \psi^{(\nu),\mu}_{\lambda_1}(\lambda_1 u_{s5}). \tag{7.3.57}$$

Plugging this ansatz into the first eigenvalue equation we obtain a differential equation for the functions $\psi^{(\nu),\mu}_{\lambda_1}$,

$$\left(\partial_x x\partial_x - (h_\phi - \mu - \delta n + \nu)\partial_x\right)\psi^{(\nu),\mu}_{\lambda_1}(x) = \psi^{(\nu),\mu}_{\lambda_1}(x)$$

This equation is solved by the functions

$$\psi^{(\nu),\mu}_{\lambda_1}(x) = \lambda_1^{-\frac{h_\phi-\mu-\delta n+\nu}{2}}\mathcal{K}_{-h_\phi+\mu+\delta n-\nu}(x) \tag{7.3.58}$$

Here, we have included a λ_1-dependent prefactor for convenience and $\mathcal{K}_\alpha(x)$ denotes the modified Bessel-Clifford function, which has an integral representation of the form

$$\mathcal{K}_\alpha\left(\frac{y^2}{4}\right) = \left(\frac{y}{2}\right)^{-\alpha} K_\alpha(y) = \frac{1}{2}\int_0^\infty \frac{\mathrm{d}t}{t^{\alpha+1}} e^{-t-\frac{y^2}{4t}}. \tag{7.3.59}$$

The modified Bessel-Clifford function satisfies the fundamental property

$$\frac{\mathrm{d}^n}{\mathrm{d}x^n}\mathcal{K}_\alpha(x) = \mathcal{K}_{\alpha+n}(x).$$

Since the function $\psi^{(\nu)}_{\lambda_1}$ diagonalizes the subleading term $\mathcal{D}_{12}^{(-1,0,0)}$ of the Casimir operator $\mathcal{C}_{12}^2$ in the u_{s3}^ν basis, it remains to solve the eigenvalue equation of $\mathcal{D}_{45}^{(-1,-1,0)}$ for the coefficients f_ν. Using the relation $\partial_x\mathcal{K}_\alpha = \mathcal{K}_{\alpha+1}$, we obtain the simple equation

$$\sum_{\nu=0}^\infty (\nu\sqrt{\lambda_1}) f_\nu u_{s3}^{\nu-1}\psi^{(\nu-1),\mu}_{\lambda_1}(\lambda_1 u_{s5}) = \sum_{\nu=0}^\infty \lambda_2 f_\nu u_{s3}^\nu \psi^{(\nu),\mu}_{\lambda_1}(\lambda_1 u_{s5}). \tag{7.3.60}$$

Up to a multiplicative constant, we thereby obtain a simple solution $f_\nu = \mathcal{N}(\lambda_2\lambda_1^{-\frac{1}{2}})^\nu/\nu!$. Using the relation

$$\mathcal{K}_{-|\alpha|}(x) = x^{|\alpha|}\mathcal{K}_{|\alpha|}(x), \tag{7.3.61}$$

we can now sum the series in ν and thereby rewrite the solution in the simple form

$$g_{(h_a,\bar{h}_a;\mu)}(u_{s2},u_{s3},u_{s5}) = (1-u_{s2})^{\mu} u_{s5}^{h_\phi-\mu-\delta n} \lambda_1^{\frac{h_\phi-\mu-\delta n}{2}} \mathcal{K}_{h_\phi-\mu-\delta n}(\lambda_1 u_{s5} + \lambda_2 u_{s3}u_{s5}),$$

which, after a rescaling of g is equivalent to

$$F_{(h_a,\bar{h}_a;n)}(u_{s2},u_{s3},u_{s5}) = \sum_{\mu} \langle \mu|n\rangle \, (1-u_{s2})^{\mu} u_{s5}^{h_\phi+\delta n+\mu} \mathcal{K}_{h_\phi+\delta n+\mu}(\lambda_1 u_{s5} + \lambda_2 u_{s3}u_{s5}). \tag{7.3.62}$$

At this stage, three unknowns remain: the domain of μ, the scaling of n, and the matrix elements $\langle\mu|n\rangle$. All of these will be obtained by the same procedure: exploiting the fact that the leading Casimirs are the same in the order of limits $\vec{\epsilon}$ (red path in Fig. 35) and $\vec{\epsilon}\,'$ (green path in Fig. 35),

$$\lim_{\epsilon_{12,45}\to 0}\lim_{\epsilon_{34}\to 0}\lim_{\epsilon_{15}\to 0} \epsilon_{15}\left(\mathcal{D}_{12}^{2,\vec{\epsilon}} - 2\lambda_1\right) = \lim_{\epsilon_{15}\to 0}\lim_{\epsilon_{34}\to 0}\lim_{\epsilon_{12,45}\to 0} \epsilon_{15}\left(\mathcal{D}_{45}^{2,\vec{\epsilon}} - 2\lambda_1\right),$$
$$\lim_{\epsilon_{12,45}\to 0}\lim_{\epsilon_{34}\to 0}\lim_{\epsilon_{15}\to 0} \epsilon_{15}\epsilon_{34}\left(\mathcal{D}_{45}^{2,\vec{\epsilon}} - 2\lambda_2\right) = \lim_{\epsilon_{15}\to 0}\lim_{\epsilon_{34}\to 0}\lim_{\epsilon_{12,45}\to 0} \epsilon_{15}\epsilon_{34}\left(\mathcal{D}_{45}^{2,\vec{\epsilon}} - 2\lambda_2\right).$$

Thus, in direct analogy to case (I) blocks, we can retrieve the form (7.3.62) from the expansion (7.3.21) of blocks around the decoupling limit (defined here at the $(0,v,x)$ node of Fig. 35 for $v=u_{s2}$, and the $(0,0,x)$ node for $v=u_{s3}$.). In this case, we observe immediately that $\mu \geq 0$, such that the eigenvalues of $\vartheta_{1-u_{s2}}$ are bounded by $\delta n = J_1 - n$ in the block. Now, to deduce the scaling of n, we make the simple observation

$$\mathcal{D}_{12}^{(-1,0,*)} - J_1^2 \propto \partial_{u_{s5}} \vartheta_{1-u_{s5}}. \tag{7.3.63}$$

On the left hand side, the Casimir and its eigenvalue $J_1^2 + \mathrm{O}(1)$ scale like $\mathrm{O}(\epsilon_{15}^{-1})$, while on the right hand side, $\partial_{u_{s5}}$ also scales like $\mathrm{O}(\epsilon_{15}^{-1})$ and $\vartheta_{1-u_{s5}}$ has eigenvalues $\delta n + \mu$, $\mu \geq 0$. There is only one way to ensure that the right hand side does not scale faster than the ϵ_{15}^{-1} to infinity, that is

$$\delta n = J_1 - n = \mathrm{O}(1). \tag{7.3.64}$$

Having determined two out of the three unknowns, we return to the coefficients $\langle\mu|n\rangle$. Looking at (7.3.62), we see that the function multiplied by $\langle\mu|n\rangle$ scales like ϵ_{15}^{μ} at higher powers of $(1-u_{s5})$. As a result, the μ-th term in the sum is only leading when $\frac{\langle\mu|n\rangle}{\langle\mu=0|n\rangle} = \mathrm{O}(\epsilon_{15}^{-\mu})$. To compare this with (7.3.21), we expand the x-dependent part into a Pochmmer sum,

$$(1-(1-u_{s5})\mathcal{S}_1\mathcal{S}_2)^{-\bar{h}_{12;\phi}} = \sum_{k=0}^{\infty} \frac{(1-u_{s5})^k}{k!} (\bar{h}_{12;\phi})_k \mathcal{S}_1^k \mathcal{S}_2^k. \tag{7.3.65}$$

In the limit $u_{s5} = \mathrm{O}(\epsilon_{15})$, the region $k = \mathrm{O}(\epsilon_{15}^{-1})$ dominates this sum[7]. Now, acting on $f_1^{\mathrm{dec}}(u_{s2})$, we find precisely

$$\mathcal{S}_1(\vartheta_{u_{s2}})^k f_1^{\mathrm{dec}}(u_{s2}) = \frac{(\bar{h}_1)_k}{(2\bar{h}_1)_k}\left(1 + (\delta n + h_\phi - h_1 - h_2)\bar{h}_1 \frac{1-u_{s2}}{k} + \mathrm{O}\left(\bar{h}_1^2 k^{-2}(1-u_{s2})^2\right)\right). \tag{7.3.66}$$

This equation means that $\frac{\langle\mu|n\rangle}{\langle\mu=0|n\rangle} = \mathrm{O}(\epsilon_{15}^{-\mu/2})$, so only the $\mu = 0$ term survives! Putting all this together, we finally arrive at the following expression for the lightcone blocks

$$\psi^{(12)3(45)}_{(h_a,\bar{h}_a;J_1-\delta n)}(u_{si}) \overset{LCL^{(2)}_{\vec{\epsilon}}}{\sim} \mathcal{N}^{\mathrm{LS,II}}_{(h_a,\bar{h}_a;n)} u_{s1}^{h_1} u_{s4}^{h_2} (u_{s2}u_{s3})^{h_\phi} (1-u_{s2})^{\delta n} u_{s5}^{h_\phi+\delta n} \mathcal{K}_{h_\phi+\delta n}\left(\lambda_1 u_{s5} + \lambda_2 u_{s3}u_{s5}\right), \tag{7.3.67}$$

[7] In analogy to the crossed channel of a CSE, one can think of k as the "spin" and $(u_{s5}-1)\partial_{u_{s5}}$ as the "crossed channel Casimir".

where

$$\mathcal{N}^{\text{LS,II}}_{(h_a,\bar{h}_a;J_1-\delta n)} = 4^{\bar{h}_1+\bar{h}_2}\sqrt{\frac{\bar{h}_2}{2\pi}}\, e^{-\bar{h}_1}\bar{h}_1^{\bar{h}_1-2(h_\phi+\delta n)}\,\bar{h}_2^{\bar{h}_1-h_\phi-\delta n}. \tag{7.3.68}$$

Taking $u_{s2}\to 0$ in this expression then yields the leading term in the limit $LCL^{(II)}_{\vec{\epsilon}}$, with scaling $J_1^2=\mathrm{O}(\epsilon_{15}^{-1})$, $J_2^2=\mathrm{O}(\epsilon_{15}^{-1}\epsilon_{34}^{-1})$ and $\delta n = J_1 - n = \mathrm{O}(1)$. The derivation of the normalization here is less intuitive than in case (I) — this is because even at all orders in u_{s2}, only the first term of the power series in $(1-u_{s2})$ survives the case (II) limit. In analogy with a derivative expansion, the sum over descendants $\mu>0$ truncates, and this sum is precisely what is counted by the second factor in the normalization (7.3.35) coming from $f_1^{\text{dec}}(0)$. At the same time, the descendants $\eta>0$ coming from higher powers of $(1-u_{s5})$ counted in the ${}_3F_2(1)$ in (7.3.35) is modified, because it depends itself the contribution of $\mu\geq 0$ descendants. With a more careful tracking of the sum over (μ,η) descendants, that is to say powers of x and u_{s2} in (7.3.21), we can obtain the normalization via limit

$$F_{(h_a,\bar{h}_a;n)} \overset{\bar{h}_2^2 u_{s2},\bar{h}_1^2\ll u_{s5}^{-1}}{\sim} \mathcal{N}^{\text{LS,II}}_{(h_a,\bar{h}_a;n)}\frac{\Gamma(h_\phi+\delta n)}{2}. \tag{7.3.69}$$

In the formula (7.3.21), this is equivalent to setting

$$(u_{s2},u_{s3})=(1,0),\quad \mathcal{S}_1^k=\frac{(\bar{h}_1)_k}{(2\bar{h}_1)_k},\quad \mathcal{S}_2^k(\vartheta)=\mathcal{S}_2^k(0). \tag{7.3.70}$$

In this case, we obtain

$$\frac{1}{2}\mathcal{N}^{\text{LS,II}}_{(h_a,\bar{h}_a;J_1-\delta n)} = \lim_{\bar{h}_1\to\infty}\frac{\Gamma(2\bar{h}_1)}{\Gamma(\bar{h}_1)\Gamma(\bar{h}_1+h_\phi+\delta n)}\lim_{\bar{h}_2\to\infty}\frac{\Gamma(2\bar{h}_2)\Gamma(\bar{h}_1-h_\phi-\delta n)}{\Gamma(\bar{h}_2)\Gamma(\bar{h}_2-\bar{h}_1+h_\phi+\delta n)}. \tag{7.3.71}$$

Note: We could also consider a case (III), where both $\lambda_1,\lambda_2=\mathrm{O}(\epsilon_{15}^{-1})$. The solution theory would the same steps as case (II), where we would now restrict to the kernel of $\mathcal{D}_{12}^{(-1,0,-1)}$ and $\mathcal{D}_{45}^{(-1,-1,0)}$ by imposing a $u_{s2}^{-\alpha_1}u_{s3}^{-\alpha_2}$ power law behavior, and we would solve the eigenvalue equations for the two Casimir operators for u_{s5}. However, we are not aware of a lightcone bootstrap setup where this third regime is relevant.

7.3.5 Five-point lightcone bootstrap revisited

We will expand both channels of the crossing equation (7.3.12) near the null polygon limit $X_{i(i+1)}=0$, with the specific hierarchy stated in eq. (7.3.13). Starting with the direct channel we observe this hierarchy ensures an expansion in leading twist in the two operator products of the direct channel. More precisely, taking both $X_{15}\ll 1$ and $X_{34}\ll 1$, we obtain

$$\begin{aligned}\sum_{\mathcal{O}_1,\mathcal{O}_2,n} P^{(n)}_{\mathcal{O}_1\mathcal{O}_2}\psi^{(15)2(34)}_{\mathcal{O}_1\mathcal{O}_2;n} &= C_{\phi\phi\phi}\left((u_{s1}u_{s3})^{\frac{\Delta_\phi}{2}}+(u_{s5}u_{s2})^{\frac{\Delta_\phi}{2}}\right)+\\ &+\sum_{n=0}^{J_\star}P^{(n)}_{\mathcal{O}_\star\mathcal{O}_\star}(u_{s1}u_{s2}u_{s3}u_{s5})^{h_\star}\, g_{\mathcal{O}_\star\mathcal{O}_\star;n}(u_{s1},u_{s2},u_{s4})+\mathrm{O}(X_{15}^{h>h_\star}).\end{aligned} \tag{7.3.72}$$

Here we have used the conventions that were stated in eq. (7.3.8), i.e. we multiplied the five-point correlation function by a factor

$$\Omega_{(15)2(34)}(X_i)=\left(X_{15}X_{34}\sqrt{\frac{X_{12}X_{23}}{X_{13}}}\right)^{\Delta_\phi}.$$

The three terms that appear on the right hand side correspond to intermediate exchange of $[\mathcal{O}_1|\mathcal{O}_2] = [\mathbf{1}|\phi], [\phi|\mathbf{1}]$ and $[\mathcal{O}_1|\mathcal{O}_2] = [\mathcal{O}_\star|\mathcal{O}_\star]$ at the top and bottom line respectively. Note that there cannot be identity exchange in both intermediate channels simultaneously. Furthermore, a single identity exchange forces the second intermediate exchange to coincide with the external operators, i.e. it forces ϕ exchange in the other operator product. The two terms with a single identity exchange are the first two terms on the right hand side of the previous equation. The third term, which may involve a sum over tensor structures n, is associated with the leading twist field $\mathcal{O}_\star$ in the operator product of ϕ with itself. We parameterize its weight and spin by $h_\star$ and $J_\star$. For this term there are a few mutually exclusive cases to distinguish. The leading twist field $\mathcal{O}_*$ may coincide with the external field ϕ itself, i.e. $[\mathcal{O}_1|\mathcal{O}_2] = [\mathcal{O}_\star|\mathcal{O}_\star] = [\phi|\phi]$. But this is not always realized especially when the appearance of ϕ in the operator product of ϕ with itself is excluded by some selection rule, as it is the case for the fundamental spin field of the Ising model, for example. It turns out that $\mathcal{O}_\star \neq \phi$ falls again into two subcases, depending on whether $h_\star > h_\phi$ or $h_\star < h_\phi$. Depending on which of the three scenarios is realized, the blocks $g_{\mathcal{O}_\star\mathcal{O}_\star;n}(u_{s1}, u_{s2}, u_{s4})$ possess the following asymptotic behavior in the lightcone limit, see subsection 3.1.

(−) In case $\mathcal{O}_\star \neq \phi$ and $h_\star < h_\phi$, then for all $0 \leq n < h_\phi - h_\star$ the blocks possess the following power law behavior in the lightcone limit,

$$\psi^{(15)2(34)}_{\mathcal{O}_\star\mathcal{O}_\star;n}(u_{si}) = \mathcal{N}_{\mathcal{O}_\star\mathcal{O}_\star;n}\left(u_{s1}u_{s2}u_{s3}u_{s5}\right)^{h_\star}\left(u_{s1}u_{s2}\right)^n\left(1+\mathrm{O}(u_{s2})\right). \tag{7.3.73}$$

Note that even when $h_\phi - h_\star > 1$, such that the direct channel sum includes $n > 0$ contributions, the latter will be subleading of relative order $(X_{12}X_{23})^n$ compared to the $n = 0$ block.

(0) In case $\mathcal{O}_\star = \phi$ the tensor structure is trivial, i.e. $n = 0$, and the blocks possesses a logarithmic divergence of the form

$$\psi^{(15)2(34)}_{\mathcal{O}_\star\mathcal{O}_\star;0}(u_{si}) = \mathcal{N}_{\phi\phi;0}\left(u_{s1}u_{s2}u_{s3}u_{s5}\right)^{h_\phi}\log u_{s1}\log u_{s2} + \mathrm{O}(u_{s2}\log u_{s1}). \tag{7.3.74}$$

(+) In case $\mathcal{O}_\star \neq \phi$ and $h_\star > h_\phi$, then for all $n = 0, 1, \ldots, J_\star$, the blocks possess the following power law behavior in the lightcone limit,

$$\psi^{(15)2(34)}_{\mathcal{O}_\star\mathcal{O}_\star;n}(u_{si}) = \mathcal{N}_{\mathcal{O}_\star\mathcal{O}_\star;n}\left(u_{s1}u_{s2}u_{s3}u_{s5}\right)^{h_\star}\left(u_{s1}u_{s2}\right)^{h_\phi-h_\star}\left(1+\mathrm{O}(u_{s2})\right). \tag{7.3.75}$$

Contrary to the case (−), the $n > 0$ blocks are not subleading.

We will now proceed to the term by term analysis of the direct channel (7.3.72) expanded up to $\mathrm{O}(X_{15}^{h>h_\star}, X_{15}^{h_\star+1})$, reproducing it term by term in the crossed channel. The third term will require a separate discussion for each of the three alternative cases $(-, 0, +)$ listed above.

$[\mathbf{1}|\phi]$-exchange in the direct channel

As we explained above, the first term on the left hand side of the direct channel decomposition (7.3.72) is associated with the exchange of $[\mathcal{O}_1|\mathcal{O}_2] = [\mathcal{O}_{15}|\mathcal{O}_{34}] = [\mathbf{1}|\phi]$ in the direct channel. Such a term can contribute non-trivially to the direct channel whenever the field ϕ appears in the operator product of ϕ with itself. If this is the case, the leading term in the direct channel is the first term in eq. (7.3.72). Taking into account the prefactor on the right hand side of the crossing symmetry equation (7.3.12) we deduce that

$$C_{\phi\phi\phi}\left(\frac{u_{s1}u_{s4}}{u_{s5}}\right)^{2h_\phi} + \ldots = \sum_{\mathcal{O}_1,\mathcal{O}_2,n} P^{(n)}_{\mathcal{O}_1\mathcal{O}_2}\psi^{(12)3(45)}_{\mathcal{O}_1\mathcal{O}_2;n}. \tag{7.3.76}$$

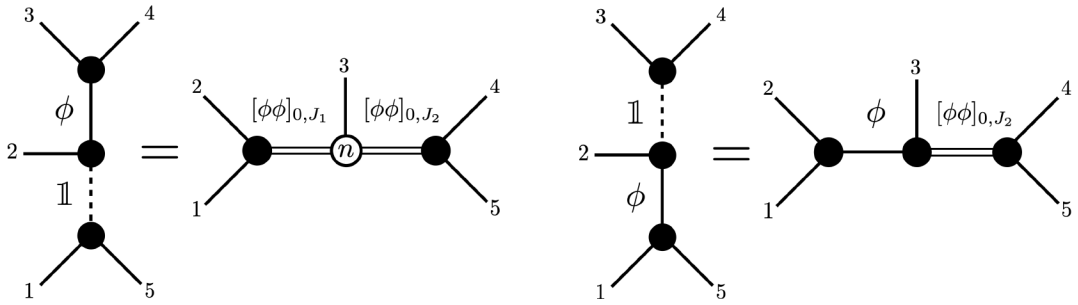

Figure 36: Lightcone bootstrap of five-point correlator with one identity exchange in the direct channel.

In our lightcone regime (7.3.13), we first take $u_{s5} \ll u_{s3} \ll u_{s2} \ll 1$. Once this limit is taken, the limiting crossed channel blocks must obey

$$\psi^{(12)3(45)}_{\mathcal{O}_1\mathcal{O}_2;n}(u_{si}) \sim (u_{s1}u_{s4})^{2h_\phi}\widetilde{\psi}^{(12)3(45)}_{h_1h_2}(u_{s2},u_{s3},u_{s5}), \tag{7.3.77}$$

to match the asymptotics in the $u_{s1} \ll u_{s4} \ll 1$ regime. This implies double-twist exchange in both operator products of the crossed channel. At the same time, it is clear that the leading contribution is $\mathcal{D}_{12}^{(-1,0,-1)}$- and $\mathcal{D}_{45}^{(-1,-1,0)}$-singular by acting on it with powers of said Casimirs defined in (7.3.37), (7.3.39),

$$\left[\mathcal{D}_{12}^{(-1,0,-1)}\right]^n u_{s5}^{-2h_\phi} = (2h_\phi)_n (h_\phi)_n u_{s5}^{-2h_\phi-n} u_{s2}^{-n}\,, \tag{7.3.78}$$

$$\left[\mathcal{D}_{45}^{(-1,-1,0)}\right]^n u_{s5}^{-2h_\phi} = (2h_\phi)_n (h_\phi)_n u_{s5}^{-2h_\phi-n} u_{s3}^{-n}\,. \tag{7.3.79}$$

More specifically, the actions of the leading Casimir operators $\mathcal{D}_{12}$ and $\mathcal{D}_{45}$ increase the singularities by an order $\mathrm{O}(\epsilon_{15}^{-1}\epsilon_{23}^{-1})$ and $\mathrm{O}(\epsilon_{15}^{-1}\epsilon_{34}^{-1})$ respectively. In direct analogy to the four-point discussion above eq. (7.2.49), this implies that the direct channel has infinite support when expanding in a basis of eigenvectors of the crossed channel differential operators. This may be understood by acting with one of the leading Casimirs (say $\mathcal{D}_{12}^{(-1,0,-1)}$) on the crossing equation (7.3.76): the order of $\epsilon_{15}^{-1}\epsilon_{23}^{-1}$ only matches on both sides when the crossed channel blocks have $\lambda_1 = \mathrm{O}(\epsilon_{15}^{-1}\epsilon_{23}^{-1})$. Similarly, acting with $\mathcal{D}_{45}^{(-1,-1,0)}$ yields a match only for $\lambda_2 = \mathrm{O}(\epsilon_{15}^{-1}\epsilon_{23}^{-1})$. In conclusion, to reproduce the correct behavior in the crossed channel, we must sum over the case (I) blocks of (7.3.41). Using the limits of blocks computed in the previous section (see (7.3.50)), we can then reproduce the correct asymptotics from a large spin and tensor structure integral[8]

$$C_{\phi\phi\phi}u_{s5}^{-2h_\phi} = (u_{s2}u_{s3})^{h_\phi}\int_{[\mathrm{O}(1),\infty)^3} \mathrm{d}\eta \frac{\mathrm{d}\lambda_1}{4\sqrt{\lambda_1}}\frac{\mathrm{d}\lambda_2}{4\sqrt{\lambda_2}}\mathcal{N}^{\mathrm{LS},I}_{(h_a,\bar{h}_a;\eta)}P^{(\eta)}_{[\phi\phi]_{0,J_1}[\phi\phi]_{0,J_2}}\, e^{-\eta u_{s5}-\frac{\lambda_1 u_{s2}+\lambda_2 u_{s3}}{\eta}}, \tag{7.3.80}$$

where $\lambda_a = \bar{h}_a^2 + \mathrm{O}(1)$ and $\bar{h}_a = J_a + \mathrm{O}(1)$ at leading order. Plugging in the general ansatz,

$$\frac{\mathcal{N}^{\mathrm{LS,I}}_{(h_a,\bar{h}_a;\eta)}}{16\sqrt{\lambda_1\lambda_2}}P^{(\eta)}_{[\phi\phi]_{0,J_1}[\phi\phi]_{0,J_2}} = C_{\phi\phi\phi}\prod_{i=1,2}\frac{\left(\eta^{-1}\lambda_i\right)^{\beta_i-1}}{\Gamma(\beta_i)}\frac{\eta^{\gamma-3}}{\Gamma(\gamma)}, \tag{7.3.81}$$

and using of the integral representation of the Gamma function, we find

$$\beta_1 = \beta_2 = \frac{\Delta_\phi}{2}, \quad \gamma = \Delta_\phi. \tag{7.3.82}$$

[8]Recall that for small ϵ_{15} we must have $n = \mathrm{O}(\epsilon_{15}^{-1})$ or larger for crossed channel blocks to be nonzero.

To relate these results to those of [67], we use the formula (7.3.48) for $\mathcal{N}^{\text{LS,I}}$ and the identification[9]

$$2^{-(J_1+J_2)} P^{(\ell)}_{[\phi\phi]_{0,J_1}[\phi\phi]_{0,J_2}}\Big|_{\text{theirs}} = P^{(\eta)}_{[\phi\phi]_{0,J_1}[\phi\phi]_{0,J_2}}\Big|^{\eta\to\ell,\lambda_i\to J_i^2}_{\text{ours}}. \tag{7.3.83}$$

We find exact agreement of the two results.

$[\phi|\mathbf{1}]$-exchange in the direct channel

The next leading term in (7.3.72) is $(u_{s2}u_{s5})^{h_\phi}$, which is subleading in X_{15}, but higher order in X_{12}. The crossing equation (7.3.76) is modified to :

$$C_{\phi\phi\phi}\Big[\left(\frac{u_{s1}u_{s4}}{u_{s5}}\right)^{2h_\phi} + \left(\frac{u_{s1}u_{s2}u_{s4}^2}{u_{s3}u_{s5}}\right)^{h_\phi}\Big] + \ldots = \sum_{\mathcal{O}_1,\mathcal{O}_2,n} P^{(n)}_{\mathcal{O}_1\mathcal{O}_2}\psi^{(12),(45)}_{\mathcal{O}_1\mathcal{O}_2;n}. \tag{7.3.84}$$

We would like to reproduce the second term on the left hand side from the crossed channel. Comparing with (7.3.77), the expected twist in the (12) OPE is lowered to $h_1 = h_\phi$. At the same time, one finds that the direct channel contribution is in the kernel of $\mathcal{D}_{12}$ at order $\mathrm{O}(\epsilon_{15}^{-1}\epsilon_{23}^{-1})$,

$$\mathcal{D}_{12}^{(-1,0,-1)}\left(\frac{u_{s1}u_{s2}u_{s4}^2}{u_{s3}u_{s5}}\right)^{h_\phi} = 0 \;\Rightarrow\; \text{DC} \in \ker \mathcal{D}_{12}^{(-1,0,-1)}. \tag{7.3.85}$$

We find the same kernel condition at $\mathrm{O}(\epsilon_{15}^{-1}\epsilon_{23}^{0})$ by applying (7.3.51),

$$\mathcal{D}_{12}^{(-1,0,0)}\left(\frac{u_{s1}u_{s2}u_{s4}^2}{u_{s3}u_{s5}}\right)^{h_\phi} = 0 \;\Rightarrow\; \text{DC} \in \ker \mathcal{D}_{12}^{(-1,0,0)}. \tag{7.3.86}$$

Therefore, the second term of the direct channel in (7.3.84) has finite support in the eigenvectors of $\mathcal{D}_{12}$, mapping precisely to a single ϕ exchange in the (12) OPE of the crossed channel. At the same time, the action of $\mathcal{D}_{45}$ is just as singular as in (7.3.79), hence the infinite support of twist $h_2 = 2h_\phi$ operators in the (45) OPE with $\lambda_2 = \mathrm{O}(\epsilon_{15}^{-1}\epsilon_{34}^{-1})$. We thereby make claim that $P^{(n)}_{\mathcal{O}_1\mathcal{O}_2} = C_{\phi\phi\phi}C^2_{\phi\phi[\phi\phi]_{0,J_2}}$, such that the CSE requires

$$(u_{s3}u_{s5})^{-h_\phi} = \int \frac{\mathrm{d}J_2}{2} C^2_{\phi\phi[\phi\phi]_{0,J_2}} \frac{\psi^{(12),(45)}_{\phi,[\phi\phi]_{0,J_2};0}}{(u_{s1}u_{s4}^2u_{s2})^{h_\phi}}. \tag{7.3.87}$$

The OPE coefficient squared $C^2_{\phi\phi[\phi\phi]_{0,J}}$ is given in e.g. [35, Eq. (12)], with $\ell \leftrightarrow J$ and $\Delta_\phi \leftrightarrow 2h_\phi$. To prove the claim (7.3.87) directly, we can use the fact that blocks in this regime satisfy the same differential equations as the case (II) in blocks (7.3.67), but with $\lambda_1 = 0 + \mathrm{O}(1)$ and $\delta n = 0$. However, since $J_1 = 0$ is finite in this case, the normalization prescription must be modified. In appendix 7.A.3, we determine the explicit normalization and obtain

$$\frac{\psi^{(12),(45)}_{\phi,[\phi\phi]_{0,J_2};0}}{(u_{s1}u_{s4}^2u_{s2})^{h_\phi}} \sim \frac{2\Gamma(2h_\phi)}{\Gamma(h_\phi)} 4^{\bar{h}_2}\sqrt{\frac{\bar{h}_2}{\pi}}\,(u_{s3}u_{s5})^{h_\phi}\mathcal{K}_{h_\phi}(u_{s3}u_{s5}J_2^2). \tag{7.3.88}$$

Sure enough, plugging this formula into the CSE and integrating over J_2 proves the claim (7.3.87).

[9] The factor 2^{-J} discrepancy comes from their alternative convention for the normalization of blocks, see [67, footnote 3].

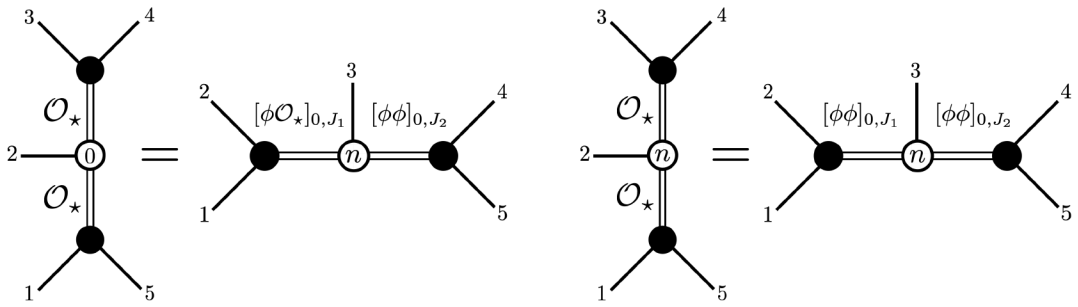

Figure 37: Lightcone bootstrap of five-point correlator with non-identity leading twist $\mathcal{O}_\star$ exchange in the direct channel. Left: lighter exchange $h_\star < h_\phi$. Right: heavier exchange $h_\star > h_\phi$.

$[\phi|\phi]$ exchange in the direct channel

Let us now consider the case where there is no identity operator in the direct channel. The simplest such situation is when there is a ϕ exchange in (15) and (34) OPE. The respective direct channel contribution is given by (7.3.72). The crossing symmetry equation (assuming $C_{\phi\phi\phi} \neq 0$) is

$$C^3_{\phi\phi\phi}(u_{s1}u_{s2}u_{s3}u_{s5})^{h_\phi}\log u_{s1}\log u_{s2}+\ldots=\left(\frac{u_{s3}}{u_{s1}}\right)^{h_\phi}\left(\frac{u_{s5}}{u_{s4}}\right)^{2h_\phi}\sum_{\mathcal{O}_1,\mathcal{O}_2,n}P^{(n)}_{\mathcal{O}_1\mathcal{O}_2}\psi^{(12),(45)}_{\mathcal{O}_1\mathcal{O}_2;n}. \tag{7.3.89}$$

Here we have not shown explicitly the leading terms involving identities, which were accounted for earlier. The powers of u_{s1}, u_{s4} impose double trace operators $[\phi\phi]_{0,J_1}, [\phi\phi]_{0,J_2}$ by the same argument as in (7.3.77). Unlike the claim made in [67], the asymptotics of this direct channel contribution *cannot* be reproduced in every single block — it is still Casimir singular for u_{s2}, u_{s3}, u_{s5} :

$$\left[\mathcal{D}^{(-1,0,-1)}_{12}\right]^n u^{h_\phi}_{s2}u^{-h_\phi}_{s5}\log u_{s2}=(n-1)!(h_\phi)_n u^{h_\phi-n}_{s2}u^{-h_\phi-n}_{s5} \tag{7.3.90}$$

$$\left[\mathcal{D}^{(-1,-1,0)}_{45}\right]^n u^{0}_{s3}u^{-h_\phi}_{s5}=(h_\phi)^2_n u^{-n}_{s3}u^{-h_\phi-n}_{s5}. \tag{7.3.91}$$

So as argued in section 7.3.5 the crossed channel blocks must have the eigenvalues $\lambda_1 = \mathrm{O}(\epsilon_{15}^{-1}\epsilon_{23}^{-1})$, $\lambda_2 = \mathrm{O}(\epsilon_{15}^{-1}\epsilon_{34}^{-1})$. So the crossing equation is similar to (7.3.80) and we use the case (I) blocks in crossed channel from (7.3.50). However, the $\log u_{s1}$ asymptotics can only be reproduced in the crossed channel via the anomalous dimension correction

$$h_1 = h_{[\phi\phi]_{0,J_1}} = 2h_\phi + \frac{\gamma}{2J_1^{2h_\phi}} + \ldots. \tag{7.3.92}$$

From (7.3.50) we see that expanding u^{h_1} around $2h_\phi$ gives the $\log u_{s1}$ at leading order. The power of $J_1^{-2h_\phi}$ together with the $\lambda_1 = J_1^2 + \mathrm{O}(1)$ dependence in the OPE coefficient $P^{(\eta)}_{[\phi\phi]_{0,J_1}[\phi\phi]_{0,J_2}}$ obtained in (7.3.81), leads to the large λ_1 integral

$$\int_{L_1^2}^{\infty}\frac{\mathrm{d}\lambda_1}{\lambda_1}e^{-\lambda_1 u_{s2}\eta^{-1}} = -\log u_{s2} + \mathrm{O}(1), \quad \forall L_1 = \mathrm{O}(1). \tag{7.3.93}$$

Here, L_1 denotes a lower limit of spins above which the large spin approximation of the blocks is valid. The rest of the crossing equation is similar to (7.3.80), i.e. the are integrals over large λ_2 and

η reproduce the $(u_{s2}u_{s5})^{h_\phi}$ asymptotics. In sum, the right hand side of (7.3.89) reduces to

$$\begin{aligned}(u_{s3}u_{s5})^{h_\phi}\int \mathrm{d}\eta \frac{\mathrm{d}\lambda_1}{4\sqrt{\lambda_1}}\frac{\mathrm{d}\lambda_2}{4\sqrt{\lambda_2}}\frac{\gamma\log u_{s1}}{2\lambda_1^{h_\phi}}\mathcal{N}^{\mathrm{LS},I}P^{(\eta)}_{[\phi\phi]_{0,J_1}[\phi\phi]_{0,J_2}}e^{-\eta u_{s5}-\frac{\lambda_1 u_{s2}+\lambda_2 u_{s3}}{\eta}}\\ =-\frac{\gamma}{\Gamma(\Delta_\phi)}C_{\phi\phi\phi}\log u_{s1}\log u_{s2}.\end{aligned} \tag{7.3.94}$$

We thus obtain universal asymptotics in the crossed channel that are independent of the finite spin part of the conformal block expansion. The result for the γ is the same as for ϕ exchange in the direct channel of the four-point crossing equation, given in e.g. [35, Eq. (41)] with $\ell_m \leftrightarrow J_1$, $\tau_m \leftrightarrow 2h_\phi$, $P_m \leftrightarrow C^2_{\phi\phi[\phi\phi]_{0,J_1}}$.

$[\mathcal{O}_\star|\mathcal{O}_\star]$-exchange in the direct channel, $h_\star < h_\phi$

We will now consider the case where the two exchanged operators in the direct channel are identical and with leading twist $h_\star < h_\phi$. In this case, we showed below (7.3.73) that the leading contribution comes solely from the block $\psi^{(15),(34)}_{\mathcal{O}_\star\mathcal{O}_\star;n=0}$, which yields

$$\cdots + u_{s2}^{h_\star}u_{s1}^{h_\phi+h_\star}u_{s3}^{h_\star-h_\phi}u_{s4}^{2h_\phi}u_{s5}^{h_\star-2h_\phi}P^{(0)}_{\mathcal{O}_\star\mathcal{O}_\star}\mathcal{N}_{\mathcal{O}_\star\mathcal{O}_\star;0}+\cdots=\sum_{\mathcal{O}_1,\mathcal{O}_2,n}P^{(n)}_{\mathcal{O}_1\mathcal{O}_2}\psi^{(12),(45)}_{\mathcal{O}_1\mathcal{O}_2;n}. \tag{7.3.95}$$

In this case, the power law $u_{s1}^{h_\phi+h_\star}u_{s4}^{2h_\phi}$ on the right hand side implies $[\phi\mathcal{O}_\star]_{0,J_1}$ exchange on the left and $[\phi\phi]_{0,J_2}$ on the right. Furthermore, the power law is $\mathcal{D}_{12}^{(-1,0,-1)}$ and $\mathcal{D}_{45}^{(-1,-1,0)}$-singular following

$$\begin{aligned}\left[\mathcal{D}_{12}^{(-1,0,-1)}\right]^n u_{s2}^{h_\star}u_{s5}^{h_\star-2h_\phi}&=(h_\phi-h_\star)_n(2h_\phi-h_\star)_n\,u_{s2}^{h_\star}u_{s5}^{h_\star-2h_\phi},\\ \left[\mathcal{D}_{45}^{(-1,-1,0)}\right]^n u_{s3}^{h_\star-h_\phi}u_{s5}^{h_\star-2h_\phi}&=(2h_\phi-h_\star)_n^2\,u_{s3}^{h_\star-h_\phi}u_{s5}^{h_\star-2h_\phi}.\end{aligned}$$

Again, as argued in the section 7.3.5, the leading direct channel evidently maps to a sum over double-twist blocks in the $\lambda_1 = \mathrm{O}(\epsilon_{15}^{-1}\epsilon_{23}^{-1}), \lambda_2 = \mathrm{O}(\epsilon_{15}^{-1}\epsilon_{34}^{-1})$ regime. Employing the asymptotics of case (I) blocks (7.3.50), the crossed channel sum reduces to

$$\begin{aligned}&\sum_{\mathcal{O}_1,\mathcal{O}_2,n}P^{(n)}_{\mathcal{O}_1\mathcal{O}_2}\psi^{(12),(45)}_{\mathcal{O}_1\mathcal{O}_2;n}=\\ &\qquad u_{s1}^{h_\star+h_\phi}u_{s4}^{2h_\phi}\int_{\mathbb{R}^3_+}\frac{\mathrm{d}\eta\,\mathrm{d}\lambda_1\mathrm{d}\lambda_2}{16\sqrt{\lambda_1\lambda_2}}\mathcal{N}^{\mathrm{LS,I}}_{(h_a,\bar{h}_a,\eta)}P^{(\eta)}_{[\phi\mathcal{O}_\star]_{0,J_1}[\phi\phi]_{0,J_2}}u_{s2}^{h_\star}u_{s3}^{2h_\phi-h_\star}e^{-\eta u_{s5}-\frac{\lambda_1 v_1+\lambda_2 v_2}{\eta}}.\end{aligned} \tag{7.3.96}$$

To reproduce the left hand side of (7.3.95), we must impose the following asymptotics at large $\eta, \lambda_1, \lambda_2$:

$$\frac{\mathcal{N}^{\mathrm{LS,I}}_{(h_a,\bar{h}_a;\eta)}}{16\sqrt{\lambda_1\lambda_2}}P^{(\eta)}_{[\phi\mathcal{O}_\star]_{0,J_1}[\phi\phi]_{0,J_2}}=P^{(0)}_{\mathcal{O}_\star\mathcal{O}_\star}\mathcal{N}_{\mathcal{O}_\star\mathcal{O}_\star;0}\frac{(\eta^{-1}\lambda_1)^{h_\phi-h_\star-1}}{\Gamma(h_\phi-h_\star)}\frac{(\eta^{-1}\lambda_2)^{2h_\phi-h_\star-1}}{\Gamma(2h_\phi-h_\star)}\frac{\eta^{2h_\phi-h_\star-3}}{\Gamma(2h_\phi-h_\star)}. \tag{7.3.97}$$

After plugging in the formulas for $\mathcal{N}^{\mathrm{LS,I}}$ in (7.3.48) and $\mathcal{N}_{\mathcal{O}_\star\mathcal{O}_\star;0}$ in (7.3.35), we retrieve the same result as [67, Eq. (48)] via the same prescription as in section 7.3.5,

$$2^{-(J_1+J_2)}P^{(\ell)}_{[\phi\mathcal{O}_\star]_{0,J_1}[\phi\phi]_{0,J_2}}\Big|_{\text{theirs}}=P^{(\eta)}_{[\phi\mathcal{O}_\star]_{0,J_1}[\phi\phi]_{0,J_2}}\Big|^{\eta\to\ell,\lambda_i\to J_i^2}_{\text{ours}}. \tag{7.3.98}$$

$[\mathcal{O}_\star|\mathcal{O}_\star]$-exchange in the direct channel, $h_\star > h_\phi$

For the exchange of two identical operators with leading twist $h_\star > h_\phi$ in the direct channel, the X_{12} and X_{23} asymptotics are modified in direct channel blocks, such that the leading contribution becomes (see (7.3.75))

$$\cdots + u_{s2}^{h_\phi} u_{s1}^{2h_\phi} u_{s3}^{h_\star-h_\phi} u_{s4}^{2h_\phi} u_{s5}^{h_\star-2h_\phi} \sum_n P^{(n)}_{\mathcal{O}_\star\mathcal{O}_\star} \mathcal{N}_{\mathcal{O}_\star\mathcal{O}_\star;n} + \cdots = \sum_{\mathcal{O}_1,\mathcal{O}_2,n} P^{(n)}_{\mathcal{O}_1\mathcal{O}_2} \psi^{(12),(45)}_{\mathcal{O}_1\mathcal{O}_2;n}. \tag{7.3.99}$$

The $(u_{s1}u_{s4})^{2h_\phi}$ power law now imposes $[\phi\phi]_{0,J_i}$ exchange at leading order in both the (12) and the (45) OPE. We also observe a kernel condition at $\mathrm{O}(\epsilon_{15}^{-1}\epsilon_{23}^{-1})$,

$$\mathcal{D}_{12}^{(-1,0,-1)} u_{s2}^{h_\phi} u_{s1}^{2h_\phi} u_{s3}^{h_\star-h_\phi} u_{s4}^{2h_\phi} u_{s5}^{h_\star-2h_\phi} = 0 \Rightarrow \mathrm{DC} \in \ker(\mathcal{D}_{12}^{(-1,0,-1)}). \tag{7.3.100}$$

The direct channel is nonetheless $\mathcal{D}_{12}^2$-singular at $\mathrm{O}(\epsilon_{15}^{-1})$ since the action of $\mathcal{D}_{12}^{(-1,0,0)}$ in (7.3.51) is non-zero and

$$\left[\mathcal{D}_{12}^{(-1,0,0)}\right]^n u_{s2}^{h_\phi} u_{s1}^{2h_\phi} u_{s3}^{h_\star-h_\phi} u_{s4}^{2h_\phi} u_{s5}^{h_\star-2h_\phi} = (2h_\phi - h_\star)_n (h_\phi)_n u_{s2}^{h_\phi} u_{s1}^{2h_\phi} u_{s3}^{h_\star-h_\phi} u_{s4}^{2h_\phi} u_{s5}^{h_\star-2h_\phi-n}.$$

At the same time, the action of $\mathcal{D}_{45}^{(-1,0,-1)}$ is singular just like in previous case:

$$\left[\mathcal{D}_{45}^{(-1,0,-1)}\right]^n u_{s2}^{h_\phi} u_{s1}^{2h_\phi} u_{s3}^{h_\star-h_\phi} u_{s4}^{2h_\phi} u_{s5}^{h_\star-2h_\phi} = ((2h_\phi - h_\star)_n)^2 u_{s2}^{h_\phi} u_{s1}^{2h_\phi} u_{s3}^{h_\star-h_\phi} u_{s4}^{2h_\phi} u_{s5}^{h_\star-2h_\phi-n}. \tag{7.3.101}$$

In comparison with the discussion in section 7.3.5, the crossed channel is now dominated by $\lambda_1 = \mathrm{O}(\epsilon_{15}^{-1})$ and $\lambda_2 = \mathrm{O}(\epsilon_{15}^{-1}\epsilon_{34}^{-1})$. This regime corresponds precisely to a sum over the case (II) blocks of (7.3.67):

$$\sum_{\mathcal{O}_1,\mathcal{O}_2,n} P^{(n)}_{\mathcal{O}_1\mathcal{O}_2} \psi^{(12),(45)}_{\mathcal{O}_1\mathcal{O}_2;n} = \tag{7.3.102}$$

$$\left(u_{s1}^2 u_{s4}^2 u_{s2} u_{s3} u_{s5}\right)^{h_\phi} \int_{\mathbb{R}_+^2} \frac{\mathrm{d}\lambda_1 \mathrm{d}\lambda_2}{16\sqrt{\lambda_1\lambda_2}} \sum_{\delta n=0}^{\infty} \mathcal{N}^{\mathrm{LS,II}}_{[\phi\phi]_{0,J_1}[\phi\phi]_{0,J_2};J_1-\delta n} P^{(J_1-\delta n)}_{[\phi\phi]_{0,J_1}[\phi\phi]_{0,J_2}} \mathcal{K}_{h_\phi+\delta n}(\lambda_1 u_{s5} + \lambda_2 v_2 u_{s5}).$$

Given that the $\epsilon_{12}, \epsilon_{23}, \epsilon_{45}$ asymptotics match on both sides of the CSE (7.3.99) with case (II) blocks (7.3.102), our remaining task is to match the ϵ_{34} and ϵ_{15} scalings by tuning the asymptotics of the crossed channel OPE coefficients in $\lambda_1\lambda_2^{-1}$ and λ_1^{-1} respectively. To this end, we will exploit the integral representation (7.3.59) of the Bessel-Clifford function and write the λ_2 integral as

$$\int_0^\infty \frac{\mathrm{d}\lambda_2}{4\sqrt{\lambda_2}} \mathcal{N}^{\mathrm{LS,II}}_\Xi P_\Xi \, \mathcal{K}_{h_\phi+\delta n}(\lambda_1 u_{s5} + \lambda_2 v_2 u_{s5}) \stackrel{!}{=}$$
$$\frac{1}{2}\int_0^\infty \frac{\mathrm{d}t}{t^{1+h_\phi+\delta n}} e^{-t-\frac{\lambda_1 u_{s5}}{t}} \int_0^\infty \frac{\mathrm{d}\lambda_2}{4\sqrt{\lambda_2}} \mathcal{N}^{\mathrm{LS,II}}_\Xi P_\Xi \, e^{-\frac{\lambda_2 v_2 u_{s5}}{t}}.$$

Here, $t \in \mathbb{R}_+$ is the variable for the integral representation and we used $\Xi := ([\phi\phi]_{0,J_1}[\phi\phi]_{0,J_2}; J_1 - \delta_n)$ as a shorthand to denote the exchanged fields and the tensor structure label $n = J_1 - \delta n$. It is of course not immediate that the t-integral and the λ_2-integral can be exchanged like this, but we are only using it as a trick to determine a plausible ansatz for $P^{(J_1-\delta n)}_{[\phi\phi][\phi\phi]}$. Once said ansatz is determined, we can plug it back into (7.3.102) in a second stage, verifying that the resulting integrals are convergent and that they solve the CSE.

Now, to match the $u_{s3} \sim \epsilon_{34}$ asymptotics after commuting the t and λ_2 integrations, we must impose

$$\frac{\mathcal{N}^{\mathrm{LS,II}}_{[\phi\phi]_{0,J_1}[\phi\phi]_{0,J_2};J_1-\delta n}}{16\sqrt{\lambda_1\lambda_2}} P^{(J_1-\delta n)}_{[\phi\phi]_{0,J_1}[\phi\phi]_{0,J_2}} = A^{(\delta n)}_{\lambda_1} \frac{\lambda_2^{2h_\phi-h_\star-1}}{\Gamma(2h_\phi - h_\star)}, \tag{7.3.103}$$

for some function $A^{(\delta n)}_{\lambda_1}$. Dividing both sides of the CSE by all of the powers of $u_{s1}, \dots, u_{s5}$ in the direct channel, we are left with

$$\cdots + \sum_{n=0}^{J_\star} P^{(n)}_{\mathcal{O}_\star \mathcal{O}_\star} \mathcal{N}_{\mathcal{O}_\star \mathcal{O}_\star; n} + \cdots = \int \mathrm{d}\lambda_1 \sum_{\delta n} A^{(\delta n)}_{\lambda_1} u_{s5}^{h_\phi + \delta n} \mathcal{K}_{h - h_\phi + \delta n}(\lambda_1 u_{s5}). \tag{7.3.104}$$

To match the $u_{s5} \sim \epsilon_{15}$ asymptotics, we must then impose

$$\frac{\mathcal{N}^{\mathrm{LS,II}}_{[\phi\phi]_{0,J_1}[\phi\phi]_{0,J_2}; J_1 - \delta n}}{16\sqrt{\lambda_1 \lambda_2}} P^{(J_1 - \delta n)}_{[\phi\phi]_{0,J_1}[\phi\phi]_{0,J_2}} = b_{\delta n} \frac{2\lambda_1^{h_\phi + \delta n - 1}}{\Gamma(h_\phi + \delta n)\Gamma(2h_\phi - h_\star)} \frac{\lambda_2^{2h_\phi - h_\star - 1}}{\Gamma(2h_\phi - h_\star)}, \tag{7.3.105}$$

where $b_{\delta n}$ are undetermined constants that must satisfy the sum rule

$$\sum_{n=0}^{J_\star} P^{(n)}_{\mathcal{O}_\star \mathcal{O}_\star} \mathcal{N}_{\mathcal{O}_\star \mathcal{O}_\star; n} = \sum_{\delta n = 0}^{\infty} b_{\delta n}. \tag{7.3.106}$$

We have thus obtained our ansatz for the OPE coefficients. Plugging (7.3.105) back into the CSE with the sum rule (7.3.106), we conclude that our ansatz is correct if

$$\int_{\mathbb{R}^2_+} \frac{\mathrm{d}x}{x} \frac{\mathrm{d}y}{y} x^\alpha y^\beta \mathcal{K}_\alpha(x + y) = \frac{1}{2}\Gamma(\alpha)\Gamma(\beta)^2, \tag{7.3.107}$$

for $\alpha = h_\phi + \delta n$ and $\beta = 2h_\phi - h_\star$. This identity is proven in appendix 7.B. In the next subsection, we will demonstrate how to determine the coefficients $b_{\delta n}$ specifying the OPE coefficients in (7.3.105) by solving the CSE at subleading orders in u_{s2}.

OPE coefficients at finite tensor structure

The above analysis of $[\mathcal{O}_\star|\mathcal{O}_\star]$ exchange with $h_\star > h_\phi$ exhibits two qualitatively new features of the lightcone bootstrap at higher points.

1. In cross ratio space, the asymptotics of individual five-point blocks with respect to X_{23} are the same as those of the direct channel.

2. In the space of crossed channel quantum numbers, the variable $\delta n = J_1 - n$ remains unconstrained. As a result, the OPE coefficients in $P^{(J_1 - \delta n)}_{\mathcal{O}_1 \mathcal{O}_2}$ in (7.3.105) are fixed only up to a δn-dependent number $b_{\delta n}$.

These two features are of course related: since the crossed channel blocks already scale correctly with respect to ϵ_{23}, there is no further ϵ_{23}-scaling imposed by the CSE on the quantum numbers. As a result, there are less independent scalings than there are quantum numbers, and some combination of the latter must be unconstrained — in this case, the combination turns out to be $\delta n := J_1 - n$. Since $X_{23} \to 0$ does not provide extra constraints on the CSE in this setup, it is natural to relax this limit as a means to compute the remaining freedom $b_{\delta n}$ in the OPE coefficients (7.3.105). In other words, we expect to determine $b_{\delta n}$ by solving the CSE in the limit

$$LCL^{(\mathrm{TS})} : X_{15} \ll X_{34} \ll X_{12} \ll X_{45}, \quad \forall\, X_{23}. \tag{7.3.108}$$

If we define $z := 1 - u_{s2}$, then the direct channel blocks take the form

$$\psi^{(15),(34)}_{\mathcal{O}_\star \mathcal{O}_\star; n} \overset{LCL^{(\mathrm{TS})}}{\sim} (u_{s1} u_{s2})^{h_\phi} (u_{s3} u_{s5})^{h_\star} g^{\mathrm{fin}}_{\mathcal{O}_\star \mathcal{O}_\star; n}(z), \tag{7.3.109}$$

where $g^{\text{fin}}_{\mathcal{O}_\star\mathcal{O}_\star;n}$ is a power series in z, given by the equation (7.A.29). On the other hand, the crossed channel blocks are given by

$$\psi^{(12),(45)}_{\Xi} \overset{LCL^{(\text{TS})}}{\sim} \mathcal{N}^{\text{LS,II}}_{\Xi}(u^2_{s1}u_{s2}u_{s3}u^2_{s4}u_{s5})^{h_\phi}(u_{s5}z)^{\delta n}\,\mathcal{K}_{h_\phi+\delta n}(u_{s3}u_{s5}J_2^2), \tag{7.3.110}$$

where $\Xi := ([\phi\phi]_{0,J_1}, [\phi\phi]_{0,J_2}; J_1 - \delta n)$. If we plug in the ansatz (7.3.105) for OPE coefficients into the CSE (7.3.12), we now obtain

$$\sum_{n=0}^{J_\star} P^{(n)}_{\mathcal{O}_\star\mathcal{O}_\star} g^{\text{fin}}_{\mathcal{O}_\star\mathcal{O}_\star;n}(z) = \sum_{\delta n=0}^{\infty} b_{\delta n} z^{\delta n}. \tag{7.3.111}$$

Evaluating (7.3.111) at $z = 1$ reproduces the sum rule (7.3.106). Now, we can determine all of the coefficients $b_{\delta n}$ from a power series expansion of g^{fin}. To summarize, the OPE coefficients for two double-twist exchanges at subleading order are given by

$$\frac{\mathcal{N}^{\text{LS,II}}_{\Xi}}{16\sqrt{\lambda_1\lambda_2}} P_\Xi \sim \frac{2\lambda_1^{h_\phi+\delta n-1}\lambda_2^{2h_\phi-h_\star-1}}{\Gamma(h_\phi+\delta n)\Gamma(2h_\phi-h_\star)^2} \sum_{n=0}^{J_\star} P^{(n)}_{\mathcal{O}_\star\mathcal{O}_\star} \frac{\mathrm{d}^{\delta n} g^{\text{fin}}_{\mathcal{O}_\star\mathcal{O}_\star;n}}{\mathrm{d}z^{\delta n}}\Big|_{z=0}, \tag{7.3.112}$$

where $\Xi = ([\phi\phi]_{0,J_1}, [\phi\phi]_{0,J_2}; J_1 - \delta n)$ and $g^{\text{fin}}_{\mathcal{O}_\star\mathcal{O}_\star;n}$ is in equation (7.A.29).

7.4 Outlook

The methodology developed here can be generalized in many directions, including different channels, higher points, and higher order corrections away from the lightcone limits. Here, we will list the most straightforward extensions in the case of five and six points.

7.4.1 Five points

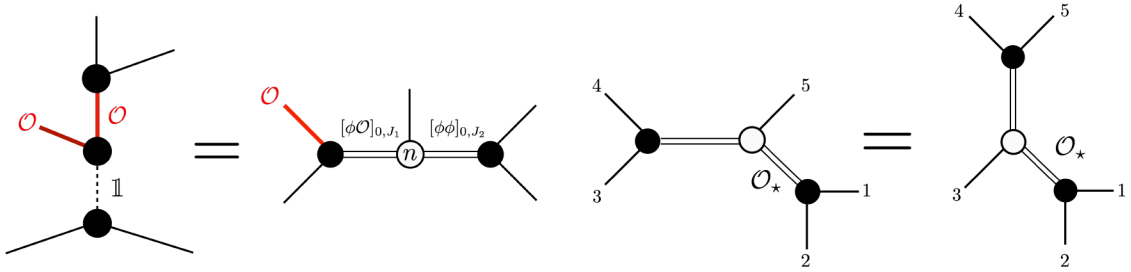

(a) Mixed correlator $\langle\phi\mathcal{O}\phi\phi\phi\rangle$.

(b) CSE of "four-point type".

Figure 38: Further extensions of the five-point bootstrap.

Mixed correlators: One simple and worthwhile generalization is to replace the external field $\phi_2 = \phi$ with another scalar field $\phi_2 = \mathcal{O}$, where $\mathcal{O}$ appears in the $\phi \times \phi$ OPE. Using the generalized prefactor (3.2.32), the CSE for the identity exchange in (51) corresponds to

$$u_{s1}^{h_\phi+h_\mathcal{O}} u_{s4}^{2h_\phi} u_{s3}^{h_\mathcal{O}-h_\phi} u_{s5}^{-2h_\phi} + \cdots = \sum_{\mathcal{O}_1,\mathcal{O}_2,n} P^{(n)}_{\mathcal{O}_1\mathcal{O}_2} \psi^{(12),(45)}_{\mathcal{O}_1\mathcal{O}_2;n}, \tag{7.4.1}$$

which is represented diagrammatically in Fig. 38a. More generally, u_{s1}, u_{s2} asymptotics in the direct channel will be controlled by $\text{sgn}(h_1 - h_\mathcal{O})$, $\text{sgn}(h_2 - h_\mathcal{O})$ respectively, while u_{s2}, u_{s3} asymptotics in the crossed channel will be controlled by $\text{sgn}(h_1 - h_\mathcal{O})$, $\text{sgn}(h_2 - h_\phi)$ respectively.

Other channels: Our choice of CSE, namely (51)2(34) = (12)3(45), was motivated by several factors, such as cyclic symmetry and the drastic simplification of the crossed channel in the $X_{15} = 0$ limit. However, there are alternative choices worth exploring. For example, the other inequivalent cyclic CSEs will look like (34)5(12) = (12)3(45), as depicted in Fig. 38b. This CSE is of "four-point type". Indeed, the direct channel and crossed channel share an OPE, namely $\phi(X_1) \times \phi(X_2)$. Thus, in the lightcone limit, both channels will have operators $\mathcal{O}_\star$ of the same twist at one internal leg, and the data probed by the lightcone bootstrap will be equivalent to that of a four-point correlator $\langle \mathcal{O}_\star(X_2, Z_2)\phi(X_3)\phi(X_4)\phi(X_5)\rangle$. However, taking e.g. $X_{15}, X_{12}, X_{23} \to 0$ instead of $X_{12} \to 0$ shows that the five-point CSE is kinematically distinct from four points — this may give rise to computational simplifications for certain $\mathcal{O}_\star$ exchanges. In general, it would be interesting to compare the spinning four-point and scalar multipoint lightcone bootstrap in these CSEs of "four-point type".

7.4.2 Six points

In our forthcoming work, we will further extend the methods and results of this chapter to six points. Indeed, the setup of Fig. 34 naturally generalizes to a six-point setup with (12)3(4(56)) as the crossed channel, and a direct channel containing the (16) OPE. In particular, the snowflake channel (16)(23)(45) leads to the planar CSE depicted in Fig. 39. There, the nine degrees of freedom in the sum over conformal blocks are divided amongst twists h, spins J, ℓ and tensor structures n at the internal legs and vertices of the OPE diagram on each side. While the theory of six-point snowflake

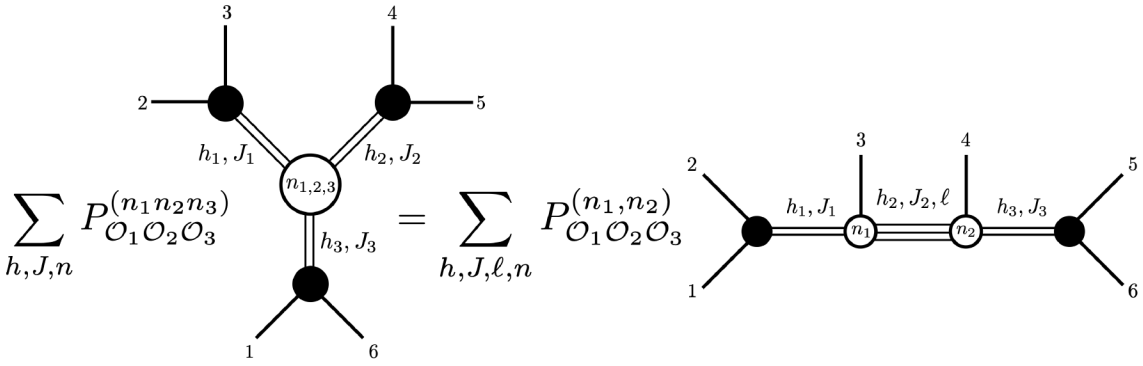

Figure 39: Graphical representation of a planar six-point crossing symmetry equation from the snowflake channel (61)(23)(45) to the comb (12)3(4(56)). Internal legs are labeled by half-twists h and spin labels J, ℓ, while vertices are labeled by tensor structures $t_{n_1 n_2 n_3}(w_1, w_2, w_3)$ in the snowflake, and $t_{n_1}(\mathcal{X}_1), t_{n_2}(\mathcal{X}_2)$ in the comb.

blocks is not fully developed, the direct channel reduces to a four-point function at leading order in the $X_{16} \ll 1$ limit, where the identity propagates through (16). Even at this order, the crossed channel already contains highly non-trivial data. In polynomial cross ratios, the CSE then becomes

$$\left(\frac{u_1\sqrt{u_2}u_3}{U^{(6)}}\right)^{2h_\phi}\left(\sum_{\mathcal{O}} C^2_{\phi\phi\mathcal{O}}\psi^{(23),(45)}(u_2, v_2) + \mathrm{O}(X_{16}^{h_\star})\right) = \sum_{\Xi} P_\Xi \psi_\Xi^{(12),(4(56))}(u, v, U^{(5)}, U^{(6)}), \tag{7.4.2}$$

where $\Xi = (\mathcal{O}_1\mathcal{O}_2\mathcal{O}_3; n_1 n_2) = (h_1 h_2 h_3 J_1 J_2 J_3 \ell; n_1 n_2)$. The sequence of lightcone limits that generalizes (7.3.13) is

$$X_{16} \ll X_{23}, X_{45} \ll X_{34} \ll X_{12}, X_{56} \ll X_{46} \ll 1. \tag{7.4.3}$$

To intuit the last limit, which ensures the suppression of higher twist exchange at the middle leg, recall the cluster decomposition limit of chapter 6.

Comb channel lightcone blocks. On the right hand side of the CSE, our computation of blocks follows the same general approach as section 7.3.2. The diagram of Fig. 35 continues to describe OPE, decoupling, and lightcone limits of six-point blocks if "(u, v, x)" now denotes the groups of cross ratios

$$u \equiv \frac{u_1}{v_2}, \frac{u_2}{v_1 v_3}, \frac{u_3}{v_2}, \quad v \equiv v_1, v_2, v_3, \quad x \equiv x_1, x_2, x_3. \tag{7.4.4}$$

In the last group, we have introduced the variables

$$(x_1, x_2, x_3) \propto (U_1^{(5)}, U_2^{(5)}, U^{(6)}) \propto (1 - w_1, 1 - w_2, \Upsilon),$$

which are simple rational functions of the polynomial cross ratios. The restriction of each lightcone limit in (7.4.3) to cross ratio space is depicted in Fig. 40. In practice, the limits $u = 0$ suppress the twist at each internal leg, the limit $v_r = 0$ couples to the large spin limits at leg r, and a polynomial equation $f(x_1, x_2, x_3) = 0$, linear in x_3, defines the (16) lightcone limit. Altogether, this sequence of limits reaches the "$(0, 0, 1)$" node in Fig. 35. Contrary to the five-point case, note that there remain two kinematical degrees of freedom in x_1, x_2, which relate to the tensor structures at the two non-trivial vertices of the comb. To compute the asymptotics of blocks, the Casimir equations are solved

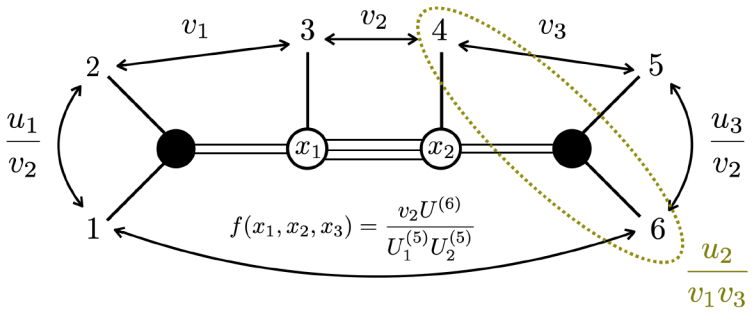

Figure 40: Description of how the lightcone limits in (7.4.3) descend to cross ratio space. To each nearest neighbor pair $i(i+1)$ is associated an independent cross ratio that scales like $\mathrm{O}(X_{i(i+1)})$. The last lightcone limit, for the next to neighboring points (46), is represented by the green lasso.

at leading order in the lightcone limits,

$$\begin{aligned}
\mathcal{D}_{12}^2 &= \epsilon_{16}^{-1} \epsilon_{23}^{-1} \mathcal{D}_{12}^{(-1,-1,0,0)} + \epsilon_{16}^{-1} \mathcal{D}_{12}^{(-1,0,0,0)} + \dots, \\
\mathcal{D}_{456}^2 &= \epsilon_{16}^{-1} \epsilon_{34}^{-1} \mathcal{D}_{456}^{(-1,0,-1,0)} + \epsilon_{16}^{-1} \mathcal{D}_{456}^{(-1,0,0,0)} + \dots, \\
\mathcal{D}_{56}^2 &= \epsilon_{16}^{-1} \epsilon_{45}^{-1} \mathcal{D}_{56}^{(-1,0,0,-1)} + \epsilon_{16}^{-1} \mathcal{D}_{56}^{(-1,0,0,0)} + \dots.
\end{aligned}$$

In particular, the factorization property (7.1.3) at $\mathrm{O}(\epsilon_{16}^{-1})$ continues to play an important role in simplifying the eigenvalue problem. Expanding around an exact result in the decoupling limit ($x = 0$), the normalization can then be determined with help of an integral formula for lightcone blocks ($u = 0$). The latter stems from a formula for the lightcone OPE of one STT and one scalar, obtained in turn from Feynman parameterizations of three-point tensor structures. It takes the general form

$$\mathcal{O}_1(X_1, Z_1)\phi_2(X_2) = \sum_{\mathcal{O}_3, n} C^{(n)}_{\mathcal{O}_1 \phi_2 \mathcal{O}_3} X_{12}^{\frac{\tau_3 - \tau_1 - \Delta_2}{2}} \int \mathrm{d}\mu(s_1, s_2, s_{2'}) \mathrm{d}\mu(s_1^{(1)}, s_2^{(1)})\, \mathcal{O}_3(X, Z, W), \tag{7.4.5}$$

where $\mathcal{O}_3$ is the leading twist operator in $\mathcal{O}_1 \times \phi_2$ and

$$X = s_1 X_1 + s_2 X_2 + s_{2'} \mathcal{Y}_{1,2}, \quad \mathcal{Y}_{1,2B} := \frac{X_2^A (X_1 \wedge Z_1)_{AB}}{X_{12}},$$
$$X \wedge Z = s_1^{(1)} X_1 \wedge Z_1 + s_2^{(1)} X_1 \wedge X_2, \quad X \wedge Z \wedge W = X_1 \wedge X_2 \wedge X_3.$$

Direct channel single-twist exchange. The first non-trivial crossed channel CFT data appears when a single leading twist operator $\mathcal{O}_\star$ is exchanged on the left hand side of the CSE (7.4.2). At this order, the crossed channel is dominated by double twist exchanges of the form given in Fig. 41. Moreover, the direct channel is $(\mathcal{D}_{12}^2, \mathcal{D}_{456}^2, \mathcal{D}_{56}^2)$-singular of orders $(\epsilon_{16}^{-1}\epsilon_{23}^{-1}, \epsilon_{16}^{-1}\epsilon_{34}^{-1}, \epsilon_{16}^{-1}\epsilon_{45}^{-1})$, which

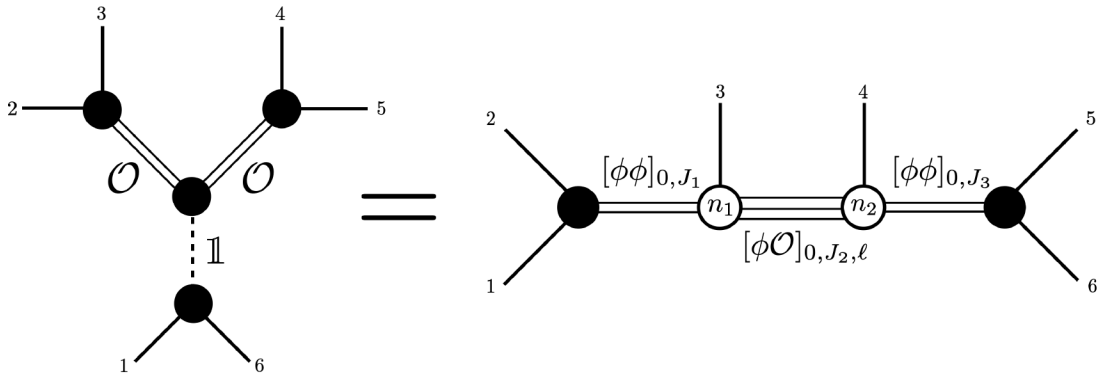

Figure 41: Leading contribution to the six-point CSE (61)(23)(45) = (12)3(4(56)). The left hand side a single four-point block for a leading twist operator $\mathcal{O}$, while the right hand side is a sum over $(J, \ell; n)$ of double-twist operators.

implores us to compute a six-point analogue of case (I) blocks. While the computation and consequent resummation of case (I) blocks for general kinematics x_1, x_2 is a difficult task, we have obtained several concrete results in reduced kinematics. The latter impose restrictions on the crossed channel quantum numbers such as $\ell \ll 1$ or $n_2 \ll 1$.

Direct channel double-twist exchange. To probe crossed channel triple-twist data, we already need double-twist exchange in the direct channel. At leading order in the $X_{34} \ll 1$ limit, this is equivalent to three identity exchanges in the (16)(34)(25) channel[10], as described by the leftward equality of Fig. 42. Reading off the power law in u_2 at leading order, we deduce the propagation of triple-twist operators at the middle leg of the comb channel. Remarkably, this shares the same qualitative properties as the $[\mathcal{O}_\star|\mathcal{O}_\star]$ exchanges with $h_\star > h_\phi$ in the five-point CSE. That is, the direct channel is $(\mathcal{D}_{12}^2, \mathcal{D}_{456}^2, \mathcal{D}_{56}^2)$-singular of orders $(\epsilon_{16}^{-1}, \epsilon_{16}^{-1}\epsilon_{34}^{-1}, \epsilon_{16}^{-1})$, meaning that all crossed channel blocks already exhibit the same asymptotics in X_{23}, X_{45} as the direct channel. Consequently, there are two less constraints on the crossed channel quantum numbers. In our investigation of six-point CSEs we have found this "case (II)" behavior to accompany all appearances of triple-twist data in the crossed channel at leading order. It may suggest that there is no analogue of the large spin limit of double-twist operators, where anomalous dimensions turn off and OPE coefficients asymptote to generalized free field theory. Harking back to an important source of inspiration for the lightcone bootstrap, it

[10] If one were to exchange the order of limits to $X_{34} \ll X_{23}, X_{45}$ in (7.4.3), this contribution would actually be the first to appear in the direct channel. This makes no difference in our setup though, since the order of limits in $X_{23,34,45}$ commute amongst themselves in the crossed channel.

would be interesting to compare this phenomenon with the physics of three-particle states in Anti de Sitter space.

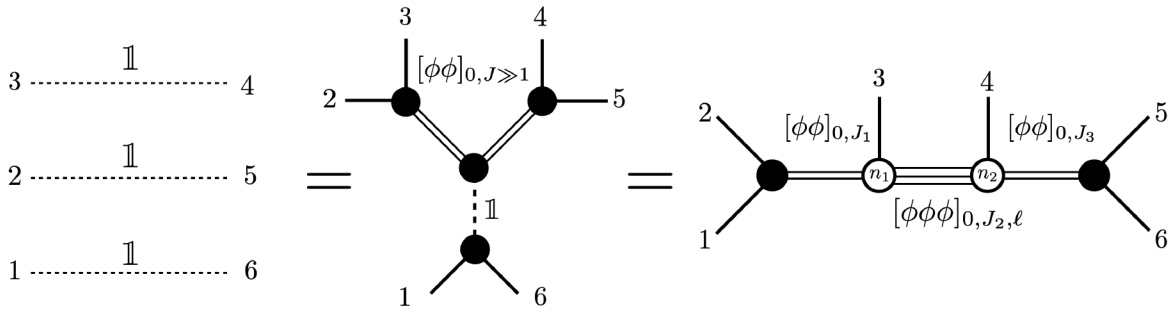

Figure 42: Leading contribution to the six-point CSE with triple-twist exchange in the crossed channel.

7.A Five-point lightcone blocks

7.A.1 Integral representation from lightcone OPE

The lightcone OPE for two scalars can be written as

$$\phi_1(X_1)\phi_2(X_2) = \sum_{\mathcal{O}_3} \frac{C_{\phi_1\phi_2\mathcal{O}_3}}{\mathrm{B}_{\bar{h}_3+h_{12},\bar{h}_3+h_{21}}|\mathbb{R}^\times|} \int_{\mathbb{R}^2_+} \frac{\mathrm{d}s_1}{s_1} s_1^{\bar{h}_3+h_{21}} \frac{\mathrm{d}s_2}{s_2} s_2^{\bar{h}_3+h_{12}} \mathcal{O}_3(X,Z), \tag{7.A.1}$$

with $X_a := s_1X_1 + s_2X_2$, $X \wedge Z := X_1 \wedge X_2$ and $\mathrm{B}_{a,b} := \Gamma(a)\Gamma(b)/\Gamma(a+b)$. From this we derive the following formula for the lightcone blocks of five identical scalars ϕ,

$$\frac{\psi^{(12),(45)}_{\mathcal{O}_1\mathcal{O}_2;n}}{X_{12}^{h_1}X_{45}^{h_2}(X_{15}X_{24}-X_{14}X_{25})^n} \overset{X_{12},X_{45}\to 0}{\sim} \int_{\mathbb{R}^4_+} \frac{\mathrm{d}^4 \log s\, (s_1s_2)^{\bar{h}_1}(s_4s_5)^{\bar{h}_2}}{\mathrm{B}_{\bar{h}_1,\bar{h}_1}\mathrm{B}_{\bar{h}_2,\bar{h}_2}|\mathbb{R}^\times|^2} X_{a3}^{h_2-\bar{h}_1-h_\phi+n} X_{b3}^{h_1-\bar{h}_2-h_\phi+n} X_{ab}^{-\bar{h}_{12;\phi}} J_{a,3b}^{J_1-n} J_{b,3a}^{J_2-n}, \tag{7.A.2}$$

where $X_a = s_1X_1 + s_2X_2$, $X_b = s_4X_4 + s_5X_5$ and $X_a \wedge Z_a = X_1 \wedge X_2$, $X_b \wedge Z_b = X_5 \wedge X_4$, such that e.g. $X_{a3} = s_1X_{13} + s_2X_{23}$. To reduce this formula to cross ratio space, we fix the gauge $X_i = X_i^\star$, with

$$X_2^\star = (1,0,\mathbf{0}), \quad X_3^\star = (0,1,\mathbf{0}), \quad X_4 = (1,1,\mathbf{n}), \tag{7.A.3}$$

in lightcone coordinates $\mathrm{d}X^2 = -\mathrm{d}X^+\mathrm{d}X^- + \mathrm{d}\mathbf{X}^2$ and for some unit vector $\mathbf{n} \in S^{d-1}$, such that

$$X_{15}^\star = U_1^5, \quad X_{14}^\star = v_1, \quad X_{13}^\star = 1, \quad X_{12}^\star = u_1 \tag{7.A.4}$$

$$X_{25}^\star = v_2, \quad X_{24}^\star = 1, \quad X_{23}^\star = 1, \tag{7.A.5}$$

$$X_{35}^\star = 1, \quad X_{34}^\star = 1, \tag{7.A.6}$$

$$X_{45}^\star = u_2. \tag{7.A.7}$$

We then evaluate the integrand at $X_{ij}^\star = X_i^\star \cdot X_j^\star$ to obtain a function of the cross ratios. In particular, we have $X_{a3}^\star = s_1 + s_2$ and $X_{b3}^\star = s_4 + s_5$ in this gauge. Finally, to extract the prefactor in (7.3.16)

from the block, we make the change of variables $\tilde{s}_1 = s_1 v_2$, $\tilde{s}_5 = s_5 v_2$. Defining $z_a := 1 - v_a$, $a = 1, 2$, we obtain

$$F^{(12),(45)}_{\mathcal{O}_1\mathcal{O}_2;n} \overset{u_{1,2}\to 0}{\sim} \int_{\mathbb{R}^4_+} \frac{\mathrm{d}^4 \log s\, (\tilde{s}_1 s_2)^{\bar{h}_1} (s_4 \tilde{s}_5)^{\bar{h}_2}}{\mathrm{B}_{\bar{h}_1,\bar{h}_1}\mathrm{B}_{\bar{h}_2,\bar{h}_2}|\mathbb{R}^\times|^2} \frac{(\tilde{s}_1 + s_2 v_1)^{h_{2\phi}+n-\bar{h}_1} (s_4 v_2 + \tilde{s}_5)^{h_{1\phi}+n-\bar{h}_2}}{(X^\star_{ab})^{\bar{h}_{12;\phi}} \left(\frac{J^\star_{a,b3}}{z_1}\right)^{n-J_1} \left(\frac{J^\star_{b,a3}}{z_2}\right)^{n-J_2}}. \tag{7.A.8}$$

7.A.2 Power series expansion of lightcone blocks

We now set $\tilde{s}_{1,5} \equiv s_{1,5}$ for simplicity, such that $X^\star_a = \frac{s_1}{v_1} X^\star_1 + s_2 X^\star_2$, $X^\star_b = \frac{s_5}{v_2} X^\star_5 + s_4 X^\star_4$ in the tensor structures. Our goal is now to expand the integrand around the decoupling limit $x = 0$, where $x = 1 - u_{s5} = 1 - \frac{U^5_1}{v_1 v_2}$. We will write this expansion as

$$e^\star(v_a, x) = e^\star(v_a, 0) \frac{e^\star(v_a, x)}{e^\star(v_a, 0)}, \quad e \in \{X_{ab}, J_{a,3b}, J_{b,3a}\}, \tag{7.A.9}$$

which translates to

$$X^\star_{ab} = (s_1 + s_2)(s_5 + s_4) \left(1 - x \frac{s_1}{s_1 + s_2} \frac{s_5}{s_5 + s_4}\right),$$
$$\frac{J^\star_{a,3b}}{z_1} = (s_5 + s_4) \left(1 + x \frac{v_1}{z_1} \frac{s_5}{s_5 + s_4}\right), \quad \frac{J^\star_{b,3a}}{z_2} = (s_1 + s_2) \left(1 + x \frac{s_1}{s_1 + s_2} \frac{v_2}{z_2}\right).$$

Factorization in the decoupling limit

Evaluating the above tensor structures $X^\star_{ab}, J^\star_{a,3b}, J^\star_{b,3a}$ at $x = 0$, we find a factorization into a product of two integrals,

$$F^{(12),(45)}_{\mathcal{O}_1\mathcal{O}_2;n} \overset{x\to 0}{\sim} \int_{\mathbb{R}_+} \frac{\mathrm{d}^2 \log s\, (s_1 s_2)^{\bar{h}_1}}{\mathrm{B}_{\bar{h}_1,\bar{h}_1}|\mathbb{R}^\times|} \frac{(s_1 + s_2 v_1)^{h_{2\phi}+n-\bar{h}_1}}{(s_1 + s_2)^{h_{2\phi}+n+\bar{h}_1}} \int_{\mathbb{R}_+} \frac{\mathrm{d}^2 \log s\, (s_4 s_5)^{\bar{h}_1}}{\mathrm{B}_{\bar{h}_2,\bar{h}_2}|\mathbb{R}^\times|} \frac{(s_5 + s_4 v_2)^{h_{2\phi}+n-\bar{h}_1}}{(s_5 + s_4)^{h_{2\phi}+n+\bar{h}_1}}.$$

Each integral is equal to one of the Gauss hypergeometric functions in (7.3.19). More generally, the 3-parameter Gauss hypergeometric function admits an integral representation

$${}_2F_1 \begin{bmatrix} a, b \\ c \end{bmatrix} (1 - v) = \int_{\mathbb{R}^2_+} \frac{\mathrm{d}s_1}{s_1} \frac{\mathrm{d}s_2}{s_2}\, {}_2f_1 \begin{bmatrix} a, b \\ c \end{bmatrix} (1 - v; s_1, s_2), \tag{7.A.10}$$

$${}_2f_1 \begin{bmatrix} a, b \\ c \end{bmatrix} (1 - v; s_1, s_2) = \frac{s_1^{c-b} s_2^b}{\mathrm{B}_{b,c-b}} \frac{(s_1 + s_2)^{a-c}}{(s_1 + s_2 v)^a}. \tag{7.A.11}$$

In this case, the formula reduces to the Euler Beta integral representation after the change of variables

$$(s_1, s_2) = (s(1 - t), st), \quad (s, t) \in (0, \infty) \times [0, 1), \quad |\mathbb{R}^\times| = \int_0^\infty \frac{\mathrm{d}s}{s}. \tag{7.A.12}$$

In our integral representation, the Euler transformation of the Gauss hypergeometric corresponds to

$${}_2f_1 \begin{bmatrix} a, b \\ c \end{bmatrix} (1 - v; s_1 v, s_2) = v^{c-a-b}\, {}_2f_1 \begin{bmatrix} c - a, c - b \\ c \end{bmatrix} (1 - v; s_2, s_1). \tag{7.A.13}$$

Expansion around the decoupling limit

By inspecting the expansion of the integrand tensor structures of the form (7.A.9), we observe that all higher order corrections to the integrand in x are proportional to

$$x^{k+m_1+m_2} \left(\frac{s_1}{s_1 + s_2}\right)^{k+m_2} {}_2f_1 \begin{bmatrix} \bar{h}_1 - h_{2\phi} - n, \bar{h}_1 \\ 2\bar{h}_1 \end{bmatrix} (1 - v; s_1, s_2)$$
$$\left(\frac{s_5}{s_5 + s_4}\right)^{k+m_2} {}_2f_1 \begin{bmatrix} \bar{h}_2 - h_{1\phi} - n, \bar{h}_2 \\ 2\bar{h}_2 \end{bmatrix} (1 - v_2; s_5, s_4).$$

At the same time, these integrand shifts $s_i^k(s_i+s_j)^{-k}$ are equivalent to

$$\left(\frac{s_1}{s_1+s_2}\right)^k {}_2f_1\begin{bmatrix}a,b\\c\end{bmatrix}(1-v;s_1,s_2)=\frac{(c-b)_k}{(c)_k}{}_2f_1\begin{bmatrix}a,b\\c+k\end{bmatrix}(1-v;s_1,s_2) \tag{7.A.14}$$

The right hand side lifts to the integral itself, and to express it in a simple way we define operators $\mathcal{S}^k$ that realize this integrand transformation,

$$\mathcal{S}^k\cdot{}_2F_1\begin{bmatrix}a,b\\c\end{bmatrix}(1-v):=\frac{(c-b)_k}{(c)_k}{}_2F_1\begin{bmatrix}a,b\\c+k\end{bmatrix}(1-v). \tag{7.A.15}$$

The operator $\mathcal{S}^k$ obviously depends on the parameters a,b,c and the variable v, but we will not need to make this dependence explicit in future uses. It is not difficult to write this integral formula as a differential operator — for example, one can cojnjugate the derivative identity for Gauss hypergeometrics by the Euler transformation as follows,

$$\begin{aligned}\frac{(c-b)_k}{(c)_k}{}_2F_1\begin{bmatrix}a,b\\c+k\end{bmatrix}&=v^{c+k-a-b}\frac{(c-b)_k}{(c)_k}{}_2F_1\begin{bmatrix}c-a+k,c-b+k\\c+k\end{bmatrix}\\&=v^{c+k-a-b}\frac{(-\partial_v)^k}{(c-a)_k}{}_2F_1\begin{bmatrix}c-a,c-b\\c\end{bmatrix}\\&=v^{c-a-b}\frac{v^k(-\partial_v)^k}{(c-a)_k}v^{a+b-c}{}_2F_1\begin{bmatrix}a,b\\c\end{bmatrix}.\end{aligned}$$

Since the differential operator acting on the ${}_2F_1$ is homogeneous of degree zero in v, it can be written as a function of $\vartheta_v:=v\partial_v$. By inspecting its action on the eigenbasis of ϑ_v, we find

$$v^k(-\partial_v)^k\cdot v^n=(-n)(-n+1)\dots(-n+k)v^n\Rightarrow v^k(-\partial_v)^k=(-\vartheta_v)_k.$$

Altogether, we obtain two useful representations of $\mathcal{S}^k$, defined in (7.A.15), as a differential operator.

$$\text{Acting on }{}_2F_1\begin{bmatrix}a,b\\c\end{bmatrix}(1-v),\quad \mathcal{S}^k=v^{c-a-b}\frac{v^k(-\partial_v)^k}{(c-a)_k}v^{a+b-c}=\frac{(c-a-b-\vartheta_v)_k}{(c-a)_k}. \tag{7.A.16}$$

Here, for the all orders expansion of lightcone blocks in x, we will use two such shift operators,

$$\mathcal{S}_a^k\cdot{}_2F_1\begin{bmatrix}\bar h_a-h_{b\phi}-n,\bar h_a\\2\bar h_a\end{bmatrix}(1-v_a):=\frac{(\bar h_a)_k}{(2\bar h_a)_k}{}_2F_1\begin{bmatrix}\bar h_a-h_{b\phi}-n,\bar h_a\\2\bar h_a+k\end{bmatrix}(1-v_a),\quad a\neq b=1,2. \tag{7.A.17}$$

The resulting formulas for $\mathcal{S}_1^k,\mathcal{S}_2^k$ as differential operators can then be read from (7.A.16) by inserting the corresponding values of (a,b,c) in the ${}_2F_1$'s. We will also adopt the notation of (7.3.19) for the product of hypergeometrics at $x=0$, that is

$$f_a^{\text{dec}}(v_a):=\frac{(\bar h_a)_k}{(2\bar h_a)_k}{}_2F_1\begin{bmatrix}\bar h_a-h_{b\phi}-n,\bar h_a\\2\bar h_a+k\end{bmatrix}(1-v_a),\quad a\neq b=1,2. \tag{7.A.18}$$

Finally, with all of the necessary conventions listed in eq. (7.A.16)—(7.A.18), the all-orders expansion of five-point lightcone blocks around the decoupling limit $x=0$ can be expressed as

$$F^{(12),(45)}_{\mathcal{O}_1\mathcal{O}_2;n}\overset{u_{1,2}\to 0}{\sim}(1-x\,\mathcal{S}_1\mathcal{S}_2)^{-\bar h_{12;\phi}}\left(1+x\frac{v_1}{z_1}\mathcal{S}_2\right)^{J_1-n}\left(1+x\,\mathcal{S}_1\frac{v_2}{z_2}\right)^{J_2-n}f_1^{\text{dec}}(v_1)f_2^{\text{dec}}(v_2). \tag{7.A.19}$$

In this formula, one should understand the three factors on the right hand side as Pochhammer power series of the form $(1-x\lambda)^{-\Delta} = \sum_{k=0}^{\infty} \frac{x^k}{k!}(\Delta)_k \lambda^k$. This culminates in a triple-sum power series expansion in x,

$$\text{RHS} = \sum_{k=0}^{\infty} \frac{(\bar{h}_{12;\phi})_k}{k!} \prod_{b\neq a=1}^{2} \sum_{m_a=0}^{J_a-n} \binom{J_a-n}{m_a} \left(\frac{v_a}{z_a}\right)^{m_a} \mathcal{S}_a^{k+m_b} f_a^{\text{dec}}\, x^{k+m_1+m_2}. \tag{7.A.20}$$

Factorization in the ϑ_x eigenbasis

In our analysis of conformal block asymptotics, we find

$$F^{(12),(45)}_{\mathcal{O}_1\mathcal{O}_2;n} \overset{u_{1,2}\to 0}{\sim} \begin{cases} \mathcal{N}(x) f_{h_{2\phi}+n}(v_1) f_{h_{2\phi}+n}(v_2) & \text{if } v_1, v_2 \to 0, \\ \mathcal{N}^{\text{LS,I}}_{\mathcal{O}_1\mathcal{O}_2;n} e^{-\frac{\bar{h}_1^2 v_1}{n}}\, e^{-\frac{\bar{h}_2^2 v_2}{n}} & \text{in case (I)}, \\ \mathcal{N}^{\text{LS,II}}_{\mathcal{O}_1\mathcal{O}_2;n} \int_0^\infty \mathrm{d}k\, k^{-(1+h_\phi+J_1-n)} e^{-k(1-x)} e^{-\frac{\bar{h}_1^2 v_1}{k}}\, e^{-\frac{\bar{h}_2^2 v_2}{k}} & \text{in case (II)}. \end{cases} \tag{7.A.21}$$

In the first case, $\mathcal{N}(x)$ is a power series with $\mathcal{N}(1) = \mathcal{N}_{\mathcal{O}_1\mathcal{O}_2;n}$ in (7.3.35). In the two other cases, we take the limit $x \to 1$ with $x^n \sim e^{-n(1-x)}$ and $x^k \sim e^{-k(1-x)}$ for (I) and (II) respectively. On the other hand, decomposing (7.A.19) in the ϑ_x eigenbasis, we do not find a separation of variables (v_1, v_2) in general,

$$F^{(12),(45)}_{\mathcal{O}_1\mathcal{O}_2;n} \overset{u_{1,2}\to 0}{\sim} \sum_{\eta=n}^{\infty} x^{\eta-n} f_\eta(v_1, v_2),$$

$$f_\eta = \sum_{k+m_1+m_2=\eta} \frac{(\bar{h}_{12;\phi})_k}{k!} \prod_{b\neq a=1}^{2} \binom{J_a-n}{m_a} \left(\frac{v_a}{z_a}\right)^{m_a} \mathcal{S}_a^{k+m_b} f_a^{\text{dec}}(v_a).$$

Factorizations similar to (7.A.21) can only occur in situations where there is not more than one triplet (k, m_1, m_2) with $k + m_1 + m_2 = \eta$ that is not subleading. In practice, the factorizations in (7.A.21) always correspond to the second and third factor in (7.A.19) being subleading, and can be obtained as a limit of the expression

$$F^{(12),(45)}_{\mathcal{O}_1\mathcal{O}_2;n} \sim (1 - x\,\mathcal{S}_1\mathcal{S}_2)^{-\bar{h}_{12;\phi}}\, f_1^{\text{dec}}(v_1) f_2^{\text{dec}}(v_2). \tag{7.A.22}$$

7.A.3 Further limits

For the remainder of this appendix, we will analyze the simplifications of formula (7.A.19) in the OPE limit, as well as the various further lightcone and/or large quantum number limits used in the paper. Most of these limits will be captured by the simplified expression (7.A.22).

OPE limit

To explicitly understand the behavior of (7.A.19) in the OPE limit, we switch to OPE cross ratios,

$$z_a = 1 - v_a + \mathrm{O}(\bar{z}_a), \quad x = \frac{z_1 z_2 \mathcal{X}}{(1-z_1)(1-z_2)} + \mathrm{O}(\bar{z}_1, \bar{z}_2), \quad \mathcal{X} := 1 - w, \tag{7.A.23}$$

with $u_a = z_a \bar{z}_a$ vanishing in the lightcone limit. Using $f_a^{\text{dec}}(1-z_a) = 1 + \mathrm{O}(z_a)$, we find

$$\left(x \frac{v_a}{z_a} \mathcal{S}_a\right)^k f_a^{\text{dec}}(1-z_a) = z_b^k \mathcal{X}^k \frac{(\bar{h}_a)_k}{(2\bar{h}_a)_k} \left(1 + \mathrm{O}(z_1, z_2)\right), \quad a \neq b = 1, 2,$$
$$(x \mathcal{S}_1 \mathcal{S}_2)^k \, f_1^{\text{dec}}(1-z_1) f_2^{\text{dec}}(1-z_2) = z_1^k z_2^k \mathcal{X}^k \frac{(\bar{h}_1)_k}{(2\bar{h}_1)_k} \frac{(\bar{h}_2)_k}{(2\bar{h}_2)_k} \left(1 + \mathrm{O}(z_1, z_2)\right).$$

It follows that all higher order terms in the expansion around $x = 0$ are subleading in the OPE limit, and the remaining x^0 term is normalized to 1,

$$F^{(12),(45)}_{\mathcal{O}_1\mathcal{O}_2;n} = 1 + \mathrm{O}(z, \bar{z}) \iff \lim_{z_a \to 0} \lim_{\bar{z}_a \to 0} \frac{\psi^{(12),(45)}_{\mathcal{O}_1\mathcal{O}_2;n}}{\prod_a \bar{z}_a^{\bar{h}_a} z_a^{\bar{h}_a} \, \mathcal{X}^n} = 1. \tag{7.A.24}$$

Direct channel lightcone limits

The formula (7.A.19) describes blocks on the $(0, v, x)$ node of Fig. 35. We will now look at $v_2 \to 0$ and/or $v_1 \to 0$ limit, corresponding to $X_{34} \ll 1$ and/or $X_{23} \ll 1$, with $x = 1 - u_{s5}$ and $\bar{h}_1, \bar{h}_2, n$ unaffected.

1. Let us begin with $v_2 \to 0$ only. In this limit, all higher order terms in x become subleading whenever $h_{1\phi} + n \leq 0$, as we discussed in subsection 3.3, and it is straightforward to take the limit of $f_1^{\text{dec}}(v_2)$ with a power law or logarithm divergence. On the other hand, when $h_1 > h_\phi - n$, we have

$$f_2^{\text{dec}}(0) = {}_2F_1 \left[\begin{matrix} \bar{h}_2 - h_{1\phi} - n, \bar{h}_2 \\ 2\bar{h}_2 \end{matrix}\right](1) = \frac{\Gamma(2\bar{h}_2)\Gamma(h_{1\phi} + n)}{\Gamma(\bar{h}_2)\Gamma(\bar{h}_2 + h_{1\phi} + n)}. \tag{7.A.25}$$

At higher orders in the x-expansion, we obtain similarly

$$\left(\mathcal{S}_2^k f_2^{\text{dec}}\right)(0) = \frac{(\bar{h}_2)_k}{(2\bar{h}_2)_k} {}_2F_1 \left[\begin{matrix} \bar{h}_2 - h_{1\phi} - n, \bar{h}_2 \\ 2\bar{h}_2 + k \end{matrix}\right](1) = \frac{\Gamma(2\bar{h}_2)\Gamma(h_{1\phi} + n + k)}{\Gamma(\bar{h}_2)\Gamma(\bar{h}_2 + h_{1\phi} + n + k)}. \tag{7.A.26}$$

In practice it's useful to encode this into the differential operator representation of $\mathcal{S}_2^k$ coming from the second equality of (7.A.16),

$$\mathcal{S}_2^k(\vartheta_{v_2}) = \frac{(h_{1\phi} + n - \vartheta_{v_2})}{(h_{1\phi} + n + \bar{h}_2)_k}. \tag{7.A.27}$$

As a result, the leading order contribution in the $v_2 \to 0$ limit is obtained by evaluating (7.A.19) at $v_2 = \vartheta_{v_2} = 0$,

$$F^{(12),(45)}_{\mathcal{O}_1\mathcal{O}_2;n} \overset{v_2 \ll u_{1,2} \ll 1}{\sim} (1 - x\, \mathcal{S}_1\mathcal{S}_2(0))^{-\bar{h}_{12;\phi}} \left(1 + x \frac{v_1}{z_1} \mathcal{S}_2(0)\right)^{J_1 - n} f_1^{\text{dec}}(v_1) f_2^{\text{dec}}(0). \tag{7.A.28}$$

In lightcone bootstrap applications, we may also consider the further limit $x = 1 - u_{s5} \to 1$. Since the sums converge, it suffices to evaluate (7.A.28) at $x = 1$. After multiplying by $z_1^{J_1 - n}$, we obtain a power series

$$g^{\text{fin}}_{\mathcal{O}_1\mathcal{O}_2;n}(z_1) = \frac{\Gamma(2\bar{h}_2)\Gamma(h_{1\phi} + n)}{\Gamma(\bar{h}_2)\Gamma(\bar{h}_2 + h_{1\phi} + n)} \sum_{k=0}^{\infty} \frac{(\bar{h}_{12;\phi})_k}{k!} \frac{(\bar{h}_1)_k}{(2\bar{h}_1)_k} \frac{(h_{1\phi} + n)_k}{(h_{1\phi} + n + \bar{h}_2)_k}$$
$${}_2F_1 \left[\begin{matrix} \bar{h}_1 - h_{2\phi} - n, \bar{h}_1 \\ 2\bar{h}_1 + k \end{matrix}\right](z_1) \, {}_2F_1 \left[\begin{matrix} n - J_1, \bar{h}_2 \\ \bar{h}_2 + h_{1\phi} + n + k \end{matrix}\right](1 - z_1). \tag{7.A.29}$$

We use eq. (7.A.29) in the case of $(\mathcal{O}_\star, \mathcal{O}_\star)$ exchange in the direct channel, where we set $h_1 = h_2 = h_\star$ and $\bar{h}_1 = \bar{h}_2 = \bar{h}_\star$.
2. If we further take $v_1 \to 0$, then we can similarly represent $\mathcal{S}_1$ as

$$\mathcal{S}_1^k(\vartheta_{v_1}) = \frac{(h_{2\phi} + n - \vartheta_{v_1})}{(h_{2\phi} + n + \bar{h}_1)_k}. \tag{7.A.30}$$

We can now evaluate the expression (7.A.19) at $v_1 = v_2 = \vartheta_{v_1} = \vartheta_{v_2} = 0$, which yields

$$F^{(12),(45)}_{\mathcal{O}_1\mathcal{O}_2;n} \overset{v_{1,2}\ll u_{1,2}\ll 1}{\sim} (1 - x\,\mathcal{S}_1(0)\mathcal{S}_2(0))^{-\bar{h}_{12;\phi}}\, f_1^{\text{dec}}(0) f_2^{\text{dec}}(0). \tag{7.A.31}$$

Performing the power series expansion around $x = 0$ and evaluating it at $x = 1$, we obtain the ${}_3F_2$ formula of (7.3.35).

Crossed channel lightcone limits

In regimes relevant to the crossed channel OPE decomposition, the quantum numbers $\bar{h}_1, \bar{h}_2, n$ diverge by a specified ϵ-scaling with the limits $v_{1,2} = \mathrm{O}(\epsilon_{23,34})$ and $1 - x = \mathrm{O}(\epsilon_{15})$. The spins $\bar{h}_1, \bar{h}_2$ are large numbers in all of these cases, and the tensor structure n may also be large. Using the differential operator representation (7.A.27), (7.A.30) of the $\mathcal{S}$-operators and their powers, we find

$$\mathcal{S}_a^k(\vartheta) = \bar{h}_a^{-k}(h_{b\phi} + n - \vartheta)_k \left(1 + \mathrm{O}(\bar{h}_a^{-1})\right). \tag{7.A.32}$$

Consequently, the two last factors in (7.A.19) will always go like

$$\left(1 + x\frac{v_a}{z_a}\mathcal{S}_b\right)^{J_a - n} = 1 + \mathrm{O}\left(\frac{(J_a - n)v_a}{\bar{h}_b}\right), \quad a \neq b = 1, 2. \tag{7.A.33}$$

These corrections will be subleading in any regime where

$$\bar{h}_2^{-2}, v_2 = \mathrm{O}(\epsilon_{34}), \quad \bar{h}_1 \ll \bar{h}_2. \tag{7.A.34}$$

This approximation applies consistently to all large spin limits considered in the crossed channel (12)3(45) that are relevant to the bootstrap analysis of section 3.

External scalar exchange in the crossed channel. Consider the special case

$$\mathcal{O}_1 = \phi, \quad n = 0, \quad \mathcal{O}_2 = [\phi\phi]_{0,J_2}, \quad J_2^2 = \mathrm{O}(\epsilon_{15}^{-1}\epsilon_{34}^{-1}). \tag{7.A.35}$$

In this case, blocks satisfy the same Casimir equations (7.3.53),(7.3.54) as case (II) blocks, but with $\lambda_2 = 0 + \mathrm{O}(1)$[11] and $\delta n = 0$. We can thus write their asymptotics as

$$F^{(12),(45)}_{\phi[\phi\phi]_{0,J_2};0} \sim \mathcal{N}^{\phi}_{\phi[\phi\phi]_{0,J_2}} (1 - x)^{h_\phi} \mathcal{K}_{h_\phi}(J_2^2 v_2(1 - x)). \tag{7.A.36}$$

In this case however, the normalization $\mathcal{N}^\phi$ cannot be computed in the same way as case (II) because we now have $h_1 = h_\phi - n$ instead of $h_1 > h_\phi - n$, meaning that the limit of the block at $v_2 J_2^2 \ll (1-x)^{-1}$ has different asymptotics than $(v_2, x) \to (0, 1)$ at finite J_2. More specifically, the hypergeometrics in the decoupling limit simplify to

$$f_1^{\text{dec}}(v_1) = 1, \quad f_2^{\text{dec}}(v_2) = {}_2F_1\left[\begin{matrix}\bar{h}_2, \bar{h}_2 \\ 2\bar{h}_2\end{matrix}\right](1 - v_2). \tag{7.A.37}$$

[11] This implies that the blocks are in the kernel of *both* $\mathcal{D}_{12}^{(-1,0,-1)}$ and $\mathcal{D}_{12}^{(-1,0,0)}$.

We can recognize on the right hand side a four-point lightcone block, with logarithmic divergence as $v_2 \to 0$. Instead, we will determine the normalization $\mathcal{N}^\phi$ by direct computation, starting from the lightcone blocks at the $(0, v_2, x)$ node[12] and following the two green arrows in Fig. 35 to the $(0, 0, 1)$ node where (7.A.36) applies. We begin with the first limit

$$\mathrm{LS}_{34}: \quad J_2^{-2}, v_2 = \mathrm{O}(\epsilon_{34}), \quad \epsilon_{34} \to 0. \tag{7.A.38}$$

In this regime, it is well known that four-point lightcone blocks reduce to modified Bessel functions,

$${}_2F_1\left[\begin{matrix}\bar{h}_2, \bar{h}_2 \\ 2\bar{h}_2\end{matrix}\right](1-v_2) \overset{\mathrm{LS}_{34}}{\sim} 2\mathrm{B}^{-1}_{\bar{h}_2}\mathcal{K}_0(v_2 J_2^2). \tag{7.A.39}$$

At this stage, we refrained from applying the Stirling formula to the Beta function $\mathrm{B}_{\bar{h}} = \Gamma(2\bar{h})^{-1}\Gamma(\bar{h})^2$ in order to keep the formula more compact. Expanding $(1 - x\mathcal{S}_1\mathcal{S}_2)^{-\bar{h}_{12;\phi}}$ into a power series and take the large $\bar{h}_2$ limit therein, we obtain

$$F^{(12),(45)}_{\phi[\phi\phi]_{0,J_2};0} \overset{\mathrm{LS}_{34}}{\sim} 2\mathrm{B}^{-1}_{\bar{h}_2}\sum_{k=0}^{\infty}\frac{(xv_2J_2^2)^k}{k!}\frac{(h_\phi)_k}{(2h_\phi)_k}\mathcal{K}_k(v_2J_2^2). \tag{7.A.40}$$

We're still not out of the woods however, because the $v_2 J_2^2 \ll (1-x)^{-1}$ asymptotics is different for $k = 0$ and $k > 0$ in this expression. This discrepancy is removed once we take the second large spin limit to the $(0, 0, 1)$ node,

$$\mathrm{LS}_{34,51}: \quad v_2 J_2^2, 1 - x = \mathrm{O}(\epsilon_{51}^{-1}), \quad \epsilon_{51} \to 0. \tag{7.A.41}$$

In this limit, the sum (7.A.40) is dominated by the regime

$$k = \vartheta_x = -\partial_{1-x} + \mathrm{O}(1) = \mathrm{O}(\epsilon_{51}^{-1}), \tag{7.A.42}$$

where we relate k on the left to the operators on the right by the action of the latter on x^k in each summand. Approximating the sum over $k = \mathrm{O}(\epsilon_{51}^{-1})$ by an integral and using the large k formulas

$$(\Delta)_k = \sqrt{\frac{\pi}{k}}\left(\frac{k}{e}\right)^{k+\Delta}\Gamma(\Delta)^{-1}\left(1 + \mathrm{O}(k^{-1})\right), \quad x^k = e^{-k(1-x)}\left(1 + \mathrm{O}(k^{-1})\right), \tag{7.A.43}$$

$$\mathcal{K}_k(kx) = \sqrt{\frac{\pi}{k}}\left(\frac{k}{e}\right)^{k} e^{-x^2}\left(1 + \mathrm{O}(k^{-\frac{1}{2}})\right), \tag{7.A.44}$$

we find

$$F^{(12),(45)}_{\phi[\phi\phi]_{0,J_2};0} \overset{\mathrm{LS}_{34,51}}{\sim} \frac{4\Gamma(2h_\phi)}{\mathrm{B}_{\bar{h}_2}\Gamma(h_\phi)}\frac{1}{2}\int_{\mathrm{O}(1)}^{\infty}\frac{\mathrm{d}k}{k^{1+h_\phi}}e^{-k(1-x)-\frac{v_2J_2^2}{k}}. \tag{7.A.45}$$

After a change of variables $t = k(1-x)$, we can identify the integral representation of the Bessel-Clifford function in (7.A.36), with the ratio of Gamma functions on the left providing the desired normalization of (7.A.36):

$$\mathcal{N}^\phi_{\phi[\phi\phi]_{0,J_2}} = 4\frac{\Gamma(2h_\phi)}{\Gamma(h_\phi)}\lim_{\bar{h}_2\to\infty}\frac{\Gamma(2\bar{h}_2)}{\Gamma(\bar{h}_2)^2} = \frac{2\Gamma(2h_\phi)}{\Gamma(h_\phi)}4^{\bar{h}_2}\sqrt{\frac{\bar{h}_2}{\pi}}. \tag{7.A.46}$$

[12] Since $f_1^{\mathrm{dec}}(v_1) = 1$, the function F is independent of v_1 in this case.

7.B Double integral computation

In this appendix, we will prove the identity (7.3.107) by direct computation of the integral on the left hand side, namely

$$I(\alpha,\beta) := \int_{\mathbb{R}^2_+} \frac{\mathrm{d}x\mathrm{d}y}{xy} x^\alpha y^\beta \mathcal{K}_\alpha(x+y). \tag{7.B.1}$$

Since $x, y \geq 0$, it is natural to intuit the argument of the Bessel-Clifford function $\mathcal{K}_\alpha$ as the square radius of a circle in the plane. To substantiate this intuition, we make the change of variables

$$x = r^2\cos^2\theta, \quad y = r^2\sin^2\theta, \quad (r,\theta) \in \mathbb{R}_+ \times [0,\pi/2). \tag{7.B.2}$$

The variables (r,θ) can be understood as polar coordinates on the plane, and the domain of θ ensures a bijection with the upper right quadrant $(\sqrt{x},\sqrt{y}) \in \mathbb{R}^2_+$. The measure transforms as

$$\frac{\mathrm{d}x\mathrm{d}y}{xy} = 4\frac{\mathrm{d}(\sqrt{x})\,\mathrm{d}(\sqrt{y})}{\sqrt{xy}} = 4\frac{r\mathrm{d}r\mathrm{d}\theta}{r^2\cos\theta\sin\theta} = 2\frac{\mathrm{d}(r^2)}{r^2}\frac{\mathrm{d}\theta}{\cos\theta\sin\theta}.$$

The double integral thereby factorizes in polar coordinates and takes the form

$$I(\alpha,\beta) = 2\int_0^\infty \frac{\mathrm{d}(r^2)}{r^2}(r^2)^{\alpha+\beta}\mathcal{K}_\alpha(r^2)\int_0^{\pi/2}\mathrm{d}\theta\,\cos^{2\alpha-1}\theta\sin^{2\beta-1}\theta. \tag{7.B.3}$$

Using $\mathcal{K}_\alpha(r^2) = r^{-\alpha}K_\alpha(2r)$, we retrieve two known integrals of special functions for $z = 2r$ and θ, namely

$$\int_0^\infty \frac{\mathrm{d}z}{z}\left(\frac{z}{2}\right)^{\alpha+2\beta} K_\alpha(z) = \frac{1}{4}\Gamma(\alpha+\beta)\Gamma(\beta), \quad \mathrm{Re}(\alpha+2\beta) > |\mathrm{Re}(\alpha)|$$
$$\int_0^{\pi/2}\mathrm{d}\theta\,\cos^{2\alpha-1}\theta\sin^{2\beta-1}\theta = \frac{1}{2}\frac{\Gamma(\alpha)\Gamma(\beta)}{\Gamma(\alpha+\beta)}, \quad \mathrm{Re}(\alpha),\mathrm{Re}(\beta) > 0.$$

In the application of this paper, $\alpha = h_\phi + \delta n$ and $\beta = 2h_\phi - h_\star$, with $h_\phi < h_\star < 2h_\phi$ and $\delta n > 0$. We conclude that the integral converges, and our ansatz for the OPE coefficients in (7.3.105) is correct.

Chapter 8

Conclusion and Future Perspectives

After a thorough investigation of the integrability based theory of multipoint blocks, we succeeded in extracting novel CFT data from lightcone limits of higher point crossing symmetry equations. The central objects of study, namely the N-point blocks of a unitary conformal field theory, were defined in part I. In part II, we then substantiated the claim that N-point blocks are eigenfunctions of a many body quantum integrable system obtained from the Gaudin model. For comb channel blocks, we further established the hierarchy of integrable systems associated to OPE subdiagrams — the full six-point hierarchy is described in Fig. 43. In particular, the three-point subsystems of five- and six-point functions were mapped explicitly to integrable $\mathbb{Z}_4$ Calogero-Moser models. In part III, we applied these results to the five-point lightcone bootstrap, using Gaudin Hamiltonians to determine the asymptotics of blocks in lightcone limits of the crossing symmetry equation. In this way, we determined the large spin OPE coefficients that are inaccessible from four-point functions. Not only did we retrieve some previous results in the literature with an independent method, thereby placing them on more solid ground, but we also performed the first computation of large spin OPE coefficients with finite tensor structures. This analysis required us to carefully examine what kind of CFT data is "universal" in a multipoint correlator, and our integrability based approach was crucially important in reaching the correct conclusion. Finally, having devised an explicit strategy to compute some first examples of triple twist data in six-point functions, we have developed here all the tools necessary to implement it in the near future.

There are many avenues thus far unexplored in the world of N-point block integrable systems and their applications to the bootstrap — we will list here only a few.

Six-point snowflake channel. In the outlook of chapter 7, we studied the first contributions to a six-point CSE with a direct channel of snowflake topology (see Fig. 39), restricting our attention to identity exchange in the (16) OPE. For the next steps, a better understanding of the hierarchy of integrable systems for the six-point snowflake would yield important information about higher order terms in the direct channel. In particular, the lightcone limits of direct channel Casimirs suggest that higher twist terms in the (16) OPE give rise to anomalous dimension corrections at the middle leg of the crossed comb channel. This would provide a first opportunity to compute anomalous dimensions of triple-twist operators from the lightcone bootstrap.

The six-point snowflake channel is represented in Fig. 44. A basis of three-point tensor structures has already been constructed [89], corresponding to a certain monomial basis of functions $t_n(w_1, w_2, w_3)$. As far as we know, the three-variable integrable system on this space of functions is not part of

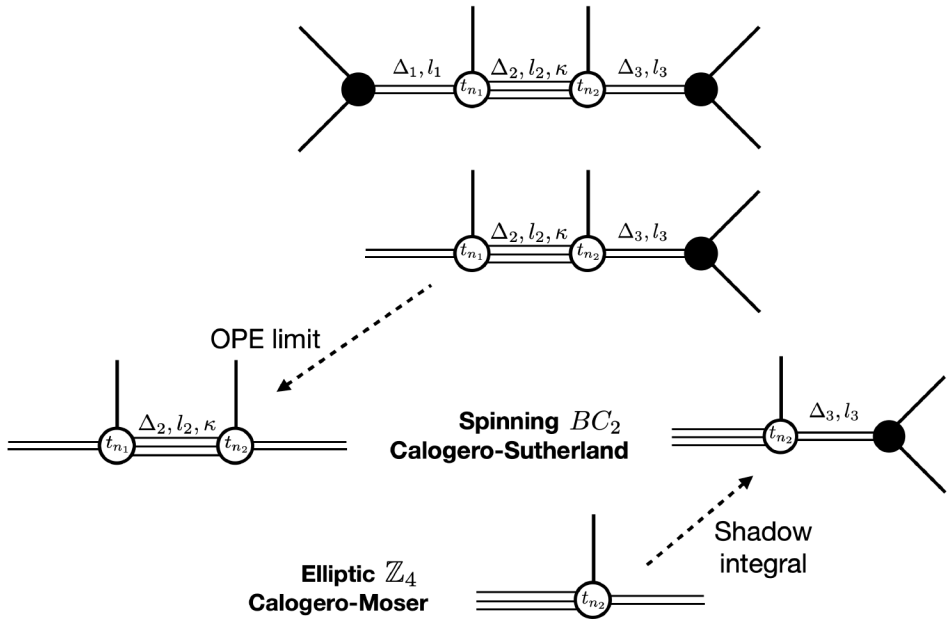

Figure 43: Hierarchy of conformal blocks integrable systems generated by the scalar six-point comb channel. The OPE limit at an internal leg realizes the reduction of a higher N, lower spin depth system to a lower N, higher spin depth subsystem, while the shadow integral representation embeds the latter into the former. The reduction to spinning CS models at $N = 4$ was demonstrated in [65], while the reduction to elliptic $\mathbb{Z}_4$ CM models at $N = 3$ was demonstrated in [64].

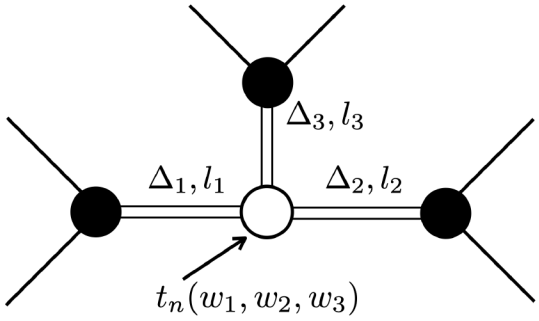

Figure 44: Diagrammatic representation of six-point snowflake channel blocks, with 3×2 edge degrees of freedom and 3 vertex degrees of freedom.

any known classification, but it behooves further investigation. On the other hand, the construction of polynomial and OPE cross ratios admits a straightforward generalization from the comb to the snowflake. All in all, the hierarchy of snowflake integrable systems associated to subdiagrams of Fig. 44 appears to be in close reach.

Multipoint Lorentzian inversion formula. The analyticity properties of higher point CFT data is an important open question to address. If the large spin expansion is convergent, then we can use our results to approximate finite spin data. Apart from its physical relevance, the finite spin regime can also be compared with numerical results. It would therefore be interesting to explore

generalizations of the Lorentzian inversion formula to higher points, as a computational tool and a means to establish that its physical data is analytic in spin. In general, the lightcone limits of higher point CSEs entail not only an expansion in large STT spin, but also analogous asymptotic expansions in MST spin and/or tensor structure labels. These limits must also be addressed to fully understand the analytic structure of higher point data. An improved understanding in this area may also shed light on the emergence of universal asymptotics in both infinite ("case (I)") and finite ("case (II)") tensor structure/MST spin regimes, the latter of which appears to describe multi-twist data. A natural starting point for tackling these questions would be the CSEs of "four-point type" discussed above Fig. 38b, which resemble spinning four-point CSEs and coincide with them in OPE limits. In these setups, we can make comparisons with the Lorentzian inversion formula for spinning blocks derived in [137, Eq. (4.45)]. Beyond this example, it may be fruitful to investigate Mellin space approaches, where AdS physics and analogies to S-matrix bootstrap are easier to decipher.

Multipoint numerical bootstrap in $d = 1$. In this thesis, we have not looked into the numerical approach to the higher point conformal bootstrap. At the current time, our knowledge of blocks in $d > 2$ is too limited for such applications, though a study of efficient Zamolodchikov-like recursion relations has yet to be carried out. That notwithstanding, even in $d = 1$, where we do have power series expansions for the blocks, an efficient algorithm to bound higher point data has not yet been found. Part of the issue is related to the opacity of the positivity conditions for the products of OPE coefficients, which resemble that of an infinite dimensional mixed correlator system. Given all of these open questions, the most promising arena for putting the numerical multipoint bootstrap to the test may be the $d = 1$ CFT living on a Maldacena-Wilson line in maximally supersymmetric Yang-Mills theory. Following the seminal work of Cavaglia et al. [143], the enhancement of standard bootstrap techniques by exact results from integrability may allow us to bootstrap six-point data even outside of the standard semi-definite programming setting. At the same time, the recent perturbative results for five- and six-point correlators derived in [144] give a valuable source of comparison in any future analysis.

Extensions to defects. The integrability of lower point defect blocks is well established [145, 146]. The conformal kinematics of defect correlators has also been well studied (see e.g. [86]). These first developments can serve as a well-founded starting point from which to investigate the integrability of N-point defect blocks. A first step would be the systematic analysis of the number of degrees of freedom in a defect correlator, and its partition into vertex and internal leg degrees of freedom in various channels. At a second stage, it would be interesting to investigate generalizations of the Gaudin construction to a general integrability based theory of higher point defect blocks.

Ultimately, we hope that the contents of this thesis may serve as a proof of concept for the multipoint lightcone bootstrap. Now that the prospect of bootstrapping triple-twist data is closer than it ever was before, we are excited to connect the results of our program with the many open questions in the CFT literature that it may help to address. Precision calculations of CFT data in O(N) models, multi-particle dynamics in Anti de Sitter space, a holistic picture of the CFT spectrum in the twist-spin plane — in all of these instances and more, we are confident that this nascent research program can significantly contribute to our understanding of conformal field theory.

Bibliography

[1] A. Polyakov, *"A View From the Island"*, Talk given at the 3rd International Symposium on the History of Particle Physics, SLAC, https://arxiv.org/abs/hep-th/9211140.

[2] H. A. Kastrup, *"On the Advancements of Conformal Transformations and their Associated Symmetries in Geometry and Theoretical Physics"*, Annalen Phys. 17, 631 (2008), arxiv:0808.2730.

[3] W. Thomson, *"Extrait d'une Lettre de M. William Thomson à M. Liouville."*, J. de Math. Pures et Appl. 10, 364 (1845).

[4] M. Smoluchowski, *"Molekular-kinetische Theorie der Opalescenz im kritischen Zustande, sowie einiger verwandter Erscheinungen"*, Ann. d. Phys. 25, 205 (1908).

[5] H. E. Stanley and V. K. Wong, *"Introduction to phase transitions and critical phenomena"*, American Journal of Physics 40, 927 (1972).

[6] E. A. Guggenheim, *"The Principle of Corresponding States"*, The Journal of Chemical Physics 13, 253 (1945).

[7] W. E. Caswell, *"Asymptotic Behavior of Nonabelian Gauge Theories to Two Loop Order"*, Phys. Rev. Lett. 33, 244 (1974).

[8] T. Banks and A. Zaks, *"On the Phase Structure of Vector-Like Gauge Theories with Massless Fermions"*, Nucl. Phys. B 196, 189 (1982).

[9] P. A. M. Dirac, *"A Remarkable representation of the 3 + 2 de Sitter group"*, J. Math. Phys. 4, 901 (1963).

[10] M. Flato, C. Fronsdal and D. Sternheimer, *"Singleton physics"*, Proceedings of the Steklov Institute of Mathematics 226, 170 (1999), hep-th/9901043, http://mi.mathnet.ru/eng/tm/v226/p185.

[11] M. Luscher and G. Mack, *"Global Conformal Invariance in Quantum Field Theory"*, Commun. Math. Phys. 41, 203 (1975).

[12] J. M. Maldacena, *"The Large N limit of superconformal field theories and supergravity"*, Adv. Theor. Math. Phys. 2, 231 (1998), hep-th/9711200.

[13] S. S. Gubser, I. R. Klebanov and A. M. Polyakov, *"Gauge theory correlators from noncritical string theory"*, Phys. Lett. B 428, 105 (1998), hep-th/9802109.

[14] E. Witten, *"Anti-de Sitter space and holography"*, Adv. Theor. Math. Phys. 2, 253 (1998), hep-th/9802150.

[15] I. Heemskerk, J. Penedones, J. Polchinski and J. Sully, *"Holography from Conformal Field Theory"*, JHEP 0910, 079 (2009), arxiv:0907.0151.

[16] A. A. Migdal, *"Conformal invariance and bootstrap"*, Phys. Lett. B 37, 386 (1971).

[17] A. M. Polyakov, *"Microscopic description of critical phenomena"*, Sov. Phys. JETP 28, 533 (1969).

[18] A. M. Polyakov, *"Conformal symmetry of critical fluctuations"*, JETP Lett. 12, 381 (1970).

[19] G. Mack and K. Symanzik, *"Currents, stress tensor and generalized unitarity in conformal invariant quantum field theory"*, Commun. Math. Phys. 27, 247 (1972).

[20] G. Mack, *"Conformal invariance and short distance behavior in quantum field theory"*, Springer Lect. Notes Phys. 17, 300 (1973).

[21] A. Polyakov, *"Non-Hamiltonian approach to conformal quantum field theory"*, Sov. Phys. JETP 66, 23 (1974).

[22] P. Liendo, Z. Liu and J. Rong, *"The old conformal bootstrap revisited"*, arxiv:2108.07295.

[23] *"Interview with Kenneth G. Wilson, 6 July 2002"*, Interview conducted by PoS collaborators: Babak Ashrafi and Sam Schweber. Edited by Alberto A. Martínez and Silvan S. Schweber., https://authors.library.caltech.edu/5456/.

[24] K. G. Wilson, *"Nonlagrangian models of current algebra"*, Phys. Rev. 179, 1499 (1969).

[25] L. P. Kadanoff, *"Operator Algebra and the Determination of Critical Indices"*, Phys. Rev. Lett. 23, 1430 (1969).

[26] A. Polyakov, *"Properties of long and short range correlations in the critical region"*, Sov. Phys. JETP 57, 271 (1969).

[27] S. Ferrara, A. F. Grillo and R. Gatto, *"Tensor representations of conformal algebra and conformally covariant operator product expansion"*, Annals Phys. 76, 161 (1973).

[28] A. Belavin, A. M. Polyakov and A. Zamolodchikov, *"Infinite Conformal Symmetry in Two-Dimensional Quantum Field Theory"*, Nucl. Phys. B 241, 333 (1984).

[29] F. Dolan and H. Osborn, *"Conformal four point functions and the operator product expansion"*, Nucl. Phys. B 599, 459 (2001), hep-th/0011040.

[30] F. Dolan and H. Osborn, *"Conformal partial waves and the operator product expansion"*, Nucl. Phys. B 678, 491 (2004), hep-th/0309180.

[31] R. Rattazzi, V. S. Rychkov, E. Tonni and A. Vichi, *"Bounding scalar operator dimensions in 4D CFT"*, JHEP 0812, 031 (2008), arxiv:0807.0004.

[32] D. Poland, S. Rychkov and A. Vichi, *"The conformal bootstrap: Theory, numerical techniques, and applications"*, Reviews of Modern Physics 91, 015002 (2019), http://dx.doi.org/10.1103/RevModPhys.91.015002.

[33] F. Kos, D. Poland, D. Simmons-Duffin and A. Vichi, *"Precision Islands in the Ising and* O(N) *Models"*, JHEP 1608, 036 (2016), arxiv:1603.04436.

[34] L. F. Alday and J. M. Maldacena, *"Comments on operators with large spin"*, JHEP 0711, 019 (2007), arxiv:0708.0672.

[35] A. L. Fitzpatrick, J. Kaplan, D. Poland and D. Simmons-Duffin, *"The Analytic Bootstrap and AdS Superhorizon Locality"*, JHEP 1312, 004 (2013), arxiv:1212.3616.

[36] Z. Komargodski and A. Zhiboedov, *"Convexity and Liberation at Large Spin"*, JHEP 1311, 140 (2013), arxiv:1212.4103.

[37] S. Ferrara, R. Gatto and A. F. Grillo, *"Conformal invariance on the light cone and canonical dimensions"*, Nucl. Phys. B 34, 349 (1971).

[38] S. Ferrara, A. F. Grillo and R. Gatto, *"Improved light cone expansion"*, Phys. Lett. B 36, 124 (1971).

[39] S. Ferrara, A. F. Grillo and R. Gatto, *"Manifestly conformal-covariant expansion on the light cone"*, Phys. Rev. D 5, 3102 (1972).

[40] D. Simmons-Duffin, *"The Lightcone Bootstrap and the Spectrum of the 3d Ising CFT"*, JHEP 1703, 086 (2017), arxiv:1612.08471.

[41] S. Caron-Huot, *"Analyticity in Spin in Conformal Theories"*, JHEP 1709, 078 (2017), arxiv:1703.00278.

[42] T. Hartman, D. Mazac, D. Simmons-Duffin and A. Zhiboedov, *"Snowmass White Paper: The Analytic Conformal Bootstrap"*, arxiv:2202.11012, in: *"2022 Snowmass Summer Study"*.

[43] J. Liu, D. Meltzer, D. Poland and D. Simmons-Duffin, *"The Lorentzian inversion formula and the spectrum of the 3d* O(2) *CFT"*, JHEP 2009, 115 (2020), arxiv:2007.07914.

[44] N. Su, *"The Hybrid Bootstrap"*, arxiv:2202.07607.

[45] S. Caron-Huot, D. Mazac, L. Rastelli and D. Simmons-Duffin, *"Dispersive CFT Sum Rules"*, JHEP 2105, 243 (2021), arxiv:2008.04931.

[46] V. Rosenhaus, *"Multipoint Conformal Blocks in the Comb Channel"*, JHEP 1902, 142 (2019), arxiv:1810.03244.

[47] S. Parikh, *"Holographic dual of the five-point conformal block"*, JHEP 1905, 051 (2019), arxiv:1901.01267.

[48] J.-F. Fortin and W. Skiba, *"New methods for conformal correlation functions"*, JHEP 2006, 028 (2020), arxiv:1905.00434.

[49] S. Parikh, *"A multipoint conformal block chain in d dimensions"*, JHEP 2005, 120 (2020), arxiv:1911.09190.

[50] J.-F. Fortin, W. Ma and W. Skiba, *"Higher-Point Conformal Blocks in the Comb Channel"*, JHEP 2007, 213 (2020), arxiv:1911.11046.

[51] J.-F. Fortin, W.-J. Ma and W. Skiba, *"Six-Point Conformal Blocks in the Snowflake Channel"*, JHEP 2011, 147 (2020), arxiv:2004.02824.

[52] J.-F. Fortin, W.-J. Ma and W. Skiba, *"Seven-Point Conformal Blocks in the Extended Snowflake Channel and Beyond"*, Phys. Rev. D 102, 125007 (2020), arxiv:2006.13964.

[53] S. Hoback and S. Parikh, *"Towards Feynman rules for conformal blocks"*, JHEP 2101, 5 (2021), arxiv:2006.14736.

[54] V. Gonçalves, R. Pereira and X. Zhou, *"20′ Five-Point Function from* $AdS_5 \times S^5$ *Supergravity"*, JHEP 1910, 247 (2019), arxiv:1906.05305.

[55] J.-F. Fortin, W.-J. Ma and W. Skiba, *"All Global One- and Two-Dimensional Higher-Point Conformal Blocks"*, arxiv:2009.07674.

[56] D. Poland and V. Prilepina, *"Recursion relations for 5-point conformal blocks"*, JHEP 2110, 160 (2021), arxiv:2103.12092.

[57] M. Isachenkov and V. Schomerus, *"Superintegrability of d-dimensional Conformal Blocks"*, Phys. Rev. Lett. 117, 071602 (2016), arxiv:1602.01858.

[58] V. Schomerus, E. Sobko and M. Isachenkov, *"Harmony of Spinning Conformal Blocks"*, JHEP 1703, 085 (2017), arxiv:1612.02479.

[59] V. Schomerus and E. Sobko, *"From Spinning Conformal Blocks to Matrix Calogero-Sutherland Models"*, JHEP 1804, 052 (2018), arxiv:1711.02022.

[60] M. Isachenkov and V. Schomerus, *"Integrability of conformal blocks. Part I. Calogero-Sutherland scattering theory"*, JHEP 1807, 180 (2018), arxiv:1711.06609.

[61] I. Burić, M. Isachenkov and V. Schomerus, *"Conformal Group Theory of Tensor Structures"*, JHEP 2010, 004 (2020), arxiv:1910.08099.

[62] I. Buric, S. Lacroix, J. A. Mann, L. Quintavalle and V. Schomerus, *"From Gaudin Integrable Models to d-dimensional Multipoint Conformal Blocks"*, Phys. Rev. Lett. 126, 021602 (2021), arxiv:2009.11882.

[63] I. Buric, S. Lacroix, J. A. Mann, L. Quintavalle and V. Schomerus, *"Gaudin Models and Multipoint Conformal Blocks: General Theory"*, JHEP 2110, 139 (2021), arxiv:2105.00021.

[64] I. Buric, S. Lacroix, J. A. Mann, L. Quintavalle and V. Schomerus, *"Gaudin models and multipoint conformal blocks. Part II. Comb channel vertices in 3D and 4D"*, JHEP 2111, 182 (2021), arxiv:2108.00023.

[65] I. Buric, S. Lacroix, J. A. Mann, L. Quintavalle and V. Schomerus, *"Gaudin models and multipoint conformal blocks III: comb channel coordinates and OPE factorisation"*, JHEP 2206, 144 (2022), arxiv:2112.10827.

[66] C. Bercini, V. Gonçalves and P. Vieira, *"Light-Cone Bootstrap of Higher Point Functions and Wilson Loop Duality"*, Phys. Rev. Lett. 126, 121603 (2021), arxiv:2008.10407.

[67] A. Antunes, M. S. Costa, V. Goncalves and J. V. Boas, *"Lightcone Bootstrap at higher points"*, JHEP 2203, 139 (2022), arxiv:2111.05453.

[68] P. Etingof, G. Felder, X. Ma and A. Veselov, *"On elliptic Calogero-Moser systems for complex crystallographic reflection groups"*, Journal of Algebra 329, 107 (2011), arxiv:1003.4689, See also erratum 2.14 in http://www-math.mit.edu/~etingof/errorsinpapers.pdf.

[69] A. Kaviraj, J. A. Mann, L. Quintavalle and V. Schomerus, *"Multipoint Comb Channel Lightcone Bootstrap - in preparation"*.

[70] *"Applications de l'analyse à la géométrie"*, *"volume I"*, 5. edition, Bachelier (1850), Paris, Note VI. *Extension au cas des trois dimensions de la question du tracé géographique* Author, G. Monge. Editor, J. Liouville.

[71] G. Lamé, *"Mémoire sur les coordonnées curvilignes"*, Journ. de Math 5, 313 (1840).

[72] P. A. M. Dirac, *"Wave equations in conformal space"*, Annals Math. 37, 429 (1936).

[73] R. Penrose, *"Zero rest-mass fields including gravitation: asymptotic behaviour"*, Proceedings of the Royal Society of London. Series A. Mathematical and physical sciences 284, 159 (1965).

[74] T. H. Go, H. A. Kastrup and D. H. Mayer, *"Properties of dilatations and conformal transformations in Minkowski space"*, Rept. Math. Phys. 6, 395 (1974).

[75] G. Mack and A. Salam, *"Finite component field representations of the conformal group"*, Annals Phys. 53, 174 (1969).

[76] J. Penedones, E. Trevisani and M. Yamazaki, *"Recursion Relations for Conformal Blocks"*, JHEP 1609, 070 (2016), arxiv:1509.00428.

[77] G. Mack, *"All unitary ray representations of the conformal group SU(2,2) with positive energy"*, Commun. Math. Phys. 55, 1 (1977).

[78] S. Minwalla, *"Restrictions imposed by superconformal invariance on quantum field theories"*, Adv. Theor. Math. Phys. 2, 783 (1998), hep-th/9712074.

[79] S. Rychkov, *"EPFL Lectures on Conformal Field Theory in D>= 3 Dimensions"*, SpringerBriefs in Physics.

[80] P. Kravchuk, J. Qiao and S. Rychkov, *"Distributions in CFT. Part II. Minkowski space"*, JHEP 2108, 094 (2021), arxiv:2104.02090.

[81] O. Aharony, S. S. Gubser, J. M. Maldacena, H. Ooguri and Y. Oz, *"Large N field theories, string theory and gravity"*, Phys. Rept. 323, 183 (2000), hep-th/9905111.

[82] J. Qiao, *"On the Wick Rotation of the Four-point Function in Conformal Field Theories"*, arxiv:2209.00285.

[83] M. S. Costa and T. Hansen, *"Conformal correlators of mixed-symmetry tensors"*, JHEP 1502, 151 (2015), arxiv:1411.7351.

[84] V. Bargmann and I. T. Todorov, *"Spaces of analytic functions on a complex cone as carriers for the symmetric tensor representations of* $\mathrm{SO}(n)$*"*, Journal of Mathematical Physics 18, 1141 (1977).

[85] V. K. Dobrev, G. Mack, V. B. Petkova, S. G. Petrova and I. T. Todorov, *"Harmonic Analysis on the n-Dimensional Lorentz Group and its Application to Conformal Quantum Field Theory"*, *"volume 63"*.

[86] E. Lauria, M. Meineri and E. Trevisani, *"Spinning operators and defects in conformal field theory"*, JHEP 1908, 066 (2019), arxiv:1807.02522.

[87] V. Fock and A. Goncharov, *"Moduli spaces of local systems and higher Teichmüller theory"*, Publications Mathématiques de l' 103, 1 (2006).

[88] I. Le, *"Cluster Structures on Higher Teichmuller Spaces for Classical Groups"*, Forum of Mathematics, Sigma 7, E13 (2019).

[89] M. S. Costa, J. Penedones, D. Poland and S. Rychkov, *"Spinning Conformal Correlators"*, JHEP 1111, 71 (2011), arxiv:1107.3554.

[90] M. S. Costa, J. Penedones, D. Poland and S. Rychkov, *"Spinning Conformal Blocks"*, JHEP 1111, 154 (2011), arxiv:1109.6321.

[91] L. Iliesiu, F. Kos, D. Poland, S. S. Pufu, D. Simmons-Duffin and R. Yacoby, *"Bootstrapping 3D Fermions"*, JHEP 1603, 120 (2016), arxiv:1508.00012.

[92] E. Elkhidir, D. Karateev and M. Serone, *"General Three-Point Functions in 4D CFT"*, JHEP 1501, 133 (2015), arxiv:1412.1796.

[93] Harish-Chandra, *"On Some Applications of the Universal Enveloping Algebra of a Semisimple Lie Algebra"*, Transactions of the American Mathematical Society 70, 28 (1951).

[94] I. R. Klebanov and E. Witten, *"AdS/CFT correspondence and symmetry breaking"*, Nuclear Physics B 556, 89 (1999), hep-th/9905104.

[95] F. Dolan and H. Osborn, *"Conformal Partial Waves: Further Mathematical Results"*, arxiv:1108.6194.

[96] G. Poschl and E. Teller, *"Bemerkungen zur Quantenmechanik des anharmonischen Oszillators"*, Z. Phys. 83, 143 (1933).

[97] S. Ferrara, A. Grillo, G. Parisi and R. Gatto, *"Covariant expansion of the conformal four-point function"*, Nucl. Phys. B 49, 77 (1972), [Erratum: Nucl.Phys.B 53, 643–643 (1973)].

[98] D. Li, D. Meltzer and D. Poland, *"Conformal Bootstrap in the Regge Limit"*, JHEP 1712, 013 (2017), arxiv:1705.03453.

[99] Harish-Chandra, *"Spherical Functions on a Semisimple Lie Group, I"*, Amer. J. Math. 80, 241 (1958).

[100] I. Buric and V. Schomerus, *"Universal Spinning Casimir Equations. Applications to Defect CFTs - in preparation"*.

[101] I. O. Burić, *"Harmonic Analysis in Conformal and Superconformal Field Theory"*.

[102] K. Symanzik, *"On Calculations in conformal invariant field theories"*, Lett. Nuovo Cim. 3, 734 (1972).

[103] S. Ferrara, A. Grillo, G. Parisi and R. Gatto, *"The shadow operator formalism for conformal algebra. Vacuum expectation values and operator products"*, Lett. Nuovo Cim. 4S2, 115 (1972).

[104] K. Koller, *"The Significance of Conformal Inversion in Quantum Field Theory"*, Commun. Math. Phys. 40, 15 (1974).

[105] D. Simmons-Duffin, *"Projectors, Shadows, and Conformal Blocks"*, JHEP 1404, 146 (2014), arxiv:1204.3894.

[106] S. Ferrara, A. F. Grillo and R. Gatto, *"Manifestly conformal covariant operator-product expansion"*, Lett. Nuovo Cim. 2S2, 1363 (1971).

[107] M. Gaudin, *"Diagonalisation d'une classe d'hamiltoniens de spin"*, Journal de Physique 37, 1087 (1976).

[108] M. Gaudin, *"La fonction d'onde de Bethe"*, Masson (1983).

[109] B. Feigin, E. Frenkel and N. Reshetikhin, *"Gaudin model, Bethe ansatz and correlation functions at the critical level"*, Commun. Math. Phys. 166, 27 (1994), hep-th/9402022.

[110] B. Feigin and E. Frenkel, *"Affine Kac-Moody algebras at the critical level and Gelfand-Dikii algebras"*, Int. J. Mod. Phys. A7S1A, 197 (1992).

[111] D. Talalaev, *"Quantization of the Gaudin system"*, hep-th/0404153.

[112] A. Chervov and D. Talalaev, *"Quantum spectral curves, quantum integrable systems and the geometric Langlands correspondence"*, hep-th/0604128.

[113] A. I. Molev, *"Feigin-Frenkel center in types B, C and D"*, Inventiones Mathematicae 191, 1 (2013), arxiv:1105.2341.

[114] A. Molev, *"Sugawara Operators for Classical Lie Algebras"*, Mathematical surveys and monographs, American Mathematical Society (2018).

[115] O. Yakimova, *"Symmetrisation and the Feigin-Frenkel centre"*, arxiv:1910.10204.

[116] A. Chervov, G. Falqui and L. Rybnikov, *"Limits of Gaudin algebras, quantization of bending flows, Jucys-Murphy elements and Gelfand-Tsetlin bases"*, Lett. Math. Phys. 91, 129 (2010), arxiv:0710.4971.

[117] A. Chervov, G. Falqui and L. Rybnikov, *"Limits of Gaudin Systems: Classical and Quantum Cases"*, SIGMA 5, 029 (2009), arxiv:0903.1604.

[118] L. Rybnikov, *"Cactus group and monodromy of Bethe vectors"*, arxiv:1409.0131.

[119] P. Argyres, O. Chalykh and Y. Lü, *"Inozemtsev System as Seiberg-Witten Integrable system"*, arxiv:2101.04505.

[120] L. Eberhardt, S. Komatsu and S. Mizera, *"Scattering equations in AdS: scalar correlators in arbitrary dimensions"*, JHEP 2011, 158 (2020), arxiv:2007.06574.

[121] G. Mack, *"Convergence of Operator Product Expansions on the Vacuum in Conformal Invariant Quantum Field Theory"*, Commun.Math.Phys. 53, 155 (1977).

[122] H. Osborn and A. Petkou, *"Implications of conformal invariance in field theories for general dimensions"*, Annals Phys. 231, 311 (1994), hep-th/9307010.

[123] A. Joseph, *"A generalization of Quillen's lemma and its application to the Weyl algebras"*, Israel Journal of Mathematics 28, 177 (1977).

[124] S. P. Smith, *"A Class of Algebras Similar to the Enveloping Algebra of* sl(2)*"*, Transactions of the American Mathematical Society 322, 285 (1990).

[125] V. V. Bavula, *"Generalized Weyl algebras and their representations"*, Algebra i Analiz 4, 75 (1992).

[126] T. J. Hodges, *"Noncommutative deformations of type-A Kleinian singularities"*, Journal of Algebra 161, 271 (1993).

[127] W. Crawley-Boevey and M. P. Holland, *"Noncommutative deformations of Kleinian singularities"*, Duke mathematical journal 92, 605 (1998).

[128] A. Oblomkov, *"Deformed Harish-Chandra homomorphism for the cyclic quiver"*, Math. Res. Lett 14, 359 (2007), math/0504395.

[129] P. Etingof, W. L. Gan, V. Ginzburg and A. Oblomkov, *"Harish–Chandra homomorphisms and symplectic reflection algebras for wreath-products"*, Publications mathémati 105, 91 (2007), math/0511489.

[130] M. P. Holland, *"Quantization of the Marsden-Weinstein reduction for extended Dynkin quivers"*, Annales Scientifiques de l'École Normale Supérieure 32, 813 (1999).

[131] P. Etingof, S. Loktev, A. Oblomkov and L. Rybnikov, *"A Lie-theoretic construction of spherical symplectic reflection algebras"*, Transformation Groups 13, 541 (2008), arxiv:0801.2339.

[132] F. W. J. Olver, A. B. Olde Daalhuis, D. W. Lozier, B. I. Schneider, R. F. Boisvert, C. W. Clark, B. R. Miller, B. V. Saunders, H. S. Cohl and M. A. McClain, *"NIST Digital Library of Mathematical Functions"*, editors listed above. Release 1.1.6 of 2022-06-30, http://dlmf.nist.gov/.

[133] E. W. Weisstein, *"'Lemniscate Function'. From MathWorld — a Wolfram Web Resource"*, https://mathworld.wolfram.com/LemniscateFunction.html.

[134] P. Etingof and E. Rains, *"On algebraically integrable differential operators on an elliptic curve"*, SIGMA 7, 062 (2011), arxiv:1011.6410.

[135] N. Reshetikhin and J. Stokman, *"Asymptotic boundary KZB operators and quantum Calogero-Moser spin chains"*, arxiv:2012.13497.

[136] F. Delduc and G. Valent, *"Classical and quantum structure of the compact Kählerian sigma models"*, Nuclear Physics B 253, 494 (1985).

[137] P. Kravchuk and D. Simmons-Duffin, *"Light-ray operators in conformal field theory"*, JHEP 1811, 102 (2018), arxiv:1805.00098.

[138] D. Mazáč, L. Rastelli and X. Zhou, *"An analytic approach to BCFT$_d$"*, JHEP 1912, 004 (2019), arxiv:1812.09314.

[139] G. J. Heckman and E. M. Opdam, *"Root systems and hypergeometric functions. I"*, Compositio Mathematica 64, 329 (1987).

[140] A. Castedo Echeverri, E. Elkhidir, D. Karateev and M. Serone, *"Seed Conformal Blocks in 4D CFT"*, JHEP 1602, 183 (2016), arxiv:1601.05325.

[141] D. Karateev, P. Kravchuk and D. Simmons-Duffin, *"Weight Shifting Operators and Conformal Blocks"*, JHEP 1802, 081 (2018), arxiv:1706.07813.

[142] T. G. Raben and C.-I. Tan, *"Minkowski conformal blocks and the Regge limit for Sachdev-Ye-Kitaev-like models"*, Phys. Rev. D 98, 086009 (2018), arxiv:1801.04208.

[143] A. Cavaglià, N. Gromov, J. Julius and M. Preti, *"Integrability and conformal bootstrap: One dimensional defect conformal field theory"*, Phys. Rev. D 105, L021902 (2022), arxiv:2107.08510.

[144] J. Barrat, P. Liendo, G. Peveri and J. Plefka, *"Multipoint correlators on the supersymmetric Wilson line defect CFT"*, JHEP 2208, 067 (2022), arxiv:2112.10780.

[145] M. Isachenkov, P. Liendo, Y. Linke and V. Schomerus, *"Calogero-Sutherland Approach to Defect Blocks"*, JHEP 1810, 204 (2018), arxiv:1806.09703.

[146] I. Burić and V. Schomerus, *"Defect Conformal Blocks from Appell Functions"*, JHEP 2105, 007 (2021), arxiv:2012.12489.